Plate kinematic evolution and regional stress history of sedimentary basins along the East African and West Madagascan continental margins

Amy Tuck-Martin

Supervisors:

Prof. Jürgen Adam

Dr. Graeme Eagles

Advisor:

Dr Ian Watkinson

A thesis submitted in fulfilment of the requirements for the degree of Doctor of Philosophy

Department of Earth Sciences,
Royal Holloway,
University of London,
Egham,
United Kingdom

Declaration of Authorship

I, Amy Tuck-Martin, hereby declare that this thesis and the work presented in it is entirely my own. Where I have collaborated with other authors or referred to the work of others, this is always clearly stated.

Signed: 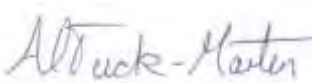

Date: 06/09/2018

Acknowledgements

I would like to thank everyone who has helped and contributed towards this Phd.

Jürgen, thank you for all your help and guidance, all the pep talks, cat stories and cups of tea. If I ever got lost, you put me back on the right track. All your hard work and attention to detail. You always helped to organise me and the often overwhelming amount of information gathered throughout this PhD.

Graeme, regardless of distance you were always there to help, even when you were in the middle of Antarctica.

Rob, thank you for all your help with the stress modelling, and your patience as I got to grips with "computer language".

I would also like to thank Lucia for all your help with the plate tectonic modelling and producing the age grid. You were a substitute 'Graeme' when I had questions that couldn't be answered by email.

I would like to thank the COMPASS research group for funding and allowing me to pursue this research in the first place.

I would also like to thank my advisor Ian, all the members of the department that keep it running smoothly, Kevin D'Souza, Dan Parsonage, Lynne White, Julie Brown and Diane Serpant.

Mark and Frank for all you IT related help. Especially Frank for your help setting up linux, I would not have had a clue. It's all computer language. Margaret Collinson who gave me a nudge towards the finish line.

My desk neighbours, Camilla and Rebecca, and to all those people who came for tea with me every day at 3pm, the ProcasTEAnation group. Alex, Adam, Zoë, Amy, Ailish. Especially Rebecca who understood the need for cake and complaining. Adam, who also took a rather alternative route towards a PhD. Everyone who bought me kinder eggs.

Sean, thank you for all your support, love and encouragement whilst I got on with my school work, and your patience with me. I'm so happy you get to continue your studies now. My family, thank you for all the years of unconditional love and support, I wouldn't be where I am now without it. Sean's family, Lin and Barry for giving me many much-needed breaks in cornwall and looking after me so well when we visit. Alfie and Doug, puppy therapy.

Abstract

Plate kinematic evolution and regional stress history of sedimentary basins along the East African and West Madagascan continental margins

by Amy Tuck-Martin

The East African and West Madagascan continental margins have been shaped by several periods of rifting, complicated by plate boundary reorganisation and oceanic ridge propagation events in the Northwest Indian Indian Ocean. The structure and evolution of the sedimentary basins along the margins were strongly controlled by the tectonic processes during margin formation. In this area, these tectonic processes originate from the fragmentation of Gondwana since the early Jurassic and the opening of the NW Indian Ocean.

This thesis presents a new comprehensive plate kinematic model for the opening of the Northwest Indian Ocean based on finite rotation poles generated by a method of visual fitting and iterative joint inversion of magnetic isochron and fracture zone data. The model presents 4 phases of tectonic development from 183-177 to the present day. It also provides a way to model the predicted first-order regional paleostress fields at key tectonic stages based on plate motion vectors and the nature and geometry of the plate boundaries.

The plate kinematic model was integrated with geological and structural data of the basins and used to allocate basin fill megasequences based on lithology, structural information and depositional environment ascertained from literature, to produce a margin scale tectono-stratigraphic framework for the East African and West Madagascan continental margins. The framework can be used to identify and correlate main stages of basin evolution to better understand the timing and distribution of petroleum system types.

The plate kinematic model was used to generate a seafloor age grid for the ocean floor at 75 Ma. This age grid, along with plate motion and boundary constraints form the kinematic model, were used as input to model the forces acting on the African plate at this time based on the assumption that the torques of the forces and balanced, and hence model the resultant stress field. The force model of Africa at 75 Ma failed to reach a solution, as a result the stress field could not be generated. Future work will focus on changed the constraints on the slab pull force to try and reach a solution.

This thesis successfully integrates plate kinematic and paleostres modelling with basin fill histories to highlight the important interplay between plate tectonics, plate boundary forces and basin formation, and the implications for petroleum system developments in these underexplored and challenging margins.

Table of Contents

List of Figures

1 Introduction

2 New Plate Kinematic Model and Tectono-stratigraphic History of the East African and West Madagascan Margins

List of Tables

Chapter 1

Introduction

1.1 Introduction

The East African and West Madagascan continental margins have evolved over the past ~180 million years as Gondwana broke apart. Prior to this, periodic, intracontinental Karoo rifting events initiated the formation of sedimentary basins all along the future margins and culminated in the eruption of the Karoo-Ferrar Large Igneous Province across South Africa (Karoo) and Antarctica (Ferrar) (Cox, 1992) After a further period of rifting in the Early to Mid-Jurassic, East Gondwana (Madagascar/India/Seychelles/Australia/Antarctica) and West Gondwana (Africa, South America) finally broke apart, accommodated by seafloor spreading in the West Somali and Mozambique basins and dextral strike-slip movement on the Davie Fracture Zone. Following the initial breakup, East Gondwana continued to fragment complicated by a number of boundary relocations and ridge propagations forming the present-day plate assembly of the Northwest Indian Ocean and its accompanying continental margins (fig. 1.1).

Since the development of plate tectonic theory and the recognition of the first conjugate magnetic anomaly data in the study region during the 1960's (e.g. Le Pichon & Heirtzler, 1968), many attempts have been made to model the plate motions that led to the opening of the Northwest Indian Ocean. As the data have improved in both quantity and quality, the complexities in the tectonic development of the area have become clearer. Individual tectonic models have been built to describe or account for these complexities, but when combined they have failed to produce a single self-consistent and coherent plate tectonic model.

Understanding the breakup between East and West Gondwana, and subsequent tectonic changes, is crucial to understanding the development of the East African and West Madagascan sedimentary basins at a time when the improving political landscape sees them emerging as frontiers for hydrocarbon exploration, and where knowledge is limited.

The East African continental margin has been largely ignored in the past in terms of hydrocarbon exploration, in favour of the western coast. Many early test wells came up dry. However, in the past couple of decades exploration has increased and the area has become a hotspot for natural gas discoveries. To build on these discoveries, it is important to understand the evolution of the area.

1.2 Motivation

The breakup between Africa, Madagascar, Antarctica and India, and the opening of the Northwest India Ocean was accomplished by a complex series of boundary changes and the opening of distinct ocean basins As a result, authors have struggled to connect the different stages into one into a complete model, from the first breakup between East and West Gondwana to the present day plate configuration. We reconcile this by producing a comprehensive plate kinematic model for all stages of development of the NW India Ocean using updated seafloor data.

Plate boundary forces drive plate motion and dominate the regional intraplate stress field. The tectonic changes in the NW Indian Ocean will have changed the boundary forces acting on the African Plate through timw and hence the intraplate stress field, which in turn effects development of the marginal sedimentary basins. For example, by causing uplift or subsidence, reactivating faults, or forming large-scale lithospheric folding. Understanding these effects and integrating them with basin fill histories allows us to investigate the link between tectonics, plate boundary forces, paleostress fields and basin evolution. This is important in reducing exploration risks and aids the identification of potential petroleum systems.

1.3 Aims

The main aims of this thesis are:

- To develop a of a new, high resolution plate kinematic model of the Northwest Indian Ocean (Chapter 2)
- To perform a 1st-order plate-kinematic stress analysis based on the plate-kinematic model (Chapter 2 & 3)
- To produce a comprehensive tectono-stratigraphic framework for the East African and West Madagascan margins by integrating the results of a new, high resolution plate kinematic model of the Northwest Indian Ocean and with geological and structural data about the area from literature (Chapter 3)
- To develop and test a workflow for the application of dynamic stress modelling to build dynamic paleostress map data being fully constrained by the plate-kinematic model (Chapter 4)

Previous plate kinematic models have been improved upon by the inclusion on an updated set of magnetic anomaly data and newly calculated rotation parameters.

Paleostress prediction maps derived from the plate kinematic model are produced for important tectonic stages and compared to the regional stress histories of sedimentary basins along the East African (Somalia to Mozambique) and West Madagascan marginal basins, which are compiled from published studies. The comparison and benchmarking will allow for a new margin-scale integration of basin histories caused by a complex rift and break-up history. The framework can be used or improved upon by industry professionals or the methods applied to other rifted margins of interest

1.4 Thesis Outline

Chapter 1 presents an introduction to the concepts and methods included in this thesis as well as an overview of the study area.

Chapter 2 is an article submitted to *Basin Research* which presents the plate kinematic model of the Northwest Indian Ocean from 183 Ma to the present day, based on seafloor spreading data. The paper presents the evolution of the area in 4 phases illustrated by a few key images that show the important changes.

Chapter 3 provides an in-depth review of the structural and stratigraphic evolution of the sedimentary basins along the East African and West Madagascan margins, correlated with the plate kinematic model of chapter 2 to produce a margin-wide tectono-stratigraphic framework for the area and paleogeographic maps for important tectonic stages.

The chapter also presents 1st-order plate-scale kinematic paleostress maps for each phase of development and discusses the potential implications of the tectonic changes in the model on the evolution of the East African and West Madagascan Margins.

Chapter 4 describes the method used for dynamic stress modelling, using the plate kinematic model as input. It also presents initial results, for example a seafloor age grid for the African Plate at 75 Ma, used in the stress modelling.

Chapter 5 comprises a review of the main results discussed in chapters 2, 3 and 4, critically evaluating their limitations and making suggestions for further work.

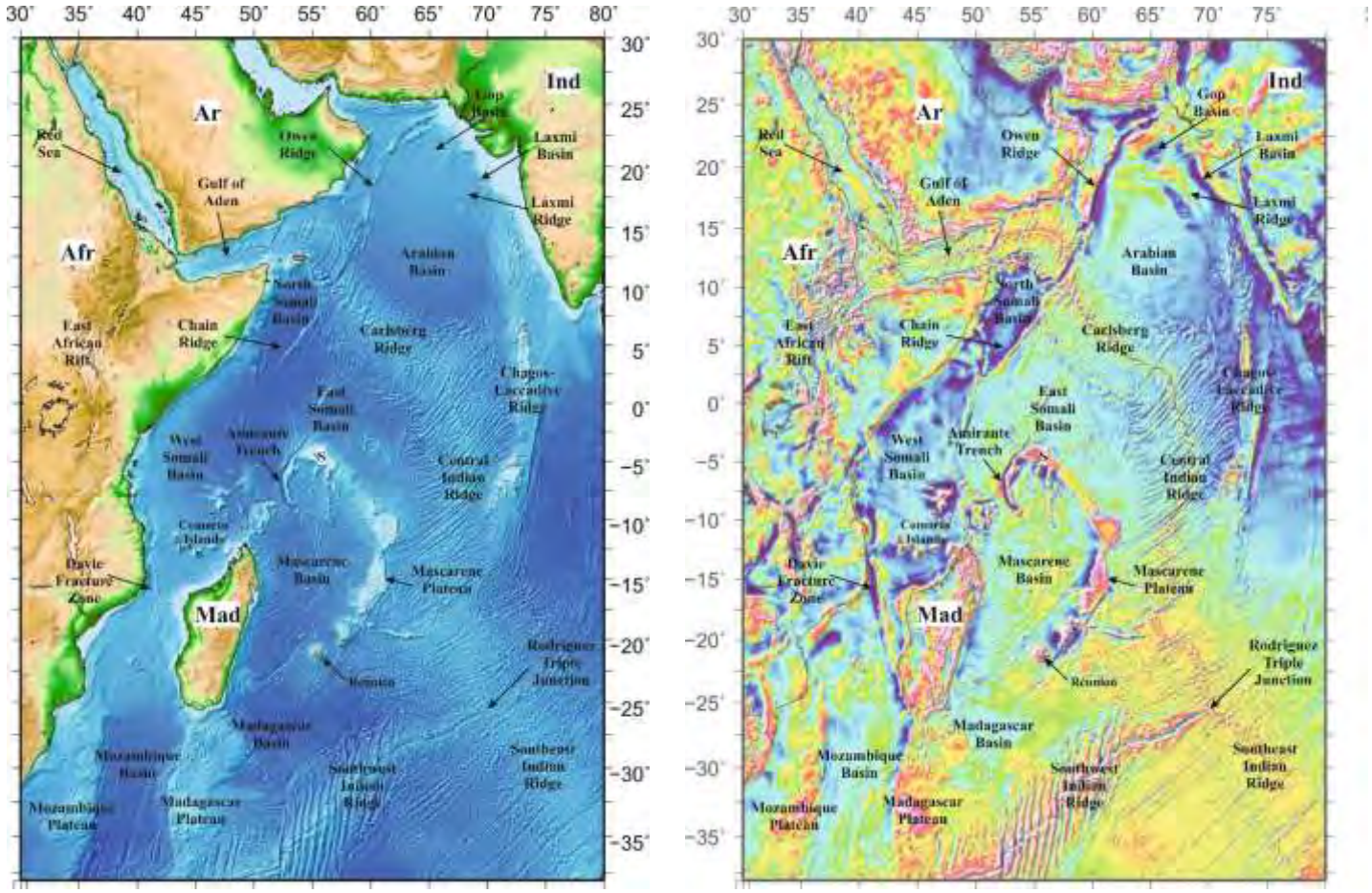

Figure 1.1: Topographic and free-air gravity maps of the study area, including important features involved in the tectonic evolution of the area. Afr – Africa, Ar – Arabia, Ind – India, Mad – Madagascar and S – Seychelles.

1.5 Plate Tectonic Theory

Plate tectonic theory revolutionised the way we view the surface of the planet in the 1960s, although its foundations were laid long before. First, Alfred Wegner suggested the theory of continental drift in 1912, after he noted the similarities between the shapes of adjacent coastlines across oceans and the correlations between palaeontological, zoological and botanical data on different continents. One of the main concerns with this theory voiced by sceptics was how can continents move when they are separated by the solid ocean floor? Despite this, work on the magnetism of continental rocks started in the 1950s and confirmed that the continents had moved relative to each other. In the early 60's both Dietz (1961) and Hess (1962) developed the theory of seafloor spreading describing how upwelling limbs of mantle convection cells create new seafloor at mid-ocean ridges, transported away by mantle convection cells and recycled into the interior of deep oceanic trenches at the downwelling limbs.

Throughout history, Earth's magnetic field has varied in strength and direction. The polarity of Earth's present day magnetic field is considered 'normal' with magnetic north lying near geographic north, but at times in that past has flipped by 180° so that magnetic north lies near geographic south, giving so-called 'reversed' polarity. When lavas erupted at mid-ocean ridges cool, magnetic domains in the minerals that form align to the Earth's magnetic field and record its direction at that point in time. As new oceanic crust is formed and moves away from the ridge to the accompaniment of a series of field polarity reversals it creates magnetic stripes of normal and reversed polarity that generally run parallel to and mostly (but not always) symmetrically to this ridge axis.

Raff and Mason (1961) were the first to produce a detailed map of magnetic anomalies of the seafloor which showed alternating stripes of normal and reversed polarity rocks (Raff and Mason, 1961) (fig. 1.2). The stripes run parallel to mid-ocean ridges and are offset by transform faults. The origin of these magnetic stripes was correctly identified by Vine and Mathews (1963) as the result of seafloor spreading and intermittent reversals in Earths field.

By the late 1960's the theory of plate tectonics had been refined and presented by a number of scientists such as McKenzie (1967) and Morgan (1968). The theory expands upon the earlier ideas of continental drift and seafloor spreading, and states that the Earth's lithosphere is broken up into nearly rigid segments or plates, which can include both continental and oceanic lithosphere, that move across the earth's surface, interacting with one another at their edges. The theory is based on a number of assumptions. First, new oceanic lithosphere is generated by seafloor spreading and second, once created it forms part of a rigid plate. Third, the generation of new oceanic lithosphere is balanced by its destruction to maintain a constant surface area of the Earth, and fourth, stresses can be transmitted through a plate over great horizontal distances without it buckling i.e. motion between plates is accommodated at distinct plate boundaries (Fowler, 2005).

Figure 1.2: One of the first magnetic anomaly maps of the total magnetic field off the west coast of North America produced by Raff & Mason, 1961.

1.6 Plate Reconstructions

Plate tectonic reconstructions depend on correctly identifying segments of active and ancient plate boundaries, dating/ understanding the movement that resulted in their present day relative locations and calculating a set of rotation parameters that accurately describes this movement. The following section briefly describes the data and methods used to produce the plate reconstructions presented in this thesis.

Euler Poles

The motions of tectonic plates around the surface of a sphere (i.e. the Earth) are described using Euler's 'fixed-point' theorem (Eulero, 1776), which states that "The most general displacement of a rigid body with a fixed-point is equivalent to a

rotation about an axis through that fixed point". In terms of plate tectonics this theory can describe the movement of rigid plates over the surface of the Earth as moving in small circles about an axis that passes through the centre of the Earth. The point where the axis cuts the surface of the Earth is called an Euler pole. The displacement of one plate with respect to another is given by degrees of rotation around a pole at a certain longitude and latitude (fig. 1.3). By convention, as seen from the inside of the planet, a clockwise rotation is a positive value and anticlockwise is negative. In map view, positive rotation angles conventionally denote anticlockwise rotations.

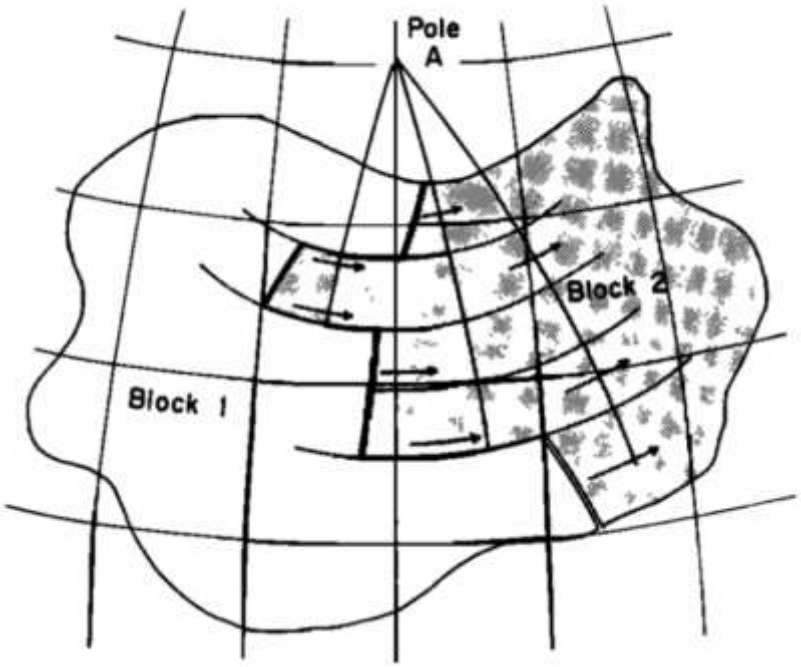

Figure 1.3: On a spherical earth, the motion of block 2 relative to block 1 must be a rotation about some pole. All the transform faults on the boundary between 1 and 2 must be small circles about pole A (Morgan, 1968).

There are three types of rotations used in tectonic reconstructions. Stage rotations describe the motion of a plate between two times assuming a constant speed and direction in between. Instantaneous rotations describe the motion at a geological instant. Reconstruction rotations, also called finite rotations, describe the sum of all plate motion between sometime in the past and some later time (usually the present) but not the individual components that make up that motion (Fowler, 2005).

Magnetic Anomaly Data

In section 1.2 we described how reversals in the Earth's magnetic field through time lead rocks of the oceanic crust to present a pattern of magnetic stripes with alternating normal and reversed polarity.

Ship-mounted or towed magnetometers can detect deviations from the magnetic field expected to be generated by convection of liquid iron in Earth's outer core. Where they pass over 'normal' polarised crust this core field is enhanced, where it is reversed the core field is reduced. These deviations are called magnetic anomalies. Given the origin of the magnetic anomaly stripes at mid-ocean ridges by instantaneous reversals of the magnetic field polarity, it is possible to 'pick' linear isochrons in the ocean floor from parts of prominent magnetic anomalies gathered by ships. Typically, these isochrons show the beginning (old) and end (young) edges of an anomaly.

To understand this magnetic anomaly pattern and date the 'stripes', it is essential to know the durations of past periods of normal and reversed polarity. With a so-called polarity reversal timescale, models of the expected magnetic variation over the ridge and its flanks can be made by multiplying these durations by the past rates of seafloor spreading at the ridge. In 1966, Vine published the first "reversal timescale" for the past 4 million years by using potassium-argon dating on a magnetic-reversal sequence measured in continental lavas and on oceanic islands. Theoretical magnetic anomalies calculated from the reversal timescale showed remarkably good agreement with those observed from the ocean floor. Since then significant improvements and additions have been made to create a geomagnetic timescale detailed enough to allow dating of the seafloor everywhere that suitable basaltic rocks exist to raise magnetic anomalies over oceanic crust. In 2012, Gradstein et al. produced the most up to date geomagnetic polarity timescale, allowing marine magnetic anomalies to be used for identifying isochrons in the so-called M-Series (Jurassic to Early Cretaceous) and the Late Cretaceous to Neogene C-series. The ages of most of these magnetic isochrons have been constrained by biostratigraphy, cyclostratigraphy and radio-isotope dating.

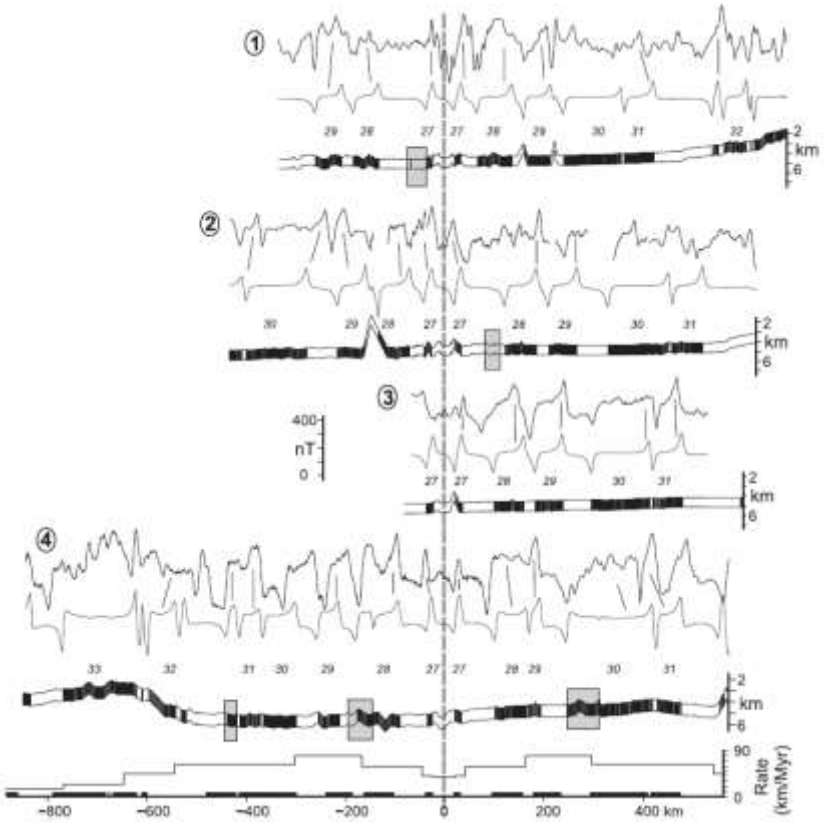

Figure 1.4: Four magnetic anomaly profiles (numbered solid lines) anomaly isochron models (dashed lines) from the Mascarene Basin. The black and white block models show the normal and reverse-polarity seafloor magnetisation (Eagles & Wibisono, 2013)

Magnetic anomaly profiles, like those for the Mascarene Basin (Indian Ocean) in figure 1.4, and the magnetic anomaly 'picks' derived from them can be used to reconstruct past plate motions and model the growth of the ocean basins between them.

Conjugate magnetic anomaly picks of the same age, separated by a mid-ocean ridge can be reconstructed back to one another by using finite rotations generated by visual fitting or by iterative joint inversion techniques (in this thesis, the main iterative technique used is that of Nankivell (1997), as described by Eagles (2004) and Livermore et al. (2005)). This method reduces the misfits of sets of small and great circle segments to the locations of fracture zones and magnetic anomaly data in the ocean floor produced by the divergence of pairs of plates. It is used and described in more detail in chapter 2.

1.7 Plate Boundary Forces

The movement of tectonic plates both relative to each other and relative to the mantle is associated with a number of different forces, some that drive plate motion and some that resist plate motion (Fowler, 2005).

Since the development of plate tectonic theory, scientists have tried to understand the forces that allow the plates to move across the earth. There are two types of forces acting on tectonic plates, those that drive plate motion and those that resist it. A plausible set of forces acting on the plates has been described by Forsyth and Uyeda (1975) and figure 1.5 illustrates these forces.

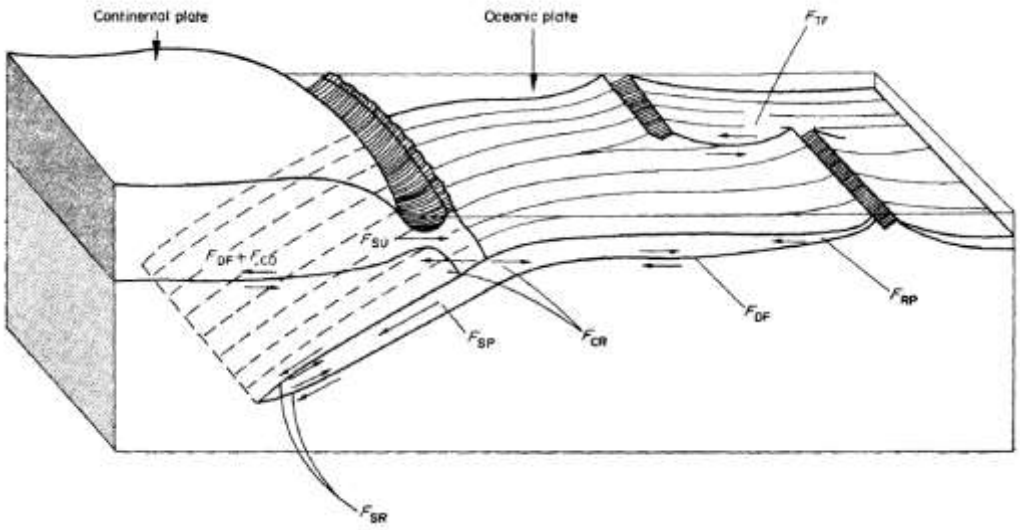

Figure 1.5: A set of possible forces that can act on lithospheric plates. F_{DF} – mantle drag, F_{CD} – extra mantle drag beneath continents, F_{RP} – ridge push, F_{TF} – transform fault resistance, F_{SP} – slab pull, F_{SR} – slab resistance, F_{CR} – colliding resistance acting on both plates with equal magnitude and opposite directions, F_{SP} – Slab pull (Forsyth & Uyeda, 1975)

Ridge Push:

Ridge push (F_{RP}) driving forces are associated with the topography of mid-ocean ridges at divergent plate boundaries. Despite the name, ridge push is not isolated to the spreading ridges, instead its effects are integrated over the entire oceanic lithosphere (Govers & Meijer, 2001). It results from a combination of the push by the upwelling mantle material and the tendency of newly formed plate to slide down the sides of the ridge due to gravity (Fowler, 2005). The ridge is topographically high, rising several kilometres above the ocean floor and this produces a significant lateral force (Fossen, 2010).

At the elevated ridge crest, the associated stress regime is extensional and dominated by normal faulting (Fossen, 2010). However, further away from the ridge the ridge push force is compressional in nature and acts horizontally through the lithosphere, perpendicular to the axis of the spreading ridge.

Hess (1962) first described the idea of a pushing force at mid-ocean ridges as a result of upwelling magma forcing the lithosphere apart. The first gravitational mechanism for spreading at mid-ocean ridges was proposed by Orowan (1964). This mechanism suggests that spreading is based on the principles of isostasy. That

is, pressure under the elevated ridge is greater, due to greater weight of overlying rock, than the pressure in the oceanic crust to either side, forcing material away from the ridge. However, the ridge material is less dense than the surrounding crust and gradually compensates for the greater volume of rock down to the isostatic compensation depth. Based on this theory, Hales (1969) proposed a model in which the raised lithosphere of the mid-ocean ridges slid down the elevated ridge. In 1970, Jacoby proposed that due to isostasy and the presence of less dense material, the ridges were uplifted, and this resulted in sliding similar to Hales' proposal. It was not until 1975 that Forsyth and Uyeda first used the term 'ridge push force'.

The importance of ridge push and the role it plays in driving plate tectonics has been debated over the years. The model of seafloor spreading proposed by Hess (1962) assumed that plate motion was primarily the result of convection currents in the mantle but further developments of the theory suggested that some form of ridge push was present in addition to mantle convection and was necessary to keep the plates moving. However, calculations indicated that slab pull (see next section) was an order of magnitude stronger than ridge push and the dominant mechanism driving plate tectonics (Forsyth & Uyeda, 1975).

However, the effects of slab pull are mostly negated by large resistive forces acting on the descending slab as it penetrates the mantle. The net force at the trench is probably comparable to ridge push (Turcotte & Schubert, 2002). In addition, mantle convection is probably too slow for drag between the lithosphere and the asthenosphere to account for the observed motion of the plates. As a result, ridge push can be considered as one of the dominant forces driving plate motion.

The method of calculating ridge push force was described by Richter & McKenzie in 1978 and the method is still used today. The equation used to estimate of the total ridge push per unit length of the ridge axis was described by Richter & McKenzie (1978) as follows:

$$F_{rp} = ge(\rho_m - \rho_w)\left(\frac{t}{3} + \frac{e}{2}\right)$$

The magnitude of ridge push is obtained by using a thermal model of a spreading ridge, such as the upwelling of hot mantle of density ρ_m at the ridge axis which then cools as it moves away from until the temperature gradient is constant across the entire thickness of the plate t. The mantle density is constant across the base of the entire plate.

As the plate cools and moves away from the ridge the elevation difference e between the ridge axis and the cooled plate increases. The pressure P_1 beneath the ridge axis at a distance z above the base of the plate is:

$$P_1 = (\rho_m - \rho_w)g(t + e - z)$$

Where ρ_w is the density of sea water. When the plate has cooled and a linear temperature gradient has become established between the mantle and the sea floor, the density within the plate ρ_p increases linearly with z:

$$\rho_p = \rho_m - \rho_w + \beta_z$$

Integration gives the pressure P_2 beneath the old sea floor

$$P_2 = g(\rho_m - \rho_w)(t - z) + \frac{g\beta}{2}(t^2 - z^2)$$

Assuming that the ridge is in hydrostatic equilibrium then P_1=P_2 when z=0, i.e. at the ridge axis. Thus

$$\beta = \frac{2(\rho_m - \rho_w)e}{t^2}$$

As a result, the ridge push equation is obtained by integration:

$$F_{rp} = \int_0^{t+e} P_1 dz - \int_0^{t} P_2 dz$$

$$F_{rp} = ge(\rho_m - \rho_w)\left(\frac{t}{3} + \frac{e}{2}\right)$$

The implications of the ridge push force on the regional first-order tectonic stress field are discussed in section 1.9.

Slab Pull:

Another major plate driving force is slab pull (F_{SP}). At subduction zones, the old, cold oceanic crust is much denser than the mantle into which it is descending, and so creates a negative buoyancy force which is called slab pull. It has been estimated that 'slab pull' is an order of magnitude greater than ridge push and as a result may be the dominant force in plate tectonics (Forsyth & Uyeda, 1975). However, it has also been suggested that slab pull may largely be balanced within the subducting slab itself by Slab Resistance (F_{SR}), which arises from viscous shear stresses acting on the top and bottom of the slab where it moves past the surrounding mantle rocks (Forsyth & Uyeda, 1975).

Resistive Forces:

Mantle drag (F_{DF}) is the resistive force along the base of the plate, assuming that the mantle is flowing slower than the plate velocity (if it is faster, then the force may drive plate motion). Mantle drag is proportional to the area of the plate and is of the same magnitude as the resistive force acting on the descending slab. These two are the main resistive forces; other minor resistive forces occur at the ridge axis and along transform faults (Transform Resistance (F_{TF}); Fowler, 2005). Mantle drag acts in the direction of absolute plate motion (Forsyth & Uyeda, 1975), therefore, where

stress fields align well with absolute plate motion it may be assumed that mantle drag is controlling the intraplate stress orientation. Where the stress field deviates from this direction, it may indicate that other forces are dominating the stress field (Zoback, 1992).

1.8 Stresses and Geological Structures

Stress (σ) is the measure of force applied to a body per unit area. This can cause internal deformation called strain (ε) that changes the shape or volume of the body. Stress acting on a plane can be subdivided into normal and shear components. Normal stresses act perpendicular to the plane, either towards each other (compressional) or away from each other (extensional). Shear stresses act in opposite directions parallel the plane (Adam, 2010). Stress at a given point is described by the stress tensor and illustrated by the stress ellipsoid. The ellipsoid gives a 2D representation of stress at a point and has three axes; σ1 maximum principal stress, σ2 intermediate principal stress, and σ3 minimum principal stress (Fossen, 2010).

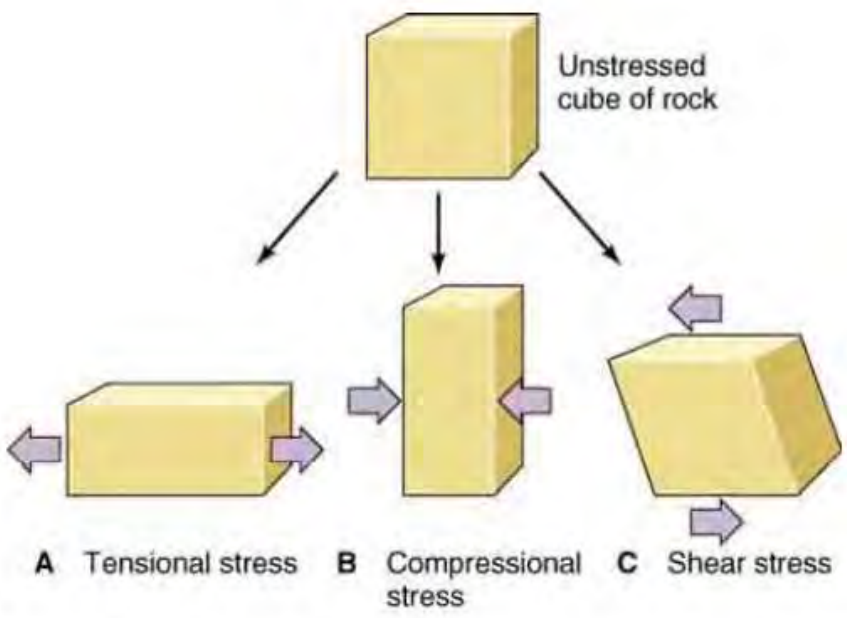

Figure 1.6: Stresses acting on a rock volume in the Earth Crust (Adam, 2010)

In mathematical terms, stress is a 2nd order tensor, a quantity with a direction, magnitude and specific plane. In total, the state of stress at a point has nine components. These comprise three normal stress vectors and six shear stress components which originate from a normal stress component and two shear stress components acting on each of the three orthogonal surfaces of an infinitesimal cube (Fossen, 2010). The cube can be oriented so that all of the six shear stresses equal zero and all that remains are the three non-zero normal stress axes, which then represent the principal stress axes (Fossen, 2010).

σ1 = Maximum principal axis

σ2 = Intermediate principal axis

σ3 = Minimum principal axis

Stresses in the lithosphere provide important information about the tectonic processes that are responsible for them. The orientation of the principal stress axis at any point in the lithosphere determines the tectonic regime that will develop at that point. The traditional classification of tectonic stress regimes came from Anderson in 1951. It assumes that there is no shear stress at the Earth's surface, which has the corollary that one of the principal stresses has to be oriented vertically and the other two horizontally (Fossen, 2010).

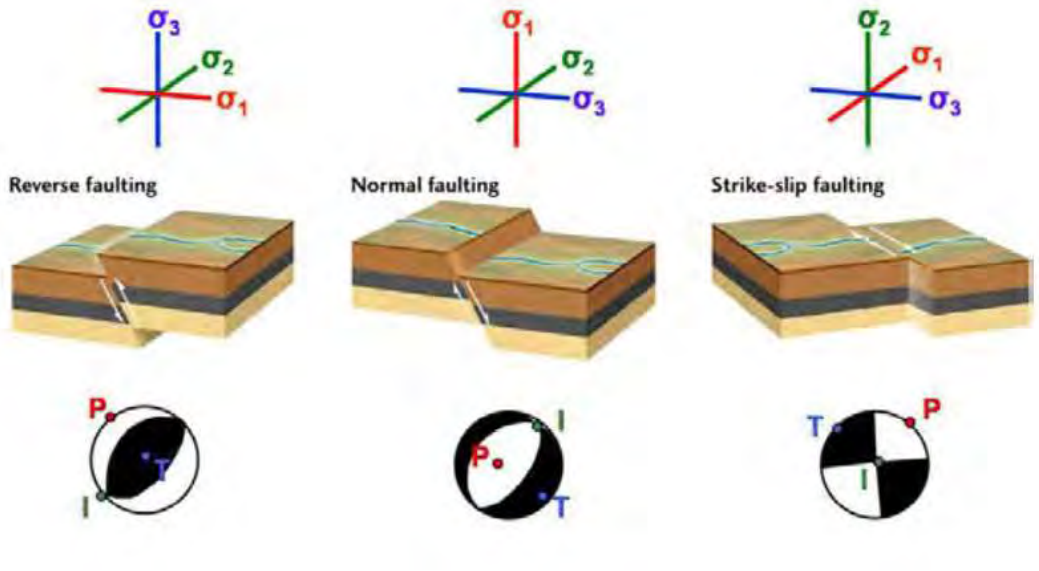

Figure 1.7: The orientations of the principal stresses and their resultant tectonic regimes according to Anderson (1951). Stereonets show fields of compression (white) and tension (black) (Adam, 2010)

The horizontal stresses have been used to estimate the paleostress field of East Africa throughout the plate kinematic model (see chapter 2).

1.9 Modelling Paleostress Fields

The tectonic processes that control structural styles and tectonic subsidence of sedimentary basins on rifted continental margins are governed by nearby regional tectonic stresses and, hence, by the plate boundaries surrounding them.

The World Stress Map Project (WSM) (fig. 1.8) has compiled present-day in-situ stress data stress data from numerous sources, e.g. earthquake focal mechanisms and borehole breakouts, and has made many important conclusions about the origin and distribution of stress in the lithosphere.

Numerous authors associated with the project (Richardson, 1992; Zoback & Zoback, 1989; Zoback, 1992) suggest that the first-order intra-plate stress field in stable plates such as North America, South America and Europe, is predominately compressional in nature and the result of compressional forces applied at the plate boundaries, namely ridge-push and slab-pull transmitted over distances of hundreds to thousands of kilometres through the seismic brittle crust into intra-plate regions. Consequently, the orientation of the stress field is determined by the geometry of plate boundaries.

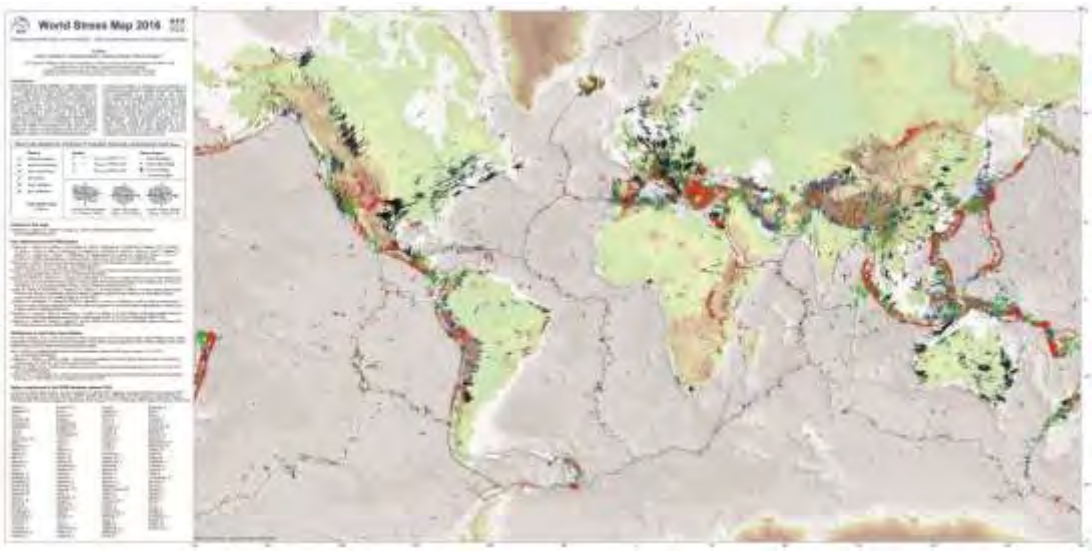

Figure 1.8: World Stress Map release 2016 (Heidbach et al., 2016)

Richardson (1992) found that there is a strong correlation between the torques arising from ridge-push forces and both the absolute velocity directions and intraplate stress field (i.e. the direction of maximum horizontal stress) of stable intraplate continental regions such as North America, Western Europe and South America. Based on the correlation between stress orientations and plate motions, he concluded that intraplate stress fields are the result of the same forces that drive plate motion. Where the relationship between boundary forces and plate motion is more complex, for example the Indo-Australian Plate, other processes must also be important.

Further analysis of WSM data reveals that short wavelength stress patterns are frequently present on a regional to basin scale (10's – 100's km). These second-order stress patterns are not controlled by plate boundary forces but instead by major intraplate forces such as gravitational forces associated with surface loads like deltas or ice sheets, or buoyancy forces related to lateral strength and density contrasts. These second-order stresses are often associated with specific geological or tectonic features like basins, detachments, and fault systems (Zoback, 1992; Heidbach et al., 2010; Tingay, 2009).

Intraplate areas of active extension are generally associated with areas of high topography, and the intraplate stress field in these areas is dominated by buoyancy stresses related to crustal thickening or thinning. This is one of several categories of second-order (regional) stresses or local perturbations (Zoback, 1992). For example, the stress orientation in the East African rift is rotated 50°-60° relative to that in the rest of western Africa due to extensional buoyancy forces caused by lithospheric thinning.

On the northeastern Canadian continental shelf, the orientation of $S_{H\ max}$ is rotated by 75°-85° compared to surrounding regions, possibly in relation to margin-normal extension in response to sediment-loading stresses (Zoback, 1992)

On a smaller scale still, second-order (regional) and third-order (local; <100 km) sources of stress become important (Heidbach et al., 2007). Active faults, local intrusions, active volcanoes, detachment horizons and density contrasts are all examples of features that refract, add to, or otherwise distort regional stress to give rise to third-order variability (Heidbach et al., 2007).

1.10 Stresses in Sedimentary Basins

Basin- and field-scale stress fields result from the complex combination of numerous factors acting at different scales, including far-field forces (e.g. plate boundary forces), basin geometry (e.g. the shape of deltaic wedges), geological structures (e.g. diapirs, faults), mechanical contrasts (e.g. near accumulations of evaporites, overpressured shales, detachment zones), topography and deglaciation (Tingay et al., 2009).

Plate boundary forces and large intra-plate sources of stress (isostatic compensation, lithospheric flexure and large topographic forces) are the main forces controlling the intra-plate stress field and, thus, the stress fields measured in basement rocks underlying sedimentary basins are commonly very similar to first- and second-order stress patterns. Hence, first- and second-order stress fields provide the background onto which local stress perturbations are superimposed (Tingay, 2009).

In general, the far-field stresses have much greater magnitudes than 'local' stresses and dominate the stress field. However, the influence of these stronger, far field stresses (acting in the basement) can be partially or totally removed from the stresses acting in the overlying sedimentary sequences by deep mechanical detachment zones. Hence, basins that contain some form of basal detachment zone typically exhibit complicated stress patterns due to the dominance of smaller intra-basin sources of stress, whereas basins whose fills are mechanically attached to the basement typically display regionally consistent stress fields resulting from far-field forces (Bell, 1996).

1.11 Sedimentary Basin Formation and Defining Features in Divergent Settings

During continental rifting, breakup and the subsequent formation of new oceanic crust between the continents, sedimentary basins form and fill along the newly formed continental margins. Their development is initially controlled by mechanical rifting and tectonic subsidence, and then later by thermal subsidence during passive margin development. The main stages in the development of sedimentary basins in such settings is described below:

1. Rifting – characterised by extensive extensional faulting, rotation of fault blocks, sedimentation in the intervening basins
2. Proto-oceanic trough development – stretching has rapidly thinned the lithosphere to allow a new ocean basin to form
3. Passive Margin – the basin continues to subside as part of a broad regional pattern of subsidence due to cooling following complete thinning of the continental lithosphere and the production of new oceanic lithosphere.

The stratigraphy of a rift basin is controlled by many different factors including tectonism, climate, sea level and sedimentary processes. In an ideal scenario, the stratigraphy of rift basins can be described as follows (by Bosence, 1998, fig. 1.9)

- **Pre-rift sequence**
- **Unconformity** – marks the onset of extension. A widespread or local erosional surface on rotated fault blocks with onlap of syn-rift strata
- **Syn-rift megasequence** – these sediments are deposed deposited during active mechanical extension and subsidence. The strata of this megasequence can be recognised by thickening into the hanging wall basins near faults to produce a fanning appearance
- **Unconformity** – marks the end of extension. Also called the 'Break-up unconformity' by Falvey (1974) and signals the onset of seafloor spreading. In more general terms, marks the onset of passive thermal subsidence phase of basin development.
- **Post-rift megasequence** – strata are deposited in the post-rift thermal subsidence phase. They often follow a sequence of shallow marine to deep marine sediments over time as the basin subsides. The sequence is commonly marked by thick onlapping and offlapping strata which may have an initial sawtooth appearance as the megasequence fills any remaining exposed half-grabens. Post-rift thermal subsidence occurs over a much wider area than mechanical subsidence due to it being controlled by cooling and increases in density of the lithosphere. It is also amplified by water and sediment loading.

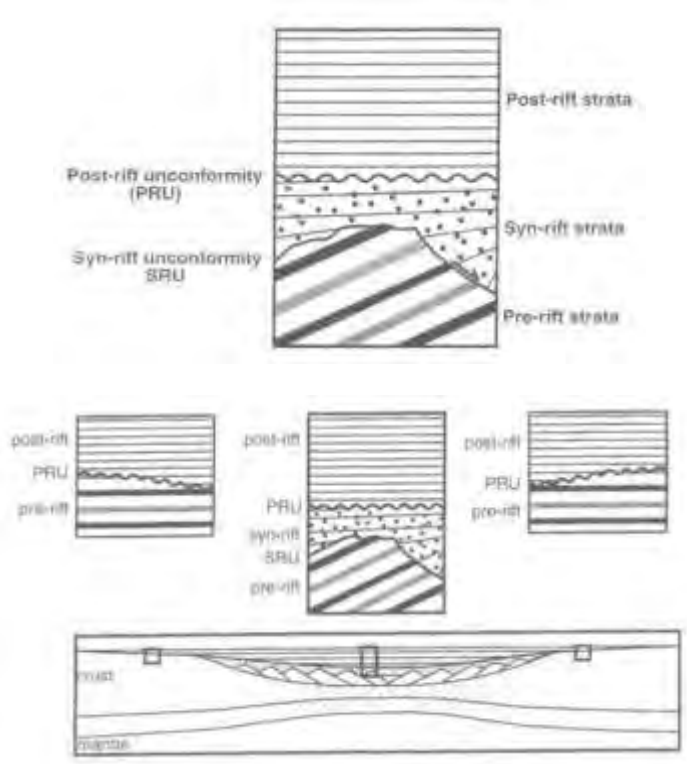

Figure 1.9: Example of tectonically controlled megasequences in rift basins (Bosence, 1998)

There are a number of key features that can affect the appearance and presence of megasequences in rift basins including location with respect to plate boundary, basin driving mechanism, heat flow and geometry. As a result, not all megasequences are present in all areas of the basins (Bosence, 1998, fig. 1.9).

This simple megasequence stratigraphy will form the basis for correlation between the sedimentary basins and plate tectonic model of the East African margins.

1.12 Lithospheric Extensional Processes

When considering the formation of continental-margin sedimentary basins it is necessary to also consider the different styles of lithospheric stretching and types of rifted margin.

Active vs Passive Rifting:

There are two end member models of continental extension, active and passive. The distinction between the two is based on the behaviour of the asthenosphere and whether or not there are active dynamic processes.

Passive rifting arises due to tensional stresses transmitted by plate boundary forces or generated by variations in the gravitational potential energy (Turcotte & Oxburgh, 1973; Coblentz et al., 1994; Coblentz & Sandiford, 1994). Lithospheric

thinning and upwelling of the asthenosphere occurs passively in response to separation in the overlying layers controlled by regional tectonic extension. However, many secondary processes are driven by passive asthenospheric upwelling such as decompression-driven melting, crustal/lithospheric magma underplating, eruption of continental flood basalts, the onset of secondary convection, and the development of large thermal gradients between extended and unextended regions (Nemčok, 2016).

Alternatively, active rifting is associated with tensile stresses produced by active asthenospheric upwelling (Houseman & England, 1986), and is often accompanied by early, possibly hotspot-related, magmatism (e.g. Şengör & Burke, 1978; Turcotte & Emerman, 1983; Storey, 1995).

Within these rifting models lie range of styles and geometries of extensional systems. Three major modes of extension were identified by Buck (1991): narrow rifts, wide rifts and a core complex mode of extension. These modes of extension are dependent on a number different factors including crustal thickness, thermal structure, strength of the lithosphere, rheological stratification, strain rates, nature and rates of sedimentation, and water content in the system (Nemčok, 2016).

The presence of magma can alter the mode of extension (Corti et al., 2003). However, even in the absence of magmatism, the system evolves in time, switching for example, a core complex mode to a rifting mode (Rosenbaum et al., 2008).

Two types of passive continental margins have been identified – volcanic and non-volcanic – based on the results of seismic studies and ocean drilling (Fowler, 2005). Volcanic (or magma-rich) margins are associated with a significant amount of mantle melting, and volcanism occurring either immediately prior to, or during, the process of continental break-up (Fowler, 2005). The presence of magma increases complexity (Rosenbaum et al., 2008). Non-volcanic (or magma-poor) margins form with no associated melting of the mantle (Fowler, 2005) and are less common than volcanic margins but less complex (Rosenbaum et al., 2008).

Non volcanic margins can become hyperextended where extensive stretching of the crust occurs such that the lower and upper crust become coupled and embrittled, allowing major faults to penetrate to the mantle, leading to partial hydration (serpentinization) of the uppermost mantle. They typified by slow extension rates (Doré & Lundin, 2015). Hyperextended crust is weak and prone to deformation and may play a role in localising subduction when oceans close. As a result, hyperextended margins may play a significant role during Wilson Cycles, i.e. process where oceans open and close along broadly similar lines during supercontinent break up (Doré & Lundin, 2015).

1.13 Overview of geological history of East Africa

Here we present a brief overview of the development of the Northwest Indian Ocean as a foundation to our plate kinematic model in chapter 2.

The Pan-African Orogeny

The term Pan-African Orogeny is used to describe the series of tectonic, magmatic and metamorphic events that led to the amalgamation of Gondwana during the period ~870 to ~550 Ma (Kröner & Stern, 2004). It cannot be considered as one true orogenic event, but a cycle of mountain building events encompassing the Brasiliano, Pan-African, Adelaidean and Beardmore orogenies, which closed a number of small oceans including the Mozambique, Adamastor, Damara and Trans-Sahara oceans (Abu-Alam et al., 2013). The Pan-African collisional belts cement together five major Archean crotons: West Africa, Congo, Tanzania, Kaapvaal and Kalahari, together with the poorly understood Saharan Metacraton (fig. 1.10) a possible mix of Proterozic microcontinents (Rino et al., 2008), and pre-Neoproterozic basement(?) remobilized during the Neoproteroic Pan-African Orogeny (Abdelsalam et al., 2002).

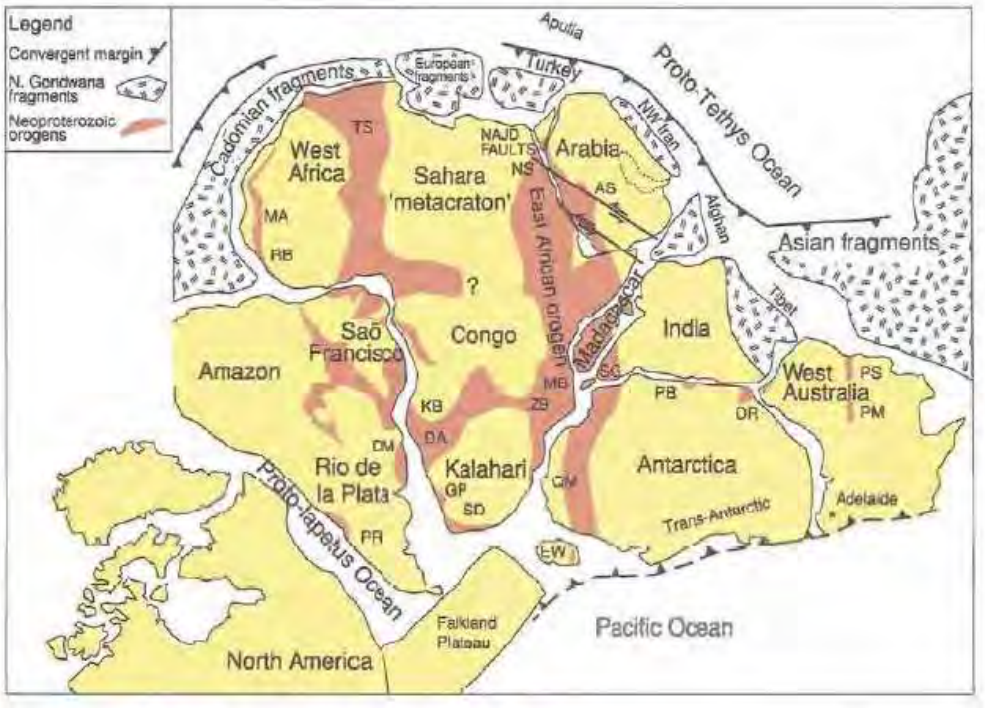

Figure 1.10: The arrangement of cratons and metamorphic mobile belts in Pangea formed by the Pan-African Orogeny. AS – Arabian Shield; BR – Brasiliano; DA – Darnara; DM – Dom Feliclano; DR – Denman Darling; EW – Eilsworth-Whitrnore Mountains; GP – Gariep; KB – Kaoko; MA – Mauretanides; MB – Mozarnbique Belt; NS – Nubian Shield; PM – Peterman Ranges; PB – Pryolz Bay; PR – Parnpean Ranges; PS – Paterson; QM – Queen Maud Land; RB – Rokelides; SD – Saldania; SG – Southern Granulite Terrane; TS – Trans-Sahara Belt; WB – West Congo; ZB – Zambezi. (Reproduced by Kröner & Stern, 2004, from Kusky et al., 2003).

The 'East African Orogen' (Kröner & Stern, 2004) consists of the Arabian-Nubian Shield in the north and the Mozambique belt further south that lies along the East African coast and forms the metamorphic basement for many of the sedimentary basins that overprinted this region as Gondwana fragmented in the Jurassic.

Karoo

The term Karoo can be used to describe a period of intracontinental tectonic activity from the Late Carboniferous to the Early Jurassic when Pangea had reached its full extent, as well as the basins that formed in that time, and the sediments deposited in them (Catuneanu et al., 2005). The Karoo tectonic activity experienced along the East African margin varied from compressional in the south, related to the convergent Panthalassan margin of Gondwana, and extensional in the north in relation to spreading along the Tethyan margin of Gondwana (Catuneanu et al., 2005) The Karoo rifting failed to separate any land masses by new oceans and in Africa culminated in the eruption of the Karoo volcanics at ~182 Ma (Encarnacion et al., 1996) which has been linked to the Karoo-Ferrar mantle plume that was also the cause of the Ferrar volcanics in Antarctica (White & McKenzie, 1989). The continental sediments of the Karoo Supergroup mark the start of deposition in the sedimentary basins that formed along what would go on to become the East African continental margin (see chapter 3).

The Breakup of Gondwana and the Opening of the Indian Ocean

The first stage of Gondwana breakup involved the separation of East Gondwana (including East Antarctica, India, Seychelles, Madagascar and Australia) from Africa, forming the West Somali and Mozambique basins (Eagles and König, 2008) between Africa and Madagascar. Madagascar/India/Antarctica initially moved southeast away from Africa (fig. 1.1). The timing of this rifting episode remains difficult to constrain. The oldest magnetic isochrons have been tentatively identified by Leinweber and Jokat (2012) as M41n (165.6 Ma) in the Mozambique Basin, which may indicate the age of breakup and the onset of seafloor spreading. Coffin and Rabinowitz (1987) dated breakup at ~165 Ma by extrapolation of marine magnetic anomalies to their interpretation of the continent-ocean boundary and Gaina et al. (2013) gave an age of ~170 Ma, based on a reassessment of gravity, seismic and magnetic data.

When oceanic spreading in the West Somali Basin stopped, at either 123 Ma (Segoufin & Patriat, 1980; Gaina et al., 2013) or during chron M10 – between 133.9 and 133.5 Ma (Coffin & Rabinowitz, 1987; Eagles & König, 2008), the plate boundary relocated to the south, separating Madagascar/Seychelles/India from Antarctica with the development of oceanic crust in the Enderby Basin off Antarctica.

After passing over the assumed 'Marion hotspot', India separated from Madagascar, accommodated by seafloor spreading at a southeast striking mid-ocean ridge, the Mascarene Ridge, and the opening of the Mascarene Basin. The Marion plume caused widespread volcanism on Madagascar (O'Neill et al. 2003) between 91.6 and 83.6 Ma (Ganerød et al. 2011). The resultant Morondava volcanics have been used to date the onset of rifting at ~89 Ma, along with the extrapolation of synthetic flowlines past magnetic anomaly 34y (84 Ma) on the African plate towards the Madagascan Margin (Eagles & Wibisono, 2013). The Mascarene ridge had a

relatively short lifespan, the reversed polarity of magnetic anomaly 26 lies directly either side of the fossil median valley of the ridge crest which dates the abandonment of the ridge at somewhere between 61.1 and 58.74 Ma (Eagles & Wibisono, 2013).

The Mascarene basin is bordered by the strikingly linear continental margin of Madagascar on the western side with a positive-negative gravity anomaly couplet that suggests the presence of extended continental crust. At the eastern margin of the basin lies the Mascarene plateau, the age and origin of which is not agreed upon. It is possible that parts of the Mascarene Plateau are underlain by continental crust, but it is completely covered by volcanic rock which youngs to the south, emplaced during the ridge's passage over the Deccan-Réunion plume.

During the abandonment of the Mascarene Ridge in favour of a new mid-ocean ridge to the east of the Mascarene Palteau, two microcontinents became isolated in the ocean interior, the Seychelles platform and the Laxmi Ridge (Müller et al. 2001).

The Seychelles are shown to consist of Precambrian granitic continental basement (Torsvik et al. 2001), a microcontinent that became isolated and rotated as part of an independent plate from approximately 64 to 61 Ma, the details of whose formation and rotation are only now coming to light (Cande et al. 2010; Ganerød et al. 2011; Eagles & Hoang, 2013).

A curved positive-negative gravity anomaly couplet called the Amirante Trench (fig. 1.1) lies to the southwest of the Seychelles and has a very unusual morphology. It has been previously suggested that it is a subduction zone (Miles, 1982), but it does not bear the detailed structure associated with traditional understanding of a subduction zone, and also lacks a chemical signature of subduction in the igneous rocks found there (Stevens et al., 2009). The structure of the Amirante Trench can more plausibly be related to crustal thickening by thrusting and folding during a convergent phase that followed its initial development as a spreading centre with a median valley during a phase of divergent motion between the Africa and Seychelles plates, which rotated rapidly about a migrating Euler pole during Palaeocene times (Eagles & Hoang, 2013).

The Laxmi ridge separates the Laxmi basin and the Arabian basin (fig. 1.1). The Laxmi basin remains something of an enigma, with many authors disagreeing on how it formed. Interpretations of linear magnetic anomalies suggest ultra-slow spreading between chron 33 and 28 (Bhattacharya et al. 1994). However, the presence of an axial volcanic plug is more reminiscent of a fast spreading ridge (Corfield et al., 2010). There are those who dispute the existence of a fossil spreading centre at all, attributing to the Laxmi basin a transitional crustal floor and its magnetic anomalies to igneous intrusions sourced from the Deccan-Réunion mantle plume (Krishna et al. 2006). In an attempt to unify the different theories on the Laxmi Basin, Eagles and Wibisono (2013) conclude that the basin evolved into a

site of oceanic accretion during chrons 29 and 28, which was probably preceded by extension of transitional crust during chron 30.

The Carlsberg Ridge is an active, slow-spreading centre in the northern Indian Ocean. Seafloor spreading on the Carlsberg Ridge began ~63.4 Ma in the north, with the oldest oceanic crust recording chron 28n (Collier et al., 2008). With Mascarene Ridge not being abandoned until ~61 Ma, it is possible the two ridges would have been active for about 2 million years at the same time, with the Seychelles isolated and moving as part of an independent plate in between.

Following the end of seafloor spreading in the Mascarene Basin, the Carlsberg Ridge propagated south, separating India from the Mascarene Plateau. Magnetic isochron interpretations show that the Seychelles was completely severed from India by the start of chron 27n (61.98 Ma). Therefore rifting was completed only a mere 3.5 Ma after the main phase of volcanic eruption from the Deccan Traps on India, from the Deccan-Réunion mantle plume (Collier et al., 2008), suggesting a tenuous link between mantle plume arrival and continental breakup.

The Deccan Traps flood basalts have been spatially and temporally linked to the separation of India and the Seychelles (Collier et al. 2008). There is some debate surrounding when the Deccan Traps eruptions began and ended, but it is generally agreed that the main tholeiitic eruption happened rapidly at 65.5 ±1 Ma (chron 29r). However, the timing of rifting between India and Seychelles is widely disagreed upon, largely due to the identification of magnetic anomalies on the Indian side, especially in the Laxmi Basin and neighbouring Gop Rift (Collier et al. 2008). The variation in dates is so large that some interpret rifting as preceding flood basalt emplacement (for example, Bhattacharya et al. 1994 date it at 79.54 Ma (chron 33n)) and others put it later (for example Miles et al. 1998 date it at 62.0 Ma (chron 27n)).

Since the Oligocene, a new phase of tectonic rifting has dominated in the region, with the development of the East African Rift System (EARS), a series of branching intracontinental rifts running through East Africa, approximately north to south, from Eritrea all the way south to Mozambique. If it does not fail, the system will eventually break the Somalian Plate away from the rest of Africa. Although, the EARS has not been modelled in this thesis its implications on the development of the sedimentary basins are profound, and will be discussed.

Chapter 2

New Plate Kinematic Model and Tectono-stratigraphic History of the East African and West Madagascan Margins

2.1. Introduction

This chapter is subdivided into two sections. The first section includes the journal article published in *Basin Research*. The second part of this chapter goes into detail about the datasets and methods, and how the tectonic model evolved throughout the course of this project in depth. It provides detail that could not be included in the publication.

2.2. Author Contributions

This chapter is written in the form of a journal article. It has been submitted to Basin Research, reviewed and sent back with corrections.

Amy Tuck-Martin drafted the majority of the manuscript (apart from the exceptions detailed below); produced all figures except figure 2 and submitted the manuscript for review.

Graeme Eagles developed the finite rotation model presented in Section 2.1 of this chapter, entitled New rotation model for ANT-AFR plate motion, drafted figure 2, and compiled the information in table 1.

Jürgen Adam drafted sections 2.4 (Paleostress maps derived from plate kinematic model) and 4 (Evolution of Regional Tectonic Stress Regimes).

All authors contributed to the proofing of the manuscript, discussion of the model's results and reviewer corrections.

Received: 10 May 2017 | Revised: 9 February 2018 | Accepted: 22 April 2018

DOI: 10.1111/bre.12294

ORIGINAL ARTICLE

WILEY Basin Research EAGE

New plate kinematic model and tectono-stratigraphic history of the East African and West Madagascan Margins

Amy Tuck-Martin[1] | Jürgen Adam[1] | Graeme Eagles[2]

[1]Department of Earth Sciences, Royal Holloway, University of London, Egham, Surrey, UK

[2]Alfred Wegner Institute, Helmholtz Centre for Polar und Marine Research, Bremerhaven, Germany

Correspondence
Amy Tuck-Martin, Department of Earth Sciences, Royal Holloway, University of London, Egham, Surrey, UK.
Email: amy.tuck-martin.2010@live.rhul.ac.uk

Abstract

The continental margins of East Africa and West Madagascar are a frontier for hydrocarbon exploration. However, the links between the regional tectonic history of sedimentary basins and margin evolution are relatively poorly understood. We use a plate kinematic model built by joint inversion of seafloor spreading data as a starting point to analyse the evolution of conjugate margin segments and corresponding sedimentary basins. By correlating megasequences in the basins to the plate model we produce a margin-scale tectono-stratigraphic framework comprising four phases of tectonic development. During Phase 1 (183–133 Ma) Madagascar/India/Antarctica separated from Africa, first by rifting and later, after breakup (at ca. 170–165 Ma), by seafloor spreading in the West Somali and Mozambique basins and dextral strike-slip movement on the Davie Fracture Zone. Mixed continental/marine syn-rift megasequences were deposited in rift basins followed by shallow-marine early postrift sequences. In Phase 2 (133–89 Ma) spreading ceased in the West Somali basin and Madagascar became fixed to the African plate. However, spreading continued between the African and Antarctic plates and deposition of the early postrift megasequence continued. The onset of spreading on the Mascarene Ridge separated India from Madagascar in Phase 3 (89–60 Ma). Phase 3 was characterized by the onset of deposition of the late postrift megasequence with continued deep marine sedimentation. At the onset of Phase 4 (60 Ma onward) spreading on the Mascarene ridge ceased and the Carlsberg Ridge propagated south to form the Central Indian Ridge, separating India from the Seychelles and the Mascarene Plateau. Late postrift deposition continued until a major unconformity linked to the development of the East African Rift System marked the change to deposition of the modern margin megasequence.

KEYWORDS

East Africa, megasequences, plate kinematics, rifted continental margins, tectonics, tectono-stratigraphy, West Madagascar

1 | INTRODUCTION

Hydrocarbon exploration along the East African margin has been going on for the past 50–60 years but it has been slow and intermittent, hampered by political instabilities and disappointing results. In the last two decades there has been a resurgence in exploration, spurred on by significant gas discoveries, for example the Pweza deep-water gas discovery offshore Tanzania. Despite the recent boom in interest, the East African margin remains underexplored

and its geodynamic and geological evolution poorly understood. We aim to develop an integrated margin-wide chronostratigraphy based on the correlation of plate kinematic processes with the regional tectonic events which can be used as potential framework for margin-scale tectonostratigraphic correlations of the basin fill histories of the sedimentary basins (Figure 1). To do this, we present a new high-resolution plate kinematic model of the Northwest Indian Ocean, interpret it in terms of geodynamic changes, and consider the implications these changes are likely to have had on the development of tectonically controlled megasequences in sedimentary basins along the East African and West Madagascan Margins.

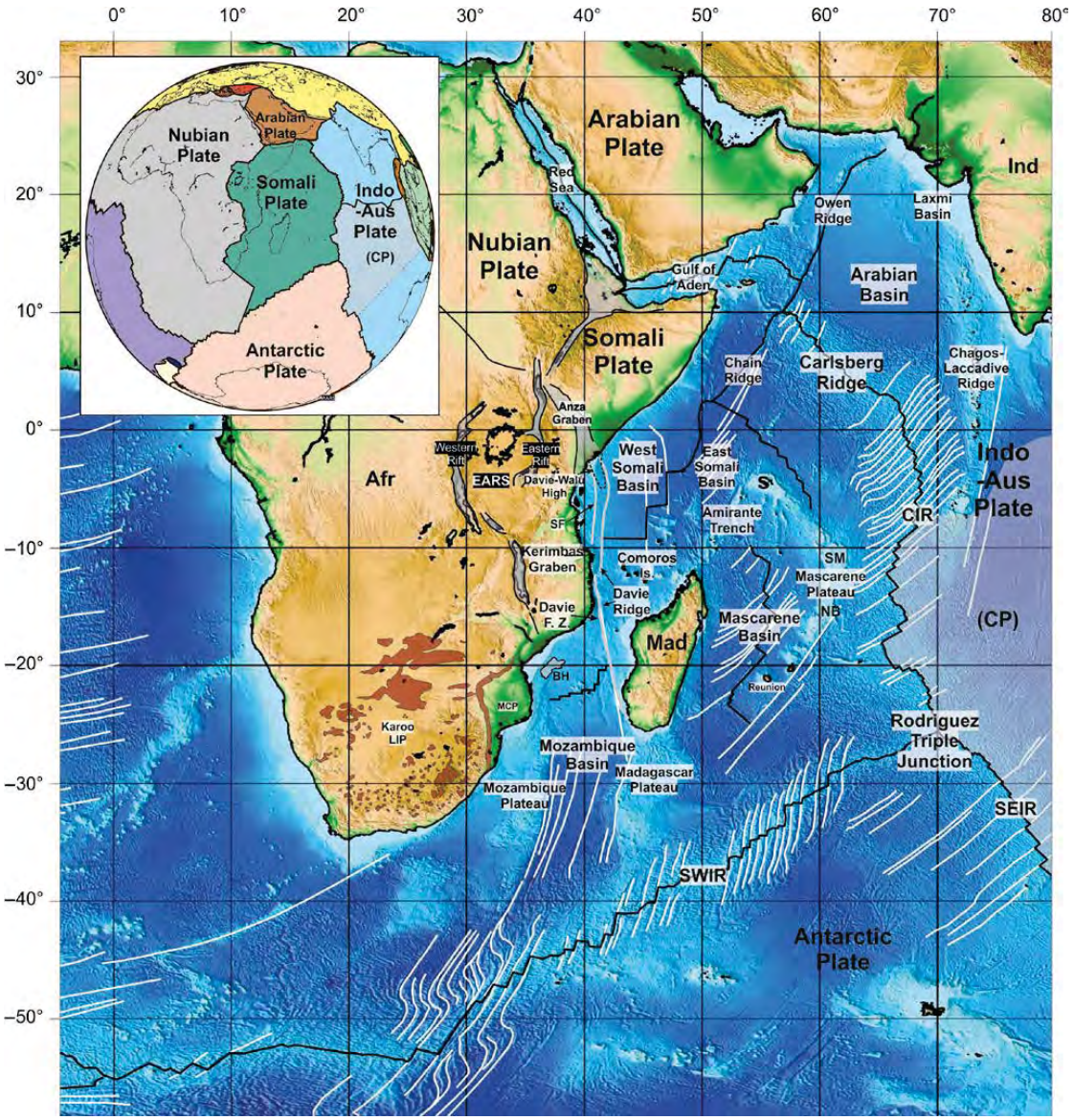

FIGURE 1 Overview of the present day Northwest Indian Ocean and key features. CIR, Central Indian Ridge; SEIR, Southeast Indian Ridge; SWIR, Southwest Indian Ridge; Mad, Madagascar; Afr, Africa; Ind, India; S, Seychelles; SM, Salha de Maya Bank; NB, Nazareth Bank; EARS, East African Rift System; S.F., Seagap Fault; BH, Beira High; MCP, Mozambique Coastal Plains; Karoo LIP (Jourdan et al., 2005); (CP) shaded area—Diffuse "Capricorn Plate" (Royer & Gordon, 1997). Inset: Present day plate boundaries

The tectonic evolution of the Northwest Indian Ocean and the present-day configuration of its accompanying continental margins (Figure 1) have been complicated by a number of major tectonic changes. Continents embedded within the region's plates, most importantly Africa, Madagascar, India, and Antarctica, formed parts of Gondwana, the southern portion of the supercontinent Pangea, from ca. 300 to 180 Ma. Throughout this time, episodic intracontinental rifting propagated through southern and eastern Africa, possibly reaching as far north as Somalia, and Madagascar (Catuneanu et al., 2005). These rifting events, often grouped as a "Karoo" rifting phase, culminated in the eruption of the Karoo-Ferrar Large Igneous Province (LIP) across South Africa (Karoo) and Antarctica (Ferrar) (Cox, 1992). Further rifting and breakup followed in the Jurassic as East Gondwana (Madagascar/India/Seychelles/Australia/Antarctica) separated from West Gondwana (Africa, South America). The timing of this breakup is widely disputed and will be addressed in this paper. Following the initial breakup, East Gondwana continued to fragment forming the present-day plate assembly (Figure 1).

As an emerging frontier for oil and gas exploration, the East African and West Madagascan Margins need to be understood in terms of their tectonic and basin fill histories, in particular how rifting, break-up and postrift phases and related petroleum systems elements can be correlated along the margins. Currently, no satisfactory and coherent plate tectonic model exists to piece together all the tectonic events and changes in the area.

This paper presents results of a new high-resolution plate rotation model for the separation of East Antarctica and Africa. The new model is an update to the study of Eagles and König (2008) incorporating new data and interpretations from the West Somali and Mozambique basins and Riiser-Larsen Sea (Davis, Lawver, Norton, & Gahagan, 2016; Leinweber & Jokat, 2012; Phethean et al., 2016; Sandwell, Muller, Smith, Garcia, & Francis, 2014). The new Africa-Antarctica rotations are combined with previously published rotations for the other pairs of plates in the region generated by a mixture of visual fitting and iterative joint inversions of magnetic isochron and fracture zone data, which allow to model the progressive development of the ocean basins in between continental fragments and to build a plate kinematic model consisting of multiple reconstruction maps.

The tectono-stratigraphic history of the rifted continental margin sedimentary basins along the East African and West Madagascan margins can be correlated and analysed by reference to the plate kinematic model. Here, we investigate the effects of these changes on the tectonically controlled megasequences of following conjugate margin segments: East Africa-India (EA-IND), East Africa-Madagascar (EA-MAD), Madagascar-East Africa (MAD-EA), and East Africa-Antarctica (EA-ANT). We have reviewed regional stratigraphy and structural information from basins on the conjugate margin segments, identifying important regional unconformities and megasequences, and integrated this information with the plate kinematic model to enable correlations along margin segments and between conjugate margin segments. The result is a margin-scale chronostratigraphic correlation chart documenting the evolution of the East African margin and its sedimentary basins. Ongoing work will provide an in-depth review of individual basins to better understand their regional tectonic and basin-fill history as well as the timing and distribution of petroleum system types (Tuck-Martin, Adam, & Eagles, 2015, 2016).

1.1 | Previous work

The first conjugate magnetic anomaly isochrons in the study region were identified in the late 1960s in the Arabian and East Somali Basins (Royer et al., 2002). Over the years, many more have been identified and refined (Cande, Patriat, & Dyment, 2010; König & Jokat, 2010; Leinweber & Jokat, 2012; McKenzie & Sclater, 1971; Norton & Sclater, 1979; Patriat & Segoufin, 1988; Schlich, 1982). On the basis of this growing data set, regional scale complexities in the formation of the Indian Ocean have been recognized, including the asymmetric accretion of oceanic crust to the African and Indian plates at different times, the action of propagating ridges, independent motion of the Seychelles plate and Miocene and younger regional deformation of the broad plate boundary zones surrounding the Capricorn plate. Accordingly, early reconstructions of the magnetic isochrons did not fully recognize these problems, and their accuracy suffered accordingly (e.g., Molnar, Pardo-Casas, & Stock, 1988). The arrival of free-air gravity anomaly maps derived from satellite altimetry in the 1980s and their subsequent improvement (see supplementary materials to Sandwell et al., 2014) give a uniform and high-resolution view of the structure of the ocean floor to complement the magnetic isochron data set. These data have helped more recent reconstructions to work in different ways to overcome the obstacles to a coherent tectonic reconstruction of the area.

Many of these recent reconstructions maintain a focus on magnetic isochron picks because of their use of the inversion method of Hellinger (1981) to calculate rotation parameters for making best fits of conjugate magnetic isochrons on the sea floor. The most up-to-date models of such reconstructions are those of Cande et al. (2010) and Cande and Patriat (2015). The authors used data from the Carlsberg (CR), Central Indian (CIR), Southwest Indian (SWIR), and Southeast Indian ridges (SEIR) in different combinations to calculate four sets of Euler rotations for

motions between the India (Capricorn), Africa (Somali), and Antarctic plates. They found that many of the data could be combined in a closed plate circuit, but that closure prior to chron 22o (49.427 Ma) locally required some degree of plate convergence within the African plate, which they related to anticlockwise rotation of a small plate bearing the Seychelles with a convergent boundary at the Amirante Trench (Figure 1).

Other recent studies (e.g., Eagles & Hoang, 2013) in the region have applied the alternative reconstruction technique of Nankivell (1997) to similar magnetic data sets together with a more rigorous treatment of the plate motion information contained in the shapes of fracture zones, evident in gravity anomaly data over regions of oceanic crust. These studies depict the separations of the African and Antarctic, African and Indian, and African and Seychelles plates without attempting to close the plate circuit, which is sensitive to the more coarsely estimated motion of the Capricorn plate (Demets, Gordon, & Royer, 2005). The kinematic history depicted in the NW Indian Ocean is smoother than that of Cande et al. (2010) and Cande and Patriat (2015), and portrays a higher resolution evolution of the Seychelles-Africa plate boundary. In the SW Indian Ocean, however, the technique has only been applied to pre-mid Cretaceous data (Eagles & K6nig, 2008), and predates the collection of new and better data in key locations (K6nig & Jokat, 2010; Phethean et al., 2016).

2 I METHOD

The joint inversion technique of Nankivell (1997), as described by Eagles (2004) and Livermore, Nankivell, Eagles, and Morris (2005), produces finite rotation poles and angles of rotation about them by minimizing the misfits of sets of small and great circle segments to the locations of fracture zones and isochron data in the ocean floor produced by the divergence of pairs of plates. Using this method, a full new model for Antarctica–Africa divergence since Jurassic times is described below in section 2.1. The intention is to provide a quantitative and up-to-date model of seafloor spreading data to combine with the similarly derived models of Eagles and Wibisono (2013) and Eagles and Hoang (2013) (sections 2.2 and 2.3), and so provide a methodologically consistent basis on which to interpret the plate kinematic history from 183 Ma to the present day.

2.1 I New rotation model for ANT-AFR plate motion

Figure 2 presents the data set for modelling of new Euler rotations describing the separation of Africa from Antarctica since Jurassic times. This data set extends that of Eagles and K6nig (2008), whose model did not address the most recent 100 million years of plate divergence, and revises its oldest parts on the basis that its M-Series anomaly picks in the Mozambique and West Somali basins have been shown to be unlikely. In the Mozambique Basin, our revision straightforwardly follows the interpretation of recently acquired magnetic data (K6nig & Jokat, 2010; Leinweber & Jokat, 2012). In the West Somali Basin, the picks required reinterpretation because of recent improvements in gravity imaging of a subtly expressed extinct mid-ocean ridge (Phethean et al., 2016). Davis et al. (2016) show that this new constraint can be consistent with existing models (e.g., Cochran, 1988; Segoufin & Patriat, 1980) of a sequence of seafloor spreading isochrons in the basin that ends shortly after the onset of the Cretaceous normal polarity superchron. In Figure 3, we show that the extinct ridge location is also consistent with alternative interpretations of that sequence as ending close to isochron M10n, around 12 Myr earlier (Eagles & K6nig, 2008; Rabinowitz, Coffin, & Falvey, 1983). The ultimate reason for the ongoing uncertainty regarding these two alternative interpretations is that detailed waveform correlations between available magnetic anomaly profiles in the basin are not possible. Following Eagles and K6nig (2008), we prefer the interpretation of extinction around M10n for two reasons: (a) that it requires relative motions between just two large plates and no unattested motion of a Madagascar plate, and (b) that its intermediate (ca. 42 km/Myr) full seafloor spreading rates at extinction are more consistent with the rather subdued appearance of the abandoned ridge crest in gravity anomaly data than the slow (ca. 26 km/Myr) rates at extinction in the alternative interpretation. In contrast, Davis et al. (2016) preferred a later extinction date because it enables reconstructions that (a) preserve correlations of interpreted prefit markers between Africa and Madagascar and (b) do not require large follow-on adjustments to the modelled geometry of the remainder of East Gondwana. The problem of the timing of seafloor spreading in the West Somali basin thus seems set to remain finely balanced until new and more reliable magnetic data become available.

The coloured symbols in Figure 2 represent the locations of magnetic isochrons as identified by Nankivell (1997) and Eagles and K6nig (2008), updated for the large new data set of K6nig and Jokat (2010), and reinterpreted in the West Somali Basin as described above. Rows of small black triangles denote our picks of fracture zone locations derived from the vertical gradient in the most recent version of Sandwell et al.'s (2014) satellite gravity data set (Figure 2a). The new data set makes the locations of fracture zones in the oldest parts of the seafloor in the Mozambique basin and Riiser Larsen Sea clearer than the data set available to Eagles and K6nig (2008). In addition,

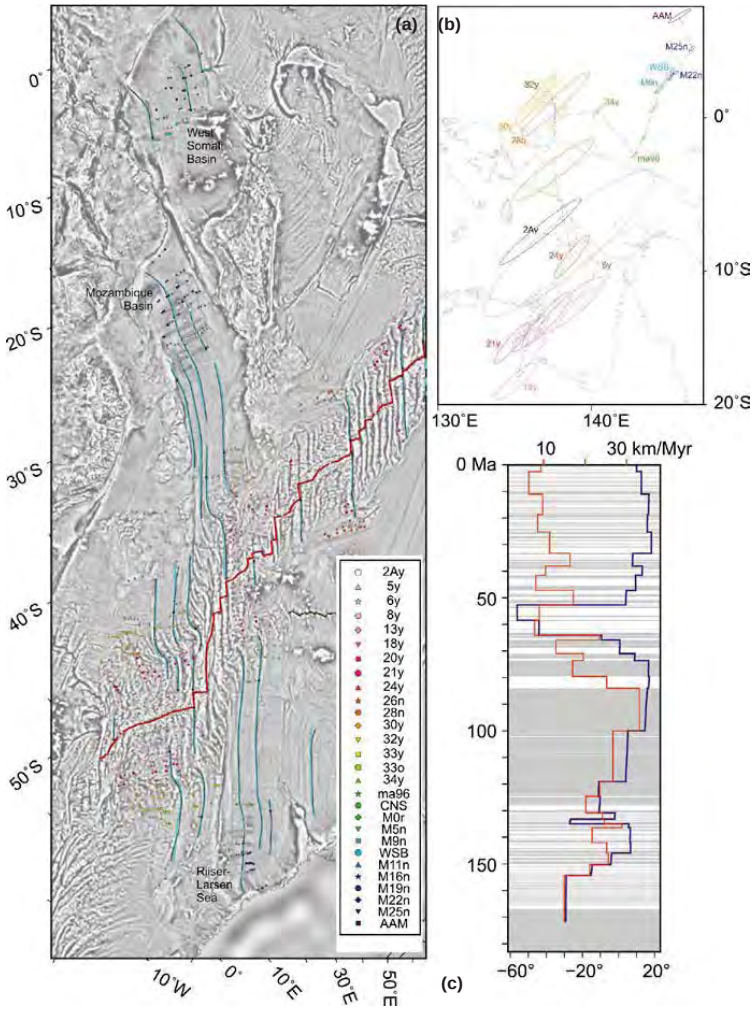

FIGU RE 2 (a) Coloured symbols: magnetic anomaly isochron picks (see key for chron names). Rotated magnetic anomaly picks appear as grey outlines. Black triangles: fracture zone picks from gravity. Blue lines: synthetic flowlines, with white dots at each constrained time. Thick grey line: present-day ridge crest (Southwest Indian Ridge). In the background is the vertical gradient from Sandwell et al.'s (2014) satellite gravity data set. (b) locations of the rotation poles and their 95% confidence ellipses. As for the isochron picks, not all poles are labelled to aid clarity. (c) Plot of the spreading directions in degrees clockwise from north (blue line), and the spreading rates in km per million years (red line) between Africa/ Madagascar and Antarctica

in the West Somali Basin we used the directionally filtered gravity anomalies of Phethean et al. (2016) to help guide our fracture zone interpretations. For the plate-kinematic model presented here, we have made no attempt to reduce the data set to reflect the Neogene relative motion of Somalian and Nubian component plates of Africa (Horner-Johnson, Gordon, & Argus, 2007).

The data set was modelled by least squares minimization of the misfits between rotated magnetic isochron picks and their conjugate and nonconjugate neighbours within shared corridors and of the misfits of synthetic ridge-crest offset flowlines to the fracture zone locations. Figure 2 represents this process by showing the rotated magnetic isochrons as grey outline symbols, and the synthetic flowlines in blue. The advantage in using nonconjugate target figures is that it permits us to include data from the African flank of the West Somali basin, as well as numerous data in less well-populated corridors, enabling a useful solution for continuous plate motion since late Jurassic times to be calculated. The disadvantage of this approach is that the use of sparse data and data without conjugates is likely to introduce populations of larger misfits into the model such that its quality in some locations or for some times is less than can be achieved by targeted modelling of the denser data set for younger periods (Horner-Johnson et al., 2007). Cande and Patriat (2015) show that this precision is of local rather than regional importance for studies of this geographical and temporal scale.

A stable solution like the one presented in Figure 2 can be generated after a few tens of iterations regardless of whether it is approached from a set of initial test rotations like those of Eagles and König (2008) or those of Leinweber and Jokat (2012). The mean of all misfits for the magnetic isochron picks is 1.1 km and their standard deviation

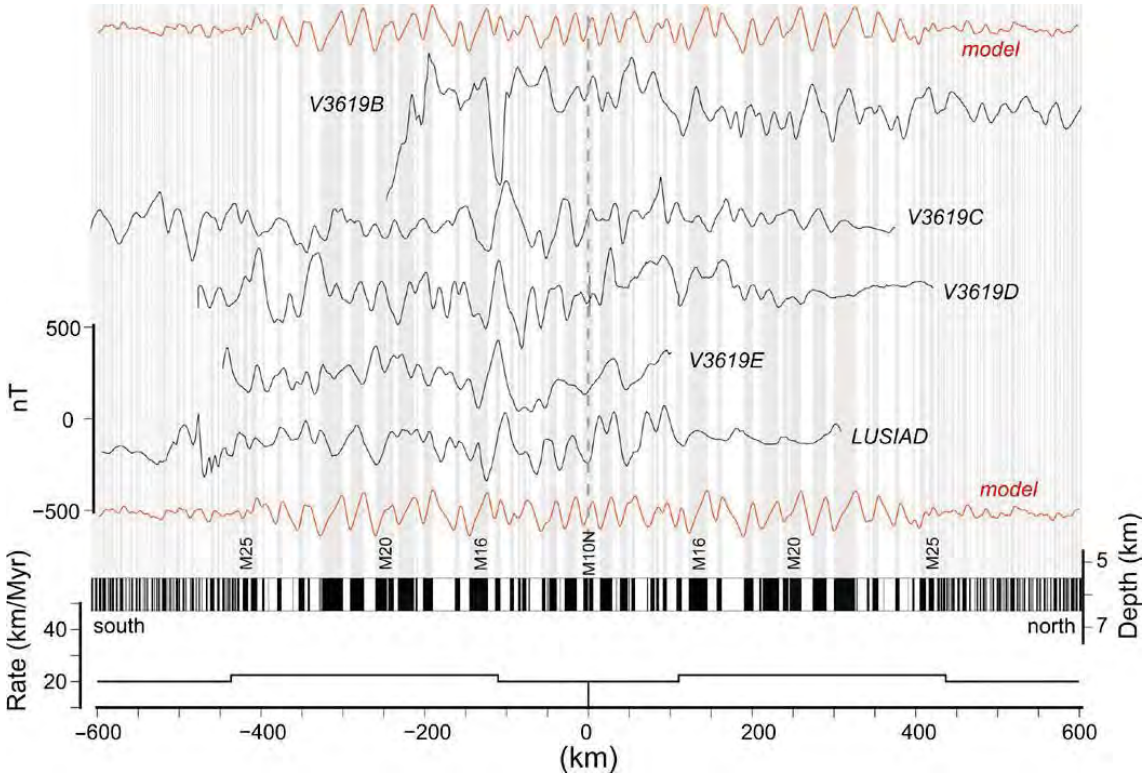

FIGU RE 3 Magnetic isochron models for five profiles crossing the West Somali Basin. The profiles are all aligned on the proposed extinct median valley (Phethean et al., 2016). Model spreading stops at the end of chron M10Nn.2r (134.98 Ma in Gradstein, Ogg, & Smith, 2004). Field inclinations are appropriate for the present-day latitude of the West Somali Basin and a palaeo-latitude of 40°S

is 18.6 km. For fracture zone picks, the mean is 0.4 km and the standard deviation is 8.8 km. The best fitting Gaussian approximation to the isochron misfit population has mean and standard deviation of 0.2 and 14.5 km, and that to the fracture zone misfits has 1.0 and 6.9 km. These values are within expected ranges for a data set and model geometry like this, comparable to a priori estimates of locational uncertainty in isochron and fracture zone picks, but mostly too large to enable the model to reliably resolve the small differences between the motions of the Somali and Nubian plates with respect to the Antarctic plate (Horner-Johnson et al., 2007). The geographical distribution of the misfits does not suggest that these data describe larger scale motion of any large plate other than those bearing Africa and Antarctica.

Figure 2b shows the locations of the finite reconstruction poles and 2-dimensional 95% confidence ellipses for them, calculated using the best-fit Gaussian misfit statistics above as estimates of the overall locational uncertainties. The full set of parameters is listed in Table 1. The rotation poles for Africa with respect to Antarctica are almost coincident at the 95% confidence level in the period between M22n and the end of spreading in the West Somali Basin (155−133 Ma; rotation WSB); the instantaneous rotation pole may have been essentially stationary throughout this period. This circumstance is consistent with a two-plate system whose relative motions were governed by an equilibrated set of driving forces. The locations of the rotation poles between M9n and ma96 (133−96 Ma), on the other hand, are statistically distinguishable from one another at 95% level, and migrate consistently towards the SSW. This coincides with an increase in the relative plate divergence velocity (Figure 2c). The onset of this epoch coincides with the loss of data from the West Somali Basin, which we assume to have ceased opening by seafloor spreading shortly before M9n. Pole locations begin to migrate towards the NW after ma96, again with statistical significance until chron 33y, and the plate divergence rate begins slowing again. This may reflect the effects of regional plate boundary reorganizations brought about by arrivals of the Bouvet and/or Marion plumes in the South Atlantic and beneath Madagascar. Slowing rates

TABLE 1 Finite rotations modelled from the flanks of the Southwest Indian Ridge, Mozambique and West Somali basins, and Riiser-Larsten Sea for reconstruction of African plate with respect to East Antarctic plate. All rotations right-handed. Azimuth refers to the orientation of the 95% confidence ellipsoid in degrees anticlockwise of east. Only 95% confidence ellipses (axes 1 and 2 and azimuth) are depicted in Figure 2

Finite rotation parameters			95% confidence ellipsoid					
Longitude	Latitude	Angle	Axis 1	Axis 2	Axis 3	Azimuth	Chron	Age
136.68	−7.46	0.44	1.37	0.16	0.02	39.38	2Ay	2.581
138.59	−8.29	1.43	3.96	0.93	0.03	40.31	5y	9.786
140.62	−9.73	2.80	2.18	0.48	0.05	41.08	6y	18.748
138.79	−12.26	3.81	1.49	0.36	0.06	40.32	8y	25.099
135.19	−17.17	5.52	0.93	0.22	0.04	41.34	13y	33.147
136.13	−14.19	6.89	0.89	0.21	0.05	44.73	18y	38.615
137.15	−13.18	7.55	1.29	0.26	0.04	48.61	20y	42.301
134.78	−14.75	8.42	0.90	0.19	0.04	49.20	21y	45.724
138.74	−9.08	10.01	0.96	0.18	0.03	51.75	24y	52.62
137.73	−3.52	10.41	1.70	0.32	0.02	36.60	26y	58.959
137.71	0.96	11.00	1.49	0.20	0.03	45.44	28o	63.494
136.48	0.98	11.68	1.13	0.15	0.05	50.48	30y	66.398
136.79	1.52	12.89	0.93	0.12	0.05	50.39	32y	71.449
137.36	1.46	13.82	0.77	0.10	0.04	50.19	33y	74.309
137.87	−0.19	15.59	0.54	0.08	0.03	49.19	33o	79.54
140.42	0.12	17.65	0.28	0.05	0.03	49.55	34y	83.64
142.61	−2.85	27.15	0.19	0.07	0.02	46.12	ma96	100
143.65	−1.20	36.49	0.19	0.14	0.02	53.83	CNS	119
143.53	−0.07	38.87	0.21	0.04	0.03	45.22	M0r	124.61
144.27	1.52	41.27	0.21	0.04	0.02	45.11	M5n	130.8
144.55	1.90	42.37	0.27	0.05	0.03	46.64	M9n	133.14
145.22	3.06	43.34	0.27	0.13	0.06	44.23	WSB	133.9–133.5
145.55	3.22	44.13	0.11	0.03	0.03	36.94	M11n	136.44
145.38	2.87	46.31	0.09	0.03	0.02	36.34	M16n	142.06
145.06	2.45	48.02	0.10	0.03	0.03	31.71	M19n	145.95
145.66	3.14	50.19	0.13	0.04	0.03	28.24	M22n	150.21
146.62	4.38	52.09	0.14	0.04	0.03	32.35	M25n	154.37
145.77	6.57	56.27	0.57	0.07	0.06	33.27	AAM	183–177

Note. CNS, Cretaceous Normal polarity Superchron; WSB, West Somali Basin extinction; AAM, African-Antarctic Margin separation.

accompany a stationary pole of rotation, within error, until chron 30y, the time of arrival of the Deccan plume beneath what was to become the India-Africa plate boundary. A new kinematic epoch is suggested by the southwards migration of finite rotation poles between chrons 30y-28o and 13y. This period might be broken down into an earlier period of rapid change in rotation parameters, ending between chrons 24y and 21y, and a later period of slower change with significant statistical overlap in pole locations. This subdivision might be related to changes in driving forces introduced as a consequence of jumps of the Carlsberg Ridge (CR) crest that resulted in the end of spreading in the Mascarene Basin (Eagles & Hoang, 2013; Eagles & Wibisono, 2013). A final epoch begins with chron 13y, and is characterized by northwards shifts between successive finite rotation poles. It is possible that this is characteristic of the introduction of new driving forces to the regional circuit by rupture of the African plate into Somalian and Nubian subplates.

2.2 I Plate kinematic reconstruction data sets

The data used for building the plate kinematic reconstruction maps include magnetic anomaly picks from Eagles and Wibisono (2013) (in the Mascarene Basin), Cande et al. (2010) and Eagles and Hoang (2013) (in the eastern

Somali basin), König and Jokat (2010) (in the Mozambique Basin), and Cande et al. (2010) (on the flanks of the SW Indian Ridge). Data in the West Somali Basin were newly interpreted for this study (see section 2.1).

Further magnetic anomaly isochrons have been tentatively identified in the Laxmi Basin according to various schemes (e.g., Bhattacharya et al., 1994; Eagles & Wibisono, 2013). These identifications vary greatly, and in view of the uncertainty we use no magnetic isochron picks from the Laxmi Basin.

In the Mozambique Basin, Leinweber and Jokat (2012) further interpreted König and Jokat's (2010) magnetic anomaly data to identify a continent-ocean-boundary (COB) that lies much closer to the coast in the Mozambique Channel than estimated by other authors (e.g., Raillard, 1990), and a continuation of the magnetic isochron sequence to much older ages in the Mozambique Basin (chron M41n; 166 Ma) than the chron M25n (154.37 Ma) identifications made with older data. We do not use these picks explicitly because they are made in very low amplitude anomalies that make the interpretation difficult to justify.

2.3 | Plate kinematic reconstruction workflow

Plate kinematic reconstruction maps were generated by cropping gridded bathymetric data within isochronous plate boundary polygons, and rotating the cropped data using *grdrotater*, *grdmask*, and *grdmath* from the GMT Suite of tools (Wessel, Smith, Scharroo, Luis, & Wobbe, 2013). The rotation parameters describing the motions of the plates are taken from Eagles and Hoang (2013), Eagles and Wibisono (2013) and from section 2.1, interpolated at 1 million year intervals (Table 1).

The plate boundary polygons (Figure 4) were generated by digitizing palaeo-ridge segments passing through the magnetic anomaly picks described in the previous section and palaeo-transform segments whose locations are preserved within fracture zones that are evident in the gravity data. To do this, we used Golden Software's *Didger 5* digitizing software and the free-air gravity data from Sandwell et al. (2014). These data image fossil fracture zones and mid-ocean ridges from the Mozambique and West Somali basins in particular more clearly than in previous data sets.

For the very oldest reconstructions, at times before the onset of seafloor spreading, prestretching continental limits were estimated from the positive and negative gravity anomaly couplets at the extended continental margin segments in the Riiser-Larsen Sea and Mozambique Basin. These estimates (labelled AAM in Figure 2) were used in the same way as the magnetic isochron picks in the rest of the inversion model. Eagles, Pérez-Díaz, and Scarselli (2015) show that the locational uncertainty of features picked in this way is similar to the numerical uncertainty in restoration of continent-ocean boundaries by quantitative palinspastic reconstruction techniques like that of Williams, Whittaker, and Müller (2011), but the location itself is independent of a starting set of rotations. The choice of such a short length of conjugate margins means there is little risk of propagating errors from unrecognized diachronous breakup into the model's earliest stage.

3 | HIGH-RESOLUTION KINEMATIC RECONSTRUCTION OF THE AFRICA-INDIA-ANTARCTICA PLATE CIRCUIT

We present the new plate kinematic model as four different phases which show distinctive periods of evolution of the Indian Ocean, separated by major tectonic changes such as ridge jumps or the initiation of new spreading ridges and the effect on the tectonic development of the conjugate East African and West Madagascan margins. The four phases are outlined in Table 2.

3.1 | Phase 1—Starting at 183–177 Ma: Separation of East and West Gondwana

The first plate tectonic phase is characterized by the separation of East Gondwana, bearing the future continents and microcontinents of Madagascar, the Seychelles, India, East Antarctica, and Australia from West Gondwana, bearing Africa and South America. This led initially to continental rifting and eventually to breakup and the onset of seafloor spreading in the newly created West Somali and Mozambique basins.

Figure 5a shows the plates of the future Africa-Antarctica-India plate system fully reassembled in their relative positions prior to fragmentation of the Gondwana supercontinent at the beginning of Phase 1 (within the time period of 183–177 Ma). The timing of this reconstruction is based on the assumption that the onset of plate divergence would have been accompanied by the eruption of the Karoo volcanics in southeast Africa (Eagles & König, 2008; Encarnación, Fleming, Elliot, & Eales, 1996) and their Ferrar counterparts in Antarctica (White & McKenzie, 1989). Alternative timings have been based on extrapolation of spreading rates from magnetic isochrons (ca. 165 Ma; Leinweber & Jokat, 2012; Roeser, Fritsch, & Hinz, 1996) and indirect dating of seaward dipping basalt flows in the Mozambique Basin (pre-169 Ma; Mueller & Jokat, 2017). In contrast, igneous rocks from the margins of the West Somali basin have not been used to determine the timing of the onset of plate divergence. These events marked the end of the intracontinental Karoo rifting episodes

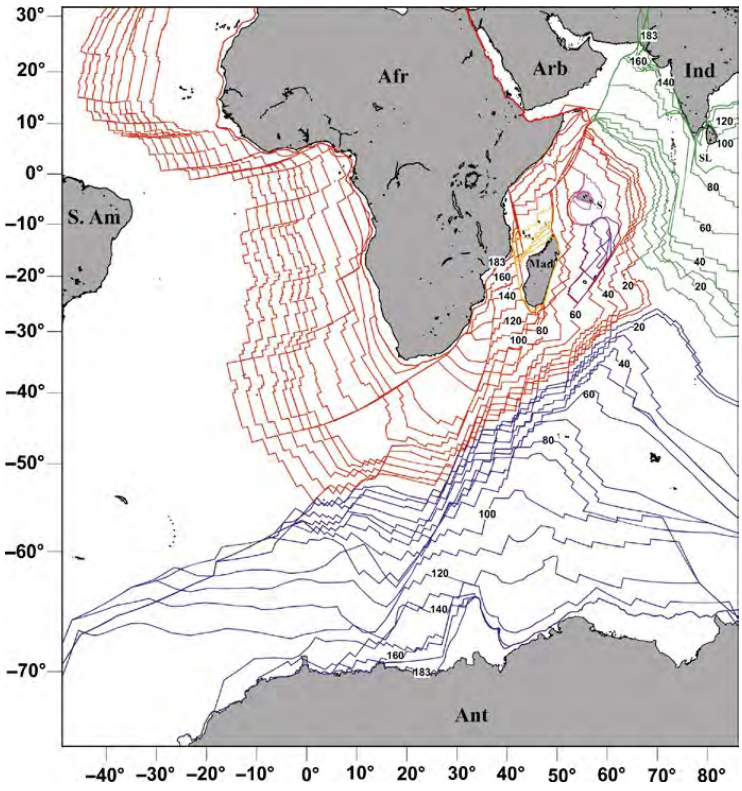

FIGURE 4 Plate outlines or isochrons used for the kinematic reconstructions. Only outlines every 10 million years are shown for clarity (outlines for Africa in the Atlantic Ocean come from Pérez-Díaz & Eagles, 2014). Afr, Africa; Arb, Arabia; Ind, India; Mad, Madagascar; S, Seychelles; SL, Sri Lanka; Ant, Antarctica; S.Am, South America

(Carboniferous to Late Triassic/Early Jurassic) and the beginning of a new, separate rifting phase that would lead to breakup of Gondwana.

The following conjugate margin segments have been identified from this initial reconstruction; (a) conjugate East African and Indian Margins (EA-IND), (b) conjugate East African and West Madagascan margins (EA-MAD), (c) the corresponding margin of West Madagascar (MAD-EA), and (d) conjugate East African and Antarctica margins (EA-ANT) (Figure 5a).

There is significant overlap between the Seychelles microcontinent and the northern part of India with Somalia (Figure 5a). Hammond, Kendall, Collier, and Rümpker (2013) documented that the Seychelles are underlain by continental crust, meaning that the overlap is an observation of significance for the plate kinematic model or its interpretation. If the model rotations are accepted as reliable, then the overlap might be interpreted as a consequence of extension of the continental margins, or as a consequenceofdiachronousriftingthatwasaccommodated by short-lived intracontinental plate boundaries, as suggested for the Muglad-Anza rift (which stretches from southern Sudan, through South Sudan and Kenya) by Pérez-Díaz and Eagles (2014).

An obvious feature worth noting in the FIT 183–177 Ma image (Figure 5a) is the overlap between East Antarctica and the Mozambique coastal plain (MCP). The overlap persists in the reconstructions for 175 (Figure 5b) and 165 Ma (Figure 5c), and is a feature of numerous alternative reconstructions (e.g., Davis et al., 2016; Eagles & König, 2008; Leinweber & Jokat, 2012). Many of these authors have suggested that the overlap signifies the MCP to be underlain by magmatic crust that did not yet exist at FIT times. Consistent with this, backstripping of the plain's thick sedimentary sequence suggests the underlying lithosphere subsided at rates reminiscent of oceanic lithosphere (Watts, 2001). However, recent seismological investigations suggest a crustal thickness of about 20 km, which would be unusually thick for oceanic crust (Domingues et al., 2016; Fonseca et al., 2014). Deep seismic data would help to confirm whether the Mozambique side of the overlap is underlain by stretched, transitional or oceanic crust with a thick volcanic cover.

With our rotations, the conjugate margins of East Africa and Madagascar reconstruct to relative positions similar to those modelled by Smith and Hallam (1970), Coffin and Rabinowitz (1987), Eagles and König (2008)

TABLE 2 Summary of the four phases of tectonic development of the Northwest Indian Ocean and their corresponding figures

Phase	Age	Tectonic events	Figures
1	183–177 to ca. 133 Ma	Rifting, breakup and drift of East Gondwana (comprising Madagascar/India/Antarctica/Seychelles) and West Gondwana (comprising Africa/South America) accommodated by seafloor spreading in the West Somali and Mozambique basins	5a. FIT183–177 Ma: All plates reassembled within the Gondwana supercontinent 5b. 175 Ma: Main rift phase 5c. 165 Ma: Breakup 5d. 150 Ma: Mature/established seafloor spreading in the West Somali and Mozambique Ocean Basins
2	ca. 133–89 Ma	Rifting and seafloor spreading on the Mascarene Ridge, opening of the Mascarene Basin and separation of India and Madagascar	6a. 133 Ma: boundary reorganization phase (seafloor spreading ends in WSB) 6b. 100 Ma: established phase 2 seafloor spreading
3	89 to ca. 60 Ma	Rifting and subsequent seafloor spreading on the Mascarene Ridge, opening of the Mascarene Basin and separation of India and Madagascar	7a. 89 Ma: boundary reorganization phase (extension to spreading in Mascarene Basin) 7b. 75 Ma: established spreading in Mascarene Basin 7c. 63 Ma: Laxmi basin opening and Seychelles microplate rotation
4	ca. 60 Ma to present day	Cessation of spreading on the Mascarene Ridge, spreading on the Carlsberg and Central Indian Ridges separating India and the Mascarene Plateau	8a. 60 Ma: early spreading on the Carlsberg Ridge 8b. 55 Ma: established spreading along the Carlsberg ridge 8c. 33 Ma: mature/established seafloor spreading on the Carlsberg and Central Indian Ridges

and Klimke and Franke (2016). Much tighter fitting reconstructions are presented by Reeves (2014), Davis et al. (2016) and Phethean et al. (2016), all of which aim to closely match the shelf outlines at times before seafloor spreading constraints become available. Outboard of the shelves, however, controversy has recently developed regarding the presence of extended continental or of oceanic crust around the Davie Fracture Zone (Danforth, Granath, Horn, & Komba, 2012; Klimke & Franke, 2016; Klimke et al., 2016; Phethean et al., 2016; Turner, Foum, & Kusznir, 2016). This controversy implies reconstruction overlaps as great as 270 km for the tighter-fit models, implausibly large to be explained by continental extension. Clearly here, as in many other settings worldwide, the difficulty of accurately and reliably locating the COB strongly limits its role in the reconstruction process.

During the rift phase (Figure 5b), plate kinematic and local plate motion vectors demonstrate extension and transtension along a 1,000 km long NNE-SSW trending future plate boundary zone between East Africa (as part of West Gondwana) and India, Madagascar and Antarctica (as parts of the East Gondwana plate). The earlier Karoo rifts followed the regional tectonic trends and inherent structures of the Precambrian basement (Catuneanu et al., 2005). However, during the later main rift stage, the regional trends of the future margin segments may not have followed the same orientations. For example, in Madagascar the rift axis migrated west (Clark, 1998; Geiger, Clark, & Mette, 2004) and in East Africa the main rift basins were superimposed discordantly over the Karoo basins (Key et al., 2008).

The age assigned to breakup and the onset of seafloor spreading in the Mozambique Basin and Riiser Larsen Sea can be estimated based on extrapolation of magnetic isochron ages towards the continent ocean boundaries. Linear extrapolation of our model's oldest dated stage (M25n-M22n) would suggest an age of 167 Ma, comparable to Leinweber and Jokat's (2012) tentative identification of anomaly M41n (165.6 Ma) near the base of the continental slope where they also placed the COB. Slower early plate divergence rates would imply earlier breakup.

The end of the main rift phase and breakup was followed by the onset of seafloor spreading in the West Somali and Mozambique Basins between East and West Gondwana (Figure 5c). Motion on the spreading ridges in the two basins was accommodated by dextral strike-slip on the Davie transform fault between parts of Tanzania, Mozambique and Madagascar. For the remainder of phase one, from the onset of seafloor spreading until the abandonment of the plate boundary in the West Somali Basin, the tectonic model describes a stable two-plate system as exhibited by the relatively stationary finite rotation poles for this time period (155–133 Ma) (see section 2.1, and Figure 2).

3.2 | Phase 2—Starting at 133 Ma: Separation of Antarctica

The second phase of tectonic activity in the Indian Ocean involved the cessation of seafloor spreading in the West

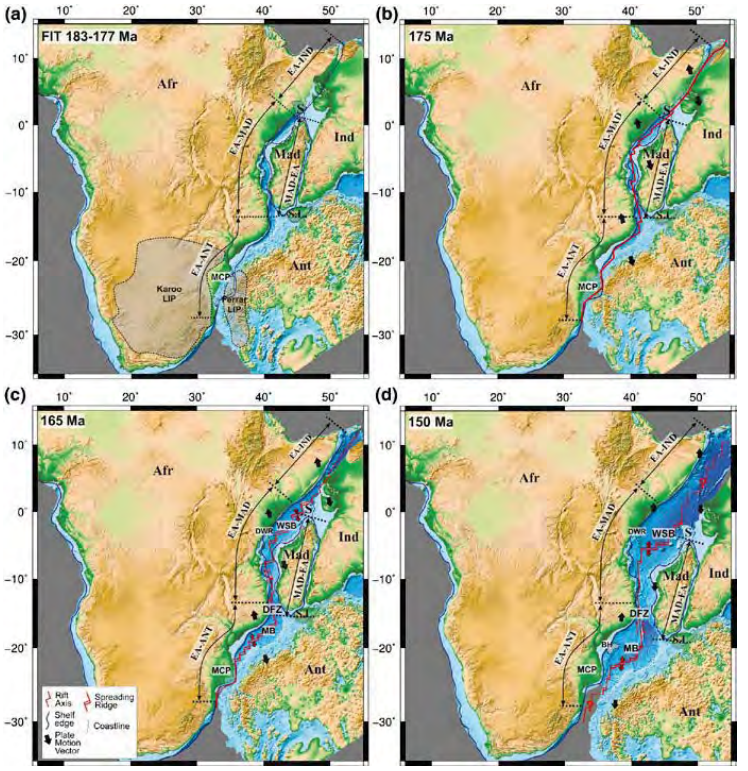

FIGURE 5 Plate reconstruction maps showing the main stages of development in Phase 1. East Gondwana (including Madagascar/India/Antarctica/Seychelles) and West Gondwana (including Africa/South America) separated, accommodated by rifting and subsequent seafloor spreading in the West Somali and Mozambique Basins. All maps use present day bathymetry data and the Mercator projection with Africa fixed in its present-day location. (a) Fully reassembled fit of all the plates in this study to their positions within the Gondwana supercontinent 183–177 Ma, with possible maximum extent of Karoo-Ferrar LIP (Riley et al., 2006), (b) 175 Ma during continental rifting, (c) 165 Ma just after breakup, with onset of seafloor spreading in West Somali and Mozambique Basins, (d) 150 Ma, established seafloor spreading. Afr, Africa; Mad, Madagascar; S, Seychelles; Ind, India; Ant, Antarctica; S.L., Sri Lanka; WSB, West Somali Basin; MB, Mozambique Basin; DFZ, Davie Fracture Zone; DWR, Davie Walu Ridge; BH, Beira High; MCP, Mozambique Coastal Plains

Somali Basin and its eventual onset in the West Enderby Basin between Madagascar and East Antarctica (Figure 6a). The timing of this change is still debated. Our model dates the boundary reorganization to sometime within chron M10n (ca. 133.9–133.5 Ma) as an explicit consequence of the assumption that the model should describe relative motions of just two large plates, East and West Gondwana. After this time, our model's finite rotation poles adopt a south-southwesterly migration path whose consistency and longevity seem difficult to explain as a mere consequence of the removal of model constraints from the West Somali Basin. As noted previously, alternative interpretations of the magnetic anomalies in the West Somali Basin place the end of spreading to just after M0 (126.30–125.93 Ma), which require motion of a third plate, remain popular and can be defended using magnetic wiggle profiles from the West Somali Basin (e.g., Davis et al., 2016; Gibbons, Whittaker, & Müller, 2013). Both timings can be seen as consistent with magnetic isochron patterns in the western Enderby Basin, which seems not to have seen seafloor spreading until around 8 Myr later than the end of spreading in the West Somali Basin (Jokat, Nogi, & Leinweber, 2010). In one scenario, the 8 Myr-long gap might be filled by continental extension prior to renewed seafloor spreading south of Madagascar; Figure 6a suggests the Mannar and Cauvery basins as locations for this extension. In the other scenario, the switch from seafloor spreading north of Madagascar to south of it could have been achieved more-or-less instantaneously. In the face of all this, and until a self-consistent scheme of isochron interpretations is set up on the basis of new and more coherent magnetic anomaly data, we continue to favour the minimum-complexity (i.e., fewest plates) view of the regional development in early Cretaceous times.

The new ENE-WSW trending spreading centre between EA-IND-MAD and EA-ANT strongly altered the orientation of the plate motion vectors and kinematics within the EA-IND-MAD plate assembly (Figure 6a). NW-SE oriented local plate motion vectors trending oblique to the N-S trending margins of the southern EA-MAD and MAD-EA indicate the potential for strike-slip or transpressional deformation along these margin segments. Accordingly, a major unconformity marks the onset of start of this phase (end Hauterivian/Barremian) along the margin segments bordering the Somali Basin, that is, the EA-IND segment (Bosellini, 1992) and the northern MAD-EA segment (Coffin & Rabinowitz, 1988). Key et al. (2008) suggest that early phase 2 deposition was controlled by renewed rifting

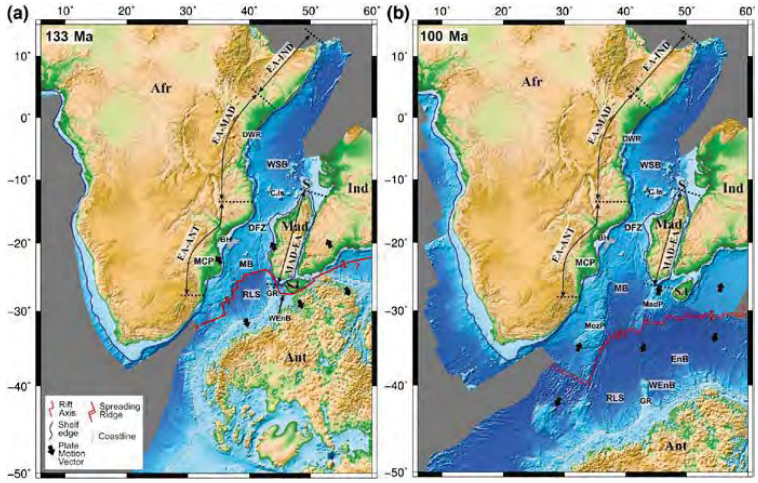

FIGU RE 6 Plate reconstruction maps showing the main stages of development in Phase 2. Seafloor spreading ceased in the West Somali Basin, the boundary relocated to the south of Madagascar separating Madagascar/India and Antarctica. (a) 133 Ma: onset of phase 2. Seafloor spreading has ceased in the West Somali Basin, relocated to western Enderby Basin, (b) 100 Ma: established phase 2. Afr, Africa; Mad, Madagascar; S, Seychelles; Ind, India; Ant, Antarctica; S.L., Sri Lanka; WSB, West Somali Basin; MB, Mozambique Basin; DFZ, Davie Fracture Zone; DWR, Davie Walu Ridge; BH, Beira High; MCP, Mozambique Coastal Plains; RLS, Riiser Larsen Sea; GR, Gunnerus Ridge; EnB, Enderby Basin; WEnB, West Enderby Basin; MozP, Mozambique Plateau; MadP, Madagascar Plateau; C.Is, Comoros Islands

and extensive inland erosion in the Rovuma Basin (southern EA-MAD), whereas in the Angoche Basin (southern EA-MAD/EA-ANT) a short-lived period of tectonic uplift followed the end of movement on the Davie Facture Zone (Mahanjane, 2014).

3.3 | Phase 3—Starting at 89 Ma: Separation of India and Madagascar

The third phase saw the continuation of Antarctica-African seafloor spreading along the SWIR, but is characterized by a dramatic change in tectonic activity in the Indian Ocean. This change was associated with the initiation of a new spreading ridge and the opening of the Mascarene Basin, separating India and Madagascar (Figure 7). The timing of activity in the Mascarene Basin is constrained mostly by the magnetic isochron interpretations described in section 2, but its earliest dated products are the ca. 89 Ma Morondava volcanics (Storey, Mahoney, & Saunders, 1997) in Madagascar, whose eruption is attributed to the arrival of the Marion mantle plume (Figure 7a). Spreading in the Mascarene Basin continued until its abandonment shortly after the young end of chron 27n (61.65 Ma) (Eagles & Wibisono, 2013).

Along Africa's southeastern plate boundary with Antarctica the spreading direction between the two plates remained in an approximately NW-SE direction along the SWIR (Figure 7b). However, further north, the regional tectonics at the East African and West Madagascan margins were more likely dominated by spreading along the newly formed N-S trending Mascarene Ridge along the eastern boundary of the African plate.

Local plate motion vectors varied from a NE-SW direction in the northern Somalia margin to an E-W direction in the Mozambique margin. Consequently, in the NE-SW oriented EA-IND, northern EA-MAD, northern and central EA-ANT segments, the local plate motion vectors were oriented mostly parallel to the continental margin segments indicating a phase of tectonic quiescence and passive margin development during the late postrift or drift stage. ENE-WSW to E-W local plate motion vectors trended perpendicular to the N-S trending margin segments of the southern EA-MAD and MAD-EA margins indicating some potential for inversion of earlier strike-slip structures in this stage. Corresponding to the opening of the Mascarene Basin, Clark (1998) describes renewed tectonic activity in the basins of western Madagascar, with strike-slip faulting and contractional folding occurring in the Late Cretaceous. Towards the end of this phase, a number of major tectonic changes and boundary relocations occurred in the oceanic crust between India and Madagascar.

3.3.1 | Opening of the Laxmi Basin and the speed of the Indian Plate

The next important boundary relocation occurred during chron 30n (66.398–68.196 Ma). Eagles and Wibisono (2013) concluded that evidence for oceanic accretion

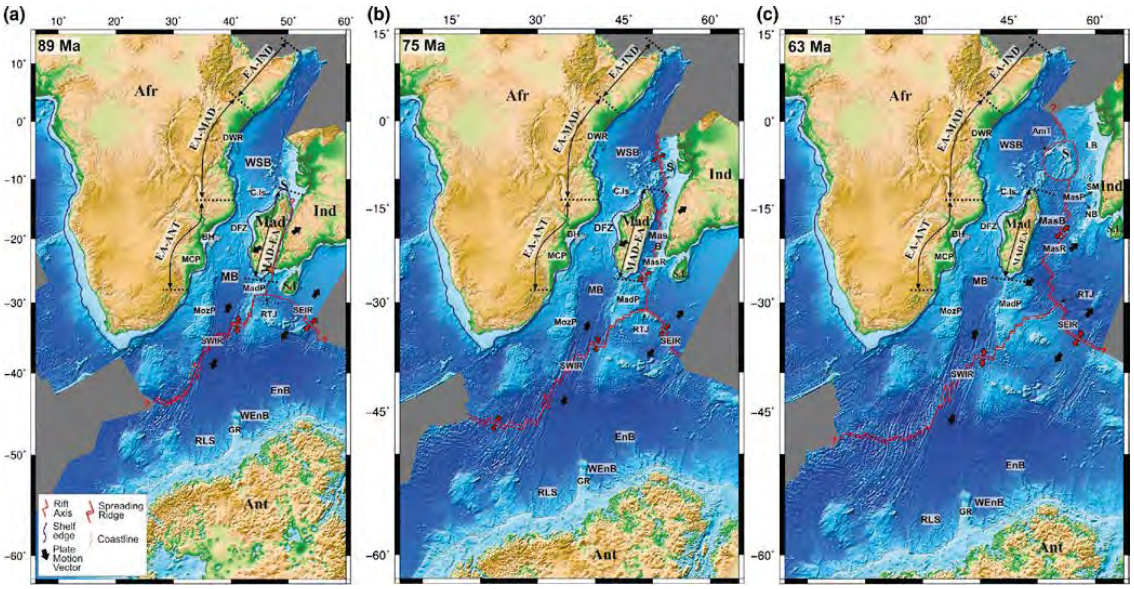

FIGU RE 7 Plate reconstruction maps showing the main stages of development in Phase 3. Seafloor spreading on the Mascarene Ridge opened the Mascarene Basin and separated India and Madagascar. (a) 89 Ma Onset of phase 3, arrival of Marion plume and eruption of Morondava volcanics on Madagascar before breakup between India and Madagascar, (b) 75 Ma established spreading in the Mascarene Basin, (c) 63 Ma rotation of Seychelles microplate. Afr, Africa; Mad, Madagascar; S, Seychelles; Ind, India; Ant, Antarctica; S.L., Sri Lanka; WSB, West Somali Basin; MB, Mozambique Basin; LB, Laxmi Basin; DFZ, Davie Fracture Zone; DWR, Davie Walu Ridge; BH, Beira High; MCP, Mozambique Coastal Plains; RLS, Riiser Larsen Sea; GR, Gunnerus Ridge; EnB, Enderby Basin; WEnB, West Enderby Basin; MozP, Mozambique Plateau; MadP, Madagascar Plateau; C.Is, Comoros Islands; SWIR, Southwest Indian Ridge; SEIR, Southeast Indian Ridge; RTJ, Rodriguez Triple Junction; MasR, Mascarene Ridge; MasB, Mascarene Basin; MasP, Mascarene Plateau; SM, Salha de Maya Bank; NB, Nazareth Bank; AmT, Amirante Trench; CR, Carlsberg Ridge; CIR, Central Indian Ridge

between chrons 30n and 28n was lacking from the Seychelles—India corridor in the very northern part of the Mascarene Basin and neighbouring flanks of the CR. They tentatively identified the missing crust to be present in the Laxmi Basin (Figure 7c), where magnetic anomaly profiles are short and had been previously interpreted in terms of much older seafloor spreading.

To further constrain the age of the Laxmi Basin, alternative reconstructions were attempted for C32n.1n and C34n using three alternative assumed ages for the initiation of plate divergence in the Laxmi Basin: C29o (65.12 Ma), 66 and 67 Ma. It was found that 67 Ma minimized overlap of the Seychelles microcontinent with the Indian-Madagascan and Somali continental margins. Therefore, the Laxmi Basin is modelled here as active between 67 (chron 30) and 64 Ma (during Chron 28n).

The Indian Plate had been accelerating northwards throughout the opening of the Mascarene Basin. This acceleration has been related to the influence of the Marion plume at the southern edge of the plate (van Hinsbergen, Steinberger, Doubrovine, & Gassmöller, 2011) or to the action of double subduction at its northern edge (Jagoutz, Royden, Holt, & Becker, 2015). During chron 30n (66.398–68.196 Ma), a further short-lived acceleration saw the speed of the Indian plate increased by 150%–200%, until it was moving faster than might be thought possible purely in response to the pull of a freely descending slab at its northern edge. Eagles and Wibisono (2013) suggested that relocation of part of the boundary between India and Madagascar from the Mascarene to the Laxmi Basin to the region above the Deccan-Réunion mantle plume led to the development of an unusually high mid-ocean ridge, from which an increased ridge push force contributed to the short period of unusually fast plate motion. They suggested that these conditions lasted for only a short while until the plate boundary in the Laxmi Basin was abandoned as the CR propagated rapidly into the region to the west of the basin. The occurrence of a similar short-lived acceleration in the new model for African-East Antarctic divergence (Figure 2c) is difficult to explain in similar terms, because of the great area of the African plate and the location of its boundary with the East Antarctic plate, opposing the direction of the proposed increase in Laxmi Basin ridge push for the African plate. A more prosaic interpretation of this event might be in terms of a timescale error affecting the dates assigned to chron 30.

3.3.2 | Rotation of Seychelles microplate and origin of the Amirante Trench

Isolation and independent movement of a small Seychelles plate (Figure 7c), was long suspected as an explanation for the islands' continental crustal composition and its intra-oceanic location. For a long time, though, the timing and details of the plate were poorly understood. Up until chron 29n (65.12–64.13 Ma) the Seychelles had been a part of the Indian plate, until the islands moved and rotated independently before becoming attached to the African plate. It is likely that the arcuate Amirante Trench to the southwest of the Seychelles platform acquired its present-day morphology during this rotation (Figure 7c), and, for a short time, formed part of the boundary between the Seychelles plate and the African plate. The present-day morphology of the trench, a deep, steep-sided, markedly arcuate trough with a rough but not tilted basement, suggests its extinction occurred while it was accommodating plate divergence at slow or ultraslow seafloor spreading rates (Eagles & Hoang, 2013), but that earlier in its development it accommodated transverse and convergent deformation as well. Our kinematic model and the rotation parameters from Eagles and Hoang (2013) suggest that this is a result of the trench forming part of a low-strain-rate "diffuse" plate boundary zone between Africa and the Seychelles. The early stages of this motion involve more widespread plate convergence and so are less confidently constrained than the later stages. As a consequence, as we noted above, it is difficult to conclude whether or not the "FIT" aged overlap between the Seychelles and the Somali margin is a result of model deficiency or should be interpreted in terms of plate boundary propagation and/or continental extension.

Isolation of the Seychelles microplate occurred as the result of a combination of ridge propagation and ridge jumping. The Mascarene Ridge became extinct at ca. 61 Ma. We date spreading in the Laxmi Basin at ca. 67 Ma until abandonment during chron 28n (64.667–63.494 Ma) following the jump to the CR. As a result, there was a period of about 6 million years during which ridges were active on either side of the Seychelles plateau, leading to the isolation of a small plate between them (Figure 7c). The Seychelles plate ceased independent motion and rotation during chron 26n (59.237–58.959 Ma) when it became attached to the African plate.

3.3.3 | Origin and position of the Mascarene Plateau

The origin of the crust beneath the Mascarene Plateau is unclear. Duncan and Hargraves (1990) wrote that it is comprised of Cenozoic basalts, which were emplaced during the passage of the Deccan-Réunion plume close the basin margin. However, more recently, Torsvik et al. (2013) and Ashwal, Wiedenbeck, and Torsvik (2017) used U-Pb dating to ascertain the ages of zircon xenocrysts separated from beach sands derived directly from young volcanic rocks on Mauritius, at the southern end of the Mascarene Plateau. They found numerous zircons with Palaeoproterozoic (>1,971 Ma) and Neoproterozoic (between 660 and 840 Ma) ages, and concluded that they were assimilated from ancient fragments of continental lithosphere beneath Mauritius and brought to the surface by plume related melts. Furthermore, crustal thickness maps from inversion of gravity data show a connecting block of anomalously thick crust that lies underneath Mauritius and the Mascarene Plateau, and extends northwards in an arc towards the Seychelles (Torsvik et al., 2013). The same authors suggest a Precambrian microcontinent, which they named Mauritia, for the origin of these xenocrysts and the reason for the anomalously thick crust, isolated by ridge jumps and covered in Cenozoic plume related lavas. They built a plate kinematic model that leaves a large space between India and Madagascar, almost as wide as Madagascar itself, for Mauritia. Most other reconstructions of the Indian and Madagascan conjugate margins leave much less space for such a microcontinent (e.g., Davis et al., 2016; Gibbons et al., 2013). Ratheesh-Kumar et al. (2014) found Mauritia to be unnecessary in their modelling supporting a fit between Madagascar and India based on flexural isostasy, elastic thickness, Moho depth data and matching tectonic lineaments, lithologies, and geochronological belts.

While accepting the significance of the zircon ages, our model shows a close fit between India and Madagascar, without the need for any significantly large intervening microcontinent blocks (Figure 7a). As a result, we consider most of the anomalous crustal thickness of the Mascarene Plateau to be a consequence of magmatic thickening during its journey over the Deccan-Réunion plume, and the area of any continental component to be too small to depict usefully in our reconstructions.

3.4 | Phase 4—Starting at 60 Ma: Separation of India and the Mascarene Plateau

The fourth tectonic phase involves the separation of India and the Mascarene Plateau, accommodated by spreading on the Carlsberg and CIR, which are still active today (Figure 8). Spreading on the CR started at the young end of chron C28n (63.10 Ma) and propagated southwards, separating India and the Mascarene Plateau between chrons C27n and C26n (61.65 and 58.38 Ma).

The rest of this phase is defined not by any significant tectonic changes within the NW Indian Ocean itself, but by changes occurring at the other margins of its plates. These include the development of the East African Rift System

(EARS) and the collisions of India and Africa with Eurasia. The latter changes led to considerable complexity in the relative movement of Africa and Antarctica in the period from ca. 58 to 53 Ma. During this time, the relative motion changes from approximately NNE-SSW to NW-SE before reverting back to NNE-SSW again. This has given rise to pronounced curves in the fracture zones on the flanks of the SWIR (Figure 8b).

Finite rotations in our model of Antarctic-Africa relative motion migrate southwards in the period after chrons 30y–28o (66.398–63.494 Ma), at first rapidly until chrons 26y to 24y (58.959–52.62 Ma), and afterwards more slowly until chron 13y (33.147 Ma) (see section 2.1, Figure 2). The initial slowdown has been interpreted in terms of the influence of the Deccan plume near the African-India plate boundary (Cande & Stegman, 2011), and its later stages in terms of the eventual continental collision between Africa and Europe (Nankivell, 1997). After chron 13, the progression of finite rotation poles adopts a northwards orientation. This abrupt change suggests a new tectonic influence beginning at 13y (33.147 Ma), which could be related to the onset of continental rifting linked to a new plate boundary in the EARS (e.g., Roberts et al., 2012).

At the beginning of this phase, three active spreading ridges existed; the CR, the CIR and the SWIR.

At this stage the local plate motion vectors along the East African and West Madagascan margins were orientated in a NE-SW direction as a consequence of active spreading on the Carlsberg and CIR. Accordingly, in the NE-SW oriented EA-IND, northern EA-MAD, northern and central EA-ANT segments, the local plate motion vectors were still oriented mostly parallel to the continental margin segments (Figure 8b) indicating tectonic quiescence and passive margin conditions. The start of this phase correlates well with the formation of the gravity-driven Lamu deep-water fold-and-thrust-belt offshore Kenya (Cruciani & Barchi, 2016). The N-S trending margin segments of the southern EA-MAD and MAD-EA margins were characterized by more oblique trending local plate motion vectors indicating potential transpressional or strike-slip deformation in this phase (Figure 9b). Further south, the direction of plate divergence rapidly flip-flopped from N to NW between 58 and 53 Ma then back to N. Figure 2c shows the spreading azimuth deviating from north by almost 60°, corresponding to a drop in the spreading rate.

Later in phase 4, the development of the East African margin is likely to have been strongly influenced by the neighbouring EARS. This may be reflected in the progression of finite rotation poles discussed earlier in this section. However, it seems the effects were largely local. Examples include: (a) Uplift and doming prior to the onset of rifting as suggested by Wichura, Bousquet, Oberhänsli, Strecker, and Trauth (2011) for the Kenya dome in the Mid-Miocene, and linked to the Oligocene by Macgregor (2015); (b) Uplift and increased sediment input triggered by the EARS may have led to loading and collapse of prograding sediment wedges, for example the Rovuma deep-water-fold-and-thrust-belt (Mahanjane & Franke, 2014)).

4 I DISCUSSION

The detailed plate tectonic model and derived plate tectonic evolutionary stages of the Northwest Indian Ocean form the basis of a chronostratigraphic chart correlating the fundamental regional tectonic events and megasequence types of the conjugate margin segments of East Africa with India, Madagascar, and Antarctica (Figure 9).

This margin-scale chronostratigraphic correlation will in turn form the basis for a more detailed future margin-scale tectono-stratigraphic framework integrating geological and geophysical data from sedimentary basins to better understand their formation and evolution along the East African and West Madagascan rifted continental margins. Here, however, we discuss possible correlations at plate margin scale.

The four main tectonic phases identified in our plate kinematic model, and the preceding Karoo phase, are shown by coloured background panels of the chart in Figure 9. For the margin-scale correlation in this paper, the chronostratigraphic chart utilizes a simplified tectono-stratigraphy of the sedimentary basins on the various East Africa and West Madagascar margin segments, compiled from literature. This tectonostratigraphy comprises the following dominant megasequences: the Karoo syn-rift, Main syn-rift, transitional, early postrift, late postrift, and modern margin. This tectono-stratigraphic classification is applied to the margin segments based on lithological and structural features and the stratigraphic boundaries described in literature and subsequently placed into the context of our plate kinematic model. The tectonic regimes of each margin segment derived from the plate kinematic model and orientation of local plate motion vectors (Chapter 3) are shown as coloured bars along the left of each margin segment and the average plate motion vectors relative to conjugate margin segments are shown by the black arrows.

The following section briefly summarizes the key tectono-stratigraphic events in the conjugate margin segments of East Africa with India, Madagascar, and Antarctica and their correlation within the newly derived margin-scale chronostratigraphic framework.

4.1 I Prephase 1: Karoo

The Karoo Phase refers to the phase of intermittent, intracontinental rifting events that affected the Pangea

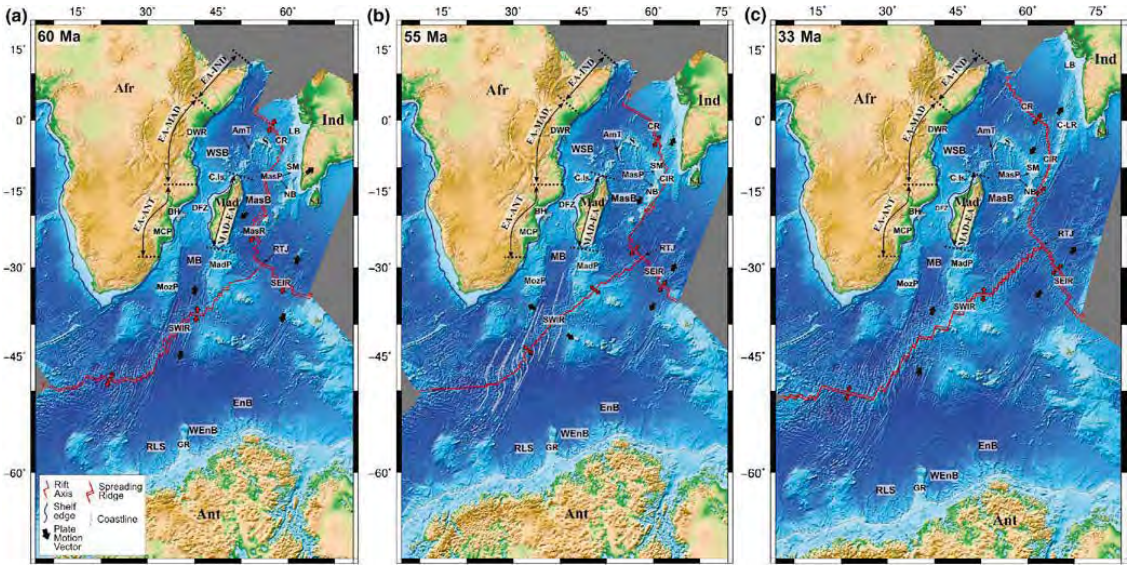

FIGU RE 8 Plate reconstruction maps showing the main stages of development in Phase 4. Seafloor spreading ended in the Mascarene Basin, spreading on the Carlsberg and Central Indian Ridges separated India and the Mascarene Plateau. (a) 60 Ma Spreading on the Carlsberg Ridge, end of spreading on the Mascarene Ridge and abandonment of Seychelles plate, (b) 55 Ma spreading on Carlsberg Ridge and Central Indian Ridge, (c) 33 Ma mature/established spreading on Carlsberg and Central Indian Ridges. Afr, Africa; Mad, Madagascar; S, Seychelles; Ind, India; Ant, Antarctica; S.L., Sri Lanka; WSB, West Somali Basin; MB, Mozambique Basin; LB, Laxmi Basin; DFZ, Davie Fracture Zone; DWR, Davie Walu Ridge; BH, Beira High; MCP, Mozambique Coastal Plains; RLS, Riiser Larsen Sea; GR, Gunnerus Ridge; EnB, Enderby Basin; WEnB, West Enderby Basin; MozP, Mozambique Plateau; MadP, Madagascar Plateau; C.Is, Comoros Islands; SWIR, Southwest Indian Ridge; SEIR, Southeast Indian Ridge; RTJ, Rodriguez Triple Junction; MasR, Mascarene Ridge; MasB, Mascarene Basin; MasP, Mascarene Plateau; SM, Salha de Maya Bank; NB, Nazareth Bank; AmT, Amirante Trench; CR, Carlsberg Ridge; CIR, Central Indian Ridge; C-LR, Chagos-Laccadive Ridge

supercontinent which were ultimately unsuccessful in reaching the final breakup stage. The age of Karoo sediments determined in the margin segments varies considerably, consistent with the idea of their deposition during a rifting phase that potentially stretched all the way from the Late Carboniferous through the Permo-Triassic and into the Early Jurassic, when Pangea had reached its maximum extent (Catuneanu et al., 2005).

Along the future margins of East Africa and West Madagascar, Karoo rifting mainly followed inherited structural basement trends, for example, the Mozambique Metamorphic Belt causing fairly discrete, linear NE trending rifts (Catuneanu et al., 2005). A number of smaller north to northwest trending pull-apart basins suggest that the East African/Malagasy Karoo Basins were formed by left-lateral transtension between India/Madagascar and Africa (Catuneanu et al., 2005; Wopfner, 1994).

The Karoo sediments are predominantly continental in nature and deposited unconformably on top of the metamorphic basement. Sporadic marine incursions from the Tethyan Ocean in the North occurred, and reached as far south as Madagascar (Wopfner, 1994). These rifting events failed to cause the breakup of Gondwana and culminated in the early Jurassic eruption of the Karoo LIP within the time period 183–177 Ma (Cox, 1992; Jourdan et al., 2005).

Dates for the boundary between the Karoo and Main Syn-rift megasequence vary greatly along the margins. Along the East African margin segment conjugate to Madagascar the boundary is dated at ca. 200 Ma (Coffin & Rabinowitz, 1988; Key et al., 2008). However, on the Madagascan margin it has been identified much later at ca. 183 Ma (Geiger et al., 2004; Papini & Benvenuti, 2008), accompanying the emplacement of the Karroo-Ferrar LIP (Cox, 1992; Jourdan et al., 2005) and the onset of Phase 1 of our plate kinematic model (see Figure 9). Along the EA-IND margin the boundary between Karoo and Main syn-rift has been placed at ca. 190 Ma (Bosellini, 1992). However, in the EA-ANT margin segment the Karoo megasequence extends into Phase 1 (Mahanjane, 2012). Variability in this order might be expected in a set of basins that have been sparsely studied using varying techniques and data sets over a 30-year period. To what extent it might also reflect the progressive break-up of Pangea or

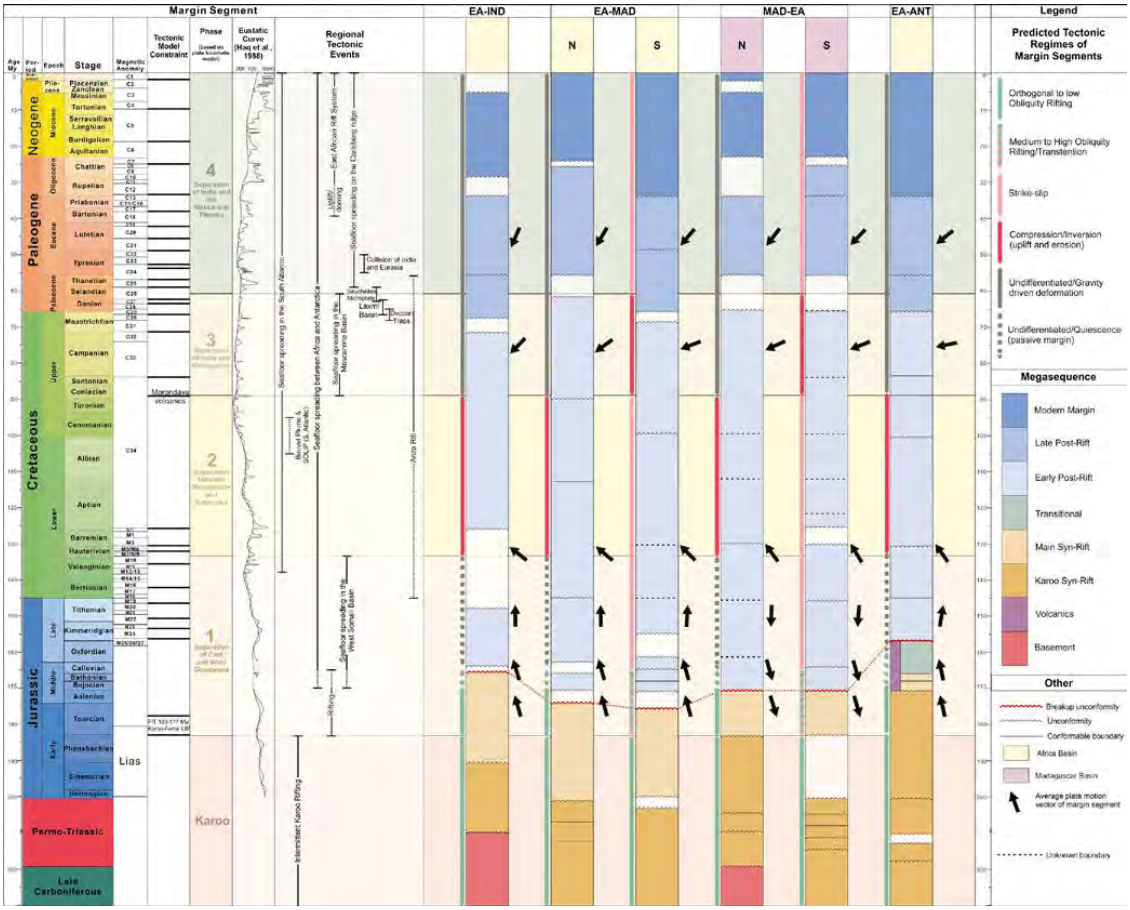

FIGU RE 9 Chronostratigraphic diagram correlating the main tectonic phases derived from the plate kinematic model, regional tectonic events, and megasequences along the East African and conjugate West Madagascan margin segments

asymmetrical rifting styles, remains to be seen on the basis of future more detailed work.

4.2 | Phase 1: Latest Karoo/main syn-rift/transitional/breakup/early postrift

As previously described in section 3.2, Phase 1 of our tectonic model includes the rifting of East Gondwana (comprising Madagascar/India/Antarctica/Seychelles) and West Gondwana (comprising Africa/South America), and their eventual breakup and subsequent seafloor spreading in the West Somali and Mozambique Basins (Figure 5a–c). Karoo syn-rift, main syn-rift, transitional, and early postrift megasequences are all either present or partially present in this phase (Figure 9).

The main syn-rift megasequence is associated with the distinct, concise stage of rifting that successfully led to the breakup of East and West Gondwana. Characteristically, syn-rift sedimentation is controlled by rift-related extensional faulting, with sediments accumulating within half grabens (Bosellini, 1992; Clark, 1998; Coffin & Rabinowitz, 1988; Geiger et al., 2004; Mahanjane, 2012; Mbede & Dualeh, 1997). Sediments were deposited under mostly shallow marine conditions along the EA-IND and MAD-EA margin segments (Bosellini, 1992; Geiger et al., 2004), with a mixture of continental, transitional and shallow water facies along EA-MAD (Coffin & Rabinowitz, 1988; Hudson & Nicholas, 2014; Mbede & Dualeh, 1997), and shelf to marine sediments along EA-ANT (Mahanjane et al., 2014). In some margin segments, the main syn-rift megasequence is easily identifiable (e.g., MAD-EA), however, in others it is difficult to distinguish from the Karoo megasequence (EA-IND, EA-MAD).

Along the conjugate Madagascan margin, the onset of the main syn-rift stage corresponds to the beginning of Phase 1 of our plate kinematic model. However, main

syn-rift deposition began earlier in the EA-IND and EA-MAD margin segments and Karoo syn-rift deposition continued well into phase 1 in the EA-ANT margin (see section 4.1 above). By nature, the main syn-rift deposition is very variable because its onset happened in isolated rift basins first. As a consequence of the staggered breakup, the main syn-rift sediments in the EA-ANT segment are younger than the EA-MAD and MAD- EA segments. However, main syn-rift sediments of similar age are found along the EA-IND segments.

A characteristic transitional megasequence has been identified in the EA-ANT segment only, where it consists of mixed marine/continental sediments deposited during an early postrift sag phase before final breakup occurred (Mahanjane, 2012).

The age of the breakup unconformity, separating the main syn-rift (or transitional) megasequence from the early postrift megasequence also is diachronous along the margins. The breakup age of the EA-MAD segment has been given at the end of the Jurassic ca. 174 Ma (Coffin & Rabinowitz, 1988) and for its conjugate MAD-EA segment the breakup age is represented by the Aalenian-Bajocian boundary, ca. 170 Ma (Geiger et al., 2004). Stratigraphic constraints in Somalia suggest breakup just to the north, along the EA-IND segment, occurred during the Callovian ca. 165 Ma (Bosellini, 1992). The discrepancy and age of these dates could be due to problems in identifying or dating the breakup unconformity, or due to erosion and removal of younger syn-rift sediments at the end of the rifting phase. Magnetic reversal isochrons in the Mozambique Basin suggest that breakup at the EA-ANT margin had occurred by 164–166 Ma (Leinweber & Jokat, 2012; Mueller & Jokat, 2017), whereas stratigraphic evidence suggests a somewhat later date of ca. 157 Ma (Mahanjane, 2012). Both interpretations agree broadly with our plate kinematic model, in which EA-ANT breakup occurs around 160 Ma, later than at the other margin segments. Interpretations of the MCPs as underlain by stretched continental crust or transitional crust (e.g., Leinweber & Jokat, 2011) are consistent with the notion of a longer lasting period of continental stretching before breakup.

The orientations of plate motion vectors during the main syn-rift is described in section 3 (Figure 5). Extension occurred in a NW-SE direction, perpendicular to most margin segments, facilitating orthogonal rifting. Exceptions to this pattern are the southern EA-MAD and MAD-EA segments characterized by dextral transtension on what was to become the Davie Fracture Zone.

Following breakup, a thick succession of postrift sediments was deposited along all margin segments. The postrift succession has been subdivided into three distinct megasequences; early postrift, late postrift, and modern margin. These subdivisions are marked by significant changes in the stratigraphic succession or tectonic development of the basins such as the sudden change in depositional facies from shallow to deep marine sediments and vice versa, or the occurrence of major regional unconformities that can be suggested to relate to phases of tectonic uplift.

The Early postrift megasequence stretches from Phase 1 through Phase 2 and into Phase 3 of our plate kinematic model. Early postrift sequences are characterized by changes of the depositional environment from shallow-marine to deep marine sediments as a consequence of thermal subsidence of the stretched continental and oceanic crust the margin segments following breakup.

Within Phase 1, the initial stages of early postrift deposition along the EA margin segments are punctuated by a number of localized unconformities followed by more consistent and sustained deposition at the start of the Cretaceous. The exception to this was observed at the EA-IND segment, where a major pre-Aptian erosional event removed early Cretaceous sediments (Bosellini, 1992).

For the rest of Phase 1, most of the Early Postrift megasequence sediments are characterized as an undifferentiated passive margin sequence, indicating relative tectonic quiescence. Local exceptions are the southern EA-MAD and southern MAD-EA margin segments, which remained close to active plate boundary segments of the future Davie Fracture Zone accommodating strike-slip tectonics. Latest Jurassic-to early Cretaceous unconformities in the EA-IND and its neighbouring northern EA-MAD margin segments cannot be directly correlated with any of the kinematic model's main events. In contrast, the neighbouring Anza Rift was a site of Berriasian-Barremian sedimentation that accompanied tectonic activity (Bosworth & Morley, 1994), effecting the development of the EA-IND and EA-MAD segments.

4.3 | Phase 2: Early postrift

Deposition of the early postrift megasequence continued throughout Phase 2 (Figure 9). Phase 2 begins with a boundary reorganization in the NW Indian Ocean caused by the cessation of seafloor spreading in the West Somali Basin and its onset in or near the West Enderby Basin separating Madagascar and India from East Antarctica (section 3.2, Figure 6). Following this reconfiguration, unconformities form within 3 million years in the MAD-EA and EA-ANT margin segments (Coffin & Rabinowitz, 1988; Mahanjane, 2014). Given their timing, these unconformities can be related to the far-field effects of the plate boundary change described in our plate kinematic model. In contrast, all of the unconformities predate the alternatively advocated later (post-M0r; 124.6 Ma) cessation of seafloor spreading in the West Somali Basin (Davis et al., 2016; Gibbons et al., 2013; sections 2.1 and 3.2).

As described in section 4.2, the boundary relocation caused a change in the orientation of the local plate motion vectors, rotating them to NW-SE. This orientation is perpendicular to the EA-IND, northern EA-MAD, northern MAD-EA, and EA-ANT margin segments, which thus were exposed to the potential for regional uplift and inversion tectonics during phase 2 (Figures 6a and 9). Regional unconformities that might be associated with this possibility are rare, potentially reflecting the relatively young age and weak associated ridge push force from the SWIR to the SW of Madagascar.

Those unconformities that have been identified in the EA-ANT and southern EA-MAD segments are limited to an Albian-Cenomanian surface (Key et al., 2008; Salman & Abdula, 1995) but might alternatively be related to the "SOLIP" LIP formation at the Agulhas Plateau south of South Africa.

4.4 | Phase 3: Early and late postrift

The beginning of Phase 3 in our plate kinematic model is defined by the initiation of the new Mascarene ridge opening the Mascarene Basin and separating India from Madagascar (section 3.3, Figure 7).

Early postrift sedimentation continued into the early stage of Phase 3. Late postrift deposition began by the end of Phase 3 in the EA-IND, southern EA-MAD, and EA-ANT margin segments. However, in the northern EA-MAD and MAD-EA margins segments, late postrift sedimentation did not start until Phase 4. The late postrift stage is dominated by generally slower thermal subsidence and basinward progradation of depositional systems consisting of deep-water sediments, for example, shales, marls, mudstones, and turbiditic sandstones (Bosellini, 1992; Key et al., 2008; Salman & Abdula, 1995).

We expect the initiation of the Mascarene Ridge to have affected the East African and West Madagascan margins. However, there is little evidence for any effects in the tectono-stratigraphy (Figure 9) besides an unconformity at a roughly corresponding time in the northern EA-MAD segment linked to renewed basement uplift (Nyagah, 1995).

The boundary between the early and late postrift megasequences is marked by a major regional unconformity ranging from Maastrichtian age (Late Cretaceous) in the EA-IND, southern EA-MAD and EA-ANT margin segments to Palaeocene age in the northern EA-MAD and the conjugate northern MAD-EA margin segments. These unconformities overlap in time with important tectonic changes throughout the Indian Ocean as identified in our plate kinematic model and described in detail in section 3. These plate tectonic events include the arrival/peak activity of the Deccan-Réunion Plume, the end of seafloor spreading in the Mascarene Basin, the rotation of the Seychelles plate, the opening of the Laxmi Basin and the initiation of seafloor spreading on the CR. All these may have had far-field effects on the East African and West Madagascan margins.

The orientation of the local plate motion vectors during phase 3 suggests the potential for inversion tectonics along the southern EA-MAD and conjugate southern MAD-EA margin segments, though the lack of regional unconformities suggests that this potential was not realized on regional basin scale and was limited to the basins of western Madagascar (Clark, 1998; see section 3.3). The local plate motion vector orientation of Phase 3 for the EA-IND, northern EA-MAD, northern MAD-EA, and the EA-ANT margin segments is mostly subparallel to the strike of the margin segments consistent with a phase of tectonic quiescence and passive margin development during the late postrift or drift stage.

4.5 | Phase 4: Late postrift and modern margin

The start of Phase 4 is marked by the end of seafloor spreading in the Mascarene Basin and the onset of spreading on the CR and CIR separating India and the Mascarene Plateau (see section 3.4, Figure 8), which continues throughout Phase 4 to the present day.

Deposition of the late postrift megasequence continues into the early stage of Phase 4. Within Phase 4, an unconformable boundary separates the Late Postrift and the Modern margin megasequences (Figure 9). The modern margin meqasequence is characterized by large prograding deltas and gravity-driven deformation (Mahanjane & Franke, 2014; Mahanjane et al., 2014).

The onset of the modern margin megasequence within Phase 4 is again discernible by another major unconformity in all margin segments, the timing of which (Oligocene) suggests a link to doming and uplift of the African plate over the Afar plume, prior to the onset of the EARS (Ebinger & Sleep, 1998; Macgregor, 2015; Wichura et al., 2011). It is expected that the EARS has increased sediment input to the East African margin segments and triggered collapse of sediment wedges at shelf margins, turbidity currents, and the formation of deep-water fold-and-thrust belts (Mahanjane & Franke, 2014; Mahanjane et al., 2014).

The plate motion vectors are orientated approximately NE-SW, subparallel to most margin segments indicating tectonic quiescence and ongoing passive margin development. The exception is the southern EA-MAD and southern MAD-EA margin segments where the local plate motion vectors trend oblique to the margin segments creating the potential for strike-slip deformation. However, in the sedimentary basins of the East African margin (e.g., Lamu Basin [Kenya], Rovuma Basin [Tanzania/Mozambique]) it

is likely that the EARS controlled the regional tectonics since its onset in the Oligocene.

5 | CONCLUSIONS

We have developed and presented a margin-scale chronostratigraphic framework for the correlation of major tectonic events and megasequences in the conjugate margin segments of East Africa and Madagascar based on the results of a new plate kinematic model and published information of related basin fill sequences.

A new plate kinematic model of the Northwest Indian Ocean from 183 Ma to the present day was built using finite rotation poles generated by visual fitting and iterative joint inversion techniques as applied to magnetic isochron and fracture zone data. The result is a comprehensive model that describes the complex evolution of the area including its multiple plate boundary reorganizations leading to the growth of numerous ocean basins between separating land masses and microplates.

The synthesis of plate kinematic results with published tectonic and stratigraphic results for specific margin segments will enable us in future to analyse the impact of margin-wide tectonic processes on sedimentary basin development. In addition, the synthesis will establish whether the plate tectonic changes and phases of plate-reconfiguration during the opening of the Indian Ocean have been recorded in the stratigraphy and structure of individual basin along the margins. This is the prerequisite for a margin-scale tectono-stratigraphic framework based on plate kinematic model data.

Four tectonic phases of development are recognized for the area:

Phase 1—Starting at 183–177 Ma: Separation of East Gondwana (including Madagascar/India/Antarctica/Seychelles) and West Gondwana (including Africa/South America) accommodated by seafloor spreading in the West Somali and Mozambique Basins.

This phase saw the deposition of the main syn-rift, transitional, and early postrift megasequences along the East African and West Madagascan margins.

Rifting occurred in a ca. NW-SE direction with dextral transtension on the Davie Fracture Zone.

After breakup, seafloor spreading in the West Somali and Mozambique Basins and strike-slip deformation along the Davie Fracture Zone.

Phase 2—Starting at 133 Ma: Cessation of spreading in the West Somali Basin, boundary relocation to the south of Madagascar and the separation of Madagascar/India and East Antarctica.

Deposition of the early postrift megasequence continued.

Phase 3—Starting at 89 Ma: Onset of seafloor spreading on the Mascarene Ridge, opening of the Mascarene Basin and separation of India and Madagascar.

Deposition of the early postrift megasequence continued, followed the late postrift megasequence at the end to this phase.

Phase 4—Starting at 60 Ma: Cessation of spreading on the Mascarene Ridge, spreading on the Carlsberg and CIR separating India and the Mascarene Plateau.

Late postrift deposition continued until a major unconformity marked the change to the deposition of the modern margin megasequence.

Future work will provide a more in-depth analysis and correlation of the stratigraphy and structures of individual sedimentary basins along the margin segments to develop a comprehensive margin-scale tectono-stratigraphic framework for the correlation of sedimentary basins and their key petroleum system elements.

ACKNOWLEDGEMENTS

The presented research is part of a PhD project of the COMPASS industry consortium (Continental Margin Process Analysis, Structures & Stratigraphy) at Royal Holloway, University of London. We thank the COMPASS consortium for project funding. We thank Stuart Clark and two anonymous reviewers for their constructive comments that have improved the quality of this paper.

REFERENCES

Ashwal, L. D., Wiedenbeck, M., & Torsvik, T. H. (2017). Archaean zircons in Miocene oceanic hotspot rocks establish ancient continental crust beneath Mauritius. *Nature Communications*, *8*, 14086. https://doi.org/10.1038/ncomms14086

Bhattacharya, G. C., Chaubey, A. K., Murty, G. P. S., Srinivas, K., Sarma, K. V. L. N. S., Subrahmanyam, V., & Krishna, K. S. (1994). Evidence for seafloor spreading in the Laxmi Basin, northeastern Arabian Sea. *Earth and Planetary Science Letters*, *125*(1–4), 211–220. https://doi.org/10.1016/0012-821X(94)90216-X

Bosellini, A. (1992). The continental margins of Somalia: Structural evolution and sequence stratigraphy. In J. S. Watkins, Z. Feng, & K. J. McMillen (Eds.), *Geology and geophysics of continental margins. AAPG Memoir*, *53*, 185–205.

Bosworth, W., & Morley, C. K. (1994). Structural and stratigraphic evolution of the Anza rift, Kenya. *Tectonophysics*, *236*(1–4), 93–115. https://doi.org/10.1016/0040-1951(94)90171-6

Cande, S. C., & Patriat, P. (2015). The anticorrelated velocities of Africa and India in the Late Cretaceous and early Cenozoic. *Geophysical Journal International*, *200*(1), 227–243. https://doi.org/10.1093/gji/ggu392

Cande, S. C., Patriat, P., & Dyment, J. (2010). Motion between the Indian, Antarctic and African plates in the early Cenozoic. *Geophysical Journal International*, *183*, 127–149. https://doi.org/10.1111/j.1365-246X.2010.04737.x

Cande, S. C., & Stegman, D. R. (2011). Indian and African plate motions driven by the push force of the Reunion plume head. *Nature*, *475*, 47–52. https://doi.org/10.1038/nature10174

Catuneanu, O., Wopfner, H., Eriksson, P. G., Cairncross, B., Rubidge, B. S., Smith, R. M. H., & Hancox, P. J. (2005). The Karoo basins of south-central Africa. *Journal of African Earth Sciences*, *43*, 211–253. https://doi.org/10.1016/j.jafrearsci.2005.07.007

Clark, D. N. (1998). Review of the exploration potential of Madagascar. *Houston Geological Society Bulletin*, *40*, 23–29.

Cochran, J. R. (1988). Somali basin, chain ridge, and origin of the northern somali basin gravity and geoid low. *Journal of Geophysical Research*, *93*(B10), 11985–12008. https://doi.org/10.1029/JB093iB10p11985

Coffin, M. F., & Rabinowitz, P. D. (1987). Reconstruction of Madagascar and Africa: Evidence from the Davie fracture zone and western Somali Basin. *Journal of Geophysical Research*, *92*, 9385–9406. https://doi.org/10.1029/JB092iB09p09385

Coffin, M. F., & Rabinowitz, P. D. (1988). Evolution of the conjugate East African-Madagascan margins and the western Somali Basin. *Geological Society of America Special Papers*, *226*, 1–79.

Cox, K. G. (1992). Karoo igneous activity, and the early stages of the break-up of Gondwanaland. *Geological Society, London, Special Publications*, *68*(1), 137–148. https://doi.org/10.1144/GSL.SP.1992.068.01.09

Cruciani, F., & Barchi, M. R. (2016). The Lamu Basin deepwater fold-and-thrust belt: An example of a margin-scale, gravity-driven trust belt along the continental passive margin of East Africa. *Tectonics*, *35*(3), 491–510. https://doi.org/10.1002/2015TC003856

Danforth, A., Granath, J., Horn, B., & Komba, K. (2012). Hydrocarbon potential of the deep offshore Tanzania Basin in Context of East Africa's Transform Margin. In *East Africa: Petroleum Province of the 21st Century, Abstr*. London: Geological Society, pp. 32–33.

Davis, J. K., Lawver, L. A., Norton, I. O., & Gahagan, L. M. (2016). New Somali Basin magnetic anomalies and a plate model for the early Indian Ocean. *Gondwana Research*, *34*, 16–28. https://doi.org/10.1016/j.gr.2016.02.010

Demets, C., Gordon, R. G., & Royer, J.-Y. (2005). Motion between the Indian, Capricorn and Somalian plates since 20 Ma: Implications for the timing and magnitude of distributed lithospheric deformation in the equatorial Indian Ocean. *Geophysical Journal International*, *161*, 445–468. https://doi.org/10.1111/j.1365-246X.2005.02598.x

Domingues, A., Silveira, G., Ferreira, A. M. G., Chang, S.-J., Custódio, S., & Fonseca, J. F. B. D. (2016). Ambient noise tomography of the East African Rift in Mozambique. *Geophysical Journal International*, *204*, 1565–1578. https://doi.org/10.1093/gji/ggv538

Duncan, R. A., & Hargraves, R. B. (1990). $^{40}Ar/^{39}Ar$ geochronology of basement rocks from the Mascarene Plateau, the Chagos Bank, and the Maldives Ridge. In R. A. Duncan, J. Backman, & L. C. Peterson (Eds.), *Proceedings of the ODP, Scientific Results* (Vol. 115, pp. 43–51). College Station, TX: Ocean Drilling Program.

Eagles, G. (2004). Tectonic evolution of the Antarctic-Phoenix Plate system since 15 Ma. *Earth and Planetary Science Letters*, *217*, 97–109. https://doi.org/10.1016/S0012-821X(03)00584-3

Eagles, G., & Hoang, H. H. (2013). Cretaceous to present kinematics of the Indian, African and Seychelles plates. *Geophysical Journal International*, *196*, 1–14.

Eagles, G., & König, M. (2008). A model of plate kinematics in Gondwana breakup. *Geophysical Journal International*, *173*, 703–717. https://doi.org/10.1111/j.1365-246X.2008.03753.x

Eagles, G., Pérez-Díaz, L., & Scarselli, N. (2015). Getting over continent ocean boundaries. *Earth-Science Reviews*, *151*, 244–265. https://doi.org/10.1016/j.earscirev.2015.10.009

Eagles, G., & Wibisono, A. D. (2013). Ridge push, mantle plumes and the speed of the Indian plate. *Geophysical Journal International*, *194*, 670–677. https://doi.org/10.1093/gji/ggt162

Ebinger, C. J., & Sleep, N. H. (1998). Cenozoic magmatism throughout east Africa resulting from impact of a single plume. *Nature*, *395*, 788–791. https://doi.org/10.1038/27417

Encarnación, J., Fleming, T. H., Elliot, D. H., & Eales, H. V. (1996). Synchronous emplacement of Ferrar and Karoo dolerites and the early breakup of Gondwana. *Geology*, *24*(6), 535. https://doi.org/10.1130/0091-7613(1996)024<0535:SEOFAK>2.3.CO;2

Fonseca, J. F. B. D., Chamussa, J., Domingues, A. L., Helffrich, G., Antunes, E., van Aswegen, G., .. . Manhica, V. J. (2014). MOZART: A seismological investigation of the East African Rift in central Mozambique. *Seismological Research Letters*, *85*, 108–116. https://doi.org/10.1785/0220130082

Geiger, M., Clark, D. N., & Mette, W. (2004). Reappraisal of the timing of the breakup of Gondwana based on sedimentological and seismic evidence from the Morondava Basin, Madagascar. *Journal of African Earth Sciences*, *38*(4), 363–381. https://doi.org/10.1016/j.jafrearsci.2004.02.003

Gibbons, A. D., Whittaker, J. M., & Müller, R. D. (2013). The Breakup of East Gondwana: Assimilating constraints from Cretaceous ocean basins around India into a best-fit tectonic model. *Journal of Geophysical Research: Solid Earth*, *118*(3), 808–822.

Gradstein, F. M., Ogg, J. G., & Smith, A. G. (eds.). (2004). *A geologic time scale 2004* (p. 589). Cambridge, UK: Cambridge University Press. https://doi.org/10.4095/215638

Hammond, J. O. S., Kendall, J.-M., Collier, J. S., & Rümpker, G. (2013). The extent of continental crust beneath the Seychelles. *Earth and Planetary Science Letters*, *381*, 166–176. https://doi.org/10.1016/j.epsl.2013.08.023

Hellinger, S. J. (1981). The uncertainties of finite rotations in plate tectonics. *Journal of Geophysical Research*, *86*(B10), 9312–9318. https://doi.org/10.1029/JB086iB10p09312

Horner-Johnson, B. C., Gordon, R. G., & Argus, D. F. (2007). Plate kinematic evidence for the existence of a distinct plate between the Nubian and Somalian plates along the Southwest Indian Ridge. *Journal of Geophysical Research*, *112*(B5).

Hudson, W. E., & Nicholas, C. J. (2014). The Pindiro Group (Triassic to Early Jurassic Mandawa Basin, southern coastal Tanzania): Definition, palaeoenvironment, and stratigraphy. *Journal of African Earth Sciences*, *92*, 55–67. https://doi.org/10.1016/j.jafrearsci.2014.01.005

Jagoutz, O., Royden, L., Holt, A. F., & Becker, T. W. (2015). Anomalously fast convergence of India and Eurasia caused by double subduction. *Nature Geoscience*, *8*(6), 475–478. https://doi.org/10.1038/ngeo2418

Jokat, W., Nogi, Y., & Leinweber, V. (2010). New aeromagnetic data from the western Enderby Basin and consequences for Antarctic-India break-up. *Geophysical Research Letters*, *37*(21).

Jourdan, F., Féraud, G., Bertrand, H., Kampunzu, A. B., Tshoso, G., Watkeys, M. K., & le Gall, B. (2005). Karoo large igneous province: Brevity, origin, and relation to mass extinction questioned by new 40Ar/39Ar age data. *Geology*, *33*(9), 745. https://doi.org/10.1130/G21632.1

Key, R. M., Smith, R. A., Smelror, M., Saether, O. M., Thorsnes, T., Powell, J. H., ... Zandamela, E. B. (2008). Revised lithostratigraphy of the Mesozoic-Cenozoic succession of the onshore Rovuma Basin, northern coastal Mozambique. *South African Journal of Geology*, *111*(1), 89–108. https://doi.org/10.2113/gssajg.111.1.89

Klimke, J., & Franke, D. (2016). Gondwana breakup: No evidence for a Davie Fracture Zone offshore northern Mozambique, Tanzania and Kenya. *Terra Nova*, *28*, 233–244. https://doi.org/10.1111/ter.12214

Klimke, J., Franke, D., Gaedicke, C., Schreckenberger, B., Schnabel, M., Stollhofen, H., .. . Chaheire, M. (2016). How to identify oceanic crust—Evidence for a complex break-up in the Mozambique Channel, off East Africa. *Tectonophysics*, *693*, 436–452. https://doi.org/10.1016/j.tecto.2015.10.012

König, M., & Jokat, W. (2010). Advanced insights into magmatism and volcanism of the Mozambique Ridge and Mozambique Basin in the view of new potential field data. *Geophysical Journal International*, *180*(1), 158–180.

Leinweber, V. T., & Jokat, W. (2011). Is there continental crust underneath the northern Natal Valley and the Mozambique Coastal Plains? *Geophysical Research Letters*, *38*(14).

Leinweber, V. T., & Jokat, W. (2012). The Jurassic history of the Africa-Antarctica corridor—New constraints from magnetic data on the conjugate continental margins. *Tectonophysics*, *530–531*, 87–101. https://doi.org/10.1016/j.tecto.2011.11.008

Livermore, R., Nankivell, A., Eagles, G., & Morris, P. (2005). Paleogene opening of Drake Passage. *Earth and Planetary Science Let- ters*, *236*(1–2), 459–470. https://doi.org/10.1016/j.epsl.2005.03.027

Macgregor, D. (2015). History of the development of the East African Rift System: A series of interpreted maps through time. *Journal of African Earth Sciences*, *101*, 232–252. https://doi.org/10.1016/j.jafrearsci.2014.09.016

Mahanjane, E. S. (2012). A geotectonic history of the northern Mozambique Basin including the Beira High—A contribution for the understanding of its development. *Marine and Petroleum Geology*, *36*(1), 1–12. https://doi.org/10.1016/j.marpetgeo.2012.05.007

Mahanjane, E. S. (2014). The Davie Fracture Zone and adjacent basins in the offshore Mozambique Margin—A new insights for the hydrocarbon potential. *Marine and Petroleum Geology*, *57*, 561–571. https://doi.org/10.1016/j.marpetgeo.2014.06.015

Mahanjane, E. S., & Franke, D. (2014). The Rovuma Delta deep-water fold-and-thrust belt, offshore Mozambique. *Tectonophysics*, *614*, 91–99. https://doi.org/10.1016/j.tecto.2013.12.017

Mahanjane, E. S., Franke, D., Lutz, R., Winsemann, J., Ehrhardt, A., Berglar, K., & Reichert, C. (2014). Maturity and petroleum systems modelling in the offshore Zambezi delta depression and Angoche basin, northern Mozambique. *Journal of Petroleum Geology*, *37*(4), 329–348. https://doi.org/10.1111/jpg.12589

Mbede, E. I., & Dualeh, A. (1997). Chapter 10: The coastal basins of Somalia, Kenya and Tanzania. *Sedimentary Basins of the World*, *3*, 211–233. https://doi.org/10.1016/S1874-5997(97)80013-5

McKenzie, D., & Sclater, J. G. (1971). The ecolution of the Indian Ocean since the Late Cretaceous. *Geophysical Journal International*, *24*(5), 437–528. https://doi.org/10.1111/j.1365-246X.1971.tb02190.x

Molnar, P., Pardo-Casas, F., & Stock, J. (1988). The Cenozoic and Late Cretaceous evolution of the Indian Ocean: Uncertainties in the reconstructed positions of the Indian African and Antarctic plates. *Basin Research*, *1*, 23–40. https://doi.org/10.1111/j.1365-2117.1988.tb00003.x

Mueller, C. O., & Jokat, W. (2017). Geophysical evidence for the crustal variation and distribution of magmatism along the central coast of Mozambique. *Tectonophysics*, *712–713*, 684–703. https://doi.org/10.1016/j.tecto.2017.06.007

Nankivell, A. P. (1997). Tectonic evolution of the Southern Ocean between Antarctica, South America and Africa over the last 84 Ma. PhD thesis, Oxford University, Oxford, UK.

Norton, I. O. I., & Sclater, J. G. (1979). A model for the evolution of the Indian Ocean and the breakup of Gondwanaland. *Journal of Geophysical Research: Solid Earth*, *84*(9), 6803–6830. https://doi.org/10.1029/JB084iB12p06803

Nyagah, K. (1995). Stratigraphy, depositional history and environments of deposition of Cretaceous through Tertiary strata in the Lamu Basin, southeast Kenya and implications for reservoirs for hydrocarbon exploration. *Sedimentary Geology*, *96*(1–2), 43–71. https://doi.org/10.1016/0037-0738(94)00126-F

Papini, M., & Benvenuti, M. (2008). The Toarcian-Bathonian succession of the Antsiranana Basin (NW Madagascar): Facies analysis and tectono-sedimentary history in the development of the East Africa-Madagascar conjugate margins. *Journal of African Earth Sciences*, *51*, 21–38. https://doi.org/10.1016/j.jafrearsci.2007.11.003

Patriat, P., & Segoufin, J. (1988). Reconstruction of the Central Indian Ocean. *Tectonics*, *155*, 211–234.

Pérez-Díaz, L., & Eagles, G. (2014). Constraining South Atlantic growth with seafloor spreading data. *Tectonics*, *33*(9), 1848–1873. https://doi.org/10.1002/2014TC003644

Phethean, J. J. J., Kalnins, L. M., van Hunen, J., Biffi, P. G., Davies, R. J., & McCaffrey, K. J. W. (2016). Madagascar's escape from Africa: A high-resolution plate reconstruction for the Western Somali Basin and implications for supercontinent dispersal. *Geochemistry, Geophysics, Geosystems*, *17*, 5036–5055. https://doi.org/10.1002/2016GC006624

Rabinowitz, P. D., Coffin, M. F., & Falvey, D. (1983). The separation of Madagascar and Africa. *Science*, *220*(4592), 67–69. https://doi.org/10.1126/science.220.4592.67

Raillard, S. (1990). *Les Marges de l'Afrique de l'est et les Zones de Fracture associées: Chaine Davie et Ride du Mozambique*, PhD thesis. Université Paris, Paris.

Reeves, C. (2014). The position of Madagascar within Gondwana and its movements during Gondwana dispersal. *Journal of African Earth Sciences*, *94*, 45–57. https://doi.org/10.1016/j.jafrearsci.2013.07.011

Ratheesh-Kumar, R. T., Ishwar-Kumar, C., Windley, B. F., Razakamanana, T., Nair, R. R., & Sajeev, K. (2014). India-Madagascar paleo-fit based on flexural isostasy of their rifted margins. *Gondwana Research*, *28*(2), 581–600.

Riley, T. R., Curtis, M. L., Leat, P. T., Watkeys, M. K., Duncan, R. A., Millar, I. L., & Owens, W. H. (2006). Overlap of Karoo and Ferrar magma types in KwaZulu-Natal, South Africa. *Journal of Petrology*, *47*(3), 541–566. https://doi.org/10.1093/petrology/egi085

Roberts, E. M., Stevens, N. J., O'Connor, P. M., Dirks, P. H. G. M., Gottfried, M. D., Clyde, W. C., .. . Hemming, S. (2012). Initiation of the western branch of the East African Rift coeval with the eastern branch. *Nature Geoscience*, *5*(4), 289–294. https://doi.org/10.1038/ngeo1432

Roeser, H. A., Fritsch, J., & Hinz, K. (1996). The development of the crust off Dronning Maud Land, east Antarctica. *Geological Society, London, Special Publications*, *108*(1), 243–264. https://doi.org/10.1144/GSL.SP.1996.108.01.18

Royer, J.-Y., Chaubey, A. K., Dyment, J., Bhattacharya, G. C., Srinivas, K., Yatheesh, V., & Ramprasad, T. (2002). Paleogene plate tectonic evolution of the Arabian and Eastern Somali basins. *Geological Society, London, Special Publications*, *195*(1), 7–23. https://doi.org/10.1144/GSL.SP.2002.195.01.02

Royer, J.-Y., & Gordon, R. G. (1997). The motion and boundary between the Capricorn and Australian Plates. *Science*, *277*(5330), 1268–1274. https://doi.org/10.1126/science.277.5330.1268

Salman, G., & Abdula, I. (1995). Development of the Mozambique and Ruvuma sedimentary basins, offshore Mozambique. *Sedimentary Geology*, *96*(1–2), 7–41. https://doi.org/10.1016/0037-0738(95)00125-R

Sandwell, D. T., Muller, R. D., Smith, W. H., Garcia, E., & Francis, R. (2014). Marine geophysics. New global marine gravity model from Cryosat-2 and Jason-1 reveals buried tectonic structure. *Science*, *346*, 65–67. https://doi.org/10.1126/science.1258213

Schlich, R. (1982). The Indian Ocean: Aseismic ridges, spreading centers, and basins. In A. E. M. Nairn & F. G. Stehli (Eds.), *The ocean basins and margins*, Vol. 6 (pp. 51–147)., The Indian Ocean New York, NY: Plenum. https://doi.org/10.1007/978-1-4615-8038-6

Segoufin, J., & Patriat, P. (1980). Existence d'anomalies mésozoiques dans le bassin de Somalie. Implications pour les relations Afrique–Antarctique–Madagascar. *Comptes Rendus de l'Académie des Sciences*, *291*(B), 85–88.

Smith, A. G., & Hallam, A. (1970). The fit of the southern continents. *Nature*, *225*, 139–144. https://doi.org/10.1038/225139a0

Storey, M., Mahoney, J. J., & Saunders, A. D. (1997). Cretaceous basalts in Madagascar and the transition between plume and continental lithosphere mantle sources. In J. J. Mahoney & M. Coffin (Eds.), *Large Igneous provinces: Continental, oceanic, and planetary flood volcanism* (pp. 95–122). Washington, DC: American Geophysical Union, Monograph.

Torsvik, T. H., Amundsen, H., Hartz, E. H., Corfu, F., Kusznir, N., Gaina, C., ... Jamtveit, B. (2013). A Precambrian microcontinent in the Indian Ocean. *Nature Geoscience*, *6*(3), 223–227. https://doi.org/10.1038/ngeo1736

Tuck-Martin, A. L., Adam, J., & Eagles, G. (2015). Correlating tectono-stratigraphic events along the East African Margin: Combining high-resolution plate kinematic models, plate-scale stress simulations and regional sedimentary basin fill histories. *The 14th HGS/PESGB Conference on African E&P* (pp. 125–126.) Abstr. London.

Tuck-Martin, A. L., Adam, J., & Eagles, G. (2016). A Tectono-Stratigraphic Framework for the East African Sedimentary Basins. *PETEX – Petroleum Geoscience Collaboration Showcase Abstr*. London. 50 pp.

Turner, J., Foum, A., & Kusznir, N. (2016). Structure of syn-breakup mini-basins, offshore Tanzania and Kenya. *The Roberts Conference – Passive Margins Abstr*. Royal Holloway, University of London, Egham, 77 pp.

van Hinsbergen, D. J. J., Steinberger, B., Doubrovine, P. V., & Gassmöller, R. (2011). Acceleration and deceleration of India-Asia convergence since the Cretaceous: Roles of mantle plumes and continental collision. *Journal of Geophysical Research*, *116*(B6), B06101.

Watts, A. (2001). Gravity anomalies, flexure and crustal structure at the Mozambique rifted margin. *Marine and Petroleum Geology*, *18*(4), 445–455. https://doi.org/10.1016/S0264-8172(00)00079-9

Wessel, P., Smith, W. H. F., Scharroo, R., Luis, J. F., & Wobbe, F. (2013). Generic Mapping Tools: Improved version released. *Eos, Transactions American Geophysical Union*, *94*, 409–410. https://doi.org/10.1002/2013EO450001

White, R., & McKenzie, D. (1989). Magmatism at rift zones: The generation of volcanic continental margins and flood basalts. *Journal of Geophysical Research*, *94*(B6), 7685. https://doi.org/10.1029/JB094iB06p07685

Wichura, H., Bousquet, R., Oberhänsli, R., Strecker, M. R., & Trauth, M. H. (2011). The Mid-Miocene East African Plateau: A pre-rift topographic model inferred from the emplacement of the phonolitic Yatta lava flow, Kenya. *Geological Society, London, Special Publications*, *357*(1), 285–300. https://doi.org/10.1144/SP357.15

Williams, S. E., Whittaker, J. M., & Müller, R. D. (2011). Full-fit, palinspastic reconstruction of the conjugate Australian-Antarctic margins. *Tectonics*, *30*, TC6012. https://doi.org/10.1029/2011TC002912

Wopfner, H. (1994). The Malagasy Rift, a chasm in the Tethyan margin of Gondwana. *Journal of Southeast Asian Earth Sciences*, *9*(4), 451–461. https://doi.org/10.1016/0743-9547(94)90056-6

How to cite this article: Tuck-Martin A, Adam J, Eagles G. New plate kinematic model and tectono-stratigraphic history of the East African and West Madagascan Margins. *Basin Res*. 2018;00:1–23. https://doi.org/10.1111/bre.12294

2.3. Further Discussion

2.3.1. Evolving datasets

This project originated as a Masters by Research project. Our first data set was a selection of magnetic anomaly data picks from Eagles & Wibisono (2013), Eagles & Hoang (2013), Eagles & König (2008) along with unpublished picks from the Somali Basin not included in the Eagles and König (2008) paper, and additional picks from Cande *et al* (2010). Originally the reconstructed plate circuit included only the movements of India and Madagascar relative to Africa.

However, it became clear that the project had far greater potential and so funding was secured to continue the project the PhD level. As a result, the motion of Antarctica relative to Africa was included in the plate circuit and the rotation data set was used to interpolated rotation parameters and plate kinematic reconstructions for 1 million year intervals. Whilst this expansion of the plate kinematic model was in progress it was became necessary to include new magnetic anomaly data picks from König & Jokat (2010) from the Mozambique basin. In addition, the magnetic anomaly picks in the West Somali Basin were reinterpreted because of recent improvements in gravity imaging of a subtly-expressed extinct mid-ocean ridge (Phethean et al., 2016). The full data set can be seen in the figure below.

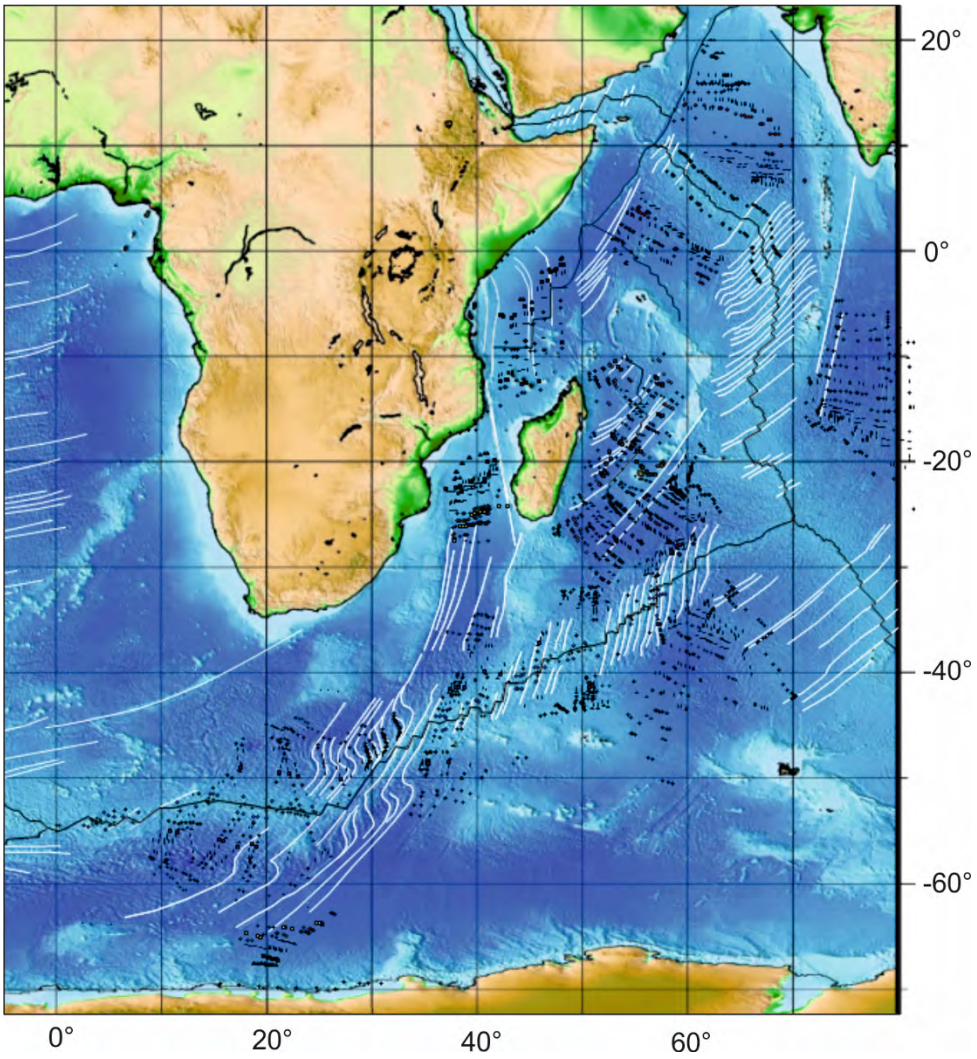

Figure A: Overview of the full magnetic anomaly data set (due to the vast spread of the data it is not possible to show it all in detail in one image).

2.3.2. Other Techniques – Refining the movement of the Seychelles

The oldest magnetic anomalies on the Carlsberg Ridge are in the very north dated to the normal polarity part of C28 (64.13 Ma) and the youngest seafloor in the northern most part of the Mascarene Basin (conjugates) is from the normal polarity part of chron 30 (65.86 Ma). Therefore, the products of C30y to C28o must have either been subducted beneath the inferred Amirante Trench or must still exist somewhere between the two points (Eagles & Wibisono, 2013). The former can be dismissed due to its location south of the trench and so it is reasonable to assume this section of seafloor is still present and its most likely location is the Laxmi Basin (Eagles & Wibisono, 2013). Magnetic anomalies have been identified in the basin by Bhattacharya et al. (1994) and interpreted as the product of ultraslow spreading between chrons 33 and 28. However, the basin's smooth surface devoid of fracture zones, its axial volcanic plug (Krishna et al. 2006) and ship track magnetic anomalies more reminiscent of those recorded over a fast spreading ridge (Eagles & Wibisono, 2013) suggest otherwise. Eagles & Wibisono (2013) conclude that extension in the Laxmi Basin began in chron 30, with seafloor spreading through chron 29 and abandonment in chron 28. At times before this the Seychelles moved as part of the Indian Plate. For the reconstructions before chron 30 new rotations

were calculated for the movement of Seychelles with respect to Africa by using the addrot program to calculate the solution from Seychelles to India and India to Africa. To support this assumption, two reconstructions were attempted at C32n.1n (70.96 Ma) and C34n (84 Ma) with three different assumed ages for the initiation of plate divergence in the Laxmi Basin; C29o (65.12 Ma), 66 Ma and 67 Ma at. It was found that 67 Ma gave the best fit in both reconstructions and so was used as the age of Laxmi Basin abandonment. In addition, it minimized the overlap of the Seychelles microcontinent with the Indian-Madagascan and Somali continental margins when fully reconstructed back to the full FIT. Therefore, the Laxmi Basin is modelled as active between from between 67 Ma (Chron 30) until 64 Ma (during Chron 28n).

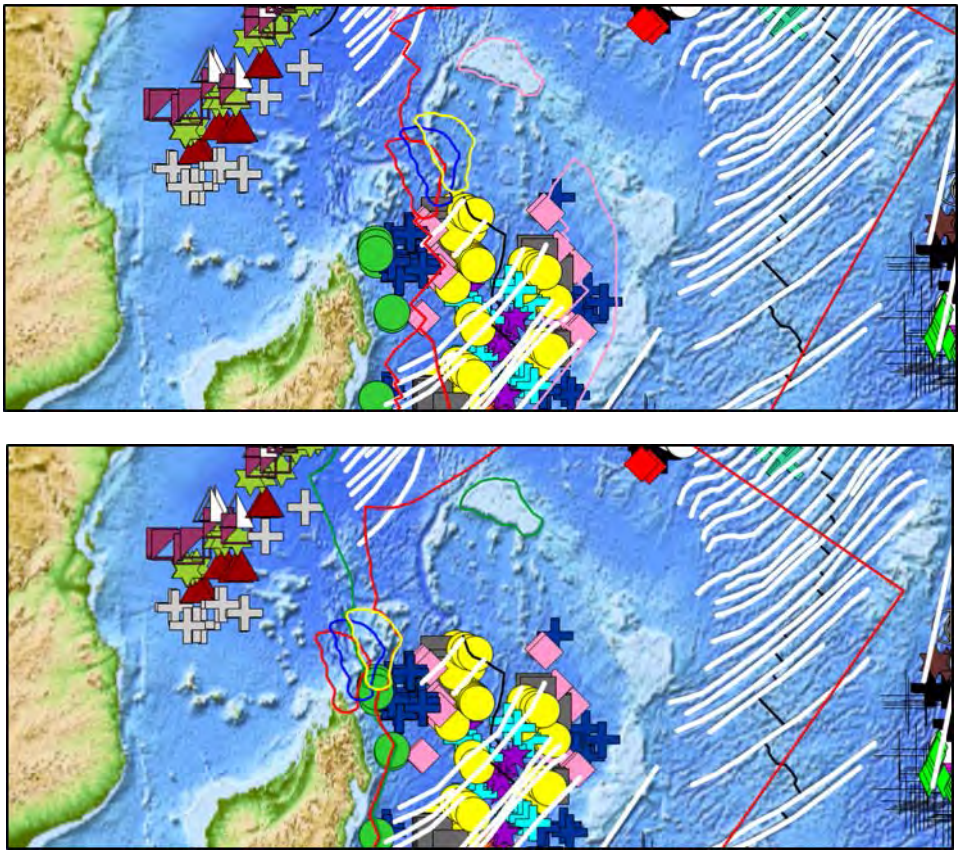

Figure B: Reconstructions used to determine the position of the Seychelles microplate based on the timing of the beginning and end of seafloor spreading in the Laxmi Basin. (Red = Laxmi basin initiation at 67 Ma; blue = Laxmi basin initiation at 66 Ma; yellow = Laxmi basin initiation at C29o (65.12 Ma).

Chapter 3

A new margin-scale tectonostratigraphic framework of East African and West Madagascan sedimentary basins based on a high-resolution plate kinematic model of the Indian Ocean

Amy Tuck-Martin, Jürgen Adam & Graeme Eagles

Author Contributions

This chapter is written in the form of a paper and presents ongoing work that will be edited and submitted to a journal after thesis submission.

The majority of this chapter was drafted by Amy Tuck-Martin, except for sections 3.1.2 and 3.2.2 which were drafted by Jürgen Adam. All images were drafted by Amy Tuck-Martin. All authors contributed to proofing and editing the text.

Abstract

The East African and West Madagascan continental margins and their sedimentary basins are gaining interest for petroleum exploration based on recent success, and large gas discoveries in Tanzania and Mozambique.

The structure and evolution of the marginal sedimentary basins are strongly controlled by the tectonic processes originating from the fragmentation of Gondwana since the early Jurassic and the opening of the NW Indian Ocean. We produce comprehensive margin-scale tectono-stratigraphic framework for the East African and West Madagascan margins based on the new high resolution plate kinematic model of the NW Indian Ocean of Tuck-Martin *et al.* (2018). Plate motion vectors and boundary geometries derived from this model were used to generate first-order regional stress patterns for distinct phases of margin formation.

We provide a review of geological and structural data of the basins and allocate basin fill megasequences based on lithology, structural information and depositional environment ascertained from literature. This information was integrated with the plate kinematic model to produce the tectono-stratigraphic framework for the East Africa – Madagascar conjugate margins, which can be used to identify and correlate main stages of basin evolution to better understand the timing and distribution of petroleum system types.

3.1. Introduction

For the past 50-60 years hydrocarbon exploration along the East African and Madagascan margins (Fig. 3.1) has been has been intermittent and hampered by political instabilities and disappointing results.

Renewed exploration interest in the past two decades following improved political conditions has led to significant gas discoveries, for example the Pweza deep-water gas discovery offshore Tanzania. Despite the accompanying growth in economic interest, the East African margin remains underexplored and its geodynamic and geological evolution poorly understood.

For a sustained drive in oil and gas exploration, the tectonic and basin fill histories of the East African and West Madagascan Margins need to be understood better. In particular, it is important to understand how the rifting, break-up and post-rift phases, and the petroleum systems elements related to them, can be correlated along the margins. A consistent and coherent tectono-stratigraphic context is essential to develop this understanding. Currently, no such context exists to correlate all the tectonic and stratigraphic changes of the sedimentary basins of the East-African and Madagascan conjugate margins (Fig. 3.1b).

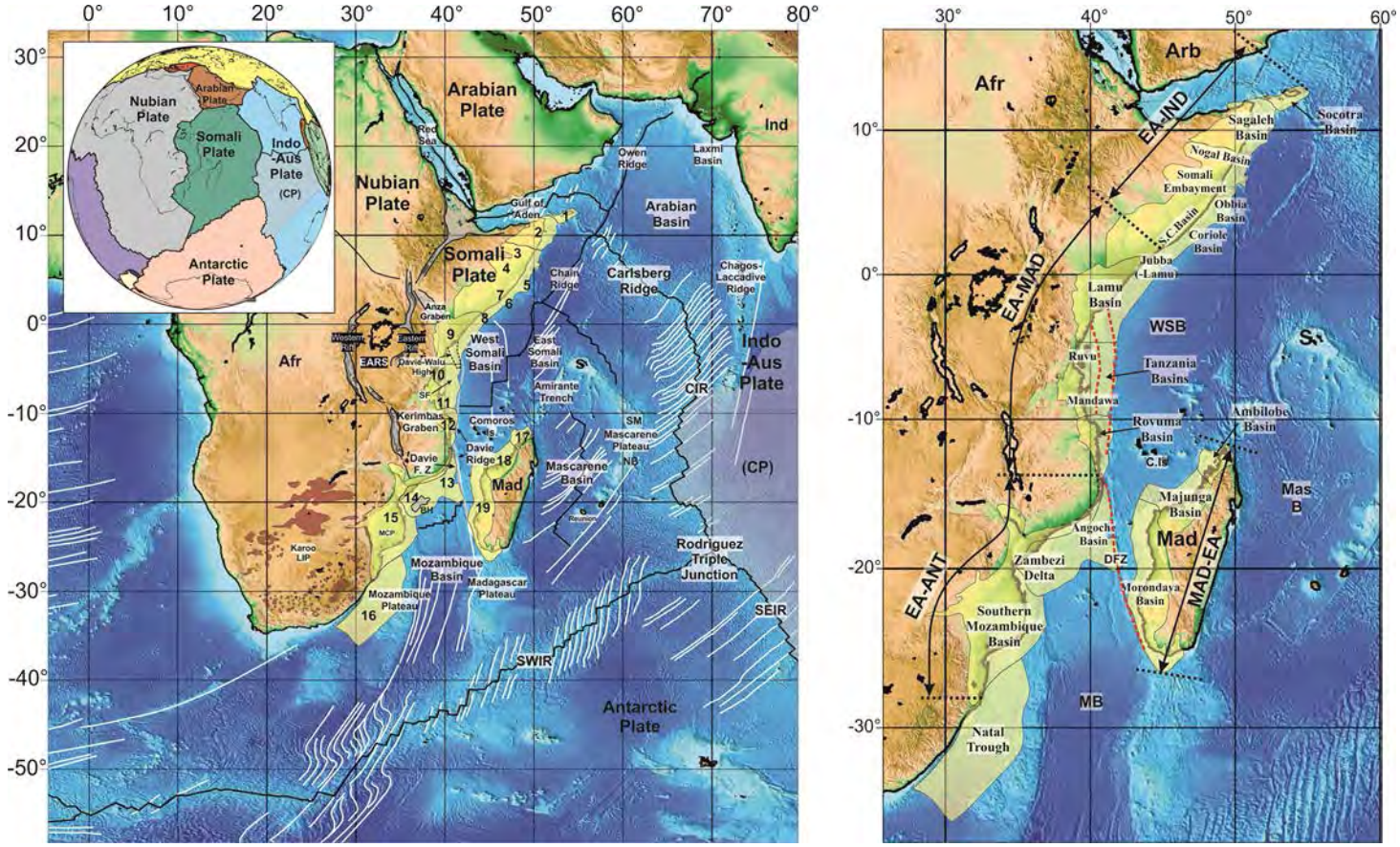

Figure 3.1: (a) Overview of the present-day Northwest Indian Ocean including key features and sedimentary basins of the East African and West Madagascan Margins (modified from Tuck-Martin *et al*., 2018). CIR – Central Indian Ridge; SEIR – Southeast Indian Ridge; SWIR – Southwest Indian Ridge; Mad – Madagascar; Afr – Africa; Ind – India; S – Seychelles; SM – Salha de Maya Bank; NB – Nazareth Bank; EARS – East African Rift System; S.F. – Seagap Fault; BH – Beira High; MCP – Mozambique Coastal Plains; Karoo LIP (Jourdan et al., 2005); (CP) shaded area – Diffuse "Capricorn Plate" (Royer & Gordon, 1997); 1 – Socotra Basin; 2 – Sagaleh Basin;, 3 – Nogal Basin; 4 – Somali Embayment; 5 – Obbia Basin; 6 – Coriole; 7 – Somali Coastal Basin; 8 – Juba(-Lamu) Basin; 9 – Lamu Basin; 10 – Ruvu Basin; 11 – Mandawa Basin; 12 – Rovuma Basin; 13 – Angoche Basin; 14 – Zambezi Delta Depression, 15 – Southern Mozambique Basin; 16 – Natal Trough; 17 – Ambilobe Basin; 18 – Mjunga Basin; 19 – Morondava Basin. Inset: Present day plate boundaries. (b) Close-up of the conjugate margin segments and their sedimentary basins.

We aim to develop an integrated margin-scale tectonostratigraphic framework enabling for the first time the correlation of the tectonic stages and basin fill histories from the rift stage to the modern passive margin. The integration and correlation of published structural and stratigraphic data describing the underlying margin-scale framework is based on a new high-resolution plate kinematic model of the Northwest Indian Ocean (Tuck-Martin et al., 2018).

The new tectono-stratigraphic model can be utilised to investigate the implications of margin-wide geodynamic changes and related regional tectonic stress fields on the regional development and petroleum systems of sedimentary basins along the East African and West Madagascan Conjugate Margins. Tuck-Martin et al. (2018) provide the introductory sketch of such an analysis in their discussion.

The East African sedimentary basins and their conjugate counterparts on the West Madagascan Margin (Fig. 3.1) formed during the rifting and breakup of Gondwana in Late Triassic and Jurassic times and the subsequent opening of the Indian Ocean. Almost all of the basins initiated with the early deposition of sediments during the intracontinental 'Karoo' rifting stage that affected much of Africa as part of the interior of the Pangea supercontinent from the Carboniferous to the Early Jurassic. Following the eruption of the Karoo-Ferrar large igneous province (LIP), a renewed rifting episode in the Early to Middle Jurassic successfully led to the breakup of East Gondwana (comprising Madagascar, India, Antarctica, the Seychelles and Australia) and West Gondwana (comprising Africa and South America). Following breakup, a sequence of plate tectonic boundary reconfigurations in the Northwest Indian Ocean led to further fragmentation of East Gondwana and the formation of the present-day plate assembly (Tuck-Martin et al., 2018). During these tectonic stages, far-field tectonic stresses transmitted into the plate interiors from topography associated with the spreading ridges in the NW Indian Ocean affected the tectono-stratigraphic development of the post-rift sedimentary basins of the conjugate E-African and Madagascan margins.

The first part of this paper provides a brief summary of the plate-kinematic model (Tuck-Martin et al., 2018), and the phases of plate tectonic and first-order stress regimes interpreted from it. The plate-kinematic model forms the framework for a set of chronostratigraphic correlations that forms the foundation on which we build the tectono-stratigraphic framework for the conjugate E-African and Madagascan sedimentary basins.

The second part provides an in-depth review of the sedimentary basins on the various East African and West Madagascan margin segments, based on information available in the public domain. As part of the review, we highlight and correlate important stratigraphic and structural changes, regional unconformities and megasequences with reference to the newly developed margin-scale plate-kinematic framework.

Finally, we integrate the regional basin histories in synoptic margin-scale paleogeographic maps and a tectono-stratigraphic correlation chart in order to discuss regional basin evolution and related petroleum systems within a fully constrained margin-scale tectonic framework.

3.2. Margin-scale Framework and derived elements

The chronostratigraphic correlation of plate tectonic events throughout the four main tectonic phases in the opening of the Indian Ocean, and the set of elementary plate-scale stress fields described in Tuck-Martin et al. (2018), form the basis for an integrated tectono-stratigraphic framework of margin-scale processes describing the regional tectonic and stratigraphic evolution of individual sedimentary basins of the East African – Madagascan conjugate margins.

The plate-kinematic model is the basis for (1) a uniform description of the timings and styles of major tectonic stages in the different conjugate margin segments (e.g. rift, transitional, break-up and drift phases); (2) analysis of the variation of the first-order plate-scale tectonic stress fields along the plate margins; and (3) the timings and characteristics of related megasequence patterns in the East African-Madagascan margin segments.

3.2.1 Plate-kinematic Model

The plate kinematic model from Tuck-Martin et al. (2018) (chapter 2) describes the tectonic history of the Northwest Indian Ocean and the surrounding continental margins of East Africa and West Madagascar. The model identifies four main phases of tectonic evolution governed by significant changes of the plate boundary configurations within the NW Indian Ocean.

The four phases are briefly summarized below:

Phase 1 - Separation of East and West Gondwana (183-177 Ma to 133 Ma) (figure 3.2a)**:**

The onset of Phase 1 is signalled by eruption of the Karoo Large Igneous Province (LIP) in southern Africa and the corresponding Ferrar LIP in Antarctica. These eruptions mark the transition from the intermittent Karoo rift phase, which affected southern and eastern Africa (Catuneau et al., 2005) to the main rift phase (identified in the tectonic model) from approximately 183-177 Ma to 170-165 Ma, which successfully resulted in the breakup of East and West Gondwana.

Subsequent breakup of East Gondwana (India, Madagascar, Seychelles, Antarctica, Australia) and West Gondwana (Africa, South America) was accommodated by rifting and seafloor spreading in the West Somali and the Mozambique basins and dextral strike-slip movement on the Davie Fracture Zone.

Phase 2 - Separation of Antarctica (133 Ma to 89 Ma) (figure 3.2b)**:**

The onset of the second tectonic phase is marked by the cessation of seafloor spreading in the West Somali Basin at approximately 133 Ma leading to the integration of Madagascar into the African plate.

The spreading centre was abandoned as part of a southwards relocation of the plate boundary between west and east Gondwana. The relocation led to rifting and seafloor spreading in the West Enderby Basin off East Antarctica, initiating the separation of Madagascar and India from East Antarctica. The exact timing of the boundary relocation is constrained by the plate-kinematic model of Tuck-Martin et al. (2018) to chron M10n (~133.9 – 133.5 Ma). In addition, the precise location of the new boundary is not well-constrained due to the relative complexity of this sector of the East Antarctic margins. Tuck-Martin et al. (2018) suggest that the Mannar and Cauvery Basins may have developed as part of the relocation process western Enderby Basin. A period of continental stretching in these basins would explain why the onset of seafloor spreading in the West Enderby Basin seems not to have occurred until around 8 Myr later than the start of Phase 2, according to the absence of seafloor spreading isochrons in the western Enderby Basin (Jokat and Leinweber, 2010).

Phase 3 (89 Ma to 60 Ma) (figure 3.2c)**:**

Whilst seafloor spreading continued relatively unchanged along the Southwest Indian Ridge (SWIR) between the Antarctica and African plates, the third phase saw a dramatic change in tectonic activity further east in the Indian Ocean. This change was associated with the initiation of a spreading ridge and the succeeding opening of the Mascarene Basin, separating India from Madagascar (Fig. 3.2c).

The onset of Phase 3 is defined by the eruption of the Morondava volcanics in Madagascar at ~89 Ma (Storey et al 1997). The Morondava volcanics are attributed to the arrival of the Marion mantle plume leading to the initiation of rifting between Africa-Madagascar and India. The timing of seafloor spreading in the Mascarene Basin is constrained mostly by marine magnetic isochrons. Spreading started shortly before chron 34y (84 Ma) and continued until the abandonment of the plate boundary in the Mascarene Basin shortly after chron 27n (61.65 Ma) (Eagles & Wibisono, 2013). The transition from Phase 3 to Phase 4 is characterized by a number of major tectonic changes and plate boundary relocations in the ocean crust between India and Madagascar.

Phase 4 (60 Ma to present) (figure 3.2d)**:**

By the beginning of Phase 4, three active spreading ridges existed in the Indian Ocean; the Carlsberg Ridge (CR), the Central Indian Ridge (CIR) and the Southwest Indian Ridge (SWIR) (Fig. 3.2 d).

Plate tectonics in Phase 4 is dominated by the onset of seafloor spreading along the Carlsberg and Central Indian Ridges (CIR) that led to the separation of India from the Mascarene Plateau and is still active today. Spreading started at the northern extremity of the Carlsberg Ridge near the young end of chron C28n (63.10 Ma) and propagated southwards to cause the final separation of India and the Mascarene Plateau between chrons C27n and C26n (61.65 and 58.38 Ma).

The later stages of Phase 4 saw the development of the East African Rift System and the collisions of India and Africa with Eurasia. These changes led to considerable complexity in the relative movement of Africa and East Antarctica in the period from ~58 to 53 Ma, as indicated by the curved fracture zones of the SWIR (Fig. 3.2 d), and the rapid southward migration of the East Antarctic-Africa rotation pole in the period between chrons 30y – 28y (66.398 Ma – 63.494 Ma) and chron 13y (33.147 Ma). This slowdown has been attributed to the influence of the Deccan plume near the African-India plate boundary (Cande & Stegman, 2011) and the eventual continental collision between Africa and Europe (Nankivell, 1997).

After chron 13, the the adoption of a northwards progression in successive finite rotation pole locations could be related to the onset of continental rifting and the development of a new plate boundary in the East African Rift System (e.g. Roberts et al., 2012).

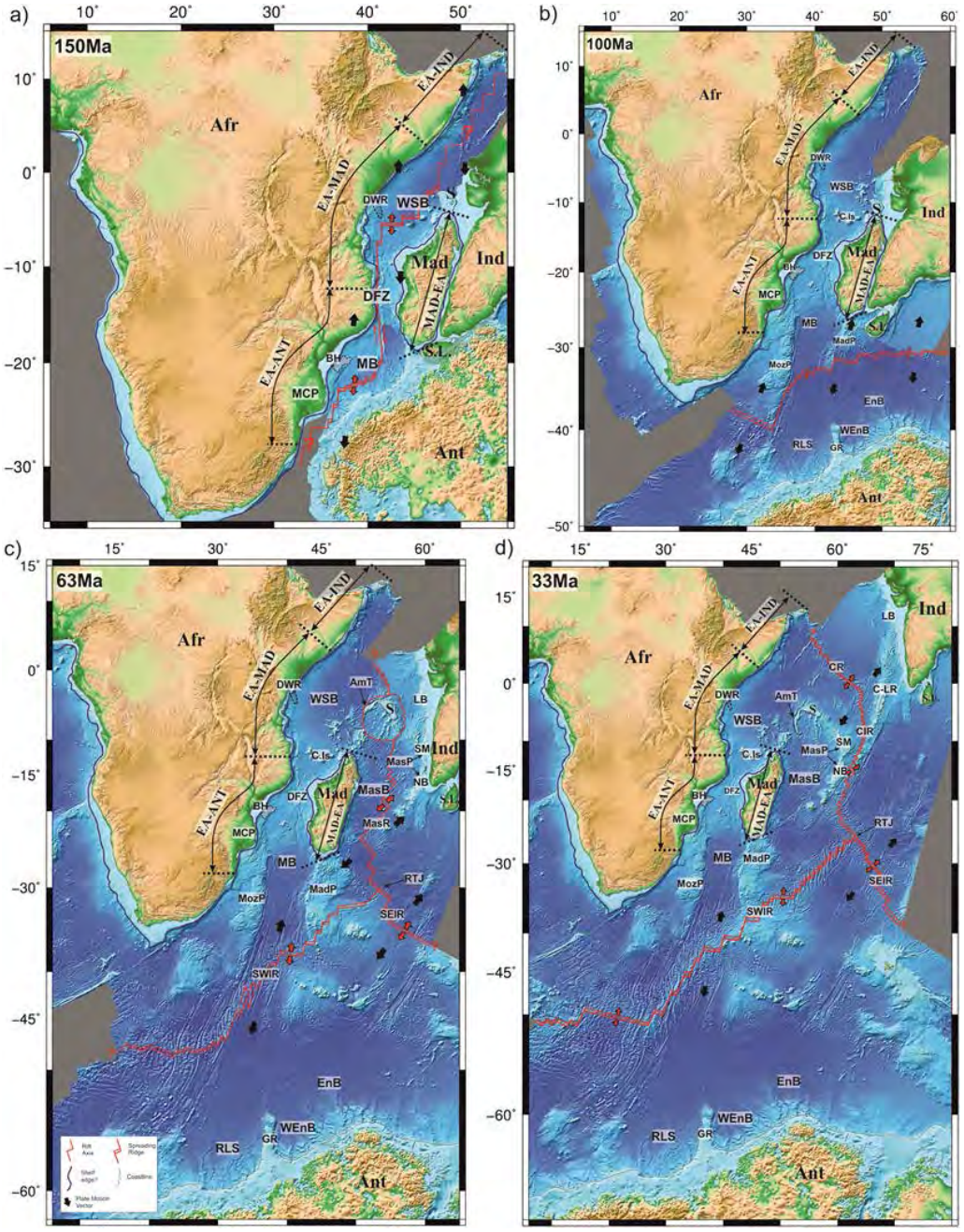

Figure 3.2: Plate tectonic reconstructions showing the 4 phases of tectonic development of the NW Indian Ocean. (a) Phase 1: 183-177 Ma to 133 Ma, Separation of East And West Gondwana, Seafloor spreading in the West Somali and Mozambique Basins, (b) Phase 2: 133 Ma to 89 Ma, end of seafloor spreading in the West Somali Basin, separation Madagascar/India and Antarctica, (c) Phase 3: 89 Ma to 60 Ma, Opening of the Mascarene Basin separating India and Madagascar, rotation of Seychelles microplate, (d) Phase 4: 60 Ma to present day, end of seafloor spreading in the Mascarene Basin, separation of India and the Mascarene Plateau accommodated by spreading on the Carlsberg and Central Indian Ridges. Afr – Africa; Mad – Madagascar; S – Seychelles; Ind – India; Ant – Antarctica; S.L. – Sri Lanka; WSB – West Somali Basin; MB – Mozambique Basin; DFZ – Davie Fracture Zone; DWR – Davie Walu Ridge; BH – Beira High; MCP – Mozambique Coastal Plains; RLS – Riiser Larsen Sea; GR – Gunnerus Ridge; EnB – Enderby Basin; WEnB – West Enderby Basin; MozP – Mozambique Plateau; MadP – Madagascar Plateau; C.Is – Comoros Islands; SWIR – Southwest Indian Ridge; SEIR – Southeast Indian Ridge; RTJ – Rodriguez Triple Junction; MasR – Mascarene Ridge; MasB – Mascarene Basin; MasP – Mascarene Plateau; SM – Salha de Maya Bank; NB – Nazareth Bank; AmT – Amirante Trench; CR – Carlsberg Ridge; CIR – Central Indian Ridge; C-LR – Chagos-Laccadive Ridge.

3.2.2 Paleostress maps derived from plate kinematic model

The architecture and evolution of sedimentary basins on rifted continental margins are strongly controlled by tectonic processes during distinct tectonic stages of margin formation, e.g. rift, transitional, break-up and drift (e.g. post-rift) phases. The tectonic processes that control structural styles and tectonic subsidence in the various stages of basin formation are governed by regional tectonic stresses.

Extensive analyses of present-day in-situ stress data by the World Stress Map Project (WSM) show that the intra-plate stress patterns in stable plates such as North America, South America and Europe, are predominately compressional and oriented subparallel to absolute plate motion vectors (Richardson, 1992; Zoback & Zoback, 1989; Zoback, 1992). This suggests that they are generated by plate boundary forces, primarily mid-ocean ridge-push, subducting slab-pull, trench-suction and traction at the base of the lithosphere (Zoback, 1992; Tingay, 2009) and are transmitted through the seismic brittle crust into intra-plate regions over distances of 100's to 1000's km, resulting in a first-order plate-scale tectonic stress field (with wavelengths greater than 500 km). Smoothed global tectonic stress maps based on WSM data confirm the existence of these long wave-length stress patterns (>2000 km) for example in North America and NE Asia (Heidbach et al., 2010).

However, further detailed analysis of WSM data reveals that short wave-length stress patterns on a regional to basin scale (10's – 100's km) are frequently present. These second-order stress patterns are not controlled by plate boundary forces but major intraplate forces related to the distributions of surface loads such as deltas or ice sheets, and intracrustal loads associated with density and thickness contrasts across geological structures like basins, detachments, and fault systems (Heidbach et al., 2010; Tingay, 2009).

Based on these concepts and our plate kinematic model, we performed a basic kinematic analysis of the first-order plate tectonic stress field of the East-African and West Madagascan conjugate margin segments during the main plate tectonic stages. The first-order plate kinematic stress analysis is derived from the orientation of local plate motion vectors and the nature of the relevant plate boundaries with the assumption that the regional maximum tectonic stress ($S_{H\,max}$) and minimum tectonic stress ($S_{h\,min}$) are trending either parallel or normal to the local plate motion vector depending on the stage of margin development and nature of nearby plate boundaries (see section below for more details). The nature of the tectonic stresses vary from tensional in areas of active rifting to compressional within the plate interior away from extensional domains. The derived local tectonic stress orientations have been integrated and depicted as stress trajectories shown in the paleostress maps for the relevant margins segments in the main plate tectonic phases (Section 3.4).

The orientations and relative magnitudes of the regional tectonic stresses are represented as paleostress maps and discussed in section 3.4. They have been

derived for specific tectonic stages of margin formation (rift, break-up, drift) based on the following assumptions:

Continental Rift Stage (Fig. 3.3 (a)) – Local plate vectors describe the direction of tectonic extension. The maximum horizontal stress ($S_{H\,max}$) trends perpendicular to the local plate vector and parallel to the rift axis, regional trend of extensional faults and syn-rift depocentres. The minimum horizontal tensional stress ($S_{h\,min}$) is parallel to the local plate vector and describes the direction of tectonic extension. This can be seen in the modern East African Rift System, where in-situ $S_{H\,max}$ follows the trend of the rift basins (Heidbach et al., 2016).

Breakup Stage (Fig. 3.3 (b)) – Drastic change in orientation of the regional stress field due to the establishment of an active spreading ridge generating "ridge push" forces along the divergent plate boundary and subsiding oceanic lithosphere. Extensional faults with similar trends as earlier rift basins are restricted to the median valleys of spreading ridges. In the oceanic crust and adjacent continental margin away from the spreading ridges, tectonic stresses are controlled by ridge push. Spreading ridges are elevated above the surrounding seafloor by the upwelling of hot mantle material (either actively or passively) which gives the ridge excess potential energy and the ridge will try to spread out as a result. In addition, as newly formed oceanic crust moves away from the ridge it cools and sinks. The result is a force (ridge-push) that acts perpendicular to the ridge axis (Forsyth & Uyeda, 1975). Therefore, the maximum horizontal compressional stress ($S_{H\,max}$) trends parallel to the local plate vector and perpendicular to ridge axis and the minimum horizontal stress ($S_{h\,min}$) is perpendicular to the local plate vector. The reversal of the tectonic stresses in comparison with the rift stage may control local uplift and inversion of rift structures on the rifted continental margin segment.

During drift or passive margin stage (Fig 3.3 (c)) the regional tectonic stresses in the oceanic and continental basement are still dominated by large-scale plate boundary forces and thus similar to those during the breakup stage. However, regional tectonic stresses may be overprinted on the continental shelf and slope by gravity-driven stresses arising from local basin features (e.g. sedimentary wedges, deltas) or geological structures (detachments, salt structures). An example for the role of detachments and gravity-driven processes is the Baram Delta and Deep-water Fold-and-Thrust Belt, NW Borneo (King et al, 2009) where stress analysis of petroleum wells have been used to ascertain the maximum horizontal stress orientation the landward extensional domain ($S_{H\,max}$ = margin parallel, normal faulting) and the basinward compressional domain ($S_{H\,max}$ = margin normal, thrust faulting).

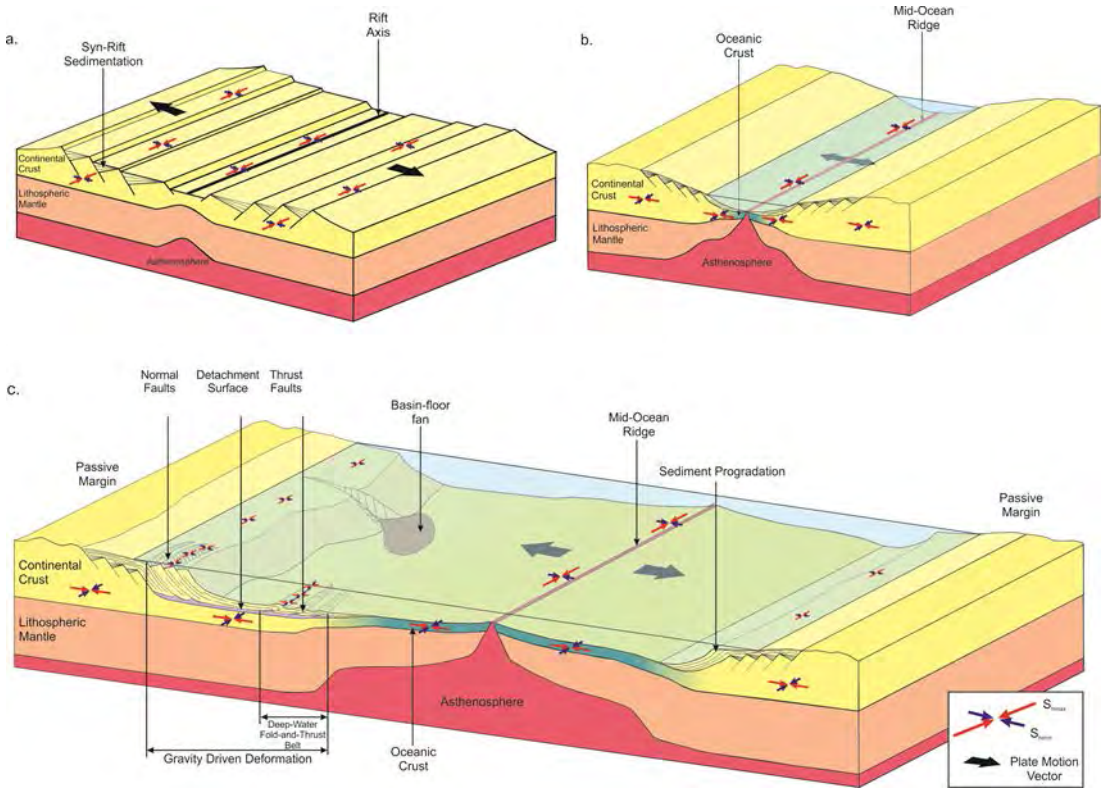

Figure 3.3: Conceptual diagram illustrating the characteristics of first-order plate-scale tectonic stress fields during continental margin formation (modified from Tuck-Martin et al., 2018). (a) Continental Rift Stage: S_{Hmax} perpendicular to plate kinematic vector and parallel rift axis. Normal faulting and syn-rift sedimentation. (b) Breakup Stage: Normal faulting and associated stress field restricted to spreading ridge. Elsewhere, S_{Hmax} parallel to plate kinematic vector and perpendicular to ridge axis. (c) Drift or Passive Margin Stage: tectonic stress field (large stress symbols) overprinted by local gravity driven stress fields at margins (small stress symbols).

3.2.3 Paleodepositional Maps

For each phase we produced paleodeposition maps based on the plate kinematic reconstruction maps of Tuck-Martin et al (2018), chapter 2. We chose time slices that were representative of each tectonic phase, which show the important tectonic changes, and also time slices that were representative of each different megasequence interpreted in this chapter (see section 3.2.4).

Simple paleodepositional/stratigraphic maps from Bosellini (1992) and Mbede & Dualeh (1997 were superimposed onto the plate kinematic reconstructions from Tuck-Martin et al. (2018). They were modified to fit the plate configurations in our reconstructions and, where necessary they were edited and updated to include more detail or new information gathered from more recent literature as described in section 3.3.

The result is maps that give a snapshot of regional depositional environments at key tectonic phases throughout the development of the East African and West Madagascan Continental Margins.

3.2.4 Megasequence Classification

For their margin-scale chronostratigraphic correlation, Tuck-Martin et al. (2018) utilise a simplified tectono-stratigraphic correlation chart for the sedimentary basins on the various East African and West Madagascan margin segments. The chart is based on the sequence of plate tectonic evolutionary stages of the Northwest Indian Ocean they interpreted from their plate kinematic model. Seven tectonically-controlled megasequences are correlated, separated by prominent basinal unconformities. Each of the megasequences describes a distinct evolutionary stage of basin evolution along the various margin segments.

The two earliest syn-rift megasequences consist of sediments laid down in the Karoo rift basins and the younger, often coincident, basins that accommodated post-Karoo extension as a prelude to Gondwana breakup and seafloor spreading. The ensuing transitional megasequence is separated from the underlying syn-rift megasequences by a diachronous breakup unconformity, reflecting propagation of the East-West Gondwana plate boundary through the rupturing supercontinent. Post-rift sediments are subdivided into three further megasequences comprising early post-rift, late post-rift and modern margin sedimentary deposits, each separated by distinctive regional unconformities related to major tectonic changes. The most recent megasequence consists of the products of ongoing tectonic influences on basin development.

Karoo Syn-Rift Megasequence (approx. 300 to 180 Ma)

The Karoo syn-rift megasequence represents the phase of intermittent, intracontinental rifting events that affected the Pangea supercontinent potentially stretching from the Late Carboniferous through the Permo-Triassic and into the Early Jurassic (Catuneanu et al., 2005). Some but not all Karoo sediments show features typical of deposition during active rifting (e.g. growth strata) while others have been deposited during tectonic quiescence between rift cycles.

The Karoo sediments are predominantly continental in nature and deposited unconformable on top of the metamorphic basement. Some shallow marine sediments document marine incursions from the Tethyan Ocean in the North occurred that reached as far south as Madagascar (Wopfner, 1991). These rifting events failed to cause the breakup of Gondwana and culminated in the early Jurassic eruption of the Karoo Large Igneous Province within the time period 183-177 Ma (Cox 1992; Jourdan et al. 2005).

Main Syn-rift Megasequence (approx. 180 Ma to 170-165 Ma)

The Main syn-rift megasequence is associated with the distinct, concise stage of rifting that successfully led to the breakup of East and West Gondwana. Syn-rift sedimentation are characterised by asymmetric growth wedges within half grabens controlled by rift-related extensional faulting (Coffin & Rabonowitz, 1988; Bosellini, 1992; Mbede & Dualeh, 1997; Clark, 1998; Geiger et al., 2004; Mahanjane, 2012).

The depositional setting of Main syn-rift Megasequence varied significantly between different margin segments. Along the EA-IND and MAD-EA margin segments, Main syn-rift sediments were deposited under mostly shallow marine conditions (Bosellini, 1992; Geiger, 2004). Along EA-MAD margin segments, a mixture of continental, transitional and shallow water facies was prominent (Coffin & Rabinowitz, 1988; Mbede & Dualeh, 1997; Hudson & Nicholas, 2014), whereas shelf to marine sediments dominated along the EA-ANT margin segment (Mahanjane et al., 2014).

Transitional Megasequence

The Transitional Megasequence was deposited in a period of tectonic quiescence and thermal subsidence following the cessation of rifting but before breakup occurred. A characteristic transitional megasequence has been identified in the EA-ANT segment only, where it consists of mixed marine/continental sediments deposited during an early post-rift sag phase (Mahanjane, 2012).

Post-rift Megasequences

The post-rift succession has been subdivided into three distinct megasequences marked by significant stratigraphic or tectonic changes in the basins such as the sudden change in depositional environments from shallow to deep marine sediments and vice versa, or the occurrence of regional unconformities related to tectonic uplift phases.

Early Post-rift

The Early Post-rift megasequence sediments is an undifferentiated passive margin sequence indicating relative tectonic quiescence with few regional unconformities indicating potential uplift due to inversion tectonics. Early post-rift sequences are characterised fully marine depositional environment gradually changing from shallow-marine sediments like carbonate platforms to deep marine clastic sediment s as consequence of slower thermal subsidence following breakup.

Late Post-rift

The late post-rift stage is dominated by generally slower thermal subsidence and basinward progradation of depositional systems and deltas. Consequently, the Late Post-rift Megasequence consists of typical shallow to deep-water sediments, e.g. shales, marls, mudstones and turbiditic sandstones (Salman & Abdula, 1995; Bosellini, 1992; Key et al., 2008).

Modern Margin

The onset of the modern margin megasequence is linked to doming and uplift of the African plate over the Afar plume, prior to the onset of the East African Rift System (Wichura et al., 2011; MacGregor, 2015; Ebinger & Sleep, 1998). The modern margin meqasequence consists of deep-water sediments, e.g. shales, marls, mudstones and

turbiditic sandstones and is characterised by large prograding deltas, collapse of sediment wedges due to gravity-driven deformation along margin segments.

3.3. Overview of tectono-stratigraphic evolution of sedimentary basins on the East Africa-Madagascan Conjugate Margins

The architecture and evolution of sedimentary basins and related petroleum system types on rifted continental margins are strongly controlled by regional tectonic processes during distinct tectonic stages of margin formation, e.g. rift, transitional, break-up and post-rift phases (Roberts & Bally, 2012; Doust & Noble, 2007; Doust & Sumner, 2007). Variations in the tectono-stratigraphic evolution of sedimentary basins caused by plate-tectonic or regional tectonic processes are reflected by differences in the subsidence history, basin fill history and petroleum system types. These regional tectonic processes and their governing regional tectonic stresses that control structural styles and tectonic subsidence in the various stages of basin formation are strongly dependent on the first-order plate-scale tectonic stress field (Zoback, 1992; Tingay, 2009).

Consequently, the new plate kinematic model and derived first-order plate-scale stress maps (Tuck-Martin et al., 2018) provide a well-constrained margin-scale chronological framework for the correlation of major tectonic events and megasequences in the conjugate margin segments of East Africa and Madagascar. The chronological framework and derived timing of megasequence types in different margin segments allows a systematic analysis and revision of published results from specific basin studies and related basin fill sequences. This in-depth analysis and correlation of the stratigraphy and structures of individual sedimentary basins along the margin segments forms the basis for the development of a margin-scale tectonostratigraphic framework for the correlation of sedimentary basins.

The synthesis of plate kinematic results with published tectonic and stratigraphic results for sedimentary basins in the specific margin segments enables us:

1. To establish whether the plate tectonic changes and phases of plate-reconfiguration during the opening of the Indian Ocean have been recorded in the stratigraphy and structure of individual basin along the margins. To analyse the control factors of margin-wide tectonic processes on regional basin evolution.
2. To correlate regional observations, stages and events of basin evolution in specific sedimentary basins within a fully constrained high-resolution plate-kinematic framework.
3. To build a margin-scale tectono-stratigraphic framework to identify important tectonic, stratigraphic and petroleum system elements in individual basins and to investigate their application potential for other comparable basin settings along the margins.

The derived comprehensive margin-scale tectono-stratigraphic framework will form the basis for the future integration of new geological and geophysical data becoming available from sedimentary basins to better understand their formation and evolution along the East African and West Madagascan rifted continental margins.

Our plate-tectonic model provides chronological and spatial input to crustal-scale architecture, tectonic evolution and megasequence type pattern along the conjugate margin segments. In addition, the literature review of the relevant geological and geophysical data of sedimentary basins provides detailed information of the regional tectono-stratigraphic evolution and basin fill history including mega-sequence subdivisions, depositional environments and sedimentary facies and their related lithofacies.

For the systematic correlation of plate-model results and published information of specific sedimentary basins we established a correlation chart summarising all relevant plate-tectonic and regional basin elements (discussed in previous paragraph) for the different basin evolutionary stages (e.g. megasequences) (Appendix B) using well-established concepts for margin-scale correlation of sedimentary basins and petroleum systems types by Roberts and Bally (2012), Doust & Noble (2007) and Doust & Sumner (2007). It is important to note that this generic correlation chart at this stage is still under development and will be further revised and expanded in the future to include new information on general basin elements and new data relevant for the East-Africa and Madagascan continental margins.

Importantly, Doust & Sumner (2007) described four distinctive types of petroleum systems which are developed widely in sedimentary basins and how they correlate with the four main stages of basin evolution (early to late syn-rift and early to late post-rift) for South-East Asia Tertiary sedimentary basins. Doust & Sumner (2007) concluded that the recognition of petroleum system types and reservoir lithofacies play types in well-explored basins can facilitate prediction of hydrocarbon prospectivity in less well-known rift/post-rift basins and plays, and thereby contribute to future exploration evaluation.

We review the stratigraphy currently available in literature, for each basin along the East African margin and the conjugate West Madagascan margin. For a systematic approach, the basins are grouped into margin segments according to their conjugate within the Gondwana supercontinent when fully reassembled (Fig 3.4) East Africa conjugate to India (EA-IND), East Africa conjugate to Madagascar (EA-MAD), Madagascar conjugate to East Africa (MAD-EA), and East Africa conjugate to Antarctica (EA-ANT). The stratigraphy of all basins is presented in figure 3.5, the tectono-stratigraphic table. All megasequences described in section 3.3 can be found in this table. For more information on how each Author gathered their stratigraphic data and how reliable their data is see Appendix C.

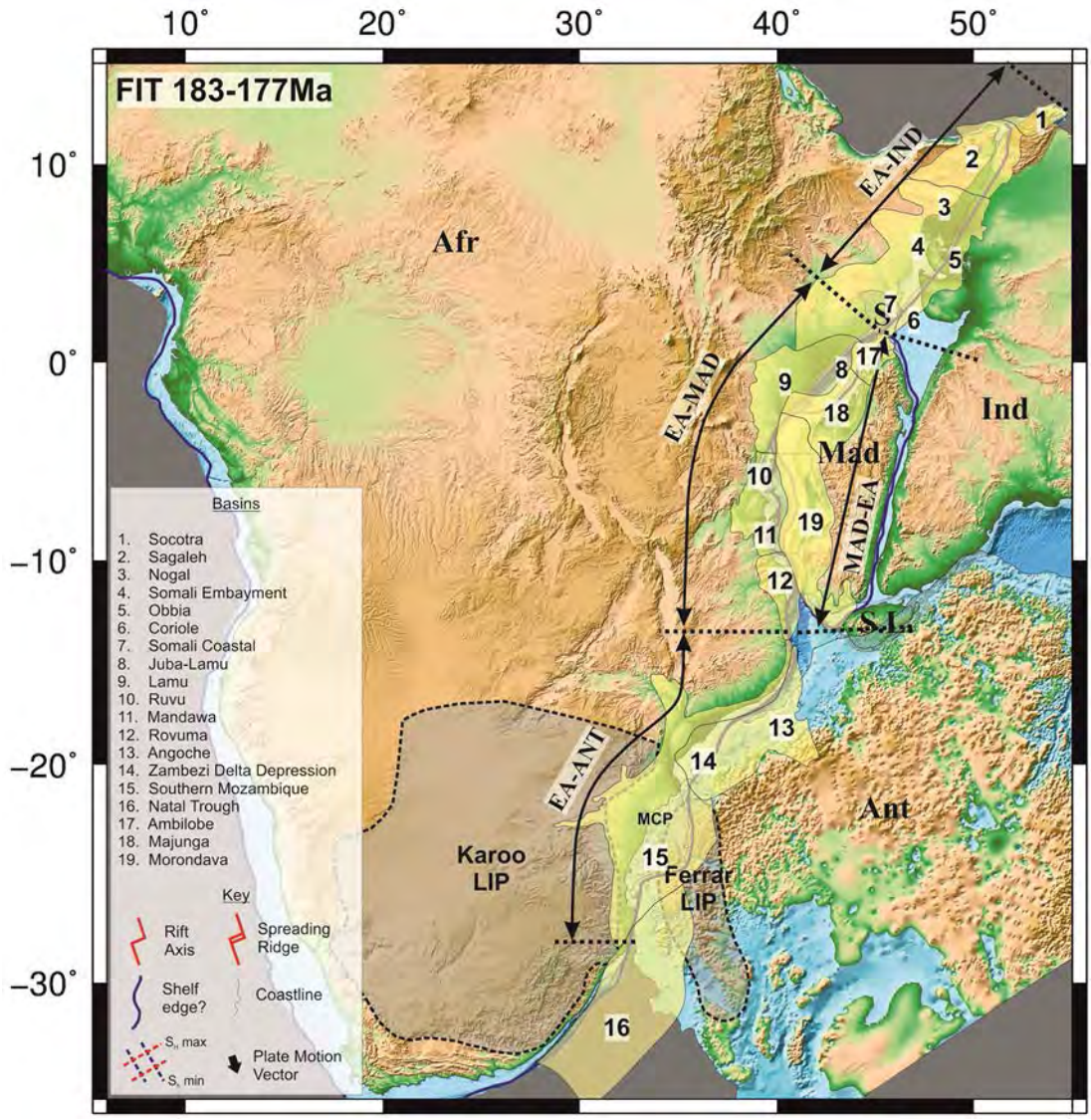

Figure 3.4: Plate reconstruction map showing the present-day location of sedimentary basins of the East-Africa and West-Madagascan margins overlain on the fully reassembled fit of all the plates to their positions within the Gondwana supercontinent 183-177 Ma using present-day bathymetry data and the Mercator projection (Africa fixed in its present-day location; modified from Tuck-Martin et al,.2018). Possible maximum extent of Karoo-Ferrar LIP after Riley et al., 2006.

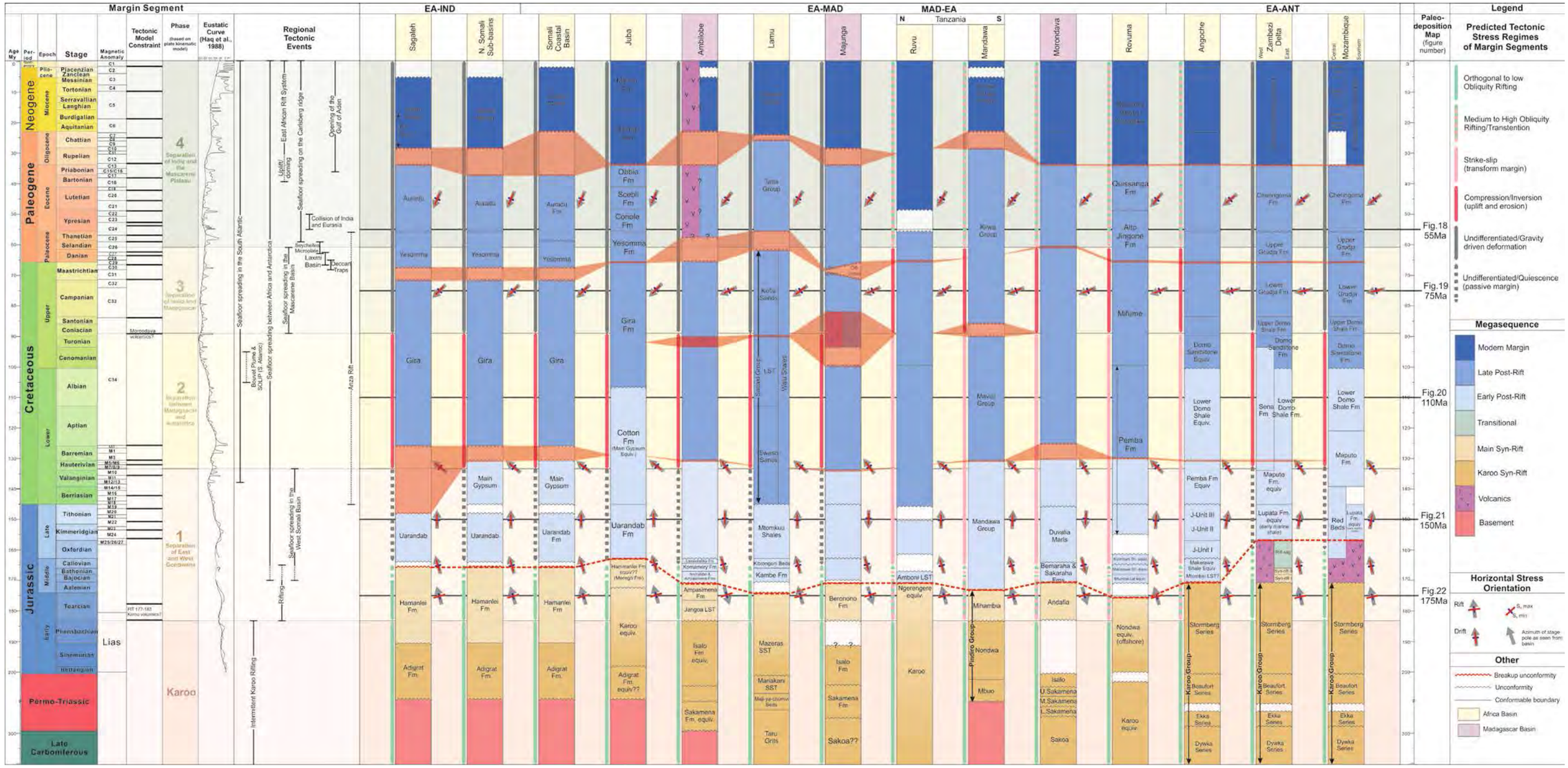
Margin Segment
EA-IND
EA-MAD
MAD-EA
EA-ANT
Age My
Period
Epoch
Stage
Magnetic Anomaly
Tectonic Model Constraint
Phase (based on plate kinematic model)
Eustatic Curve (Haq et al., 1988)
Regional Tectonic Events
Sagaleh
N Somali Sub-basins
Somali Coastal Basin
Juba
Ambilobe
Lamu
Majunga
N Tanzania
S Tanzania
Ruvu
Mandawa
Morondava
Rovuma
Angoche
Zambezi Delta
Mozambique
Paleo-deposition Map (figure number)
Legend
Predicted Tectonic Stress Regimes of Margin Segments
Orthogonal to low Obliquity Rifting
Medium to High Obliquity Rifting/Transtention
Strike-slip (transform margin)
Compression/Inversion (uplift and erosion)
Undifferentiated/Gravity driven deformation
Undifferentiated/Quiescence (passive margin)
Megasequence
Modern Margin
Late Post-Rift
Early Post-Rift
Transitional
Main Syn-Rift
Karoo Syn-Rift
Volcanics
Basement
Horizontal Stress Orientation
Rift
Drift
Other
Breakup unconformity
Unconformity
Conformable boundary
Africa Basin
Madagascar Basin
Fig.18 55Ma
Fig.19 75Ma
Fig.20 110Ma
Fig.21 150Ma
Fig.22 175Ma
Paleogene
Neogene
Cretaceous
Jurassic
Permo-Triassic
Late Carboniferous
Lias
Karoo
Seafloor spreading in the South Atlantic
Seafloor spreading between Africa and Antarctica
East African Rift System
Seafloor spreading on the Carlsberg ridge
Opening of the Gulf of Aden
Collision of India and Eurasia
Deccan Traps
Arza Rift
Rifting
Intermittent Karoo Rifting
Separation of India and the Mascarene Plateau
Separation of India and Madagascar
Separation between Madagascar and Antarctica
Separation of East and West Gondwana

Figure 3.5: (*Previous Page)* Tectono-stratigraphic chart for the East African and West Madagascan sedimentary basins. (See table 1 for full list of references)

Basin	References
Sagaleh	Bosellini, 1992 Coffin & Rabinowitz, 1988
Northern Somali Sub-Basins	Bosellin, 1992 Coffin & Rabinowitz, 1988
Somali Coastal Basin	Bosellin, 1992 Coffin & Rabinowitz, 1988
Juba(-Lamu) Basin	Kearns et al., 2016 Bosellini, 1992
Lamu Basin	Cruciani & Barchi, 2016 Rais-Assa, 1998 Mbede & Dualeh, 1997 Coffin & Rabinowitz, 1988 Nyagah, 1995 Nyraberi & Rop, 2014
Ruvu Basin	Mbede & Dualeh, 1997
Mandawa Basin	Hudson & Nicholas, 2014 Nicholas et al., 2007 Nicholas et al., 2006
Rovuma Basin	Salman and Abdula, 1995 Key et al.,2008 Key and Reeves (2012) Mahanjane and Franke, 2014 Franke et al., 2015.
Angoche Basin	Mahanjane et al., 2014 Salman and Abdula, 1995 Mahanjane, 2014
Zambezi Delta Depression	Salman & Abdula, 1995 Salazar et al 2013 Mahanjane, 2012 Mahanjane et al., 2014
Southern Mozambique Basin	Salman & Abdula, 1995 De Buyl & Flores, 1986
Ambilobe Basin	Coffin & Rabinowitz, 1988 Papini & Benvenuti, 2008 Rerat, 1964 Besairie & Collignon, 1972 Wescott & Diggens, 1998
Majunga Basin	Coffin & Rabinowitz, 1988 Jeans & van Meerbeke, 1995 Razafindrazaka et al., 1999 Papini & Benvenuti, 2008
Morondava Basin	Wescott & Diggens, 1997 Geiger et al., 2004 Clark, 1998

Table 1: Full list of references used to construct the Tectono-stratigraphic table.

3.3.1. East African Basins conjugate to India

In the pre-breakup assembly of the Gondwana supercontinent, the northern Somali segment of the East African margin was attached to the Indian conjugate margin (EA-IND in Figure 3.4). Subsequent rifting and breakup during the early and middle Jurassic let to the formation of the Sagaleh basin, the Somali Embayment (also called the Mudugh Basin), the Nogal Basin and Obbia basins (2-5 in Fig. 3.4, Fig. 3.6).

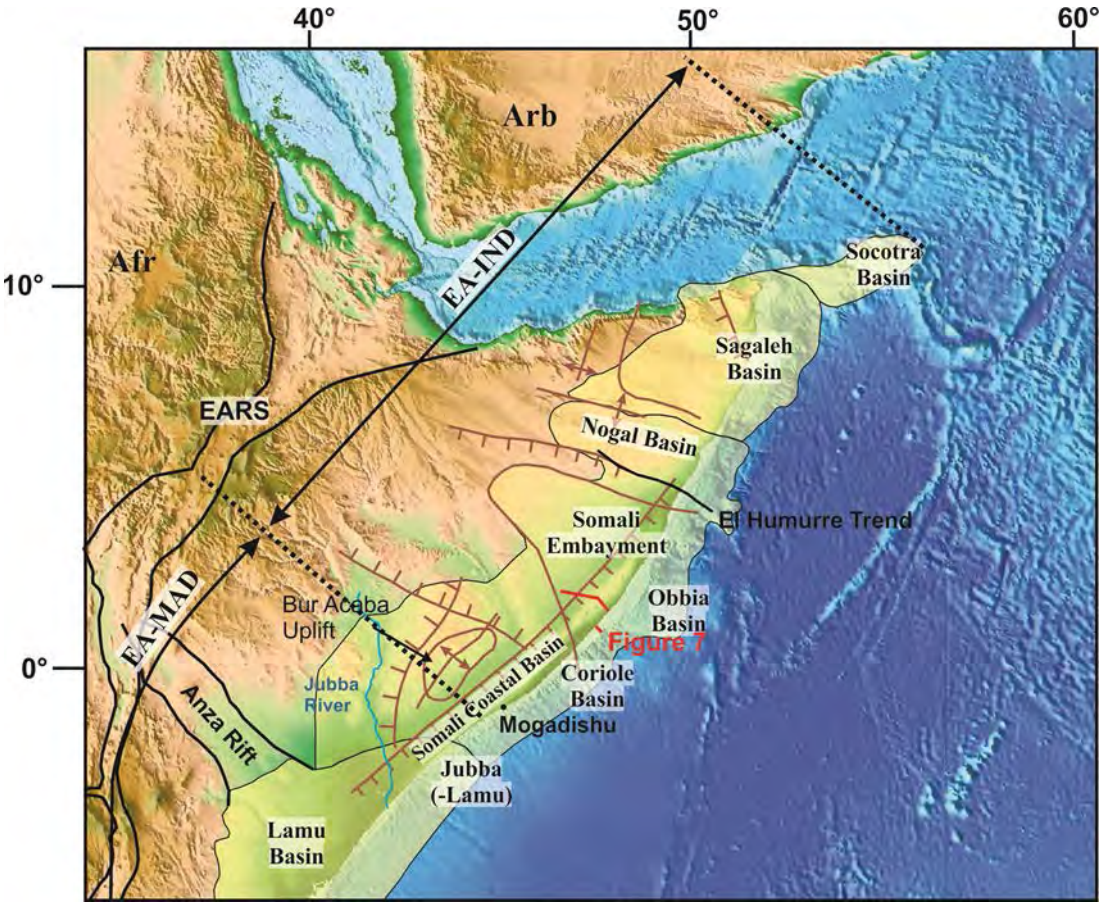

Figure 3.6: Regional overview of the East Africa continental margin belonging to the Western EA-IND conjugate margin segments showing the location respective sedimentary basins of regional structural elements (Modified from Bosellini, 1992; Zhou et al., 2013).

Our knowledge of these basins largely depends on regional studies from the late 1980's (Coffin & Rabinowitz, 1988) and the early 1990s (Bosellini, 1992) because no regional research studies and exploration efforts took place for 20-30 years due to political instabilities in the Horn of Africa. Only with the improving political conditions in recent years, new exploration efforts have been initiated. However, new results are not yet in the public domain. For more detailed stratigraphic descriptions for the EA-IND margin segment see Appendix D.

3.3.1.1. Sagaleh Basin

The Sagaleh Basin in northern Somalia covers the very northeast tip of the Horn of Africa and is sometimes referred to as the Daroor or Dharoor Basin. The basin fill history comprises six megasequences or some equivalents and the younger basin evolution is partly influenced by the opening of the Red Sea.

Karoo syn-rift

The oldest sediments in the Sagaleh Basin consist of the Triassic - early Jurassic (Sinemurian) continental Adigrat Formation which rests unconformably on the pre-rift basement of Precambrian to early Palaeozoic crystalline and metamorphic rocks (Bosellini, 1992). Initial deposition was strongly controlled by the Karoo rifting events during Triassic to early Jurassic and palaeotopography, and both upper and lower boundaries of the Adigrat Fm. are diachronous and difficult to date due to poor fossil control (Bosellini, 1992). However, the Adigrat Fm. is considered to be the 'Karoo' equivalent succession in northeast Africa. Thus, in this study the Adigrat Fm. has been assigned to the Karoo rift stage, but due to age uncertainties an early main syn-rift age cannot be precluded.

The Adigrat Fm. ranges from continental alluvial, fluvial and coastal plain sediments with coarse-grained clastics at the base and shale units towards the top. They were deposited in a vast arid land with changeable depositional environments dominated by alluvial and fluvial settings with local lacustrine and coastal plain-deltaic areas as well as inland sabkas and eolian dune fields (Bosellini, 1992).

The top boundary of the Adigrat Fm. was controlled by rifting during the Jurassic (Bosellini, 1992).

Main syn-rift

The main syn-rift stage in the Somalia marginal basins led to the deposition of an early to middle Jurassic shallow marine transgressive sequence called the Hamanlei Formation. This significant change in depositional environment from continental Karoo sediments to shallow marine indicates the onset of tectonic subsidence. The Hamanlei Formation (Pliensbachian to Bathonian) consists of mainly oolitic limestones deposited in a shallow-marine carbonate platform setting (Bosellini, 1992).

The lower boundary is diachronous (Bosellini, 1992) caused by the gradual onlapping of shallow marine sediments on the top of the Adigrat Formation whereas the top boundary is formed by a coeval unconformity over the whole of Somalia (Bosellini, 1992), assigned as the breakup unconformity (fig. 3.5).

Despite being classified as Syn-rift Megasequence, no evidence of synkinematic thickness changes have been observed in the Sagaleh basin but further south the

Hamanlei Fm. exhibits fault-controlled thickness changes (Bosellini, 1992) due to active faulting and subsidence (Coffin & Rbinowitz, 1988).

Breakup and Early post-rift

Over most of the East African margin, a major regional transgression from late Callovian to Oxfordian is related to the final break-up of East and West Gondwana and subsequent phase of regional thermal subsidence (Bosellini, 1992).

In the Somali basins further south this is documented by basinal deep-marine shales of the Uarandab Sequence overlying the shallow-marine shelf carbonates of the Hamanlei Fm. indicating foundering and drowning of the carbonate platform (Bosellini, 1992) during the early post-rift stage.

However, in the Sagaleh Basin the Urandab equivalent sediments remain of shallow water origin, consisting of restricted-marine lagoonal evaporites and coastal carbonate-clastic shoals (Bosellini, 1992) indicating no significant change in depositional environment from the late main syn-rift megasequence without a transgressive stage. Further offshore the Uarandab equivalent strata are mostly missing (Bosellini, 1992).

The lower Cretaceous (Berriasian – Barremian or Neocomian) sediments are missing in the Sagaleh basin due to either non-deposition or erosion caused by regional tilting and erosion, possibly enhanced by low eustatic sea levels (Bosellini, 1992). Further south, sediments of this age are represented by the early post-rift Main Gypsum Sequence (Bosselini, 1992; see section 3.3.1.2).

Late post-rift

The Mid Post-rift deposition of the Sagaleh Basin follows a major regional unconformity (Berriasian – Barremian) and documents the onset of the passive margin stage. It includes the transgressive Gira Supersequence (Aptian – Senonian) which lies above the unconformity and transgresses from east to west over Jurassic sediments (Bosellini, 1992).

Above this, the Gira Supersequence shows a west to east facies change across the Sagleh Basin, from continental fluvial sandstones in the far west, to a vast shallow-marine carbonate shelf consisting of shallowing-up cycles and then marginal high-energy carbonates (e.g. shoals, reefs) and finally deep-water facies (mudstone and shale) including turbiditic sandstones in the east in the Aptian/Albian interval (Bosellini, 1992). This period of deposition was marked by relative tectonic quiescence, with a stable shallow–marine carbonate shelf and open deep-marine conditions in the most easterly part of the basin (Bosellini, 1992).

The transgressive Yesomma sequence (Late Maastrichtian – Paleocene) follows a major early Maastrichtian unconformity caused by regional uplift and block

faulting, and the formation of east – west trending horsts and grabens. Along the margin the event was accompanied by shallow intrusions and basaltic lava flows.

The sequence shows a typical facies change from continental fluvial sandstones in the west through marginal, shallow-marine shelf carbonates to deep-water basinal shales in the east (Bosellini, 1992). The early Maastrichtian deformation event was more pronounced in the west, but along the Indian Ocean coast the mid-Cretaceous carbonate platform drowned suddenly and was replaced by open deep-marine sediments – Sagaleh Fm (Bosellini, 1992). Bosellini (1992) suggest the cause of this tectonic event could be related to the drift of the Indian Plate northward, and more speculatively, to a rebound effect caused by the failure of Oman subduction.

A late Paleocene/early Eocene marine transgression created an open-shallow marine carbonate shelf across the horn of Africa (Bosellini, 1992). The Auradu Supersequence (Eocene) unconformably overlies the Yesomma sequence and is part of the late post-rift megasequence.

The Auradu Ss. records a cycle of both eustatic movements and tectonic movements, as shown by the thickness of the Auradu sequence, related to the onset of the opening of the Gulf of Aden at the end of the Eocene (Bosellini, 1992). The sequence records two regional transgressions; one in the early Eocene covered northern Somalia and the Sagaleh Basin in shallow-marine limestones (Auradu Limestone) and one in the Late Eocene which deposited the Karkar Formation – limestone, with alluvial and deltaic successions in the Northeast. The two transgressive formations were separated by the middle Eocene regressive Taleh Fm – mostly evaporites with shelf carbonates and dolomite (Bosellini, 1992). In the deep offshore basin, the Aruadu Ss. consists of clays and shales of the Obbia Formation, spanning the entire Eocene Epoch (Bosellini, 1992)

Modern margin

A major angular unconformity separates the Late Post-rift megasequence and the Modern Margin megasequence. In the Sagaleh basin the early Oligocene sediments are missing, possibly due to tectonic uplift and deformation (Bosellini, 1992), most likely related to the development of the East African Rift System.

The modern margin megasequence of the Sagaleh Basin consists of the Late Oligocene to Miocene Hafun Series, mainly consisting of carbonates. At this time most of Somalia is subaerially exposed, and deposition occurs in narrow belts along the margin (Bosellini, 1992). The Eil Sequence (Late Oligocene – Miocene) is part of the Hafun Series series (Bosellini, 1992; 1987) consisting of a narrow and thin prograding carbonate platform that grades into deep-water mudstones and shales offshore to the east (the Garad Fm) (Bosellini, 1992).

3.3.1.2. Northern Somali Sub-basins

The Northern Somali Sub-basins incorporate the areas along the EA-IND margin segment south of the Sagaleh basin including the Nogal basin, the Somali Embayment (e.g. Mudugh Basin) and the offshore Obbia Basin (Fig. 3.6).

The El Hamurre lineament (active during the Jurassic) is an important structural feature formed by a fault scarp that separates theses northern Somali subbasins (El Humurre Trend in Fig. 3.5). The Nogal Basin lies north of the El Hamurre lineament, whereas the onshore Somali Emabaymentand offshore Obbia basin both lie south of the El Hamurre lineament.

The tectonic and stratigraphic development of Northern Somali Sub-basins is similar to the Sagaleh basin further north with the the same 6 megasequences or some equivalents being present. Thus, the summary emphasises the differences in the tectonic and stratigraphic history from the Sagaleh Basin.

Karoo Syn-rift

The Triassic - early Jurassic equivalent to the Karoo syn-rift megasequence is the same in this area as in the Sagaleh basin. The Adigrat Formation consists mostly of continental alluvial, fluvial and coastal plain sediments and unconformibly overlays the metamorphic basement (Bosellini, 1992).

Main Syn-rift

A significant change of the depositional environment from the Karoo to the Main-Syn rift megasequence is documented by the shallow-marine platform carbonates of the early - middle Jurassic Hamanlei Formation indicating the onset of regional tectonic subsidence a marine ingression from the Tethys in the northeast as a result of rifting (Bosellini, 1992).

The Hammanlei Fm. covers the northern Somali sub-basins and the Sagaleh basin. The difference in this area is the presence of the Meregh Formation in the deeper parts of the basin. The Meregh formation (Sinemurian – Hettangian) was deposited by turbidity currents and is composed primarily of micrite, dolomite and oolitic limestones (Bosellini, 1992).

Early Post-rift

The El Hamurre lineament (El Humurre Trend in Fig. 3.6) acted as an important depositional divide in northeast Somalia. Bosellini (1986; 1992) interpreted the El Hamurre lineament as a transform fault during the breakup of Gondwana which accommodated the separation of the Madagascar block. This led to structural and depositional differences to the north and south across the lineament.

As previously mentioned in sections 3.3.2.1, following breakup, the Sagaleh Basin and Nogal Basin to the north of the El Hamurre lineament remained structurally

high as documented by shallow marine sediments of the Urandab Fm. equivalent in the Early Post-rift stage (Bosellini, 1992).

South of the El Hamurre trend the Uarandab Fm. is consists of transgressive shales (Urandab Fm – late Callovian to late Oxfordian) and regressive limestones (Gabredarre Fm – late Oxfordian/Kimmeridgian to early Tithonian) in the landward Somali Embayment and deep-water basinal shales in the offshore Obbia Basin (Bosellini, 1992) suggesting marine transgression due to thermal subsidence in the Early Post-rift phase. Bosellini (1992) attributed the late Callovian/Oxfordian transgression and the sudden flooding of the Hamanlei carbonate platform south of the El Hamurre escarpment to structural sag following final continental breakup.

The Main Gypsum sequence of the Somali Embayment unconformably above the Uarandab Fm. and consists of dolostones and sulphates deposited in a sabka and lagoonal environment. In basinward direction it is replaced by shallow-marine carbonates of a paleo shelf margin and basinal mudstones and shales of the deep-marine Obbia basin (Bosellini, 1992).

Late Post-rift

The Late Cretaceous Gira Supersequence rests on a Hauterivian – Barremian unconformity. In the offshore Obbia basin, south of the El Hamurre lineament, the sediments of the Gira Supersequence consists of deep-marine mudstones, shales, and turbidite fan deposits (Bosellini, 1992).

The major Maastrichtian unconformity at the base of the Yesomma Sequence previously described for the Sagaleh Basin in section 3.3.1.1. is also present in this area contemporaneous with shallow intrusions and basaltic lava flows Indian Ocean continental margin (Bosellini, 1992). It may be related to the tilting of the entire northern Somali block and the El Hamurre lineament may have been reactivated (Bosellini, 1992). Whilst the crustal movements were affecting the area to the north, further south in the Mudugh Basin was crustal stability and a steady regression (Bosellini, 1992).

The mid-Cretaceous carbonate platform drowned suddenly (more pronounced in the west) and was replaced by pelagic sediments offshore (Bosselini, 1992).

During the deposition of the Auradu supersequence (Eocene) the Auradu LST and Obbia Fm are the same as in the Sagaleh basin. However, there was no evaporitic sequence (Taleh formation) in this area, instead the Taleh equivalent formation is replaced by transitional sediments and a carbonate platform. The overlying Karkar Fm. and the Late Eocene of the Obbia Fm. have been eroded and are missing in this area (Bosellini, 1992).

Modern Margin

The late Oligocene/Miocene sediments in this area are more typical of the Somal/Merca sequence with transgressive, shallow water carbonates followed by the regressive deltaic and shelf clastic / carbonate platform of the Merca formation and basinward deep-sea fans (Bosellin, 1992).

3.3.1.3. Somali Coastal Basin

The Somali coastal basin stretches along the southeast coast of Somalia (Fig. 3.7). Coffin & Rabinowitz (1988) and Bosellini (1992) have both described the stratigraphy which is similar to the North Somalia basins (sections 3.3.1.1 and 3.3.1.2) with only a few minor differences highlighted below.

The stratigraphy of the Karoo Syn-rift to Early Post-rift megasequences as well as the Modern Margin Megasequence is the same as the basins further north but is characterised by a variation in depositional environment from the late Early Post-rift phase.

Late Post-rift

The Mid Post-rift Megasequence of the Somali Coastal Basin is represented by the Gira Supersequence, similar to the basins further north. However, it shows more deltaic influence and transitional shelf to open-marine deep-water turbiditic depositional environments (Bosellini, 1992).

Part of the Auradu Sequence in the Somali Coastal basins consist of shallow-marine sands rather than limestones of the the equivalent of the Taleh formation and the top of the Auradu Sequence (Late Eocene) has been eroded (Bosellini, 1992).

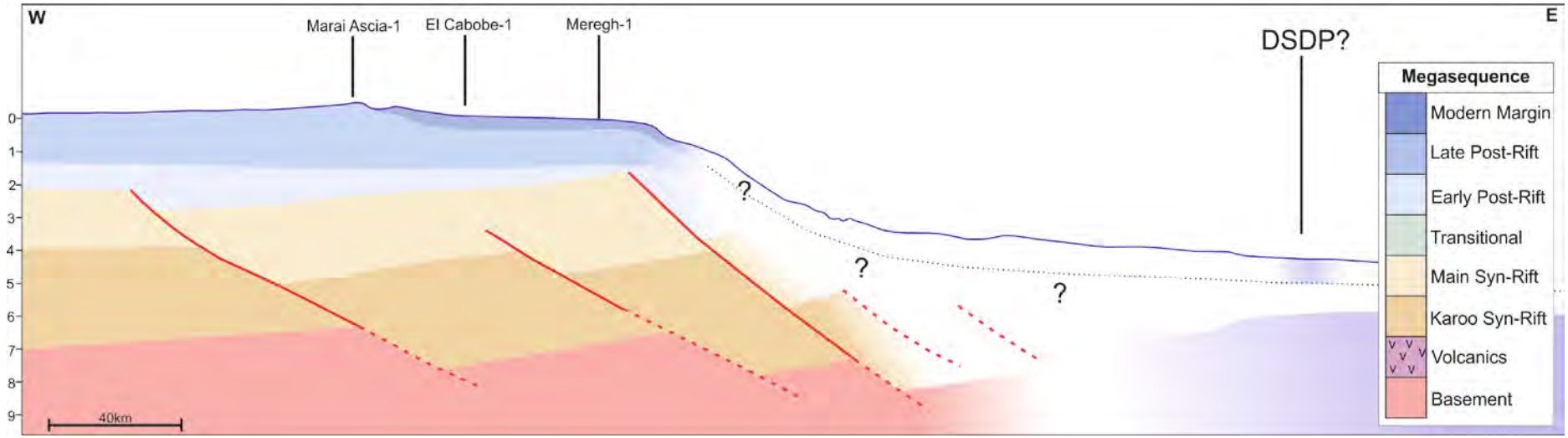

Figure 3.7: Cross-section of the Somali continental margin showing regional structures, well locations and megasequences in a W-E transect through the Somali Coastal Basin (after Bosselini, 1992).

3.3.2. East Africa Basins conjugate to Madagascar

The sedimentary basins of the East African margin are conjugate to Madagascar in the fully reassembled Gondwana continent (EA-MAD in Fig. 3.4). They include the Juba(-Lamu) Basin (Somalia), the Lamu Basin (Kenya), the Ruvu and Mandawa Basins (Tanzania), and the Rovuma basin (Tanzania/Mozambique boundary) (See Figure 3.8).

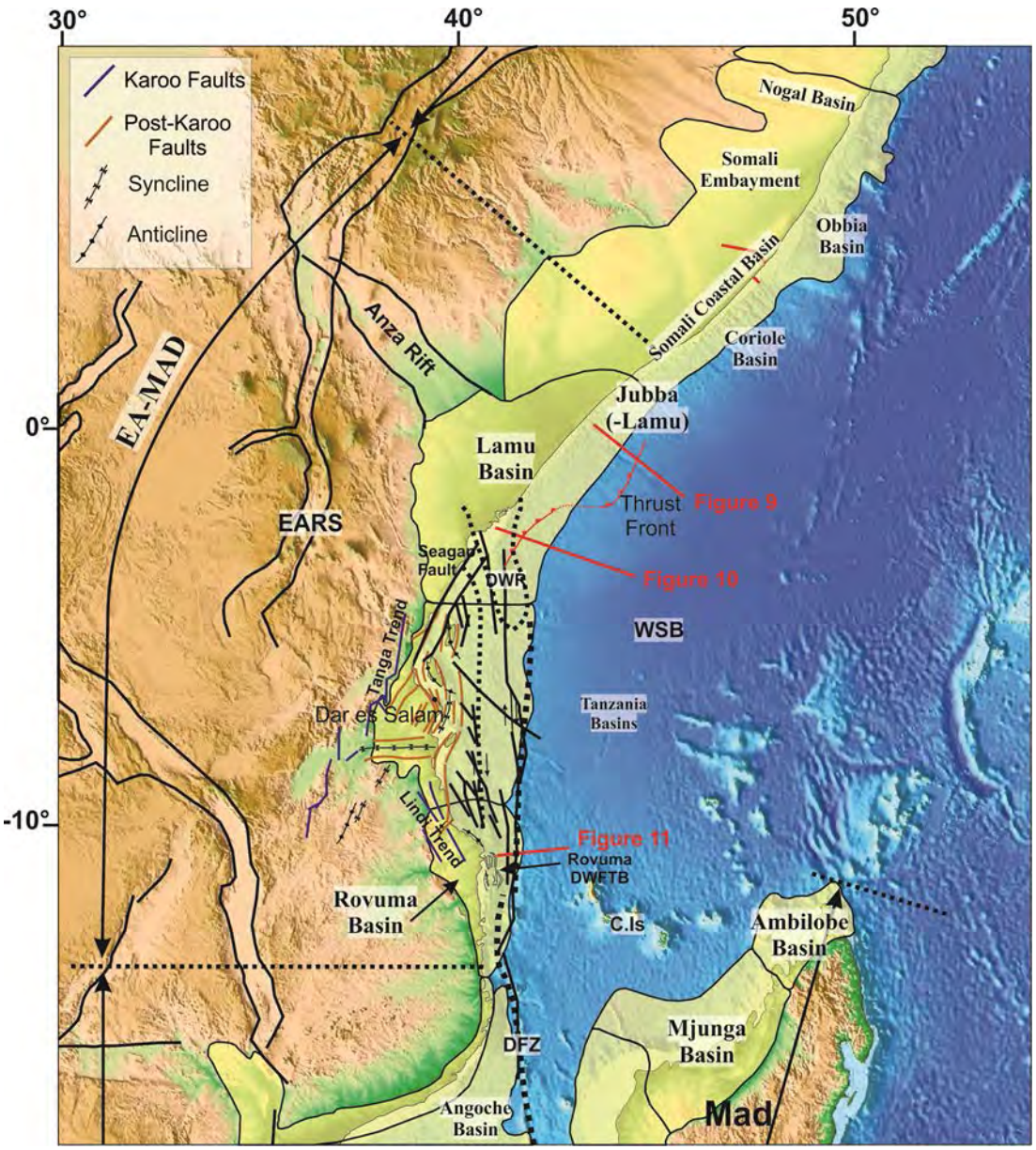

Figure 3.8: Regional overview of the East Africa continental margin conjugate to the West Madagascan margin segment, showing the location of respective sedimentary basins and regional structural elements (after Kapilima, 2003; Nicholas, 2007; Zhou et al., 2013; Mahanjane & Franke, 2014; Cruciani & Barchi, 2016).

Some of these have a more complicated history than previously encountered in the Somali Basins. The Somali Coastal Basin and the Juba Basin developed in a similar

way to the Somali Basins further north. However, the Tanzanian Basins and the Rovuma Basin formed along the Davie Fracture Zone, a transform margin between East Africa and Madagascar that remained active form ~180 Ma to 130 Ma (Tuck-Martin *et al.,* 2018), and which may have been reactivated since (Franke et al., 2015). As a result the stratigraphic and structural development of these basins is likely to be different and highly complex. For detailed stratigraphic descriptions of the EA-MAD marginal sedimentary basins see Appendix E.

3.3.2.1. Juba Basin

The Juba basin is located in the offshore area of the southern tip of Somalia (Fig. 3.7). Frequently, it is also referred to as the Juba-Lamu basin due to its connection to the Lamu basin offshore Kenya. The stratigraphy and basin history is quite different from the other Somali basins in the North due to the influence of the prevalent Juba-Shabeele Rivers in the Early Cretaceous and related large delta complexes. The stratigraphy of the Juba Basin has not been clearly described in the literature. The cross-section has been modified from recent work by Spectrum Geo Ltd. (Kearns et al., 2016).

Karoo Syn-Rift

The Karoo Syn-Rift megasequence of the Juba basin is similar to the other Somali basins to the north (sections 3.3.1.1, 3.3.1.2, 3.3.2.1.), with Karoo sediments unconformably overlying crystalline/metamorphic basement. Karoo Syn-rift deposition continued at least into the Early Jurassic (Mbede & Dualeh, 1997; Bosellini, 1992), although no published formal description of these sediments in the Juba Basin currently exists.

Main Syn-Rift

The distinction between Karoo, Main Syn-rift and Early Post-rift megasequences is less clear in the Juba basin the basins further north. Assuming the stratigraphic history is similar until the onset of Juba/Shabelle river delta deposition then the Main Syn-rift megasequence is represented by the Hamanlei Formation (Middle Jurassic) which in the Juba basin also includes evaporites (Bosellini, 1992) and shallow marine limestone (Kearns et al., 2016).

Early Post-Rift

The Early Post-rift megasequence of the Juba Basin consists of the Uarandab Formation (Upper Jurassic) and the Cotton Formation (Lower Cretaceous) which both consist of marine shale and limestone (Kearns et al., 2016).

Late Post-Rift

The Late Post-rift of the Juba Basin begins with the Gira Supersequence, bounded to the top and bottom by unconformities and spanning the entire Upper Cretaceous. Similar in nature to the Gira Supersequence across the rest of Somalia, it consists of

deltaic and transitional facies on the shelf and deep-water mudstone and shale in the basin (Kearns et al., 2016; Bosellini, 1992).

The Yesomma Sequence of the Juba Basin is also different to the rest of the Somali coastal basins, with continental Yesomma sandstone in the west and deltaic-marine sandy successions in the east (Bosellini, 1992). The tectonic deformation that affected the central and northern parts of Somali, north of the El Hamurre lineament, did not affect the Juba basin (e.g. Mudugh & Mogadishu basins) and the structural stability is marked by these prograding deltas represented by the Yesomma Sequence located along the edge of the shelf (Bosellini, 1992).

This deltaic influence is linked to the prograding Juba delta which dominated deposition in the Juba basin at this time. Due to very high sedimentation rates of the Juba delta the tectonic and eustatic movements observable in the other basins along the eastern coast of Somalia were subdued and actually masked completely (Bosellini, 1992).

Above the Yesomma Formation lies an Eocene aged sequence of three formations, named the Coriole, Scebli and Obbia formations. These all consist of marine shales, limestones and sandstones (Kearns et al., 2016).

Modern Margin

The Somal and Merca Formations (or Eil Sequence) in the Juba Basin are similar in nature to the rest of Somalia, and lie on the Early Oligocene unconformity that has been recognised in the other Somali Basins. The Somal Formation (late Oligocene to mid-Miocene) represents a general marine transgression (Bosellini, 1992) and the Merca Fm is mid-Miocene to recent (Kearns et al., 2016) and represents a depositional regression during highstand (Bosellini, 1992). In the east, in the deeper parts of the basin are the deep-water mudstones and shales of the Garad Formation (Bosellini, 1992).

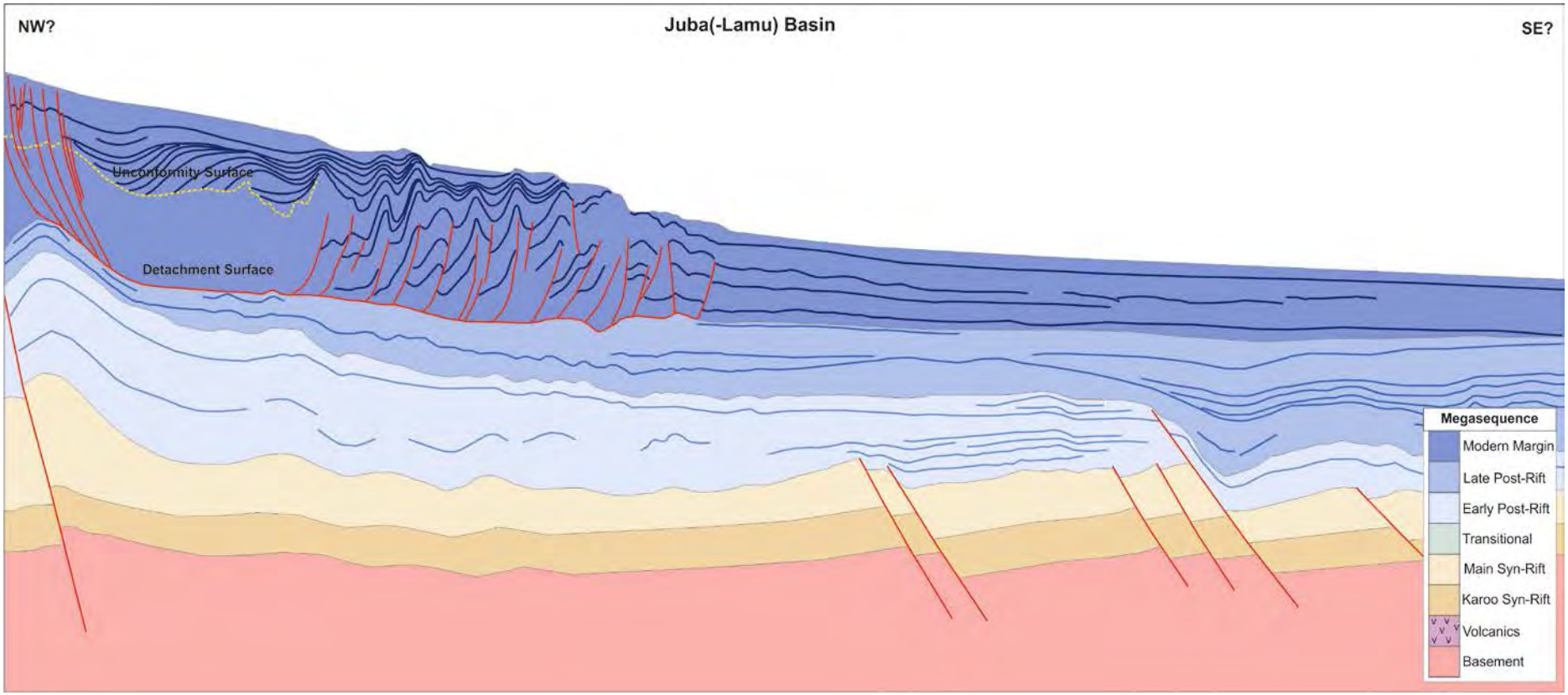

Figure 3.9: Regional cross-section of the Somali-Kenya continental margin showing regional structures and megasequences in a NW-SE transect through the Juba-Lamu Basin (modified from Kearns et al., 2016).

3.3.2.2. Lamu Basin

The Lamu Basin, or Lamu Embayment, covers both onshore and offshore Kenya and has a very complicated structural and tectonic history (Fig. 3.8). It forms one of the arms of a failed triple rift system that formed during the Jurassic Main rifting and Gondwana breakup (Nyagah, 1995). The other arms of this tri-radial rift system stretched to the NE along the Somali coast, and down to the south along the Kenyan/Tanzanian coast, these are the arms that successfully reached breakup and allowed East Gondwana to break away. The Anza rift forms the third arm/failed rift segment that stretches NW into the interior of Kenya/African continent (Bosworth & Morley, 1994; Greene et al., 1991; Reeves et al., 1987). Figure 3.10 shows a cross-section through the Lamu basin, modified from Cruciani & Barchi (2016).

Karoo Syn-Rift

In the Lamu Basin, the Karoo Syn-rift megasequence contains at least 3 formations which record a succession of predominantly continental sediments, beginning with the peri-glacial and fluviatile sediments of the Taru Grits, the lacustrine sandstones and shales of the Maji-ya-Chumvi Formation (potential source rock) and the deltaic shales, coals and sandstones of the Mariakani Fm. (Rais-Assa, 1998). According to Coffin & Rabinowitz (1988) this phase of deposition was initiated by major faulting in the Late Carboniferous or Early Permian.

Main Syn-Rift

Significant faulting occurred between the deposition of the Mariakani Formation and the overlying Mazeras Sandstone (Coffin & Rabinowitz, 1988). As the name suggest, the predominantly continental Mazeras sandstone consists coarse-grained, cross-bedded sandstones, the lower part deltaic in origin and the upper part aeolian (Mbede & Dualeh, 1997). Another major episode of faulting accommodated the end of the deposition of the Mazeras Sandstone at the end of the Early Jurassic (Coffin & Rabinowitz, 1988), producing numerous syn-sedimentary faults and synclinal structures throughout the top of the unit (Mbede & Dualeh, 1997), which we assign as the breakup unconformity (fig 3.5). Coffin and Rabinowitz (1988) suggest this is still part of the Karoo Megasequence but we suggest it is, at least in part, the main syn-rift sequence.

Early Post-Rift

Marine conditions were fully established in the Middle Jurassic. The Early Post-rift Megasequence lies unconformably on the Mazeras Sandstones and begins with limestones and shales of the Kambe formation (Bajocian-Bathonian), shallow-water deltaic sediments of the Kibiongoni Beds (Callovian) and the Late Jurassic marine shales of the Mtomkuu formation (Coffin & Rabinowitz, 1988; Rais-Assa, 1988; Nyagah, 1995).

Also early post-rift is the Sabaki Group (Neocomian through earliest Paleocene) deposited in a tide-influenced shelf and marine setting (Nyagah, 1995). The Group begins with a deltaic succession of sandstones, siltstone and shales (Ewaso Sands: Neocomian-Albian), followed by the Hagarso limestones (Albian-Maastrichtian) and the Freetown Limestones (Cenomanian?). The final unit of the Sabaki Group is the the Kofia sands (Turonian-Early Paleocene) which we assign to the Mid Post-rift Megasequence below. Whilst these sediments were deposited on the continental margin and shelf, in the deep offshore basin a thick succession of shales was deposited that stretches across the entire timespan of the Sabaki Group, called the Walu shales (Nyagah, 1995). Similar shales were deposited all along the East African margin at this time, related to regional mid-Cretaceous transgressive phase (Nyagah, 1995).

Mid Post-Rift

The Lamu basin experienced renewed basement uplift from the Turonian to the Paleocene creating the Davie-Walu Ridge (D-WR in Fig. 3.8) and its northwards onshore continuation (i.e., Walu-Kipini and Garissa axis; [Nyagah 1995]). The Davie-Walu Ridge is an uplifted structure (Cruciani & Barchi, 2016) which lies at the northern termination of the Davie Ridge-fracture zone (DFZ in Fig. 3.8). Jeans et al. (2012) and Osicki et al. (2015) recognised it as a tranpressional structure, with the main phase of uplift/inversion occurring in the Late Cretaceous (Cruciani & Barchi, 2016). The uplift caused increased erosion of the hinterland in the west and the rapid deposition of the deltaic Kofia sands in the east. Cruciani & Barchi (2016) suggest that the rapid clastic sediment input (Kofia sands) may have caused the underlying Walu Shales to become overpressured, and hence trigger the main phase of gravity-spreading deformation in the Lamu deep-water fold-and-thrust belt (DW-FTB) (see Fig. 3.10). The cross-section (fig. 3.10) shows the deformation of the Early and Mid Post-rift Megasequences in the oldest DW-FTB, above a detachment unit in the Early Post-rift. The main phase of shortening in the Lamu DW-FTB occurred in about 15 Myr (from the Maastrichtian-Paleocene), although the landward areas may have experienced gravity tectonics all the way up to the Early Miocene (Cruciani & Barchi, 2016).

Late Post-Rift

Above the late Paleocene unconformity lies the late post-rift Tana Group (Eocene to Oligocene [Cruciani & Barchi, 2016]) which marks the establishment of a new depositional regime. The lithospheric assemblage comprises shelf-carbonates and fluvio-deltaic facies (Kipini Fm.), deposited by a paleo Tana river distributary system (Nyagah, 1995), during three pulses of sea level change three pulses of sea-level rise and a single regressive phase of deposition, which coincide with tectonics in the Afar region (Cruciani & Barchi, 2016). The shelf carbonate facies that built up between periods of siliciclastic deposition are related to a tectonically influenced depositional pattern involving episodic uplift and subsidence which prevailed during the Palaeogene (Nyagah, 1995).

Modern Margin

The Modern Margin megasequence, the Coastal group lies on a major Late Oligocene unconformity, marked offshore by starved-basin conditions (Nyagah, 1995). Deposited in the course of three major cycles of sea-level change in a variety of settings including restricted shelf, middle to outer shelf, deep-marine and fluvial settings. Carbonate sequence associated with marine shales and an overlying siliciclastic sequence (Nyagah, 1995). It consists of limestones (Baratumu Fm.) deposited on the continental shelf associated with gradual subsidence during Early to Late Miocene. Lamu reefs on the shelf edge, both topped by Marafa fm. sandstones. In the deeper subsiding parts of the basin are the deep marine Simba shales (Nyagah, 1995).

A second, younger DWFTB became active during this phase and superimposed above the older DWFTB described above (fig. 3.10). The main phase of deformation on this belt was during the Late Miocene and Early Pliocene, linked to uplift of Kenya-Somalia coastal regions after the middle Miocene due to movements in the Kenya Rift Valley (Cruciani & Barchi, 2016).

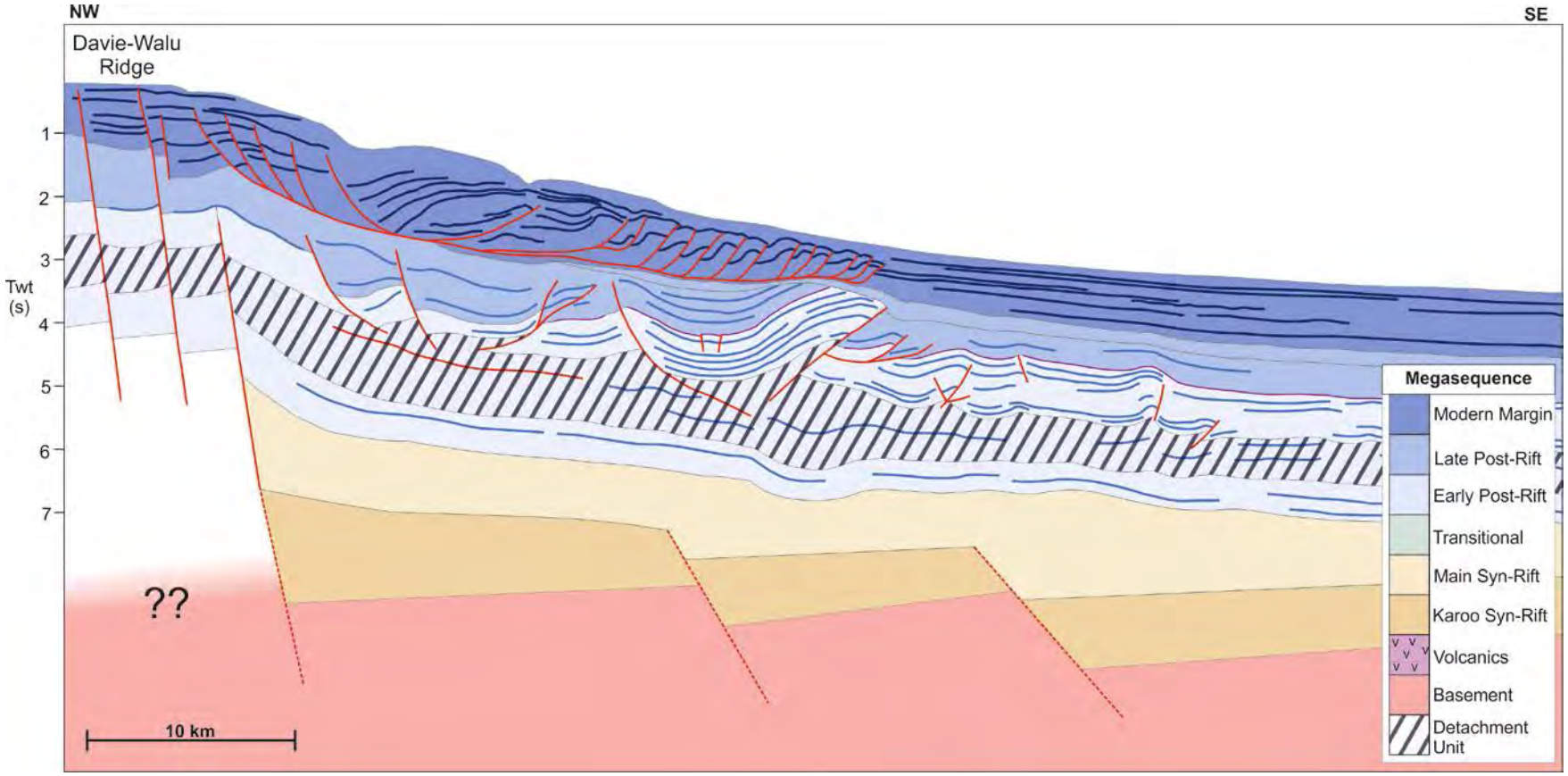

Figure 3.10: Regional cross-section of the Kenya continental margin showing regional structures and megasequences in a NW-SE transect through the Lamu Basin (modified from Cruciani & Barchi, 2016).

3.3.2.3. Tanzania

There are numerous basins in Tanzania, in this paper we focus on the two main basins that lie along the coast, the Ruvu Basin, on the Northern coast, and the Mandawa basin, on the southern coast (fig. 3.8).

Ruvu Basin

The Ruvu basin lies along the northern coast of Tanzania, within the NNE-SSW Tanga fault trend rift system (Mbede & Dualeh, 1997). Stratigraphy is mostly gathered from the work of Mbede & Dualeh (1997).

Karoo Syn-rift

The evolution of the Ruvu basin also began with the deposition of the mainly continental Karoo sediments during the Late Carboniferous to Early Mid Jurassic in a variety of environments. The movement of faults caused erosion of the rift shoulders and deposition of complex fluvial systems along the downthrown flanks of normal faults, including braided and meandering streams, flood plains, deltaic and swampy deposits and lacustrine shales. There is evidence of rare marine incursions in the faster subsiding sections of the basin (Mbede & Dualeh, 1997).

Mbede & Dualeh (1997) recognise at least two Karroo megacycles within the Ruvu Basin. The first cycle, and the oldest Karoo deposits found in this basin, is the Lower Permian Hatambulo Formation comprising sandstones of deltaic and lacustrine origin, interbedded with deltaic shales and sandstones. Throughout Early Karoo sedimentation the rift zones were reactivated by a number of tectonic pulses (Mbede & Dualeh, 1997).

Main Syn-rift

Mbede & Dualeh (1997) suggest the second megacycle, referred to as the Ngerengere Beds, represent the youngest Karoo sediments and are correlatable with the Mazeras Sandstones. However, we suggest these beds, or the upper portion of them, form the Main Syn-rift megasequence.

The topmost section of the Karoo group, the Ngerengere beds is composed of a number of sequences separated by disconformities indicating a number of different deposition cycles in response to tectonic control by bounding faults (Mbede & Dualeh, 1997).

Along the coast in the north, the Ngerengere beds consist of interbedded continental sandstones, siltstones and shales of Late Triassic to Early Jurassic age. Further south the sediments are more continental in nature, comprising interbedded quartzitic, red, silty sandstones deposited in lacustrine and braided stream environments. The Ngerengere Beds of the central basin consist of arkosic sandstones, with occasional limestones, and shales deposited in a high energy

environment but becoming quieter with time, and indicating regular marine incursions (Mbede & Dualeh, 1997).

Early Post-rift

Fully marine conditions became established in the Bajocian/Bathonian with the deposition of the Amboni limestones on the continental margin and shelf, and deep marine shales offshore. By this point rifting had ceased, but subsidence continued, the Karoo grabens along the coast were flooded by a shallow epicontinental sea and the Amboni limestone marks the start of the early post-rift sequences (Mbede & Dualeh, 1997).

The Late Jurassic was a tectonically quiet phase with continuing marine transgression. Across most of coastal Tanzania there was low energy marine environment with mainly marine clastic sediments and sandstones, limestones and mudstones, whilst in the east, deep marine shale deposition continued in the offshore basin (Mbede & Dualeh, 1997).

A Neocomian regression resulted in the deposition of fluviatile sandstones, described by Mbede & Daleh (1997) as a major reservoir. In some areas the Neocomian sediments are present as deltaic bituminous sandstones interbedded with clay, and Mbede & Dualeh (1997) also suggest the possibility of tectonic activity at this time due to the presence of an outcrop of septarian limestones and conglomeratic sandstones.

A prominent Barremian regional unconformity at the end of the Mid Post-rift has been attributed by to tectonic activity related to continued wrench faulting, as Madagascar moved southwards, and far-field effects of the breakup of South America and Africa (Mbede and Dualeh, 1997).

Late Post-rift

Above the unconformity, the late post-rift megasequence was deposited during a period of fluctuating sea level in the middle Cretaceous. Gradual subsidence combined with rising sea levels led to open marine conditions and the deposition of various outer shelf marls, mudstones, siltones and clays. This was followed by a full Late Cretaceous marine transgression and the deposition of deep water clays which continued into the Paleocene (Mbede & Dualeh, 199

Regression followed, beginning in the Mid Eocene, which Mbede & Daleh (1997) attribute to the development of the Owen Fracture Zone and associated seafloor spreading. This manifested itself in the Ruvu basin by the build-up of clastic sediments (Mid – Late Eocene) on a broad continental shelf and slope, which exceeded the rate of subsidence (Mbede & Daleh, 1997).

Modern Margin

Oligocene strata are mostly missing from the Ruvu basin, and Miocene sediments lie unconformably above Late Post-rift sediments. The Miocene sediments consist of marine limestones, mudstones and sands deposited during another marine transgression, overstepping older beds and contemporaneous with renewed tectonic activity associated with the development of the EARS (Mbede & Daleh, 1997).

The development of the EARS resulted in the uplift and basinward tilting of hinterlands, intensive erosion and rapid basinal subsidence and resulted in the deposition of large prograding deltas across the Dar-es-Salaam Embayment and Zanzibar channel and accompanied by synsedimentary faults. (Mbede & Daleh, 1997)

A late Miocene unconformity was followed by regressive Pliocene to recent sediments. Regressive estuarine fluviatile Plio-Pleistocene sands were deposited in existing depressions in the west continental areas, meanwhile marine deposits were limited to present day offshore areas (Mbede & Dualeh, 1997).

Mandawa Basin

The Mandawa Basin covers the southern coast of Tanzania, but its stratigraphic evolution is different the Ruvu basin in the north due to presence of salt.

Karoo Syn-Rift

The "Karoo" equivalent syn-rift megasequence in this basin is called the Pindiro Group (Late Triassic to Early Jurassic) which lies unconformably above Precambrian basement. It comprises three formations. The first formation, the Mbuo Formation, is mainly continental in nature, comprising clastic sediments, deposited in alluvial, fluvial and lacustrine environments, before marine incursion (Hudson & Nicholas, 2014).

During the Late Triassic, the southern and central parts of the Mandawa Basin subsided at a much higher rate than adjacent areas. Marine incursions from the Tethys Ocean in the Northeast had already reached as far south as the Mandawa Basin, but the deepest parts were cut off from the future Indian Ocean by structural highs to the east and south. As a result, the Mandawa Basin became a restricted marine environment and the middle formation of the Pindiro Group, the Nondwa formation, was deposited which comprises mainly evaporites and subordinate shales (Hudson & Nicholas, 2014).

Main Syn-rift

It is difficult to differentiate between Karoo Syn-rift and Main Syn-rift megasequences in the Mandawa Basin. It is possible that the upper unit of the Pindiro Group the Mihambia Formation (Toarcian – Aalenian) is part of the Main

Syn-rift megasequence. It consists of clastic sediments with subordinate limestones and indicates a change in deposition from a restricted marine environment (Nondwa Fm.) to a shallow and marginal marine environment following a further period of rifting (Hudson & Nicholas, 2014). The top of the Pindiro group is marked by an Intra-Aalenian unconformity which has been suggested as the breakup unconformity (Said et al. 2015; Hudson & Nicholas, 2014).

The major fault trend in the Mandawa basin and southern coastal Tanzania is the NNW-SSE trending "Lindi fault trend" which produced Mesozoic faults associated with breakup and the dextral strike-slip movement of Madagascar. It basin possibly formed as a transtensional wrench zone associated with later stage of movement, and may have been reactivated since (Nicholas et al., 2007).

Early Post-rift

Early post-rift begins with the Mandawa Group which includes a number of different formations stretching from the Aalenian to the Hauterivian and is topped by a Barremian aged unconformity. The lower part of the Mandawa Group was deposited in a range of shallow marine and lagoonal environments. Continental conditions returned to the north of the Mandawa Basin during the Late Jurassic indicated by the deposition of fluvial to fluvio-deltaic sandstones. The group is topped by a mix of shallow-water limestones continental alluvial to fluvial sandstones (Hou, 2015).

Mid Post-rift

Above the Barremian unconformity is the Mid Post-rift Mavuji Group aged Late Barremian to Turonian/Coniacian (Hudson 2011), which consists of a lower limestone member deposited in a clastic-dominated shallow marine environment and a middle sandstone member deposited in an alluvial to fluvial environment. Then rest of the Mavuji Group consists of three laterally equivalent formations deposited during the Aptian to Mid Turonian. In the west are deltaic, mouth bar sandstones, which are replaced by shallow marine reefal limestones on the shelf. Finally in the east are outer shelf marine clay/siltstones with itercalations of thin turbiditic sandstone beds (Hou, 2015).

Late Post-rift

The late Cretaceous (Santonian) to mid Oligocene the Mandawa Basin was a true passive margin (and along most of East African margin) and a period of tectonic stability marked by the accumulation of a thick, outer-shelf, clay-dominated succession called the Kilwa Group (Nicholas et al., 2007; Nicholas et al., 2006). Uniform Subsidence across the shelf and slope and the Kilwa group had very little or no lateral facies change across the margin. The Kilwa group itself can be subdived into four formations (Nangurukuru Fm, Kivinji Fm, Masoko Fm, Pande Fm) but mostly consists of over 1 km of a broadly homogenous, mid- to outer-shelf

clay-dominated succession, Upper Cretaceous to Paleogene in age that lies disconformably on Albian marls (Nicholas et al., 2006).

Modern Margin

The Songo Songo Group directly overlies the Kilwa Group with a marked angular unconformity, which marks the end of the tectonically stable passive margin stage and a renewed period of extension along the coast, with new normal faults and reactivation of "Lindi" faults (Nicholas et al., 2007). The Songo Songo Group consists of syn-tectonic Upper Miocene clays and nodular limestones, deposited during a period of active extension along the coast, development of new normal faults and reactivation of older NNW trending Mesozoic faults. Oligocene sediments are missing and it is possible they were eroded during tectonic activity (Nicholas et al., 2007).

Significant uplift and erosion occurred in southern Tanzania after the Late Miocene and contemporaneous with this was the deposition of the Pliocene Mikindani Beds, a series of fluvial and terrestrial sediments. These were followed by thin marine sands and patchy reefs deposited in a shallow shelf environments in the Pleistocene, the deposition of which was constrained by lack of accommodation space, reinforcing the theory of a period of inversion, which Nicholas et al. (2007) suggest is due to thermal doming and tilting of the Tanzanian craton prior EARs rift initiation.

3.3.2.4. Rovuma

The Rovuma Basin lies on the boundary between Tanzania and Mozambique, and covers both onshore and offshore, reaching water depths of between 550 and 2000 metres (Ledesma, 2013). It experienced a complicated tectonic history, being subjected first to transtensional rifting followed by a change to a transform controlled passive margin

The Rovuma basin has been the site of successful gas discoveries, such as in the Windjammer well and already an actively producing gas fields, the Mnazi Bay gas field. Significant investment has been made in the area. For example, ENI has approval from the Government of Mozambique for the installation of a floating unit for the treatment, liquefaction and storage of natural gas to produce up to 5 TCF.

Stratigraphic information for the Rovuma Basin comes from Salman and Abdula (1995) Key et al. (2008), Key and Reeves (2012) and Mahanjane and Franke (2014). The cross-section (fig. 3.11) was modified from Mahanjane & Franke, 2014, and Franke et al., 2015.

Karoo Syn-rift

Karoo sediments of the Rovuma Basin rest on basement of Late Paleozoic Mozambique metamorphic belt and their distribution is controlled by basement rift

topography (Salman & Abdula, 1995). Although, Karoo sediments do not crop out in the Rovuma Basin, Salman and Abdula (1995) infer their presence based on interpretations of seismic sections and correlation with the Selous and Mandawa Basins of southern Tanzania.

Based on these correlations, Salman and Abdula (1995) assume Karoo facies similar to both basins to be present in the Rovuma Basin. In the west the facies would be syn-rift continental sediments, Permo-Triassic in age like the Selous Basin, including conglomerate and sand with shale bands. In the East it is possible the salt which is characteristic of the Mandawa Basin at this time extends south into the Rovuma Basin, deposited in lagoonal, restricted basins (Salman & Abdula, 1995).

Main Syn-rift

The Main Syn-rift megasequence of the Rovuma Basin is represented by the Rio Mecole and N'Gapa Formations, both continental in nature and late Triassic to Early Jurassic in age (Key et al., 2008). These sediments filled in small, isolated, fault-controlled (north-northwest to south-southeast trending) basins (Key *et al.,* 2008) that were discordant with the underlying Karoo half-grabens, indicating a separate phase of rifting (Key & Reeves, 2012). Both formations consist on red continental conglomerates deposited in high-energy, fluviatile environments, in alluvial fans or on scree slopes, in small, isolated rift basins, with paleoflow directions from rift shoulders in the NE and NW (Key et al., 2008).

Early Post-rift

Offshore, the early post-rift began with a marine succession of limestones and shales, the Mtumbei limestone equivalent, Makarawe shale equivalent and the Kizimbani shale equivalent. All middle Jurassic in age (Mahanjane & Franke, 2014).

The rest of the Early Post-rift Megasequnce is typified by high sedimentation rates throughout the Late Jurassic and Cretaceous, with the deposition of the Pemba, Macomia (onshore) and Mifume formations (Key *et al*., 2008).

The Pemba Formation lies above a Callovian/Oxfordian unconformity and in its entirety, stretches all the way from the Oxfordian (Late Jurassic) to the Albian (Early Cretaceous) and represents coastal progradation into an open marine environment (i.e. deltaic to shallow shelf settings) (Key *et al.,* 2008). The Lower Pemba Formation consists of Late Jurassic shallow marine sediments with deposition controlled by incipient rifting (Key et al., 2008). The Middle Pemba Fm is Earliest Cretaceous is age and comprises deltaic to open marine sandstones deposited during active seafloor spreading. The Upper Pemba fm. is assigned Mid Post-rift.

Mid Post-rift

The first unit of the Mid Post-rift is the Upper Pemba Formation fluvial to shallow marine shoreface sequence (Late Berremian – Albian) deposited during sea-floor spreading (Key et al., 2008).

Contemporaneous with the deposition of the Upper Pemba Formation in the east, the Macomia Formation (Aptian to Albian) was being deposited onshore, in the west of the basin as a high-energy reworked, proximal fluviatile sequence of sandstones and conglomeratic beds, deposited in a braided channel system (Key *et al.*, 2008). Some localised organic-rich mudstones suggest areas of lagoonal or lacustrine deoposition, with very little marine influence. Extensive kaolinisation suggest a hot and humid paleoclimate (Key et al., 2008).

Key et al. (2008) suggest that both the Macomia and Upper Pemba Formations were deposited as the result of renewed rifting in the Rovuma Basin and extensive inland erosion, which continued throughout the Late Cretaceous, and fed the sandstone beds in the west.

The Mifume Formation (Upper Cretaceous: Cenomanian to Maastrichtian) is separated from the underlying Pemba formation by a diachronous angular unconformity and marked change in lithology. It consists of a uniform sequence of strongly bioturbated marls/clays deposited during a widespread Late Cretaceous marine transgression which affected most of eastern Africa, in a continental margin/shelf and slope environment (Key *et al*., 2008).

Late Post-rift

Following the thick successions of the Cretaceous, the Cenozoic was marked by reduced sedimentation rates (Key *et al*., 2008). The shallow water carbonates and coastal sediments of the Alto Jingone and Quissanga Formations with a reefal facies along the outer edge of the shelf, were deposited during this time, Paleocene and Eocene (Key *et al*., 2008). According to Key et al. (2008) sedimentation throughout the Cenozoic was accompanied by active faulting but the relative thinness of the Alto Jingone and Quissanga Formations suggests there was little movement (Key *et al*., 2008).

Modern Margin

The Rovuma basin also experienced an early Oligocene unconformity associated with the development of the East Africa Rift System (EARS). Key *et al.,* (2008) suggest that the renewed rifting along the EARs at ~35Ma not only produced the unconformity but also initiated delta progradation in the Rovuma basin, which was then followed by a Miocene transgression. The Modern Margin Megasequence consists of three formations which are lateral facies equivalents of one another. Onshore, the continental sandstones of the Chinda Fm were deposited in alluvial to possibly estuarine environments during Neogene uplift. On the shelf, shallow

marine/estuarine sandstones, with basal conglomerate beds overlying an unconformity, and unconsolidated red sand bars of the Mikindani Fm were deposited. Offshore, the Rovuma Delta Complex consists of a thick, eastward prograding wedge of Cenozoic fluvial deltaic deposits (continental and paralic clasts) to shallow-water marine and deep-marine strata that overlie unconformably the interface of Palaeocene–Eocene successions (Key et al., 2008; Salman and Abdula, 1995).

Since the Oligocene and the development of the East African Rift System, sediment loading and tilting of the hinterland led to the formation of the Rovuma Deep-Water Fold-and-Thrust Belt (fig. 3.11). The DWFTB formed by gravity-driven deformation above a detachment unit that is most likely under-compacted and over-pressured shale of Early Cenozoic age (Mahanjane & Franke, 2014).

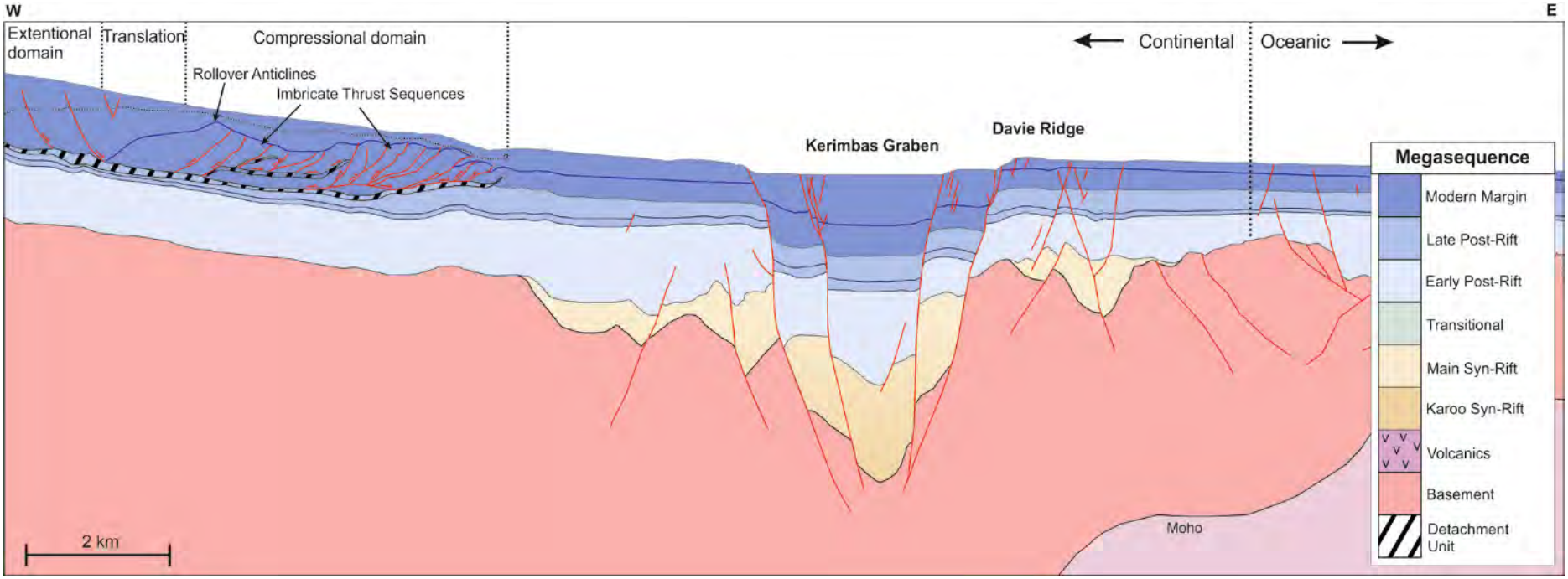

Figure 3.11: Regional cross-section of the Tanzania-Mozambique continental margin showing regional structures and megasequences in a W-E transect through the Rovuma Basin (modified from Mahanjane & Franke, 2014; Franke et al., 2015).

3.3.3. Madagascar Basins conjugate to East Africa

More than 180 Ma Madagascar was in the middle of Gondwana, betwixt Africa and India, which formed the southern portion of the supercontinent Pangea (see fig 3.4 183-177 Ma reconstruction). Connected in the east to India, Antarctica to the south and Africa to the west. During breakup (described by Tuck-Martin *et al.,* 2018) 5 coastal basins formed around Madagascar, with three of these situated on the west coast, conjugate to East Africa; the Ambilobe basin (sometimes called the Diego or Antsiranana Basin), the Mjunga (Majunga) Basin and the Morondava basin (fig. 3.12). These three basins have a similar geological history and a similar evolution during the breakup of Gondwana. On the east coast is the narrow, linear East coast basin and in the south, is the Cap St. Marie basin. These two basins are not discussed here because they have a different evolution history. For detailed stratigraphic descriptions of the EA-MAD marginal sedimentary basins see Appendix F.

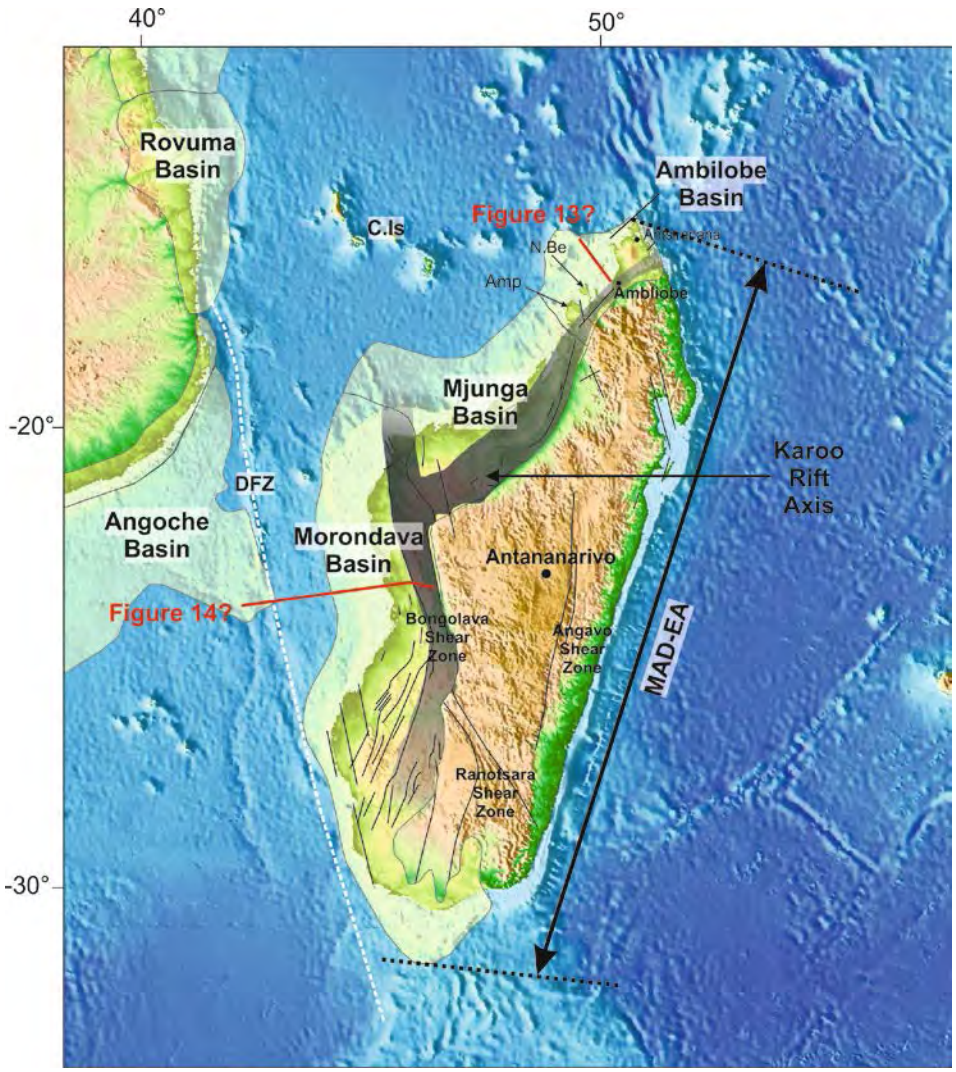

Figure 3.12: Regional overview of the West Madagascan continental margin belonging to the East African conjugate margin segment, showing the location of respective sedimentary basins and regional structural elements (Modified from Giger et al., 2004; Emmel et al., 2006; Clark, 2008; Papini & Benvenuti, 2008; Zhou et al., 2013).

3.3.3.1. Ambilobe

The Ambilobe Basin (also called the Diego Basin or Antsiranana Basin), is located on the northwest corner of Madagascar and covers both onshore and offshore.

The stratigraphic information available in the public domain at the moment describes the onshore or very shallow offshore sediments and very little is known about the offshore stratigraphy. The stratigraphy described below has mostly been gathered from Coffin & Rabinowitz (1988) and Papini & Benvenuti (2008). Papini & Benvenuti (2008) in turn updated and refined the work of Rerat (1964) and Besairie & Collignon (1972).

Karoo Syn-rift

Similarly to the basins along East Africa, the sedimentary basins of Western Madagascar also begin their stratigraphic record with 'Karoo' sediments. According to Coffin and Rabinowitz (1988) the basement through the upper Triassic of the Ambilobe Basin bares similarities to the Sakamena Group of the other Madagascar basins, although there is no mention of the Sakoa group, which is only present in the Morondava basin of Madagascar further south. There is an angular unconformity between Late Permian and Early Triassic due to vertical crustal movement (Coffin & Rabinowitz, 1988) during Karoo rifting.

Although Karoo rifting was intracontinental and never reached breakup, it was sufficient to allow marine incursions through the Permian and Early Triassic, accompanied by the deposition of Upper Permian and Early Triassic shales. Another unconformity separates these marine sediments from overlying continental sandstones of the Isalo Formation (Coffin & Rabinowitz, 1988) deposited in alluvial fan and fluvial environments until the earliest Jurassic (Papini & Benvenuti, 2008). It is possible salt was deposited at this time (Clark 1998) in a more basinward direction.

Main Syn-rift

At the end of the Early Jurassic, an early Toarcian regional transgression caused a dramatic facies change (Coffin & Rabinowitz, 1988) and the following successions of the Main Syn-rift megasequence were deposited unconformably on Karoo deposits (Wescott & Diggens, 1998).

Significant tectonic activity during the Late Toarcian – Early Aalenian, produced two asymmetric sub-basins bounded by steep faults, the Ampasindava sub-basin to the SW and the Ankarana-Analamera sub-basin to the NE. The two sub-basins were separated by a major structural high just NE of Ambilobe and experienced different subsidence rates and depositional environments (Papini & Benvenuti, 2008).

The SW was a zone of strong subsidence and the first unit deposited here was Unit B (or Jangoa Limestone by Rerat (1964)), deposited on a mixed carbonate-terrigenous ramp. This unit marks an increase in marine influence from underlying continental Isalo sandstones (Papini & Benvenuti, 2008). In the NE, Unit 2 (Marivorahona Series and the Ankarabo Sandstone, Rerat, 1964; Besairie & Collignon, 1972) was deposited in a mixed carbonate – terrigenous ramp followed by fluvio-deltaic input. Both Units B and 2 are lower to middle Toarcian in age (Papini & Benvenuti, 2008).

In the SW, subsidence was more intense than the NE. Deposition of Unit C (or Ampasimena Fm according to Rerat, 1964) experienced an increase in marine influence, and represents a coastal plain and shallow marine environment of Toarcian to Aalenian age (Papini & Benvanuti, 2008).

During the Aalenian, Units 3 and 4 were deposited in the NE during more pronounced subsidence and block tilting. Both units were deposited on a mixed carbon-terrigenous ramp controlled by relative sea-level fluctuations (Papini & Benvenuti, 2008). A widespread marine transgression flooded to NE sub-basin at the Aalenian/Bajocian boundary (Papini & Benvenuti, 2008).

At the same time as the transgression in the NE, Unit D (Bathonian to Early Callovian) was deposited in the SW sub-basin. The unit rests on an unconformable, erosional boundary with the underlying Unit C (Papini & Benvenuti, 2008). Deposited under marine influence in an overall alluvial-coastal environment with some fluvial/floodplain settings. Mud volcanoes and fluid escape structures in Unit D suggest the basin was still tectonically active at this time. Deposition was controlled by high-frequency pulses in basin subsidence and increases in accommodation space due to tectonism (Papini & Benvenuti, 2008).

Papini & Benvenuti (2008) suggest that, in agreement with Geiger *et al.* (2004), effective separation of East Africa took place only from the Toarcian. This was preceded by a period of Permo-Triassic pre-Gondwana breakup rifting (Geiger *et al.*, 2004) and was followed by a subsequent drifting stage active from the Bajocian (post Gondwana breakup stage).

Early Post-rift

Following breakup, the SW sub-basin subsided more rapidly than the NE. In the NE, Unit 5 was the first Early Post-rift unit to be deposited which records numerous sea level fluctuations (Papini & Benvenuti, 2008). No evidence given to suggest the changes in sea level are related to tectonic activity (Papini & Benvenuti (2008). Unit 5 has been correlated by Papini and Benvenuti (2008) to the Bemaraha and Sakarha formations of the Morondava Basin further south, as described by Geiger *et al.* (2004). These formations are discussed in detail later, but Geiger *et al.* (2004) suggest they represent a post rift carbonate platform, suggesting a similar depositional environment for Unit 5.

In the SW the first units of the early post-rift megasequence are described by Papini & Benvenuti (2008) as Units E (Bathonian to early Callovian) deposited in fluvial channels incised in the floodplain and crevasse splays and Unit F (Callovian), deposited on a coastal plain (Papini & Benvenuti, 2008).

Throughout the Late Jurassic, the different deposition environments between the SE and the NW continued with sediments described by Coffin & Rabinowitz (1988). In the east, are interfingered marine and continental sediments, whilst in the west, epicontinental and marine sediments were deposited. By the early Cretaceous, sediments (upper Valanginian through upper Hauterivian) topped by an angular unconformity (Coffin & Rabinowitz, 1988).

Mid Post-rift

Above the end Hauterivian unconformity lies 600m of sandstone, which is in turn overlain by Lower Albian shale and Middle and Upper Albian marl (Coffin & Rabinowitz, 1988).

During the Upper Cretaceous, marl rich in microfauna was deposited in the Cenomanian followed by a sudden change to fossiliferous continental sandstone during the lower Turonian, contemporaneous with an important episode of volcanism as illustrated by the presence of trachyte in early Turonian conglomerates (Coffin & Rabinowitz, 1988).

By the late Turonian, marine conditions returned indicated by sandstone succeeded by shaly limestones. The unit stretches throughout the Senonian (comprising the Coniacian, Santonian, Campanian, and Maastrichtian Ages) (Coffin & Rabinowitz, 1988).

Late Post-rift

Paleocene aged rocks in the Ambilobe Basin are ambiguous. Dolomite at the base of the Eocene section may be Paleocene in age, however no sedimentary rock has been formally identified as Paleocene in the Ambilobe Basin (Coffin & Rabinowitz, 1988)

Two units have been identified as Eocene in age in the Ambilobe Basin, and lower unit of dolomite and basaltic tuff and an upper unit of karst limestone of Lutetian age. Volcanism was prevalent at this time with the eruption of alkaline intrusives in the western part of the basin (Coffin & Rabinowitz, 1988).

Modern Margin

Oligocene sediments are mostly missing in the Ambilobe Basin although there are indications of volcanic activity continuing from Eocene time (Coffin & Rabinowitz, 1988).

Miocene sediments lie unconformably above Eocene sediments, consisting of alternating layers of limestone, sandstone, and basaltic tuff (Aquitanian to Burdigalian), topped by lava flows of late Miocene age.

Pliocene sediments are missing from the Ambilobe Basin, although volcanism may have continued from the Miocene (Coffin & Rabinowitz, 1988). The Quaternary period was dominated by coastal dune and reef development; along with volcanism (basalt flows) that is probably continuous since Eocene time (Coffin & Rabinowitz, 1988).

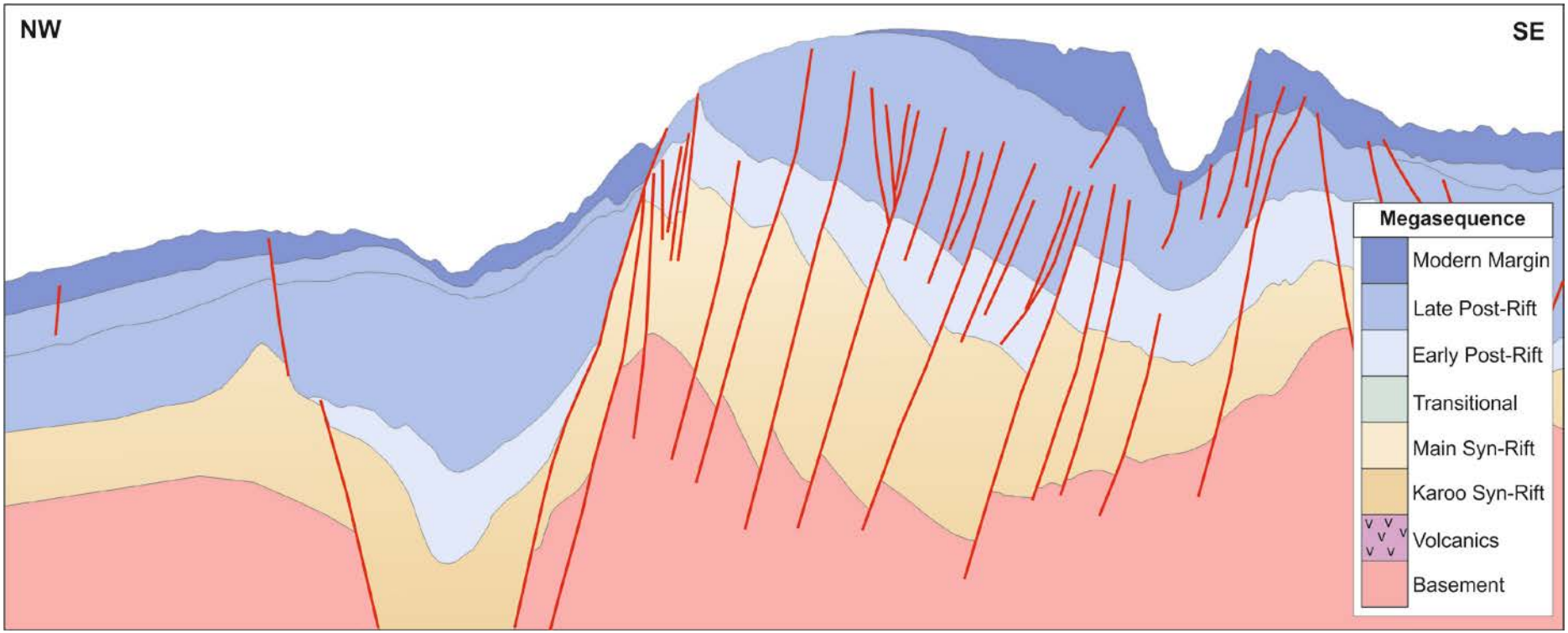

Figure 3.13: Regional cross-section of the West Madagascar continental margin showing regional structures and megasequences in a NW-SE transect through the Ambilobe Basin (modified from Dirkx, 2016. Exact location and scale are unknown).

3.3.3.2. Majunga

The Majunga Basin lies on the northwest coast of Madagascar and covers both onshore and offshore. There has been very little exploration in this basin with a total of 8 wells drilled, only 2 of which are offshore (Mariarano-1 & Mahajamba-1, 1971-72) (Spectrum).

The nature of the basin offshore varies from north to south. In the north there is a deep Karoo aged rift basin with well imaged horst and graben structures that were reactivated during the Jurassic rifting episode. In the middle there is a Jurassic aged salt basin, and in the south, there is a broad shelf with a steep slope down to the basin (Dirkx, 2016)

Stratigraphy is similar to the Ambilobe Basin to the north and the Morondava basin to the South and the information below has been gathered from Coffin & Rabinowitz (1988), Jeans & van Meerbeke (1995), Razafindrazaka et al. (1999) and Papini & Benvenuti (2008).

Karoo Syn-rift

The stratigraphy of the Majunga Basin again begins with the Karoo Supergroup, although it is not clear whether the first unit, the Sakoa Group, is present in the Majunga Basin. The Sakoa Group is absent in the Ambilobe Basin to the north, but present in the Morondava Basin to the south. If present, it has been described by Jeans and Meerbeke (1995) in combination with the Lower Sakamena group as thick sequences of fluvio-deltaic, coal swamp, and terrestrial immature clastics deposited in grabens during extensional faulting.

The Sakamena Group (Late Permian/Early Triassic) can be subdivided into 3 units (Razafindrazaka et al., 1999). The Lower Sakamena Group has already been described above. The Middle Sakamena group consists of (Upper Permian to Early Triassic) bituminous argillites and limestones (Razafindrazaka et al., 1999), deposited as tectonic movement slowed during the Upper Permian, and record a marine incursion (Jeans and Meerbeke, 1995). The Upper Sakamena group records a return to continental conditions with the deposition of predominantly fine red, cross-laminated sandstones (Razafindrazaka et al., 1999).

Above a weak angular unconformity (Razafindrazaka et al., 1999) lies the Isalo Formation (Lower Jurassic). The Isalo Formation varies from continental fluviatile, cross-bedded sandstones (Razafindrazaka et al., 1999) with local flood plain shales (Jeans and Meerbeke, 1995) at the base (Isalo I) followed by increasing marine influence in the Middle Isalo II Fm, topped by Isalo III: lagoonal and marine beds intercalated with terrestrial sandstone (Razafindrazaka et al., 1999). At this time, it has been suggested that salt was deposited in the Ambilobe Basin to the north (Clark, 1998), so it is possible that the salt in the Majunga Basin was also deposited at this time.

Main Syn-rift

During the Early Jurassic times, the old NE-SW and N-S Karoo trends were re-activated by the onset of rifting of the Somali Basin (Jeans & Meerbeke, 1995). As a result, the Main Syn –rift megasequence was deposited, the Beronono Formation, which is described by Geiger (2004) as the lateral equivalent to the syn-rift Andafia Formation in the Morondava Basin further south. By correlation to the Andafia fm. we assume the Beronono Fm. consists of shallow-marine marls, sandstones and shales aged Toarcian to Aalenian (Geiger et al., 2004; Clark, 1998).

Early Post-rift

By the end of the Middle Jurassic, the West Madagascan Margin was covered by shallow-water carbonate platforms which most likely extended to the Majunga Basin. Razafindrazaka et al., (1999) describe open marine facies comprising marls, limestones (Ankara and Kelifely Limestones) and argillites.

A major Upper Jurassic transgression flooded the carbonate platform and led to the deposition of marine clastics, limestones, marls and clays often containing glauconite or gypsum during the Late Jurassic reflecting post-rift subsidence (Coffin & Rabinowitz, 1988; Jeans & Meerbeke, 1995). Marine deposition continued into the earliest part of the Cretaceous (Neocomian) (Coffin & Rabinowitz, 1988).

Mid Post-rift

The deposition of the Mid Post-rift megasequence marks a change from open marine conditions of the Early Post rift to predominantly continental conditions during the Hauterivian and Aptian times, with Hauterivian continental cross-bedded sandstone followed by a predominantly continental Aptian section with several marine horizons (Coffin & Rabinowitz, 1988).

The Albian marks a return to marine conditions with shale and marl rich in fossils (Coffin & Rabinowitz, 1988) following an Aptian transgression (Razafindrazaka et al., 1999).

In the Cenomanian, marine conditions prevailed in the northern parts of the basin, but to the south conditions reverted to continental once more with the deposition of the Ankarafantsika sandstones (Coffin & Rabinowitz, 1988).

Late Post-rift

A major Turonian unconformity marks the start of the Late Post-rift, accompanied by widespread basaltic magmatism, including subaerial lava flows and extrutions in lacustrine and marine environments (Coffin & Rabinowitz, 1988). Magmatism is linked to the separation of India/Seychelles from Madagascar in the east (Coffin & Rabinowitz, 1988; Jean & Meerbeke, 1995; Razafindrazaka et al., 1999) and continued into the Campanian, whilst accompanying uplift of the hinterland resulted in a long period of deltaic – fluviomarine clastic progradation. Uplift and

tilting of the Madagascan mainland continued throughout much of the tertiary (Jeans & Meerbeke, 1988).

The lava flows were followed by predominantly continental sediments from the Conacian to Campanian, with some thin, well-defined marine intervals deposited in a lagonal environment (Coffin & Rabinowitz, 1988). Fully marine conditions became established again during the Maastrichtian with a unit of fossiliferous marly limestone or chalky marl that persisted through to the Eocene (Coffin & Rabinowitz, 1988). Offshore, the Maastrictian is usually missing and middle to upper Eocene sediments rest unconformably on Coniacian through Campanian marine marls (Coffin & Rabinowitz, 1988).

Onshore, Paleocene sediments are predominantly marine, commonly topped by a layer of red clay (Coffin & Rabinowitz, 1988; Razafindrazaka et al., 1999), whereas, offshore, the Epoch is represented by calcareous shale (Coffin & Rabinowitz, 1988).

The Eocene begins with fossil-rich Ypresian age limestone and marl, with sandy horizons (Coffin & Rabinowitz, 1988; Razafindrazaka et al., 1999). Offshore, the middle and upper Eocene sediments, including marl and limestones lie unconformably above Campanian marl or above Paleocene shale. Deposition of the Eocene sediment likely continued into the early Oligocene (Coffin& Rabinowitz, 1988).

Modern Margin

An Oligocene unconformity separates the Late Post-rift and the Modern Margin megasequences. Miocene sediments have been recognised along the shore of the basin as marine marls and limestone rich in fossils (Razafindrazaka et al., 1999; Coffin & Rabinowitz, 1988). Offshore, lower Miocene dolomite and limestone lie unconformably over mid-Oligocene sediments (Coffin & Rabinowitz, 1988).

A regression during the Pliocene led to the deposition of continental cross-bedded sandstones intercalated with silty clay or rare sandy lacustrine limestone, followed by Quaternary alluvial deposits (Coffin & Rabinowitz, 1988).

3.3.3.3. Morondava Basin

The Morondava Basin covers the southwestern coast of Madagascar, both onshore and offshore.

Karoo Syn-Rift

Stratigraphy begins with the Karoo syn-rift megasequence (Late Carboniferous to Late Triassic) including the Sakoa Group, the Sakamena Group and the Isalo Formation. The Sakoa Group is mainly continental, deposited in a range of environments including lacustrine, swamp, alluvial fans and stream deposits with possible, with rare marine incursions (Wescott & Diggens, 1997). Greater marine influence in the Sakamena Group resulted in the deposition of sediments in a

variety of environments including marine, fluvio-deltaic and lacustrine at the base to shallow marine, shoreface, deltaic and fluvial at the top (Wescott & Diggens, 1997; Geiger et al., 2004). The Sakamena Group is topped by continental fluvial channel and braided stream sandstones of the Isalo Formation (Geiger et al., 2004).

Clack (1998) describes the Morondava Basin as two tectonic provinces: 1) a western passive margin and 2) an eastern Permo-Triassic failed rift, the "Karoo" rift (fig. 3.12). When Karoo rifting failed, the extension centre shifted to the west, leading to break up and continued development of the Morondava basin. As a result, the two provinces may have different histories and different play types (Clark, 1998). If this is the case then Karoo sediments may be missing in the west of the basin and offshore, including the Sakamena source rock.

Main Syn-Rift

The Main Syn-rift megasequence has been identified as the Andafia Formation (Toarcian-Aalenian) separated from underlying Isalo sandstones by an erosional unconformity. Mainly shallow marine marls and shales, the formation shows typical features of being syn-rift in seismic, borehole and outcrop data, show it forms wedge-shaped bodies in half-grabens and that the Andafia sediments onlap tilted and roatated Isalo sandstone fault blocks (Clark, 1998). The Andafia formation is the lateral equivalent to the Beronono formation of the Majunga basin (Geiger et al., 2004)

Early Post-Rift

Early post-rift begins in the Bajocian to Bathonian with shallow water carbonate platform sediments of the Bemaraha formation and the coastal plain sediments of the Sakaraha formations, lying unconformably over the Andafia formation. Both formations have been removed by erosion in the north (Geiger et al., 2004).

A period of forced regression followed and the deposition of sandstones of the Ankazoaba and Sakanavaka formations during the late Bathonian stage (Geiger & Schwelgert, 2006). An erosional unconformity separates the sandstones from the underlying carbonates of the Bemaraha and Sakaraha formations (Geiger et al., 2004).

The term Duvalia has been used to refer to a number of different sequences of various ages. It was originally applied to Early Cretaceous mudstones (Valangian – Hauterivian) by Besairie & Collignon, 1972 and Coffin & Rabinowitz, (1988). Some authors also include Middle to Late Jurassic sediments as well as Early Cretaceous sediments under the name Duvalia (Geiger, 2006). We use the term to refer to a sequence of marls of Late Jurassic age.

Early Cretaceous sediments are missing in the onshore, southern part of the Morondava basin. In the north they are present as dark marine shales, and/or continental sandstones overlain by marine shale. Offshore, the Early Cretaceous

consists of interbedded sand and shale with evidence of volcanic activity indicated by basaltic lava flows, pyroclastics, tuffs and ignimbrites (Coffin & Rabinowitz, 1988).

Mid Post-rift

Clark (1998) noted renewed tectonic activity in the basins of western Madagascar, including the Morondava Basin, during the Late Cretaceous. Expressed as wrench faulting and associated compressional folding it has tentatively associated with the lateral movements either along the Davie fracture zone or the Ile Sainte Marie lineament on the eastern side of Madagascar, as a result of the separation of India and Madagascar (Clark, 1998). Significant igneous activity continued throughout the basin from the Early Cretaceous into the beginning of the late Cretaceous, peaking during the Turonian (Coffin & Rabinowitz, 1988).

Thick, continental to marine sand of Cenomanian to Turonian age are present in the central and southern parts of the basin and grade rapidly offshore to shale. By the end of the Turonian, conditions were predominantly marine (Coffin & Rabinowitz, 1988).

Late Post-rift

In the northern Morondava Basin, Paleocene sediments are mostly missing and Eocene sediments lie unconformably above Upper Cretaceous sediments. In the southern and central areas marine sediments including limestone, dolomite and marl are present, with some shale in places (Coffin & Rabinowitz, 1988).

Eocene sediments consist of interbedded carbonate and shale sequence with evidence of minor volcanic activity, and shallow-water marls in the offshore central part of the basins (Coffin & Rabinowitz, 1988).

Modern Margin

Once again, Oligocene sediments are missing from the northern part of the basin, but are present as marine limestones, shales and marls present in the south. Shallow marine conditions continued for the rest of the Neogene, replaced by continental sandstones onshore and shales offshore during the Quaternary (Coffin & Rabinowitz, 1988).

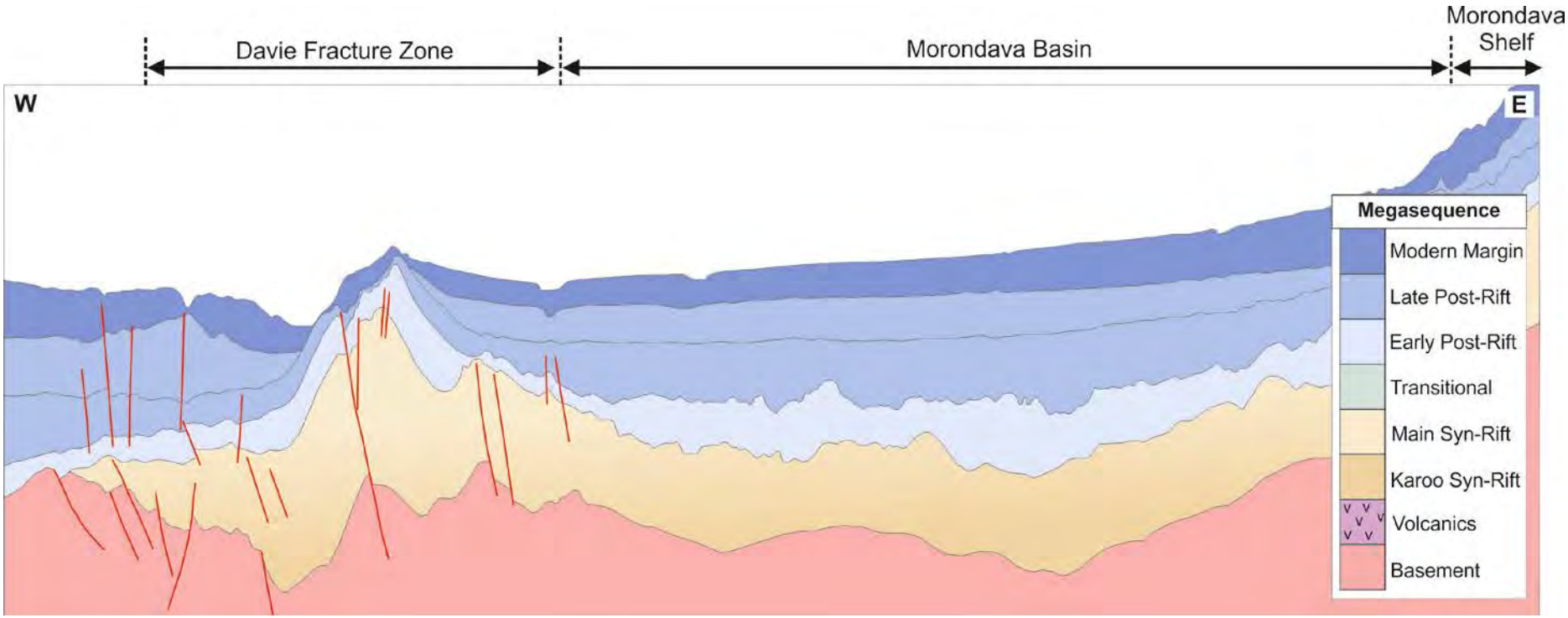

Figure 3.14: Regional cross-section of the West Madagascar continental margin showing regional structures and megasequences in a W-E transect through the Morondava Basin (modified from Dirkx, 2016. Exact location and scale are unknown).

3.3.4. East African Basins conjugate to Antarctica

In the 183-177 Ma reconstruction (fig. 3.4) Antarctica was joined to Africa and the basins on the East Africa margin conjugate to Antarctica is the Mozambique Basin

The Mozambique Basin covers central and southern parts of the Mozambique margin, both onshore and offshore including the margin shelf and slope (Salman & Abdula 1995). It varies considerably from north to south and can be subdivided further into three other basins whose evolution differs from one another. In the north is the Angoche basin, then the Zambezi Delta Depression, and then to the south you have what we call the Southern Mozambique Basin (fig. 3.15).

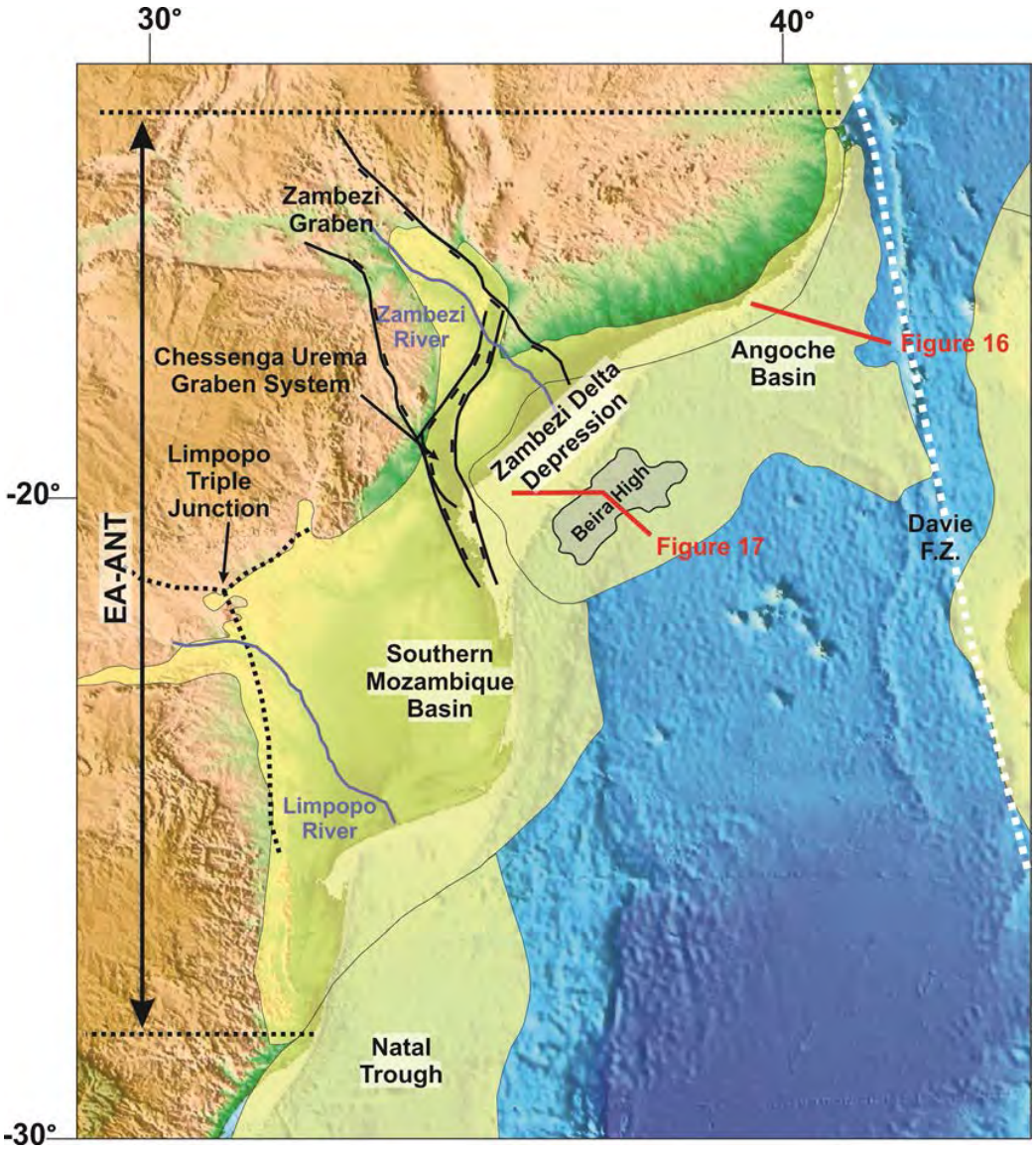

Figure 3.15: Regional overview of the East African continental margin conjugate to the Antarctica margin segment, showing the location of respective sedimentary basins and regional structural elements (Modified from Mahanjane, 2014; Salazar et al., 2013; Mahanjane 2012; Zhou et al., 2013).

Significant work has been carried out on these basins in recent years, and stratigraphic information comes from Salman & Abdula (1995), Mahanjane et al. (2014), Mahanjane (2014), Mahanjane (2012), Salazar et al. (2013). For detailed stratigraphic descriptions of the EA-MAD marginal sedimentary basins see Appendix G.

3.3.4.1. Angoche Basin

The Angoche Basin lies offshore along the northern Mozambique Margin, bound to the northeast by a compressional zone associated with the Davie Fracture Zone (Mahanjane *et al.*, 2014), the west (landward) by the Angoche volcanic zone, a dyke swarm orientated ~ NE-SW forming part of the Karoo-Ferrar LIP ~180 Ma (Mahanjane, 2014), and to the southwest by the Beira high and the Zambezi Delta.

The stratigraphy of the Angoche Basin is not well known due to lack of well control, but is believed to be similar to the better understood/explored Zambezi Delta to the south and the Rovuma Basin to the north. Stratigraphic information has been gathered from Salman and Abdula (1995), Mahanjane et al., (2014) and Mahanjane (2014), who interpreted seismic reflection line and correlated it to regional stratigraphic information and wells from the Zambezi Delta and the Rovuma Basin.

Karoo Syn-Rift

Stratigraphy is believed to begin with Karoo sediments resting on precambian metamorphic basement, although they have not been recognised offshore. They have been found in onshore rifts, in the Lower and middle Zambezi Grabens, but it is unlikely they are present offshore (Mahanjane *et al.*, 2014).

If present it is likely the to be a sequence of continental, coaly sediments like the Dwyka, Ekka, and Beaufort series that are common across Mozambique and South Africa, and described further south (Salman & Abdula, 1995) see sections 3.3.4.2 and 3.3.4.3.

Main Syn-rift or Transitional

Main syn-rift sediments are not clearly recognised or described anywhere in the literature for the Angoche Basin. Mahanjane (2014) suggests that at this time the Angoche Basin was affected by strike slip deformation due to early movement of the Davie Fracture Zone and the Basins close proximity to it.

The middle Jurassic sediments are described by Mahanjane (2014) as shelf carbonates of the Mtumbei Lst and the Makarawe Shales, Bathonian to Bajocian in age (Mahanjane, 2014). Salman and Abdula (1995) correlated the Mid-Jurassic sediments of the Mozambiqian side of the Rovuma basin with the Makarawe Fm, Mtumbet LST, and Kizimbani Shale of the Tanzanian side. It is possible these sediments extend south into the Angoche Basin.

Mahanjane (2014) maps more than 1km of Middle Jurassic succession as post breakup, and correlated to the Makarawe Shale (Bajocian-Bathonian), and topped by what Mahanjane (2014) refers to as a 'drift onset unconformity' which marks the onset of seafloor spreading in the Mozambique ocean basin. So, these are interpreted as transitional sediments in this basin and that Main Syn-rift sediments are missing or have not been imaged.

Early Post-rift

The Upper Jurassic sediments of the Angoche Basin have subdivided into 3 units by Mahanjane (2014) J-Unit I and J-Unit III are both shale layers separated by a layer of paralic sandstone J-Unit II. The three units stretch from the Oxfordian up to and including the Tithonian, and are bound top and bottom by major unconformities. The basal unconformity has been referred to as the "drift onset" unconformity by Mahanjane (2014) and has already been discussed in the section above. The unconformity at the top of the J-Units marks the boundary between the Jurassic and the Cretaceous (Upper Jurassic Unconformity 145.5Ma, Mahanjane, 2014). The J-units were deposited as the Angoche Basin experienced a period of transpression and tectonic subsidence (Mahanjane, 2014).

Tectonic subsidence continued throughout the Neocomian with the deposition of shale and paralic sandstones (Pemba Fm. equiv.) which show good correlation with the Pemba formation of the Rovuma Basin (see section 3.3.2.5) and the Domo series of the Mozambique basins (see section 3.4.1.2.) (Mahanjane, 2014).

Mid Post-rift

The unconformity bounded Lower Domo Shale equivalent unit was deposited during the Barremian, Aptian, and Albian during a short-lived period of tectonic uplift following the end of movement of the DFZ (Mahanjane, 2014). Further south in the Mozambique Basin the Domo shale is regarded as a potential sources rock, dark grey to black, thinly bedded, marly shale (Nairn et al., 1991).

Above a major top Albian unconformity is a unit of paralic sandstone with deposited during a marine regression during the Cenomanian and Turonian called the Domo Sand equivalent (Mahanjane, 2014). Mounded patterns within the sandstones suggest slope fan or basin floor fan deposits (Mahanjane, 2014), similar to the Domo sandstones in the south (Salman & Abdula, 1995).

Conformably above the Domo sandstones is a unit of shales (Coniacian – Santonian) correlated with the Upper Domo Shale further south in Mozambique (Mahanjane, 2014). The final unit of the upper Cretaceous is the Lower Grudja Equiv. (Campanian, Maastrichtian) described as a unit of shale deposited in slope and basin floor fans in the lower half, and passing up into deep-water marly-shale in the top half (Mahanjane, 2014).

Late Post-rift

Another major unconformity at the top of the Lower Grudja equivalent unit marks the Cretaceous-Tertiary boundary and the change to Late Post-rift deformation. According to Mahanjane (2014), the unconformity formed during the late Cretaceous due to erosion associated with a major regression.

The Paleocene and Eocene sediments were deposited during tectonic quiescence, and consist of a sequence of deep-water sediments typical of a passive margin such as shales, siltstone, marls and limestones with slope and basin floor fans. Eocene sediments consist mainly of shale with slope and basin floor fans topped by a major regional unconformity at the Eocene/Oligocene boundary (Mahanjane, 2014)

Modern Margin

Above the Oligocene unconformity, sediments were deposited contemporaneously with activity of the East African Rift System (EARS) in the west. Sediments include a series of limestones, shaly siltstones with basin floor fans in the south. During the Miocene paralic and channel fill sandstones were deposited followed by Pliocene limestones and Quaternary shallow water and shelf terrigenous sediments (Mahanjane, 2014).

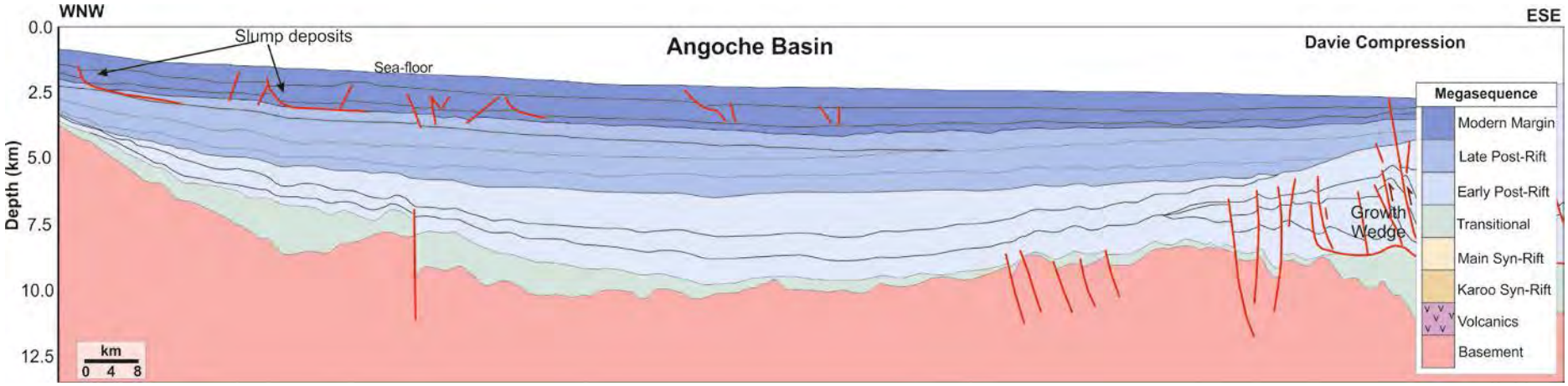

Figure 3.16: Regional cross-section of the East Africa continental margin showing regional structures and megasequences in a WNW-ESE transect through the Angoche Basin (modified from Mahanjane, 2012. For cross-section location see fig. 3.15).

3.3.4.2. Zambezi Delta Depression

The Zambezi Delta Depression lies offshore Mozambique at the mouth of the Zambezi River, bound to the west by the Limpopo triple junction and to the east by the Angoche Basin (fig. 3.15). Also includes the Beira high and the outer Beira high which acted as a barrier to sedimentation until the Early Tertiary when it finally became buried by sediments (Hollebeek et al., 2016).

Mahanjane (2012) suggest the breakup between Mozambique and Antarctica and the formation of the Zambezi Delta Depression / Basin occurred in two stages. Rift Stage 1 created a narrow v-shaped failed rift within the Zambezi Delta Depression itself, containing thick lava flows. Then Rift stage 2, were the rift axis jumped to the outer eastern edge of the Beira High and eventually led to breakup.

Sedimentary fill consist of Upper Jurassic, Cretaceous and Cenozoic rocks discordantly overlying Karoo rocks (Salman & Abdula 1995). Stratigraphic information has been gathered from Salman & Abdula (1995), Salazar et al (2013), Mahanjane (2012) and Mahanjane et al. (2014). The cross-section in 3.17 was modified from Mahanjane (2012).

Karoo Syn-rift

The presence of Karoo sediments in the ZDD is difficult to ascertain. Salazar et al (2013) recognise a thick sedimentary sequence that stretches deeper than imaged by the currently available seismic data that exhibits active fault growth that could be Karoo. Within the deepest parts of the ZDD is a thick layer of lava flows which are limited on both sides by normal faults, as a result the sediments below the lava are difficult to image (Mahanjane, 2012). However, Mahanjane (2012) identifies a thick, tilted pre-rift unit on the outer Beira High, between the continental basement and the rift unit, which is likely Karoo sediments.

The lava flows only occur within one stratigraphic level, at the breakup unconformity reflection, which suggests they are associated with the end of rifting (Mahanjane, 2012) and are mainly concentrated in the in the southwest ZDD (Salazar et al, 2013). It is reasonable to assume that Karoo sediments lie under here if this was the centre of rift-phase I according to Mahanjane (2012), and if the volcanics are associated with the Karoo-Ferrar LIP at the end of the Karoo rift phase. They may be part of the Stormberg series described by Salman and Abdula (1995) for the rest of Mozambique.

Prominent rotated fault blocks are visible in the seismic, in the basement of the outer Beira High. The fault planes mostly lie parallel to the coast in a NE-SW direction suggesting a south easterly extension direction (Mahanjane, 2012).

Main Syn-rift

According to Mahanjane (2012), rift phase II involved a rift "jump" to the Southeastern edge of the Beira High, and the deposition of two syn-rift units on the outer, eastern Beira High which we assign to the Main Syn-rift Megasequence. Syn-rift I is a unit of Bajocian aged shale and Syn-rift II consists of Bathonian shallow water and shelf terrigenous rocks (Mahanjane et al., 2014).

The outer Beira high is strongly faulted and the Syn-rift units exhibit a wedge-shaped geometry separated by a distinct unconformity. Listric normal faults have cut and tilted the pre-rift succession into asymmetric half-grabens, the orientation of which suggests extension in a southeast direction (Mahanjane, 2012).

Transitional/breakup

Sag sediments have been recognised by Mahanjane (2012) on the outer edge of the Beira High (Mahanjane 2012) comprising paralic sandstones of Oxfordian age, followed by the Breakup unconformity at approximately 155 Ma (Mahanjane et al., 2014)

Early Post-rift

The Early Post-rift stratigraphy begins a Tithonian to Kimmeridgian aged succession (Salman & Abdula, 1995; Mahanjane et al., 2014) of continental sandstones of the Lupata Formation in the west and its offshore equivalents in the east, ancient deltaic clays and marine shale (Mahanjane et al., 2014). The Lupata Fm is equivalent to the Red Beds Fm further south, described in section 3.4.3 (Salman & Abdula, 1995).

During the Neocomian the Maputo Formation equivalent was deposited in the Zambezi Basin as predominantly marine sandstones, limestones, shale (possible source rock), and volcanics (Mahanjane, 2012).

The Sena Formation is found onshore in the central and northernwest parts of Mozambique and is particularly widespread in the Lower Zambezi Graben (Salman & Abdula, 1995). It is Lower Cretaceous to Cenomanian in age (Salman & Abdula, 1995; Mahanjane et al., 2014) and comprises a continental sequence of fluvial and alluvial sandstones, conglomerates and argillites enriched with coaly detritus (Salman & Abdula, 1995).

Unconformably above the Sena Formation is the Barremian to Albian aged Lower Domo Shale formation (Mahanjane et al., 2014). In the west, it consists of dark marine argillites and arkose sandstone. To the east it grades into continental slope and rise sediments with widespread fan complexes (Salman & Abdula, 1995) and eventually deep marine shale (Mahanjane et al., 2014).

Mid Post-rift

Above an erosional unconformity lies the first unit of the Mid Post-rift, the Domo Sandstone Formation which consists of paralic sandstones deposited during a marine regression during the Cenomanian to Turonian (Salman & Abdula, 1995; Mahanjane et al., 2014). It consists of primarily quartzose sandstone, interbedded with dark argillite. Towards the south and the east the sandstones become increasingly replaced by argillites (Salman & Abdula, 1995).

A conformable boundary separates the Domo Sandstone Fm. from the overlying Upper Domo shale formation (Coniacian – Turonian) (Mahanjane et al., 2014).

At the top of the Mid Post-rift is the Lower Grudja Formation which shows a west to east facies change from continental sands and conglomerates in the west, to a thick layer of clay with bands of sandstone in the east, deposited as shoals and bars in a shallow water shelf environment. Further east still, the sandy bodies are replaced by thick shale deposited on a continental paleoslope (Salman & Abdula, 1995).

Late post-rift

The Cenozoic sediments of Mozambique display the features characteristic of a passive continental margin, i.e. progradation towards the outer edge of the paleoshelf and continental slope. The late post-rift consists two formations. The Upper Grudja Formation (Paleocene) is of a sequence of glauconitic sand, clay and marl with bands of limestone resting on an erosional unconformity (Salman & Abdula, 1995). Unconformably above the Upper Grudja is the Cherigoma Formation which in the Zambezi, comprises limestones with bands of clay and calcareous sandstones deposited of the shelf slope or fore reef (Salman & Abdula, 1995). Towards the east the limestones are replaced by basin floor fans and deep-water marl/shale deposits (Mahanjane et al, 2014) and underwater slumping processes (Salman & Abdula, 1995).

Modern Margin

Since the Oligocene to the present day the Modern margin phase of deposition in the ZDD has been dominated the Zambezi Delta, the largest delta on the east coast of Africa, which is fed by the Zambezi, Punge and Buzi rivers (Salman & Abdula, 1995). The Zambezi Delta complex consists of interbedded conglomerate, sand and clay. The rate of sedimentation far exceeded the rate of subsidence so the delta prograded to the east (Salman & Abdula, 1995).

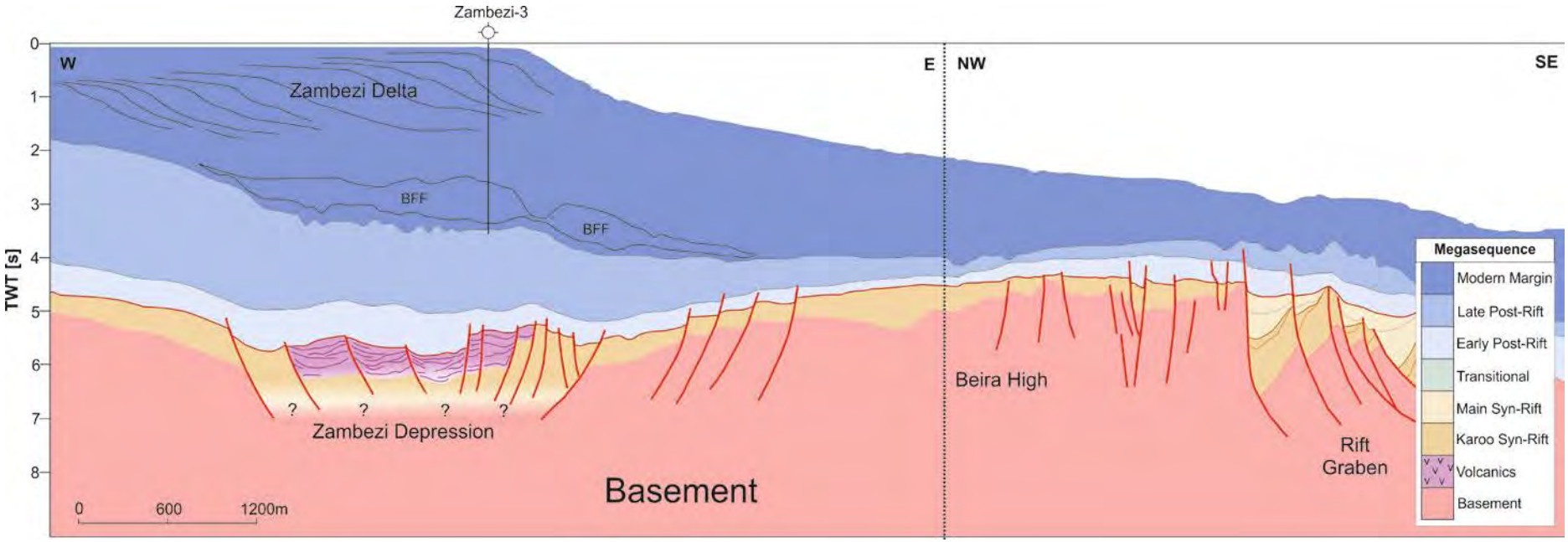

Figure 3.17: Regional cross-section of the East Africa continental margin showing regional structures and megasequences in a ~W-E transect through the Zambeze Delta Depression and the Beira High (modified from Mahanjane, 2012. For cross-section location see fig. 3.15).

3.3.4.3. Southern Mozambique Basin

The Southern Mozambique Basin refers to everything south of the Zambezi Delta Basin, which includes the Limpopo Delta, and the area between the Zambezi and Limpopo Deltas.

Karoo Syn-Rift

The oldest sediments of the Southern Mozambique Basin are complex due to a higher level of volcanism in this area than the other basins along the margin. The presence of a Karoo Section below the Stormberg Lavas has been inferred by De Buyl & Flores (1986), and described by Salman and Abdula (1995). They consist of the terrigenous coal bearing Dwyka series. Next, is the shale, siltstone, and sandstone (De Buyl & Flores, 1986) of the Ekka Series, with widely developed seams of hard coal (Salman & Abdula), deposited contemporaneously with the Sakamena Fm in Madagascar. To the east, the Ekka series increases in marine character suggesting a possible marine incursion as early as the Middle Permian (De Buyl & Flores, 1986). Finally, is the Beaufort Series characterised by sandstone and shale (De Buyl & Flores, 1986) and containing a lot of coaly material dispersed throughout the series (Salman and Abdula, 1995; Nairn et al., 1991).

At the top of the Karoo section is a thick sequence of volcaniclastics, lava flows, and sandstones called the Stormberg Series which correlates with the Isalo Fm in Madagascar. The volcanics appear to underlie the plain of Mozambique (De Buyl & Flores, 1986).

Main Syn-Rift, Transitional and Breakup

The Main Syn-rift megasequence is no clear, there is nothing described in the literature that can be confidently assigned as Main Syn-rift. The Stormberg volcanic series continued into the Late Jurassic.

Early Post-Rift

The first unit of the Early Post-rift is the Upper Jurassic to Lower Cretaceous Red Beds formation which is resting on basalt. It is mainly continental in nature with increasing marine influence towards the east (De Buyl & Flores, 1986), indicated by a sandy clay layer deposited in an ancient delta. (Salman & Abdula, 1995)

A marine transgression at the beginning of the Cretaceous led to the deposition of the Maputo Formation (Neocomian) comprising a sequence of sandstones and limestones deposited in a shallow water environment by Salman & Abdula (1995). In the east, the Maputo clastics grade upwards into a lower Cenomanian sandstones characterised by local turbiditic facies and rich ammonitic fauna (De Buyl & Flores, 1986). Onshore the Maputo Fm grades to the northwest into the thick, continental Sena Formation (De Buyl & Flores, 1986), comprising fluvial and alluvial

formations: arkose sandstones, conglomerates and argillites enriched with coaly detritus (Salman & Abdula, 1995).

During the Aptian to Cenomanian the Lower Domo Shales Formation was deposited across the Central and Southern Mozambique Basin both onshore and offshore (Salman & Abdula, 1995) consisting of dark marine argillites with occasional sandstones beds, deposited in a pelagic environment and under anaerobic conditions (De Buyl & Flores, 1986).

The Maputo Fm and the Lower Domo Shales are the marine equivalent of the Sena Fm (Salman & Abdula, 1995). At the same time as the Red Beds Fm, Lupata Fm and the Sena Fm and its marine equivalents were deposited was also a time of intense volcanic activity, with volcanic lava flows along graben boundaries (Salman & Abdula, 1995).

Mid Post-Rift

The Middle Post-rift Megasequence lies above an erosional unconformity and consists of a self-contained cycle of sedimentation characterised by a consistent marine transgression, during the Upper Ceomanian to Maastrichtian (Salman & Abdula, 1995). It consists of three formations. First, the Domo Sands (Upper Cenomanian to Turonian) quartzose sandstone, interbedded with dark argillite, becoming more argillaceous towards the south and east, Second, the Upper Domo Shales (Turonian – Lower Senonian), a sequence of dense clays which grades into the continental Sena Fm in the northwest. Finally, the Lower Grudja formations (Campanian – Maastrichtian), a layer of clay with bands of glauconitic-quartzose sandstones deposited as buried shoals and bars in a shallow water shelf environment. Towards the east the sandstone beds are gradually replaced by a thick uniform layer of Upper Cretaceous shale, deposited on a continental palaeoslope. To the west the Lower Grudja grades into continental sands and conglomerates (Salman & Abdula, 1995).

Subsequent erosion resulted in truncation of the Lower Grudja Formation offshore (De Buyl & Flores, 1986) and its absence from the buried elevated areas and horsts in the southern parts of the basin (Salman & Abdula, 1995).

Late Post-Rift

The Late Post-rift megasequence lies above an erosional unconformity and consists of two units deposited in a predominantly shallow-water shelf environment. In the east these units are replaced by deeper-water formations of the continental slope (Salman & Abdula, 1995).

The first unit is the Upper Grudja Formation which comprises a sequence of glauconitic sand, clay and marl with bands of limestone. Above this is middle to late Eocene reefs of the Cheringoma formation, which comprises stacked nummulitic limestones and marl, with bands of clay and calcareous sandstone,

deposited on a shallow-water carbonate shelf. Eastwards it changes to deeper-water formations, which are calcarenitic and calcilutitic and formed in along the continental slope and rise. A chain of reef massifs lies along the outer edge on the shelf (Salman & Abdula, 1995).

Modern Margin

An unconformity separates the Late Post-rift from the Modern Margin Megasequences. In central Mozambique, sediments deposited were not influenced by the Zambezi or Limpopo deltas and consist of a sequence of shallow-water shelf deposits, mainly Miocene in age and consists of the three formations. The Inharrime consists of red dolomite, red clay and sandstone with bands of anhydrite deposited in a restricted lagoonal environment. In the central part there exists a thick gypsum bearing sequence called Temane Formation. Above the Inharime formation is the Jofane formation, a unit of marine carbonate including limestones, calcarinite and arenaceous limestone (Salman & Abdula, 1995).

To the south the above formations are replaced by the Limpopo Delta which was deposited predominantly in the coastal plain and formed a sub-areial delta and exhibits a noticeable reduction in the amount of terrigenous material (Salman & Abdula, 1995)

The Pliocene deposits were deposited during extensive marine regression in predominantly continental environments such as ancient dunes, river terraces and lakes. Marine sediments were deposited along the modern shelf and reach maximum thickness further north in the Zambezi Delta (Salman & Abdula, 1995).

3.4. Tectono-stratigraphic correlation of East Africa & Madagascar margin basins: Basin Fill versus Plate Kinematic Model

Based on the basin summary presented in section 3.3 and the plate-kinematic model presented in Tuck-Martin et al. (2018), we present margin-scale synthesis of sedimentary basin formation of the East Africa-Madagascan conjugate margins utilising a series of paleodepositional maps alongside platekinetmatic stress maps (Figs. 3.18 – 3.22) and margin-scale tectonostratigraphic synthesis (Figure 3.5). We also present a series of paleodepostional maps alongside the plate kinematic maps (with qualitative stress analysis).

We discuss the Karoo rifting events and the deposition of the Karoo megasequence followed by the four tectonic phases identified in Tuck-Martin *et al.* (2018). For each phase, we discuss the following:

- The link between the important/major unconformities and plate-tectonic processes and events derived from the plate model. Are they related to major tectonic changes or could they be due to sea level changes
- Regional uplift and tectonic inversion events linked to changes in the plate tectonic stress regime.

- We also describe the orientations and relative magnitudes of regional tectonic stresses with reference to re-organisations of the first-order plate-scale paleostress field for each tectonic phase and its predicted effect on the tectonic development of the conjugate East African and West Madagascan margins based on the concepts described in section 3.2.4.
- What is the effect diachronous opening of margin segments as seen in the plate tectonic model of the basin fill and timing of rifting and breakup in regional basins?
- Correlation of regional tectono-stratigraphic elements between conjugate margin sedimentary basins

3.4.1. Karoo

The present-day sedimentary basins along the East Africa and West Madagascar continental margins likely all began their life during the intermittent intracontinental "Karoo" rifting events that occurred from late Carboniferous to the Early Jurassic times. The main Karoo Basin was located in South Africa, but isolated or segmented Karoo rift basins and associated syn-rift depocenters likely occurred along the future conjugate margins of East Africa and Madagascar, reaching as far north as Somalia.

Karoo rifting was controlled by flexural subsidence mechanisms in the south related to subduction and orogenesis along the paleo-Pacific margin, and extensional processes in the north, related to the divergent Tethyan margin (Catuneanu *et al.,* 2005). As a result, a series of discrete, linear NE trending rifts formed along the future margins of East Africa and West Madagascar which followed the regional tectonic trends and inherent structures of the Precambrian basement (Catuneanu *et al.,* 2005). Across East Africa and Madagascar, sinistral strike-slip movement created a number of smaller north to northwest trending pull-apart basins (Catuneau et al., 2005; Schandelmeier *et al*., 2004; Wopfner et al., 1993).

These rifting events failed to initiate the breakup of Gondwana and culminated in the early Jurassic eruption of the Karoo Large Igneous Province (Fig. 3.4) within the time period 183-177 Ma (Cox, 1992; Jourdan *et al.*, 2005).

Along the future East African and West Madagascan Continental Margins, the Karoo sediments were predominantly continental in nature and deposited unconformably on top of the metamorphic basement. Some marine incursions from the Tethyan Ocean in the North occurred, and reached as far south as Madagascar (Wopfner, 1991).

Along the future EA-IND margin segment (in Somalia) the Karoo rifting formed a series of segmented basins, such as the Somali Coastal Basin, separated by structural highs e.g. the Bur-Acaba, the Nogal and Hargesya-Ergavo uplifts (Mbede & Dualeh, 1997). The Somali Coastal Basin trends in a NE – SW direction parallel to

the margin and is bound to the north by a major NE –SW fault (Mbede & Dualeh, 1997). Karoo sedimentation across most of Somalia is documented by the continental Adigrat Sandstones (Bosellini, 1992).

Along the EA-MAD margin segment, Karoo sedimentation was a mix of peri-glacial, lacustrine and deltaic sediments (Rais-Assa, 1998) in the Lamu Basin and fluvial systems, flood plains, deltas, swamps, lakes (Mbede & Dualeh, 1997) in the Ruvu Basin of northern Tanzania. In the south of Tanzania the Karoo of the Mandawa Basin begins with continental sediments but turns into restricted marine evaporites and shallow/marginal marine sediments indicating marine incursions most likely from the Tethys in the Northeast in the rift basins. The marine influence is also documented in the conjugate basins of Madagascar (MAD-EA). The Sakamena Formation of the Morondava Basin documents marine influence in the Upper Permian – Triassic (Wescott & Diggens, 1997; Geiger, 2004).

Further south (EA-ANT), the sedimentary basins of Mozambique are much closer to the "centre" of Karoo rifting and the Karoo-Ferrar mantle plume. As result the Karoo sediments are similar to those of the Main Karoo Basin in South Africa including the continental Dwyka, Ekka and Beufort series and the end of the Karoo phase is marked by considerable volcanic activity, topped by the sequence of volcaniclastics, lava flows, and sandstones of the Stormberg series.

3.4.2. Synthesis Phase 1 – Starting at 183–177 Ma: Separation of East and West Gondwana Figures 3.18 & 3.19

The first plate tectonic phase involves the separation of East (consisting of Madagascar, the Seychelles, India, East Antarctica and Australia) and West Gondwana (consisting Africa and South America).

The eruption of the Karoo–Ferrar volcanics within the time period from 183 – 177 Ma (Cox, 1992; Jourdan *et al*., 2005) marks the end of the Karoo rifting events and differentiates it from a separate phase of rifting which we identify as the Main Syn-rift phase, which finally led to the breakup of Gondwana. In some basins the distinction between the two different rifting phases is clear, illustrated by both structure and stratigraphy. Whilst earlier Karoo rifts followed the regional tectonic trends and inherent structures of the Precambrian basement (Catuneau et al., 2005), rifts associated with the main syn-rift phase may not have followed the same trends in all basins. For example, in the Morandava Basin (Madagascar), Clark (1997 and Geiger et al. (2004) suggest that after the end of Karoo rifting, the rift axis migrated west, leaving an older Karoo aged rift graben onshore to the east, whilst younger Jurassic rifting relocated to the Davie Fracture Zone to the west. In the Rovuma Basin, Key *et al.* (2008) identified that the later syn-rift basins (aka. main syn-rift basins in the terminology of this paper) were superimposed discordantly over the earlier Karoo rift basins. Stratigraphically, the Madagascan basins show a clear distinction between the Karoo Syn-rift and the Main Syn-rift megasequences. However, in other basins, such as those along the EA-MAD and EA-ANT margins,

it is currently not possible to distinguish the Main Syn-rift megasequence and the Karoo Syn-rift megasequence from the literature.

A separate period of rifting occurred following the eruption of the Karoo-Ferrar Volcanics, one that would eventually lead to break up. During this period rifting occurred in a NNW-SSE direction between two plates; East Gondwana comprising Madagascar, India, Antarctica, Seychelles and Australia, and West Gondwana comprising Africa and South America. Extension occurred between East Africa and India, and between East Africa and Antarctica accommodated by transtension along the future Davie Fracture Zone between East Africa and Madagascar. The large-scale tectonic stress field in the rift zones of the three future margin segments was controlled by the divergence between the two parts of Gondwana. As a result, the regional minimum horizontal stress ($S_{h\,min}$) trended mainly in a NNW-SSE direction, parallel to the local plate motion vector (i.e. extension direction). The regional maximum horizontal stress ($S_{H\,max}$) trended ENE-WSW, normal to the local plate motion vector and extension direction (see fig. 3.18).

The rift axes between the future EA-IND segment and the northern EA-MAD segment were characterised by an overall NE-SW orientation, producing rift margins with strike trends oblique to the regional tectonic extension ($S_{h\,min}$). In contrast, the rift segment of the southern EA-MAD margin trended NNW-SSE, subparallel to the regional tectonic extension ($S_{h\,min}$), forming a margin-scale transfer zone between the northern and southern oblique rift segments that was likely dominated by transtensional deformation. Only the rift margins of the ENE-WSW striking northern EA-ANT segment were oriented subparallel to the regional maximum horizontal stress trends ($S_{H\,max)}$ and normal to regional tectonic extension ($S_{h\,min}$) and most likely expressed deformation by orthogonal to slightly oblique rifting. The rift trends of the southern EA-ANT segment again rotated back to NE-SE in the central segment (oblique rifting) and NNE-SSW direction in the southern segment (transtensional deformation). As a result, the stress field was favourable for normal faulting in the basins of EA-IND, northern EA-MAD/MAD-EA, and EA-ANT, but results in transtensional deformation in the basins of southern EA-MAD/MAD-EA such as the Tanzanian basins, the Rovuma basin and the Morondava Basin.

During the deposition of the Main Syn-rift megasequence, the sea flooded the EA-IND margin from the Tethys Ocean in the Northeast, following the deepest parts of the subsiding basins to form long, branching marine sounds (Bosellini, 1992). Shallow-marine carbonate shelves formed along the Somali Margin controlled by down to the basement faults and rotated fault blocks (Bosellini, 1992).

Further south (along the EA-MAD margin segment), in the Lamu basin of Kenya however, sedimentation was predominantly continental still over most of the basin, the top and bottom boundaries controlled by major periods of rifting (Coffin & Rabinowitz, 1988; Mbede & Dualeh, 1997). In Tanzania, continental conditions

dominated in the Ruvu basin with some rare marine incursions. Numerous sequences separated by disconformities, deposition cycles controlled by tectonism (Mbede & Dualeh, 1997). More marine influence in the southern Mandawa Basin. Mesozoic faults trending NNW-SSE (the Lindi fault trend) associated with breakup and dextral strike-slip of Madagascar. Developed in a possible transtensional wrench zone (Hudsone & Nicholas, 2014; Nicholas, 2007).

In the south of the East African margin (the EA-ANT segment) the Mozambique was mostly exposed to volcanics of the Stormberg series.

In Madagascar (MAD-EA) the conditions were predominantly marine already, with a coastal plain and shallow-marine environment in the Ambilobe Basin (Units C & D) in asymmetric sub-basins bound by steep faults, and controlled by numerous pulses of tectonic subsidence. Further south shallow marine sediments of the Beronono Fm (Majunga Basin) and the Andafia Fm (Morondava).

Breakup

Based on the linear extrapolation of the oldest magnetic isochron ages (M25n-M22n) towards the continent ocean boundaries, the plate kinematic model of Tuck-Martin et al. (2018) estimates the age of breakup and the onset of seafloor spreading in the Mozambique Basin and Riiser Larsen Sea at167 Ma, comparable to Leinweber and Jokat's (2012) tentative identification of anomaly M41n (165.6 Ma) near the base of the continental slope where they also placed the continent-ocean boundary. In the West Somali Basin we would expect the timing of breakup to be the same/similar due to both basins opening as a result of the separation of a two-plate system and both basins are linked by the Davie Fracture Zone.

The exception to this is the southern Mozambique Basin (southern EA-ANT margin segment), where stretching of the continental crust that forms the Mozambique Coastal Plains may have delayed breakup in this area until ~157 Ma (Tuck-Martin et al., 2018).

The sedimentary basins of the East African and West Madagascan Margins record a range of breakup ages in the stratigraphy that vary from the Aalenian to the Kimmeridgian. The oldest ages for breakup are recorded in the EA-MAD and conjugate MAD-EA margin segments. In the Mandawa Basin of Tanzania where the top of the Pindiro group is marked by an Intra-Aalenian unconformity (~173 Ma) (Said et al. 2015; Hudson & Nicholas, 2014). Further north in Tanzania, in the Ruvu Basin, the breakup unconformity lies between the Ngerengere Beds and the Amboni Limestone at the Aalenian/Bajocian boundary ~170 Ma. The unconformity separates tectonically controlled continental sediments from transgressive marine sediments deposited during tectonic quiescence (Mbede & Dualeh, 1997). At the southern end of the EA-MAD segment, in the Rovuma Basin, the breakup unconformity lies at the boundary between the N'Gapa Fm deposited in a continental rift setting and the Mtumbei Limestone equiv., which was depositied

under fully marine conditions at the Toarcian/Aalenian boundary, approximately 174 Ma (Key et al., 2008). At the northern end of the EA-MAD segment the breakup unconformity lies within the Aalenian, e.g. the final stages of deposition of the Mazeras Sandstones in the Lamu Basin was contemporaneous with syn-sedimentary faulting. No faulting was reported in the formations that followed the Mazeras Sandstone (Mbede & Dualeh, 1997; Coffin & Rabinowitz, 1988).

In the conjugate margin of Madagascar (MAD-EA) the breakup unconformities in the basins are of a similar age. In the Ambilobe Basin it lies at the Aalenian/Toarcian boundary, ~174 Ma (Papini & Benvenuti, 2008). In the Majunga and Morondava basins it is interpreted as slightly younger, at the Aalenian/Bajocian boundary, ~170 Ma (Clark, 1998; Geiger et al., 2004).

In the Somali Basins the breakup unconformity is recognised at the top of the Hammanlei formation, at the Bathonian/Callovian boundary at ~166 Ma, contemporaneous with a major regional transgression (Bosellini, 1992). In the Lamu Basin, breakup is assigned to the end of the Mazeras sandstone, earlier, within the Aalenian. In Mozambique, the breakup unconformity has been recognised by Mahanjane et al., (2014) at approximately 155 Ma, much younger than the rest of the margin to the north. Therefore, it is clear the age of breakup described in the literature coincides well with the interpretation from our plate kinematic model (Tuck-Martin et al., 2018, chapter 2).

Early Post-rift

After breakup, seafloor spreading became active in the West Somali and Mozambique Ocean Basins as East Gondwana moved South-Southeast relative to West Gondwana, accommodated dextral strike-slip movement along the Davie Fracture Zone. The initiation of active spreading ridges at approximately ~165 Ma led to a change in the stress field across East Africa the plate boundary forces were controlled by ridge push which caused a dramatic change in the orientation and relative magnitude of the regional tectonic stresses in the various margin segments. Ridge Push exerted a compressional force perpendicular to the axis of the spreading ridge as the newly created oceanic crust cooled and subsided (Forsyth & Uyeda, 1975). However, at this early stage, with such young oceanic crust it is unlikely that the ridge push stress was strong enough to cause any deformation on the margins.

The active ridge segments were mainly oriented perpendicular to the regional plate vector exerting a compressive ridge push force perpendicular to the ridge axis and parallel to the plate vector, giving rise to a dramatic reorientation of the large-scale tectonic stresses. During the drift stage (Fig. 3.19) maximum horizontal tectonic stresses ($S_{H\,max}$) were orientated approximately N-S along the EA-IND and EA-MAD continental margin segments. Along the EA-ANT margin segment the ridges rotated in a more NNE-SSW direction (Fig. 3.19).

Marine conditions prevailed along the East African and West Madagascan margins at this time, and just after breakup most of the basins were dominated by carbonate platforms and shallow marine deposition (see fig. 3.19). As subsidence continued, the carbonate platforms were drowned and replaced by marls and shales.

Figure 3.19 shows the plate reconstruction at 150 Ma during well-established seafloor spreading in the West Somali and Mozambique basins. (a) shows the position of the plates, the basins and the stress field predicted by the plate kinematic model (Tuck-Martin et al., 2018). North of the el Hamurre lineament, northern Somalia (including the Sagaleh and Nogal Basins) remained relatively elevated and as a result sediments of the Urandab remained shallow-marine in nature. Across Somalia to the south of the El Hamurre lineament a clear transgression during the late Callovian to late Oxfordian followed breakup which resulted in the deposition of shales. By 150 Ma regressive limestones were deposited onshore in the west, however offshore to the east were deep-marine basinal shales (Bosellini, 1992). The rest of the basins along the margins mostly show a similar facies change from landward/onshore continental clastics to deep-marine shales in a basinward direction separated by a thin band of carbonates. Deposition in the basins along the Davie Fracture Zone (e.g. the Rovuma Basin) was still affected by rifting due the continued strike-slip movement along the DFZ. This area of the DFZ between the Rovuma Basin on East Africa and the Morondava Basin of Madagascar remained structurally higher than the WSB to the north and the MB to the south so deposition here was shallow-marine clastics and probably formed a barrier to any deep water ocean currents. In the Angoche basin there was a unit paralic clastics and/or J-Unit III shale deposited during transpression (Mahanjane, 2014)

Antarctica and Africa had fully separated by this point but onshore Mozambique basin still experienced extensive continental sedimentation, but no more volcanism at this time.

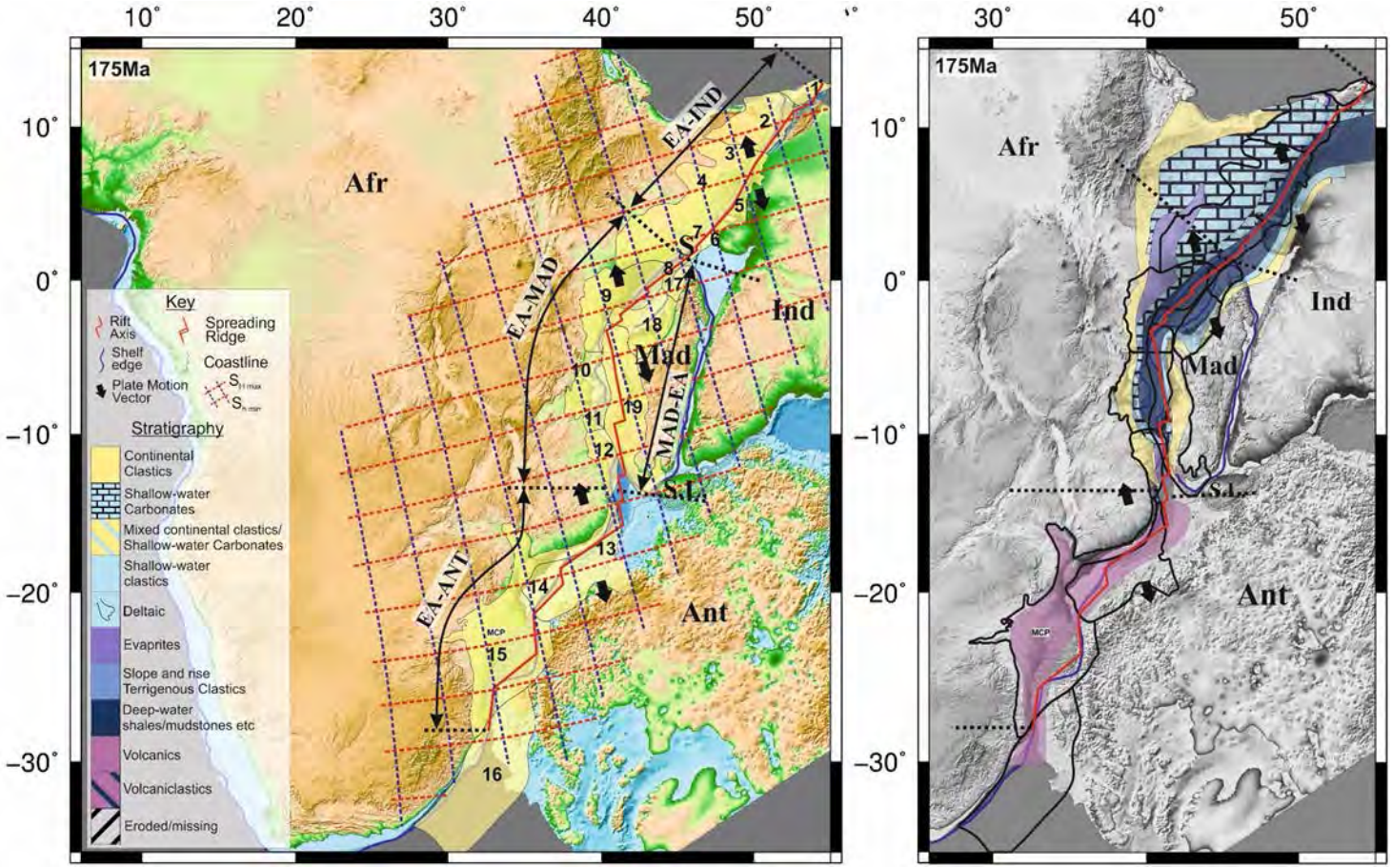

Figure 3.18: Paleostress map derived from the plate kinematic model (Tuck-Martin et al., 2018) and paleodeposition map (modified from Bosellini, 1992 and Salman & Abdula, 1995) for the East African and West Madagascan sedimentary basins at 175 Ma. 1 – Socotra Basin; 2 – Sagaleh Basin;, 3 – Nogal Basin; 4 – Somali Embayment; 5 – Obbia Basin; 6 – Coriole Basin; 7 – Somali Coastal Basin; 8 – Juba(-Lamu) Basin; 9 – Lamu Basin; 10 – Ruvu Basin; 11 – Mandawa Basin; 12 – Rovuma Basin; 13 – Angoche Basin; 14 – Zambezi Delta Depression, 15 – Southern Mozambique Basin; 16 – Natal Trough; 17 – Ambilobe Basin; 18 – Mjunga Basin; 19 – Morondava Basin.

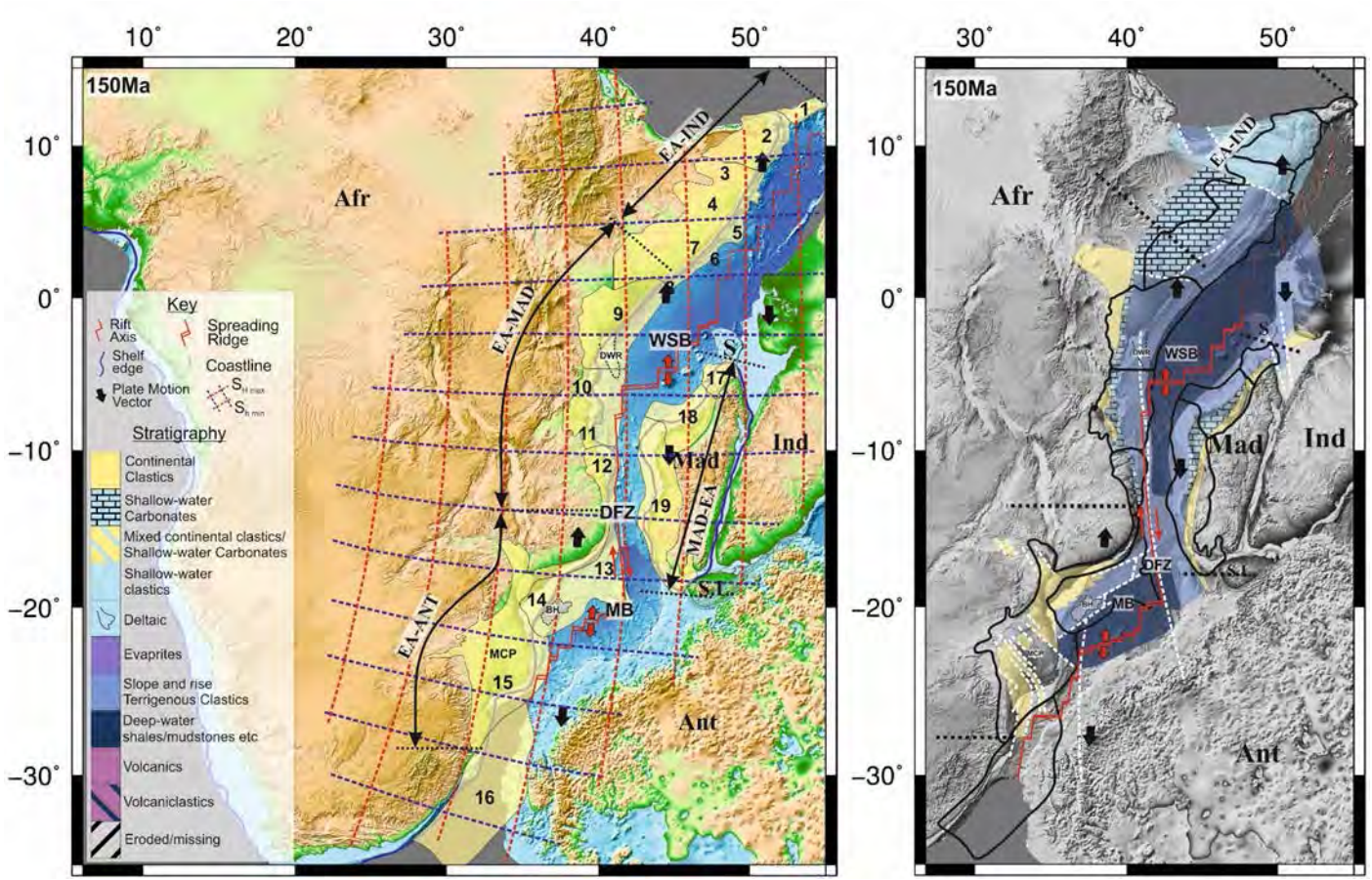

Figure 3.19: Paleostress map derived from the plate kinematic model (Tuck-Martin et al., 2018) and paleodeposition map (modified from Bosellini, 1992 and Salman & Abdula, 1995) for the East African and West Madagascan sedimentary basins at 150 Ma. 1 – Socotra Basin; 2 – Sagaleh Basin;, 3 – Nogal Basin; 4 – Somali Embayment; 5 – Obbia Basin; 6 – Coriole Basin; 7 – Somali Coastal Basin; 8 – Juba(-Lamu) Basin; 9 – Lamu Basin; 10 – Ruvu Basin; 11 – Mandawa Basin; 12 – Rovuma Basin; 13 – Angoche Basin; 14 – Zambezi Delta Depression, 15 – Southern Mozambique Basin; 16 – Natal Trough; 17 – Ambilobe Basin; 18 – Mjunga Basin; 19 – Morondava Basin.

3.4.3. **Synthesis Phase 2 – Starting at 133 Ma: Separation of Antarctica to 89 Ma (Figure 3.20).**

Phase 2 involved the cessation of seafloor spreading in the West Somali Basin at sometime within chon M10n (~133.9 – 133.5 Ma). Madagascar became fixed to the African Plate and the boundary relocated, leading to eventual onset of spreading in the West Enderby Basin between Madagascar and East Antarctica, allowing for the separation of Madagascar/India from Antarctica and continued spreading in the Mozambique Basin. The new ENE-WSW trending spreading centre between the Africa/India/Madagascar and Antarctica controlled the far-field stresses within the EA-IND-MAD plate assembly (Fig. 3.20), producing a compressional stress field orientated parallel to the local plate motion vector. For the continental margin basins of East Africa, India and Madagascar, this far-field tectonic stress field was dominated by ridge push forces and was characterised by maximum horizontal stresses ($S_{H\,max}$) trending parallel to the local plate motion vector. Near the spreading centre, $S_{H\,max}$ was oriented in a NNW-SSE orientation. These maximum horizontal far-field stresses were transmitted northward through the EA-IND-MAD plate assembly rotating to a more NW-SE direction along the East-African margin. Consequently, maximum horizontal stresses in the NE-SW-oriented EA-IND, northern EA-MAD, northern and central EA-ANT segments were oriented perpendicular to the continental margin, giving rise to the potential for inversion. A major unconformity has been recognized at the start of this Phase (end Hauterivian/Barremian) along the margin segments bordering the Somali Basin i.e. the EA-IND segment (Bosellini, 1992) and the northern MAD-EA segment (Coffin & Rabinowitz, 1988). NW-SE compressional far-field stresses trended oblique to the N-S trending margins of the southern EA-MAD and MAD-EA margins with the potential for strike-slip or transpressional deformation. Key et al. (2008) suggest that early phase 2 deposition was controlled by renewed rifting and extensive inland erosion in the Rovuma Basin (southern EA-MAD) whilst in the Angoche Basin (southern EA-MAD/EA-ANT) a short-lived period of tectonic uplift followed the end of movement on the Davie Facture Zone (Mahanjane 2014).

At the start of this phase, a number of the sedimentary basins bordering the West Somali Ocean Basin exhibit a prominent end Neocomian/Barremian unconformity which also marks the change from Early Post-rift sediments to mid post rift. We suggest this could be a direct consequence of the extinction of the spreading ridge in the West Somali Basin, and supports our assumption that this took place during the Hauterivian (~133 Ma, Tuck-Martin et al., 2018).

Along the EA-IND segment, this unconformity has been attributed to pre-Aptian tilting and erosion, possibly exacerbated by low sea-levels (Bosellini, 1992). The unconformity extends south along the EA-MAD margin segment, although it is not documented in the Juba and Lamu Basins. In Tanzania, a pre-Aptian unconformity has been recognised in the Ruvu basin by Mbede and Dualeh (1997), and in the Mandawa Basin and an unconformity at the Valangian/Hauterivian boundary

separates early post-rift megasequence from late post-rift (Hudson, 2011). Key et al. (2008) suggest that sedimentation in the Rovuma Basin, corresponding to early phase 2 of our tectonic model was controlled by renewed rifting and extensive inland erosion, whilst in the Angoche Basin (southern EA-MAD/EA-ANT) a short-lived period of tectonic uplift followed the end of movement on the Davie Facture Zone (Mahanjane 2014) and resulted in a corresponding unconformity at the Hauterivian/Barremian boundary.

In the conjugate basins of Madagascar (MAD-EA) similar unconformities have been identified, for example (Coffin & Rabinowitz, 1988) identify an angular unconformity in the Ambilobe Basin at the northern MAD-EA segment.

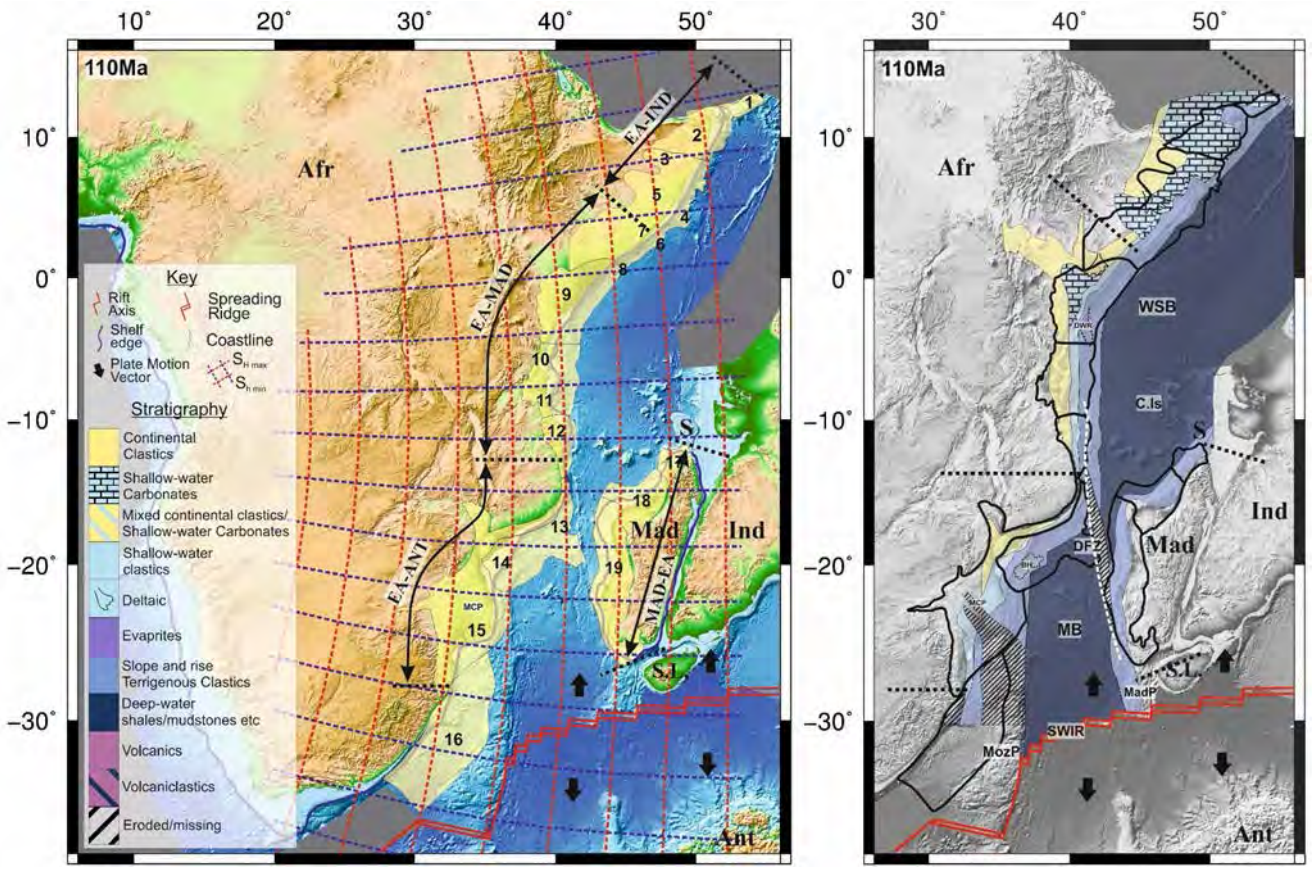

Figure 3.20: Paleostress map derived from the plate kinematic model (Tuck-Martin et al., 2018) and paleodeposition map (modified from Bosellini, 1992 and Salman & Abdula, 1995) for the East African and West Madagascan sedimentary basins at 110 Ma. 1 – Socotra Basin; 2 – Sagaleh Basin;, 3 – Nogal Basin; 4 – Somali Embayment; 5 – Obbia Basin; 6 – Coriole Basin; 7 – Somali Coastal Basin; 8 – Juba(-Lamu) Basin; 9 – Lamu Basin; 10 – Ruvu Basin; 11 – Mandawa Basin; 12 – Rovuma Basin; 13 – Angoche Basin; 14 – Zambezi Delta Depression, 15 – Southern Mozambique Basin; 16 – Natal Trough; 17 – Ambilobe Basin; 18 – Mjunga Basin; 19 – Morondava Basin. WSB – West Somali Basin; MB – Maozambique Basin; DFZ – Davie Fracture Zone; SWIR – Southwest Indian Ridge.

3.4.4. Synthesis Phase 3 – Starting at 89 Ma: Separation of India and Madagascar to 60 Ma (Figure 3.21)

At the start of this Phase, the arrival of the Marion mantle plume beneath the southeast corner of Madagascar led to the eruption of the Morondava volcanics on Madagascar at ~89 Ma (Storey et al., 1997). Contemporaneous with this was the initiation of rifting and subsequent seafloor spreading on the Mascarene Ridge, the opening of the Mascarene Basin and the separation of India and Mascarene Plateau. Seafloor spreading continued between Africa and Antarctica, with the new ridge connecting to the Southwest Indian Ridge (SWIR) at the Rodriguez Triple junction. Spreading in the Mascarene Basin continued until its abandonment shortly after the young end of chron 27n (61.65 Ma) (Eagles & Wibisono, 2013).

Across the SWIR, between Africa and Antarctica, spreading direction remained in an approximately NW-SE direction and therefore the stress field in this area was dominated by the NW – SE compressive ridge-push forces (fig. 3.21). Further north the East African and West Madagascan margins were dominated by the compressional $S_{H\,max}$ stresses produced by the newly formed Mascarene Ridge, parallel to the spreading direction, orientated NE-SW at the northern end of the margin and E-W at the southern end. As a result, the NE-SW oriented EA-IND, northern EA-MAD, northern and central EA-ANT margin segments were subjected to $S_{H\,max}$ oriented mostly in strike direction and $S_{H\,min}$ in dip direction of the continental margin segments similar to gravity-driven stress fields acting on the continental shelves during passive margin development. Along the N-S trending southern EA-MAD and MAD-EA margin segments, $S_{H\,max}$ was compressional and orientated ENE-WSW to E-W indicating the potential for inversion of earlier strike-slip structures (Tuck-Martin et al., 2018).

A major tectonic/volcanic event affected East Africa and West Madagascar during the Turonian, at the same time as the start of this phase.The conjugate margins of EA-MAD and MAD-EA both underwent significant tectonic and volcanic activity during the Turonian which we attribute to far-field effects from the breakup of India and Madagascar in the east. In the Lamu Basin, renewed basement uplift during the Turonian to the Paleocene caused uplift and erosion of the hinterland and rapid deposition of the Kofia sands. This rapid deposition caused the underlying Walu shales to become overpressured and triggered the deformation of the Lamu DWFTB at the beginning of Phase 4 (Cruciani & Barchi, 2016).

Clark (1998) describes renewed tectonic activity in the Basins of Western Madagascar, with wrench faulting and compressional folding occurring in the Late Cretaceous. The Turonian is also associated with extensive volcanism across the basins of Madagascar, indicated by the presence of trachyte in the in the Turonian sediments of the Ambilobe Basin, and basaltic lava flows and extrusions in the Majunga Basin (Coffin & Rabinowitz, 1988). In the Majunga Basin, volcanism continued into the Campanian and was accompanied by uplift of the hinterland and

deltaic progradation (Coffin & Rabinowitz, 1988). Along the EA-ANT margin segment, there was no obvious features suggesting tectonic control but there was a stratigraphic/depostional change from Domo sands deposited during regression (Cenomanian-Turonian) to Upper Domo shales (transgression) (Salman & Abdula, 1995).

Figure 3.21 shows the plate reconstruction of Tuck-Martin et al. (2018) at 75 Ma, during phase 3 with well-established spreading on the Mascarene Ridge, with the associated stress field (already described above) and the paleodeposition of the basins at this time. Following the Turonian/Conacian uncoformities that marked the start of this phase in the EA-MAD and MAD-EA margins segments, the rest of this phase was one of tectonic quiescence in all but the Lamu Basin (Kenya, EA-MAD) and the Madagascar Basins (MAD-EA).

The exception is the basins of the EA-IND margin segment (Sagaleh, N. Somali, and Somali Coastal Basins) do not show anything in the stratigraphy that suggests this tectonic change had any effect on the development of the basins.

In the basins of EA-IND margin the Gira supersequence showed a west to east facies change from fluvial sandstone, to carbonate platform to deep-water mudstones (Bosellini, 1992). In the Juba(-Lamu) and Lamu Basins (northern EA-MAD segment) the continental shelfs were dominated by terrigenous, deltaic sedimentation and deep-water shales, offshore in the east (Mbede & Dualeh, 1997; Nyagah, 1995; Cruciani & Barchi, 2016). Further south, thick deep-water clays were deposited along in the Ruvu and Mandawa basins of Tanzania (Mbede & Dualeh, 1997; Nicholas et al., 2007; Nicholas et al., 2006). At the southern end of the EA-MAD margin segment the Rovuma basin and a west to east facies change similar to the EA-IND segment western near-shore sediments to eastern open-marine sediments of the Mifume Fm. deposited during Late Cretaceous marine transgression (Key et al 2008). In the basins of the EA-ANT margin segment (including the Angoche, Zambezi Delta and Southern Mozambique Basins) was deposited the Lower Grudja Fm which varies from shallow water shelf clays and sandstones in the west to thick, deep-water shale in the east with slope and basin floor fans (Mahanjane, 2014; Salman & Abdula, 1995).

The exceptions to this tectonic quiescence are the Lamu Basin and the basins of western Madagascar. In the Lamu Basin, uplift of the hinterland in the west continued throughout the Late Cretaceous at the same time as the deposition of the deltaic Kofia Sands in the east (Cruciani & Barchi, 2016).

In the basins of the MAD-EA margin segment, volcanism associated with the separation of Madagascar and India continued until the Campanian, and concomitant uplift and tilting of the Madagascan mainland continued throughout the Late Cretaceous of Phase 3 and into Phase 4 (Jeans & Meerbeke, 1995).

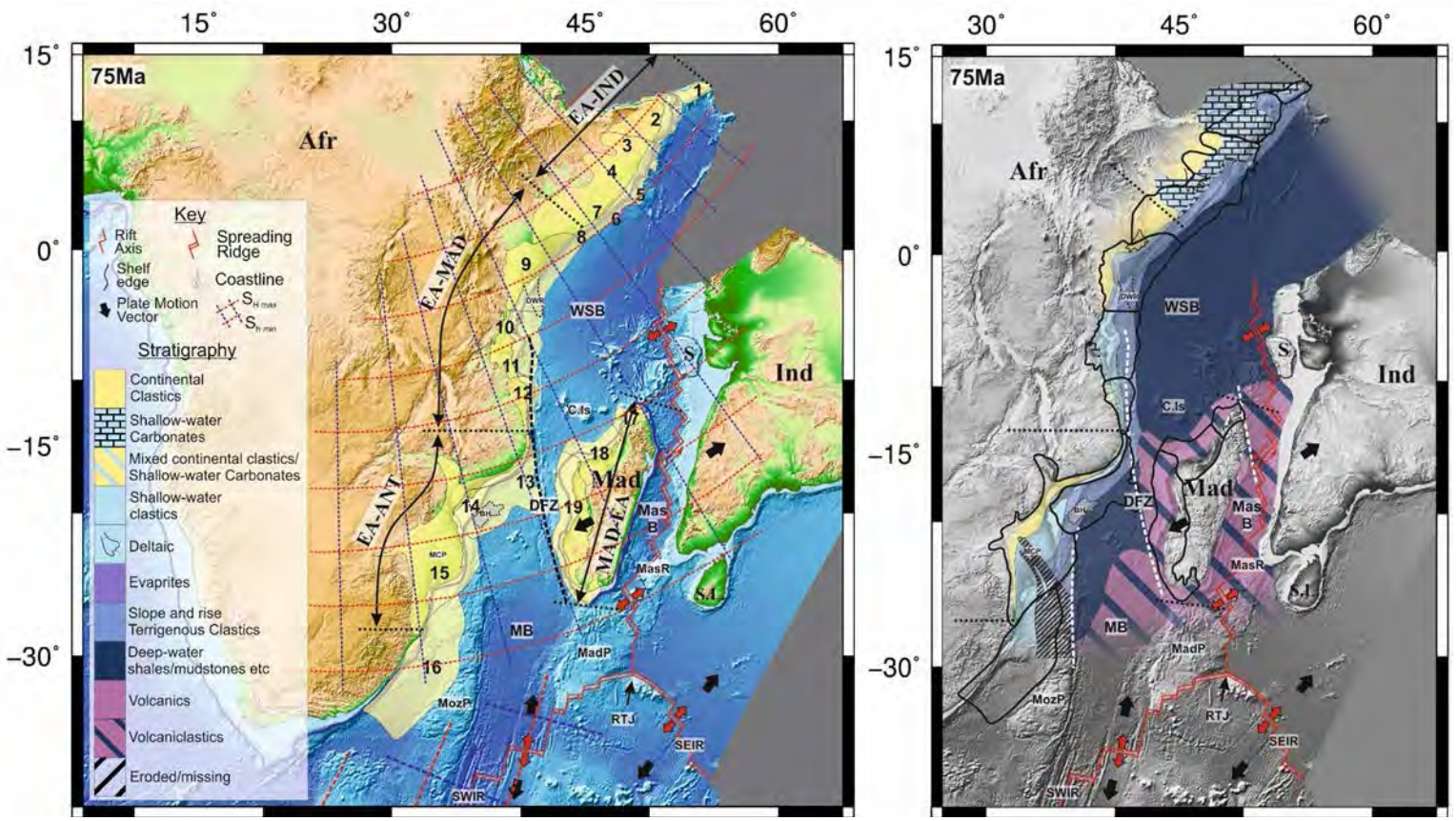

Figure 3.21: Paleostress map derived from the plate kinematic model (Tuck-Martin et al., 2018) and paleodeposition map (modified from Bosellini, 1992 and Salman & Abdula, 1995) for the East African and West Madagascan sedimentary basins at 75 Ma. 1 – Socotra Basin; 2 – Sagaleh Basin;, 3 – Nogal Basin; 4 – Somali Embayment; 5 – Obbia Basin; 6 – Coriole Basin; 7 – Somali Coastal Basin; 8 – Juba(-Lamu) Basin; 9 – Lamu Basin; 10 – Ruvu Basin; 11 – Mandawa Basin; 12 – Rovuma Basin; 13 – Angoche Basin; 14 – Zambezi Delta Depression, 15 – Southern Mozambique Basin; 16 – Natal Trough; 17 – Ambilobe Basin; 18 – Mjunga Basin; 19 – Morondava Basin. WSB – West Somali Basin; MB – Maozambique Basin; DFZ – Davie Fracture Zone; SWIR – Southwest Indian Ridge; SEIR – Southeast Indian Ridge; Mas. B. – Mascarene Basin; RTJ – Rodriguez Triple Junction; Mas. R. – Mascarene Ridge.

3.4.5. Synthesis Phase 4 – Starting at 60 Ma: Separation of India and the Mascarene Plateau (Figure 3.22)

During Phase 4, seafloor spreading on the Carlsberg Ridge (CR) propagated south to form the Central Indian Ridge (CIR) separating India and the Mascarene Plateau. Seafloor spreading continued on the Southwest Indian Ridge (SWIR). These three spreading ridges remained active throughout phase 4 and continue to present day. Later in Phase 4 more recent tectonic events be dominated the development of the continental margins, namely the collision of India and Africa with Eurasia and the development of the East African Rift System (EARS) (Tuck-Martin et al., 2018).

The plate kinematic model from Tuck-Martin *et al.* (2018) During the first part half of this phase the finite rotation pole migrated south after chrons 30y – 28y (66.398 Ma – 63.494 Ma). Initially the migration was very rapid until chrons 26y to 24y (58.959 Ma – 52.62 Ma) and associated with the influence of the Deccan plume near the African-India plate boundary (Cande & Stegman, 2011). From chrons 26y to 24y (58.959 Ma – 52.62 Ma) until chron 13y (33.147 Ma) the migration was much slower linked to the eventual continental collision between Africa and Europe (Nankivell, 1997).

They also identified an abrupt change in the progression of the finite rotation poles to a northwards direction beginning at chron 13y (33.147 Ma), indicative of a new tectonic influence which may be related to the onset of the EARS (Tuck-Martin et al., 2017). Corresponding prominent Oligocene unconformities are present of the majority of the marginal sedimentary basins.

During this phase the far-field maximum horizontal tectonic stress produced by the ridge-push forces along the Carlsberg and Central Indian Ridges was orientated NE-SW and affected most of the East African and West Madagascan margins. $S_{H\ max}$ was orientated NE-SW (see figure 3.22), in strike or moderately oblique to the NE-SW oriented EA-IND, northern EA-MAD, northern and central EA-ANT margin segments. The minimum horizontal stresses ($S_{h\ min}$) lies mostly in dip direction of the continental margins which may allow potential shelf extension by margin-parallel normal faults and associated deep-water thrust faults. The beginning of Phase 4 corresponds to the main phase of deformation on the oldest Deep-Water Fold-and-Thrust Belt (DWFTB) in the Lamu Basin, Kenya (EA-MAD) during the Paleocene, facilitated by a major period of basement uplift from the Turonian to Early Paleocene (Cruciani & Barchi, 2016).

The N-S trending margin segments of the southern EA-MAD and MAD-EA margins were affected by more oblique trending maximum and minimum far-field stresses with a NE-SW compressional $S_{H\ max}$ stresses and NW-SE $S_{h\ min}$ indicating potential strike-slip deformation in this phase (fig. 3.22).

During the latter part of Phase 4, the neighbouring East African Rift System (EARS) likely had a strong influence on the stress field along the East African margin.

This may be reflected in the progression of finite rotation poles discussed in Tuck-Martin et al., (2018) in chapter 2. However, it seems the effects were largely local. Examples include: (i) Uplift and doming prior to the onset of rifting as suggested by Wichura et al. (2011) for the Kenya dome in the Mid-Miocene, and linked to the Oligocene by MacGregor (2015); (ii) Uplift and increased sedimentation triggered by the EARS may have caused the first-order tectonic stress field to be overprinted by localised gravity-driven stress fields due to loading and collapse of prograding sediment wedges, for example the Rovuma DWFTB (Mahanjane & Franke, 2014)). Paleostress maps illustrating the effect of the East African Rift System on the regional stress field are beyond the scope of this paper which focuses on the effects of tectonic changes in the Northwest Indian Ocean directly related to the breakup of Gondwana.

In the Somali Basins (EA-IND margin segment) the Early Oligocene sediments are missing, possible removed by uplift and erosion, the Modern Margin megasequence rests on a major angular unconformity (Bosellini, 1992). This unconformity continues south into the EA-MAD margin segment. In the Lamu Basin, the unconformity is dated as Late Oligocene and resulted in sediment starved conditions in the offshore part of the basin (Nyagah, 1995). In the Ruvu Basin (Tanzania) Oligocene strata, and deposition of Miocene deltas were amplified by uplift, tilting and erosion on the hinterland, associated with EARS development (Mbede & Dualeh, 1997). The same conditions affected the Mandawa Basin in the south of Tanzania with missing Oligocene sediments and uplift/erosion after the Late Miocene (Nicholas et al., 2007). At the southern end of the EA-MAD margin segment, the development of the EARS resulted in an early Oligocene unconformity and initiated the progradation of the Rovuma Delta Complex in the Rovuma basin (Key et al., 2008). In the basins of Mozambique, Angoche, Zambezi, Southern, (EA-IND) an early Oligocene unconformity runs through all of them, and since deposition has been dominated by the Zambezi and Limpopo Deltas (Salman & Abdula, 1995). In Madagascar (MAD-EA) the same Oligocene unconformity is present all along the western margin and Oligocene sediments are missing in all basins except the southern Morondava Basin (Coffin & Rabinowitz, 1988).

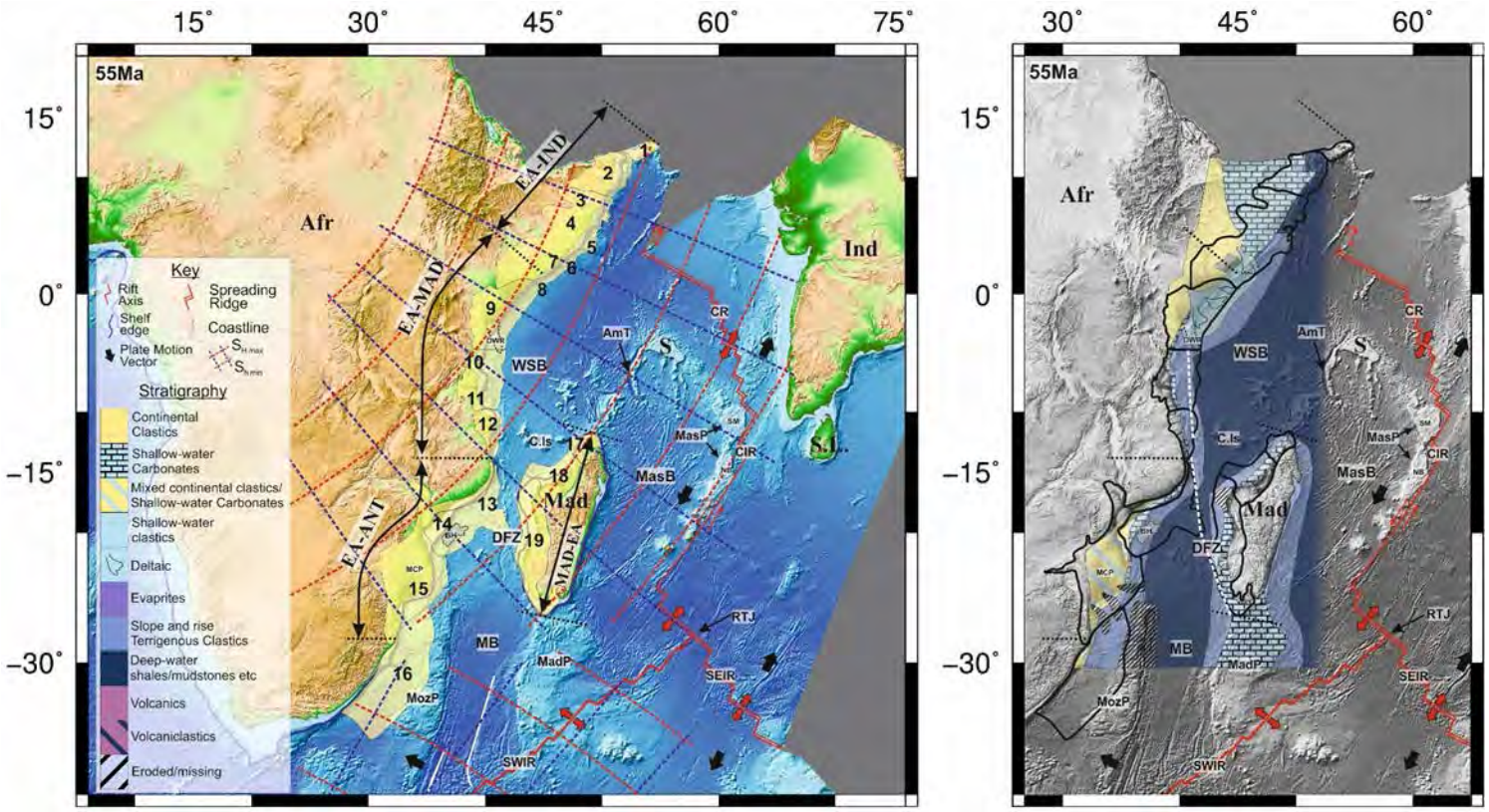

Figure 3.22: Paleostress map derived from the plate kinematic model (Tuck-Martin et al., 2018) and paleodeposition map (modified from Bosellini, 1992 and Salman & Abdula, 1995) for the East Afican and West Madagascan sedimentary basins at 55 Ma. 1 – Socotra Basin; 2 – Sagaleh Basin;, 3 – Nogal Basin; 4 – Somali Embayment; 5 – Obbia Basin; 6 – Coriole Basin; 7 – Somali Coastal Basin; 8 – Juba(-Lamu) Basin; 9 – Lamu Basin; 10 – Ruvu Basin; 11 – Mandawa Basin; 12 – Rovuma Basin; 13 – Angoche Basin; 14 – Zambezi Delta Depression, 15 – Southern Mozambique Basin; 16 – Natal Trough; 17 – Ambilobe Basin; 18 – Mjunga Basin; 19 – Morondava Basin. WSB – West Somali Basin; MB – Maozambique Basin; DFZ – Davie Fracture Zone; SWIR – Southwest Indian Ridge; SEIR – Southeast Indian Ridge; Mas. B. – Mascarene Basin; RTJ – Rodriguez Triple Junction; Mas. R. – Mascarene Ridge; CR – Carlsberg Ridge, CIR – Central Indian Ridge; Mas P – Mascarene Plateau; AmT – Amirante Trench; C. Is – Comoros Islands.

3.5. Conclusions

Here we present a margin-scale tectonostratigraphic framework for the correlation of major tectonic events and megasequences in the sedimentary basins of the conjugate East Africa and Madagascar margins based on the results of a new plate kinematic model, first-order regional kinematic stress analysis and published information of related basin fill sequences.

The framework highlights a number of links between plate tectonic changes and phases of plate-reconfiguration described by the plate kinematic model of the opening of the NW Indian Ocean and stratigraphy and structure of individual basin along the margins, expressed as unconformites and tectonically controlled megasequences.

By correlating regional observations, stages and events of basin evolution in specific sedimentary basins within a fully constrained high-resolution plate-kinematic model allows us to analyse the impact of margin-wide tectonic processes on sedimentary basin development.

The framework has the potential to investigate the effect of important tectonic changes on the stratigraphy and structure of sedimentary basins and the development of petroleum system elements in individual basins and correlate them with similar basin settings along the margins.

Chapter 4

Dynamic Paleostress Modelling of Africa

Amy Tuck-Martin[1] & Rob Govers[2]

[1]Royal Holloway, University of London, Egham, Surrey, UK. TW20 0EX

[3]Utrecht University, Heidelberglaan 2, Utrecht, NL.

Author Contributions

This work was carried out in collaboration with Dr Rob Govers of Utrecht University, Netherlands, using methods and computer programs designed and written by him. In addition figure 4.8 was drafted by Rob.

The text and the rest of the images were drafted by Amy Tuck-Martin

Abstract

The structure and evolution of sedimentary basins at rifted continental margins are controlled by tectonic processes at distal plate boundaries. Forces such as ridge push and slab pull, are transmitted from the boundaries to the plate interior, controlling the first-order, plate-scale stress field. The modern day stress field is relatively easy to constrain by in-situ measurements such as earthquake focal mechanisms and borehole breakouts. However, paelostress fields cannot be measured directly and can only be determined by fault plane solutions or by numerical modelling.

We present a numerical approach to modelling the paeleostress field of Africa at 75 Ma. 'Known' toques ridge push, slab pull and basal drag were calculated and used to constrain the 'unknown' torques viscous resistance, transform ridge resistance and plate contact resistance. By assuming the plate was in dynamic equilibrium i.e. neither accelerating nor decelerating, the sum of the torques are required to cancel out (Forsyth & Uyeda, 1975).

The African plate was modelled using finite element mesh with its geometry, oceanic lithospheric age and relative motion of adjacent plate controlled by the tectonic models of Tuck-Martin *et al* (2018), Perez-Diaz & Eagles, (2014, 2017) and Seton *et al* (2012).

Two models were produced for different sets of forces, one for resistive mantle drag and the other for driving mantle drag. We found that no solution was possible for either model. The failure of each model to produce a solution may lie with the assumptions used to constrain the slab pull force. Specifically, modelling slab pull as a function of age produced an anomalously large force along the Northeastern boundary, where very old Tethyan lithosphere was subducting beneath Eurasia.

Additional models were carried out with varying slab dip angles and slab lengths. Slab dip angle was found to have little effect on the slab pull torque, however changing the slab length had an effect but not enough to reach a solution.

4.1. Introduction

The African Plate and its present day boundaries have evolved as a result of the breakup of Gondwana since the Early Jurassic, beginning with the opening of the Central Atlantic at ~ 195 Ma (Gaina *et al.*, 2013). This was followed by the breakup between East Gondwana (comprising India, Madagascar, Seychelles, Antarctica, and Australia) and West Gondwana (comprising Africa and South America) by rifting and seafloor spreading in the West Somali and Mozambique basins. Finally, breakup in the South Atlantic between Africa and South America began at ~138 Ma (Perez-Diaz & Earles, 2014).

In the Northwest Indian Ocean, East Gondwana continued to fragment. After seafloor spreading ceased in the West Somali Basin at approximately 133 Ma, the plate boundary relocated to the south of Madagascar, which became fixed to the African Plate. As a result, Madagascar/India separated from Antarctica (133 Ma to present), then India and Madagascar (89 – 60 Ma) and India and the Mascarene

Plateau (60 Ma – present) (see Tuck-Martin *et al.*, 2018, chapter 2 for more details). Throughout this time the eastern boundary of African plate was bounded by spreading ridges.

The northern boundary of Africa has a more complicated history, the full history of which stretches back further than our 195 Ma starting point considered in this chapter. From 195 Ma onwards the northern African boundary lay along the mid-ocean ridge in the Tethys Ocean, until approximately 95 Ma when Africa began to subduct beneath Eurasia (Gaina *et al*, 2013).

The sedimentary basins which formed as result of the breakup of Gondwana, along the margins of East Africa and West Madagascar are of interest for hydrocarbon exploration. Throughout their development, they have been affected by a number of regional unconformities that may be linked to far-field effects of changing plate boundaries and their boundary forces (see chapters 2 and 3).

We have previously described a model for qualitatively predicting paleostress fields from our plate kinematic model, described in chapter 3, based on the findings of the World Stress Map Project. In this model we suggest that the first-order tectonic intraplate stress field is mostly compressional in nature and a direct result of plate boundary forces (see chapter 3, and section 1.1 below).

To assess the validity of this model we study the forces acting on the plate by modelling the dynamics of the African Plate as a whole. The set of forces is constrained by the idea that the plate is neither accelerating nor decelerating at this time and is therefore mechanically balanced, as a result the sum of their torques is required to vanish (Forsyth & Uyeda, 1975). We use instantaneous Euler poles at 75 Ma from our plate kinematic model and the assumption that Africa is. The advantage of this approach is that the better known edge forces can be used to solve for the less well known forces. The resulting force model will be used to compute the intraplate paleostress field which will be compared with the stress field derived from the plate kinematic model in chapter 3. We aim to investigate to what extent the plate boundary forces can explain the intraplate stress field, and how the stress field produced by this method compares to our earlier predictions.

We choose to focus on one time slice during Phase 3 of the kinematic model (chapter 2), at 75 Ma, because the African plate boundaries at this time are well known and the initiation of the Mascarene Ridge should have an interesting effect on the regional stress field.

4.1.1. Qualitative Stress Field of Africa at 75 Ma

Here we provide a summary of the paleostress field for the East African and West Madagascan Margins at 75 Ma as predicted by the Plate Kinematic model of Tuck-Martin *et al* (2018) and described in chapter 3

The spreading direction between Africa and Antarctica was approximately NW-SE and the stress field in this area, stretching into South Africa, was dominated by the NW–SE compressive ridge-push forces exerted by the SWIR and orientated perpendicular to the ridge axis and parallel to spreading direction (fig. 4.1).

Further north, the East African and West Madagascan margins were more likely dominated by far-field stresses produced by the newly formed Mascarene Ridge along the eastern boundary of the African plate. Ridge-push forces due to this new dominantly N-S trending spreading zone resulted in Maximum horizontal stresses ($S_{H\,max}$) oriented perpendicular to the ride axis and parallel to the local plate vectors varying from a NE-SW direction in the northern Somalia margin to an E-W direction further south, in the Mozambique margin (fig. 4.1).

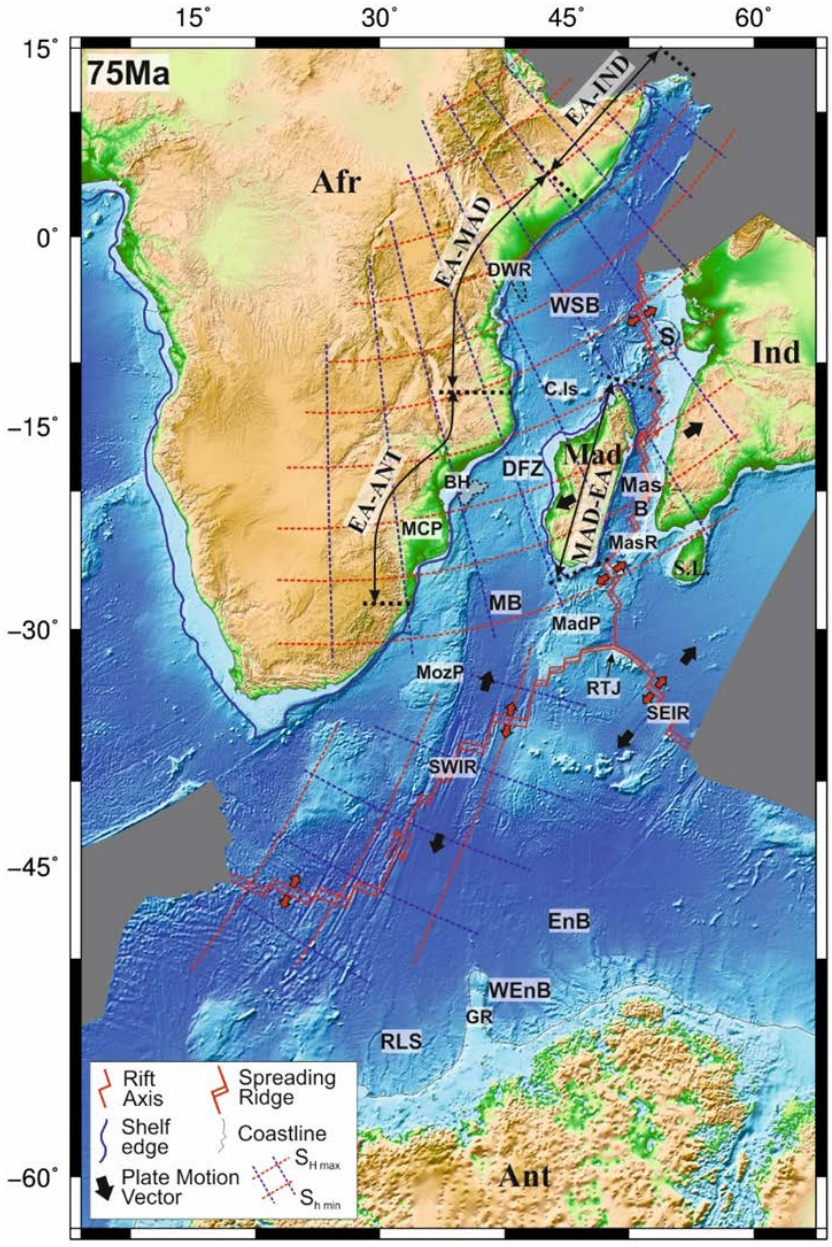

Figure 4.1: Plate tectonic reconstruction at 75 Ma with associated paleostress field (Tuck-Martin *et al.,* 2018).

4.2. Methods

4.2.1. Model geometry and plate boundaries: The Africa Plate at 75 Ma

At 75 Ma, this was in the middle of the third phase of tectonic development of the Northwest Indian Ocean as described by (Tuck-Martin *et al.,* 2018, in chapter 2) and summarised here.

During this phase, seafloor spreading continued between Antarctica and Africa along the Southwaet Indian Ridge (SWIR), but a dramatic change in tectonic activity occurred along the eastern boundary, associated with the initiation of a new spreading ridge and the opening of the Mascarene Basin, separating India and Madagascar. The earliest products of this change are the Morondava volcanics dated at approximately 89 Ma (Storey *et al* 1997) in Madagascar, whose eruption is attributed to the arrival of the Marion mantle plume. Extension and subsequent seafloor spreading in the Mascarene Basin most likely began contemporaneously with the emplacement of the Morondava volcanics and continued until the abandonment of the Mascarene ridge shortly after the end of chron 27n (61.65 Ma) (Eagles & Wibisono, 2013), constrained by the magnetic isochron interpretations described in Tuck-Martin *et al* (2018) and Chapter 2.

At 75 Ma, most of the boundaries around the African Plate at this time were divergent mid-ocean ridges, including ridges in the Central/Northern Atlantic Ocean (Seton *et al.,* 2012), the Southern Atlantic Ocean (Pérez-Díaz *et al.,* 2014) and the Southwest Indian Ridge (SWIR) between Antarctica and South Africa (Tuck-Martin *et al.,* 2018). The eastern boundary was a ridge and transform boundary in the Mascarene Basin (Tuck-martin *et al.,* 2018) connected to the Rodriduez triple between the Mascarene Ridge, the Southwest Indian Ridge (SWIR) and the Southeast Indian Ridge (SEIR). According to Seton *et al.* (2012) the Mascarene Ridge was connected to the Tethys Subduction Zone by a long transform boundary.

The northern boundary however, was convergent at 75 Ma. Along this boundary the Tethys Oceanic crust of the African Plate was subducting beneath the Eurasian Plate (fig. 4.2). The movement of Iberia and the nature/position of the boundary between Africa and Eurasia at this time were complicated. Towards the Northwest at some point the boundary stops being a true subduction zone and changes into a transform boundary that links the subduction zone to the mid-ocean ridge in the North Atlantic. Seton *et al.* (2012) show no relative movement between Africa and Iberia at 75 Ma and during the 1 million years before, but they do show relative movement between Eurasia and Iberia. Therefore, Iberia has been included as part of the Africa plate at 75 Ma, with a transform boundary with Eurasia lying to the north.

4.2.2. Euler Poles

Instantaneous Euler poles were calculated for all the plates in the circuit. For Africa, this was the pole of absolute plate motion at 75 Ma relative to hotspots, and was taken from O'Neill *et al* (2005). For the other plates, all instantaneous Euler poles were taken as the plate's movement relative to Africa. The movement of India and

Antarctica were taken from the tectonic model of Tuck-Martin *et al* (2018) by subtracting the pole at 74 Ma from the pole at 75 Ma to get the movement during the 1 million year interval immediately prior to 75 Ma. The Euler pole for South America was taken from the tectonic model of Perez-Diaz *et al* (2014). Both these models use a data-rich, robust method to determine plate movement by joint iterative inversion of seafloor magnetic anomaly picks and fracture zone traces.

The instantaneous Euler poles for North America and Eurasia relative to Africa come for the tectonic model of Seton *et al* (2012).

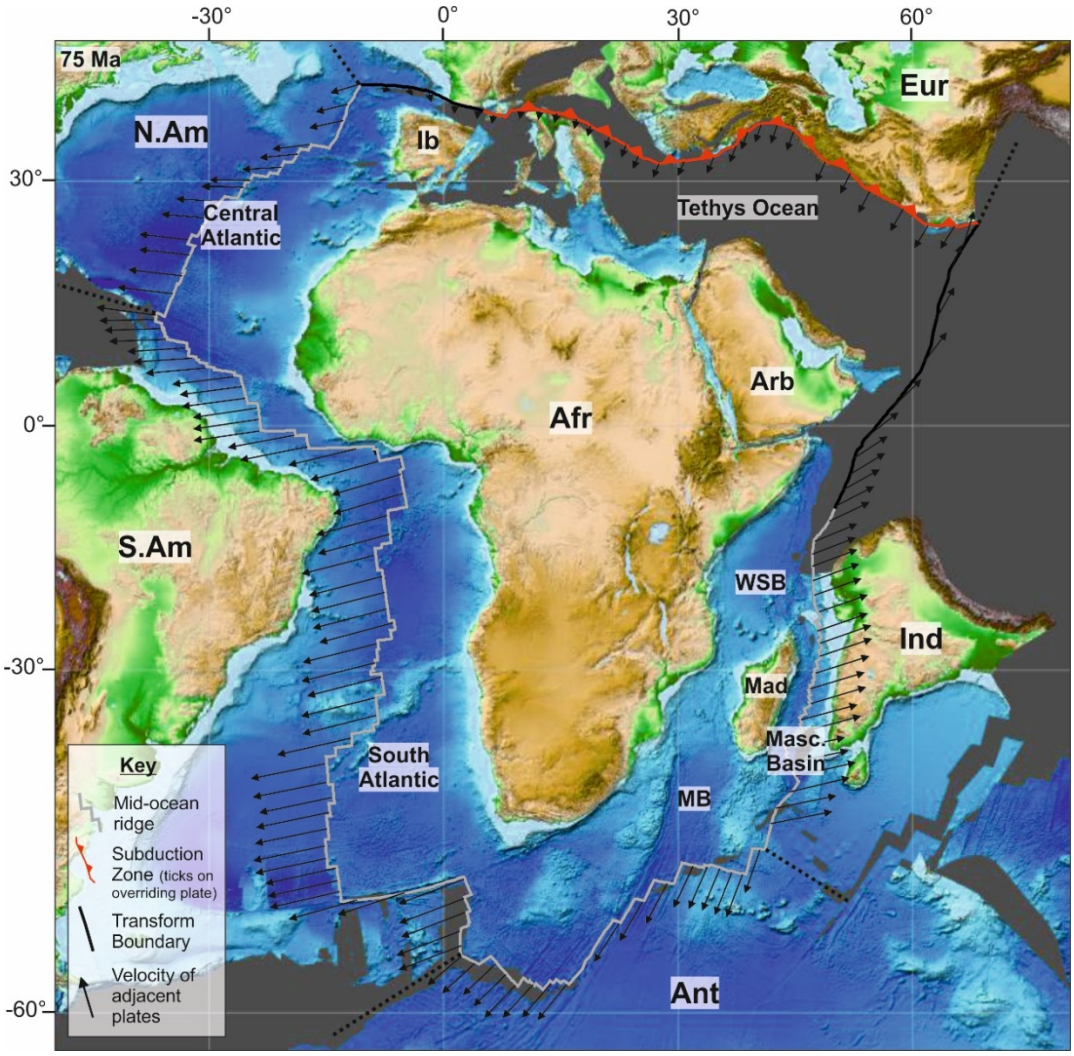

Figure 4.2: The position of the African plate and all adjacent plates at 75 Ma with their relative velocities (indicated by the arrows). The outline and position of Africa, and the relative velocity of India and Antarctica are based on the tectonic model of Tuck-Martin *et al.*, 2018. Information for the South Atlantic comes from Perez-Diaz & Eagles, 2014; Information for the Central Atlantic and Eurasia comes from Seton *et al.*, 2012; the background image has been created with GPlates and the model of Seton *et al.*, 2012. Eur – Eurasia, Ib – Iberia, N.Am – North America, S.Am – South America, Afr – Africa, Arb – Arabia, WSB – West Somali Basin, MB – Mozambique Basin, Mad – Madagascar, Ind – India, Ant – Antarctica.

4.2.3. Age Grid

Using the plate kinematic model from Tuck-Martin *et al* (2018) we produced a new high resolution age grid for the northwest Indian Ocean at 75 Ma.

The age grid is based on magnetic anomaly data points interpolated onto isochrons constrained within the model of Tuck-Martin *et al.* (2018) and further points interpolated visually at 5 Myr intervals between the isochrons, guided by seafloor gravity fabric. The full set of picks can be seen in figure 4.3. The age of the magnetic anomaly data were interpreted according to the magnetic reversal time scale of Gradstein *et al* (2004). Also included were fracture zone traces digitised from free air gravity and bathymetric data (Sandwell *et al.,* 2014) and extinct mid-ocean ridges in the West Somali Basin.

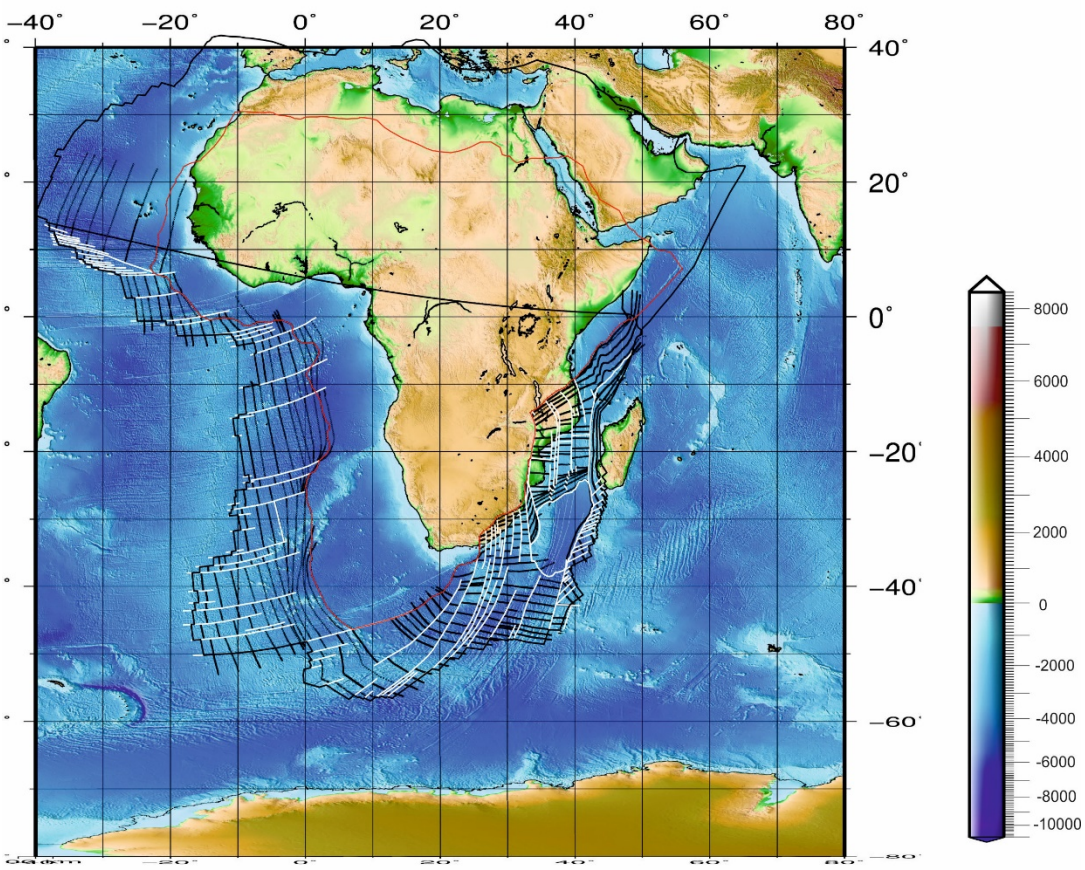

Figure 4.3: Data set used to create the age grid for the South Atlantic and the Northwest Indian Ocean, rotated to their position 75 million years. Data for the Northwest Indian Ocean comes from Tuck-Martin *et al* (2018) and data for the South Atlantic comes from Pérez-Díaz & Eagles (2017).

The data points are used to create the grid of seafloor age using the minimum curvature gridding method in Surfer 14 (Golden Software), a mapping, contouring and surface modelling software package. The minimum curvature method interpolates a smooth surface comparable to a thin, linearly elastic plate that passes through each of the input data points with minimum bending. We set our

interpolation to complete after 10,000 iterations, with each iteration applying the minimum curvature algorithm in an attempt to smooth the grid. The internal tension and boundary tension were both set to 0.8 to allow control over the amount of smoothing and reduce high magnitude artefacts in areas of no data. The values of the grid nodes were recalculated until the misfit between the node values and the input data points between iterations was less than the maximum residual value (set at 0.5), or the maximum number of iterations is reached. The fracture zone traces were used to show breaks in age on the grid surface, and no interpolation was calculated for portions of the grid that cross the digitised fracture zone traces.

Our age grid was then combined with an age grid for the South Atlantic Ocean by Pérez-Díaz and Eagles (2017), and the North Atlantic and Tethys Ocean age grid from Seton *et al* (2012) to produce an age grid for the entire African Plate at 75 Ma. All age grids had to be resized and resampled before they were able to be combined. Figure 4.4 shows the complete age grid for Africa at 75 Ma.

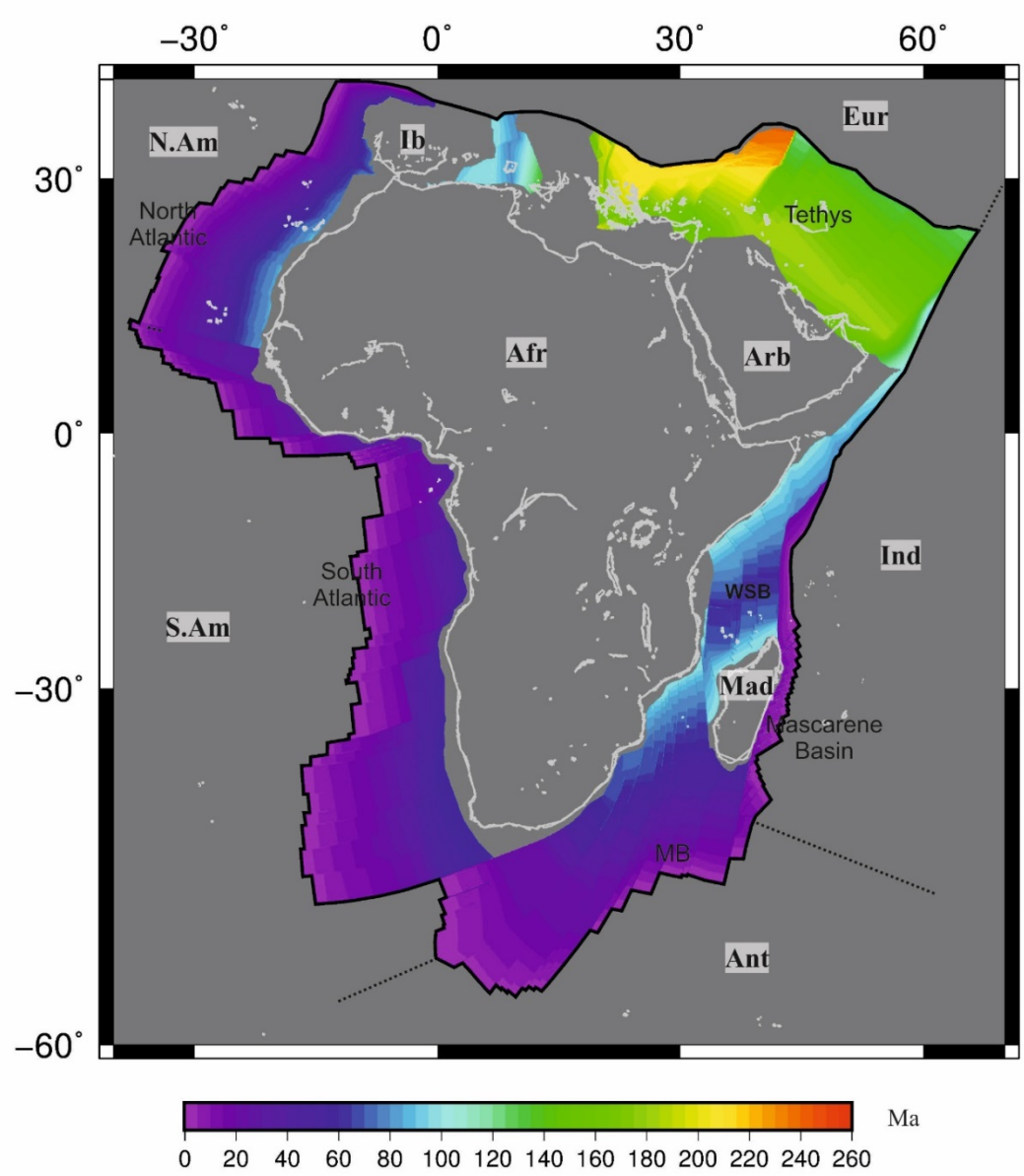

Figure 4.4: Seafloor age grid for the African Plate at 75 Ma (South Atlantic age grid from Perez-Diaz & Eagles 2017, Central Atlantic and Tethys Ocean age grid from Seton *et al.*, 2012).

4.2.4. Model Forces

Figure 4.5 shows the forces considered in this paper, acting on the African plate. Below we describe the origin of these forces and the assumptions we have used to constrain them.

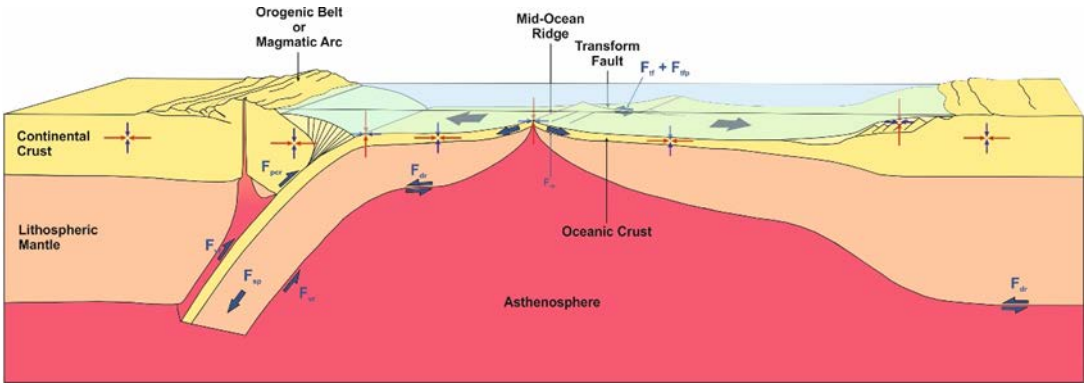

Figure 4.5: Forces in the lithosphere used in this paper. (Redrawn and modified from Fossen, 2010; Foryth & Uyeda, 1975)

Ridge Push (F_{rp})

One of the most important driving forces acting on the African Plate is ridge push. The term ridge push is misleading; the force is not isolated at the ridge axis but is a pressure gradient integrated horizontally across the whole of the plate (Lister, 1975). The force arises as the result of 2 effects; 1) when new oceanic material is produced at mid-ocean ridges it is elevated above the surrounding lithosphere, hence it has gravitational potential energy and the tendency to spread out and sink to a lower energy and 2) as oceanic lithosphere ages, it cools and becomes denser, causing it to subside (Lister, 1975; Forsyth & Uyeda, 1975). It is compressional in nature and acts perpendicular to the spreading direction.

The ridge push calculation for a section (of unit width) of lithosphere from spreading ridge to age *t* comes from Richter & McKenzie (1978):

$$F_{rp} = gh(\rho_m - \rho_w)\left(\frac{1}{3}L + \frac{1}{2}h\right) \quad (1)$$

g = gravitational acceleration
h = difference in elevation between the ridge crest and the ocean floor
L = lithospheric thickness
ρ_w = density of seawater
ρ_m = density of sublithospheric mantle

For Africa at 75 Ma, the plate is surrounded on three sides by mid-ocean ridges, so ridge push force is likely to have a major effect on the intraplate stress field. Oceanic lithosphere ages for the African plate at 75 Ma were taken from the age grid described above (section 2.3, figure 4.4). The age grid is used to compute the age gradient a.k.a. the change in age per kilometre of crust (fig. 4.6). Both L and h increase with age t. Ridge push is then calculated from the age gradients based on

the GDH1 thermal model of Stein & Stein (1992), which describes the average variation in depth and heat flow with lithospheric age. Where depth (m) is related to the age (Myr) by

$$d(t) = 2{,}600 + 365t^2 \qquad t < 20\ Myr \qquad (2)$$

$$= d_r + d_s\left[1 - \left(\frac{8}{\pi^2}\right)\exp\left(\frac{-\kappa\pi^2 t}{a^2}\right)\right] \qquad t \geq 20\ Myr \qquad (3)$$

$$= 5651 - 2473\exp(-0.0278t) \qquad (4)$$

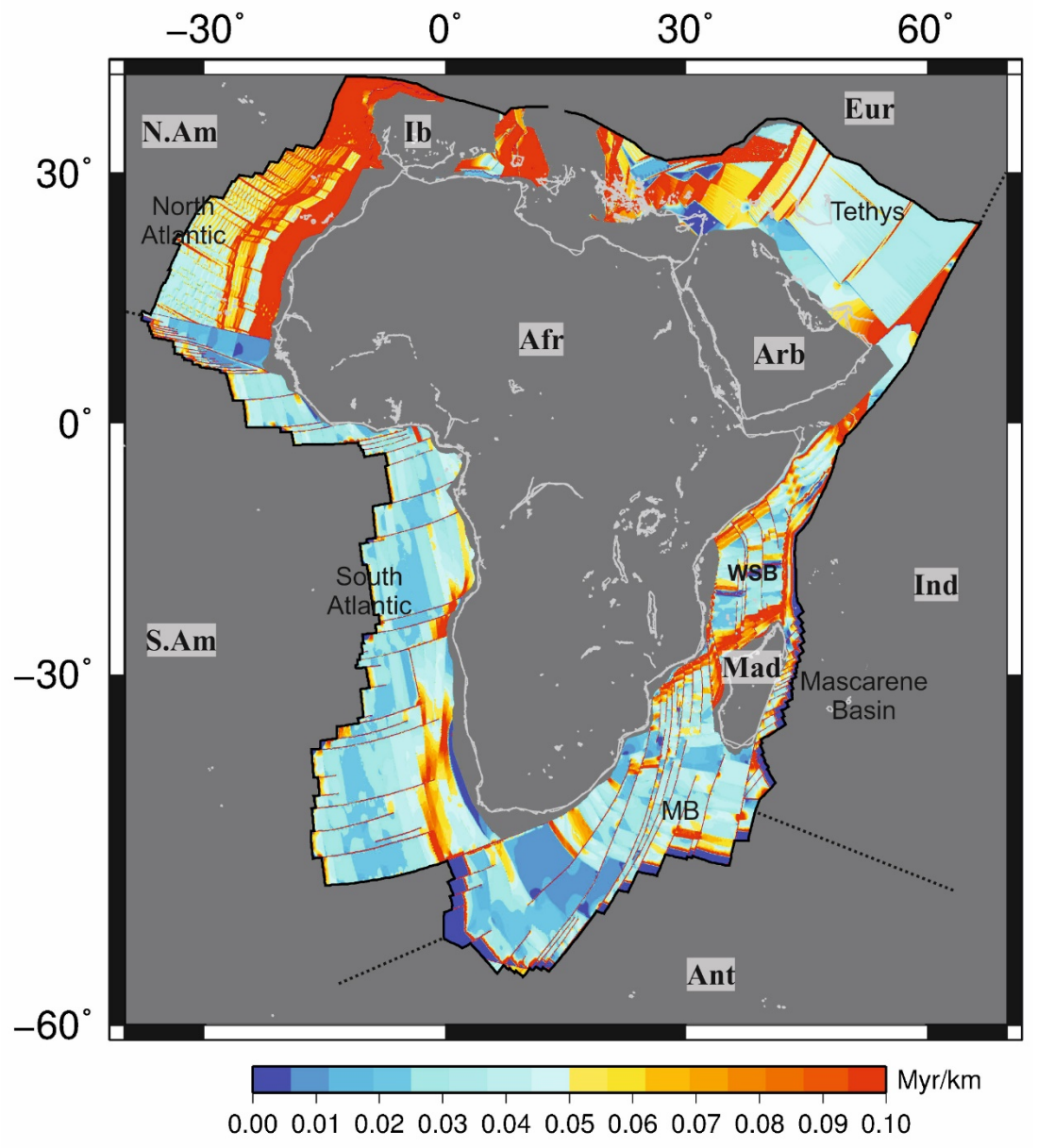

Figure 4.6: Age Gradients for the oceanic lithosphere of the African Plate at 75 Ma derived from the age grid in figure 4.4.

Slab Pull (Fsp)

Another major driving force acting on the African Plate at 75 Ma is slab pull (F_{SP}), acting at subduction boundaries. In our model, Africa at 75 Ma, a large portion of the northern boundary is the subduction zone between Africa and Eurasia. Slab pull results from the density contrast between the sinking slab and the surrounding mantle. The oceanic slab is much colder and denser than the surrounding mantle creating a downward pull, which can be transmitted to the horizontal part of the plate to drive its motion (Forsyth & Uyeda, 1975). Similarly, to ridge push, slab pull can be considered as a lithospheric body force that is integrated throughout the plate.

Slab pull is a lithospheric body force that acts horizontally throughout the lithosphere and is calculated by integrating density anomalies from the trench to the end of the slab. Slab length The GDH1 thermal model (Stein & Stein, 1992) is used to calculate the density anomalies of the slab at the trench, assuming the slab is heated by conduction after it has sunk beneath the overriding plate (Govers & Meijer, 2001). Integration is taken up to the end of the slab length, which is calculated as a function of age and assumed to be the end of the seismic zone, predicted by oceanic age and convergence velocity (Wortel *et al.,* 1991).

While slab length can be estimated due to its age-dependent relationship, slab dip angle is much more difficult constrain, it does not appear to show any correlation to the magnitude of slab pull, the age of subducting lithosphere at the trench, the thermal regime of the subducting lithosphere, the convergence rate, or the subduction polarity (Lallemand *et al.,* 2005). However, the absolute motion of the overriding plate has been suggested to play an important role on slab dip (Lallemand *et al.,* 2005). Average slab dip angles beneath continental plates have been suggested to be in the range of 50° ± 20° (Lallemand *et al.,* 2005). We assume a slab dip angle towards the higher end of this range, 60°. The age of the lithosphere at this subduction zone is quite old and also very dense which justifies the use of a slightly higher angle.

The derivation of the slab pull calculations used in this chapter originate from the work of Wortel *et al* (1991) and are described below.

Slab pull, which constitutes the downdip component of the gravitational body force acting on the dense subducted slab, is calculated using the thermal model of McKenzie (1969) where slab pull per unit length in the direction of the trench is given by:

$$F_{sp} = g \sin \phi \int_0^L \int_0^{s_{sz}} \Delta\rho \, dx \, dz \qquad (5)$$

Φ = dip
L = thickness of downgoing slab
$\Delta\rho$ = density contrast between slab and surrounding mantle
x = direction downdip to the upper (dipping) interface between the slab and the upper mantle.
z = direction perpendicular to the upper (dipping) interface between the slab and the upper mantle.

The downdip integration is limited to the end of the seismic zone (S_{SZ}), which is given by Wortel & Vlaar, (1988), this is combined with McKenzie's (1969) thermal model to give:

$$F_{sp} = \left(\frac{4g\alpha\rho_m T_m L^3}{\kappa\pi^4}\right) v_c \sin\emptyset \left[1 - \exp\left(\frac{-\pi^2\kappa S_{SZ}}{v_c L^2}\right)\right] \quad (6)$$

v_C = rate of plate convergence.
α = coefficient of thermal expansion.
ρ_m = density of the asthenosphere.
T_m = temperature of the asthenosphere.
κ = the thermal diffusity of the asthenosphere/lithosphere.

All the parameters are assumed to be constant, and using the age dependence of L (see above), κ = 0.9 x 10^{-6} m^2s^{-1} and S_{SZ} = 0.12 $v_c t$ (see Wortel & Vlaar, 1988), Richter & McKenzie (1978) obtain the following:

$$\left[1 - \exp\left(\frac{-\pi^2\kappa S_{SZ}}{v_c L^2}\right)\right] = 0.29 \quad (7)$$

Consequently, the factor between brackets does not depend on either v_c or on the age of the lithosphere. Putting $v_c \sin\phi = v_z$, they found that:

$$F_{sp} \propto v_c L^3 \quad (8)$$

Finally, they took into account the age-dependence of L to give:

$$F_{sp} = c_{sp} v_z t^{\frac{3}{2}} \quad (9)$$

Where c_{sp} is a constant and the age of the oceanic lithosphere is taken from the age grid, described above in section 2.3.

The slab pull force is reduced by the compositional buoyancy of the subducted slab following England and Wortel (1980). The compositional buoyancy acts in the up-dip direction of the subducting slab and arises from the petrological stratification of the oceanic crust and upper mantle created during the sea floor spreading (Vlaar & Wortel 1976; Oxburgh & Parmentier 1977; England & Wortel 1980); both the basaltic crust and the depleted uppermost mantle are less dense than the adjacent upper mantle an equivalent temperature and pressure.

This compositional buoyancy force (F_{cb}) counteracts the force resulting from the cooling and densification of the lithosphere which is represented by slab pull (F_{sp}, Wortel *et al.*, 1991). England & Wortel (1980) suggest that the compositional buoyancy of the descending lithosphere is removed by phase changes at less than 100 km depth. Therefore, the magnitude of this force is estimated by integrating the (compositional) density difference of the dipping oceanic lithosphere down to a depth of 100 km. The value of the compositional buoyancy is estimated as 3.0 x 10^{12} N m^{-1} based of model results obtained by vanden Beukel (1990), and this is used to reduce the slab pull force (Wortel *et al.*, 1991).

Basal Drag (F_{dr})

Basal drag (F_{dr}) is a force that acts on the base of the plate and is distributed over the entire area of the plate, also referred to as a shear traction. It arises from the relative motion between the plate and the mantle (Gover & Meijer, 2001). Very little is understood about this force, even whether it drives plate motion, if there is active flow (i.e. thermal convection) in the asthenosphere or resists it, when the asthenosphere is passive with regards to plate motion (Forsyth & Uyeda, 1975).

Basal drag is assumed to act parallel to the direction of the absolute plate motion and to have a magnitude in the order of a few MPa only (Govers & Meijer, 2001). As a result, the mantle drag acting on the African Plate should be proportional to the area and to the velocity of the plate relative to the asthenosphere (Forsyth & Uyeda, 1975).

Due to the size of the African plate, it is likely that mantle drag contributed to the force balance. We assume a value for basal drag of either +1 MPa when assuming the force is driving plate motion (acting parallel to plate motion), or -1 MPa when assuming it is resisting plate motion (acting anti-parallel to plate motion).

Transform Push (F_{tfp})

Transform Push (F_{tfp}) is a driving force resulting from normal stresses transmitted across transform faults and it is proportional to the relative velocity perpendicular to transform segments (Govers & Meijer, 2001).

It is generally thought that the contribution of transform push is insignificant, because the shear resistance at transform faults is assumed to be low and the two forces are considered to be proportional (Govers & Meijer, 2001). However,

Transform Resistance (F_{tf})

Transform fault resistance is a shear resistive force acting at transform faults as a result of the shear stress at strike-slip motion. It acts on all transform faults in our model (Govers & Meijer, 2001).

Plate Contact Resistance (F_{pcr}).

There are a number of resistive forces that act on the slab at subduction zones. One of them is the plate contact resistance (F_{pcr}). It is a shear stress between the subducting and the overriding plate integrated along the contact area. F_{pcr} acts in the direction of relative plate motion so a positive value means frictional resistance. (Govers & Meijer, 2001).

Viscous Resistance (F_{vr})

Viscous resistance (F_{vr}), sometimes referred to as slab resistance, is the resistive force arising from mantle shear stresses acting on the top and bottom of the slab (Govers & Meijer, 2001). It depends on the velocity of the downgoing slab and is proportional to the viscosity of the surrounding mantle. F_{vr} is orientated perpendicular to the strike of the trench and resists the advance of the plate into the mantle (Forsyth & Uyeda, 1975).

4.2.5. Torque Balance

As the African plate moves across the spherical Earth, the forces acting on the plate, described above, are considered to be rotational about an axis that passes through the centre of the Earth, i.e. a torque. The torques are described as vectors in a Cartesian co-ordinate system (Forsyth & Uyeda, 1975), and the location where their poles intersect the Earth can be plotted to assess the likelihood of a torque balance solution.

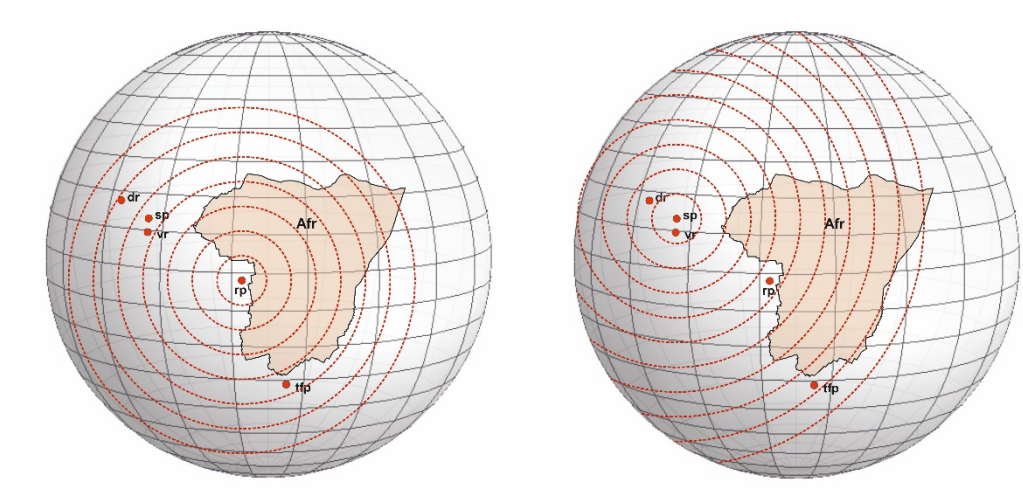

Fig 4.7: Example of the poles of the boundary force torques plotted on a sphere, (left) the red circles indicate orientation of the sum of the ridge push force and (right) the orientation of the sum of the slab pull force.

Our model rests on the assumption that the plate is in dynamic equilibrium i.e. it is neither accelerating nor decelerating. As a result, the sum of the torques of forces acting on the plate are required to sum to zero (Forsyth & Uyeda, 1975).

The torque balance is solved by the following equation, from Govers and Meijer (2001):

$$\sum_i T_i = \sum_i \int_O R \times F_i dO = 0 \qquad (1)$$

Where $\sum_i$ is the sum over the total set of torques vectors, and the integration is over the boundaries or the area of the plate O, depending on the nature of the force involved, i.e. surface force or boundary force. Of the forces considered in our model, ridge push and mantle drag are distributed over the surface area of the plate, all other forces are modelled as boundary forces. F_i is the force type and R is the radius vector from the centre of the Earth to the surface location where a force acts on the African plate.

We assume that the ridge push, slab pull, and mantle drag are understood well enough to be considered as "known" torques in the force balance calculations and hence can be used to solve for the unknown forces namely in our model plate contact resistance, viscous resistance, transform fault push and resistance, using equation (1).

4.2.6. Finite Element Modelling

The calculations were carried out on a finite element mesh, consisting of an assembly of triangular elements in a spherical shell (GTECTON, Govers & Meijer 2001). The Africa Plate is assumed to consist of lithosphere of uniform thickness at 100km thick with a poisons ratio of 0.3 and a Young's modulus of $7.5x10^3$.

4.3. Results

Figure 4.8 shows the location of the torque vectors which is used to determine whether or not a solution is possible, whether balance is possible. For mechanical equilibrium of the plate to be achieved the driving forces must be balanced by the resistive forces. The red dots are the poles of the driving force torques and the red area outlines the region where the sum of the driving torques will lie. The blue dots are the antipodes of the driving torques and the blue area is the region where the antipode of the driving torque will occur. The sum of the resistive torques will lie in the grey area. A solution will exist where the grey and blue curves intersect. The Afr-absolute motion pole was calculated using Africa's motion with respect to India Ocean hotspots (O'Neill *et al.*, 2003).

When mantle drag (dr) is modelled as resistive (fig. 4,8 (top)), the anti-driving (blue) and resistive (grey) curves do not intersect, therefore there is no solution for this set of forces.

When the mantle drag (dr) is modelled as driving plate motion (fig. 4.8 (bottom)) there are only two resistive forces plate contact resistance (pcr) and transform fault resistance (tf), connected by single line and no longer the shaded grey area. The sum of the resistive forces will lie somewhere along the connecting line. In this model the blue area still does not intersect this line, so based on these torques there is no solution either.

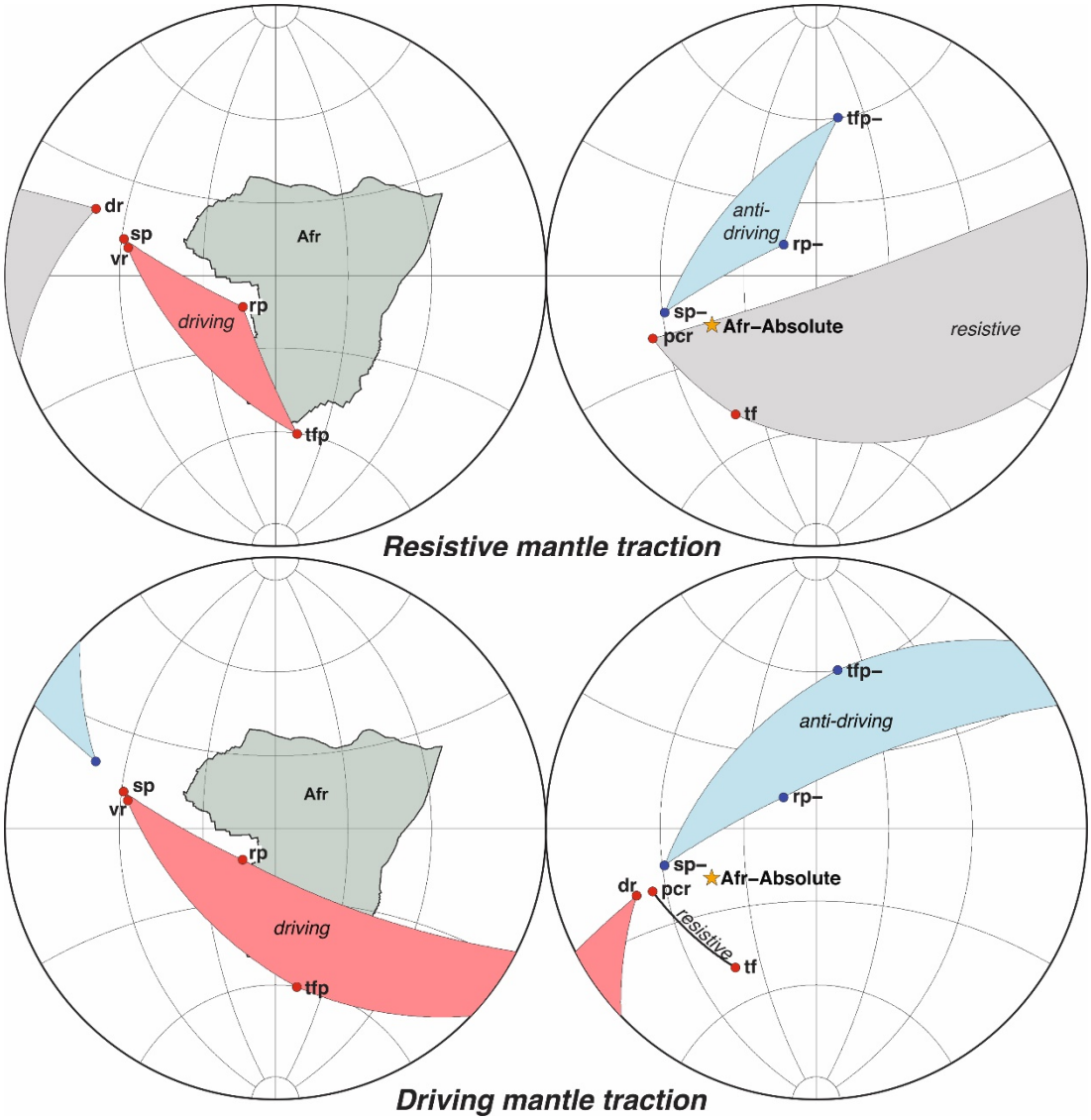

Figure 4.8: (top) torque results when mantle drag (F_{dr}) is resistive; (bottom) torque results when mantle drag (F_{dr}) is driving.

Further iterations of the above, plotting the torque vectors was carried out (see fig 4.9) by varying the constraints on slab pull in order to try and find a solution; a point where the resistive forces and the antipodes of the driving forces intersect. However, still no solution could be found.

a)

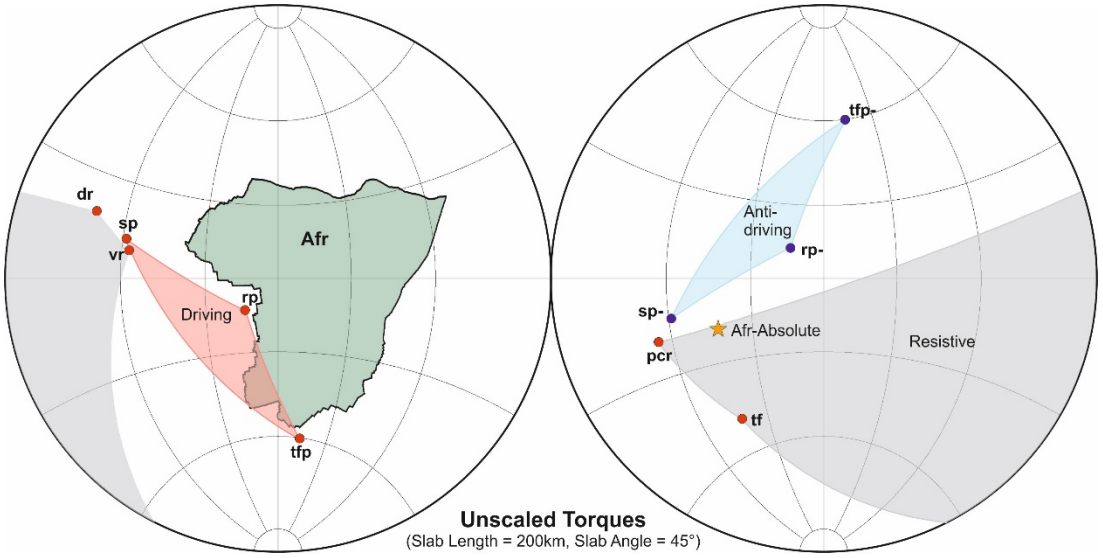

Unscaled Torques
(Slab Length = 200km, Slab Angle = 45°)

b)

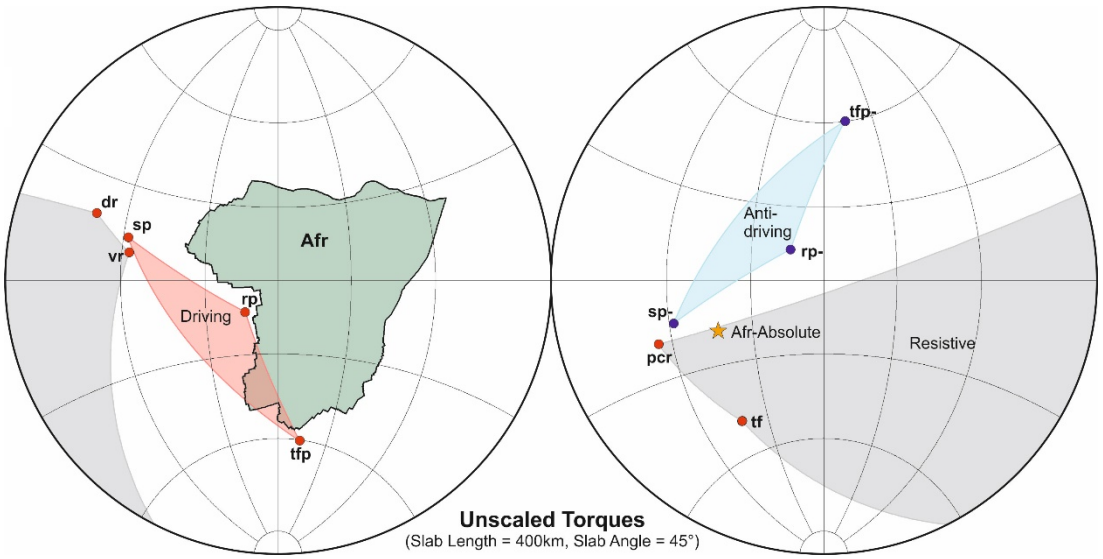

Unscaled Torques
(Slab Length = 400km, Slab Angle = 45°)

c)

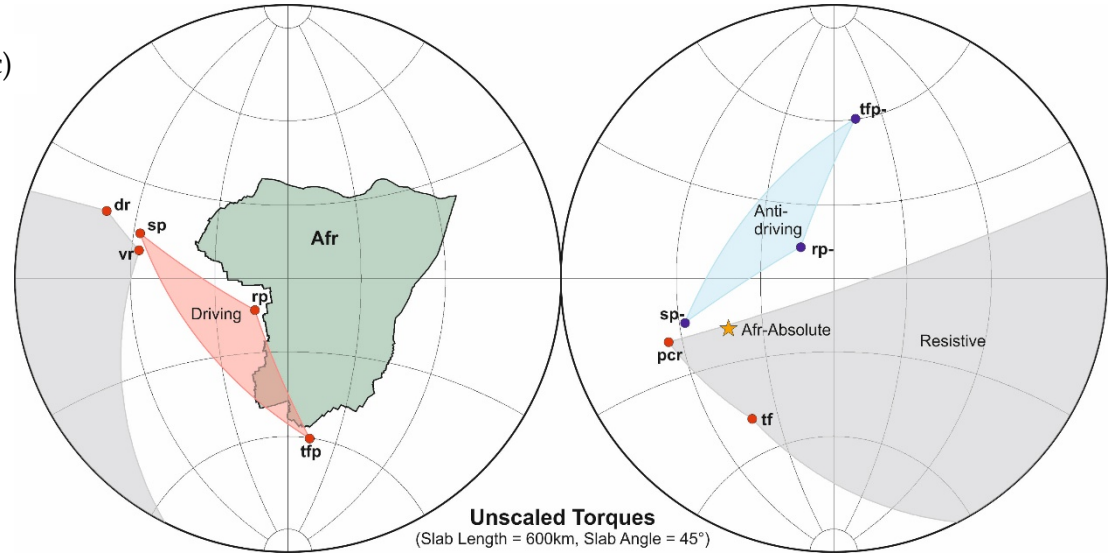

Unscaled Torques
(Slab Length = 600km, Slab Angle = 45°)

d)

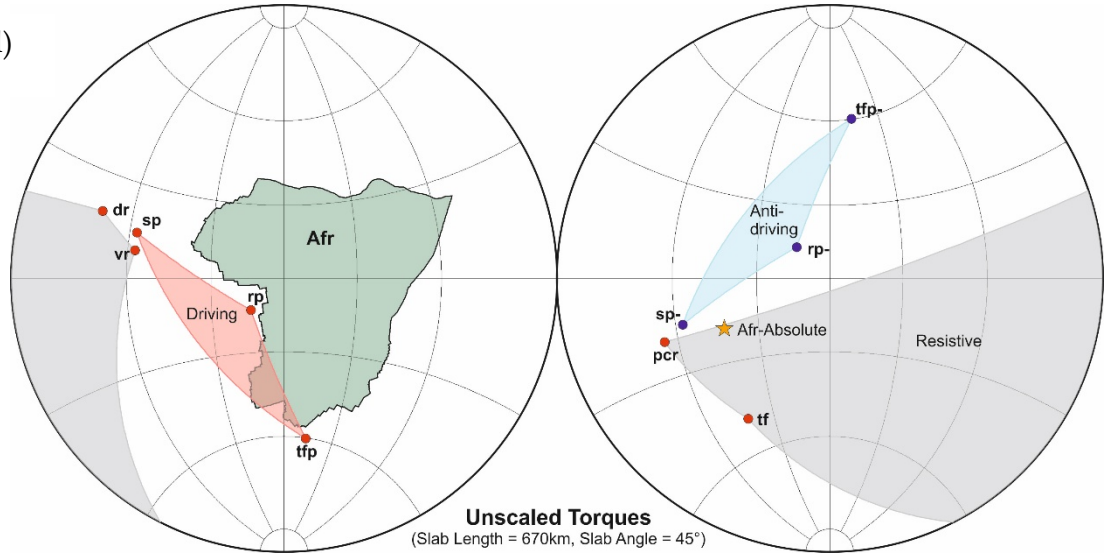

Figure 4.9: torque results plotted of a sphere with varying slab lengths and slab angles. (Previous page) a) Slab length 200 km and slab angle = 45°, b) slab length = 400 km and slab angle = 45°, c) slab length = 600 km and slab angle = 45°, (this page) d) slab length = 670 km and slab angle = 45°.

It was found from other model results that changing the slab angle had very little effect on the where the pole of the slab pull torque plotted, and so changing this angle would not lead to an overlap between the resistive forces and the antipodal area of the driving forces, and so would not lead to a solution. However, it was found that the slab length did have an effect of the slab pull torque location. Instead of allow the slab length to be determined as a function of age, a number of model iterations were made to calculate the location of the slab pull torque pole by manually varying the length of the slab (see figure 4.9). By increasing the length of the slab, the slab pull torque pole moved closer to the area in which the sum of the resistive forces lies. However, the slab length is limited to the end of the seismic zone at 670 km (see section 2.4. Slab Pull) and even with these changes there is still no overlap and hence no solution.

4.4. Discussion

Due to the fact that no solution exists for this current model set of forces, we were unable to calculate the force balance and the resultant stress field.

In modelling of this kind, many assumptions need to be made about the magnitude and direction of the forces acting on the plate. Uncertainties in these assumptions can result in the failure to reach a solution. In our set of forces, it is most likely that the uncertainties lies within the choices made to constrain slab pull, and how these affect its position.

During the first Slab length is calculated as a function of age. The age grid from Seton *et al.* (2012) gives very old ages for the Tethys Oceanic lithosphere subducting beneath Eurasia (fig. 4.3). As a result, such old lithosphere would give a very long slab length and hence a very large slab pull force, which was corroborated by early

attempts to calculate the force balance. Such an unrealistically large slab pull force would need to be balanced by equally unrealistically high resistive forces.

We are confident in the accuracy and resolution of the age grid of the NW Indian Ocean produced in this thesis (chapter 4) and the similar age grid of the South Atlantic by Perez-Diaz and Eagles (2017). Both grids are based on large data sets and robust kinematic models which closely replicate seafloor spreading and therefore closely approximate the true seafloor age (Perez-Diaz & Eagles, 2017). These models represent a significant improvement in confidence in comparison to the age grid of Seton *et al* (2012), specifically when compared to the latter's determinations of the Neotethys oceanic lithosphere in the Northeast of the African Plate.

The ocean floor of the Neotethys formed when the Cimmerian blocks rifted off Gondwana in the Late Permian and drifted north across the Paleo-Tethys Ocean (Muttoni *et al.,* 2008). The Neotethys opened behind the Cimmerian blocks until they collided with Eurasia, causing Neotethys to buckle and begin subducting beneath Eurasia.

Most of the Neotethys oceanic lithosphere has since been destroyed by subduction, although there are indications that parts of the Ionian Sea and the east Mediterranean basins may represent the old preserved in-situ Neotethys ocean floor, ranging in age from ~270 Ma (Late Permian) to 230 Ma (Middle Triassic) (Müller *et al.,* 2008). As a result, age grid for this area cannot be produced in the same way as those in chapter 4 and Perez-Diaz *et al* (2017), using seafloor data. The age grid from Seton et al (2012) is mostly based on the work of Müller *et al* (2008), who produced synthetic Neotethys ocean floor isochrons based on Stampfli and Borel's (2002) tectonic model of the opening of the Neotethys Ocean.

Uncertainty in the northeast area of the age grid derives from uncertainty in the timing of Neotethys opening, which is poorly unconstrained. The timing and rates of motion of the Cimmerian terranes are poorly constrained because paleomagnetic based estimates of paleolatitude obtained with modern techniques are minimal for these areas (Muttoni *et al.,* 2008). Paleomagnetic poles could help retrace the relative motion of the Cimmerian terranes and hence the opening of the Neotethys behind it.

Due to the destruction of the Neotethyan Oceanic lithosphere beneath Eurasia it is difficult to produce an accurate, detailed age grid for this part of the African Plate, so there is significant uncertainty in the age of the subducting lithosphere.

In addition to the uncertainties surrounding slap pull, there may also be errors associated with mantle drag and absolute plate motion direction. As mantle drag is dependent on absolute plate motion, any uncertainty in the location of the Afr-Absolute pole translates to uncertainty in the position of the mantle drag (dr) pole as well. However, from figures 4.8 and 4.9 it is clear that moving the dr pole slightly will still not likely result in an intersection.

4.5. Conclusion

We created two models using a set of plate forces including ridge push, slab pull, mantle drag, transform push and resistance, and subduction related resistive forces. The two models differed in the nature of mantle drag, in one model it was assumed to be driving plate motion, in the other it was assumed to be resisting it. By calculating and plotting the torque vectors for each force it became apparent that no solution for the force balance was possible for either model. As a result, we were unable to calculate the force balance required for Africa to be in a state of dynamic equilibrium at 75 Ma or the stress field at this time using the chosen set of forces and constraints. I addition, changing the constraints on slab pull, such as the age of the subducting lithosphere, the slab length and the slab dip angle still did not result in a solution.

Chapter 5

Discussion

5.1 Introduction

The main aim of this thesis is the development of a high resolution, comprehensive plate kinematic model of the Northwest Indian Ocean from the initial rifting of Gondwana in the Early Jurassic to the present-day. The new plate kinematic model has been utilised as basis for further analytical and correlative studies including:

- A first-order plate-kinematic paleostress analysis,
- A new margin-scale tectono-stratigraphic correlation of the conjugate margin basins,
- The investigation of the applicability of plate-scale dynamic paleostress analysis based on time-series paleo-plate and plate boundary geometries of main tectonic stages identified in the plate kinematic model.

This chapter presents a brief summary of the results described in detail in chapters 2, 3 and 4, followed by a discussion of the wider implications of these results and assessment of the limitations. Finally, the possible direction of future work is considered and the main conclusions are briefly summarised.

5.2 Summary of Results

The following sections summarise, in chronological order, the four phases of tectonic development and related paleo-stress fields of the East African and West Madagascan Margins, with reference to the evolution of the sedimentary basins along those margins and paleostress fields. All of the events reviewed here have been discussed in depth and in the context of other published studies in chapters 2, 3 and 4.

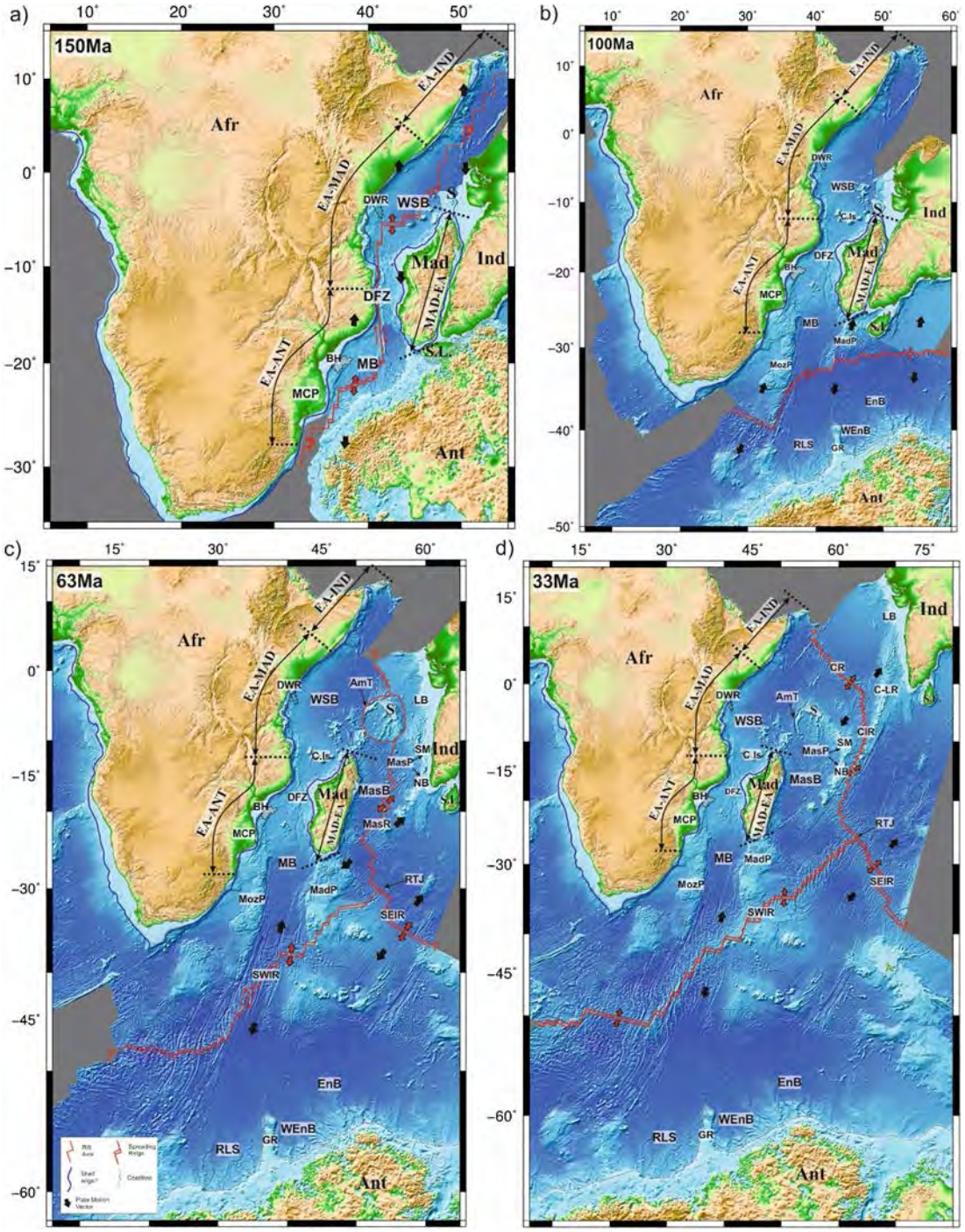

Figure 5.1: Summary image showing the 4 Phases of tectonic development, a) Phase 1, b) Phase 2, c) Phase 3, d) Phase 4. See text for detailed descriptions.

5.2.1 Phase 1 Early Jurassic (Toarcian) to Early Cretaceous (Hauterivian): 183-177 Ma to 133 Ma

Phase one begins with a separate distinct period of rifting, following the end of the Karoo intracontinental rifting and the eruption of the Karoo-Ferrar LIP at approximately 183 Ma. Rifting occurred in a NW – SE direction in the West Somali and Mozambique Ocean Basins, between East Gondwana (comprising Madagascar, India, Seychelles, Antarctica, and Australia) and West Gondwana (comprising Africa and South Africa), linked by dextral movement on the Davie Fracture Zone (DFZ). $S_{H\,max}$ in the sedimentary basins of the EA-IND, northern EA-MAD and MAD-EA, and EA-ANT margin segments trended sub-parallel to margin, suggesting orthogonal rifting. $S_{H\,max}$ trended highly oblique to southern EA-MAD and MAD-EA segments accommodating dextral transtension on the Davie Fracture Zone. Frequent marine incursions from the (Neo)Tethys Ocean in the north east deposited syn-rift sediments in developing half-grabens of mixed shallow-water terrigenous and marine shales in the sedimentary basins.

Breakup occurred between East and West Gondwana at approximately 167 Ma, based on the oldest magnetic anomalies and their extrapolation back to the continental margins. Ages assigned to breakup unconformities in the sedimentary basins vary from 165 Ma in Somalia, ~171/174 Ma between East Africa and Madagascar, and 157 Ma between Mozambique and Antarctica.

Breakup was followed by active seafloor spreading in the West Somali and Mozambique ocean basins constrained by magnetic anomaly data (chapter 2). The initiation of active spreading ridges resulted in a compressional ridge push force, perpendicular to the ridge axis. As a result, $S_{H\,max}$ changed to NE-SW, perpendicular to the EA-IND, northern EA-MAD and MAD-EA, and EA-ANT margin segments. $S_{H\,max}$ trended highly oblique to southern EA-MAD and MAD-EA margins segments – giving rise to strike-slip along the Davie Fracture Zone. The ridge push force from such young lithosphere seems not to have been strong enough to give rise to any tectonic inversion on the extended continental margins.

Deposition of the Early Post-rift megasequence followed breakup in the marginal sedimentary basins, which consisted of mainly shallow marine, carbonate platforms, giving way to shales in the deeper parts of the basins.

5.2.2 Phase 2 Early Cretaceous (Hauterivian) to Late Cretaceous (Coniacian): 133 Ma to 89 Ma

Seafloor spreading in the West Somali Basin ceased just after chron M10n (133.9 – 133.5 Ma), and the boundary between the west and east Gondwana plates relocated to the West Enderby Basin, to the south of Madagascar, which became fixed to the African plate and separated together with India from Antarctica. Contemporaneous with this change was a major end Hauterivian/Barremian unconformity, which has

been recognised in the basins bordering the West Somali Basin and the Davie Fracture Zone (Bosellini, 1992; Coffin & Rabinowitz, 1988).

Seafloor spreading in the Mozambique Basin continued now connected to the spreading ridge in the West Enderby Basin. The lack of data pertinent to the movement of Sri Lanka makes it difficult to say when it moved to its present-day position relative to India. We modelled its movement between 120 Ma and 89 Ma when enough space had formed between India, Madagascar and Antarctica to accommodate the movement. After 89 Ma, Sri Lanka became fixed to India.

$S_{H\,max}$ was orientated in an approximately NW-SE orientation produced by the compressional ridge push force originating from the Southwest Indian Ridge (SWIR). In the sedimentary basins along the EA-IND, northern EA-MAD, northern and central EA-ANT segments $S_{H\,max}$ was orientated perpendicular to the continental margin, giving rise to the potential for inversion, which may be the cause of the regional Hauterivian/Barremian unconformity mentioned above. Along the southern EA-MAD and MAD-EA segments, $S_{H\,max}$ trended oblique to the strike of the margin with the potential for strike-slip or transpressional deformation. Key et al. (2008) suggest that early phase 2 deposition was controlled by renewed rifting and extensive inland erosion in the Rovuma Basin (southern EA-MAD) whilst in the Angoche Basin (southern EA-MAD/EA-ANT) a short-lived period of tectonic uplift followed the end of movement on the Davie Facture Zone (Mahanjane 2014).

5.2.3 Phase 3 Late Cretaceous (Coniacian) to Middle Paleocene (Selandian): 89 Ma to ~60 Ma

The start of Phase 3 is marked by the eruption of the Morondava volcanics on Madagascar, linked to the arrival of the Marion mantle plume beneath the South-eastern tip of the island at ~89 Ma. This was followed by continental rifting and then seafloor spreading at the Mascarene Ridge, and the opening of the Mascarene Basin, separating India and Madagascar.

The spreading direction along Africa's southeastern plate boundary with Antarctica remained in an approximately NW-SE direction and the stress field in this area, stretching into South Africa, was still dominated by the NW – SE compressive ridge-push forces exerted by the SWIR.

Further north, far-field stresses produced by the newly formed Mascarene Ridge along the eastern boundary of the African plate, likely dominated the stress field along the East African and West Madagascan margins. Ridge-push forces due to this new dominantly N-S trending spreading zone resulted in $S_{H\,max}$ oriented parallel to the local plate vectors varying from a NE-SW direction in the northern Somalia margin to an E-W direction in the Mozambique margin.

Consequently, in the NE-SW oriented EA-IND, northern EA-MAD, northern and central EA-ANT segments $S_{H\,max}$ was oriented mostly along-strike of the continental margin and $S_{h\,min}$ in the dip direction. The resulting passive margin stress fields gave rise to the potential for shelf extension by local gravity-driven deformation.

Along the southern EA-MAD and MAD-EA segments, compressional far-field stresses were orientated perpendicular to the margin, indicating the potential for inversion of earlier strike-slip structures in this stage. Accordingly, Clark (1998) describes renewed tectonic activity in the basins of western Madagascar, with wrench faulting and compressional folding occurring in the Late Cretaceous. Turonian times also saw a major period of volcanism in Madagascar, which continued throughout the Late Cretaceous and into the Paleocene.

Early post-rift sedimentation continued into the early part of Phase 3. Late post-rift deposition began by the end of Phase 3 in the EA-IND, southern EA-MAD and EA-ANT margin segments. However, in the northern EA-MAD and MAD-EA margins segments, late post-rift sedimentation did not start until Phase 4. The late post-rift stage is dominated by generally slower thermal subsidence and basinward progradation of depositional systems consisting of deep-water sediments e.g. shales, marls, mudstones and turbiditic sandstones (Salman & Abdula, 1995; Bosellini, 1992; Key et al., 2008).

The boundary between the early and late post-rift megasequences is marked by a major regional unconformity ranging from Maastrichtian (Late Cretaceous) in the EA-IND, southern EA-MAD and EA-ANT margin segments to Paleocene age in the northern EA-MAD and the conjugate northern MAD-EA margin segments. Towards the end of this phase, the arrival and peak activity of the Deccan-Réunion mantle plume coincides with a number of plate boundary changes in the Northwest Indian Ocean e.g. the end of seafloor spreading in the Mascarene Basin, the rotation of the Seychelles plate, the opening of the Laxmi Basin and the initiation of seafloor spreading on the Carlsberg Ridge.

Stress Modelling at 75 Ma

The initiation of the Mascarene Ridge provides addition ridge push force along the eastern boundary of the African plate and hence, affects the distribution and magnitude of driving forces acting on the plate.

For a proof of concept as part of this thesis, I chose a time slice from this phase, 75 Ma, to further process paleo-plate geometry data and to test the dynamic stress modelling approach described in chapter 4. After successfully implementing all work steps, the first attempt at force balance calculations was unsuccessful. It is likely that the slab pull force used in the balance was unreasonably strong, and so dominated the force balance. The reason for this is most likely uncertainties in slab age, length and dip angle, affecting the magnitude of slab pull. A further iteration

was not possible in the time frame of the thesis but will be part of ongoing project work for future publication.

5.2.4 Phase 4 Middle Paleocene (Selandian) to present: ~60 Ma to present

The start of Phase 4 is marked by the end of seafloor spreading in the Mascarene Basin and the onset of spreading on the Carlsberg Ridge (CR) and Central Indian Ridge (CIR) separating India and the Mascarene Plateau which continues throughout Phase 4 to the present day.

Late post-rift deposition continued into Phase 4 until the Oligocene, where a major regional unconformity separates it from the overlying modern margin megasequence. The Oligocene unconformity has been attributed to doming and uplift of the African plate over the Afar plume, prior to the onset of the East African Rift System (EARS; Wichura et al., 2011; MacGregor, 2015; Ebinger & Sleep, 1998). Development of the EARS caused uplift of the African continental hinterland and an increased rate of sediment deposition to the East African marginal basins. The influx of sediment triggered collapse of shelf margin sediment wedges, turbidity currents, and the formation of deep-water fold-and-thrust belts (Mahanjane & Franke, 2014; Mahanjane et al., 2014). The modern margin meqasequence is characterised by large prograding deltas and gravity-driven deformation (Mahanjane & Franke, 2014; Mahanjane et al., 2014).

The orientation of $S_{H\,max}$ in Phase 4 is approximately NE-SW, subparallel to most margin segments allowing local stress fields to be controlled by gravity-driven deformation. The exception to this is the southern EA-MAD and southern MAD-EA margin segments where the stress is oblique to the trend of the margin creating the potential for strike-slip deformation. However, in the sedimentary basins of the East African margin (e.g. Lamu Basin (Kenya), Rovuma Basin (Tanzania/Mozambique)) it is likely that the EARS controlled the first-order regional tectonic stress field since its onset in the Oligocene, with local basin-scale stress patterns overprinting it along the margins.

5.3 Critical Evaluation of Project Outcomes

There have been many advances in paleogeographic and paleo-tectonic modelling since the theories of continental drift (Wegner, 1912) and plate tectonics (McKenzie, 1967; Morgan, 1968) were first proposed in the twentieth century. As a result it is now possible to model the motion of plates on a global scale and with ever tighter constraint. These plate kinematic models are invaluable to not only academics in the field, but have wider implications and uses such as understanding of the development of continental margins and their sedimentary basins, geodynamic modelling, and the importance this has for hydrocarbon prospectivity. This section represents an evaluation of the methods used in this thesis and discusses the wider implications of their results.

5.3.1 Plate Kinematic Model

A number of plate tectonic models over the years have addressed the fragmentation of Africa, Madagascar, India and Antarctica based on a range of different data sets and methods (e.g. Reeves et al., 2016; Cande & Patriat, 2015; Gibbons et al., 2013; Patriat & Segoufin, 1988). However, even with the increasing volume of higher quality data and advances in computer-assisted modelling, detailed understanding of the timings of key stages in plate motions, such as breakup and the onset and end of seafloor spreading in diverse ocean sub-basins remains elusive.

Magnetic anomaly isochrons in the area were first interpreted in the Arabian and East Somali Basins in the 1960s. Since then many more have been interpreted and the interpretations refined in areas including the West Somali and Mozambique Basins (see chapter 2 and references therein). Most recent additions include magnetic data in the Mozambique Basin (König and Jokat, 2010; Leinweber and Jokat, 2012), which allowed us to produce the updated model of Africa – Antarctica divergence described in chapter 2. However, the magnetic anomaly database in the West Somali Basin has not been added to since the 80s (Segoufin and Patriat, 1980; Cochran, 1988) and has only been reinterpreted since then. Given the controversy over whether the Mozambique and West Somali basins opened simultaneously between the same pair of plates, with most models assuming they did but few actually using the assumption as a constraint, new magnetic anomaly data in the West Somali Basin would be highly beneficial to understand the earliest plate motions and the formation of these margins. It would also help to clarify when seafloor spreading ended in the West Somali Basin which is the source of ongoing disagreement amongst plate modellers. Understanding these early tectonic events is vital to understanding the timing and distribution of petroleum systems.

The method of using magnetic anomaly data and fracture zone traces, and the joint inversion technique produces a robust model, free from the uncertainties of identifying pre-breakup features and reuniting them (Perez-Diaz & Eagles, 2014, and references therein). Each stage of ocean floor development and the related plate movements is tightly constrained and dated, and models produced in this way can depict the entire period and area of an ocean's growth, including fracture zone interpretations in the method provides additional constraint that benefits from the high and consistent density of data available from over 30 years of satellite altimetry measurements. Despite this, targeted new magnetic data acquisition will remain essential for continuing progress in plate kinematic modelling.

5.3.2 Age Grid and Dynamic Paleostress Modelling

As discussed in chapter 4, the failure to reach a solution for the torque balance calculations and hence, calculate the stress field may arise from uncertainties in slab pull. Specifically, in the age of the subducting slab. The uncertainty in age affects our dynamic stress modelling because it affects the distribution and magnitude of ridge push and slab pull forces. The limitations of our dynamic stress model of the

African Plate at 75 Ma have already been discussed in chapter 4. No solution could be reached for our chosen set of forces, and our chosen constraints on those forces. The failure to reach a solution is most likely linked to the age of the subducting lithosphere in the Neotethys due to the generation of uncertainties in the constraints on slab pull. Specifically, the assumption that slab length is a function of age (of the subducting lithosphere).

The oceanic lithosphere being subducted along the northeastern boundary is from the Neotethys Ocean. The age grids for the NW Indian Ocean produced in this thesis (chapter 4) and the South Atlantic by Perez-Diaz and Eagles (2017) are based on large data sets and robust kinematic models which closely replicate seafloor spreading and therefore closely approximate the true seafloor age (Perez-Diaz & Eagles, 2017). However, most of the Neotethys oceanic lithosphere has since been destroyed by subduction, although there are indications that parts of the Ionian Sea and the east Mediterranean basins may represent the old preserved in-situ Neotethys ocean floor, ranging in age from ~270 Ma (Late Permian) to 230 Ma (Middle Triassic) (Müller et al., 2008). As a result, age grid for this area cannot be produced in the same way as those in chapter 4 and Perez-Diaz et al (2017), using seafloor data. The age grid from Seton et al (2012) is mostly based on the work of Müller et al. (2008), who produced synthetic Neotethys ocean floor isochrons based on Stampfli and Borel's (2002) tectonic model of the opening of the Neotethys Ocean.

The age of the Neothys oceanic lithosphere on the African Plate subducting beneath Eurasia given by the age grid of Seton et al (2012), lithosphere is very old, which would give a very long slab length and possibly generate a greatly exaggerated slab pull force. This abnormally large slab pull force may be the reason why no solution could be found in chapter 4.

The dynamic stress modelling based on the torque balance method has, in other cases, proven to be effective at predicting the present day balance of torques acting on the plates and the resultant stress field, which shows good correlation with observed present-day stress fields, e.g. the Juan de Fuca plate (Govers & Meijer, 2001) and the Eurasian Plate (Warner-Ruckstuhl et al., 2013).

Convection in the mantle causes vertical displacement at the Earth's surface, called dynamic topography (Richards & Hager, 1984). The dynamic topography is expressed as areas of uplift and subsidence. In continental areas, this can cause uplift and increased erosion of the hinterland and increased sediment delivery to the ocean, and progradation of sediment wedges and deltas along the margins. An example is the enhanced rates of sediment delivery by the Zambezi River to its coastal delta caused by pulses of dynamic uplift of southern Africa in the late Cenozoic (Walford et al., 2005). Dynamic uplift of the ocean affects volumetric capacity of the ocean basins and may have a eustatic effect (Allen & Allen, 2013).

Plate tectonics must be considered as a surface expression of mantle convection with both intrinsically linked. Dynamic topography at the Earth's surface is important in basins analysis as it can result in topographic uplift of the hinterland, increasing erosion and a subsequent increase in sediment supply to the basins. Subsidence caused by dynamic topography creates more accommodation space in the basins (Allen & Allen, 2013).

Mantle convection has repercussions on the dynamic stress modelling, because the interaction between the mantle and the overlying plate, and its effect on plate motion is poorly understood, so difficult to model. Currently, our dynamic stress model takes a lithosphere focused approach that simplifies the plate's interaction with the underlying mantle (chapter 4). Conversely, a number of studies have instead focussed on the convecting mantle, and either oversimplified the edge forces due to plate interactions or ignored them completely (Ricard & Vigny, 1989; Steinberger et al., 2001; Lithgow-Bertelloni & Guynn., 2004; Ghosh et al., 2008). Recent studies show the need to integrate the two approaches, combining lithosphere dynamics and mantle flow to produce a holistic plate-scale approach to better understand the role of the mantle in driving (or resisting) plate motion (Warners-Ruckstuhl et al., 2012).

Topography caused by mantle convection and uplift along with the thickness of the lithosphere results in Gravitational Potential Energy (GPE) which is expressed as a horizontal force resulting from lateral variations GPE.

One of the reasons why our torque balance calculations in chapter 4 may have been unsuccessful could be due to our failure to take into account GPE. It may be necessary to include GPE to balance the large slab pull forces along the northeastern boundary.

5.3.3 Implications for Petroleum Industry

The recent interest in East Africa for hydrocarbon exploration has been spurred on by oil finds in the Cenozoic rifts of the EARS and major gas discoveries offshore Tanzania and Mozambique. But we must not forget the long, complicated and often disappointing history of exploration in this area, and the challenges it presents.

There was significant interest from petroleum companies during the 50s, 60s, 70s and 80s and as a result, most exploration work was carried out during this time. Interest declined in the 90s due to the plummeting oil price in the late 1980s and political instability throughout the region as well as civil wars in Mozambique (1977-1992) and Somalia (1991-ongoing). In recent years, things are slowly improving, with new governments installed in Mozambique (1994), Kenya (2002) and Somalia (2012). Madagascar has also had its issues such as several coups, violent unrest and disputed elections since its independence from France in the 1960s, but democracy was re-established in 2013. Tanzania has mostly avoided the political problems that affected the over countries. Despite these improvements the

political situation across East Africa and Madagascar remains fragile. For these reasons exploration efforts have floundered in the past few decades, and as a result there is a lack of geological information from the marginal sedimentary basins. In particular is a lack of boreholes/well and seismic offshore, and a lot of what is available both on and off shore is dated, or not available in the public domain.

Basin Evolution and Changing Plate Boundaries

The main concerns of the petroleum industry lie in the earliest stages of rift basin formation and breakup, namely the basin-forming mechanisms and timing and distribution of restricted lacustrine and marine source rocks. Unfortunately, this is where most of the uncertainty in the plate kinematic modelling lies. This early stage cannot rely directly on magnetic anomaly data, but instead the extrapolation of the spreading rates back to a sensible breakup point providing a realistic pre-rift assembly of all modern continental plates and their rift basin fragments.

Another thing to consider is the effect of the tectonic changes described in Tuck-Martin et al (2018), chapter 2, and their effect on the development of the basins after initial breakup. Large scale stratigraphic cycles in the basins fill history are controlled by changes in things such as tectonic subsidence / uplift, changes in horizontal stress, dynamic topography and changes in base level caused by eustatic mechanisms (Allen & Allen, 2013).

In chapters 2 and 3, we discussed how changes in plate boundaries control the first-order tectonic stress field across East Africa, in chapter 4 we tried to quantify the forces acting at the boundaries which produce the stress-field.

Variations in the horizontal in-situ stress field in the lithosphere may cause vertical movements large enough to have a major impact on stratigraphy and may also produce long wavelength lithospheric folding. Cloetingh et al (1985) found that changing the horizontal stresses on a passive continental margin with an overlying sedimentary load and an age-dependent elastic thickness caused vertical motion in the continental lithosphere. For example, a change from tensile to compressive stress produces a net uplift of the basin margin, forcing a stratigraphic offlap and a change from compressive to tensile stress produces a net subsidence and enhanced stratigraphic onlap. These patterns of offlap and onlap can often be mistaken for the effects of eustatic sea-level change.

We believe that tectonic changes at the plate boundaries, outlined in our tectonic model, cause changes in the horizontal stress field of significant magnitude over a sufficiently short time period to significantly influence stratigraphic packaging. Therefore it is really important to understand the changing stress field through time to understand basin stratigraphy.

Importance of Margin-scale Tectonostratigraphic Framework

It is essential to understand how the rifting, break-up and post-rift phases effect the timing and distribution of petroleum systems and how systems can be correlated along the margins. The tectono-stratigraphic framework describe in chapters 2 and 3, provides a way to correlate all the tectonic and stratigraphic changes of the sedimentary basins of the East-African and Madagascan conjugate margins from the rift stage to the modern passive margin.

By utilising the plate-kinematic model (chapter 2), the derived paleostress fields (chapter 3) the timings and characteristics of related megasequence patterns, the tectono-stratigraphic model can be developed to investigate the implications of margin-wide geodynamic changes and related regional tectonic stress fields on the regional development of potential petroleum systems of sedimentary basins.

Being able to integrate new geological and geophysical data from field work, seismic surveys or well data, as it becomes available and place this information in an already well-established tectonostratigraphic framework is essential for future exploration. The framework can be updated and expanded as needed.

Doust & Sumner (2007) concluded that the recognition of petroleum system types and reservoir lithofacies play types in well-explored basins can facilitate prediction of hydrocarbon prospectivity in less well-known basins and plays, and thereby contribute to future exploration evaluation. In this way, the framework allows information from the well-known sedimentary basins/areas to be extrapolated along the East African and conjugate West Madagascan margins to aid understanding and exploration in the poorly understood frontier basins where there is little geological data. Other rifted continental margins could also benefit from the application of these methods.

In chapter 3, we highlighted a number of regional unconformities and tectonically controlled megasequences that correlated with major boundary change in our plate tectonic model (chapter 2). For example a major regional Hauterivian/Barremian unconformity has been recognised in most basins bordering the West Somali Basin and along the Davie Fracture Zone, corresponding to the end of seafloor spreading in the West Somali Basin.

With some unconformities the origin is harder to identify and correlate with tectonic changes, which may be due to the influence of other factors such as changing sea levels or dynamic topography linked to mantle convection. A way of solving this problem would be to calculate backstripped subsidence curve to distinguish between subsidence due to tectonics and subsidence due to sediment loading, and then corrected for paleobathymetric and eustatic variations, to investigate the basin-forming mechanisms. Previous attempts were made to do this all along the East African margin by Janssen (1995), but with more information becoming available in recent years this should be attempted again, to correlate the tectonic subsidence with the plate kinematic events and changing plate boundaries.

Performing tectonic subsidence studies e.g. backstripping, would enable greater constraint on the timing of important tectonic events along the margins.

5.4 Outlook / Future Work

The future for East Africa mostly depends on more data being gathered or made available which we have already mentioned in the critical evaluation above. More magnetic anomaly data in the West Somali Basin would help with understanding/modelling the earliest stages of seafloor spreading which are crucial to hydrocarbon exploration. More geological information from the basins will allow us to correlate the tectonic changes in the NW Indian Ocean described in our plate kinematic model with sedimentary basin evolution and stratigraphic fill. However, until industry can be confident in the political landscape and security improves, it may remain too dangerous. Spectrum managed to shoot more seismic offshore Somalia in 2D seismic acquisition programmes undertaken in 2014 and 2016, but the resurgence in piracy off the coast of Somalia in March and April 2017, the first attacks in 5 years, present a worrying step backwards.

We discussed in chapter 4 how no solution was possible for the force balance, a fundamental step in the dynamic stress modelling workflow. Future work would need to rectify this by repeating the process with different constraints on the slab pull force (see chapter 4 and section 5.3.2. above).Further constraints may need to be included, for example the gravitational potential energy arising from topography and variations in crustal thickness may have an effect on the stress field. In addition, the dynamic stress modelling should be extended further to investigate how the stress field across Africa has changed with time, in response to changing plate boundaries. The modelling will be applied to time slices from each of the 4 tectonic phases described in the plate kinematic model (Tuck-Martin et al., 2018; chapter 2), to investigate how the boundary changes in the NW Indian Ocean affected the plate boundary forces acting on the African Plate and therefore, how they changed the paleostress field. These results will be compared to the paleostress predictions from the tectonic model and the basin fill histories to investigate the effect of changing plate boundaries on basin development.

As previously mentioned subsidence analysis would be a good way to correlate the plate tectonic changes, and hence the changes in paleostress field to basin development by improving the constraints on the timing and extent of the tectonic subsidence in the basins. If tectonic subsidence curves could be generated for all the sedimentary basins then it could provide a greater understanding of how different tectonic changes influenced the different margin segments.

5.5 Conclusions

- The plate-kinematic model of Tuck-Martin et al. (2018), chapter 2, describes the opening of the Northwest Indian Ocean from the Early Jurassic to the present day, constrained by seafloor magnetic anomaly isochron data and fracture zone traces, providing a well constrained, detailed model of the fragmentation of East Gondwana and ocean floor growth.
- The plate kinematic model was used to produce a high resolution seafloor age grid for the NW Indian Ocean at 75 Ma, and used along with plate boundary constraints and relative motions of plates adjacent to the African plate, as input for dynamic stress modelling.
- The plate kinematic model can be correlated with geologic information from the sedimentary basins along the margins of the NW Indian Ocean, of East Africa and West Madagascar to create a margin-wide tectonostratigraphic framework, to show the effect of tectonic changes on basin formation.
- Divergent plate boundary forces are believed to drive plate motion and related ridge-push forces control the first-order regional intraplate stress field since breakup.
- The major tectonic changes in the NW Indian Ocean, at the African plate boundary, causes changes to the forces acting on the African plate. The horizontal stresses these forces produce are transmitted through the lithosphere to the plate interior, controlling the intraplate stress field.
- Changes in the stress field can cause vertical movements, which may be expressed in the marginal sedimentary basins as unconformities due to uplift or subsidence.
- We find a tentative link between major plate boundary changes in the Northwest Indian Ocean and regional unconformities in the basins along the East African and West Madagascan continental margins.
- Efforts to quantify the forces acting on the African plate and their resultant stress filed have so far been unsuccessful due to uncertainties in the relationship between the age of the subducting lithosphere, slab length, slab dip angle and the magnitude of slab pull along Africa's northeastern boundary with Eurasia.

Bibliography

Abdelsalam, M.G., Liégeois, J. & Stern, R.J. (2002) The Saharan Metacraton. *Journal of African Earth Sciences,* **34,** 119-136

Abu-Alam, T.S., Santosh, M., Brown, M. & Stüwe, K. (2013) Gondwana Collision. *Mineralogy and Petrology,* **107**(5), 631-634

Adam, J. (2010): Rock Mechanics and Petroleum Geomechanices. MSc Petroleum Geoscience course notes, Royal Holloway University, (unpublished)

Allen, P.A. & Allen, J.R. (2013) *Basin Analysis: Principles and Application to Petroleum Play Assessment.* 3rd ed. Oxford: Wiley-Blackwell.

Ashwal, L.D., Wiedenbeck, M. & Torsvik, T.H. (2017) Archaean Zircons in Miocene Oceanic Hotspot Rocks Establish Ancient Continental Crust beneath Mauritius. *Nat Commun*, **8,** 14086.

Bell, J. S. (1996), In situ stresses in sedimentary rocks (part 2): Applications of stress measurements, *Geosci. Canada*, **23**(3), 135–153

Bhattacharya, G. C., Chaubey, A. K., Murty, G. P. S., Srinivas, K., Sarma, K. V. L. N. S., Subrahmanyam, V. & Krishna, K. S. (1994), Evidence for seafloor spreading in the Laxmi Basin, northeastern Arabian Sea, *Earth Planet. Sci. Lett.*, **125**(1–4).

Bosellini, A. (1992), The continental margins of Somalia: structural evolution and sequence stratigraphy, *Geol. Geophys. Cont. margins*, 185–205.

Bosence DWJ. (1998) *Stratigraphic and sedimentological models of rift basins.* In: Purser BH, Bosence DWJ, editors. Sedimentary and tectonic evolution of rift basins—the Red Sea–Gulf of Aden. London (UK)7 Chapman Hall-Kluwers; p. 9 – 25.

Bosence, D.W.J. ed. *Sedimentation and Tectonics in Rift Basins. Red Sea – Gulf of Aden.* London: Chapman & Hall. Bosworth, W. & Morley, C. K. (1994), Structural and stratigraphic evolution of the Anza rift, Kenya, *Tectonophysics*, **236(**1–4), 93–115.

Buck, W. R. (1991), Modes of continental lithospheric extension. *J. Geophys. Res.*, **96**, 20161-78.

Cande, S.C., Patriat, P. & Dyment, J. (2010) Motion between the Indian, Antarctic and African Plates in the Early Cenozoic. *Geophysical Journal International*, **183,** 127-149.

Cande, S. C. & Patriat, P. (2015), The anticorrelated velocities of Africa and India in the Late Cretaceous and early Cenozoic, *Geophys. J. Int.*, **200**(1), 227–243.

Cande, S.C. & Stegman, D.R. (2011) Indian and African Plate Motions Driven by the Push Force of the Reunion Plume Head. *Nature*, **475,** 47-52.

Catuneanu, O., Wopfner, H., Eriksson, P.G., Cairncross, B., Rubidge, B.S., Smith, R.M.H. & Hancox, P.J. (2005) The Karoo Basins of South-Central Africa. *Journal of African Earth Sciences*, **43,** 211-253.

Clark, D. N. (1998), Review of the exploration potential of Madagascar, *Houston Geol. Soc. Bull*., 40, 23–29.

Cloetingh, S., McQueen, H., & Lambeck, K., (1985) On a tectonic mechanism for regional sea level variations, *Earth Planet. Sci. Lett*., **75**, 157-166.

Coblentz, D. D., Richardson, R. M. & Sandiford, M. (1994), On the gravitational potential of the Earth's lithosphere. *Tectonics*, **13**, 929-945.

Coblentz, D. D. & Sandiford, M. (1994), Tectonic stresses in the African plate: Constraints on the ambient lithospheric stress state. *Geology*, **22**, 831-834.

Cochran, J. R. (1988) Somali basin, chain ridge, and origin of the northern Somali basin gravity and geoid low, *J. Geophys. Res*., **93**(B10), 11,985 – 12,008.

Coffin, M. F., & Rabinowitz, P. D. (1987), Reconstruction of Madagascar and Africa: Evidence from the Davie fracture zone and western Somali Basin, *J. Geophys. Res*., 92, 9385–9406, doi:10.1029/JB092iB09p09385.

Coffin, M. F. & Rabinowitz. P. D. (1988), Evolution of the conjugate East African-Madagascan margins and the western Somali Basin, *Geol. Soc. Am. Spec. Pap*., 226,1–79.

Collier, J.S., Sansom, V., Ishizuka, O., Taylor, R.N., Minshull, T.A., & Whitmarsh, R.B. (2008) Age of Seychelles – India break-up. *Earth and Planetary Science Letters*, **272**, 264-277

Corfield, R.I., Carmichael, S., Bennett, J., Akhter, S., Fatimi, M. & Craig, T. (2010) Variability in the crustal structure of the West Indian Continental Margin in the Northern Arabian Sea. *Petroleum Geoscience,* **16,** 257-265.

Corti, G., Bonini, M., Conticelli, S., Innocenti, F., Manetti, P. & Sokoutis, D. (2003), Analogue modelling of continental extension: a review focused on the relations between the patterns of deformation and the presence of magma. *Earth Sci. Rev*., **63(3-4),** 169-247.

Cox, K. G. (1992), Karoo igneous activity, and the early stages of the break-up of Gondwanaland, *Geol. Soc. London, Spec. Publ*., **68**(1), 137–148.

Cruciani, F. & Barchi, M. R. (2016), The Lamu Basin deepwater fold-and-thrust belt: An example of a margin-scale, gravity-driven trust belt along the continental passive margin of East Africa, *Tectonics*, **35(3),** 491-510.

Danforth, A., Granath, J., Horn, B. & Komba, K. (2012) Hydrocarbon potential of the deep offshore Tanzania Basin in Context of East Africa's Transform Margin, *East Africa: Petroleum Province of the 21st century, abstr. Vol.,* 32-33.

Davis, J.K., Lawver, L.A., Norton, I.O. & Gahagan, L.M. (2016) New Somali Basin Magnetic Anomalies and a Plate Model for the Early Indian Ocean. *Gondwana Research*, **34,** 16-28.

De Buyl, M. & Flores, G. (1986) Southern Mozambique Basin: The most promising hydrocarbon province offshore east Africa. *AAPG Memoir*, **40,** 399-425.

Demets, C., Gordon, R.G. & Royer, J.-Y. (2005) Motion between the Indian, Capricorn and Somalian Plates since 20 Ma: Implications for the Timing and Magnitude of Distributed Lithospheric Deformation in the Equatorial Indian Ocean. *Geophysical Journal International*, **161,** 445-468.

Besairie, H., Collignon, M., (1972). Géologie de Madagascar; I. Les terrains sédimentaires. *Annales Géologiques de Madagascar* **35**, 1–463.

Dietz, R. (1961). "Continent and ocean basin evolution by spreading of the sea floor", *Nature* **190**, pp. 854–857.

Dirkx, R. (2017) Observations on Tectonic Evolution and Prospectivity of Madagascar Offshore Basins Based on Interpretation of New Seismic Data. *AAPG/SEG International Conference and Exhibition*, Barcelona, Spain, April 3-6, 2016.

Domingues, A., Silveira, G., Ferreira, A.M.G., Chang, S.-J., Custódio, S. & Fonseca, J.F.B.D., (2016), Ambient noise tomography of the East African Rift in Mozambique. *Geophys. J. Int.* **204**, 1565–1578.

Doré, T. & Lundin, E. (2015), Hyperextended continental margins—Knowns and unknowns. *Geology*, **43(1),** 95-96.

Doust, H. & Sumner, H. S. (2007) Petroleum systems in rift basins – a collective approach in Southeast Asian basins, *Petroleum Geoscience*, **13**, 127–144

Doust, H. & Noble, R. A. (2008) Petroleum systems of Indonesia, *Marine and Petroleum Geology,* **25**, 103–129

Duncan, R. A, & R. B. Hargraves, R. B. (1990), $^{40}Ar/^{39}Ar$ geochronology of basement rocks from the Mascarene Plateau, the Chagos Bank, and the Maldives Ridge, *In: Proceedings of the ODP, Sci. Results,* **115**, 43–51, eds Duncan, R.A. et al., College Station, TX (Ocean Drilling Program)

Eagles, G. (2004) Tectonic Evolution of the Antarctic–Phoenix Plate System since 15 Ma. *Earth and Planetary Science Letters*, **217,** 97-109.

Eagles, G. & König, M. (2008) A Model of Plate Kinematics in Gondwana Breakup. *Geophysical Journal International*, **173,** 703-717.

Eagles, G. & Hoang, H.H. (2013) Cretaceous to Present Kinematics of the Indian, African and Seychelles Plates. *Geophysical Journal International*, **196,** 1-14.

Eagles, G. & Wibisono, A.D. (2013) Ridge Push, Mantle Plumes and the Speed of the Indian Plate. *Geophysical Journal International*, **194,** 670-677.

Eagles, G., Pérez-díaz, L. & Scarselli, N. (2015) Getting over Continent Ocean Boundaries. *Earth-Science Reviews*, **151,** 244-265.

Ebinger, C. J. & Sleep, N. H. (1998), Cenozoic magmatism throughout east Africa resulting from impact of a single plume, *Nature*, **395**, 788–791.

Emmel, B., Jacobs, J., Katowski, M. & Graser, G. (2006) Phanerozoic upper crustal tectono-thermal development of basement rocks from central Madagascar: An integrated fission-track and structural study, *Tectonophysics*, **412,** 61-86.

Encarnación, J., Fleming, T. H., Elliot, D. H. & Eales, H. V. (1996), Synchronous emplacement of Ferrar and Karoo dolerites and the early breakup of Gondwana, *Geology*, **24**(6), 535.

England, P. & Wortel, R. (1980), Some consequences of the subduction of young slabs. *Earth planet. Sci. Lett.* **47**, 403-415.

Eulero, L. (1776). "Formulae generales pro translatione quacunque corporum rigidorum", *Novi Commetarii academiae scientiarum Petropolitanae* **20**, pp. 189–207.

Falvey, D.A., 1974. The development of continental margins in plate tectonic theory. *Aust. Petrol. Explor. Assoc. J.*, **14**, 95-106.

Fonseca, J.F.B.D., Chamussa, J., Domingues, A.L., Helffrich, G., Antunes, E., Van Aswegen, G., Pinto, L. V., Custódio, S. & Manhica, V.J. (2014), MOZART: A Seismological Investigation of the East African Rift in Central Mozambique. *Seismol. Res. Lett.* **85,** 108–116.

Fontaine, F. R., Barruol, G., Tkalčié, H., Wölbern, I., Rümpker, G., Bodin, T. & Haugmard, M. (2015), Crustal and uppermost mantle structure variation beneath La Réunion hotspot track, *Geophys. J. Int*., **203**, 107-126.

Forsyth, D. & Uyeda, S. (1975), On the Relative Importance of the Driving Forces of Plate Motion, *Geophys. J. R. astr. Soc.,* **43,** 163-200.

Fossen, H. (2010) *Structural Geology*. Cambridge: Cambridge University Press.

Fowler. C.M.R. (2005), *The Solid Earth. An Introduction to Global Geophysics.* 2nd ed. Cambridge: Cambridge University Press.

Franke, D., Jokat, W., Ladage, S., Stollhofen, H., Klimke, J., Lutz, R., Mahanjane, E. S., Ehrhardt A., & Schreckenberger, B. (2015) The offshore East African Rift System: Structural framework at the toe of a juvenile rift, *Tectonics,* **34**, 2086–2104, doi:10.1002/2015TC003922.

Gaina, C., Torsvik, T.H., Van Hinsbergen, D.J.J., Medvedev, S., Werner, S.C. & Labails, C. (2013) The African Plate: A History of Oceanic Crust Accretion and Subduction since the Jurassic. *Tectonophysics*, **604,** 4-25.

Ganerød, M., Torsvik, T.H., van Hinsbergen, D.J.J., Gaina, C., Corfu, F., Werner, S., Owen-Smith, T.M., Ashwal, L.D., Webb, S.J. & Hendricks B.W.H. (2011) Palaeoposition of the Seychelles microcontinent in relation to the Deccan

Traps and the Plume Generation Zone in Late Cretaceous-Early Palaeogene time. *Geological Society, London, Special Publications,* **357**, 229-252.

Geiger, M., Clark, D. N. & Mette, W. (2004), Reappraisal of the timing of the breakup of Gondwana based on sedimentological and seismic evidence from the Morondava Basin, Madagascar, *J. African Earth Sci.*, **38**(4), 363–381.

Ghosh, A., Holt, W.E., Wen, L., Haines, A.J. & Flesch, L.M., 2008. Joint modeling of lithosphere and mantle dynamics elucidating lithosphere mantle coupling, *Geophys. Res. Lett.*, **35,** doi:10.10292008GL034365.

Gibbons, A.D., Whittaker, J.M. & Müller, R.D. (2013) The Breakup of East Gondwana: Assimilating Constraints from Cretaceous Ocean Basins around India into a Best-Fit Tectonic Model. *Journal of Geophysical Research: Solid Earth*, **118**(3), 808-822.

Gover, R. & Meijer, P. T. (2001) On the dynamics of the Juan de Fuca plate, *Earth Planet. Sci. Lett.*, **189,** 115-131.

Gradstein, F. M., Ogg, J. G. & Smith, A. G. (2004) A Geologic Time Scale 2004, 3rd ed., Cambridge: Cambridge University Press.

Hales, A. L., (1969), Gravitational sliding and continental drift, *Earth planet. Sci. Lett.,* **6**, 31-34.

Hammond, J. O. S., Kendall, J-M., Collier, J. S. & G. Rümpker, G. (2013), The extent of continental crust beneath the Seychelles, *Earth Planet. Sci. Lett.*, **381,** 166–176.

Heidbach, O., Reinecker, J., Tingay, M., Müller, B., Sperner, B., Fuchs, K. & Wenzel, F. (2007), Plate boundary forces are not enouh: Second- and third-order stress patterns highlighted in the World Stress Map database, *Tectonics,* **26**, TC6014, doi:10.1029/2007TC002133.

Heidbach, O., Tingay, M., Barth, A., Reinecker, J., Kurfeß, D. & Müller, B. (2010), Global crustal stress pattern based on the World Stress Map database release 2008, *Tectonophysics*, **482**(1–4), 3–15.

Heidbach, O., Rajabi, M., Reiter, K. & Ziegler, M. WSM Team (2016), World Stress Map Database Release 2016. GFZ Data Services, doi:10.5880/WSM.2016.001.

Hellinger, S. J. (1981), The Uncertainties of Finite Rotations in Plate Tectonics, *J. Geophys. Res.*, **86**(B10), 9312–9318.

Hess, H. (1962). "History of Ocean Basins", *Petrologic studies: A volume to honor A. F. Buddington.* Princeton University Press: Princeton, pp. 599–620.

Horner-Johnson, B. C., Gordon, R. G. & Argus, D. F. (2007), Plate kinematic evidence for the existence of a distinct plate between the Nubian and Somalian plates along the Southwest Indian Ridge, *J. Geophys. Res.*, **112**(B5).

Houseman, G. & England, P. (1986), A dynamical model of lithosphere extension and sedimentary basin formation. *J. Geophys. Res*., **91**, 719-729.

Hudson, W. E. & Nicholas, C. J. (2014), The Pindiro Group (Triassic to Early Jurassic Mandawa Basin, southern coastal Tanzania): Definition, palaeoenvironment, and stratigraphy, *J. African Earth Sci.*, **92,** 55–67.

Jacoby, W. B., (1970), Instability in the upper mantle and global plate movements, *J. geophys. Res*., **75**, 5671-5680.

Jagoutz, O., Royden, L., Holt, A. F. & Becker, T.W. (2015), Anomalously fast convergence of India and Eurasia caused by double subduction, *Nat. Geosci.*, **8**(6), 475–478

Janssen, M. E., Stephenson, R. A. & Cloetingh, S. (1995) Temporal and spatial correlations between changes in plate motions and the evolution of rifted basins, *GSA Bulletin*; **107**(11), 1317–1332.

Jeans, P. J. & Van Meerbeke, G. L. E., (1995) Geological evolution and hydrocarbon habitat of the Majunga Basin and Karroo Corridor, Madagascar, in *International earth-science congress*; 1027-1032

Jokat, W., Nogi, Y. & Leinweber, V. (2010), New aeromagnetic data from the western Enderby Basin and consequences for Antarctic-India break-up, *Geophys. Res. Lett.*, **37**(21).

Jourdan, F., Féraud, G., Bertrand, H., Kampunzu, A. B., Tshoso, G., Watkeys, M. K. & LE Gall, B. (2005), Karoo large igneous province: Brevity, origin, and relation to mass extinction questioned by new 40Ar/39Ar age data, *Geology*, **33**(9), 745.

Kapilima, S. (2004) Tectonic and sedimentary evolution of the coastal basin of Tanzania during the Mesozoic times, *Tanz. J. Sci*., **29**(1), 1-16.

Kearns, H., Berryman, J., Hodgson, N. & Rodriguez, K. (2016) Offshore Somalia: East Africa's Oil Frontier, *GeoExPro,* **13**(2), 50-54.

Key, R. M., Smith, R. A., Smelror, M., Saether, O. M., Thorsnes, T., Powell, J. H., Njange, F. & Zandamela, E. B. (2008), Revised lithostratigraphy of the Mesozoic-Cenozoic succession of the onshore Rovuma Basin, northern coastal Mozambique, *South African J. Geol.*, **111**(1), 89–108.

Key, R. M. & Reeves, C. V. (2012) The post-Gondwana development of East Africa's coastline with emphasis on the development of the Rovuma Basin, Extended abstract. Geological Society meeting, London, October 24-26.

King, R. C., Hillis, R. R., Tingay, M. R. P. & Morley, C. K. (2009), Present-day stress and neotectonic provinces of the Baram Delta and deep-water fold-thrust belt, *J. Geol. Soc.,* **166,** 197-200.

Klimke, J., & Franke, D. (2016). Gondwana breakup: no evidence for a Davie Fracture Zone offshore northern Mozambique, Tanzania and Kenya. *Terra Nova*, **28**, 233-244.

Klimke, J., Franke, D., Gaedicke, C., Schreckenberger, B., Schnabel, M., Stollhofen, H., Rose; J., & Chaheire, M. (2016). How to identify oceanic crust—Evidence

for a complex break-up in the Mozambique Channel, off East Africa. *Tectonophysics*, **693**, 436-452.

König, M. & Jokat. W. (2010), Advanced insights into magmatism and volcanism of the Mozambique Ridge and Mozambique Basin in the view of new potential field data, *Geophys. J. Int.*, **180**(1), 158–180.

Krishna, K.S., Gopala Rao, D. & Sar, D. (2006) Nature of the crust in the Laxmi Basin (14°-20° N), western continental margin of India. *Tectonics,* **25,** 1-18

Kröner, A. & Stern, R.J. (2004) Pan-African Orogeny. *Encyclopedia of Geology,* **1,** 1-12

Kusky, T. M., Abdelsalam, M., Stern, R. J. & Tucker, R. D. (eds.) (2003) Evolution of the East African and related orogens, and the assembly of Gondwana. *Precambrian Res*. **123**, 82-85.

Lallemand, S., Heuret, A. & Boutelier, D. (2005) On the relationships between slab dip, back-arc stress, upper plate absolute motion, and crustal nature in subduction zones, *Geochem. Geophys. Geosyst.,* 6, Q09006, doi:10.1029/2005GC000917.

Leinweber, V. T. & Jokat, W. (2011), Is there continental crust underneath the northern Natal Valley and the Mozambique Coastal Plains?, *Geophys. Res. Lett.*, **38**(14).

Leinweber, V. T. & Jokat, W. (2012), The Jurassic history of the Africa–Antarctica corridor — new constraints from magnetic data on the conjugate continental margins, *Tectonophysics*, **530–531**, 87–101.

Le Pichon, X. & Heirtzler, J. R. (1968) Magnetic Anomalies in the Indian Ocean Sea-Floor Spreading, *J. Geophys. Res*., **73**(6), 2101-2117.

Lithgow-Bertelloni, C.& Guynn, J.H., 2004. Origin of the lithospheric stress field, *J. geophys. Res.,* **109,** doi:10.1029/2003JB002467.

Lister, C. (1975), Gravitational drive on oceanic plates caused by thermal contraction, *Nature,* **257,** 663-665.

Livermore, R., Nankivell, A., Eagles, G. & Morris, P. (2005), Paleogene opening of Drake Passage, *Earth Planet. Sci. Lett.*, **236**(1–2), 459–470.

MacGregor, D. (2015), History of the development of the East African Rift System: A series of interpreted maps through time, *J. African Earth Sci.*, **101**, 232–252.

Mahanjane, E. S. (2012), A geotectonic history of the northern Mozambique Basin including the Beira High – A contribution for the understanding of its development, *Mar. Pet. Geol.*, **36**(1), 1–12.

Mahanjane, E. S. (2014), The Davie Fracture Zone and adjacent basins in the offshore Mozambique Margin – A new insights for the hydrocarbon potential, *Mar. Pet. Geol.*, **57**, 561–571.

Mahanjane, E. S. & Franke, D. (2014), The Rovuma Delta deep-water fold-and-thrust belt, offshore Mozambique, *Tectonophysics*, **614**, 91–99.

Mahanjane, E. S., Franke, D., Lutz, R., Winsemann, J., Ehrhardt, A., Berglar, K. & Reichert, C. (2014), Maturity and petroleum systems modelling in the offshore Zambezi delta depression and Angoche basin, northern Mozambique, *J. Pet. Geol.*, **37**(4), 329–348.

Mbede, E. I. & Dualeh, A. (1997), Chapter 10: The coastal basins of Somalia, Kenya and Tanzania, in *Sedimentary Basins of the World*, **3**, 211–233.

McKenzie, D. P. (1967). "Some remarks on heat flow and gravity anomalies", *Journal of Geophysical Research* **72**(24), pp. 6261–6273. DOI: 10 . 1029 / JZ072i024p06261.

McKenzie, D. P. (1969) Speculations on the consequences and causes of plate motion. *Geophys. J. R. astr. Soc.* **18**, 1-32.

McKenzie, D. & Sclater, J. G. (1971), The ecolution of the Indian Ocean since the Late Cretaceous, *R. Astron.Soc.,Geophys.J.*, **24**(5), 437–528.

Miles, P. R., Munschy, M. & Ségoufin, J. (1998), Structure and early evolution of the Arabian Sea and East Somali Basin, *Geophys. J. Int.*, **134**, 876–888

Miles, P.R. (1982) Gravity models of the Amirante Arc, western Indian Ocean. *Earth and Planetary Sciences Letters,* **61**(1), 127-135.

Molnar, P., Pardo-Casas, F. & Stock, J. (1988), The Cenozoic and Late Cretaceous evolution of the Indian Ocean: uncertainties in the reconstructed positions of the Indian, African and Antarctic plates, *Basin Res.*, **1**, 23–40.

Morgan, W. J. (1968). "Rises, Trenches, Great Faults and Crustal Blocks". *Journal of Geophysical Research*, **73**(6), pp. 1959–1982.

Müller, R.D., Gaina, C., Roest, W.R. & Hansen, D.L. (2001) A recipe for microcontinent formation. *Geology,* **29**(3), 203-206.

Müller, R. D., Sdrolias, M., Gaina, C. & Roest, W. R. (2008) Age, spreading rates, and spreading asymmetry of the world's ocean crust, *Geochem. Geophys. Geosys.*, **9**(4), Q04006, doi:10.1029/2007GC001743.

Mueller, C. O., & Jokat, W. (2017). Geophysical evidence for the crustal variation and distribution of magmatism along the central coast of Mozambique. *Tectonophysics*, **712-713**, 684-703.

Muttoni, G., Gaetani, M., Kent, D. V., Sciunnach, D., Angiolini, L., Berra, F., Garzanti, E., Mattei, M. & Zanchi, A. (2008) Opening of the Neo-Tethys Ocean and the Pangea B to Pangea A transformation during the Permian, *GeoArabia*, **14**, (4), 17-48.

Nankivell, A. P. (1997), Tectonic Evolution of the Southern Ocean between Antarctica, South America and Africa over the last 84 Ma, PhD thesis, Oxford Univ., Oxford, U. K.

Nemčok, M. (2016), Rifts and Passive Margins: Structural Architecture, Thermal Regimes, and Petroleum Systems. 1st edition. Cambridge University Press, New York, USA.

Nicholas, C. J., Pearson, P. N., Brown. P. R., Jones, T. D., Huber, B. T., Karega, A., Lees, J. A., McMillan, I. K., O'Halloran, A., Singano, J. M. &Wade, B. S. (2006) Stratigraphy and sedimentology of the Upper Cretaceous to Paleogene Kilwa Group, southern coastal Tanzania, *J. Afr. Earth Sci*., **45,** 431-466.

Nicholas, C. J., Pearson, P. N., McMillan, I. K., Ditchfield, P. W. & Singano, J. M. (2007) Structural evolution of southern coastal Tanzania since the Jurassic, *J. Afr. Earth Sci*., **48,** 273-297.

Norton, I. O. I. & J. G. Sclater, J. G. (1979), A model for the evolution of the Indian Ocean and the breakup of Gondwanaland, **84**(9), 6803– 6830.

Nyaberi, M. D. & Rop, B. K. (2014) Petroleum Prospects of Lamu Basin, South-Eastern Kenya *J. Geol. Soc. India*, **83,** 414-422.

Nyagah, K. (1995), Stratigraphy, depositional history and environments of deposition of Cretaceous through Tertiary strata in the Lamu Basin, southeast Kenya and implications for reservoirs for hydrocarbon exploration, *Sediment. Geol.*, **96**(1–2), 43–71.

O'Neill, C., D. Mu¨ller, and B. Steinberger (2005), On the uncertainties in hot spot reconstructions and the significance of moving hot spot reference frames, *Geochem. Geophys. Geosyst.,* **6**, Q04003, doi:10.1029/2004GC000784.

O'Neill, C., Müller, D. & Steinberger, B. (2003) Geodynamic implications of moving Indian Ocean hotspots. *Earth and Planetary Science Letter,* **215**, 151-168.

Orowan, E., (1964) Continental drift and the origin of mountains, *Science*, **146**, 1003-1010.

Oxburgh, R. & E. M. Parmentier (1977), Compositional and density stratification in oceanic lithosphere. *J. geol. Soc. Lond.* **133**, 343-355.

Papini, M. & Benvenuti, M. (2008) The Toarcian–Bathonian succession of the Antsiranana Basin (NW Madagascar): Facies analysis and tectono-sedimentary history in the development of the East Africa-Madagascar conjugate margins, *J. Afr. Earth Sci.*, **51,** 21-38.

Patriat, P. & J. Segoufin. J (1988), Reconstruction of the Central Indian Ocean, *Tectonics*, **155**, 211–234.

Pérez-Díaz, L. & Eagles, G. (2017), A new high-resolution seafloor age grid for the South Atlantic, *Geochem. Geophys. Geosyst,* **18**, 457–470, doi:10.1002/2016GC006750.

Pérez-Díaz, L. & Eagles, G. (2014), Constraining South Atlantic growth with seafloor spreading data, *Tectonics*, **33**(9), 1848–1873.

Phethean, J.J.J., Kalnins, L. M., Van Hunen, J., Biffi, P. G., Davies, R. J. & McCaffrey, K. J. W. (2016), Madagascar's escape from Africa: A high-resolution plate reconstruction for the Western Somali Basin and implications for supercontinent dispersal, *Geochem. Geophys. Geosyst.*, **17**, 5036–5055.

Raff, A. and R. Mason (1961). "Magnetic survey off the west coast of North America, 40 N latitude to 52 N latitude", *Geological Society of America Bulletin*, **72**, pp. 1267–1270. DOI: 10.1130/0016-7606(1961)72.

Rais-Assa, R. (1988) Stratigraphy and geodynamics of the Mombasa Basin (Kenya) in relation to the genesis of the proto-Indian Ocean, *Geol. Mag.* **125** (2), 141-147.

Ratheesh-Kumar, R. T., Ishwar-Kumar, C., Windley, B. F., Razakamanana, T., Nair, R. R. & Sajeev, K. (2014), India–Madagascar paleo-fit based on flexural isostasy of their rifted margins, *Gondwana Res.*, **28**(2), 581–600.

Razafindrazaka, Y., Randriamananjara, T., Pique, A., Thouin, C., Laville, E., Malod, J. & Rehault, J-P. (1999) Extension et sédimentation au Paléozoïque terminal et au Mésozoïque dans le bassin de Majunga (Nerd-Ouest de Madagascar), *J. Afr. Earth Sci*., **28**(4), 949-959.

Reeves, C. V., Teasdale, J. P. & Mahanjane, E. S. (2016) Insight into the Eastern Margin of Africa from a new tectonic model of the Indian Ocean, *From:* Nemcˇok, M., Ryba´r, S., Sinha, S. T., Hermeston, S. A. & Ledve´nyiova´, L. (eds) *Transform Margins: Development, Controls and Petroleum Systems*. Geological Society, London, Special Publications, **431**, http://doi.org/10.1144/SP431.12

Rerat, J.C., (1964). Note sur les variations de faciès des sèries jurassiques du nord de Madagascar. *Comptes Rendus Semaine gèologique, Tananarive*, 15–22.

Ricard, Y.& Vigny, C., 1989. Mantle dynamics with induced plate tectonics, *J. geophys. Res.,* **94**(B12), 17543–17560.

Richardson, R. M. (1992), Ridge Forces, Absolute Plate Motions, and the Intraplate Stress Field, *J. Geophys. Res.*, **97**(B8), 11,739-11,748.

Richards, M. A. & Hager, B. H. (1984) Geoid anomalies in a dynamic Earth. *J. Geophys. Res.,* **89**, 5487-6002.

Richter, F. M. & McKenzie, D. P. (1978) Simple plate models of mantle convection. *J. Geophys*. **44**, 441-471.

Riley, T. R., Curtis, M. L., Leat, P.T., Watkeys, M. K., Duncan, R. A., Millar I. L. & Owens, W. H. (2006), Overlap of Karoo and Ferrar Magma Types in KwaZulu-Natal, South Africa, *J. Petrol.*, **47**(3), 541–566.

Rino, S., Kon, Y., Sato, W., Maruyama, S., Santosh, M. & Zhao, D. (2008) The Grenvillian and Pan-African orogens: World's largest orogenies through geologic time, and their implications on the origin of superplume. *Gondwana Research,* **14,** 51-72

Roberts, D. G. & Bally, A. W. (2012), 4 - Some remarks on basins and basin classification and tectonostratigraphic megasequences, In R*egional Geology and Tectonics: Principles of Geologic Analysis, Elsevier,* Amsterdam, 76-92

Roberts, E. M., Stevens, N. J., O'Connor, P. M., Dirks, P. H. G. M., Gottfried, M. D., Clyde, W. C., Armstrong, R. A., Kemp, A. I. S. & Hemming, S. (2012), Initiation of the western branch of the East African Rift coeval with the eastern branch, *Nat. Geosci.*, **5**(4), 289–294.

Roeser, H.A., Fritsch, J., & Hinz, K. (1996). The development of the crust off Dronning Maud Land, east Antarctica. *Geological Society, London, Special Publications*, **108(1**), 243-264.

Rosenbaum, G., Weinberg, R. F. & Regenauer-Lieb, K. (2008), The geodynamics of lithospheric extension. *Tectonophysics*, **458(1-4),** 1-8.

Royer, J-Y. & Gordon, R. G. (1997), The Motion and Boundary Between the Capricorn and Australian Plates, *Science,* **277**(5330), 1268–1274.

Royer, J.-Y., Chaubey, A. K., Dyment, J., Bhattacharya, G. C., Srinivas, K., Yatheesh, V. & Ramprasad, T. (2002), Paleogene plate tectonic evolution of the Arabian and Eastern Somali basins, *Geol. Soc. London, Spec. Publ.*, **195**(1), 7–23.

Salazar, M. U., Baker, D., Francis, M., Kornpihl, D. & West, T. (2013) Frontier exploration offshore the Zambezi Delta, Mozambique, *First Break,* **31,** 135-144.

Salman, G. & I. Abdula, I. (1995), Development of the Mozambique and Ruvuma sedimentary basins, offshore Mozambique, *Sediment. Geol.*, **96**(1–2), 7–41.

SandwelL, D.T., Muller, R.D., Smith, W.H., Garcia, E. & Francis, R. (2014) Marine Geophysics. New Global Marine Gravity Model from Cryosat-2 and Jason-1 Reveals Buried Tectonic Structure. *Science*, **346,** 65-67.

Schlich, R., (1982), The Indian Ocean: Aseismic ridges, spreading centers, and basins, *In: The Ocean Basins and Margins, Volume 6: The Indian Ocean,* eds. Nairn, A. E. M., Stehli, F. G. 51–147, Plenum, New York, 1982.

Segoufin, J. & Patriat, P. (1980) Mesozoic anomalies in the Somali Basin ‐ inferences concerning the relationships between Africa-Antarctica-Madagascar. *Compte Rendus de l'Académie des Science, Série B Physique,* **291,** 85-88.

Sengör, A. M. C. & Burke, K. (1978), Relative timing of rifting and volcanism on Earth and its tectonic implications. *Geophys. Res. Lett.*, **5**, 419-421.

Seton, M., Müller, R. D., Zahirovic, S., Gaina, C., Torsvik, T., Shephard, G., Talsma, A., Gurnis, M., Turner, M., Maus, S. & Chandler, M. (2012), Global continental and ocean basin reconstructions since 200 Ma, *Earth-Science Reviews*, **113**, 212-270.

Smith, A. G., & Hallam, A., 1970, The fit of the southern continents, *Nature*, **225**, 139–144.

Stampfli, G. M., and G. D. Borel (2002), A plate tectonic model for the Paleozoic and Mesozoic constrained by dynamic plate boundaries and restored synthetic oceanic isochrons, *Earth Planet. Sci. Lett.*, **196**, 17–33.

Stein, C. A. & Stein, S. (1992) A model for the global variation in oceanic depth and heat flow with lithospheric age, *Nature,* **359,** 123-129.

Steinberger, B., Schmeling, H. & Marquart, G., 2001. Large-scale stress field and topography induced by global mantle circulation, *Earth planet. Sci. Lett.,* **186,** 75–91.

Stevens, W.E., Storey, M., Donaldson, C.H., Ellam, R.M., Lelikov, E., Tararin, G. & Garbe-Schoenberg, C. (2009) Age and origin of the Amirante ridge-trench structure , western Indian Ocean. In: *Proceedings of the Fall meeting 2009,* San Francisco, CA, USA. American Geophysical Union, Abstract T23A-1885

Storey, M., Mahoney, J. J. & Saunders, A. D. (1997), Cretaceous basalts in Madagascar and the transition between plume and continental lithosphere mantle sources, *In: Large Igneous provinces: Continental, Oceanic, and Planetary Flood Volcanism*, 95–122, eds Mahoney, J.J. & Coffin,M., *Am. Geophys. Union*, Monogr, Washington, DC.

Storey, B. C. (1995), The role of mantle plumes in continental breakup: case histories from Gondwanaland. *Nature*, **377**, 301-308.

Tingay, M. (2009), State and origin of present-day stress fields in sedimentary basins, *ASEG Ext. Abstr.*, *2009*(1), 1.

Tingay, M. R. P., Hillis, R. R., Morley, C. K., King, R. C., Swarbrick, R. E. & Damit, A. R. (2009), Present-day stress and neotectonics of Brunei: Implications for petroleum exploration and production, *AAPG Bulletin*, **93**(1), 75–100.

Torsvik, T. H., Amundsen, H., Hartz, E. H., Corfu, F., Kusznir, N., Gaina, C., Doubrovine, P. V., Steinberger, B., Ashwal, L. D. & Jamtveit, B. (2013), A Precambrian microcontinent in the Indian Ocean, *Nat. Geosci.*, **6**(3), 223–227.

Torsvik, T. H., Ashwal, L. D., Tucker, R. D. & Eide, E. A. (2001), Neoproterozoic geochronology and palaeogeography of the Seychelles microcontinent: the India link, *Precambrian Res.,* **110,** 47-59.

Tuck-Martin, A. L., Adam, J. & Eagles, G. (2018) New Plate Kinematic Model and Tectono-stratigraphic History of the East African and West Madagascan Margins, *Basin Research,* 2018;00: 1-23. https://doi.org/10.1111/bre.12294

Tuck-Martin, A. L., Adam, J. & Eagles, G. (2016) A Tectono-Stratigraphic Framework for the East African Sedimentary Basins, *PETEX – Petroleum Geoscience Collaboration Showcase Abstr. Vol.,* p. 50.

Tuck-Martin, A. L., Adam, J. & Eagles, G. (2015) Correlating tectono-stratigraphic events along the East African Margin: Combining high-resolution plate kinematic models, plate-scale stress simulations and regional sedimentary

basin fill histories. *The 14th HGS/PESGB Conference on African E&P Abstr. Vol.,* pp. 125 – 126.

Turcotte, D. L. & Emerman, S. H. (1983), Mechanisms of active and passive rifting. *Tectonophysics*, **94**, 39-50.

Turcotte, D. L & Schubert, G. (2002), Geodynamics (second ed.), Cambridge University Press, New York, USA.

Turcotte, D. L. & Oxburgh, E. R. (1973) Mid-plate Tectonics, *Nature,* **244**, 337-339.

Turner, J., Foum, A. & Kusznir, N. (2016) Structure of syn-breakup mini-basins, offshore Tanzania and Kenya. *The Roberts Conference – Passive Margins Abstr. Vol.,* 77

vanden Beukel, J. (1990), Thermal and mechanical modelling of convergent plate boundaries (Ph.D. thesis, University of Utrecht). Geologica Ultraiectina 62. (126 pages.).

Van Hinsbergen, D. J. J., Steinberger, B., Doubrovine, P. V. & Gassmöller, R. (2011), Acceleration and deceleration of India-Asia convergence since the Cretaceous: Roles of mantle plumes and continental collision, *J. Geophys. Res.*, **116**(B6), B06101.

Vine, F. and D. Matthews (1963). "Magnetic anomalies over oceanic ridges", *Nature* **199,** pp. 947–949.

Vlaar, N. J. & Wortel, M. J. R. (1976), Lithospheric aging, instability and subduction. *Tectonophys.* **32,** 331-351.

Walford, H. L., White, N. J. & Sydow, J. C. (2005) Solid sediment load history of the Zambezi Delta, *Earth and Planetary Science Letters,* **238**, 49– 63.

Warners-Ruckstuhl, K. N., Meijer, P. T., R. Govers, R. & Wortel, M. J. R. (2010), A lithosphere-dynamics constraint on mantle flow: Analysis of the Eurasian plate, *Geophys. Res. Lett.*, **37**(18).

Warners-RuckstuhL, K. N., Govers, R. & Wortel, R. (2012), Lithosphere-mantle coupling and the dynamics of the Eurasian Plate, *Geophys. J. Int.*, **189**(3), 1253–1276.

Warners-RuckstuhL, K. N., Govers, R. & Wortel, R. (2013), Tethyan collision forces and the stress field of the Eurasian Plate, *Geophys. J. Int.*, **195**(1), 1-15.

Wortel, M. J. R. & Vlaar, N. J. (1988) Subduction zone seismicity and the thermo-mechanical evolution of downgoing lithosphere. *Pageoph.* **128,** 625-659.

Watts, A. (2001), Gravity anomalies, flexure and crustal structure at the Mozambique rifted margin, *Mar. Pet. Geol.*, *18*(4), 445–455.

Wegener, A. (1912). "Die Entstehung der Kontinente", *Geologische Rundschau* **3**(4), pp. 276–292. DOI: 10.1007/BF02202896.

Wescott, W.A. & Diggens, J.N., (1998). Depositional history and stratigraphical evolution of the Sakamena Group (Middle Karoo Supergroup) in the southern Morondava Basin, Madagascar. *J. Afr. Earth Sci.,* **27,** 461–479.

Wessel, P., Smith, W. H. F., Scharroo, R., Luis, J. F. & Wobbe, F. (2013) Generic Mapping Tools: Improved version released, *EOS Trans. AGU*, **94**, 409-410, 2013.

White, R. & McKenzie, D. (1989), Magmatism at rift zones: The generation of volcanic continental margins and flood basalts, *J. Geophys. Res.*, **94**(B6), 7685.

Wichura, H., Bousquet, R., Oberhänsli, R., Strecker, M. R. & Trauth, M. H. (2011), The Mid-Miocene East African Plateau: a pre-rift topographic model inferred from the emplacement of the phonolitic Yatta lava flow, Kenya, *Geol. Soc. London, Spec. Publ.*, **357**(1), 285–300.

Williams, S.E., Whittaker, J.M., & Müller, R.D. (2011), Full- fit, palinspastic reconstruction of the conjugate Australian- Antarctic margins, *Tectonics*, **30**, TC6012, doi:10.1029/2011TC002912.

Wopfner, H. (1994), The Malagasy Rift, a chasm in the Tethyan margin of Gondwana, *J. Southeast Asian Earth Sci.*, **9**(4), 451–461.

Wortel, M. J. R., Remkes, M. J. N., Govers, R., Cloetingh, S. A. P. L., Meijer, P. T. & Bott, M. H. P. (1991), Dynamics of the Lithosphere and the Intraplate Stress Field [and Discussion], *Philos. Trans. R. Soc. A Math. Phys. Eng. Sci.*, **337**(1645), 111–126.

Zoback, M. L. (1992), First- and second-order patterns of stress in the lithosphere: The World Stress Map Project, *J. Geophys. Res.*, **97**(B8), 11703.

Zoback, M. L., and M.D. Zoback, (1989), Tectonic stress field of the conterminous United States, *Mem. Geol. Soc. Am.*, **172**, 523-539.

Zhou, Z., Tao, Y., Li, S. & Ding, W. (2013) Hydrocarbon potential in the key basins in the East Coast of Africa, *Petrol. Explor. Develop.,* **40(**5): 582–591.

Blank

Page

Blank

Page

Appendix A: Plate kinematic reconstructions

(All maps use present day bathymetry data and the Mercator projection with Africa fixed in its present day location.)

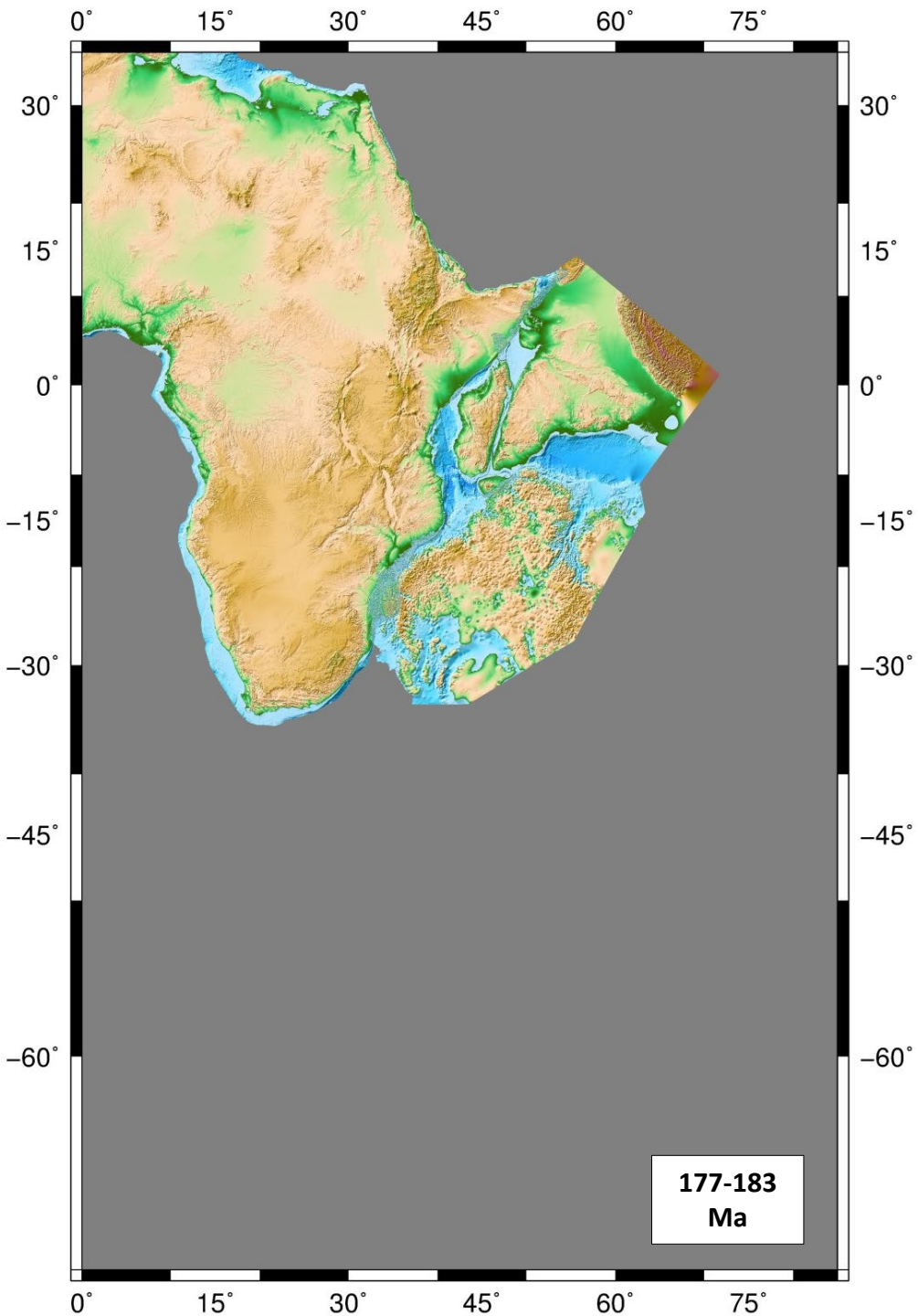
0˚
15˚
30˚
45˚
60˚
75˚
30˚
15˚
0˚
–15˚
–30˚
–45˚
–60˚
177-183
Ma

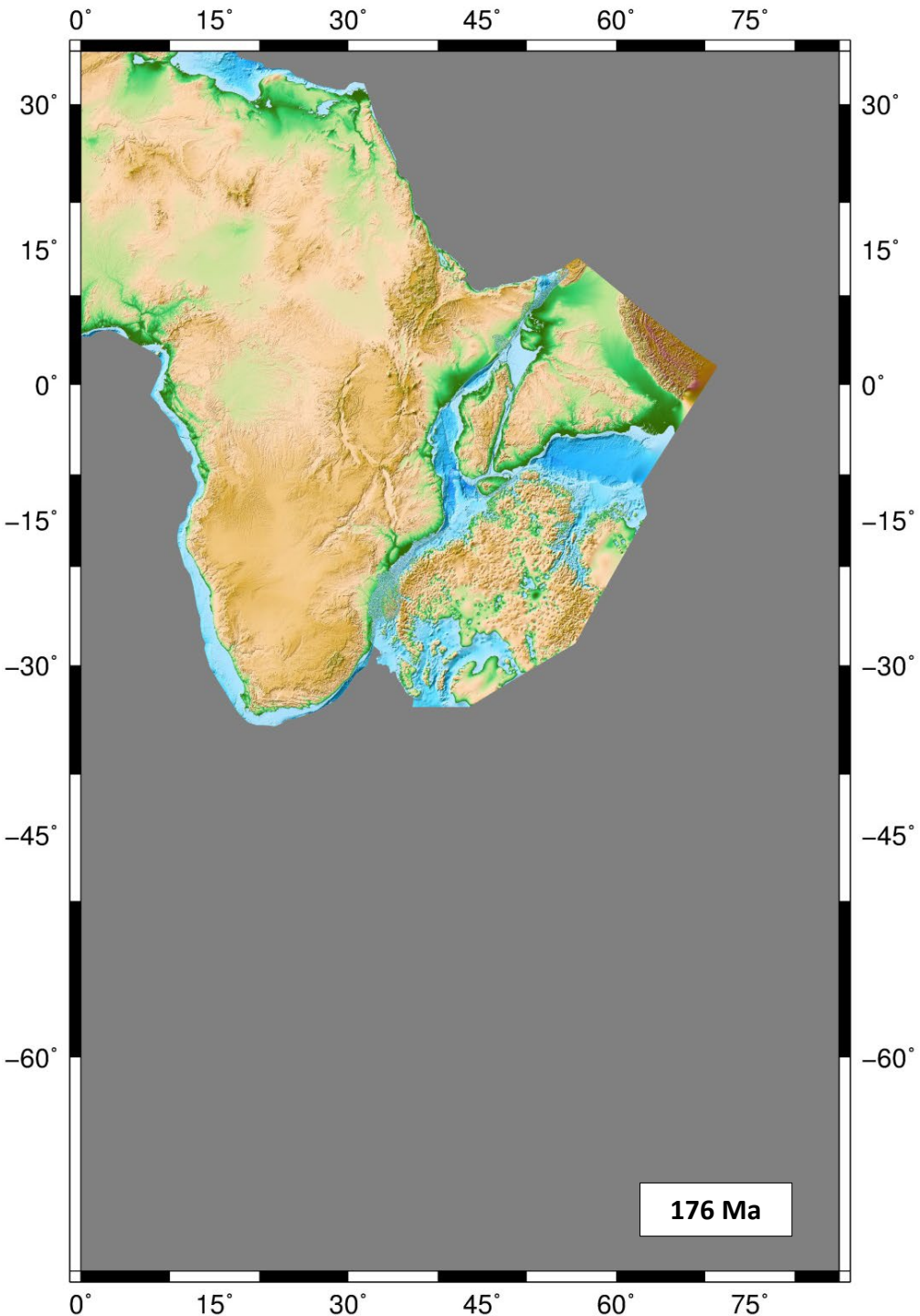
0˚
15˚
30˚
45˚
60˚
75˚
30˚
15˚
0˚
–15˚
–30˚
–45˚
–60˚
176 Ma

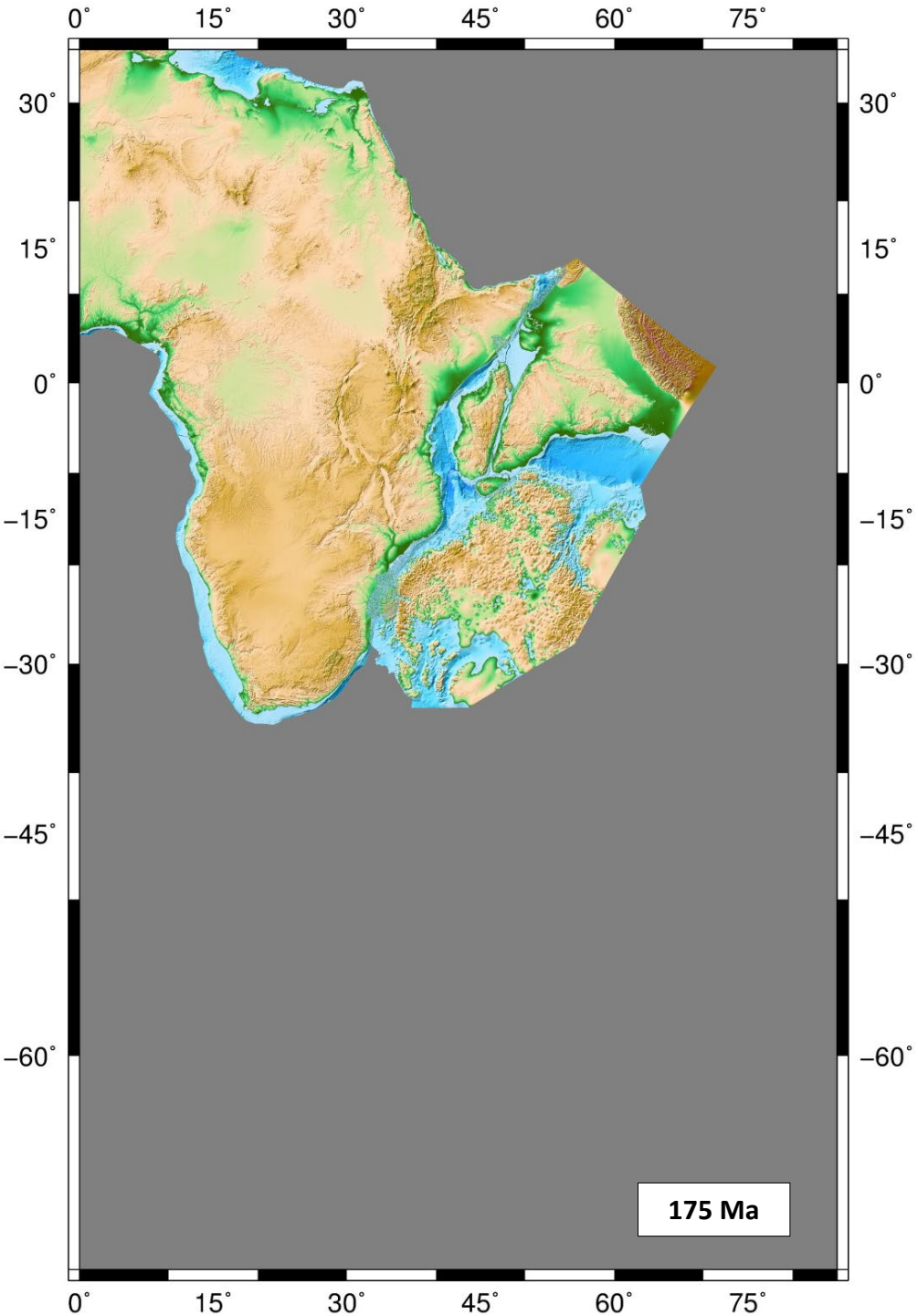
0°
15°
30°
45°
60°
75°
30°
15°
0°
−15°
−30°
−45°
−60°
175 Ma

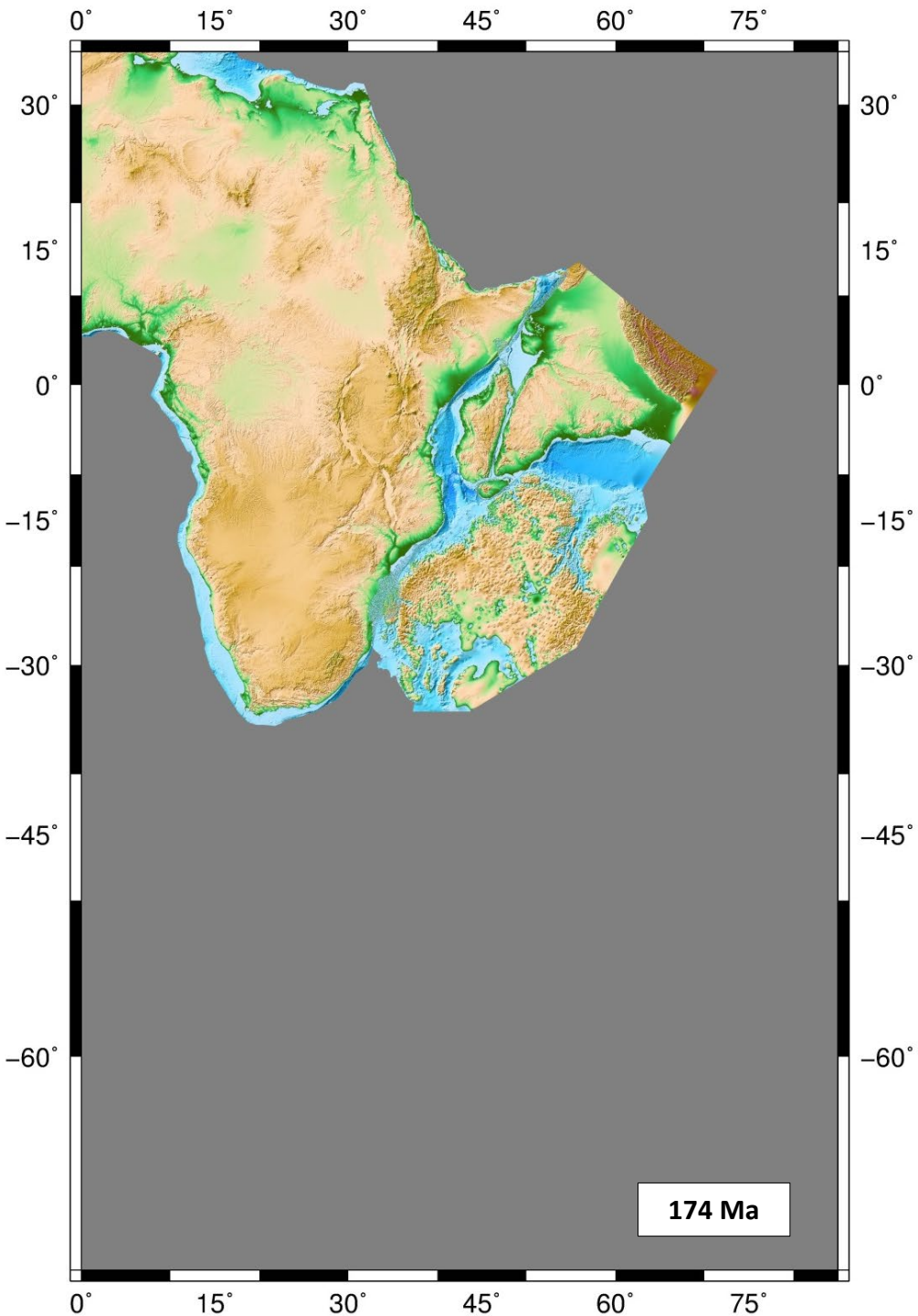
0˚
15˚
30˚
45˚
60˚
75˚
30˚
15˚
0˚
–15˚
–30˚
–45˚
–60˚
174 Ma

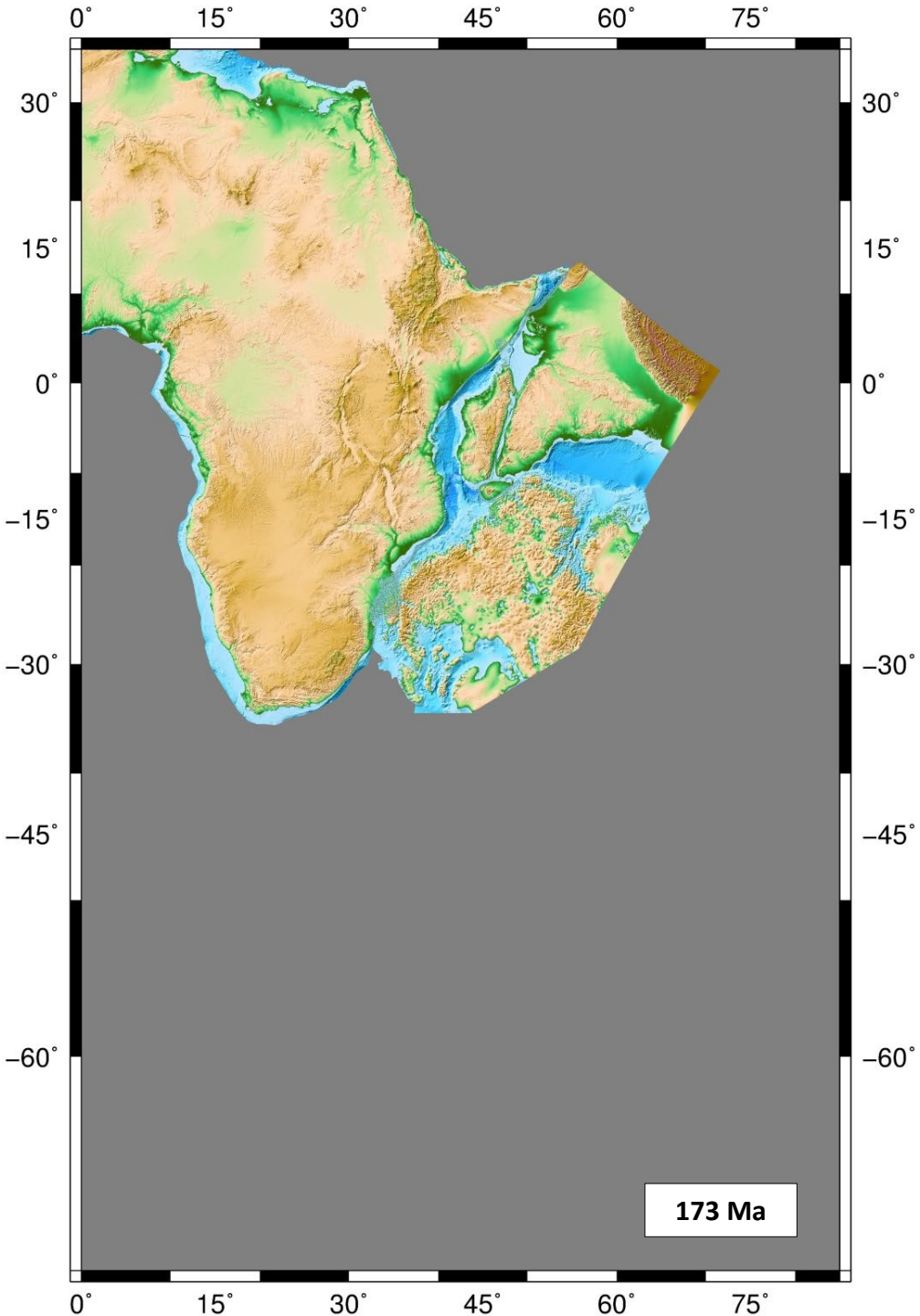
0°
15°
30°
45°
60°
75°
30°
15°
0°
−15°
−30°
−45°
−60°
173 Ma

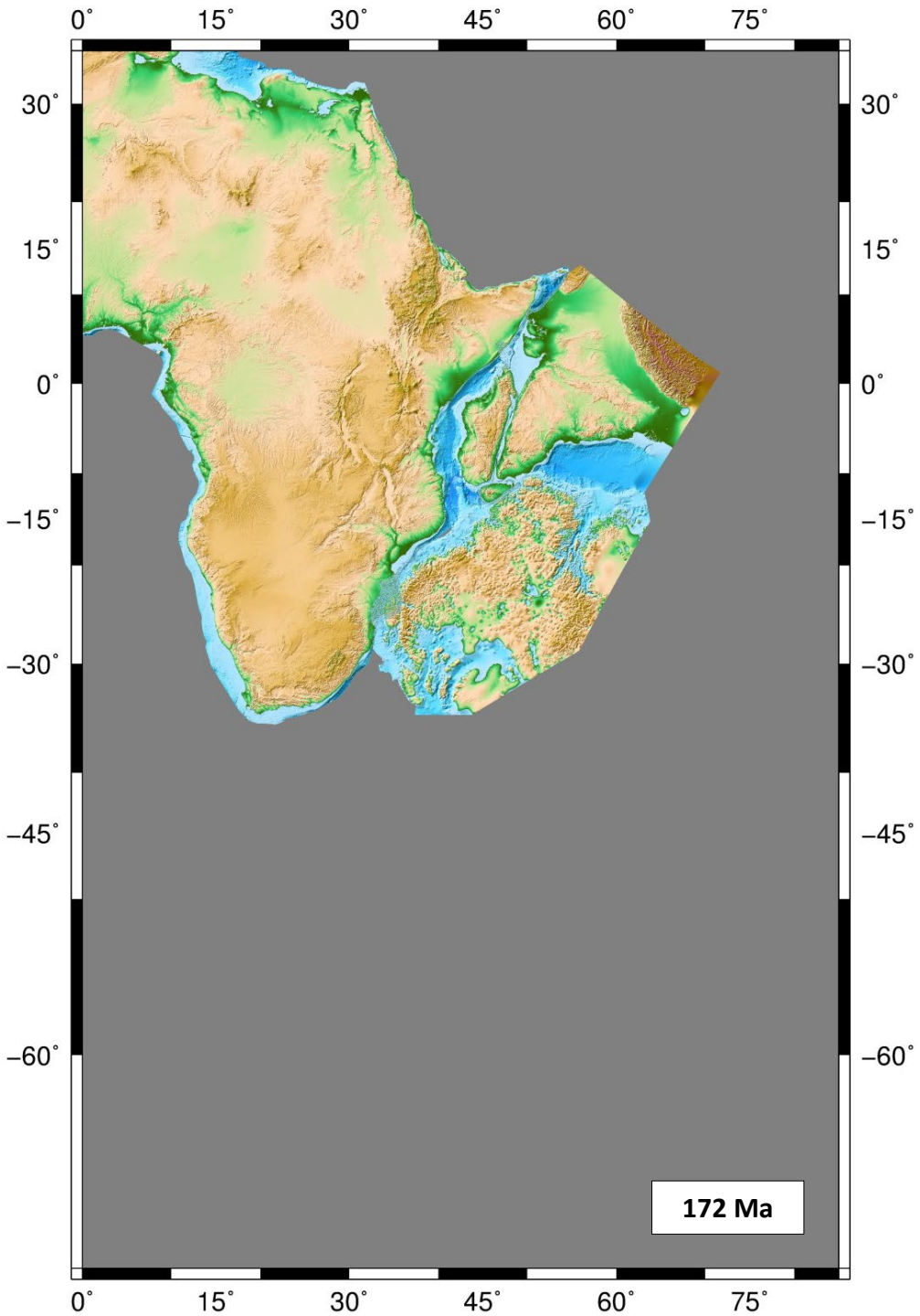
0˚
15˚
30˚
45˚
60˚
75˚
30˚
15˚
0˚
–15˚
–30˚
–45˚
–60˚
172 Ma

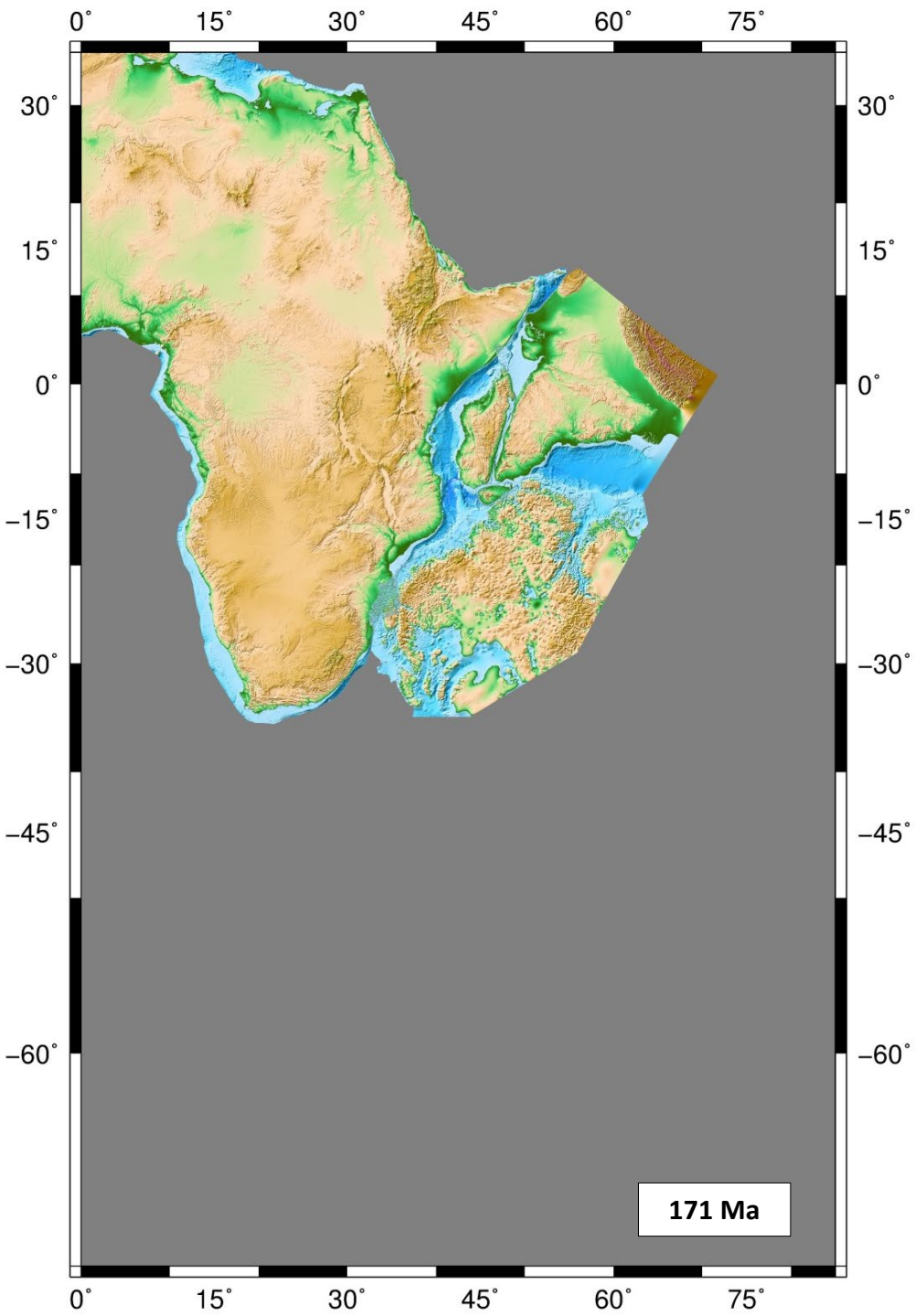
0˚
15˚
30˚
45˚
60˚
75˚
30˚
15˚
0˚
–15˚
–30˚
–45˚
–60˚
171 Ma

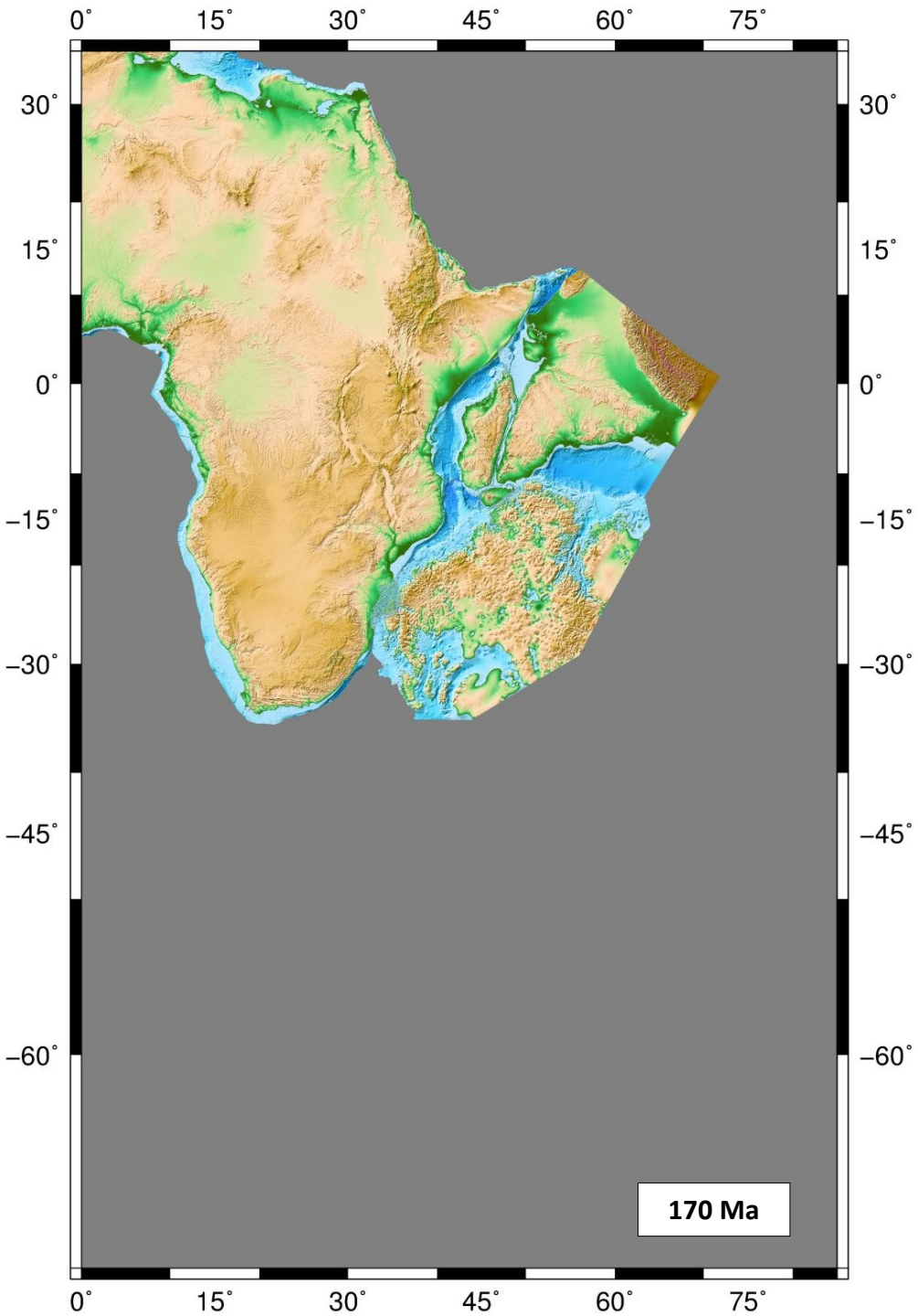
0˚
15˚
30˚
45˚
60˚
75˚
30˚
15˚
0˚
–15˚
–30˚
–45˚
–60˚
170 Ma

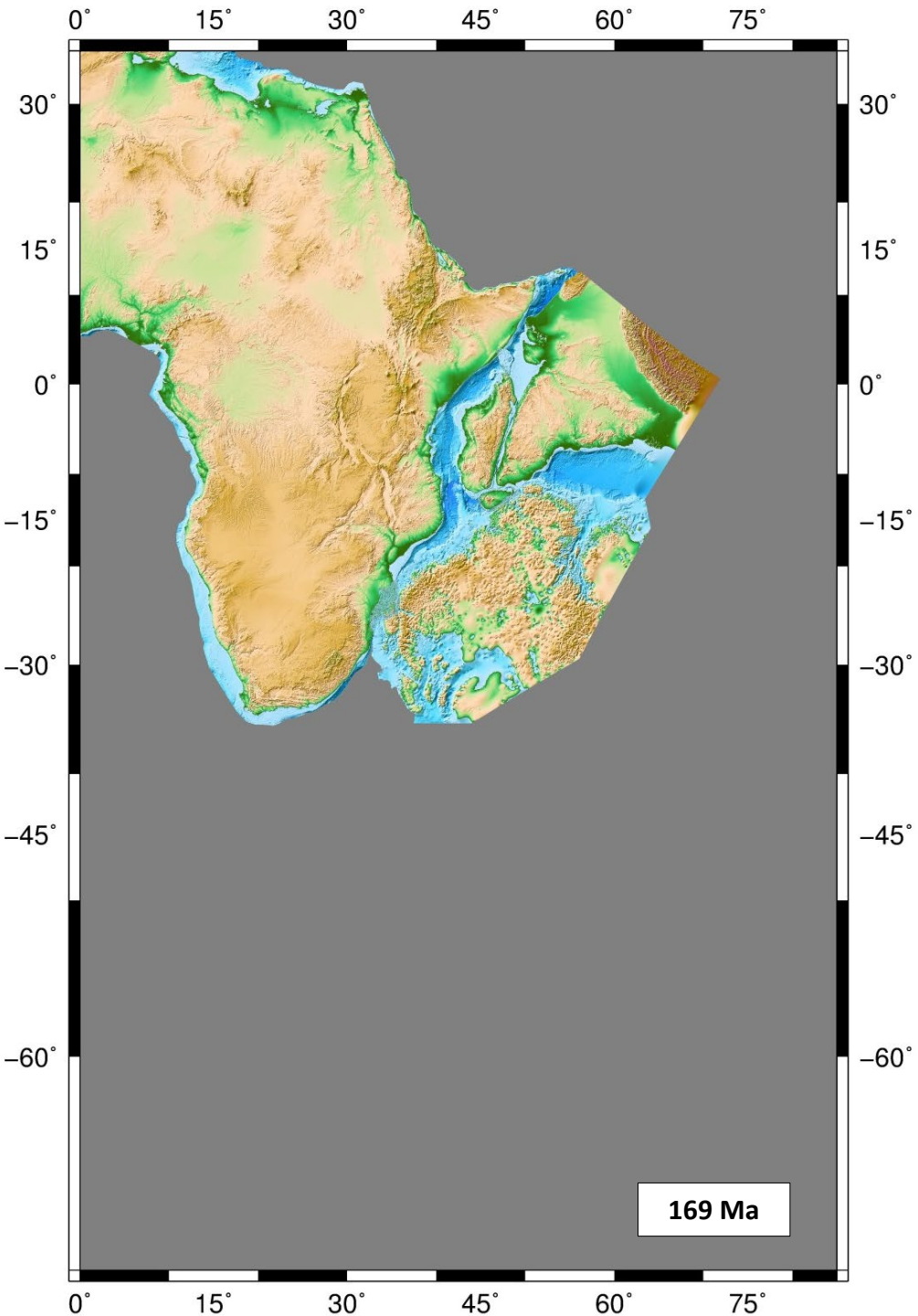
0˚
15˚
30˚
45˚
60˚
75˚
30˚
15˚
0˚
–15˚
–30˚
–45˚
–60˚
169 Ma

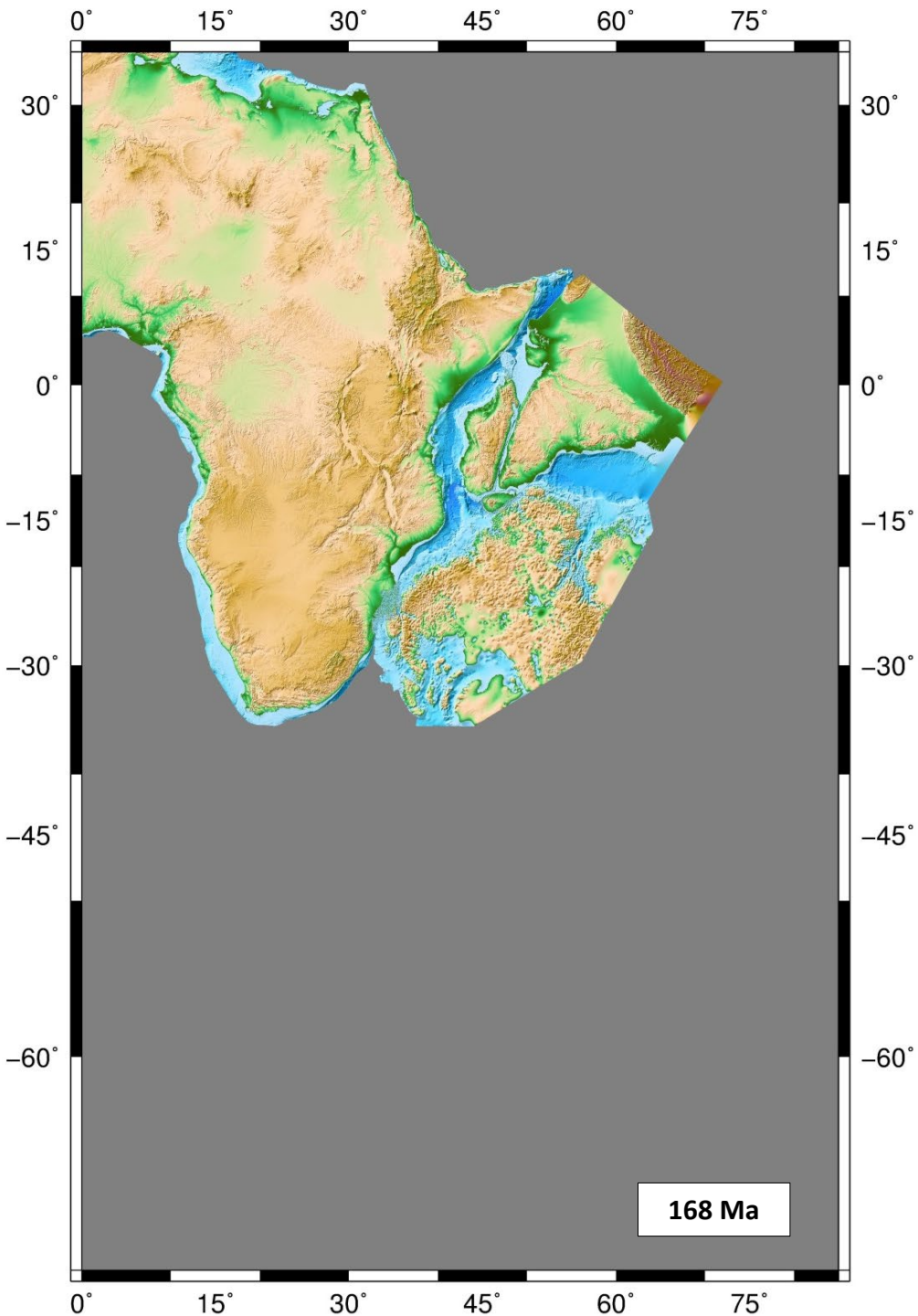
0˚
15˚
30˚
45˚
60˚
75˚
30˚
15˚
0˚
–15˚
–30˚
–45˚
–60˚
168 Ma

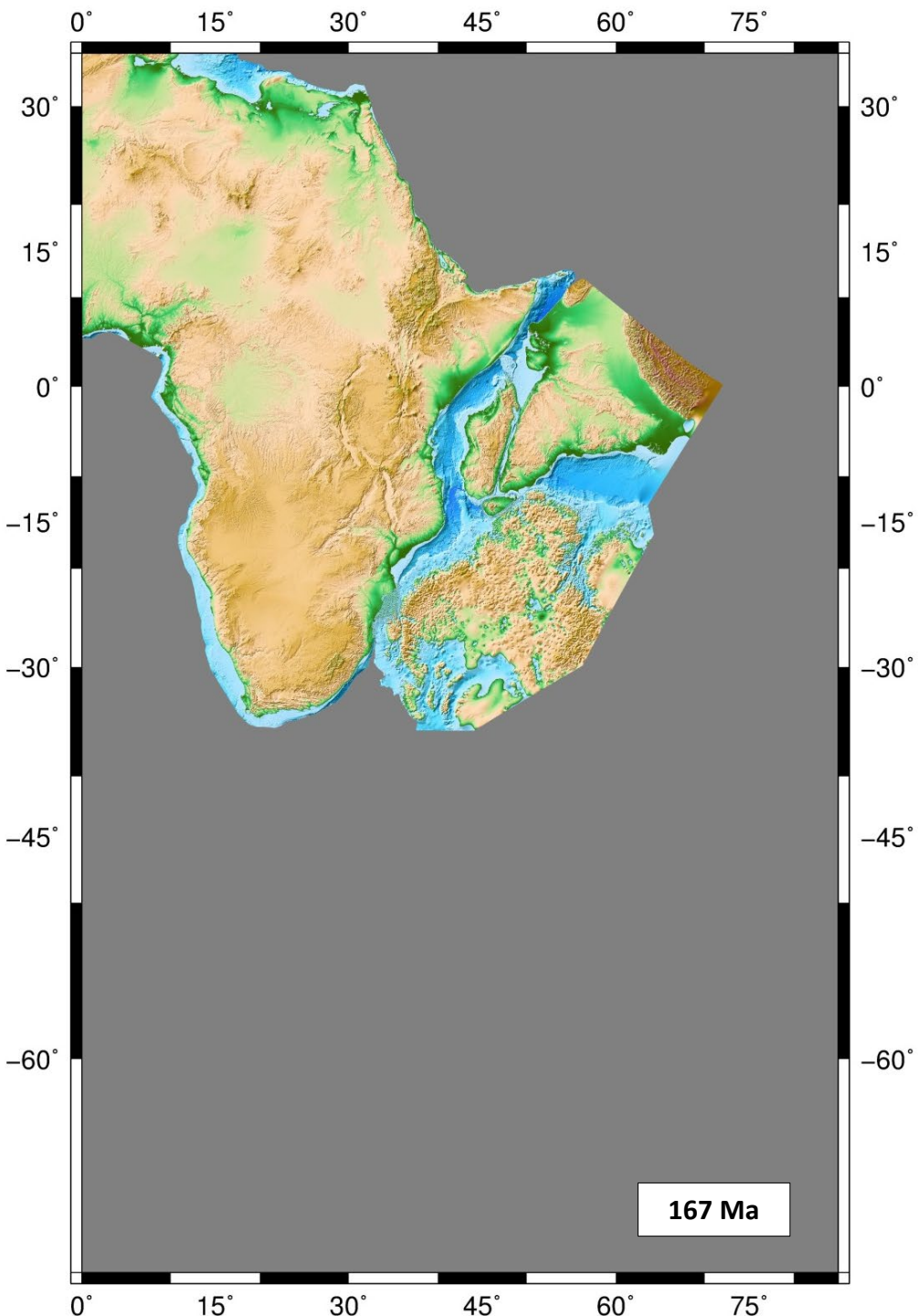
0˚
15˚
30˚
45˚
60˚
75˚
30˚
15˚
0˚
–15˚
–30˚
–45˚
–60˚
167 Ma

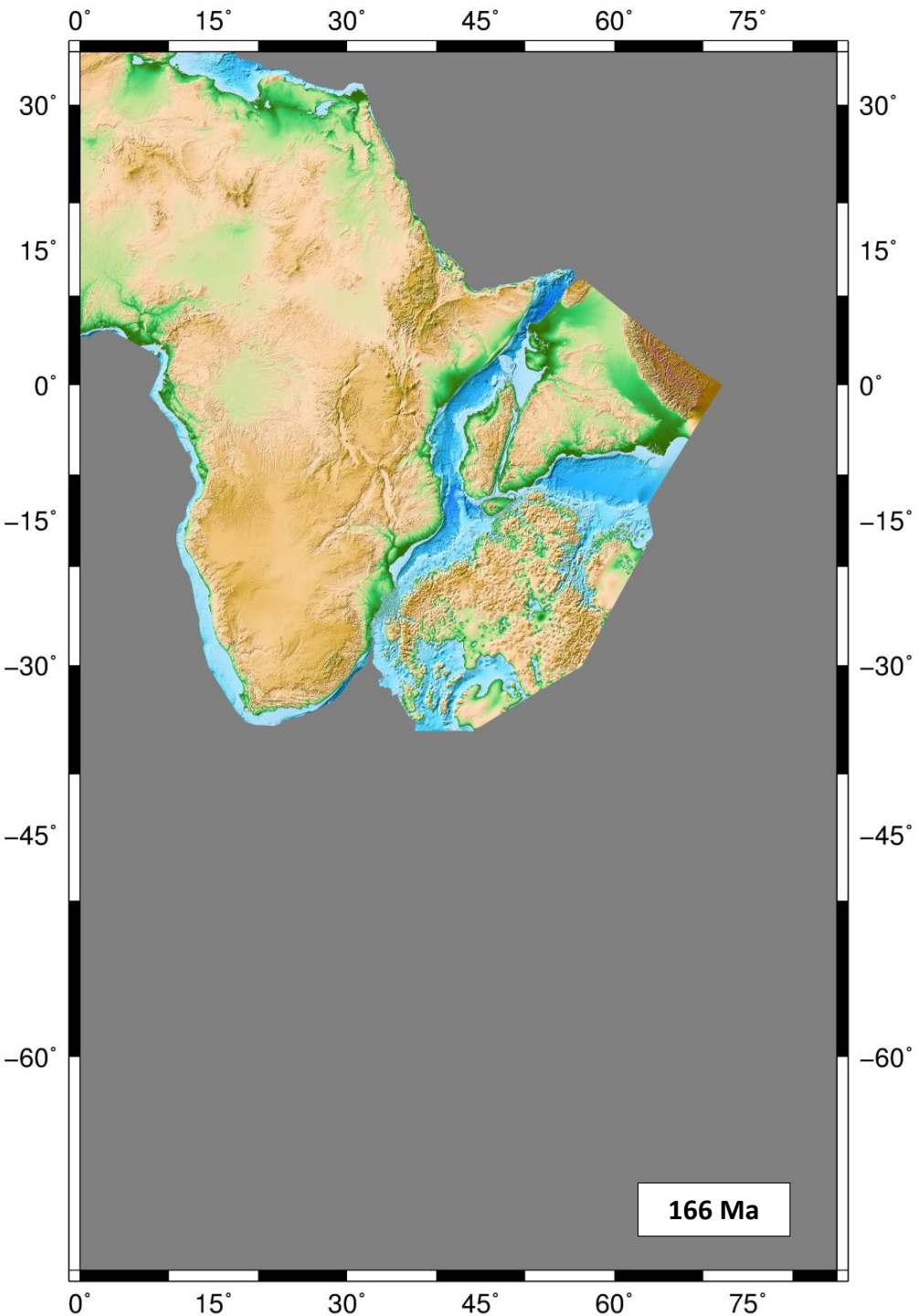
0˚
15˚
30˚
45˚
60˚
75˚
30˚
15˚
0˚
–15˚
–30˚
–45˚
–60˚
166 Ma

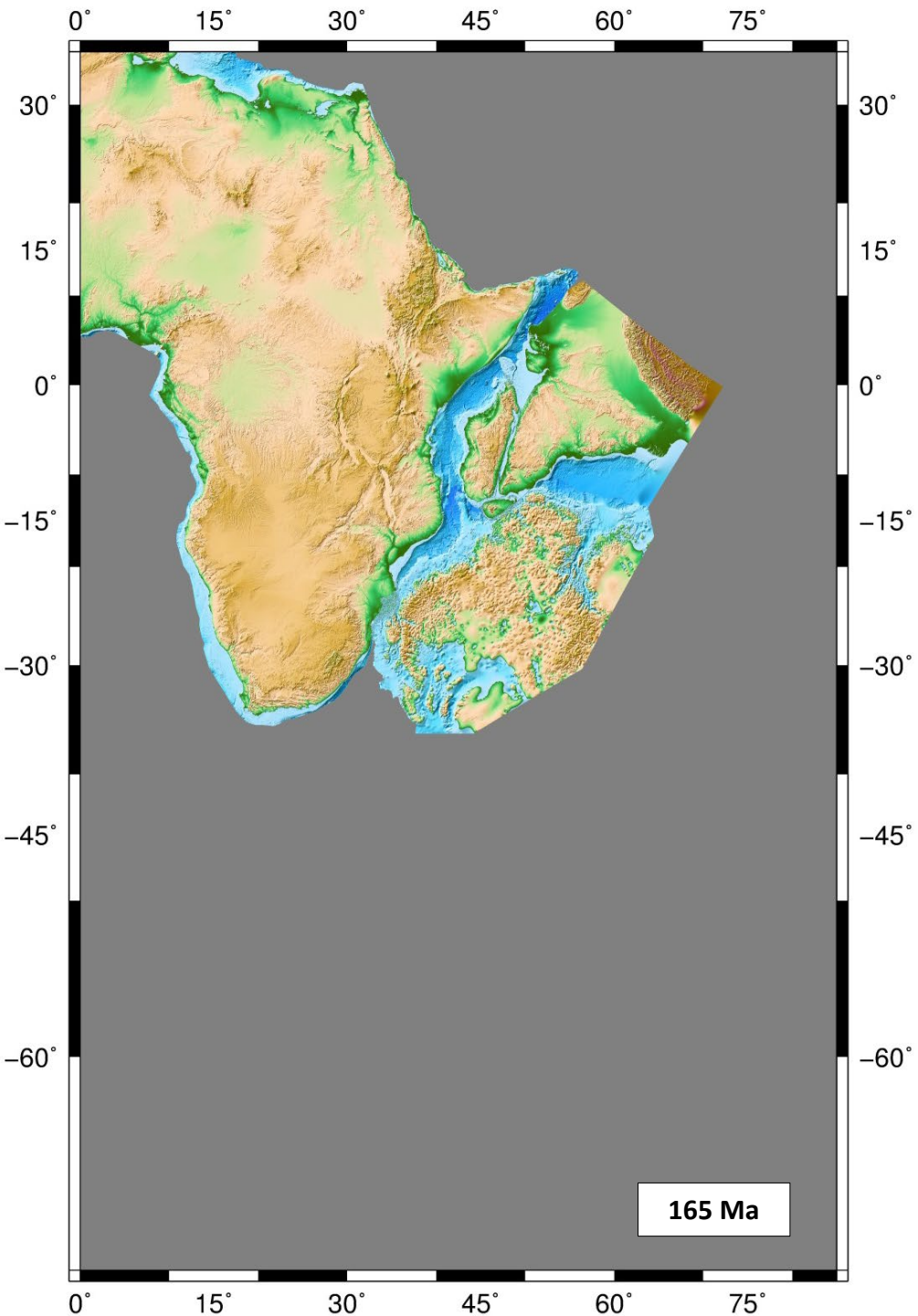
0˚
15˚
30˚
45˚
60˚
75˚
30˚
15˚
0˚
−15˚
−30˚
−45˚
−60˚
165 Ma

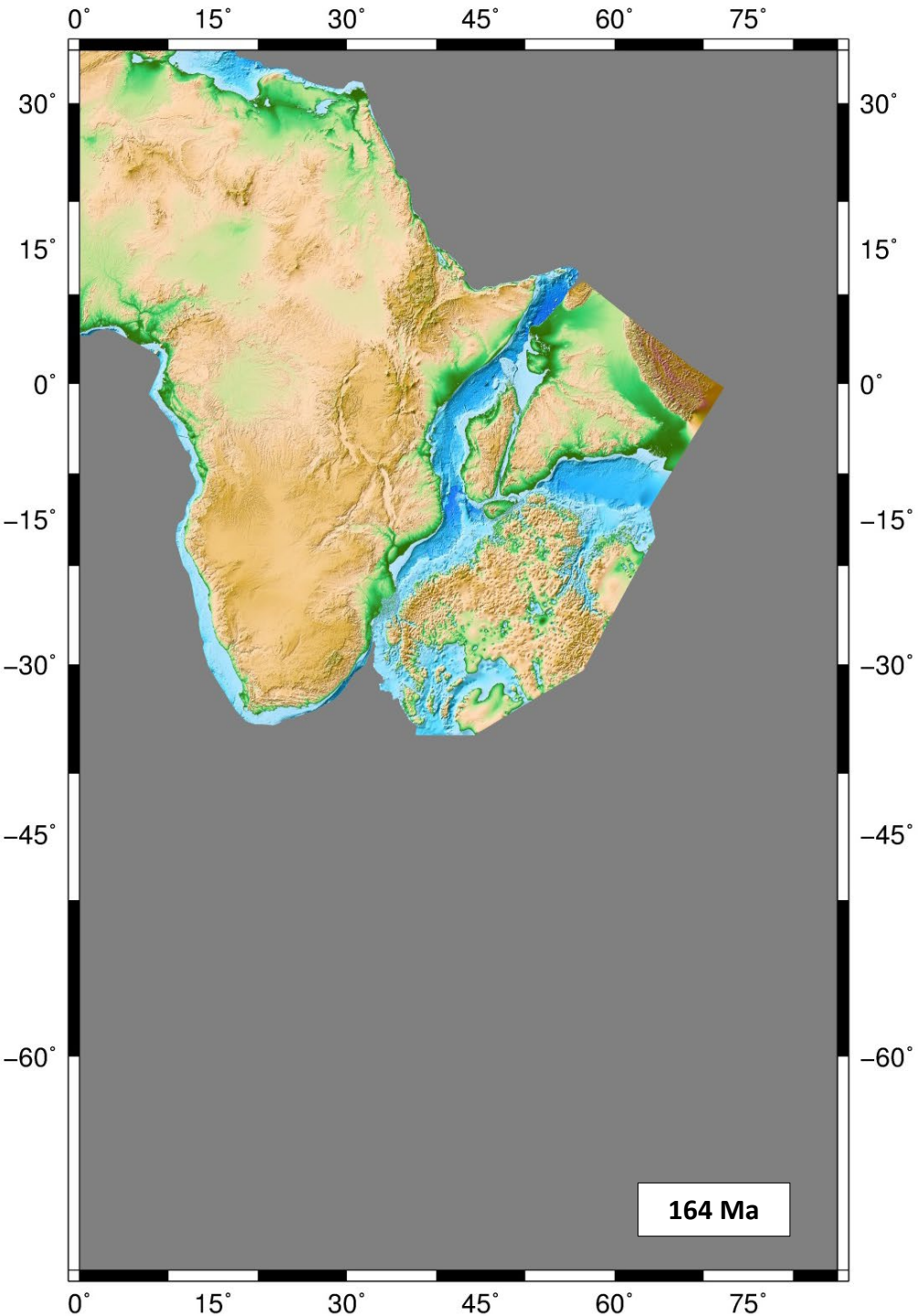
0˚
15˚
30˚
45˚
60˚
75˚
30˚
15˚
0˚
–15˚
–30˚
–45˚
–60˚
164 Ma

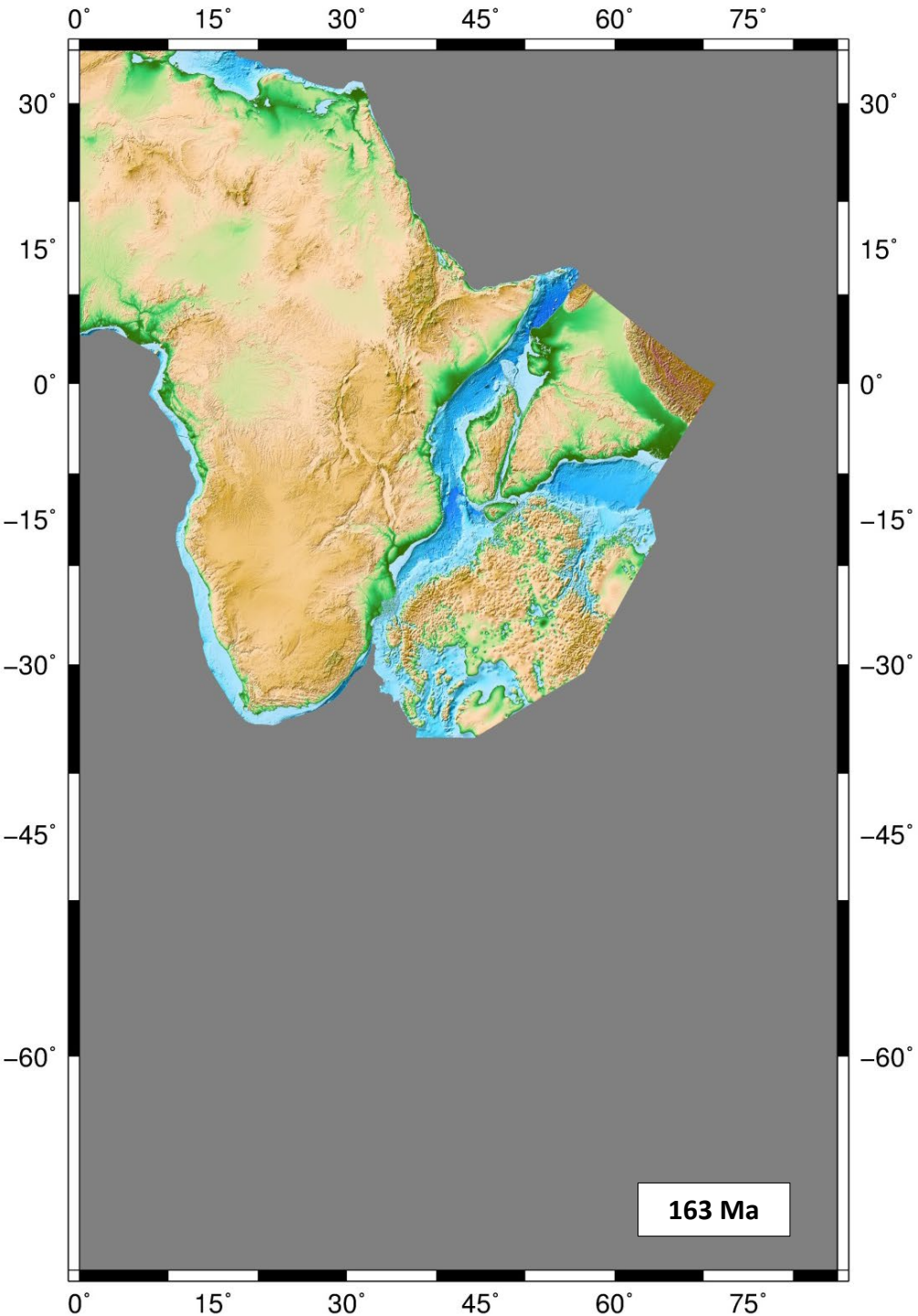
0˚
15˚
30˚
45˚
60˚
75˚
30˚
15˚
0˚
–15˚
–30˚
–45˚
–60˚
163 Ma

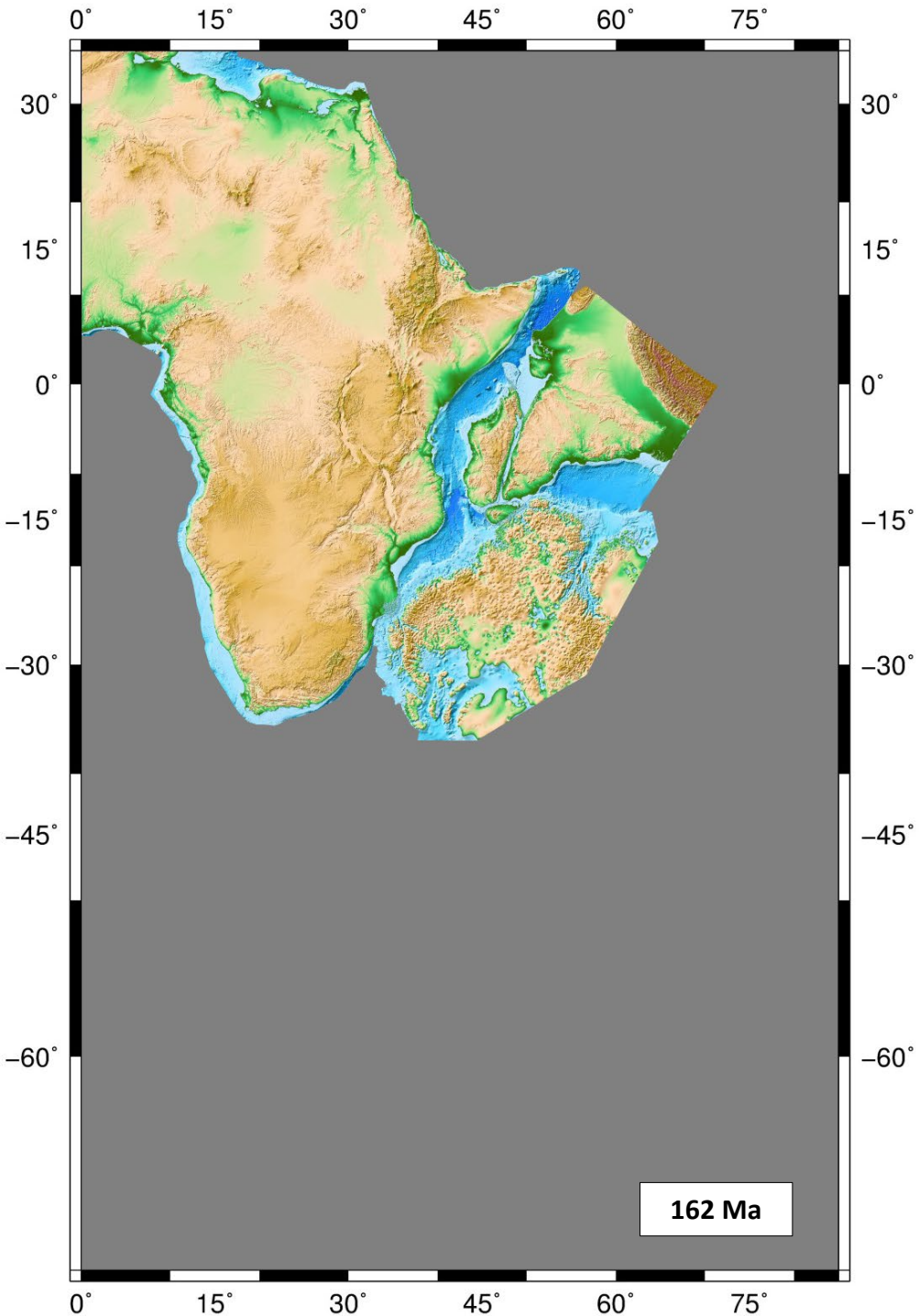
0˚
15˚
30˚
45˚
60˚
75˚
30˚
15˚
0˚
–15˚
–30˚
–45˚
–60˚
162 Ma

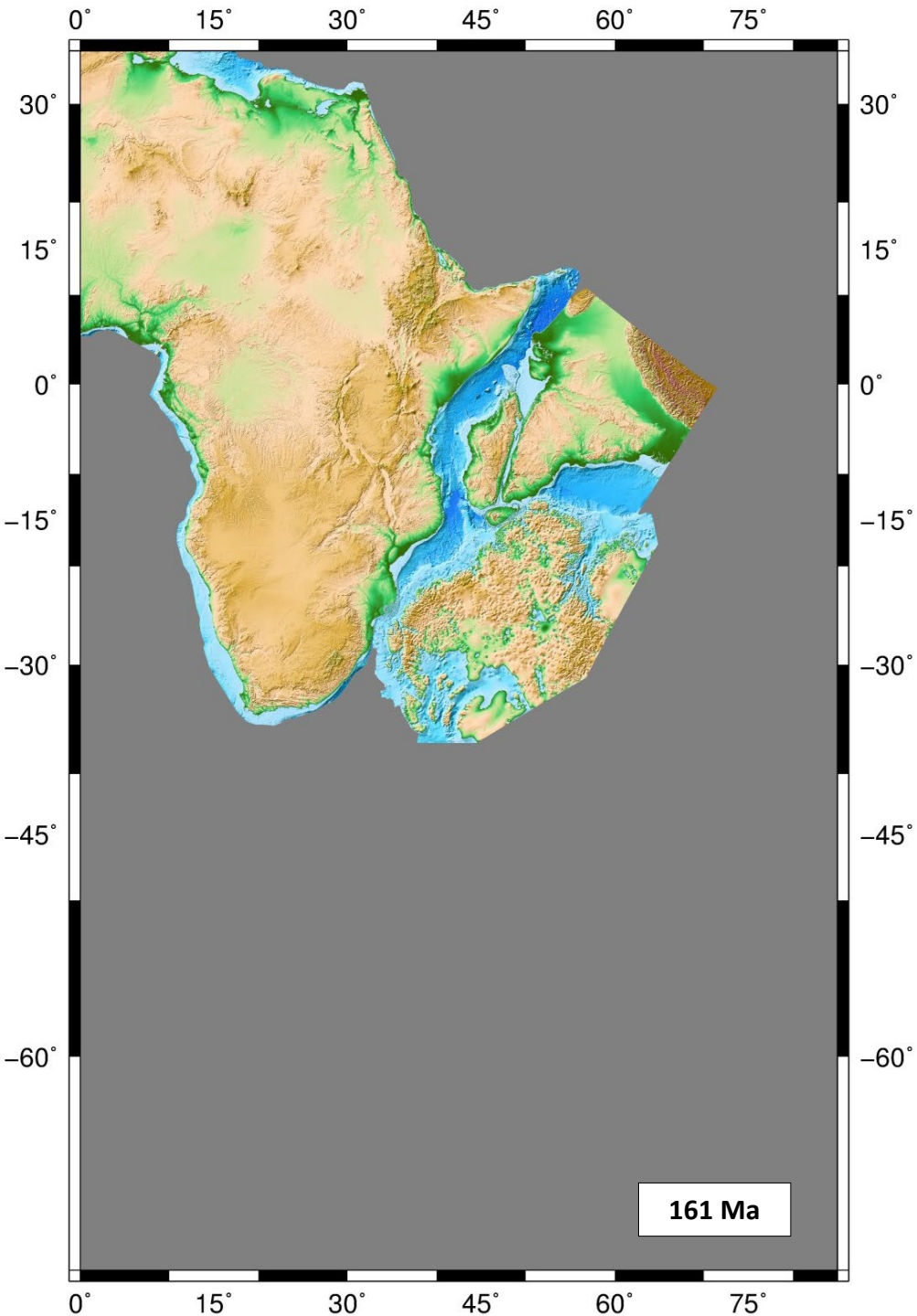
0˚
15˚
30˚
45˚
60˚
75˚
30˚
15˚
0˚
–15˚
–30˚
–45˚
–60˚
161 Ma

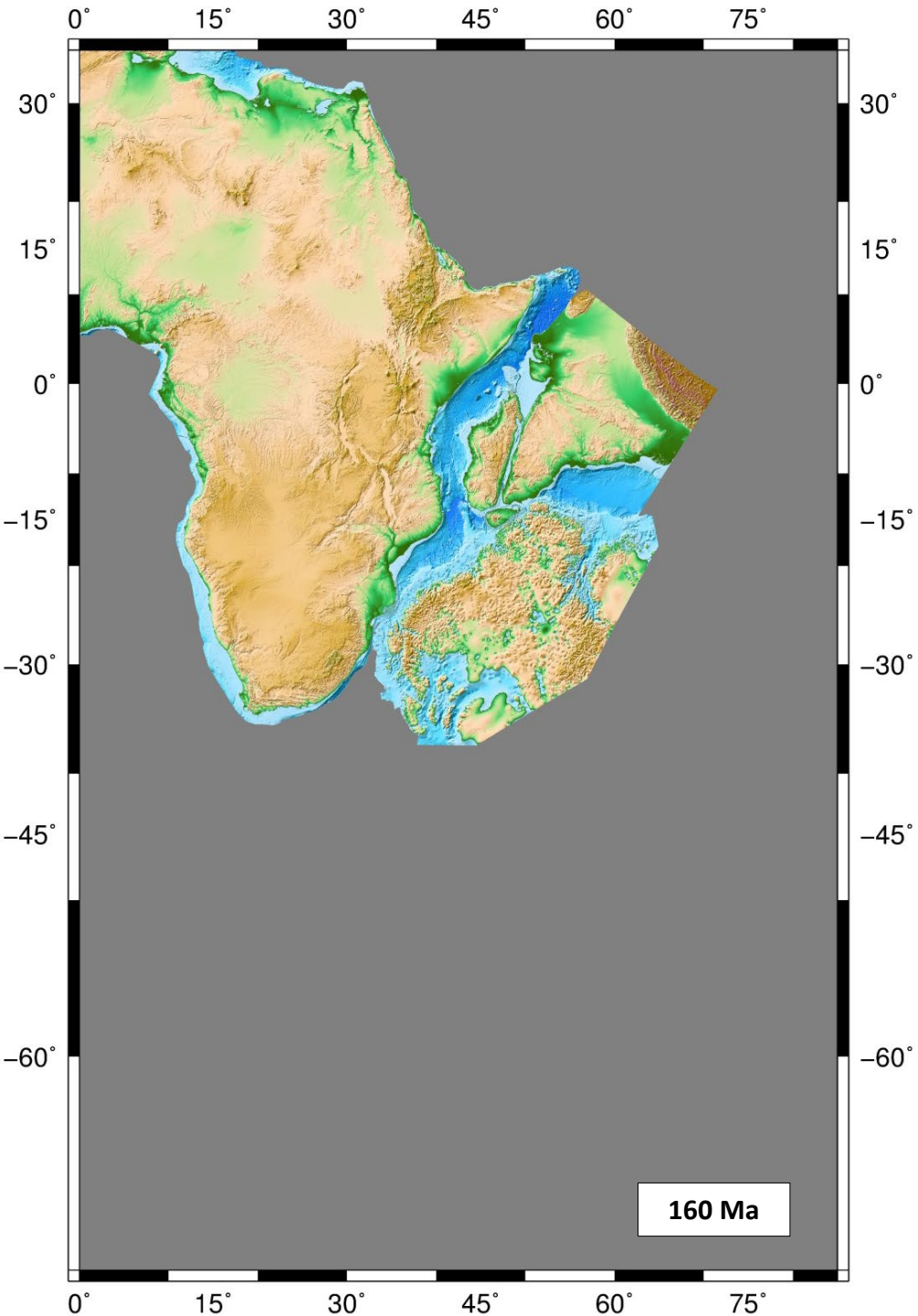
0˚
15˚
30˚
45˚
60˚
75˚
30˚
15˚
0˚
–15˚
–30˚
–45˚
–60˚
160 Ma

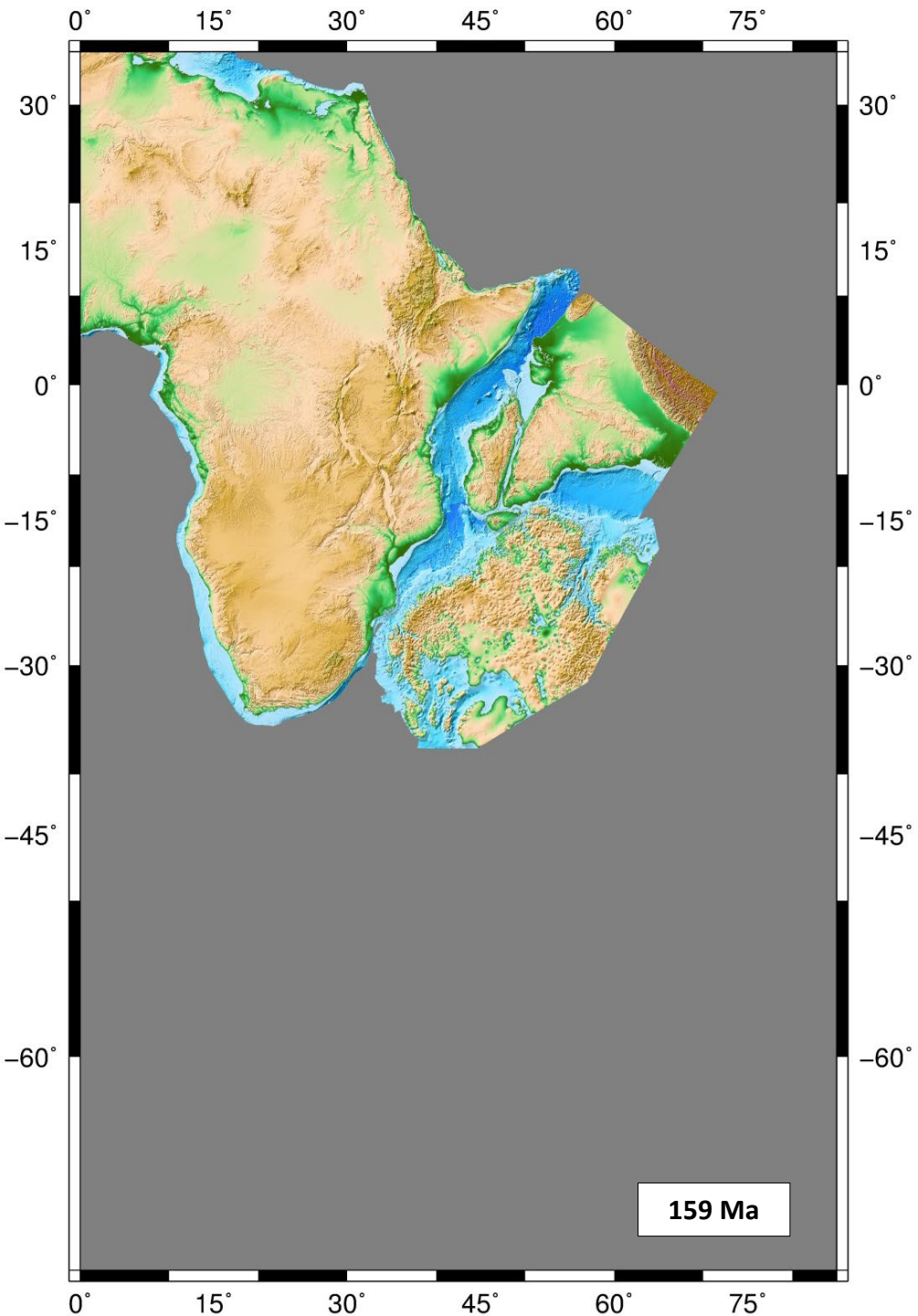
0˚
15˚
30˚
45˚
60˚
75˚
30˚
15˚
0˚
−15˚
−30˚
−45˚
−60˚
159 Ma

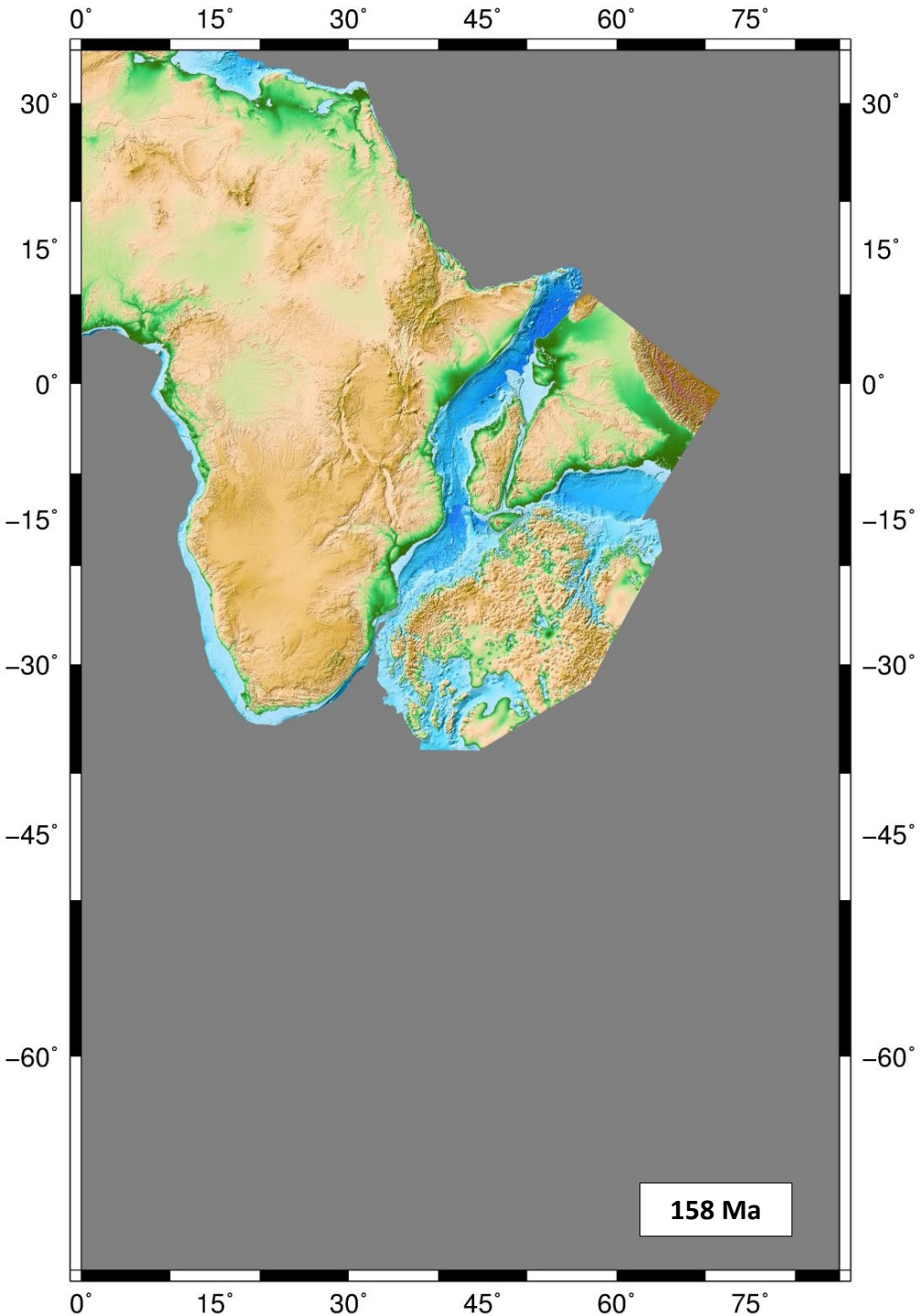
0˚
15˚
30˚
45˚
60˚
75˚
30˚
15˚
0˚
–15˚
–30˚
–45˚
–60˚
158 Ma

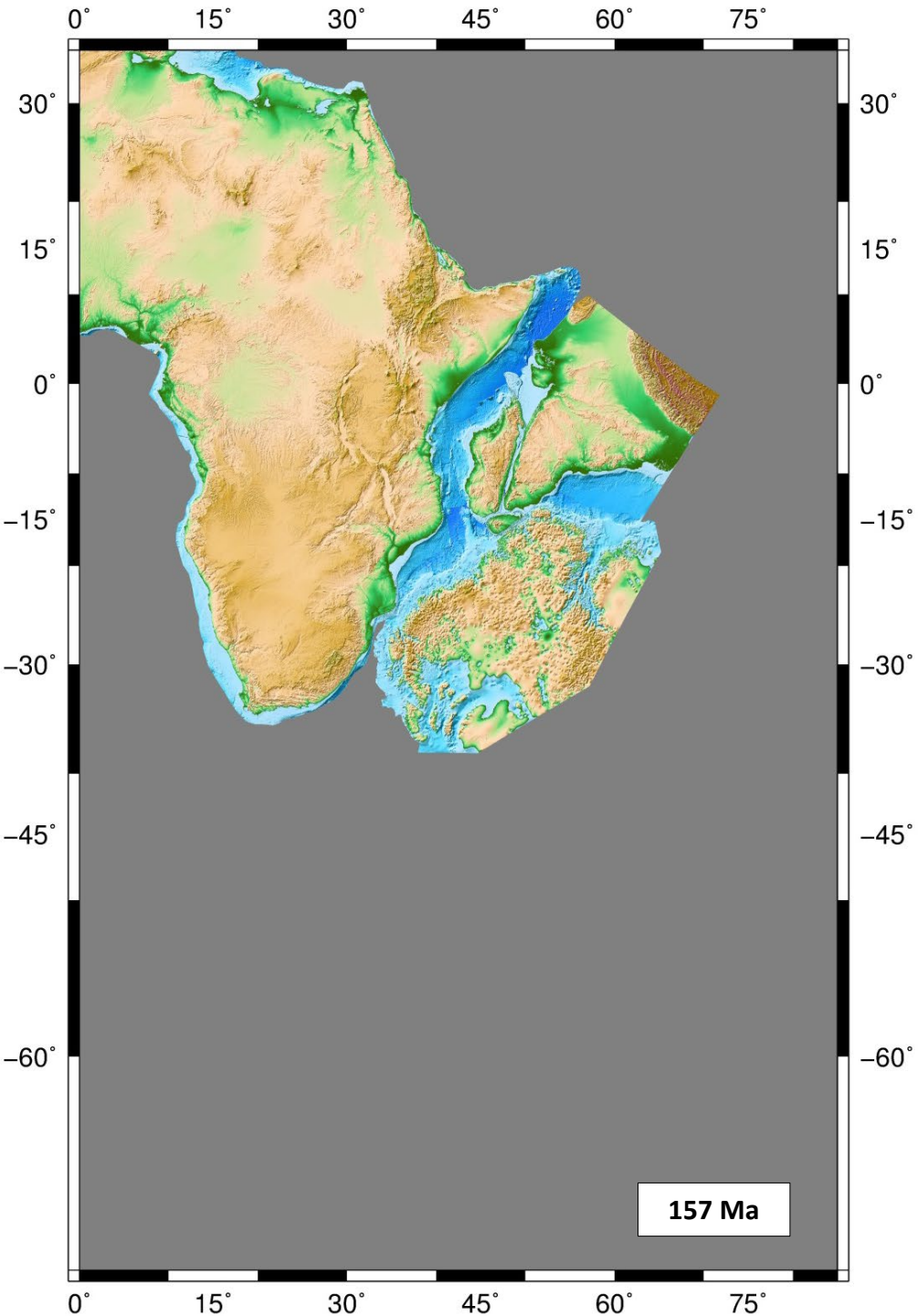
0˚
15˚
30˚
45˚
60˚
75˚
30˚
15˚
0˚
–15˚
–30˚
–45˚
–60˚
157 Ma

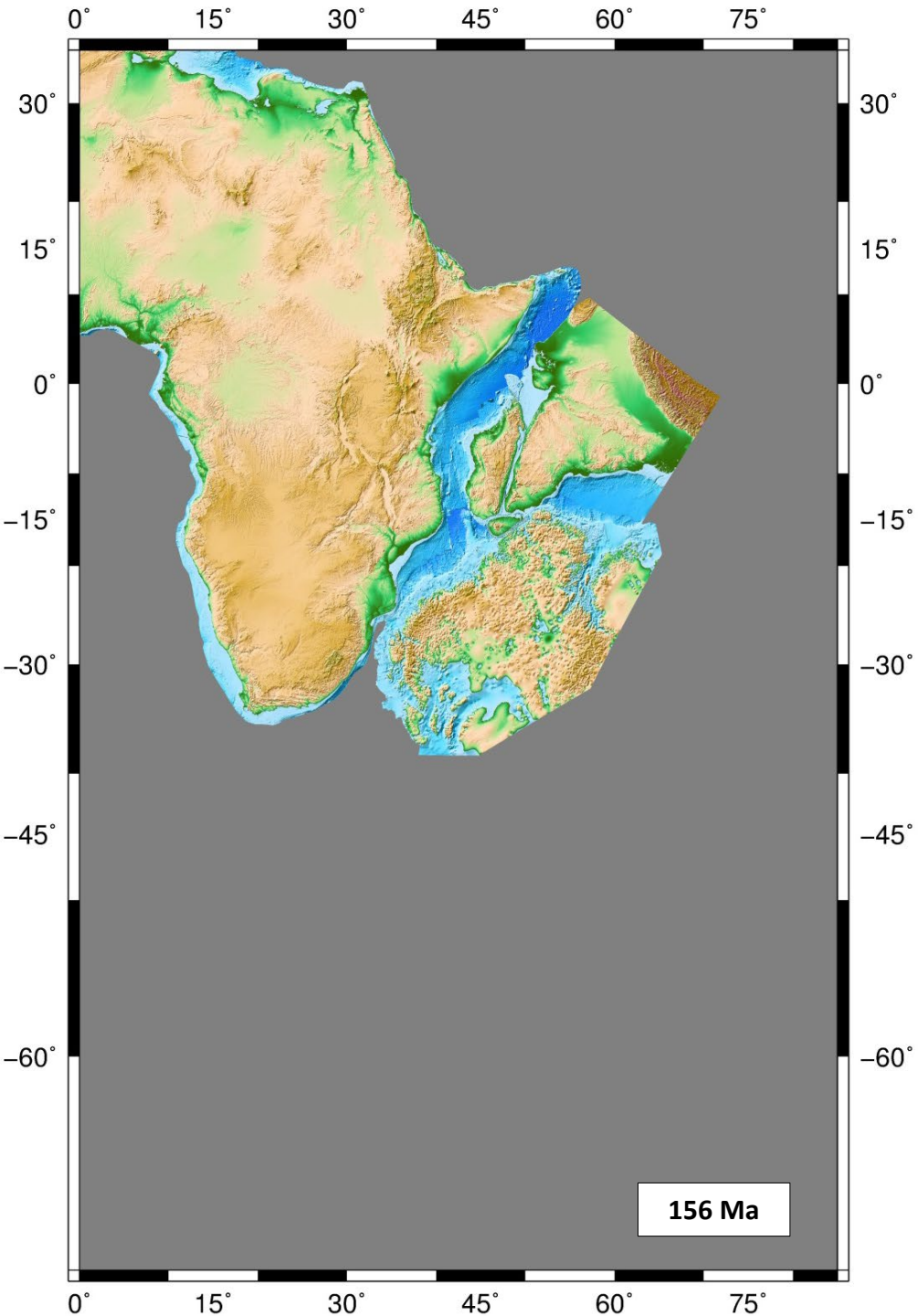
0°
15°
30°
45°
60°
75°
30°
15°
0°
−15°
−30°
−45°
−60°
156 Ma

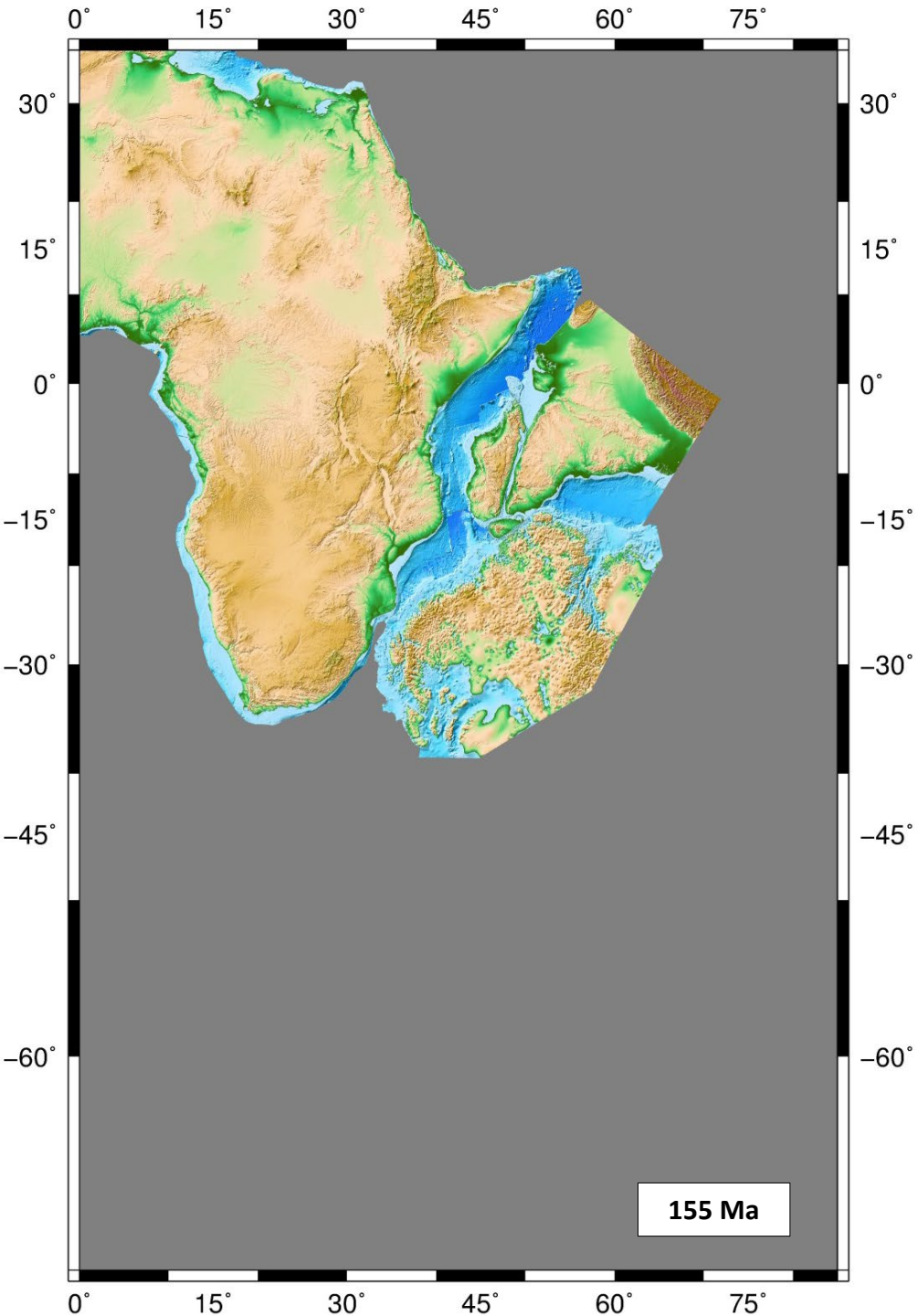
0˚
15˚
30˚
45˚
60˚
75˚
30˚
15˚
0˚
–15˚
–30˚
–45˚
–60˚
155 Ma

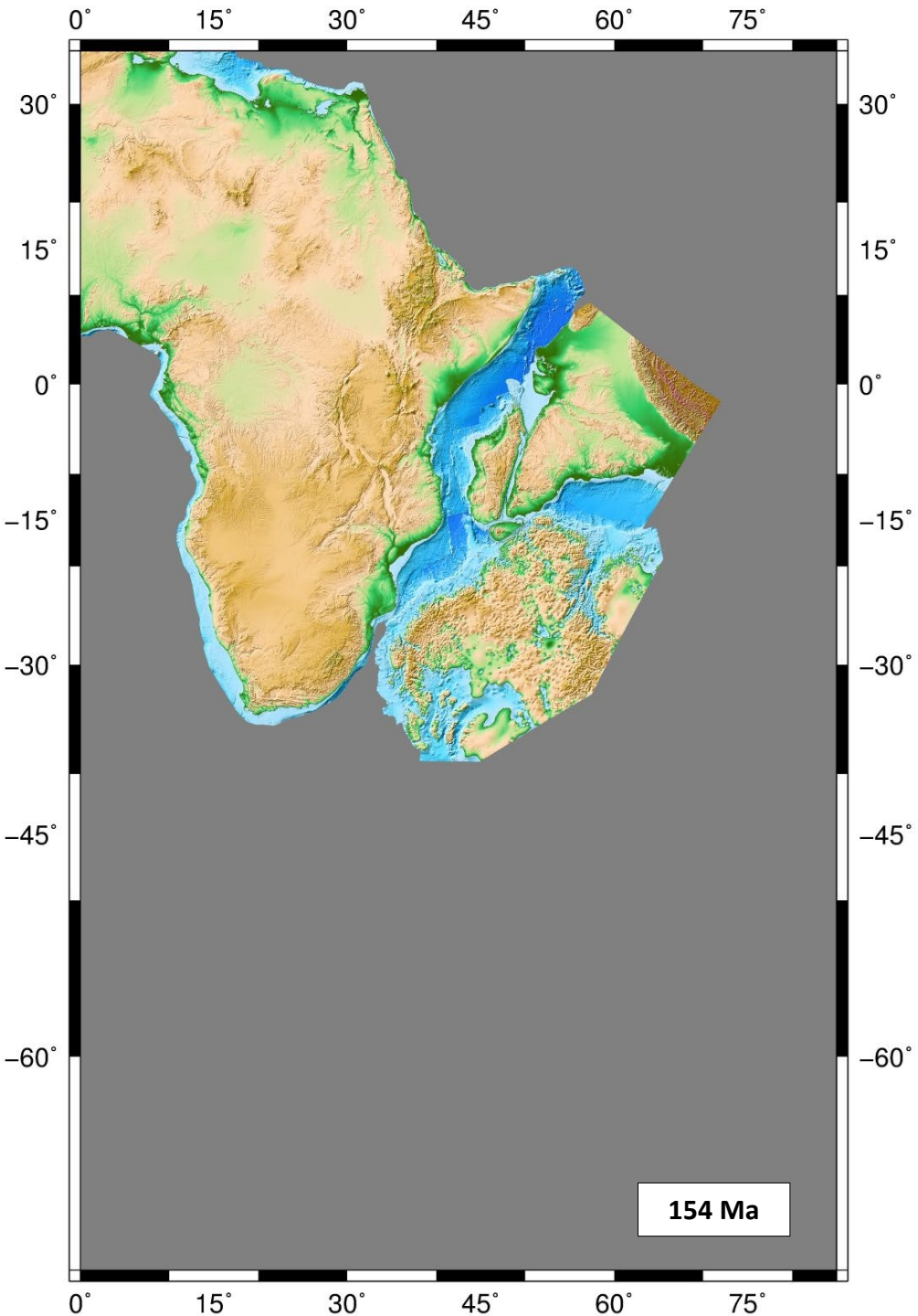
0˚
15˚
30˚
45˚
60˚
75˚
30˚
15˚
0˚
–15˚
–30˚
–45˚
–60˚
154 Ma

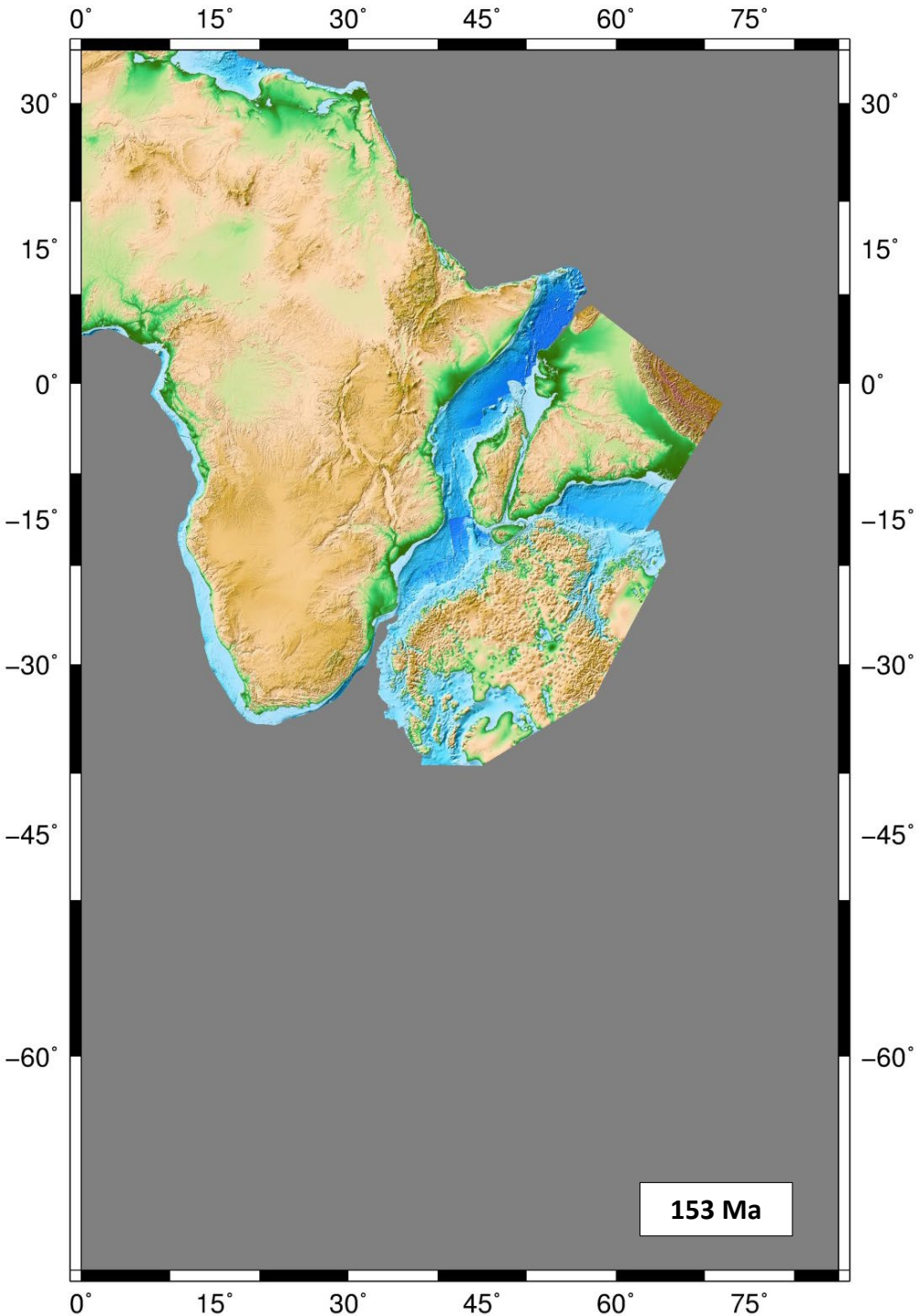
0˚
15˚
30˚
45˚
60˚
75˚
30˚
15˚
0˚
−15˚
−30˚
−45˚
−60˚
153 Ma

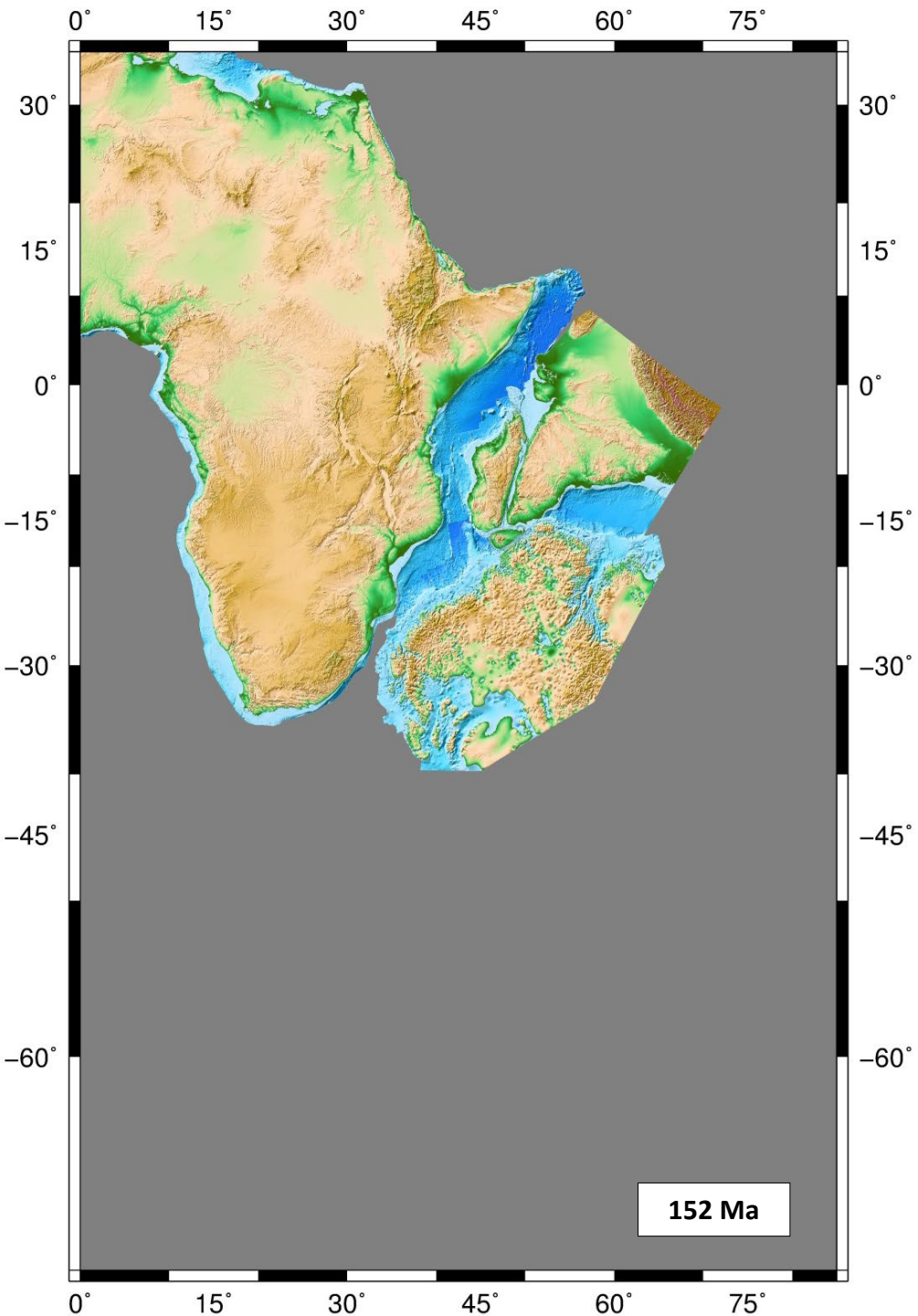
0˚
15˚
30˚
45˚
60˚
75˚
30˚
15˚
0˚
−15˚
−30˚
−45˚
−60˚
152 Ma

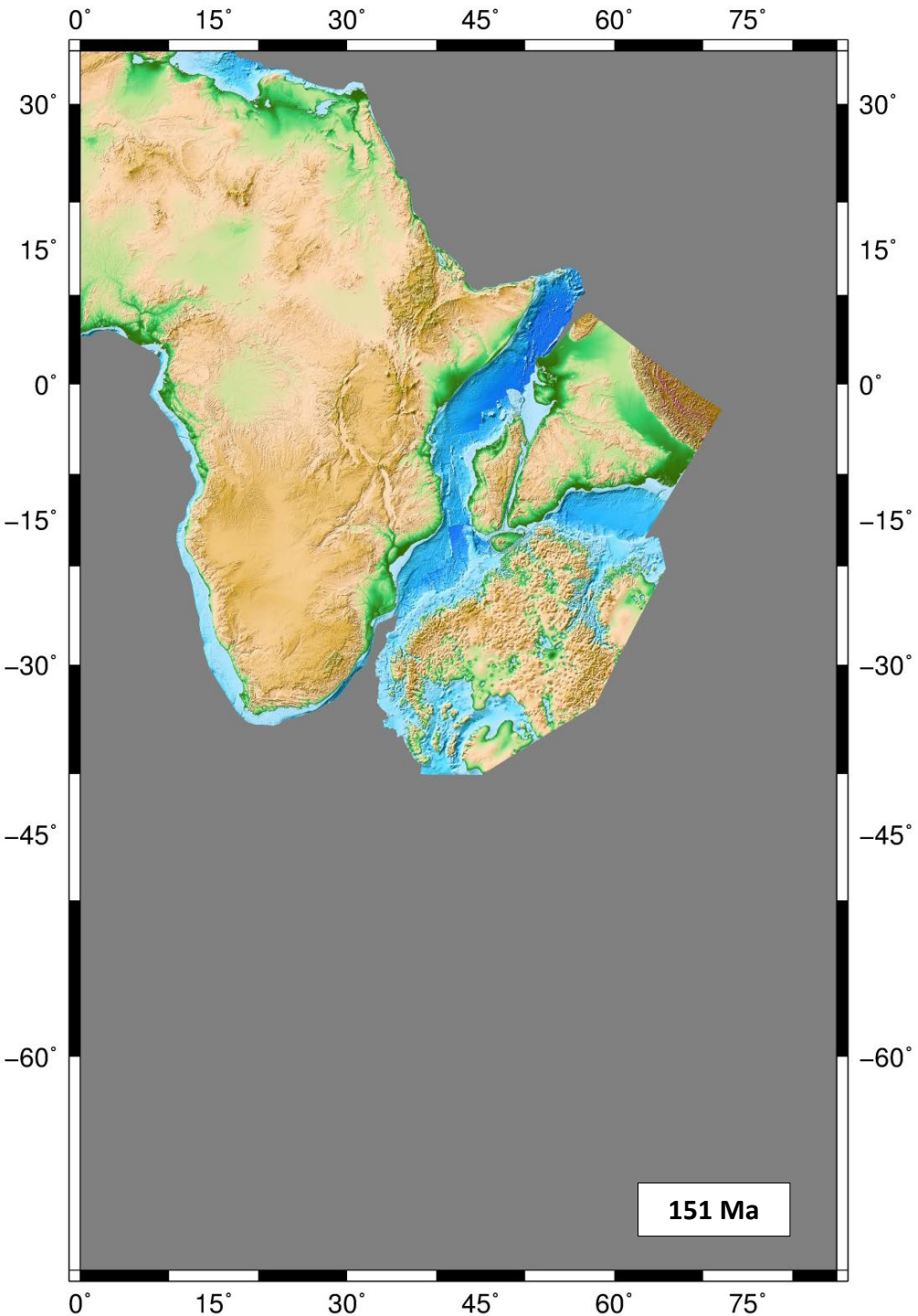
0°
15°
30°
45°
60°
75°
30°
15°
0°
−15°
−30°
−45°
−60°
151 Ma

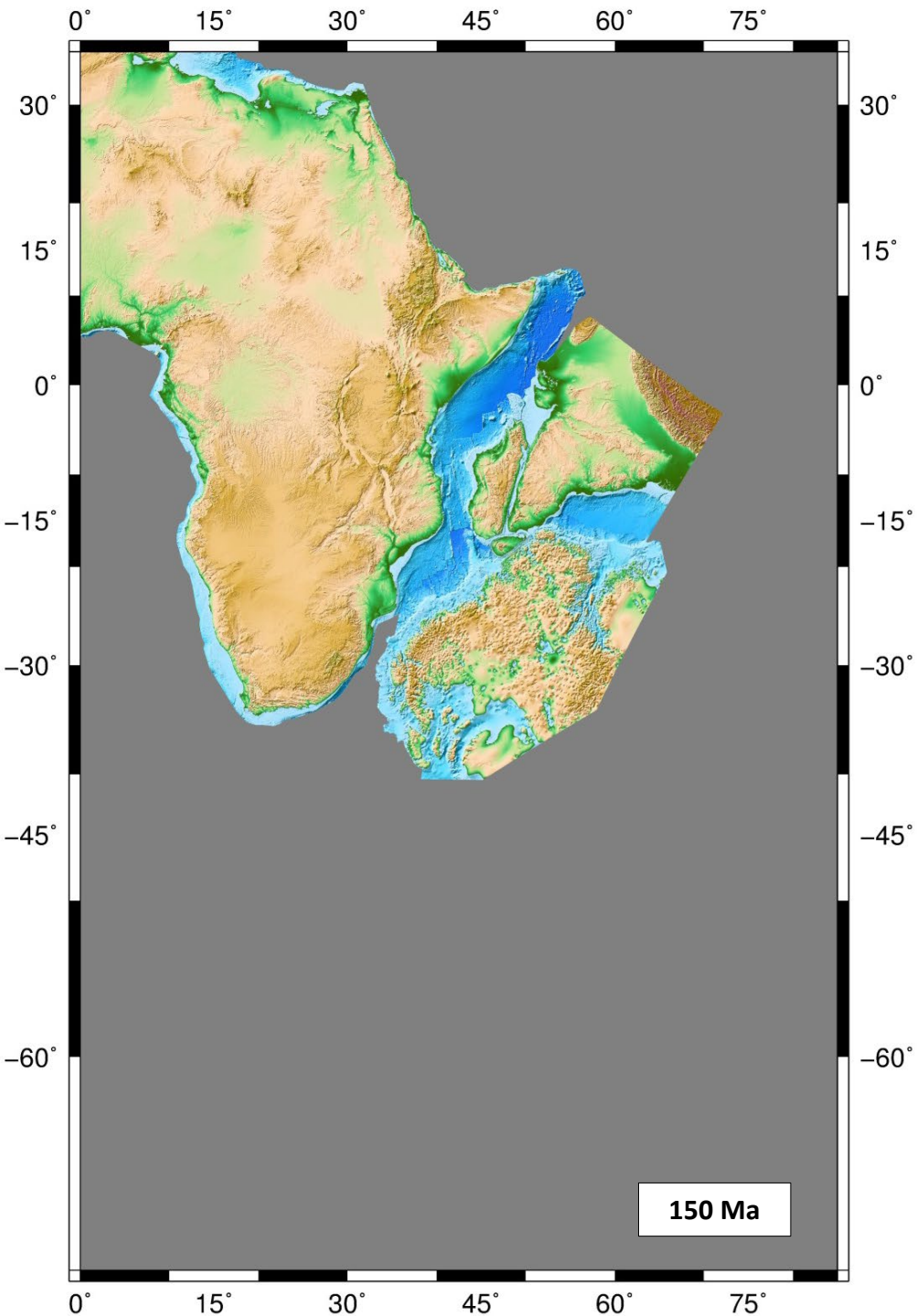
0˚
15˚
30˚
45˚
60˚
75˚
30˚
15˚
0˚
−15˚
−30˚
−45˚
−60˚
150 Ma

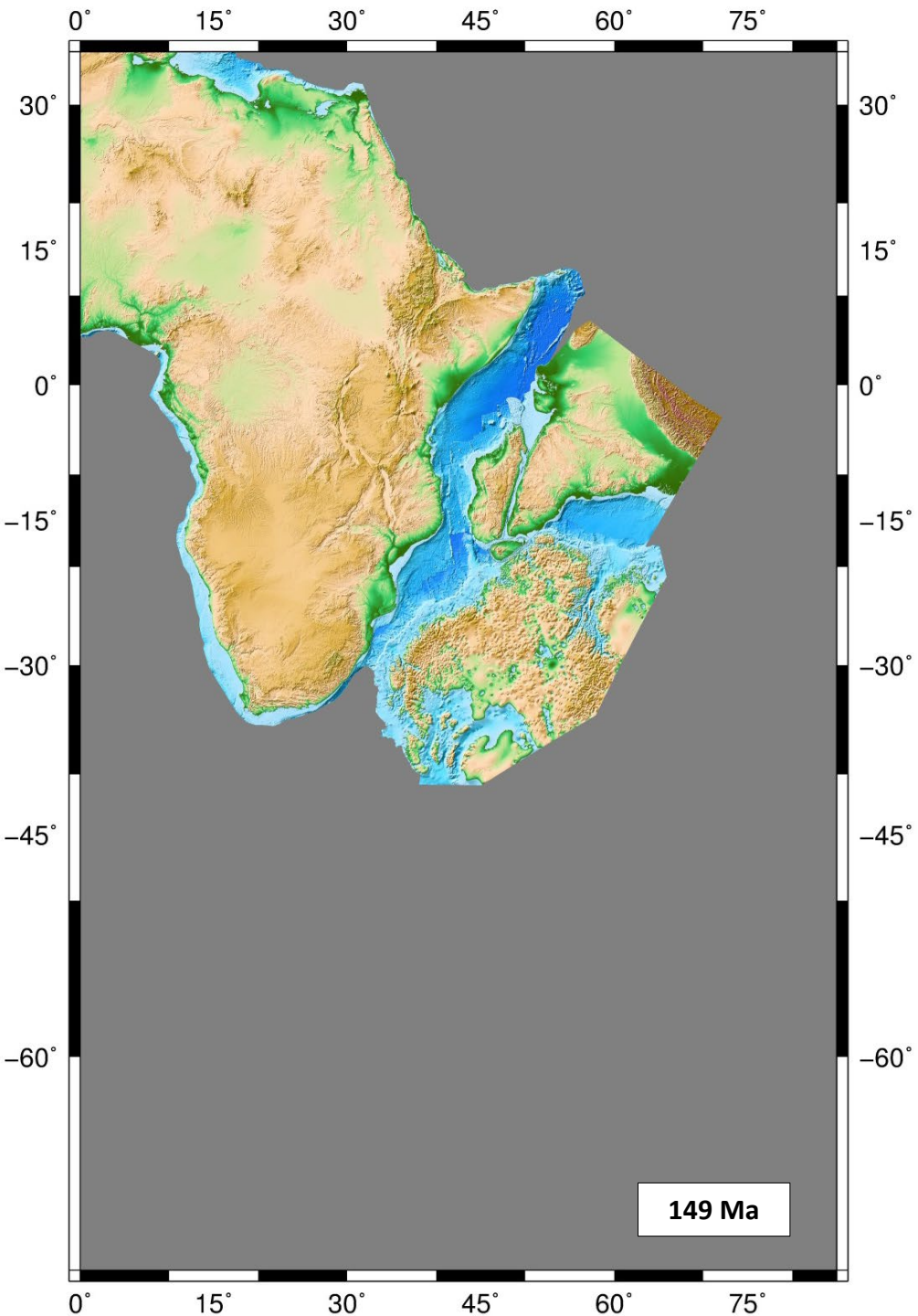
0˚
15˚
30˚
45˚
60˚
75˚
30˚
15˚
0˚
–15˚
–30˚
–45˚
–60˚
149 Ma

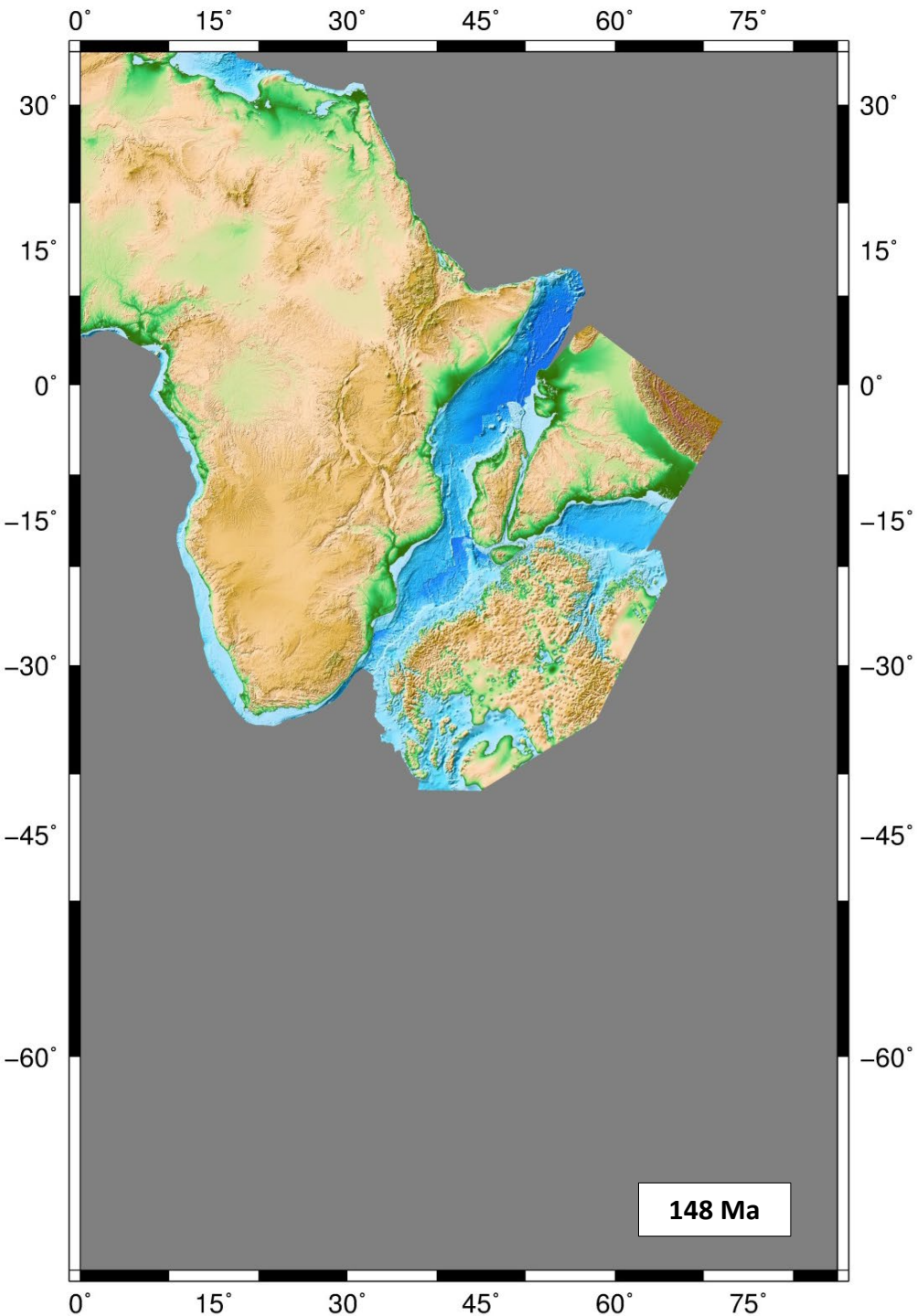
0˚
15˚
30˚
45˚
60˚
75˚
30˚
15˚
0˚
−15˚
−30˚
−45˚
−60˚
148 Ma

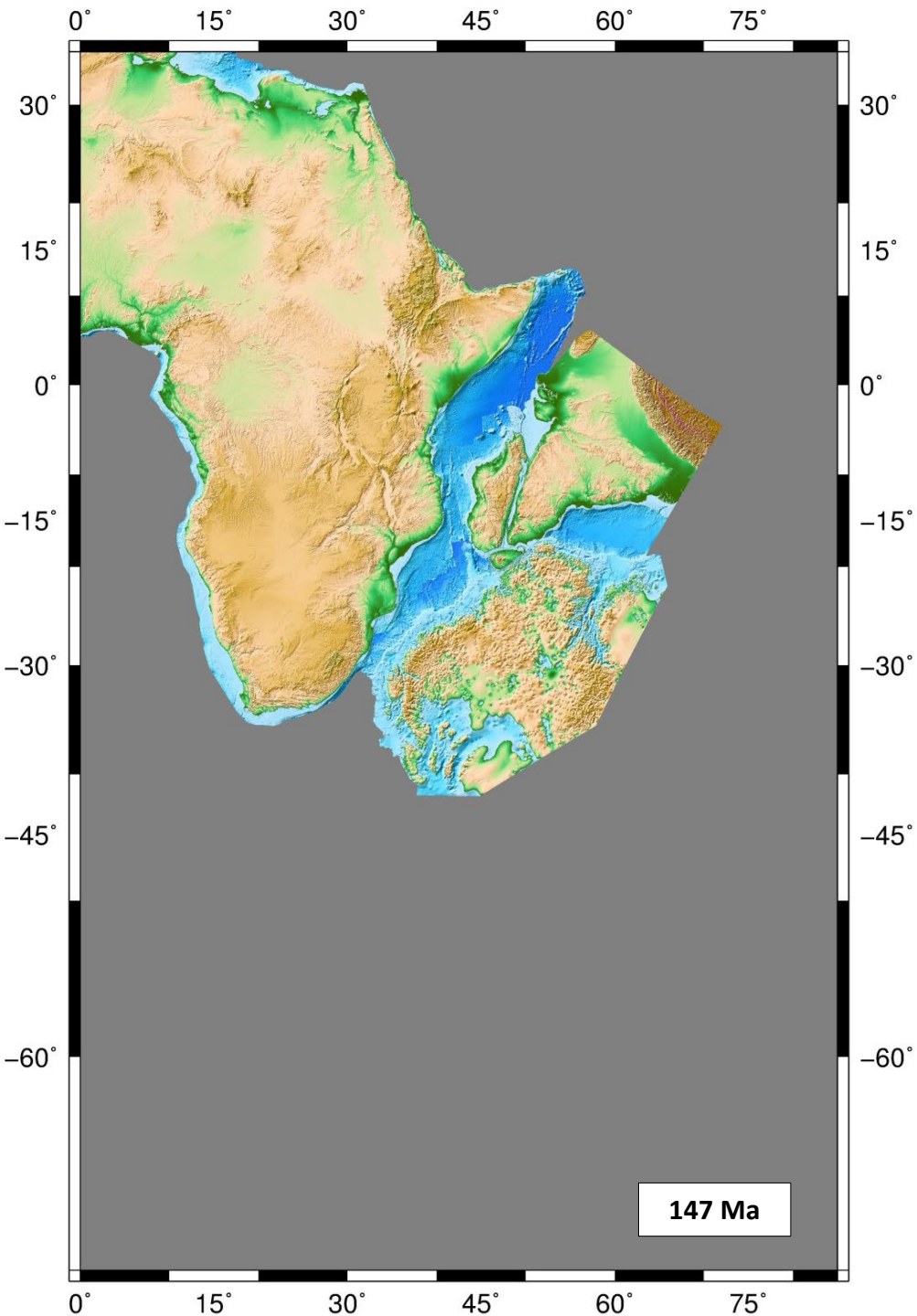
0˚
15˚
30˚
45˚
60˚
75˚
30˚
15˚
0˚
–15˚
–30˚
–45˚
–60˚
147 Ma

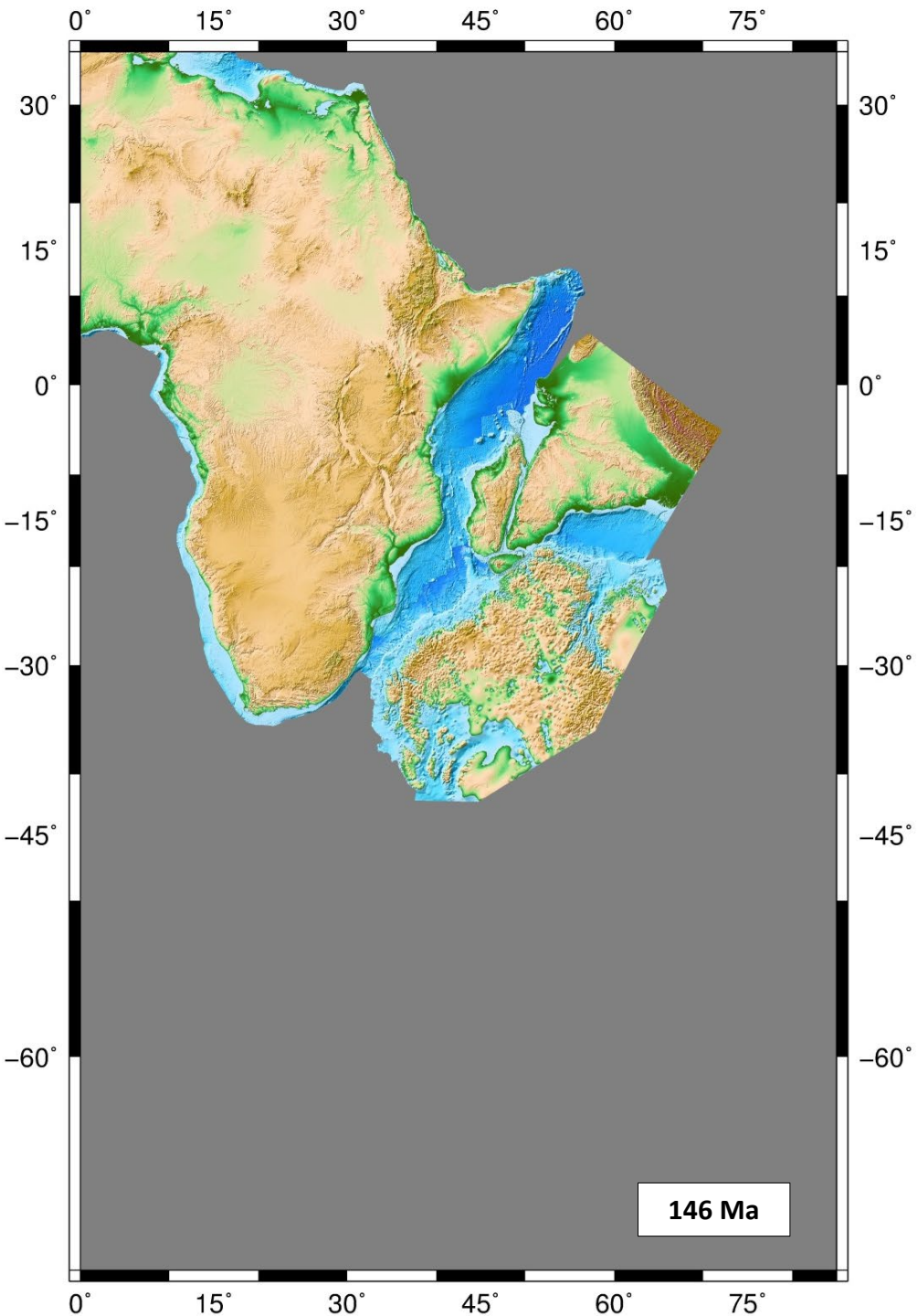
0˚
15˚
30˚
45˚
60˚
75˚
30˚
15˚
0˚
–15˚
–30˚
–45˚
–60˚
146 Ma

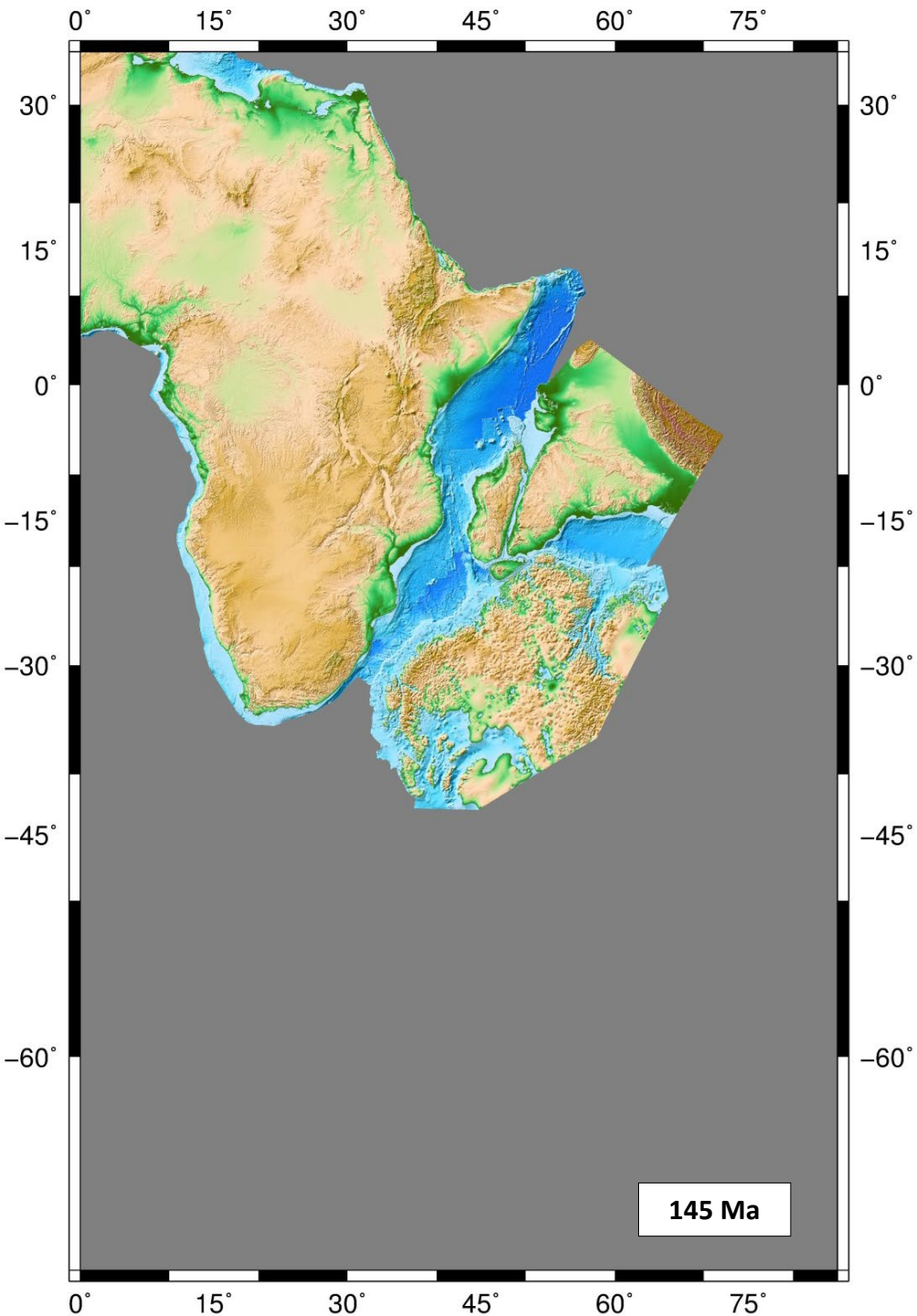
0˚
15˚
30˚
45˚
60˚
75˚
30˚
15˚
0˚
–15˚
–30˚
–45˚
–60˚
145 Ma

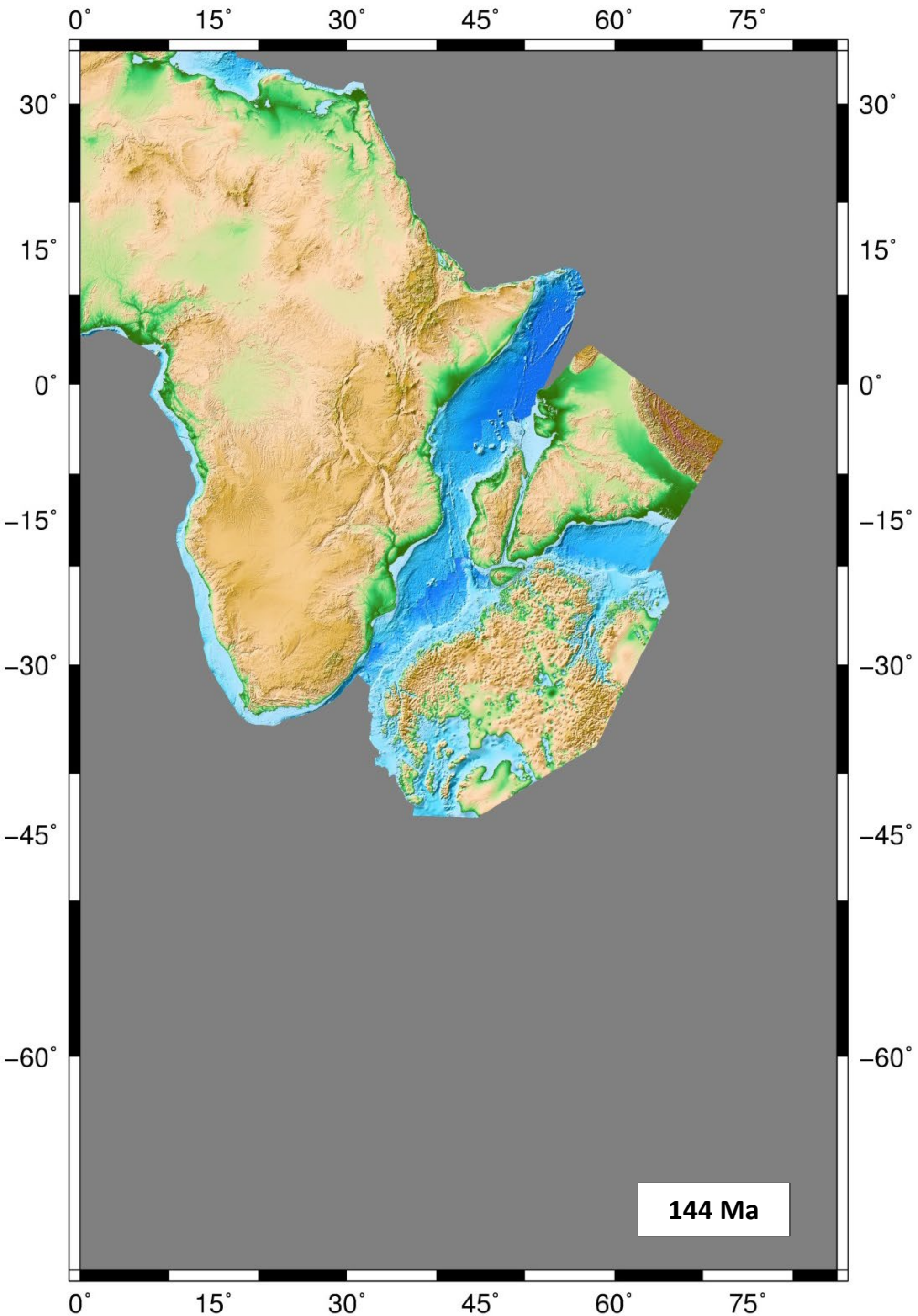
0°
15°
30°
45°
60°
75°
30°
15°
0°
−15°
−30°
−45°
−60°
144 Ma

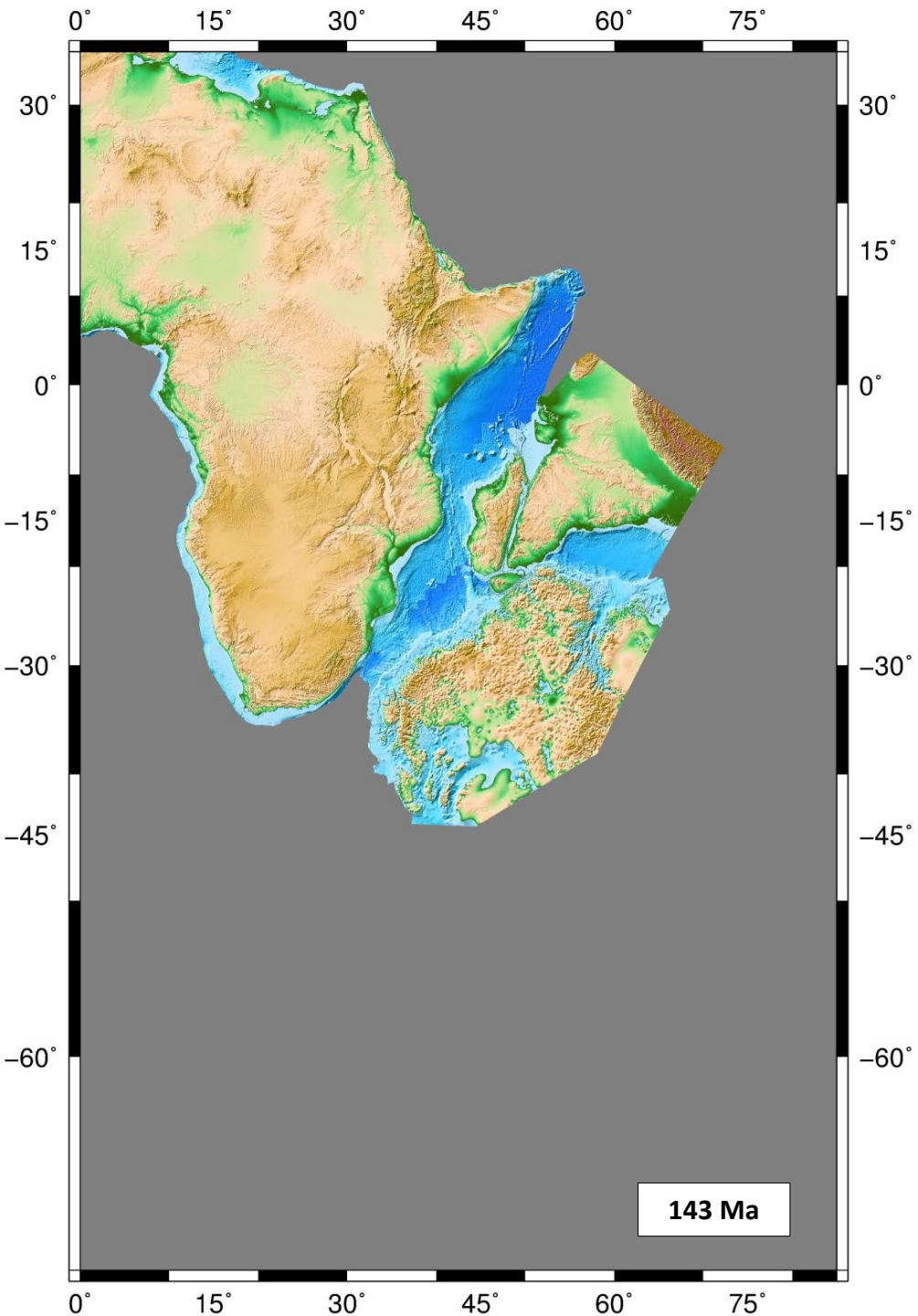
0°
15°
30°
45°
60°
75°
30°
15°
0°
−15°
−30°
−45°
−60°
143 Ma

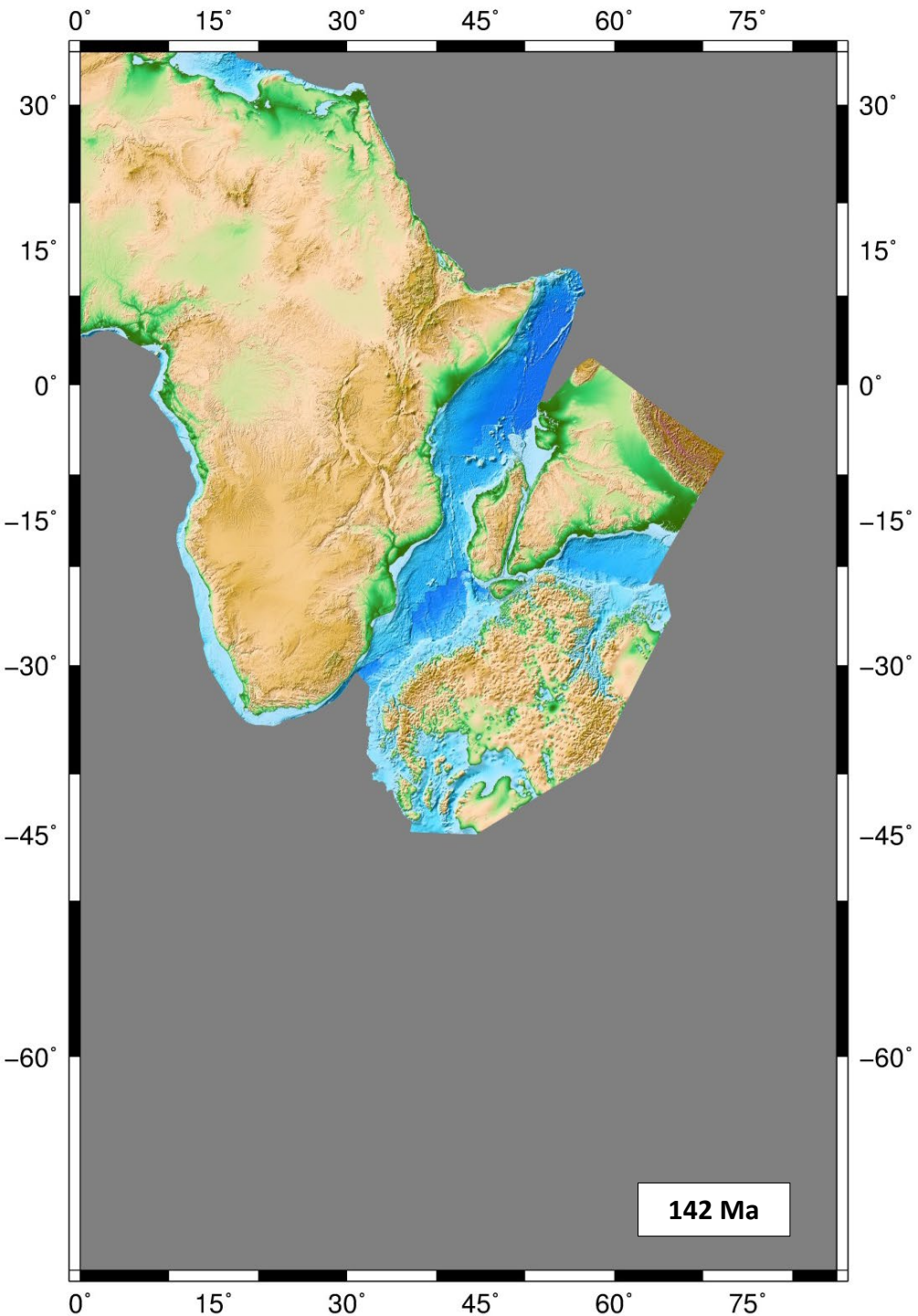
0˚
15˚
30˚
45˚
60˚
75˚
30˚
15˚
0˚
–15˚
–30˚
–45˚
–60˚
142 Ma

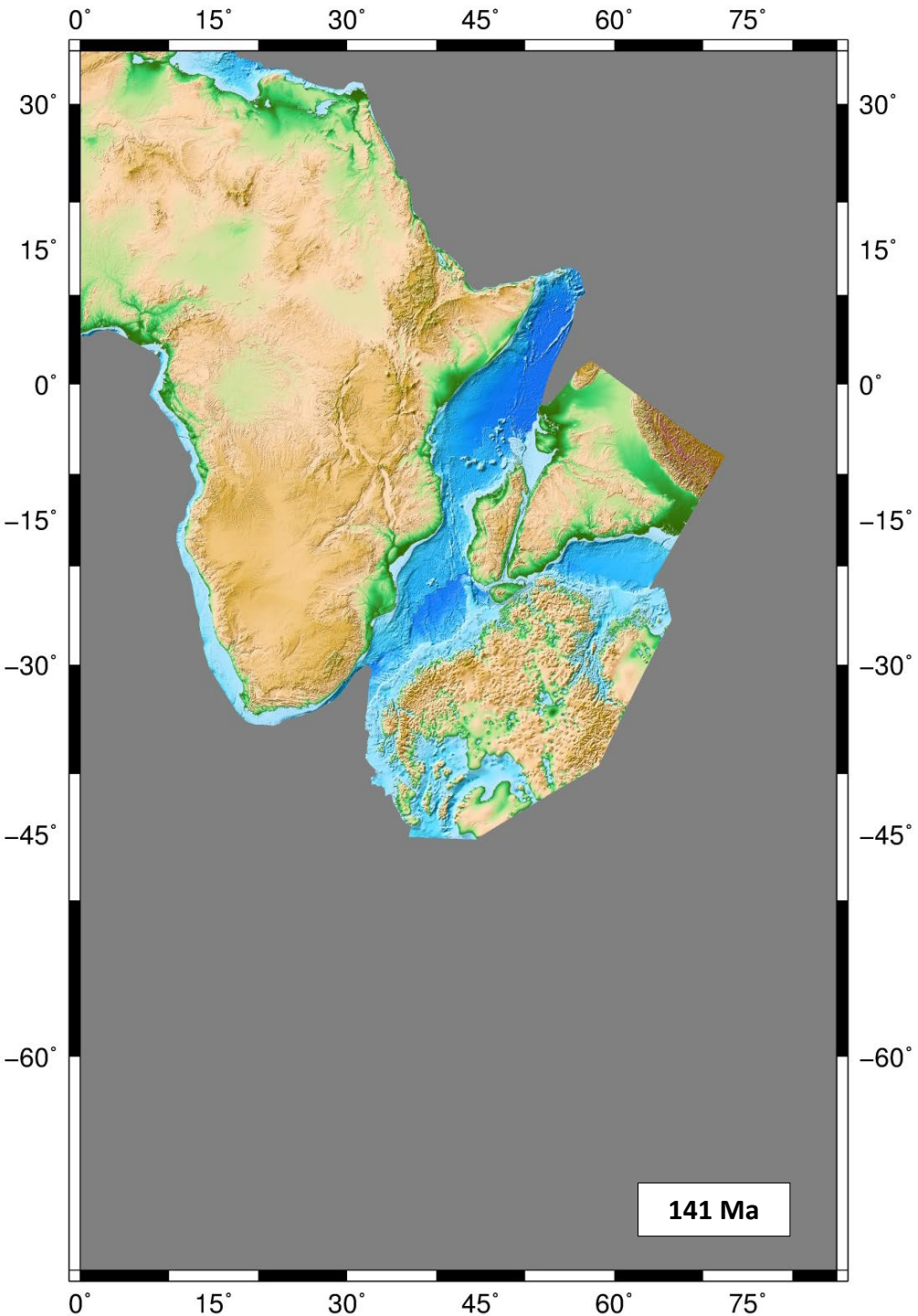
0°
15°
30°
45°
60°
75°
30°
15°
0°
−15°
−30°
−45°
−60°
141 Ma

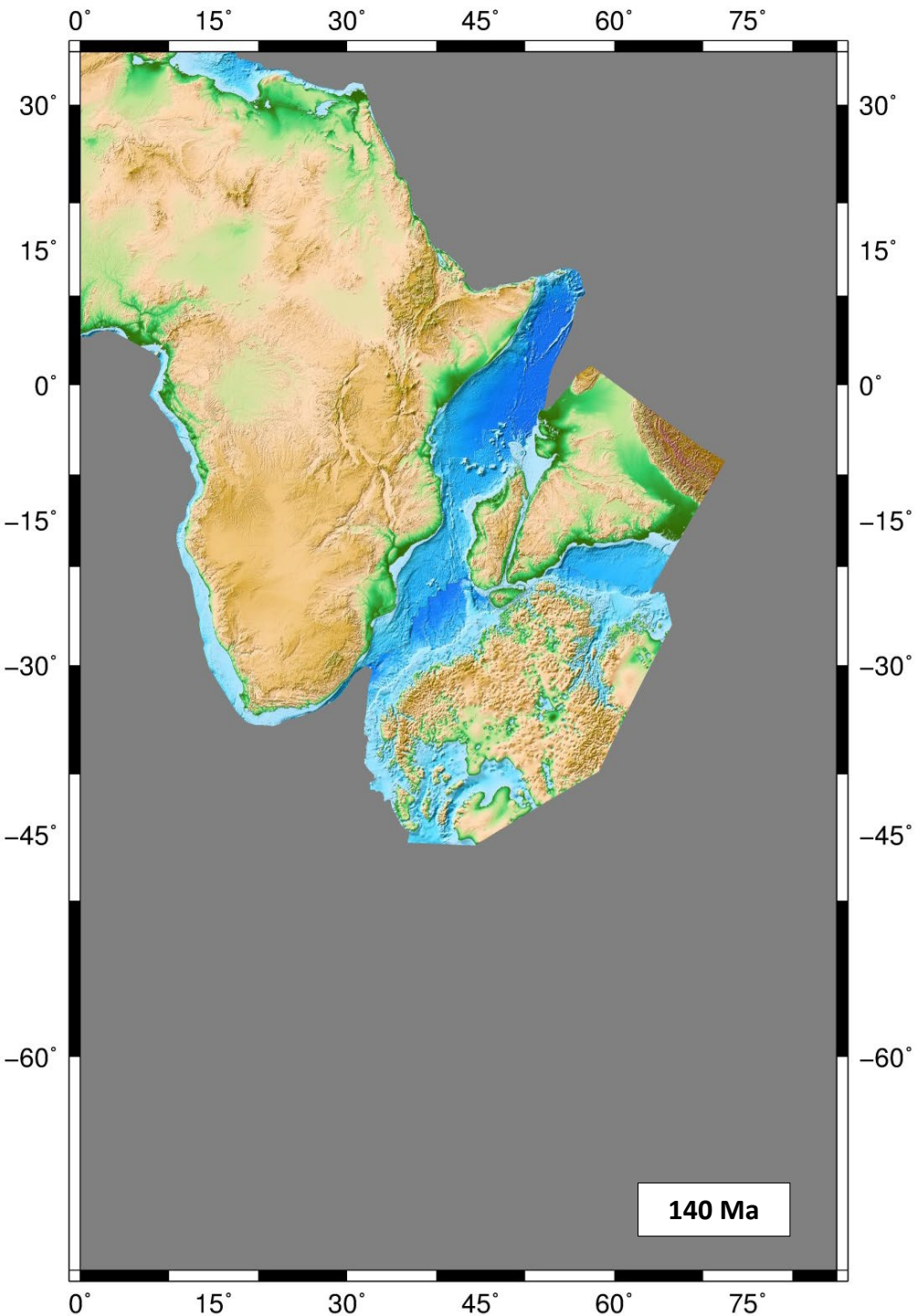
0°
15°
30°
45°
60°
75°
30°
15°
0°
−15°
−30°
−45°
−60°
140 Ma

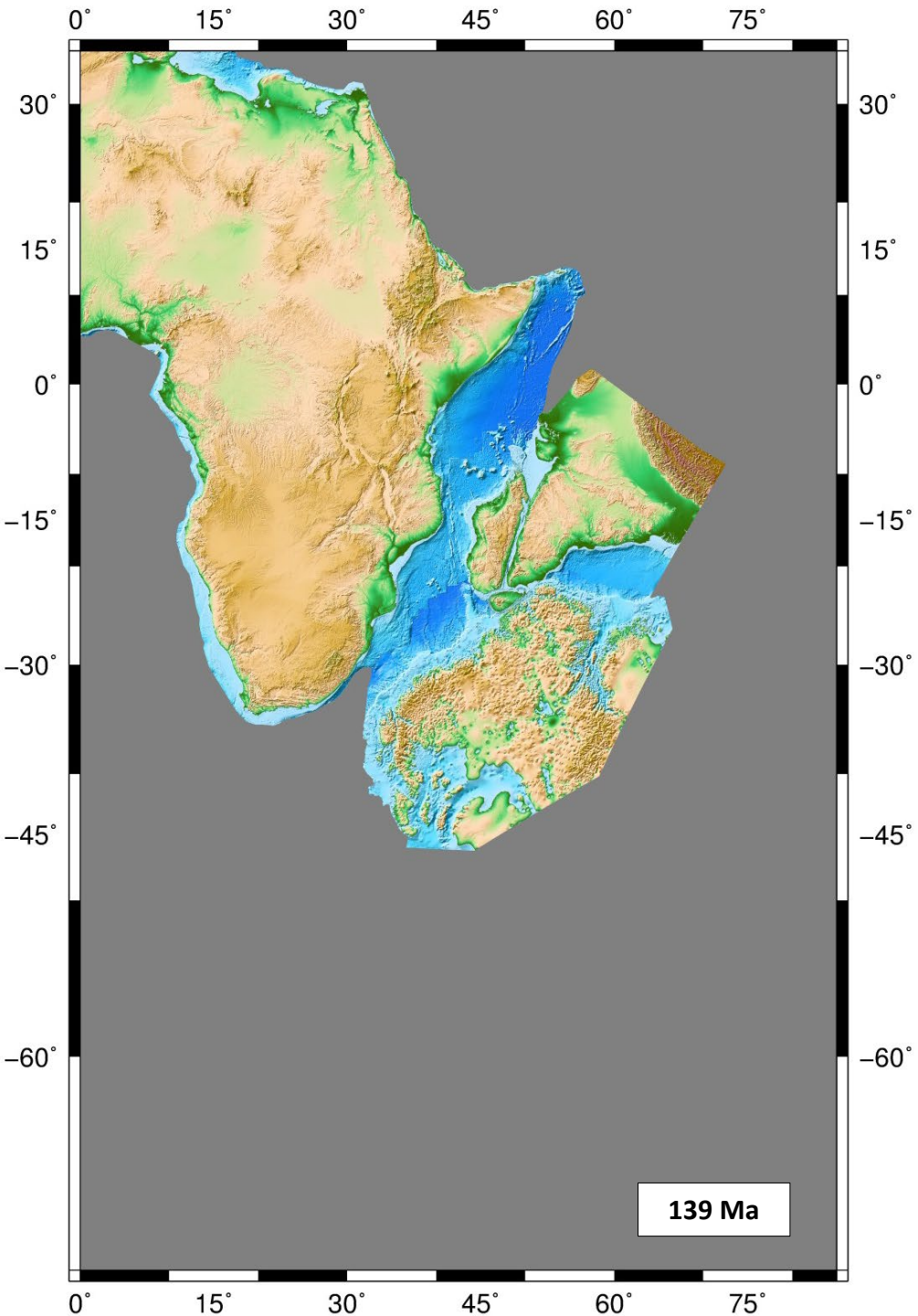
0°
15°
30°
45°
60°
75°
30°
15°
0°
−15°
−30°
−45°
−60°
139 Ma

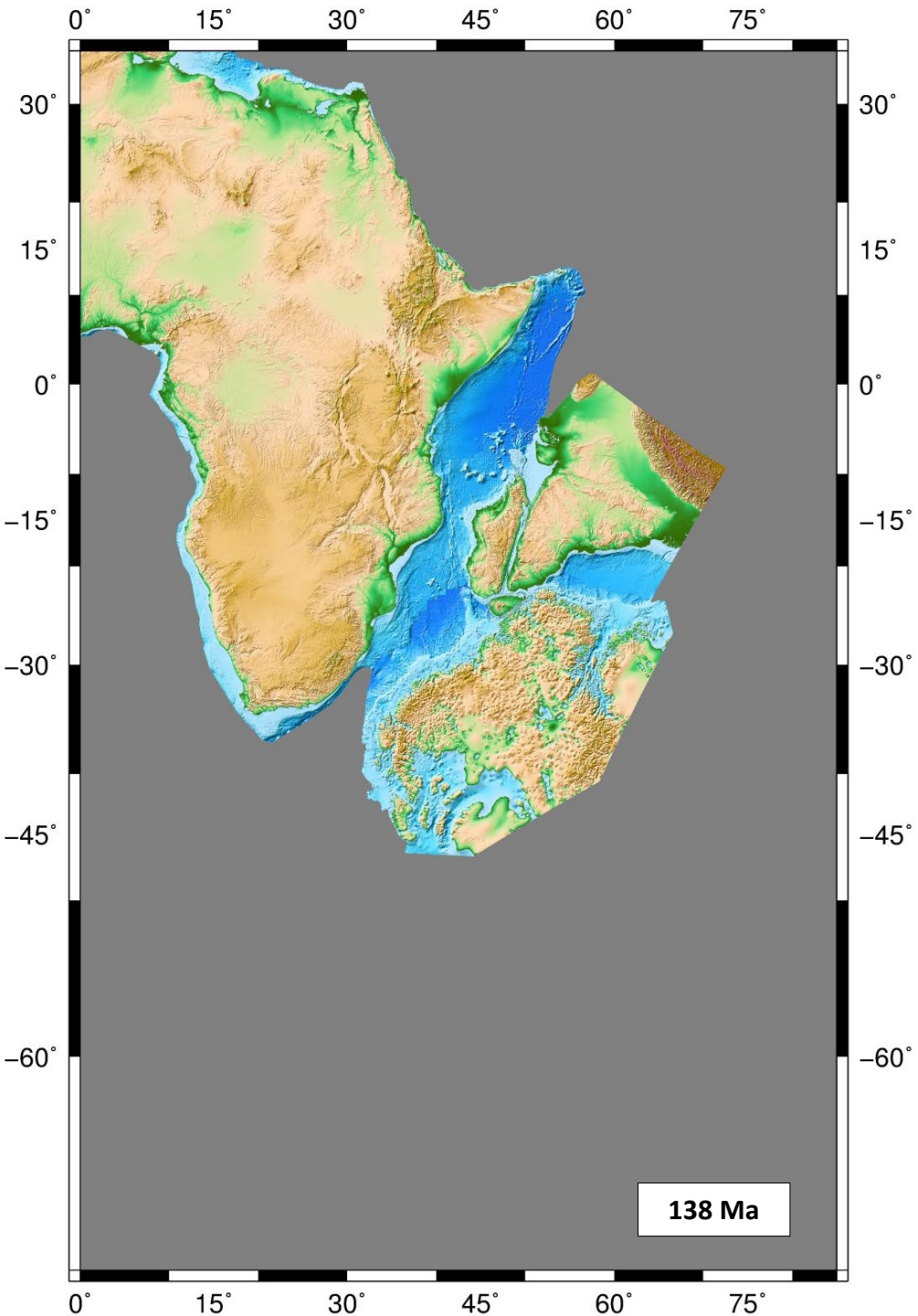
0°
15°
30°
45°
60°
75°
30°
15°
0°
−15°
−30°
−45°
−60°
138 Ma

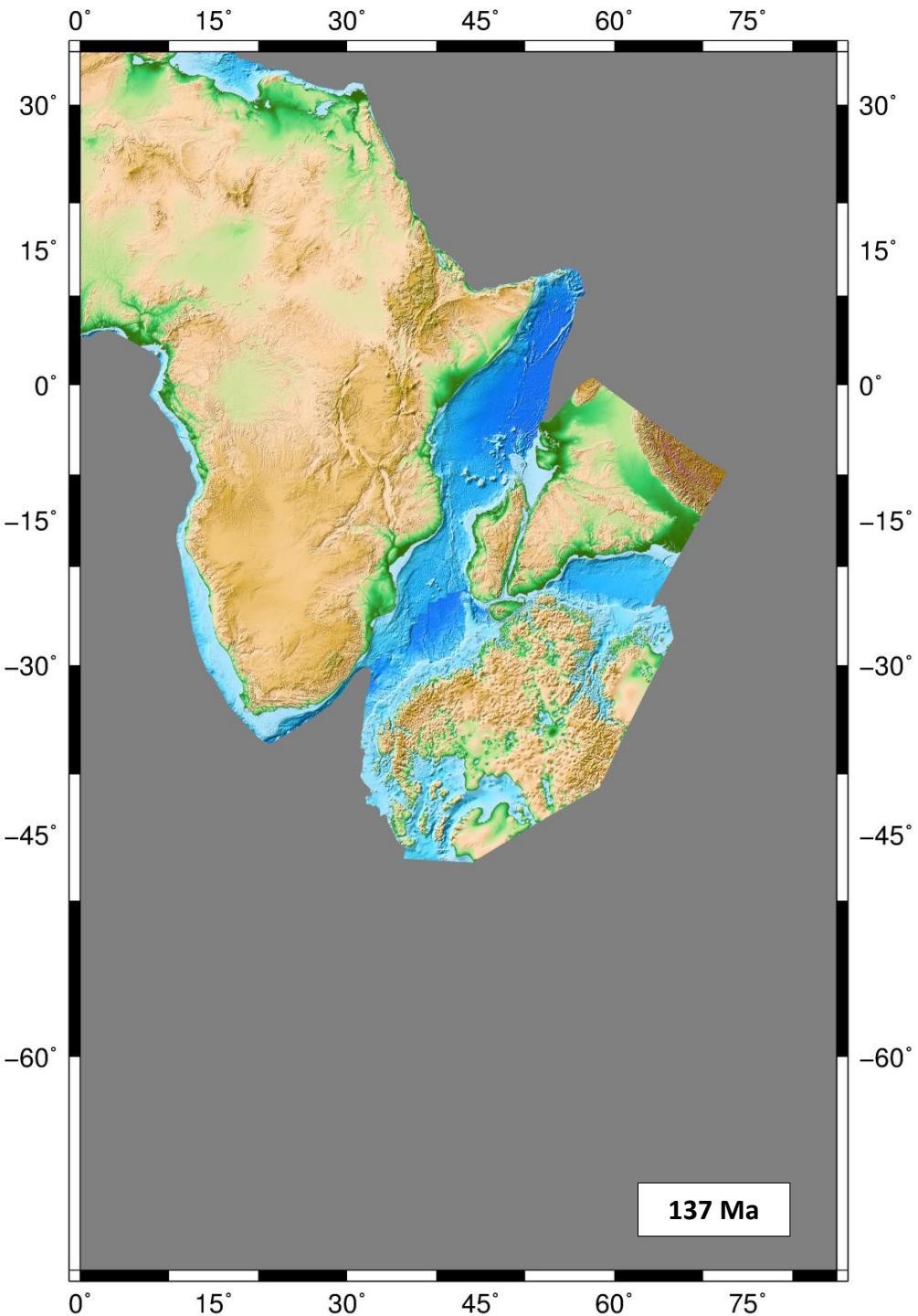
0˚
15˚
30˚
45˚
60˚
75˚
30˚
15˚
0˚
–15˚
–30˚
–45˚
–60˚
137 Ma

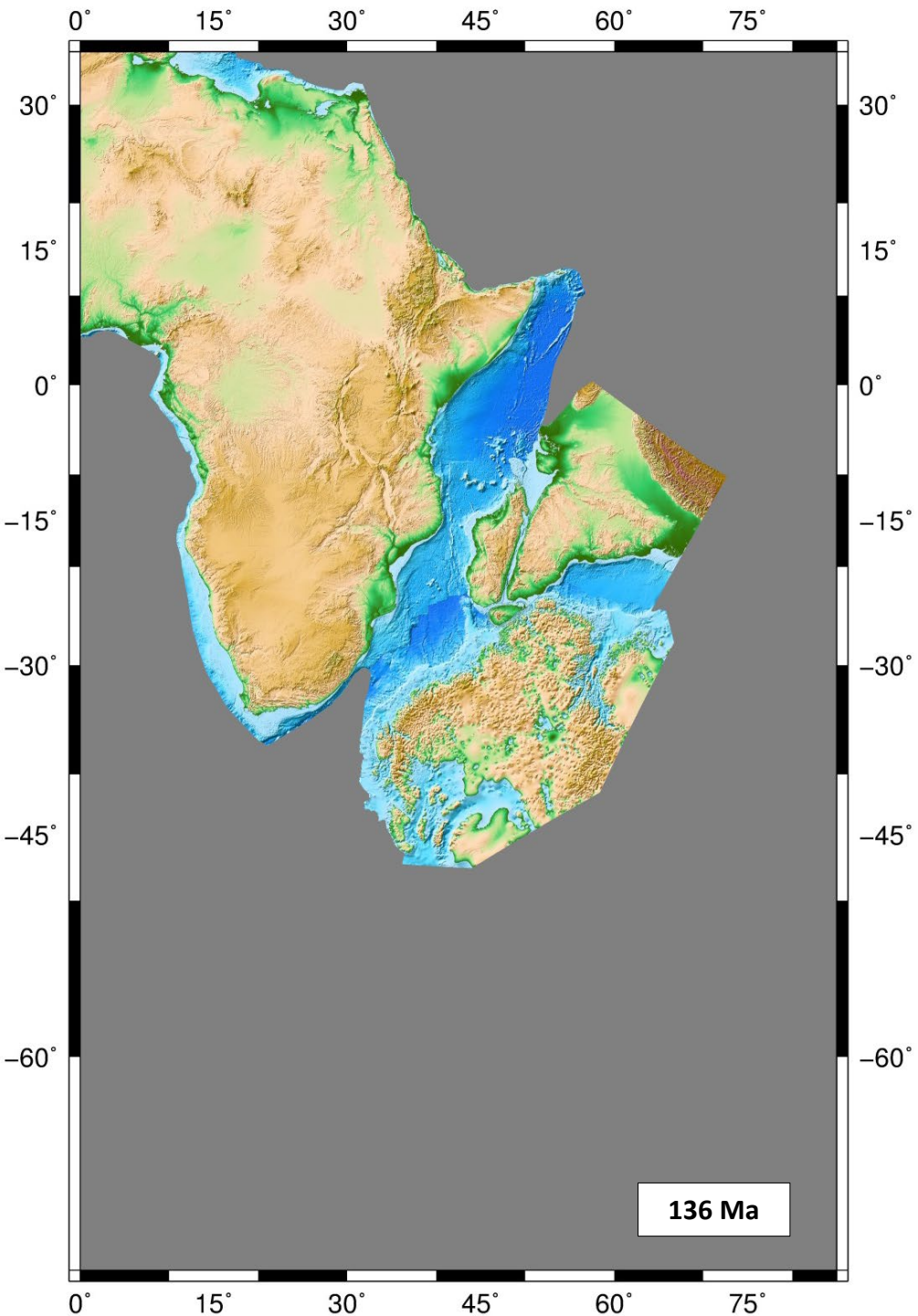
0°
15°
30°
45°
60°
75°
30°
15°
0°
−15°
−30°
−45°
−60°
136 Ma

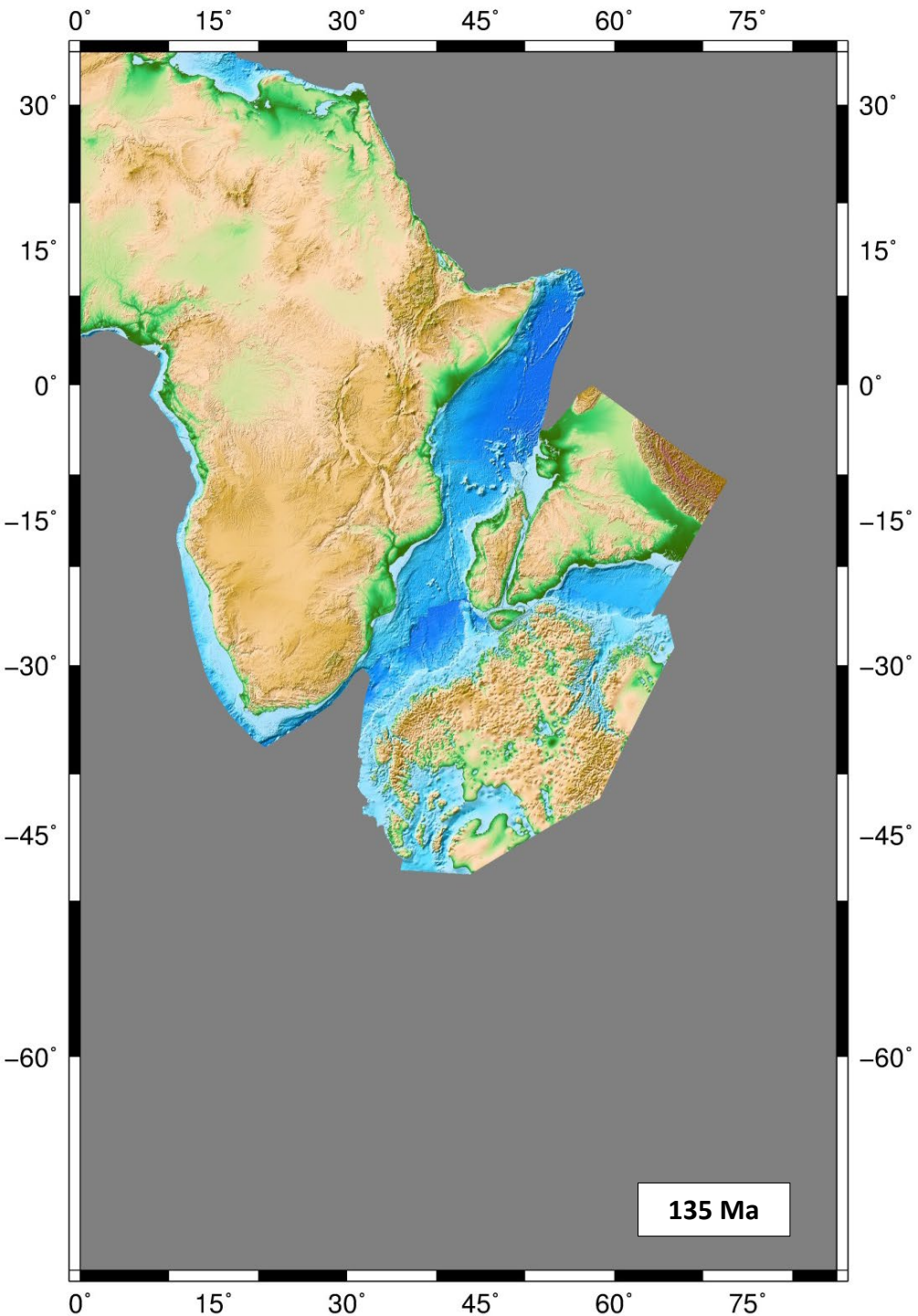
0°
15°
30°
45°
60°
75°
30°
15°
0°
−15°
−30°
−45°
−60°
135 Ma

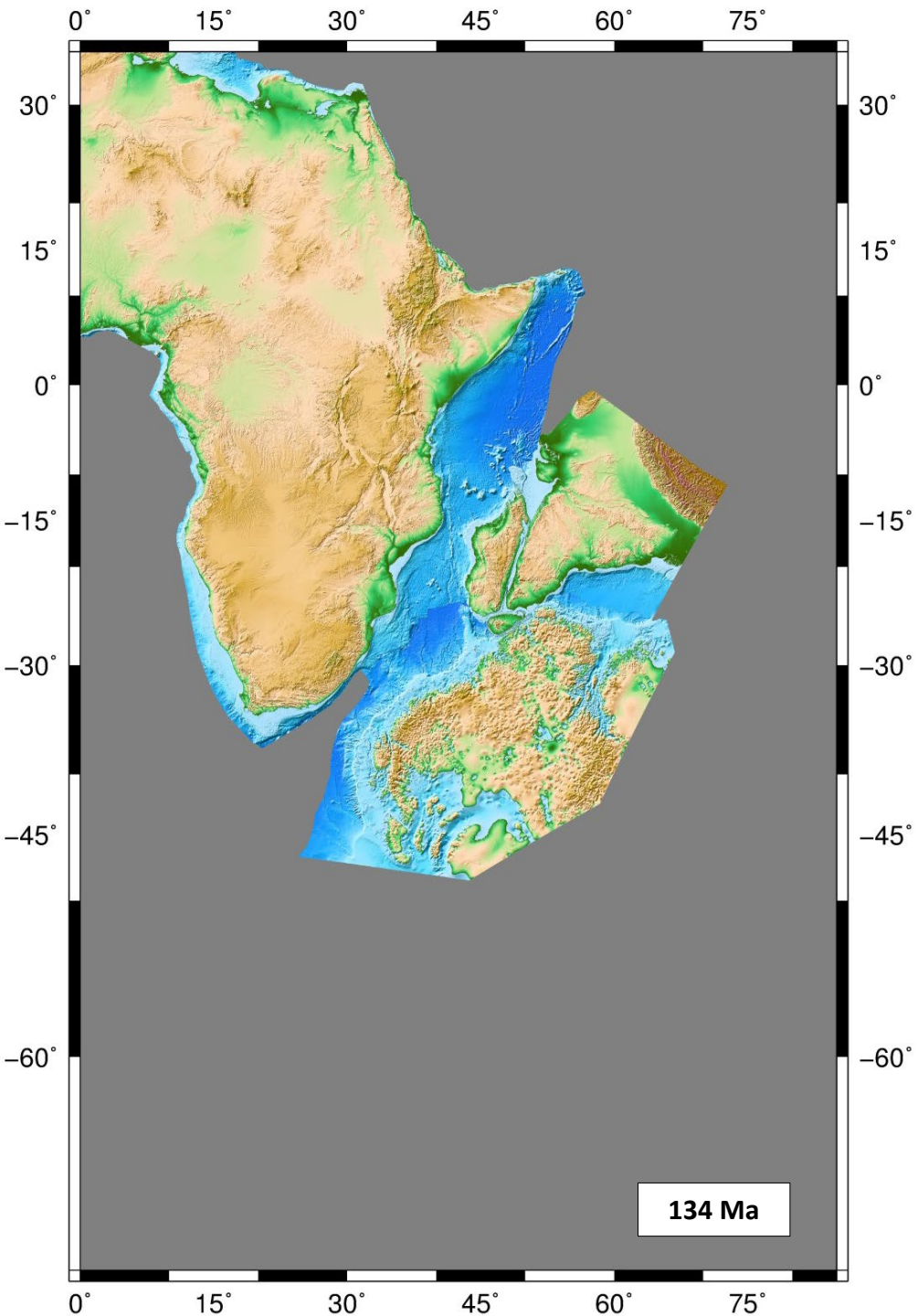
0°
15°
30°
45°
60°
75°
30°
15°
0°
−15°
−30°
−45°
−60°
134 Ma

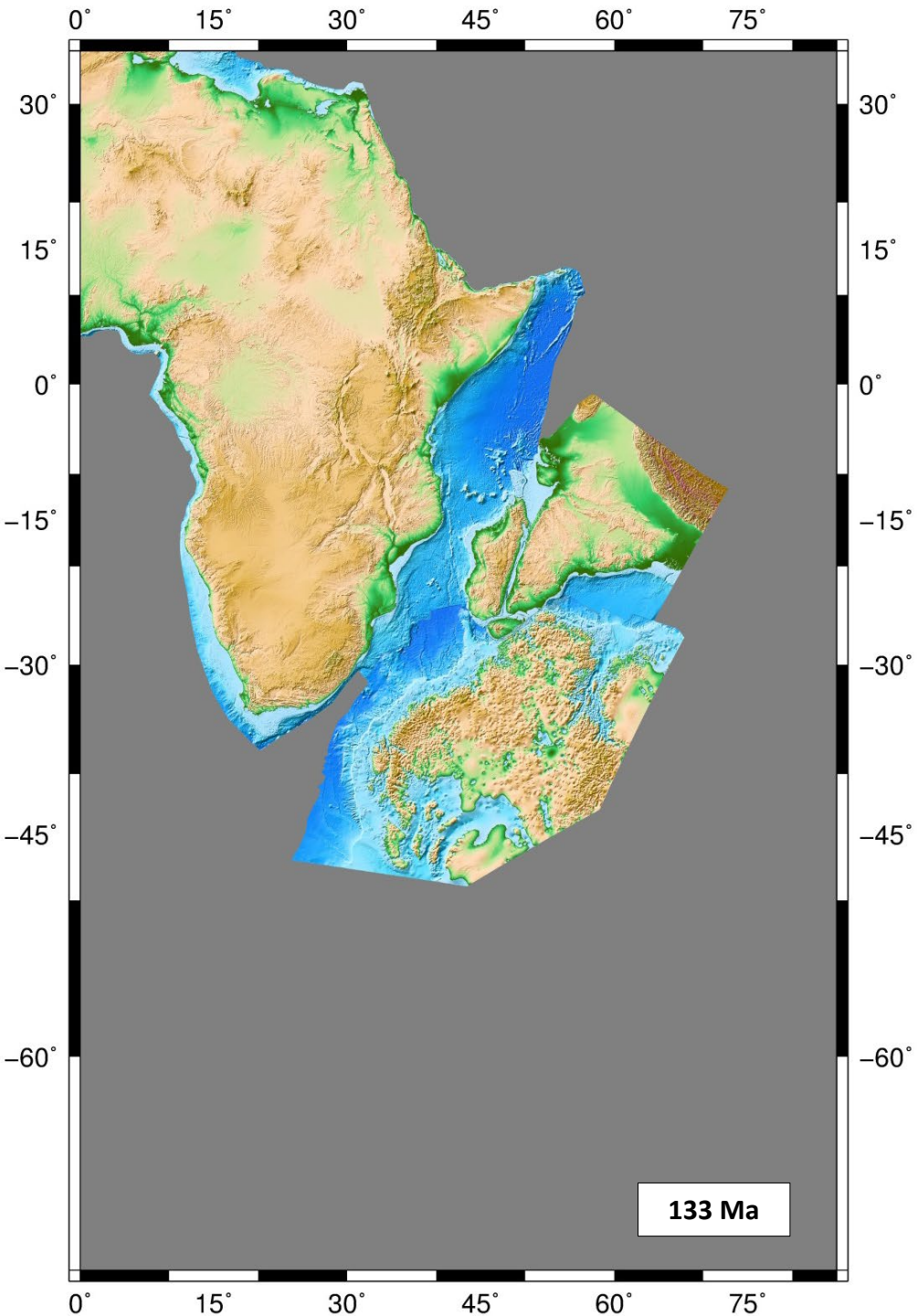
0˚
15˚
30˚
45˚
60˚
75˚
30˚
15˚
0˚
–15˚
–30˚
–45˚
–60˚
133 Ma

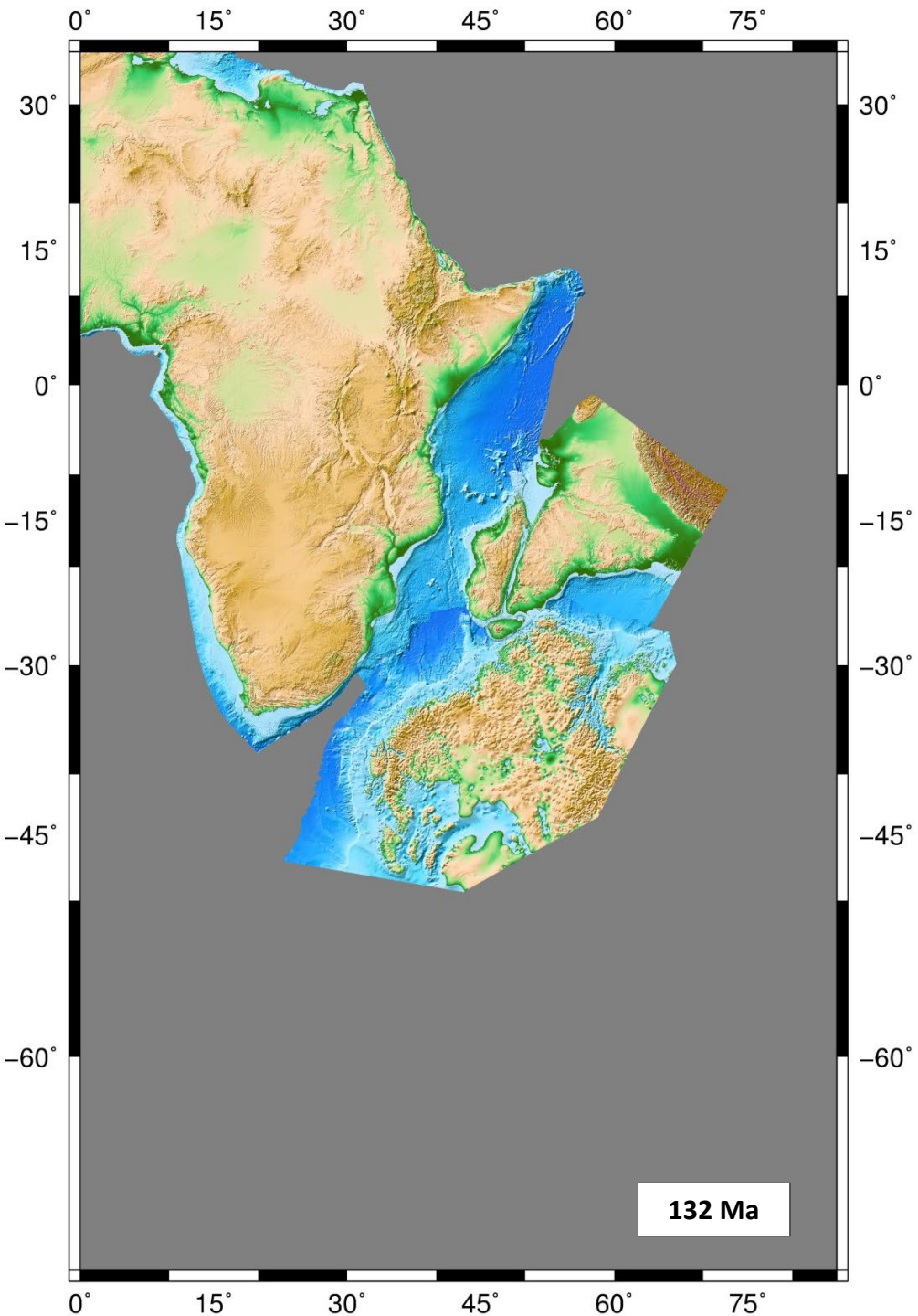
0°
15°
30°
45°
60°
75°
30°
15°
0°
−15°
−30°
−45°
−60°
132 Ma

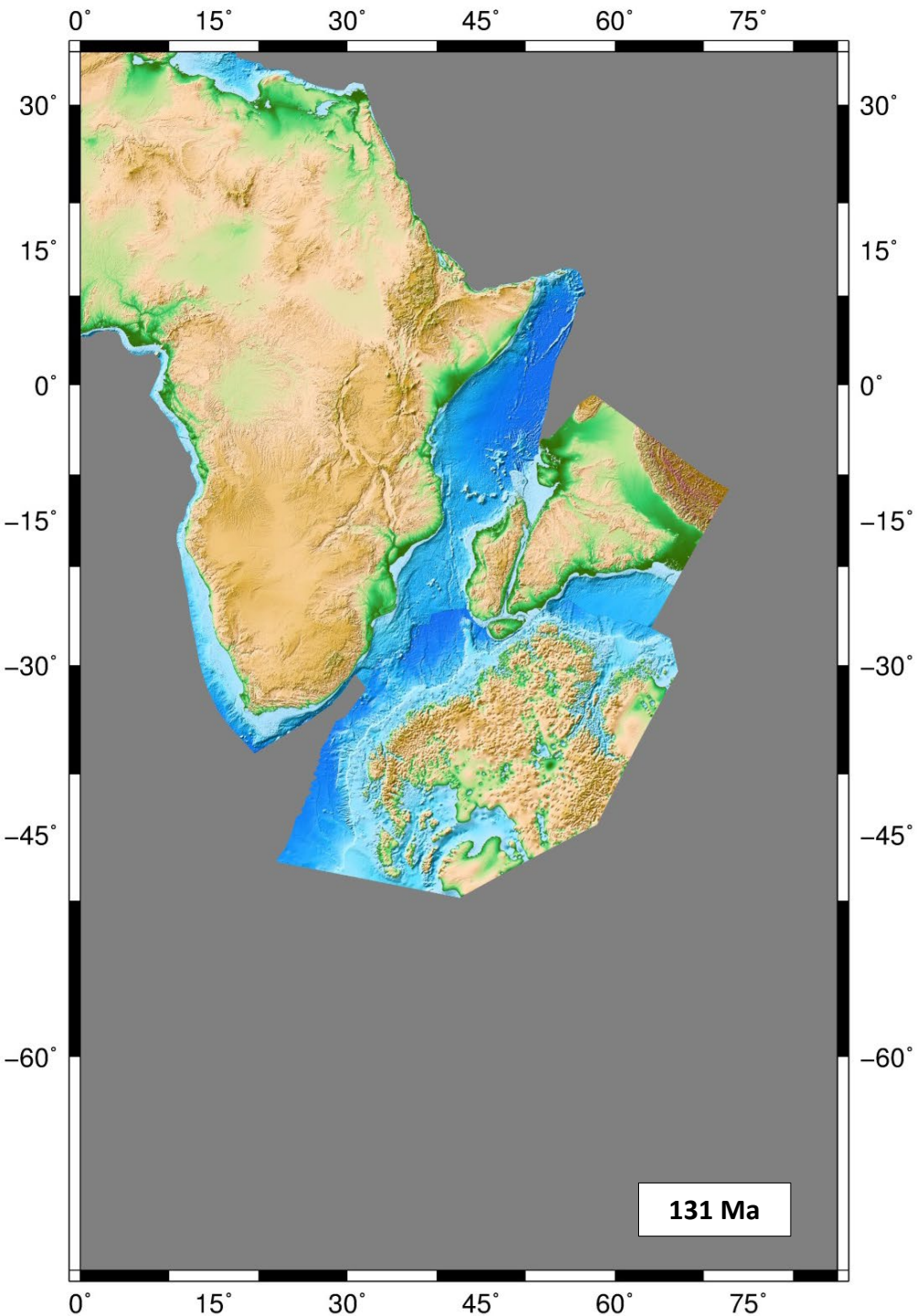
0°
15°
30°
45°
60°
75°
30°
15°
0°
−15°
−30°
−45°
−60°
131 Ma

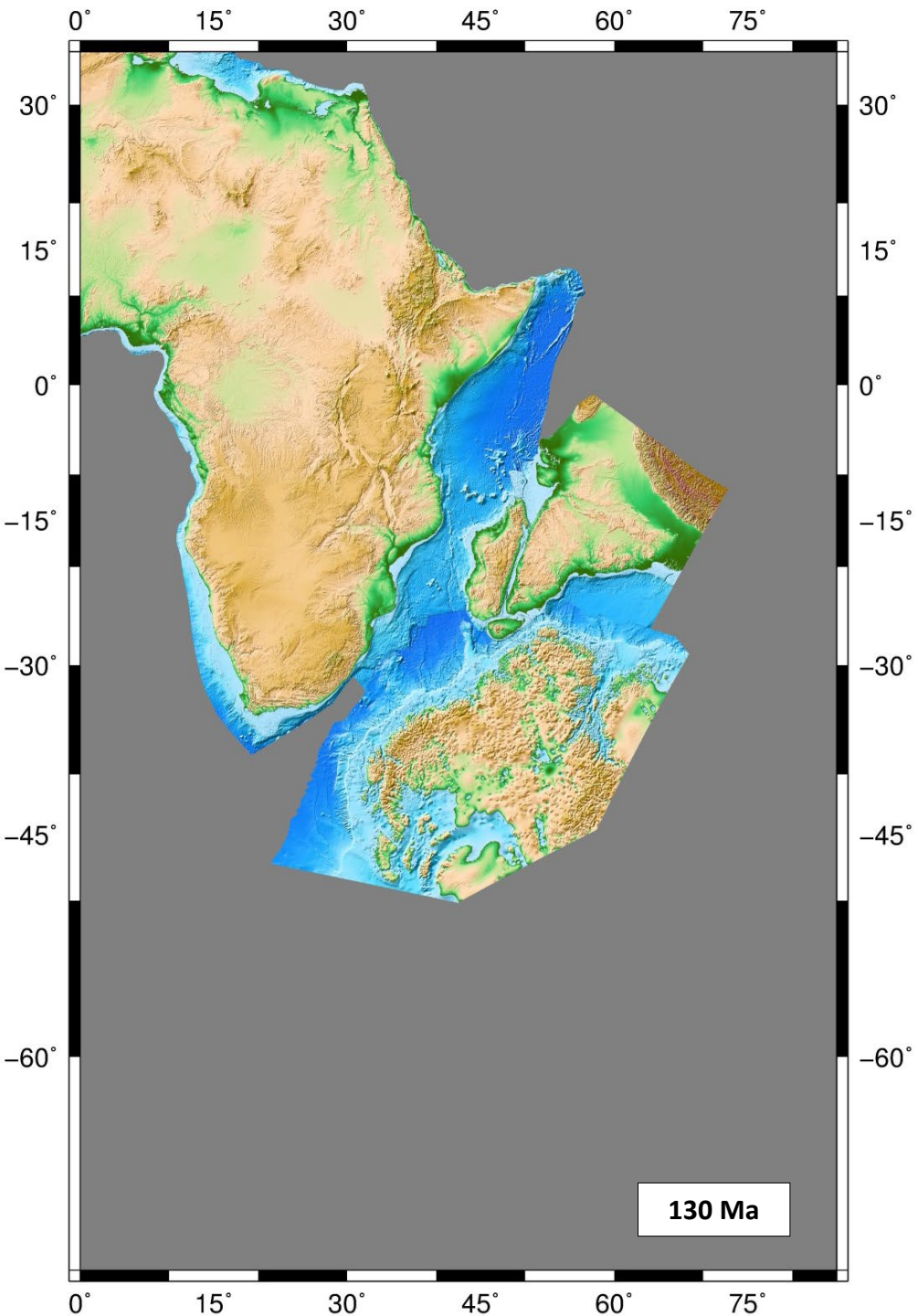
0˚
15˚
30˚
45˚
60˚
75˚
30˚
15˚
0˚
–15˚
–30˚
–45˚
–60˚
130 Ma

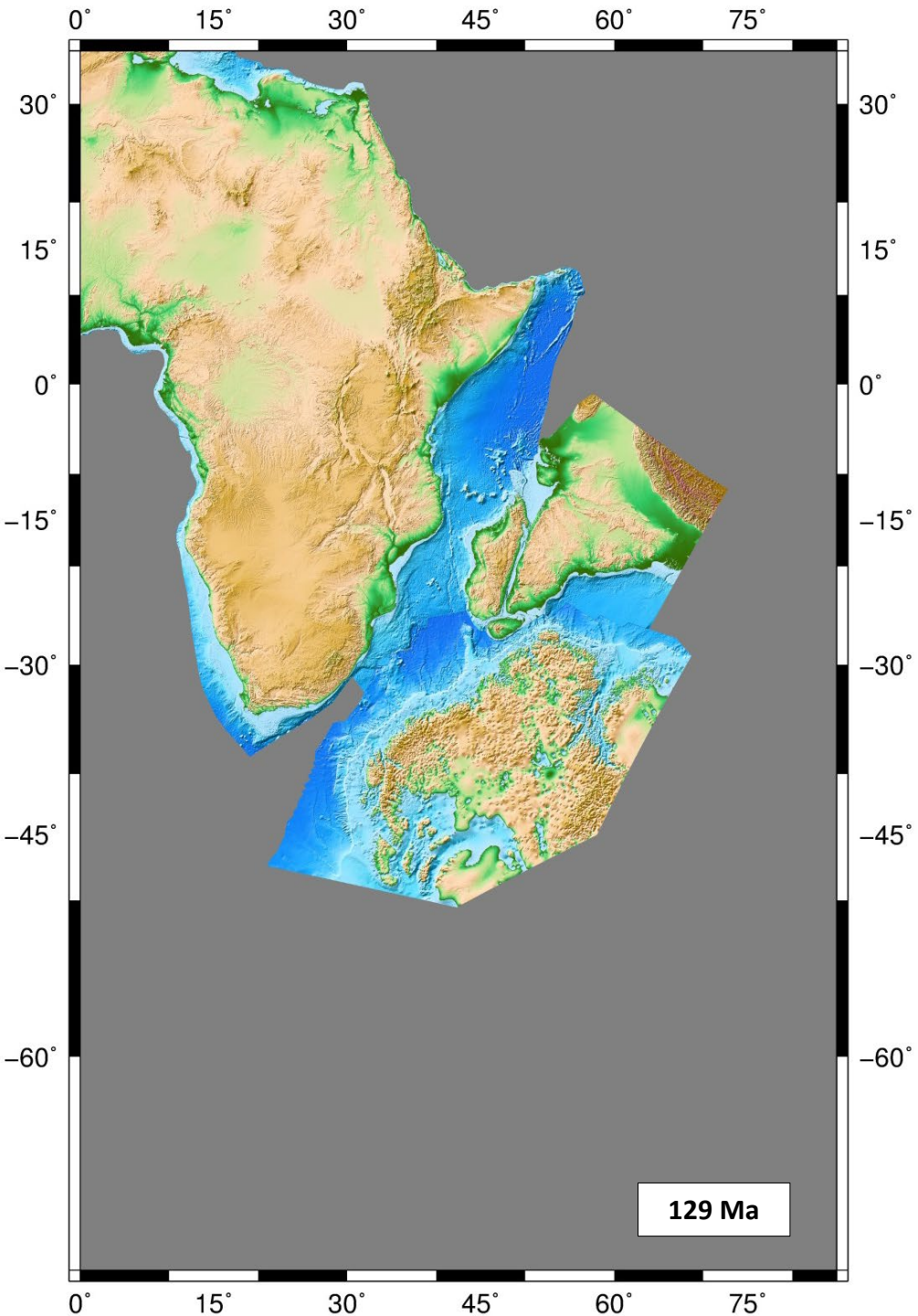
0˚
15˚
30˚
45˚
60˚
75˚
30˚
15˚
0˚
–15˚
–30˚
–45˚
–60˚
129 Ma

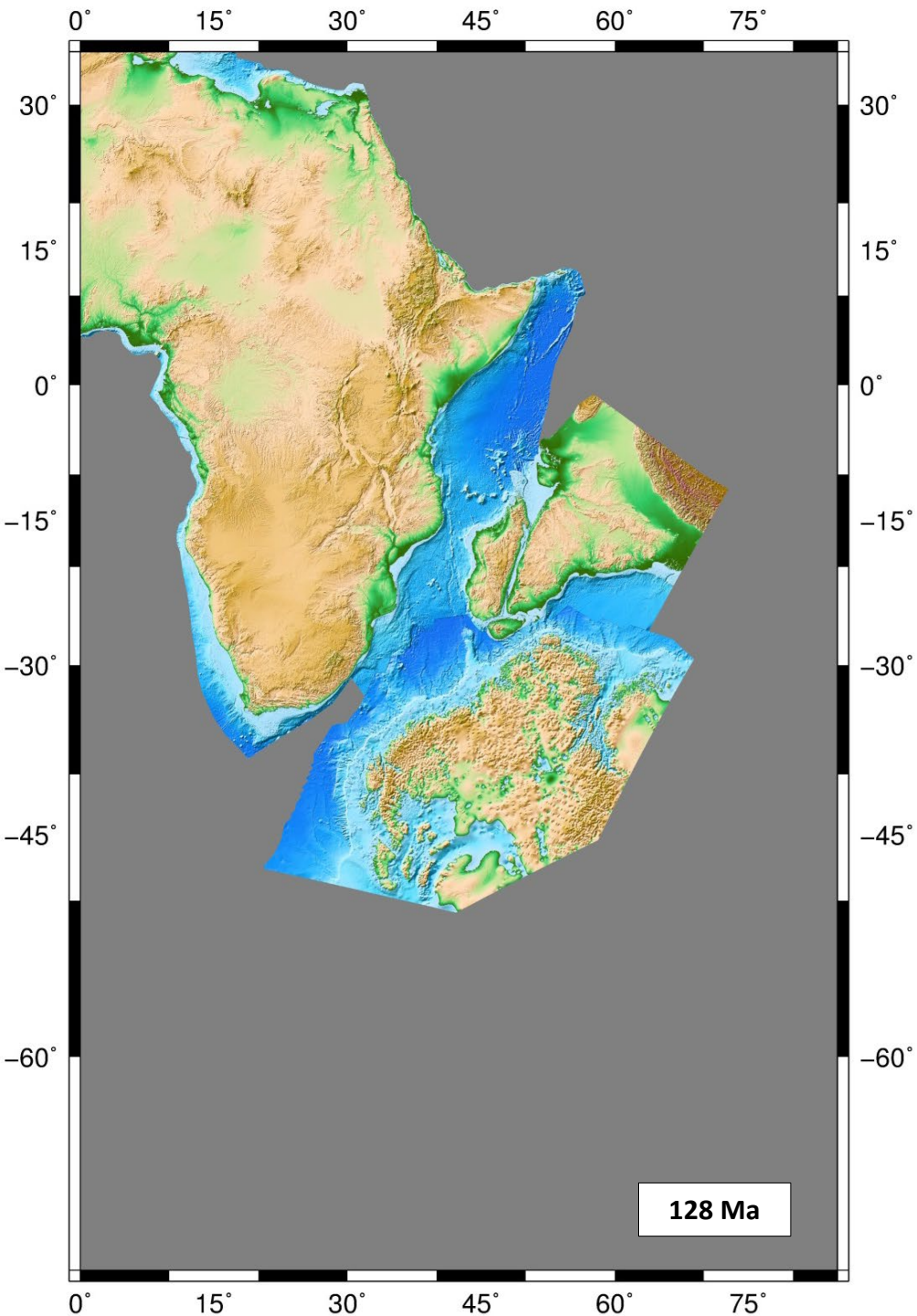
0°
15°
30°
45°
60°
75°
30°
15°
0°
−15°
−30°
−45°
−60°
128 Ma

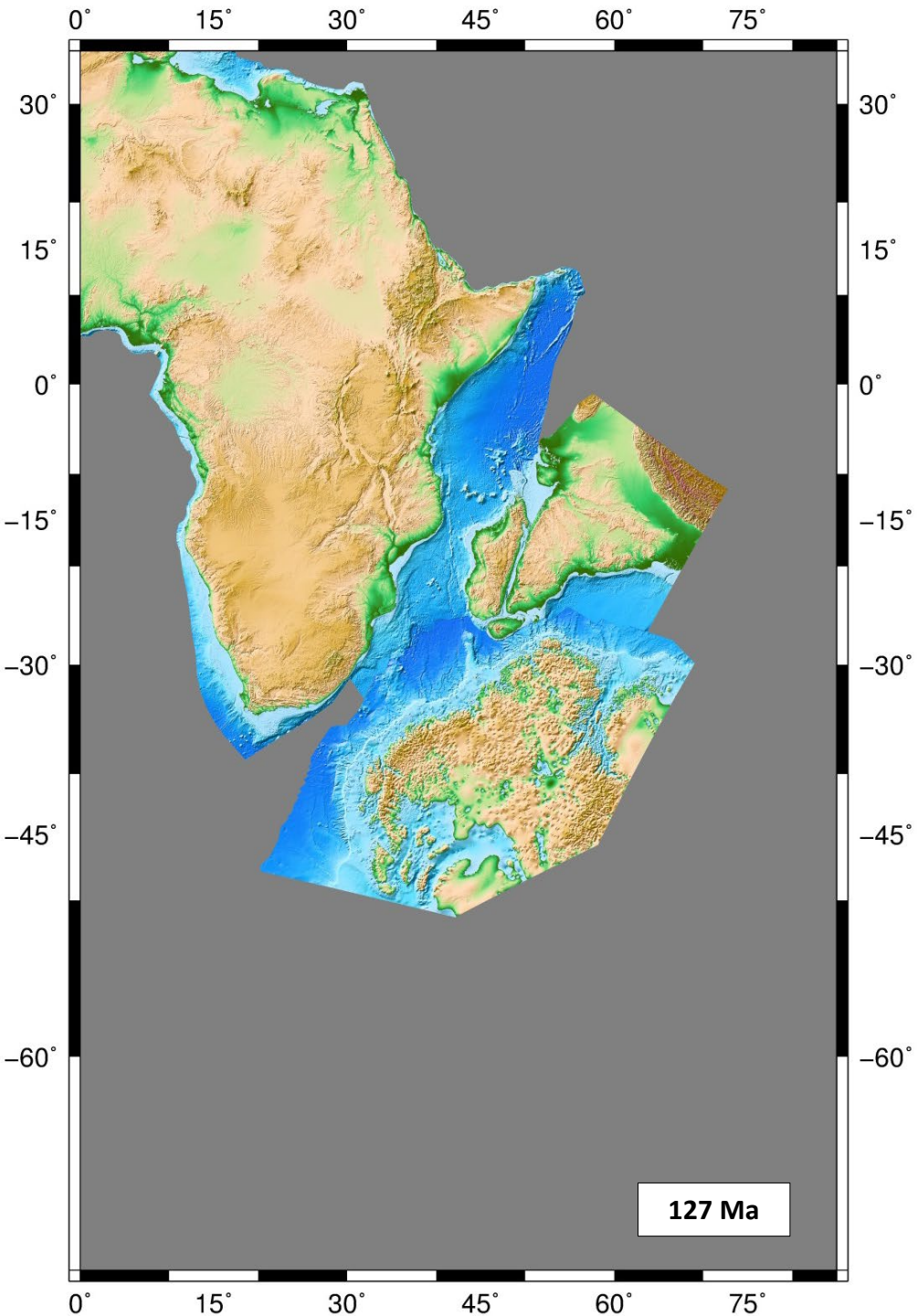
0°
15°
30°
45°
60°
75°
30°
15°
0°
−15°
−30°
−45°
−60°
127 Ma

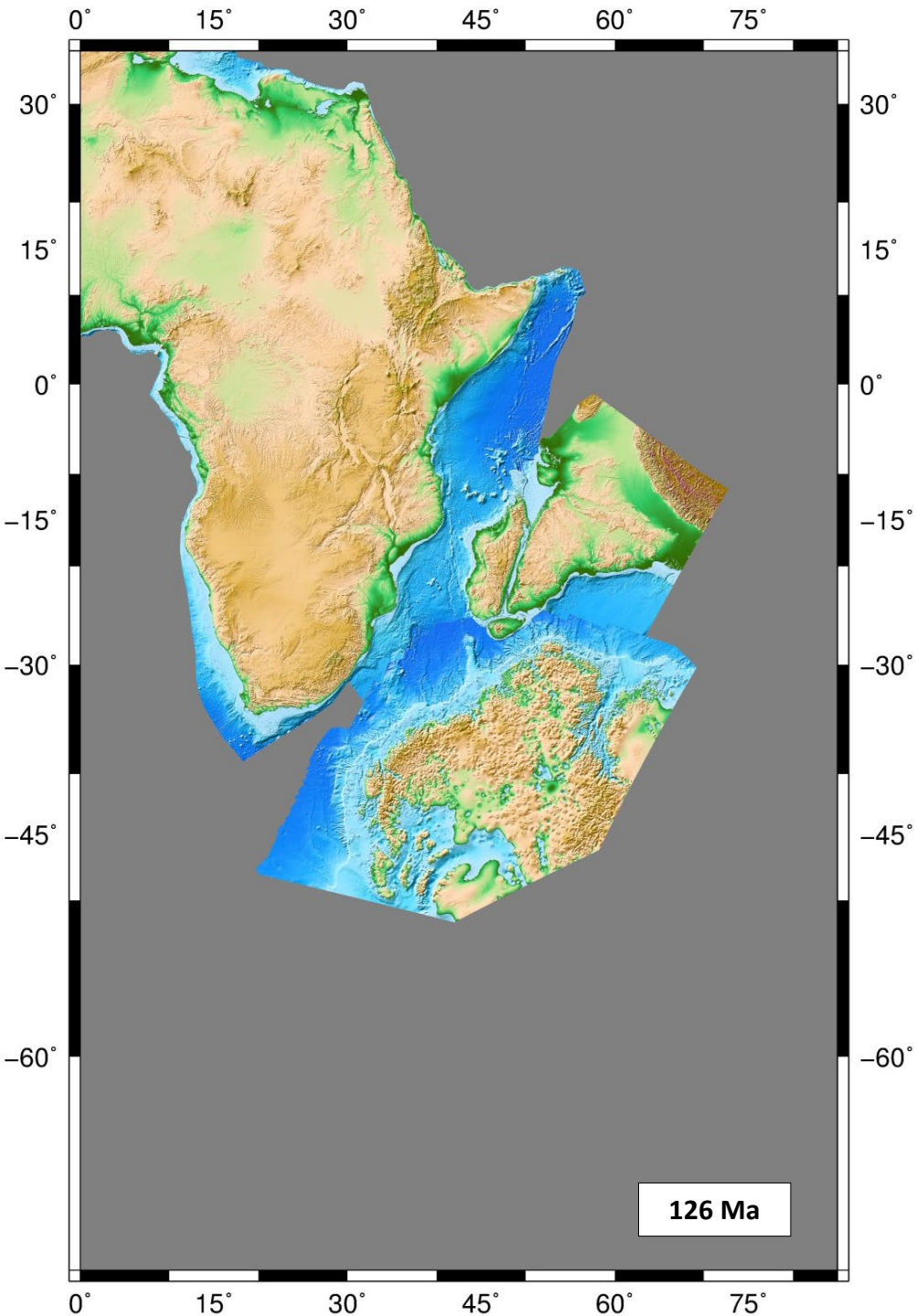
0˚
15˚
30˚
45˚
60˚
75˚
30˚
15˚
0˚
–15˚
–30˚
–45˚
–60˚
126 Ma

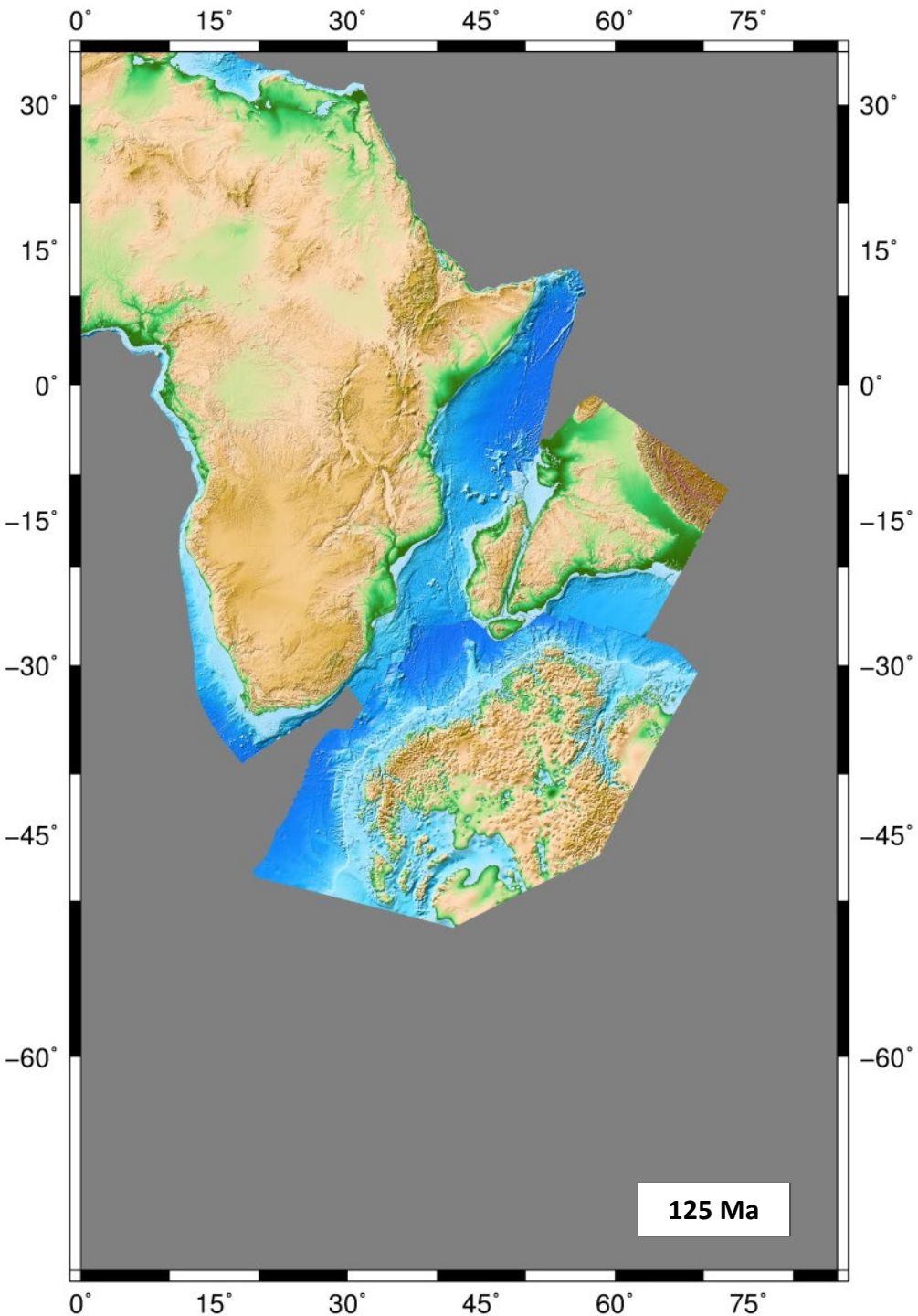
0°
15°
30°
45°
60°
75°
30°
15°
0°
−15°
−30°
−45°
−60°
125 Ma

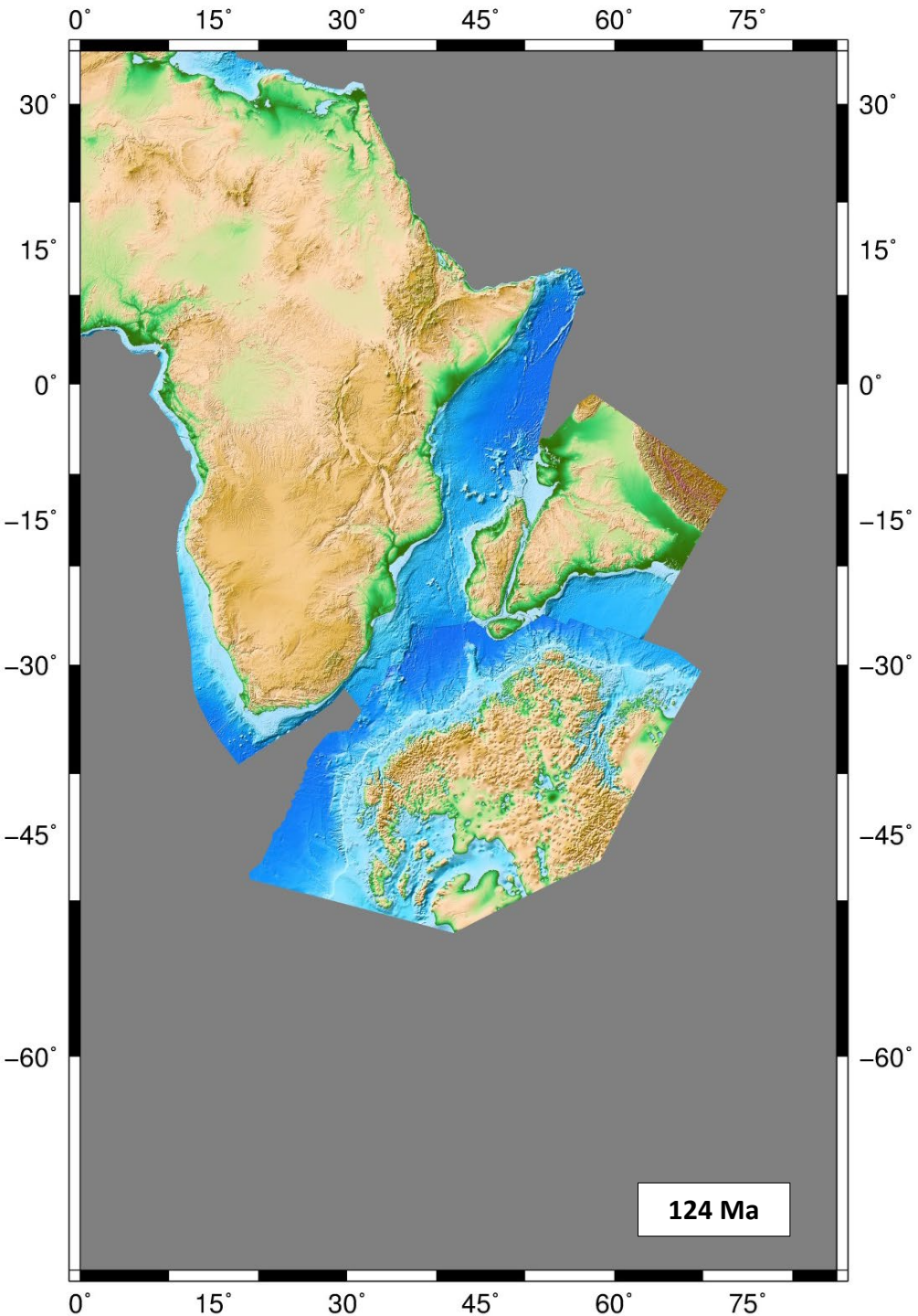
0˚
15˚
30˚
45˚
60˚
75˚
30˚
15˚
0˚
–15˚
–30˚
–45˚
–60˚
124 Ma

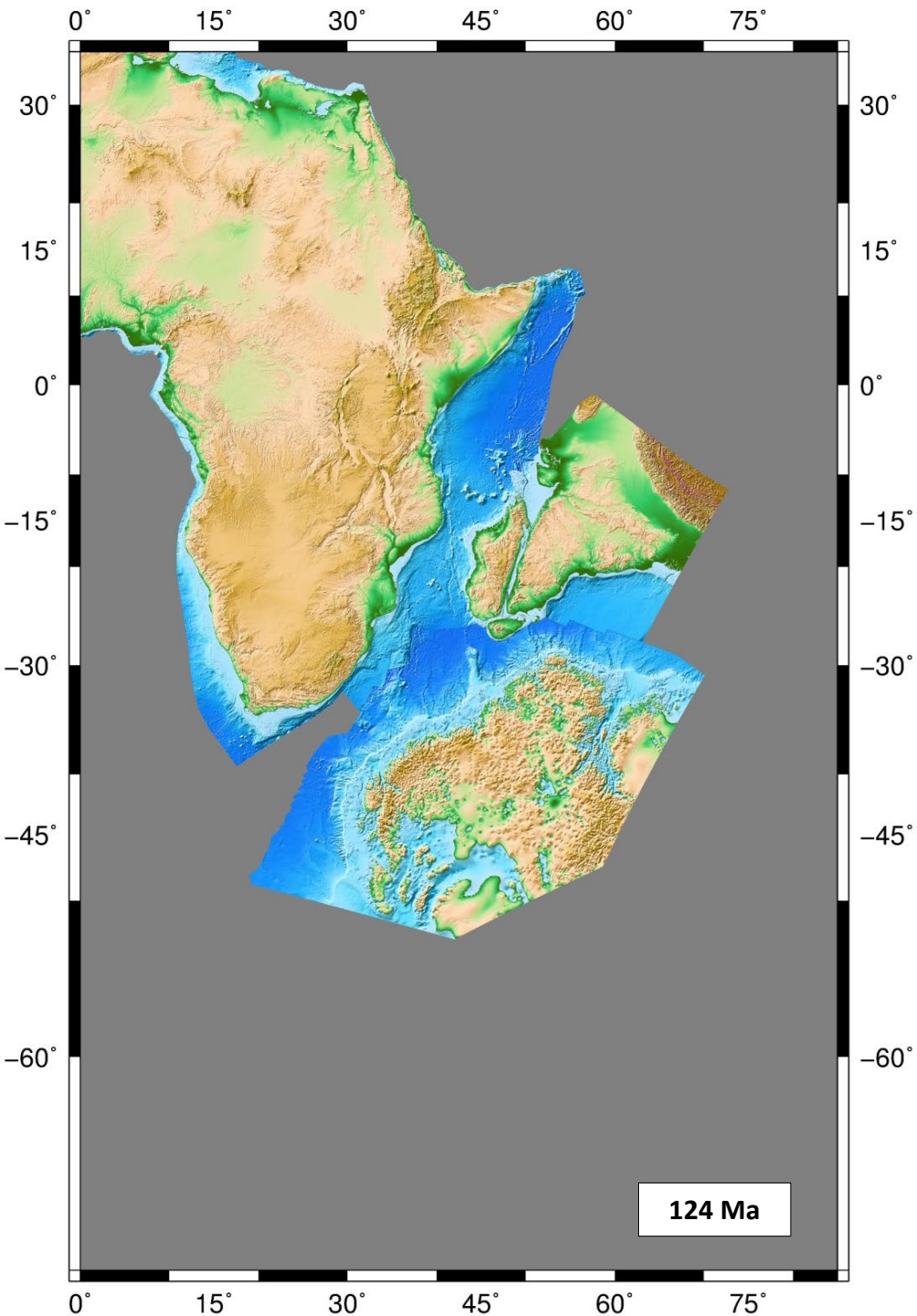
0°
15°
30°
45°
60°
75°
30°
15°
0°
−15°
−30°
−45°
−60°
124 Ma

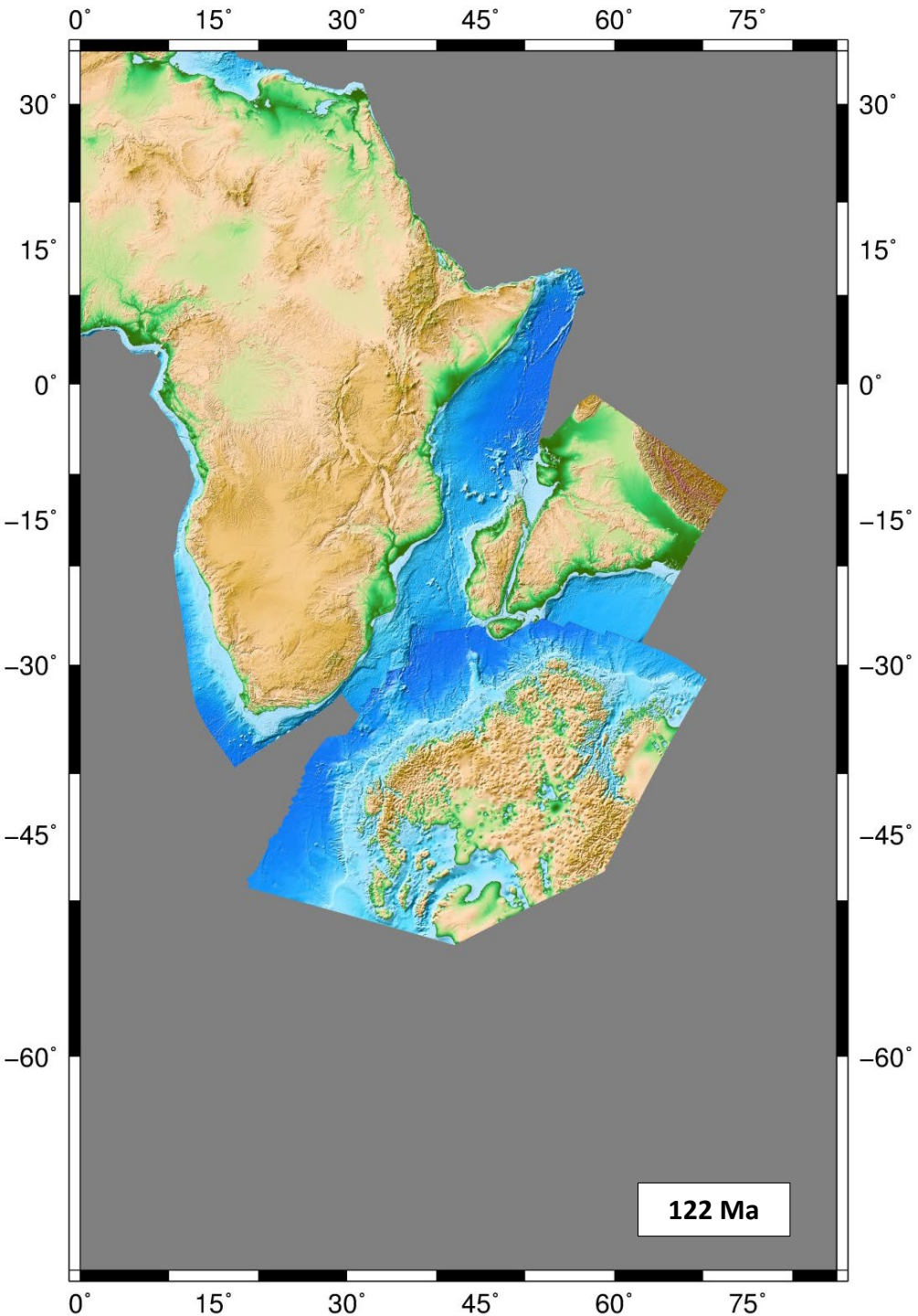
0˚
15˚
30˚
45˚
60˚
75˚
30˚
15˚
0˚
–15˚
–30˚
–45˚
–60˚
122 Ma

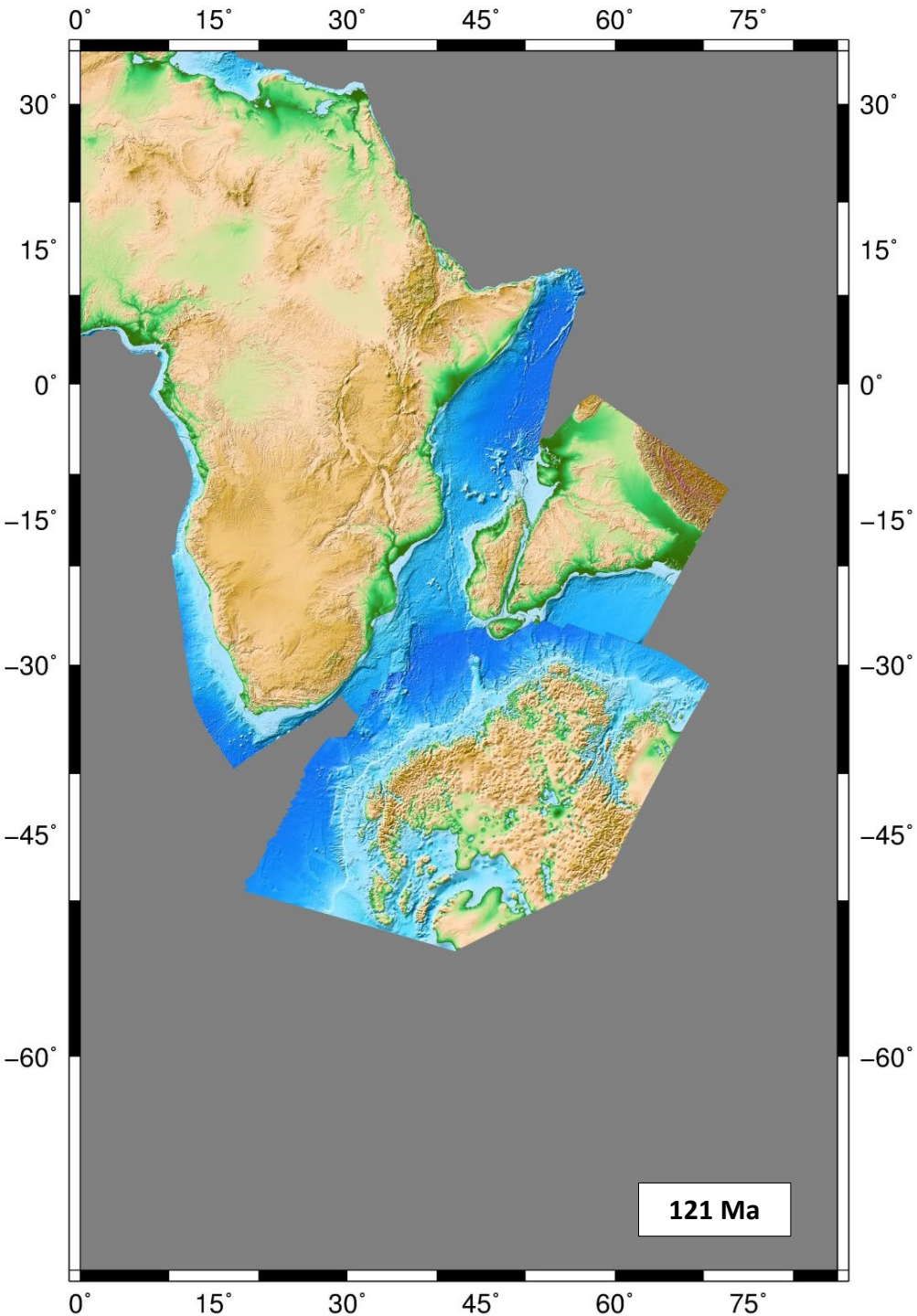
0˚
15˚
30˚
45˚
60˚
75˚
30˚
15˚
0˚
–15˚
–30˚
–45˚
–60˚
121 Ma

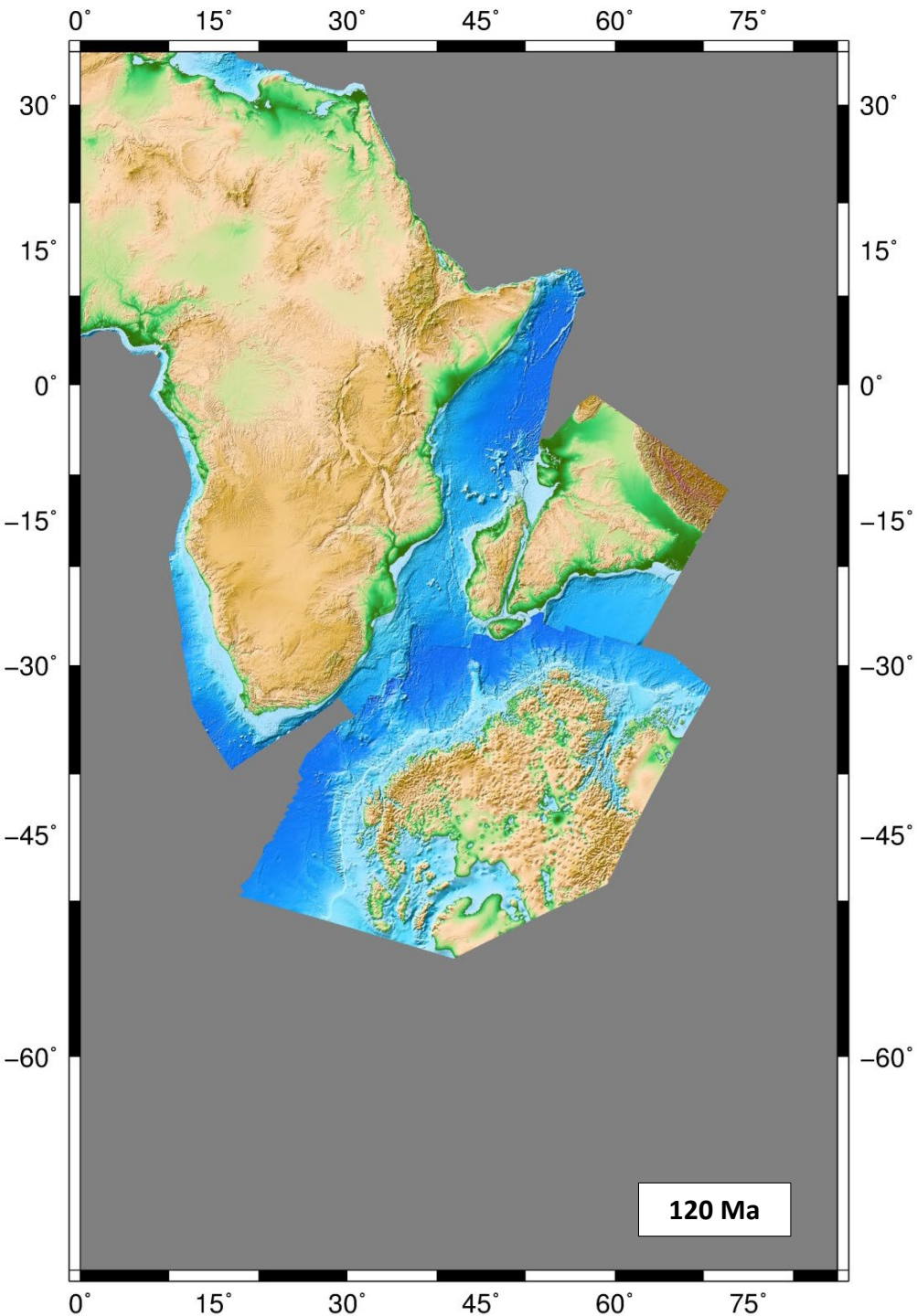
0˚
15˚
30˚
45˚
60˚
75˚
30˚
15˚
0˚
–15˚
–30˚
–45˚
–60˚
120 Ma

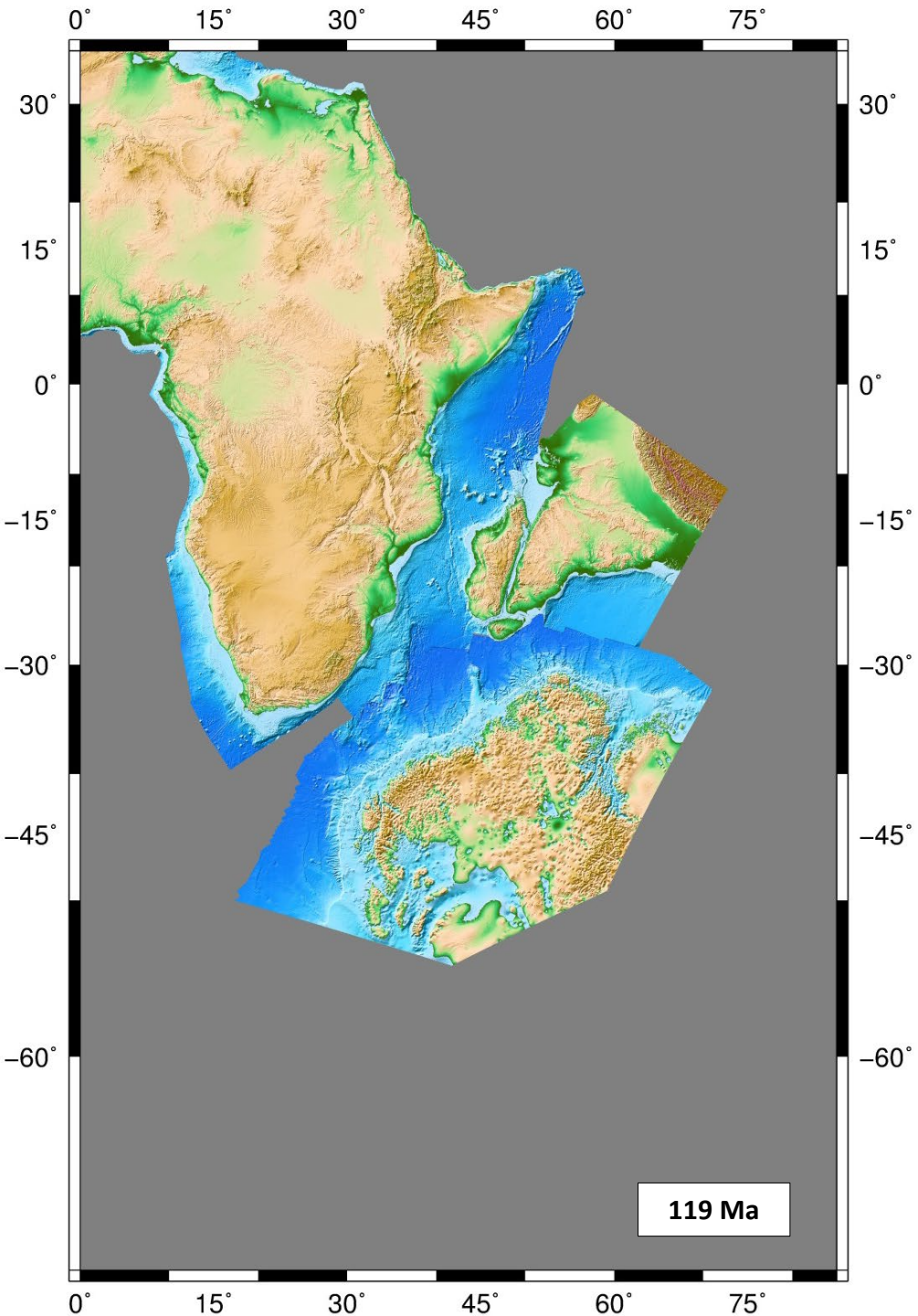
0˚
15˚
30˚
45˚
60˚
75˚
30˚
15˚
0˚
–15˚
–30˚
–45˚
–60˚
119 Ma

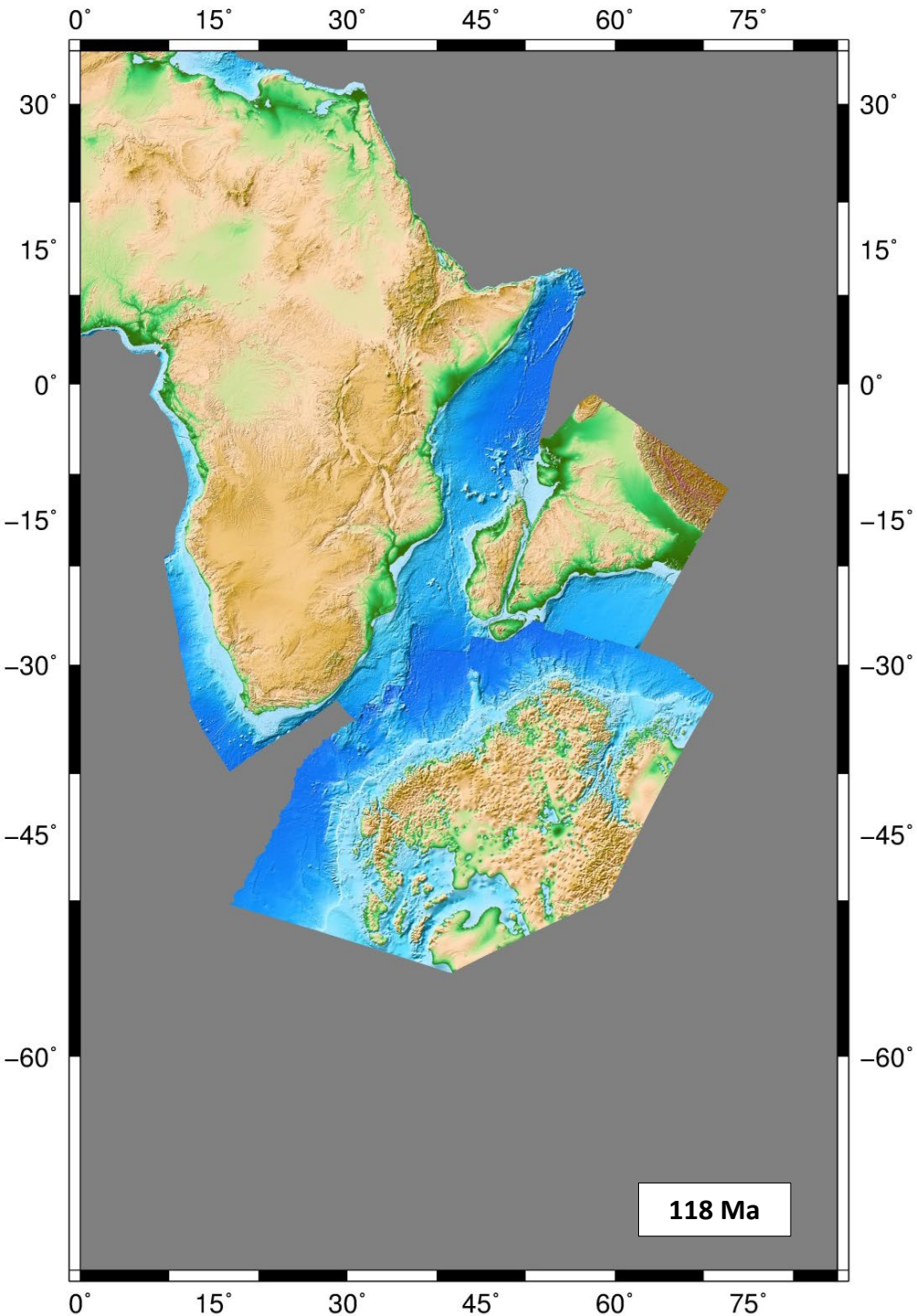
0˚
15˚
30˚
45˚
60˚
75˚
30˚
15˚
0˚
–15˚
–30˚
–45˚
–60˚
118 Ma

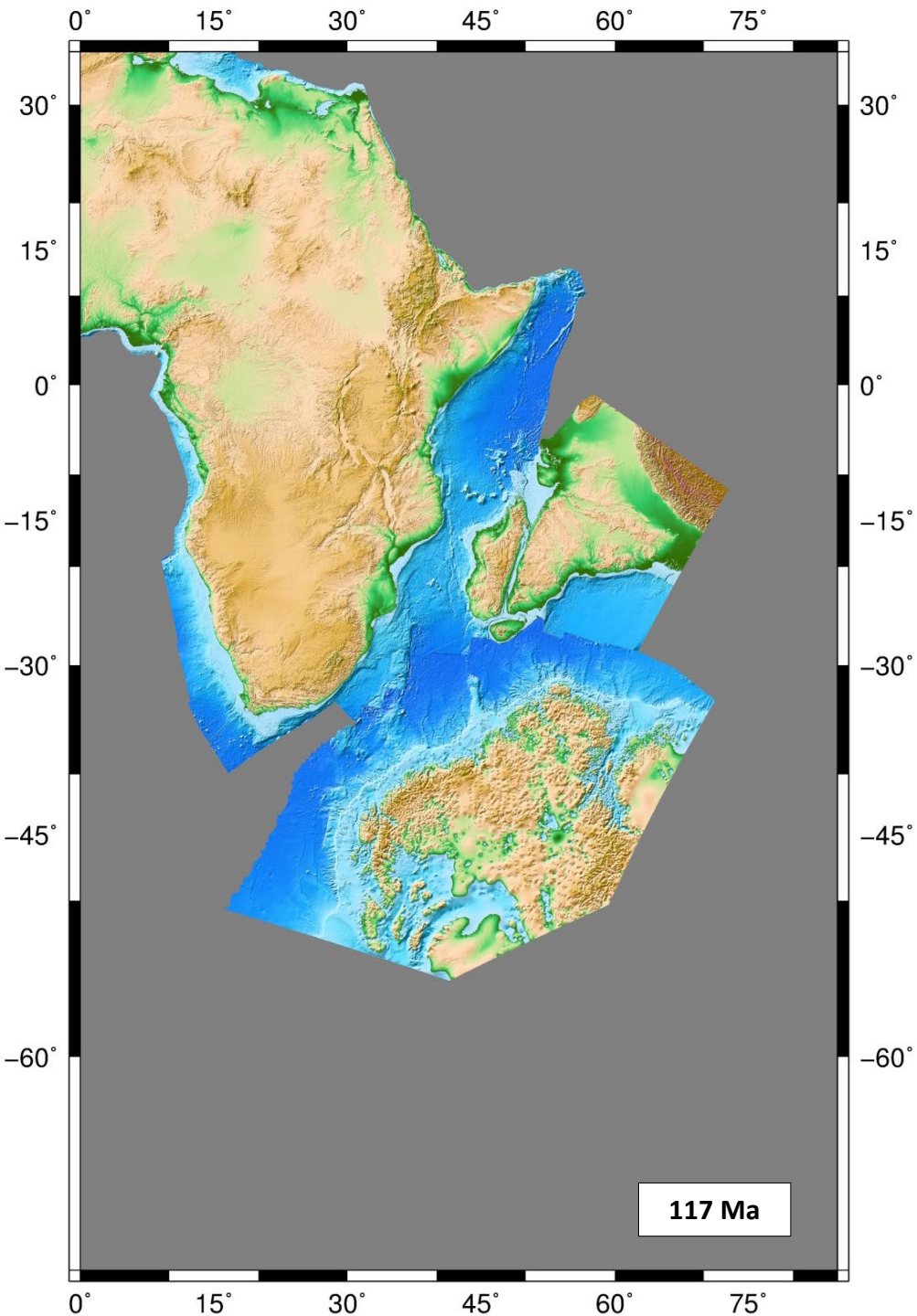
0˚
15˚
30˚
45˚
60˚
75˚
30˚
15˚
0˚
–15˚
–30˚
–45˚
–60˚
117 Ma

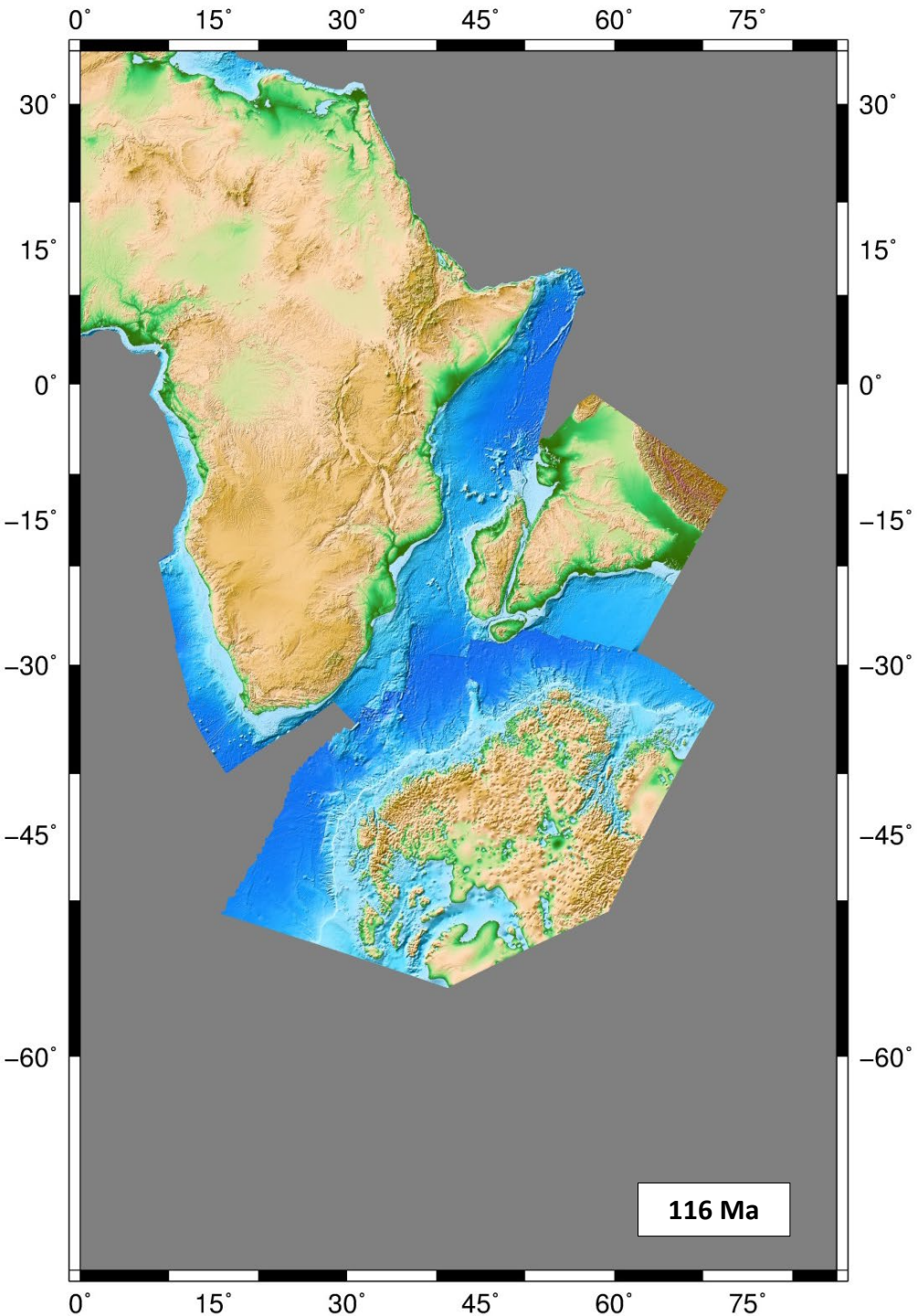
0˚
15˚
30˚
45˚
60˚
75˚
30˚
15˚
0˚
–15˚
–30˚
–45˚
–60˚
116 Ma

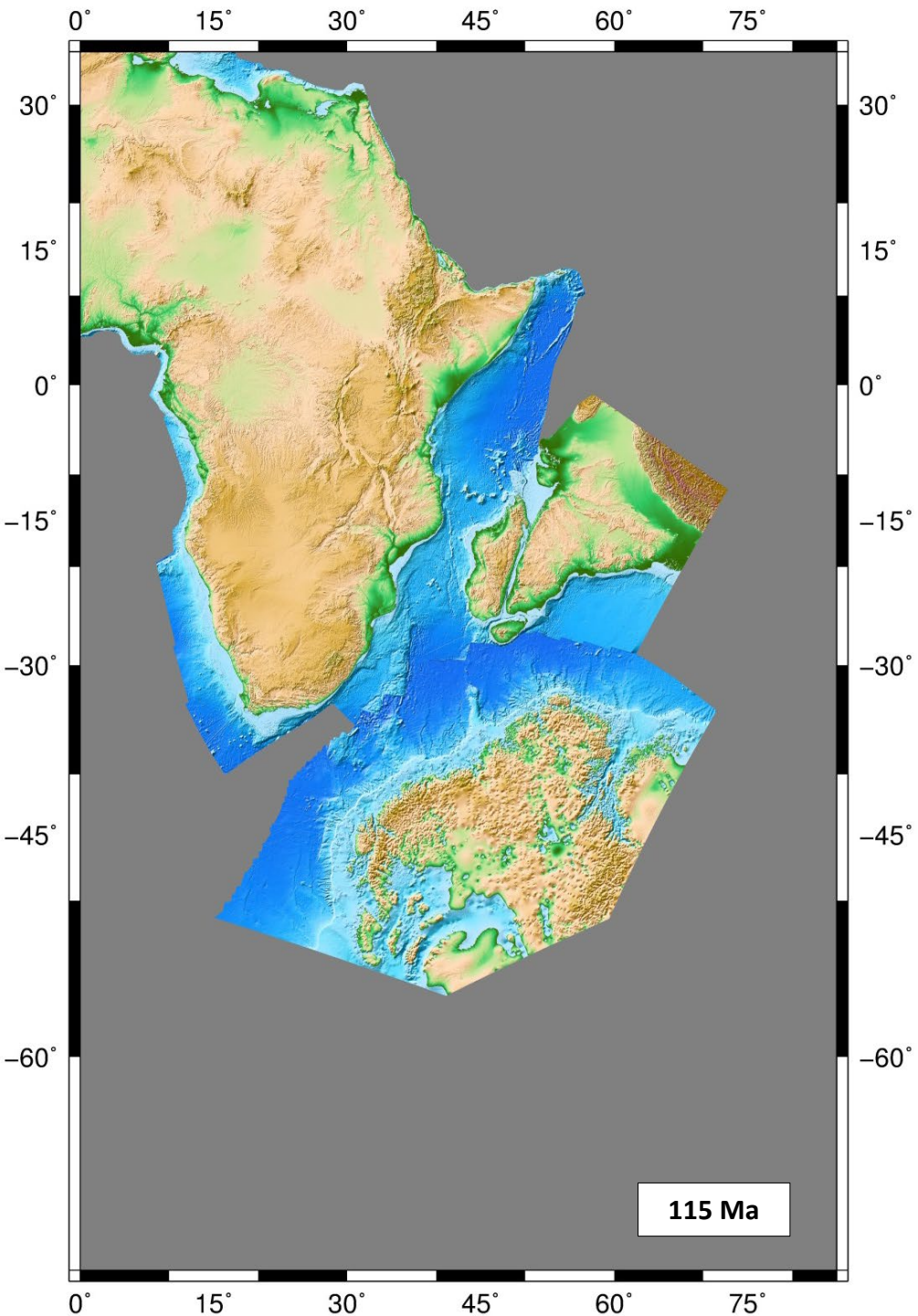
0˚
15˚
30˚
45˚
60˚
75˚
30˚
15˚
0˚
–15˚
–30˚
–45˚
–60˚
115 Ma

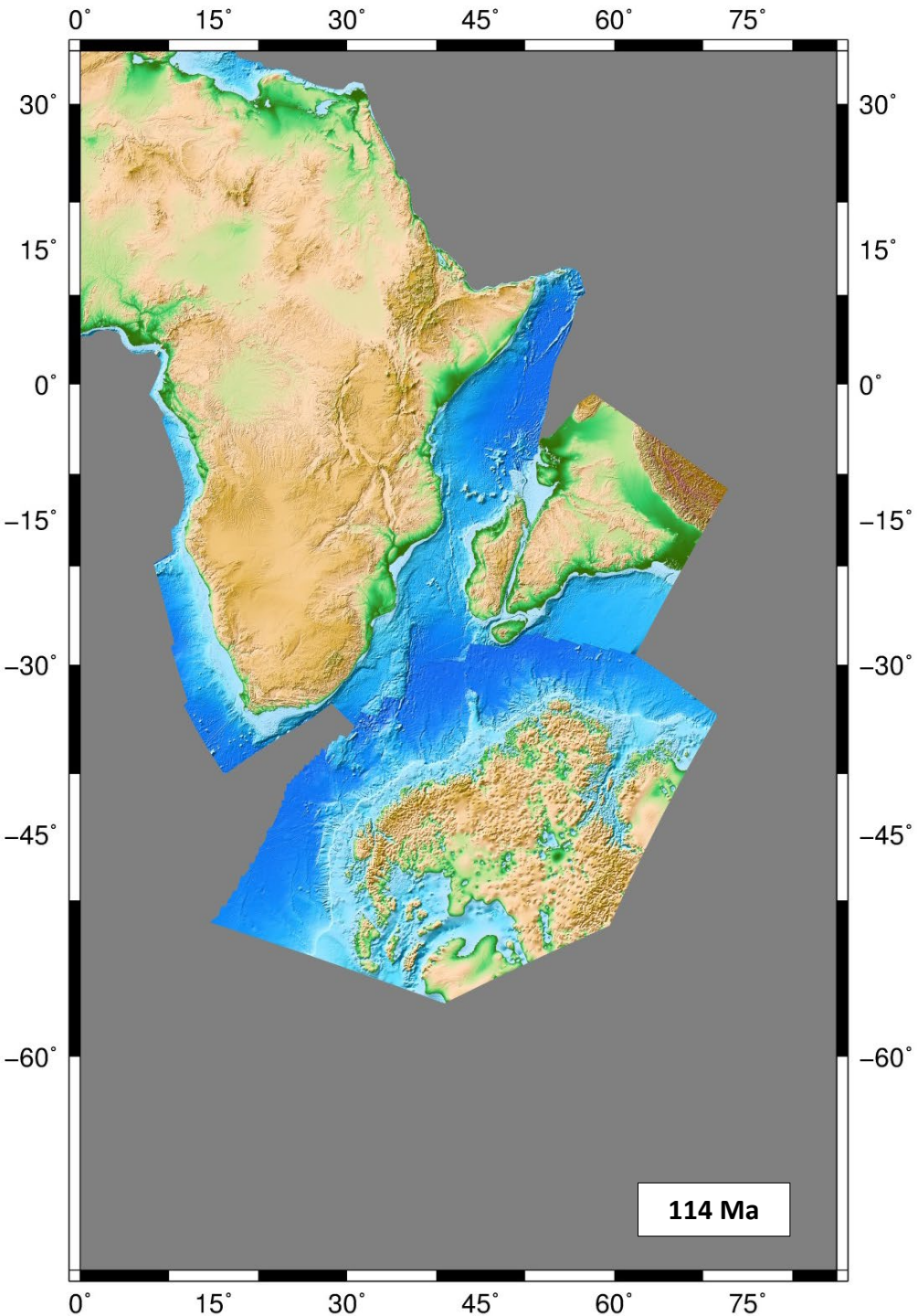
0˚
15˚
30˚
45˚
60˚
75˚
30˚
15˚
0˚
–15˚
–30˚
–45˚
–60˚
114 Ma

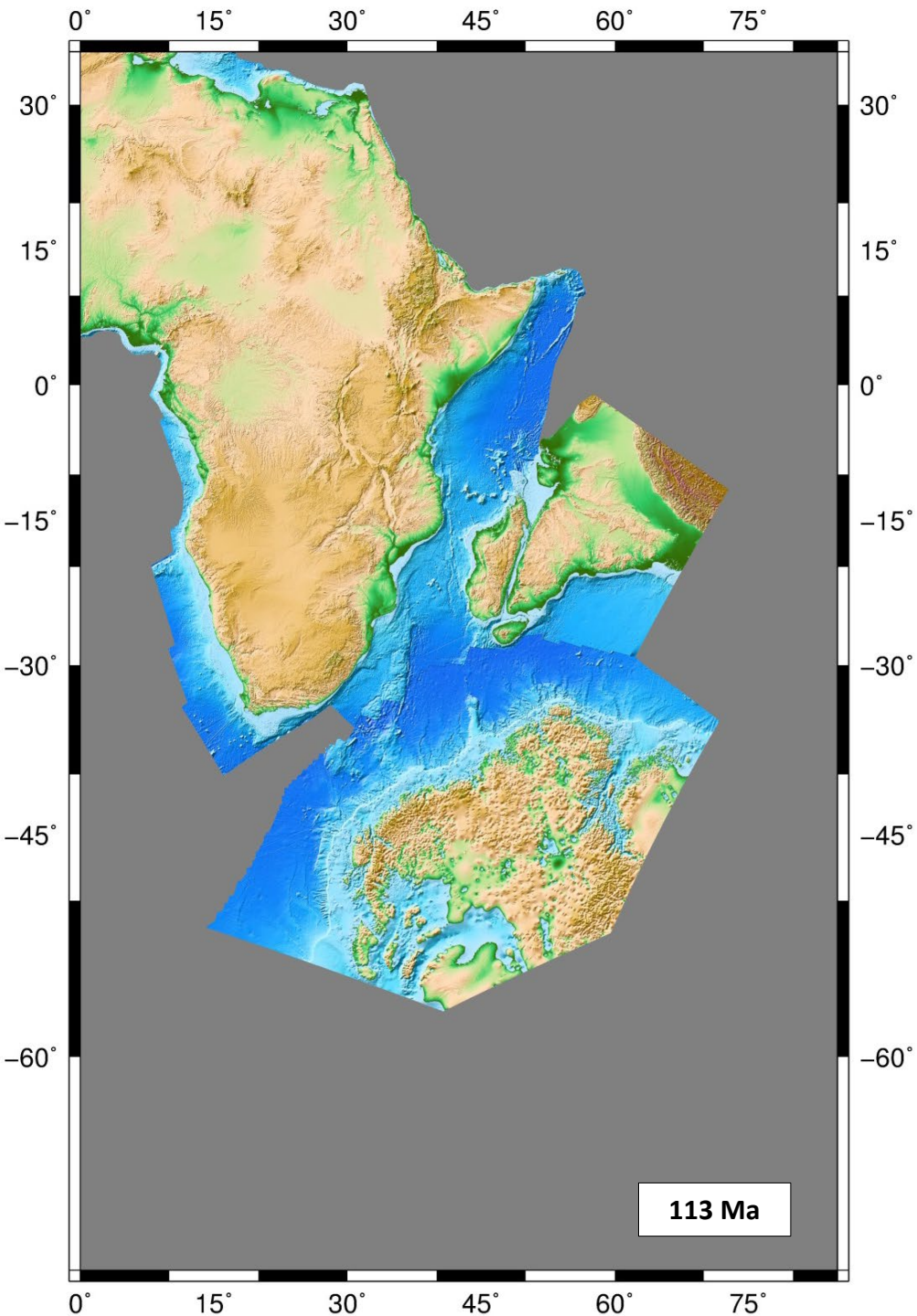
0°
15°
30°
45°
60°
75°
30°
15°
0°
−15°
−30°
−45°
−60°
113 Ma

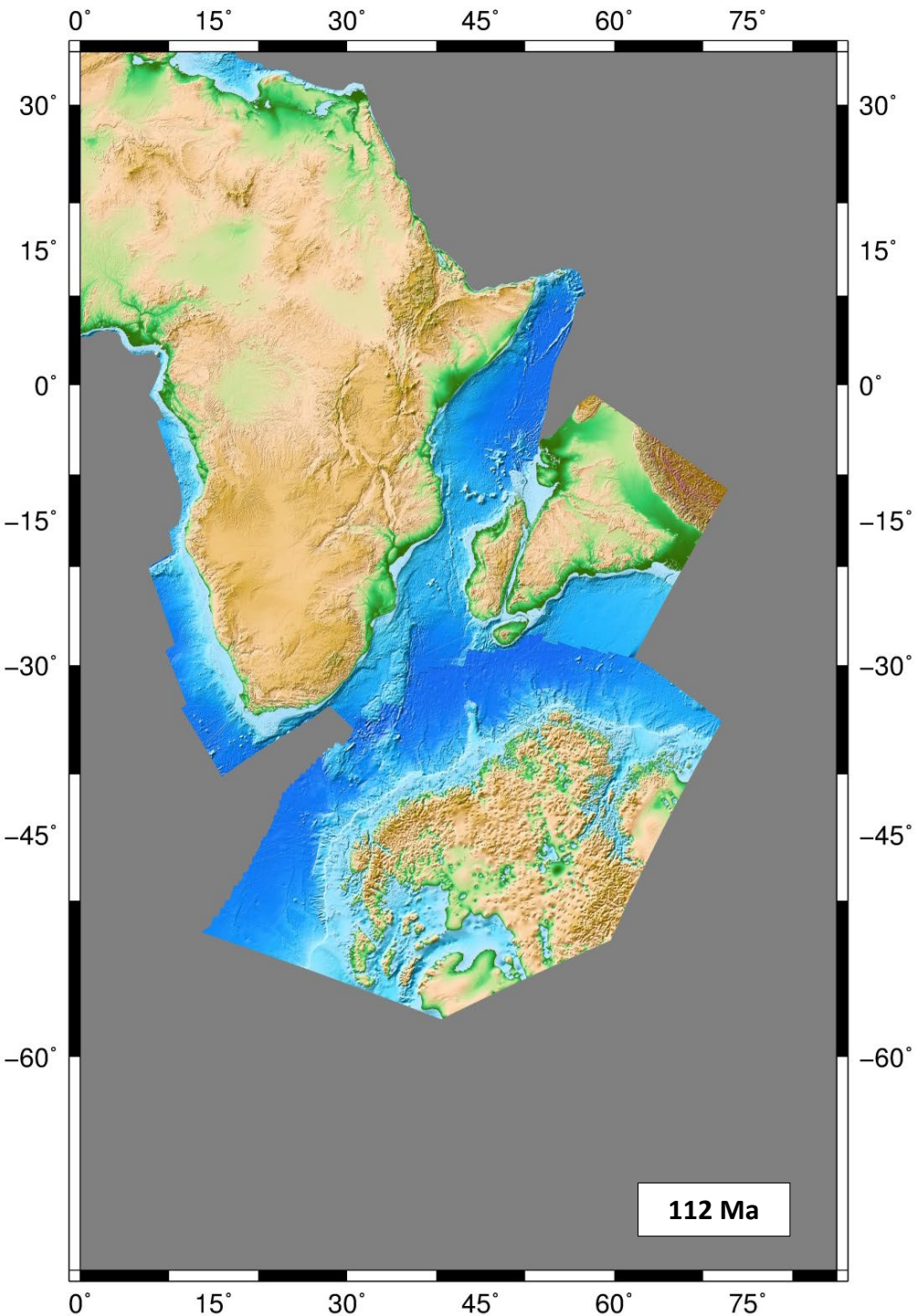
0˚
15˚
30˚
45˚
60˚
75˚
30˚
15˚
0˚
–15˚
–30˚
–45˚
–60˚
112 Ma

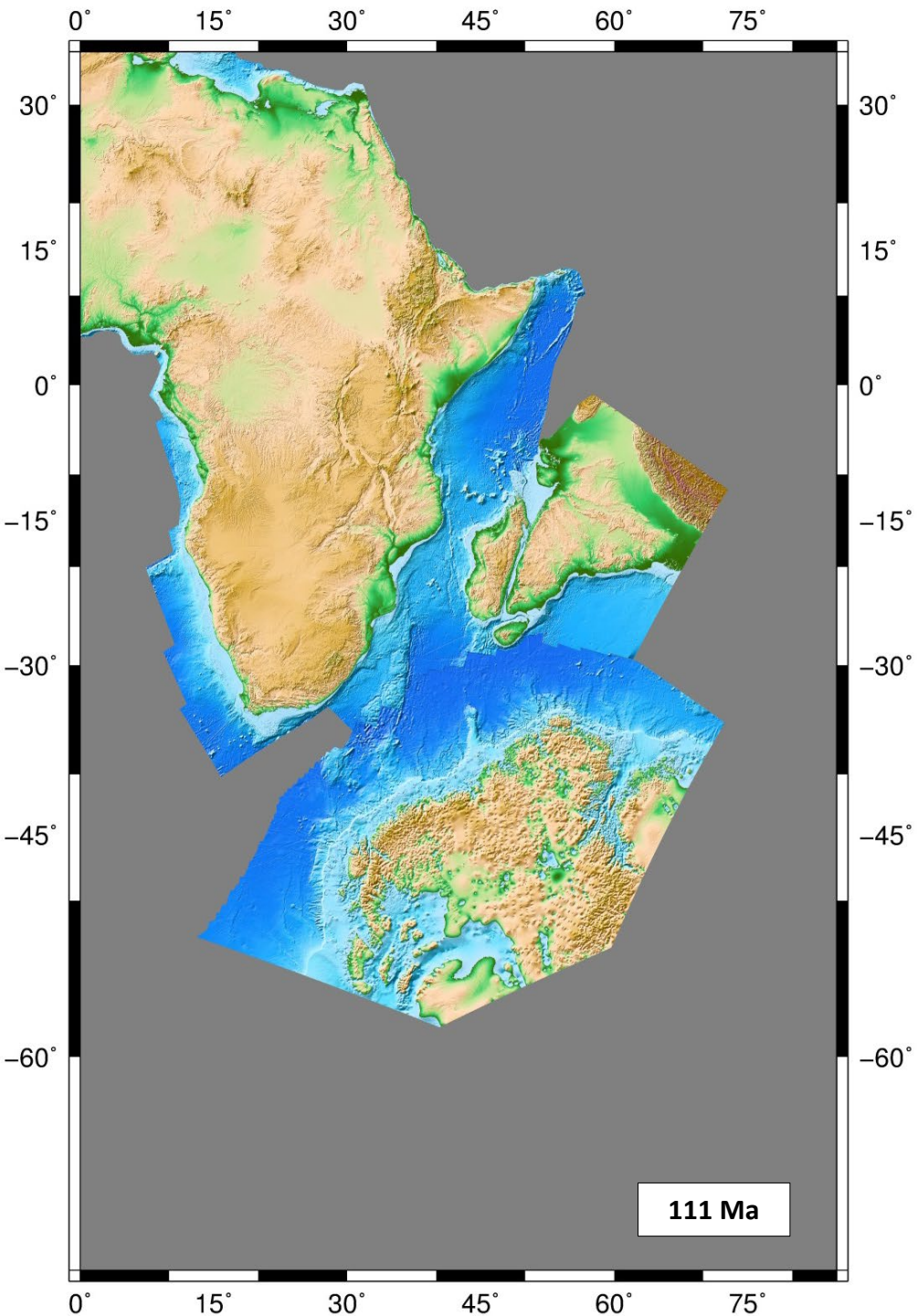
0˚
15˚
30˚
45˚
60˚
75˚
30˚
15˚
0˚
–15˚
–30˚
–45˚
–60˚
111 Ma

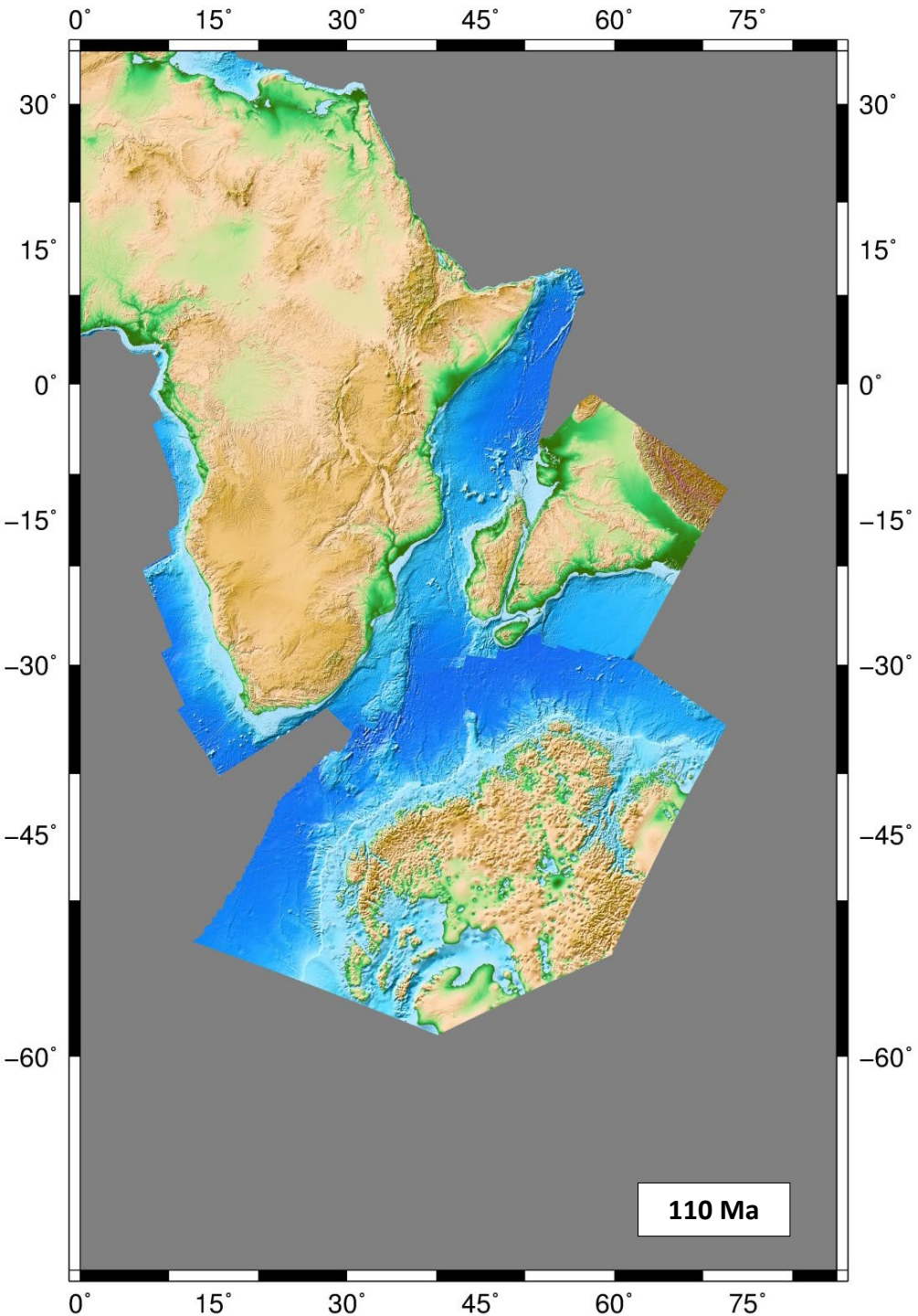
0˚
15˚
30˚
45˚
60˚
75˚
30˚
15˚
0˚
–15˚
–30˚
–45˚
–60˚
110 Ma

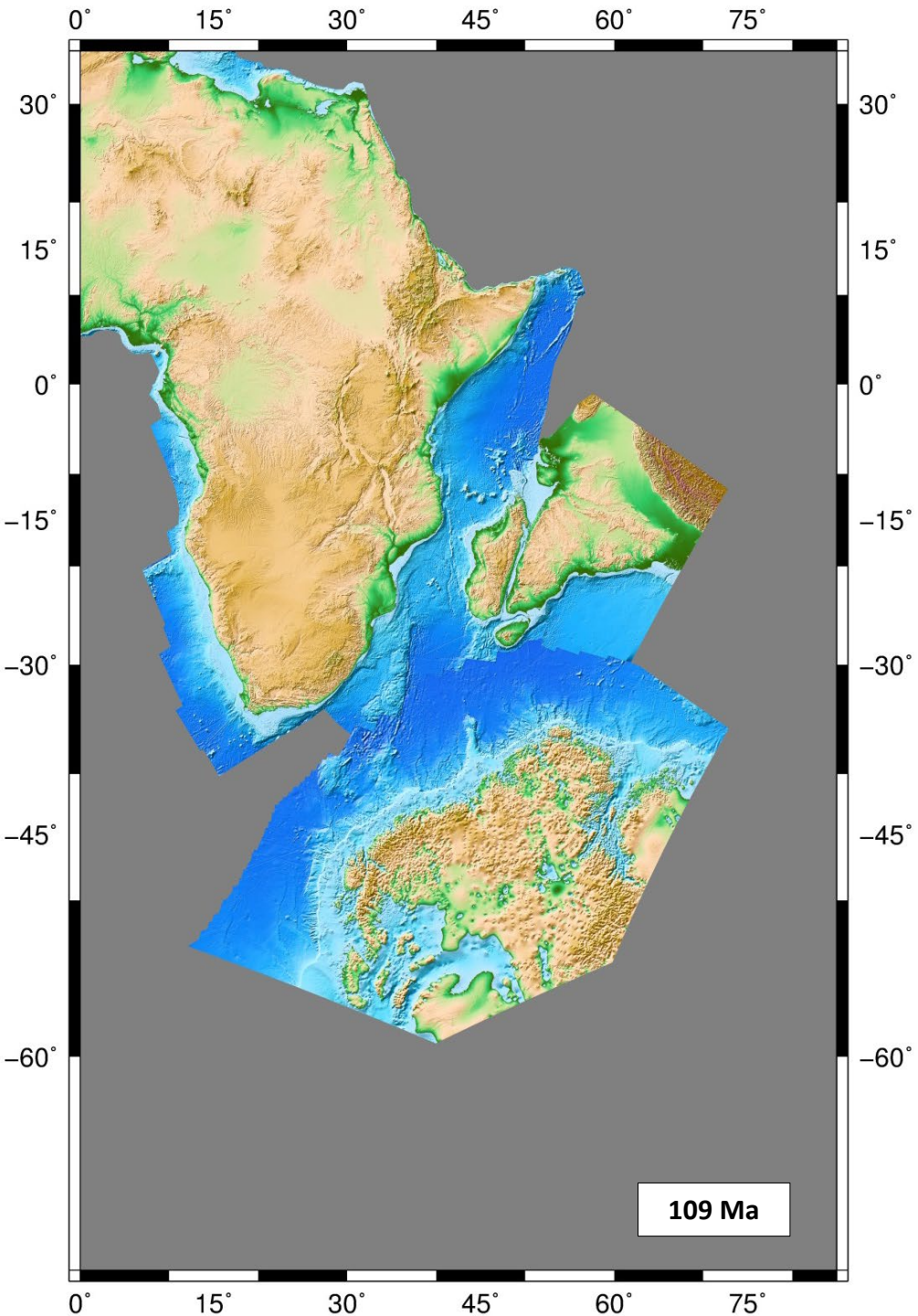
0˚
15˚
30˚
45˚
60˚
75˚
30˚
15˚
0˚
–15˚
–30˚
–45˚
–60˚
109 Ma

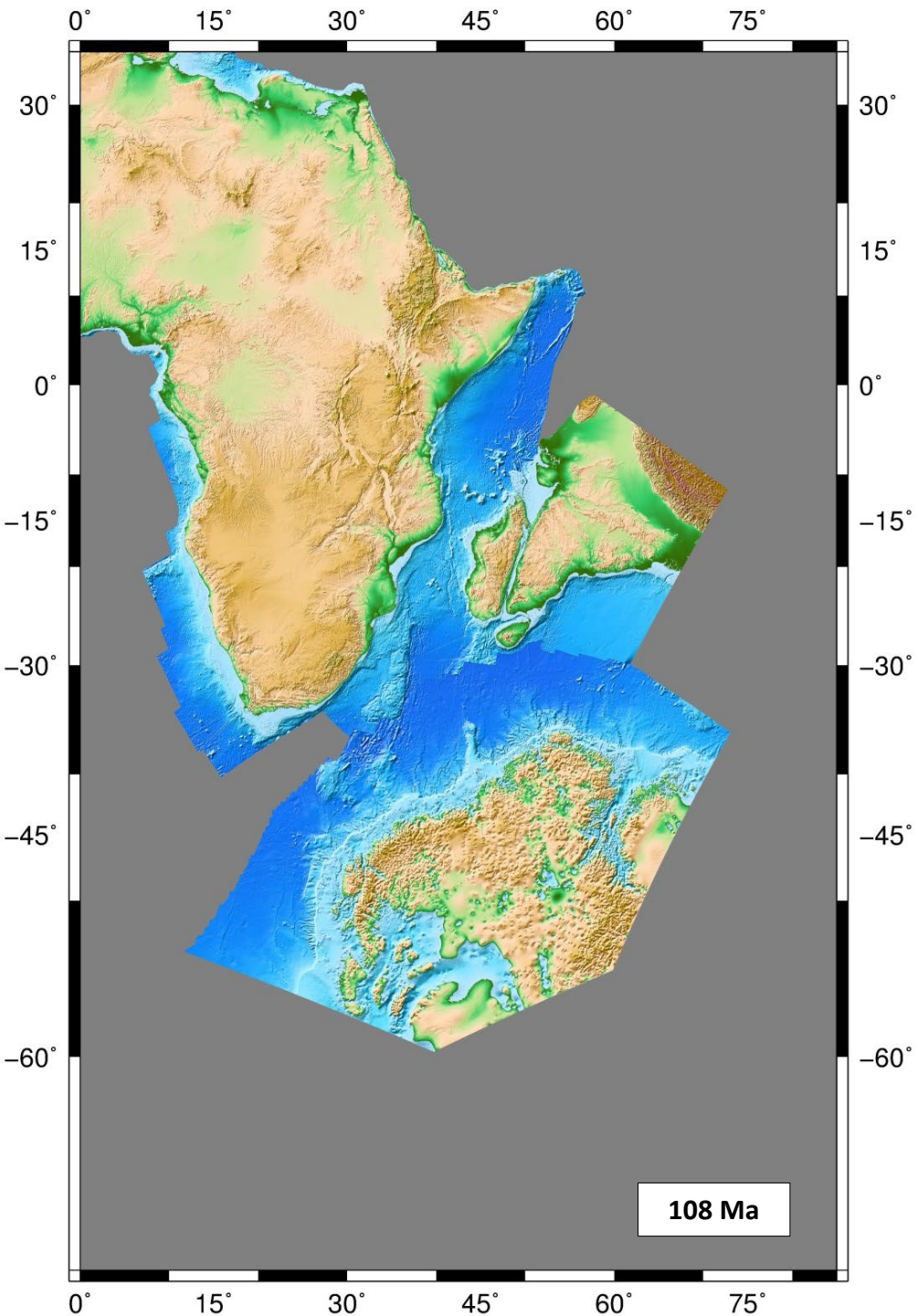
0°
15°
30°
45°
60°
75°
30°
15°
0°
−15°
−30°
−45°
−60°
108 Ma

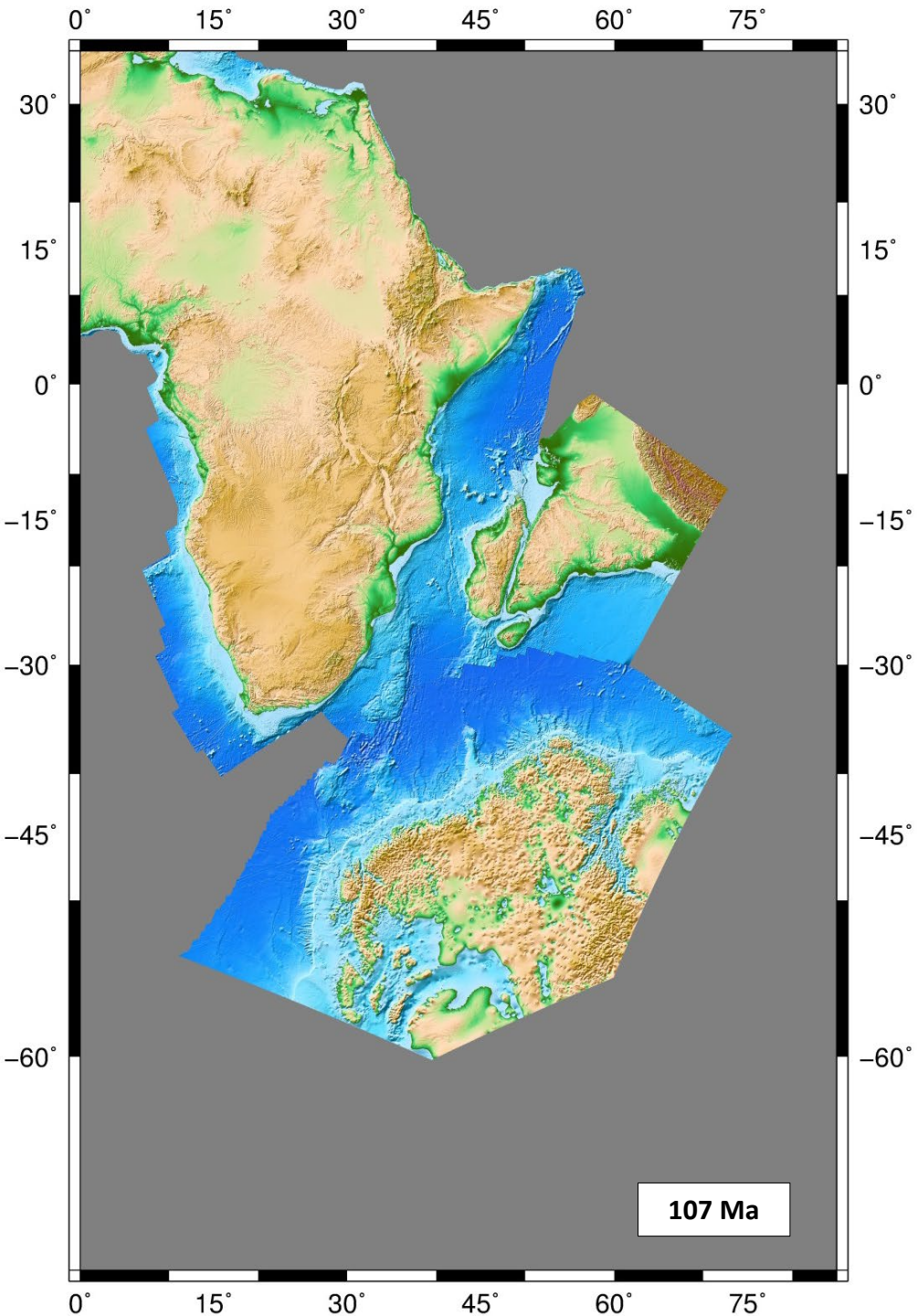
0˚
15˚
30˚
45˚
60˚
75˚
30˚
15˚
0˚
–15˚
–30˚
–45˚
–60˚
107 Ma

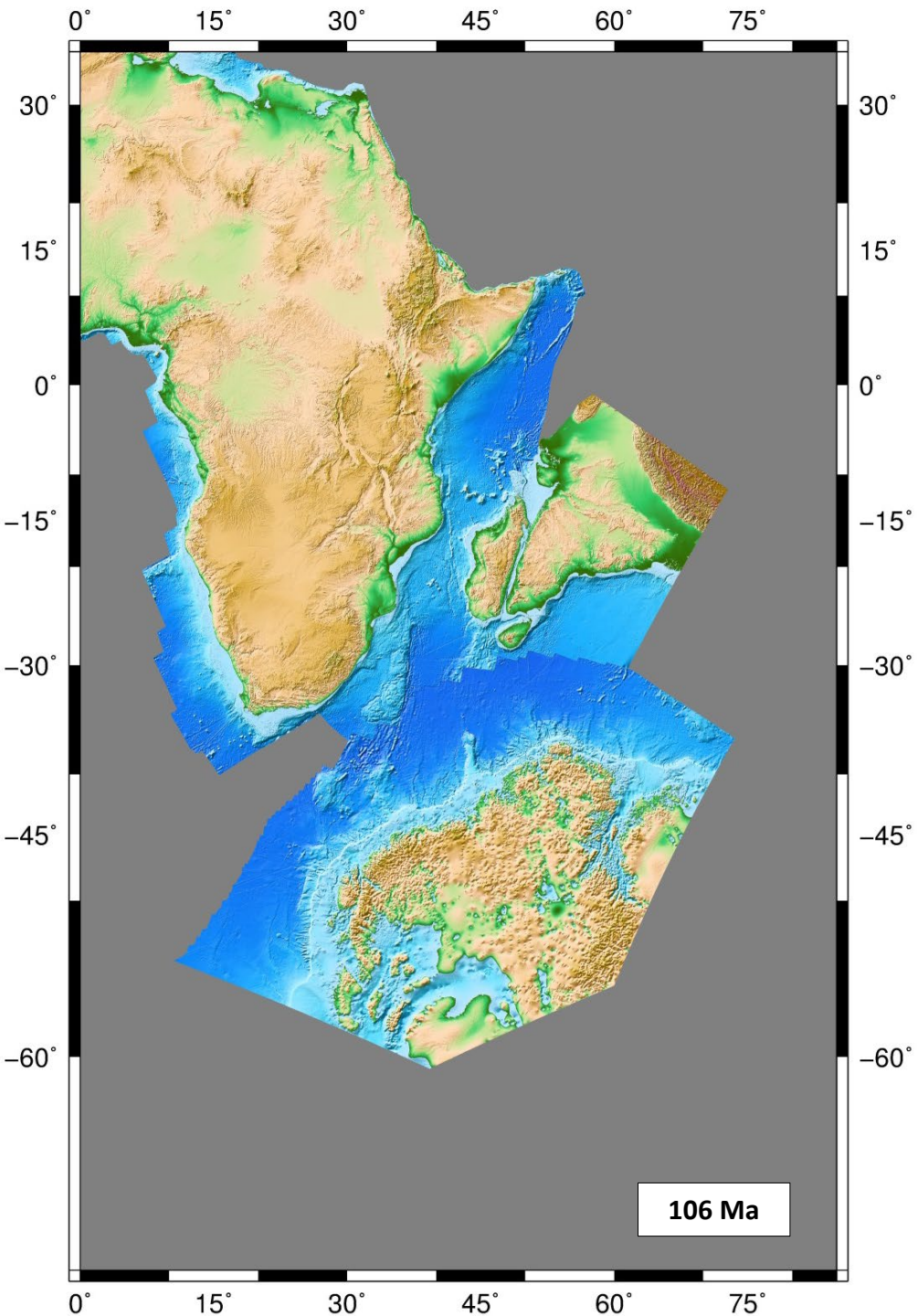
0˚
15˚
30˚
45˚
60˚
75˚
30˚
15˚
0˚
–15˚
–30˚
–45˚
–60˚
106 Ma

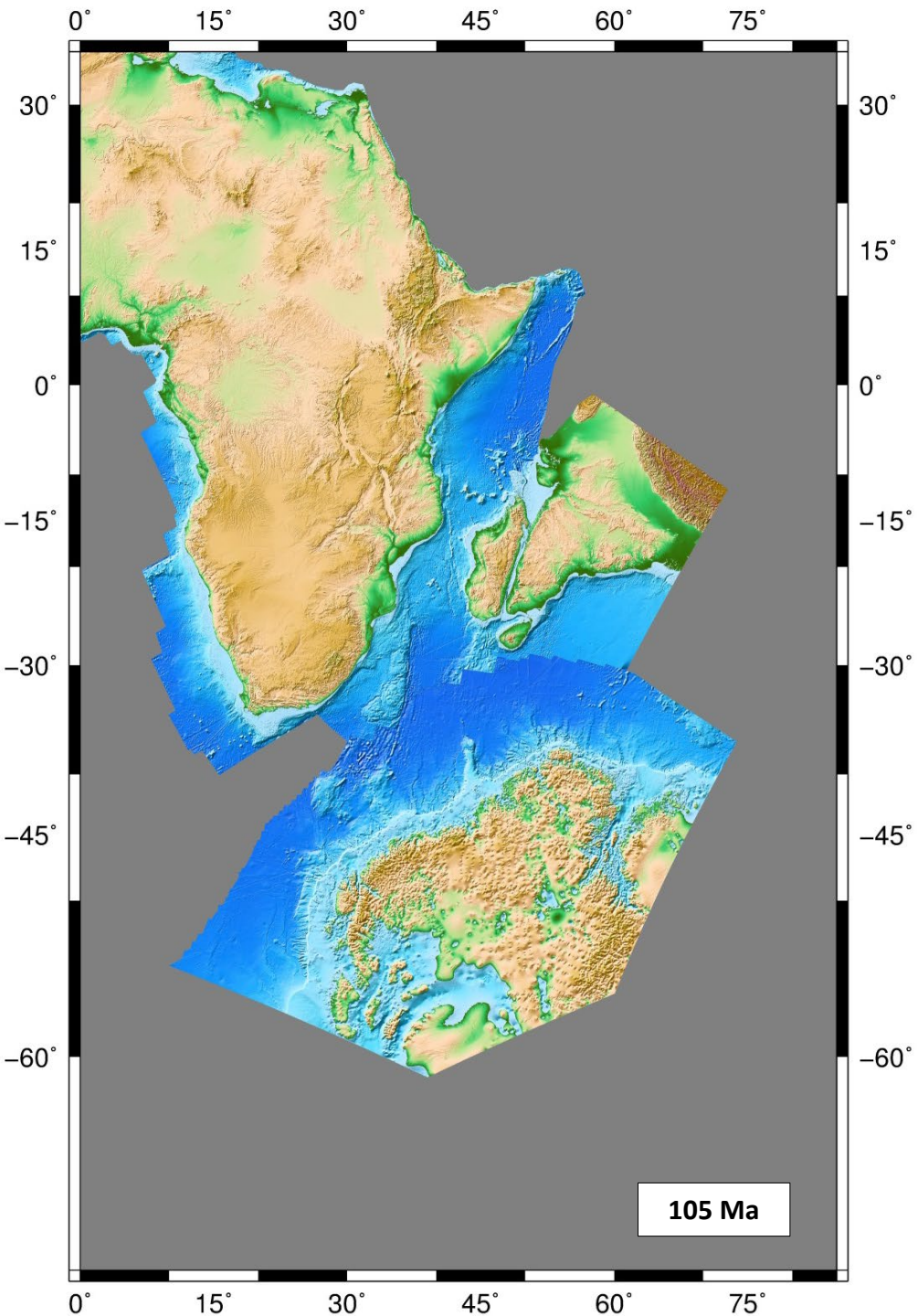
0°
15°
30°
45°
60°
75°
30°
15°
0°
−15°
−30°
−45°
−60°
105 Ma

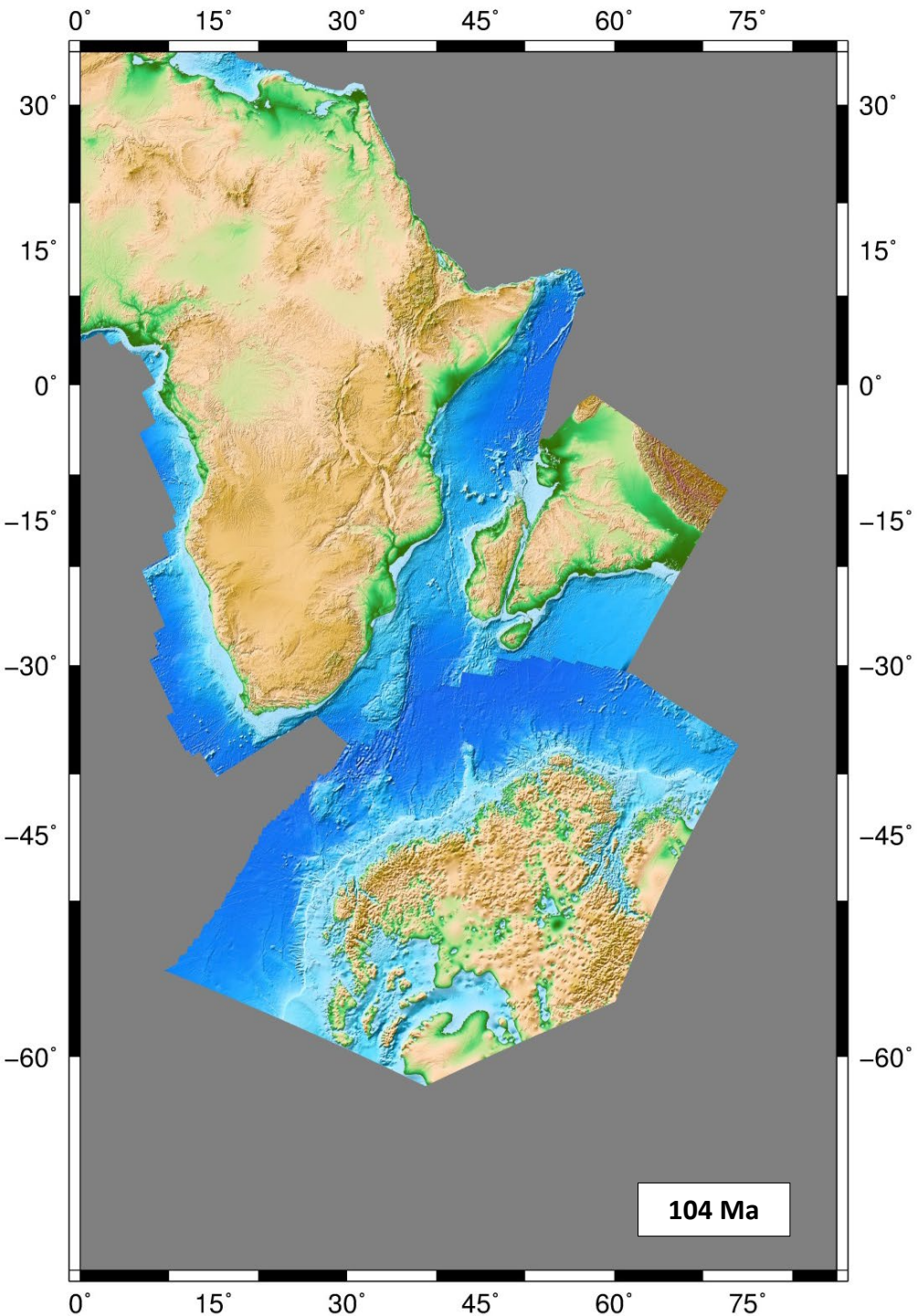
0°
15°
30°
45°
60°
75°
30°
15°
0°
−15°
−30°
−45°
−60°
104 Ma

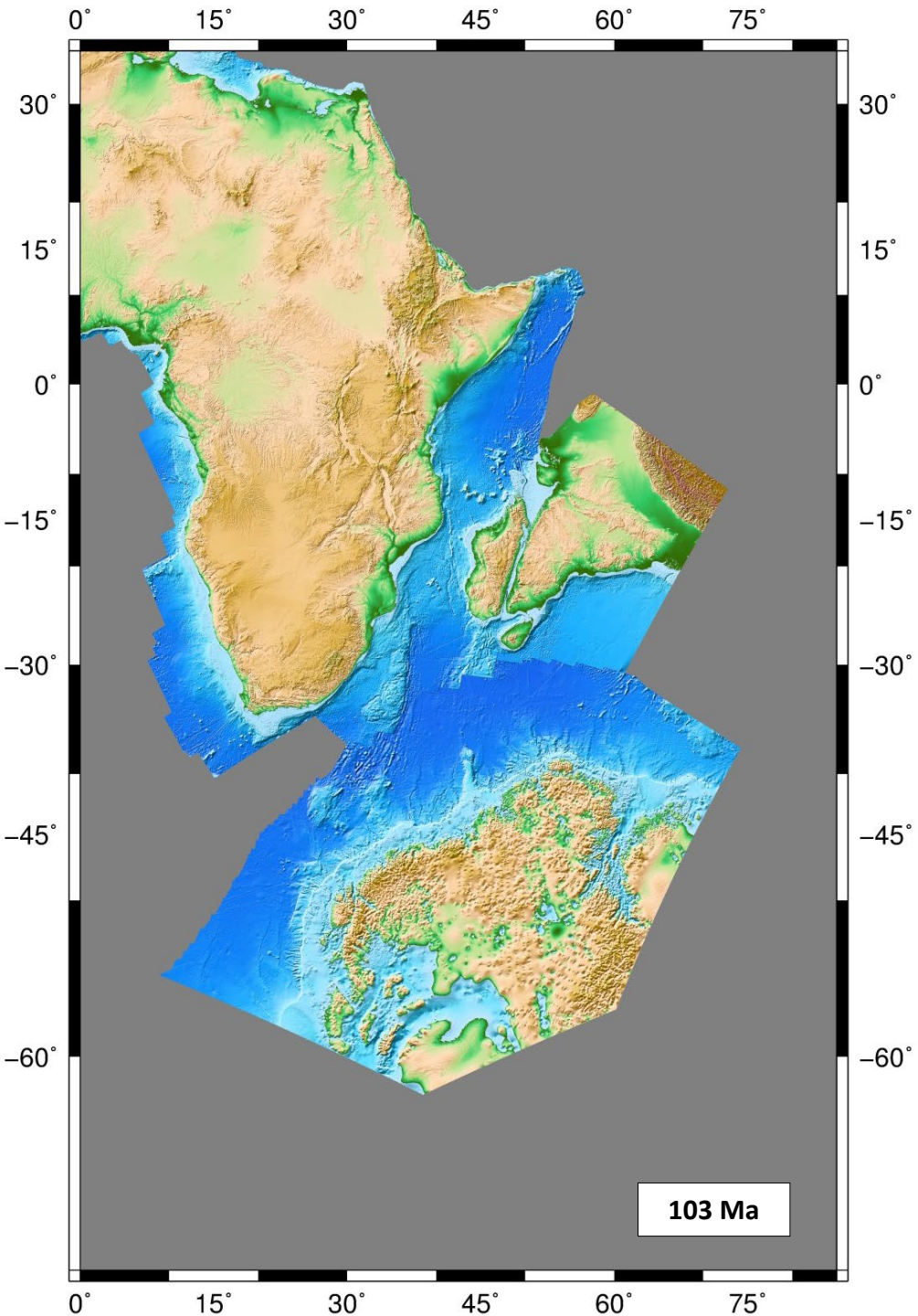
0°
15°
30°
45°
60°
75°
30°
15°
0°
−15°
−30°
−45°
−60°
103 Ma

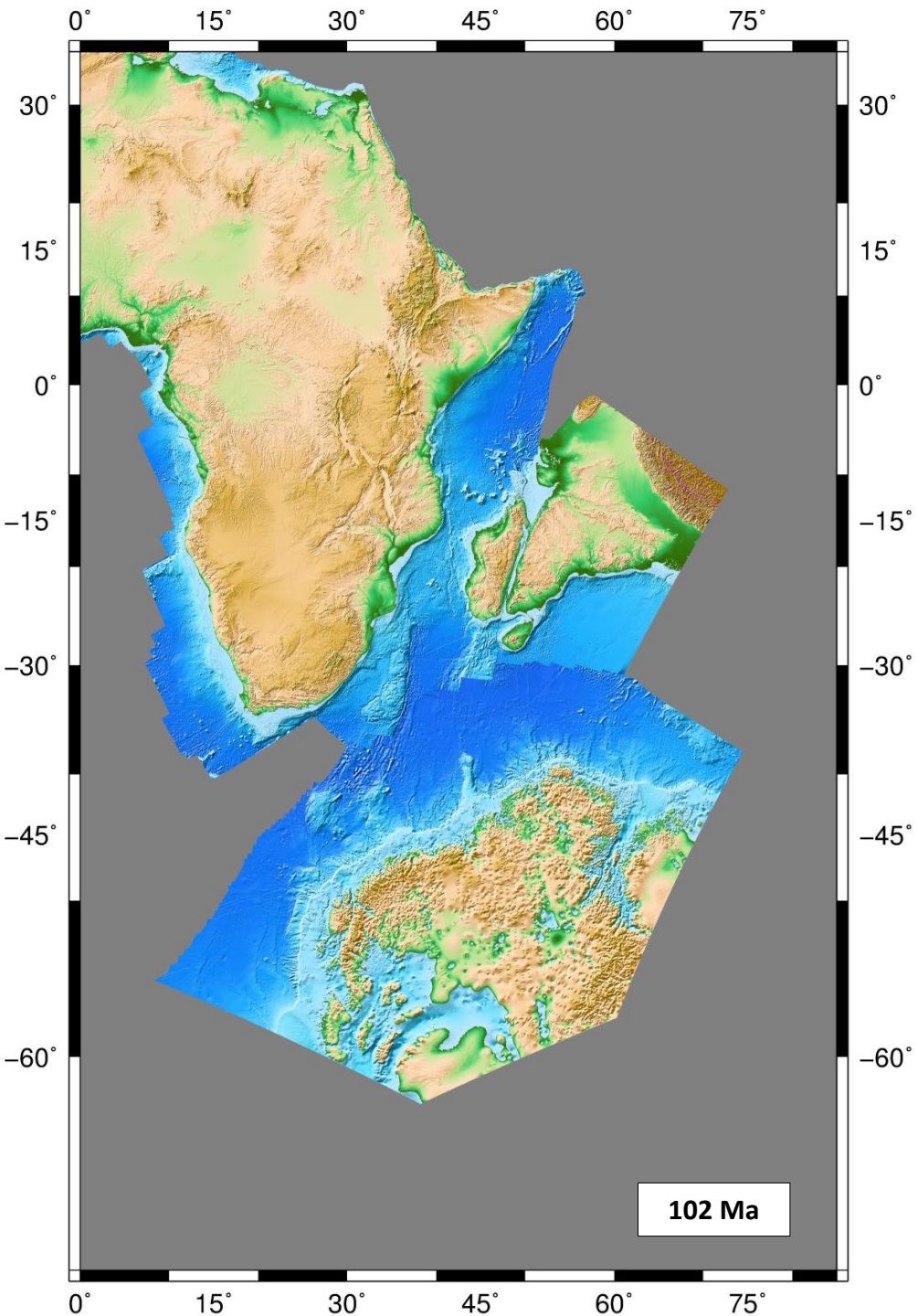
0˚
15˚
30˚
45˚
60˚
75˚
30˚
15˚
0˚
–15˚
–30˚
–45˚
–60˚
102 Ma

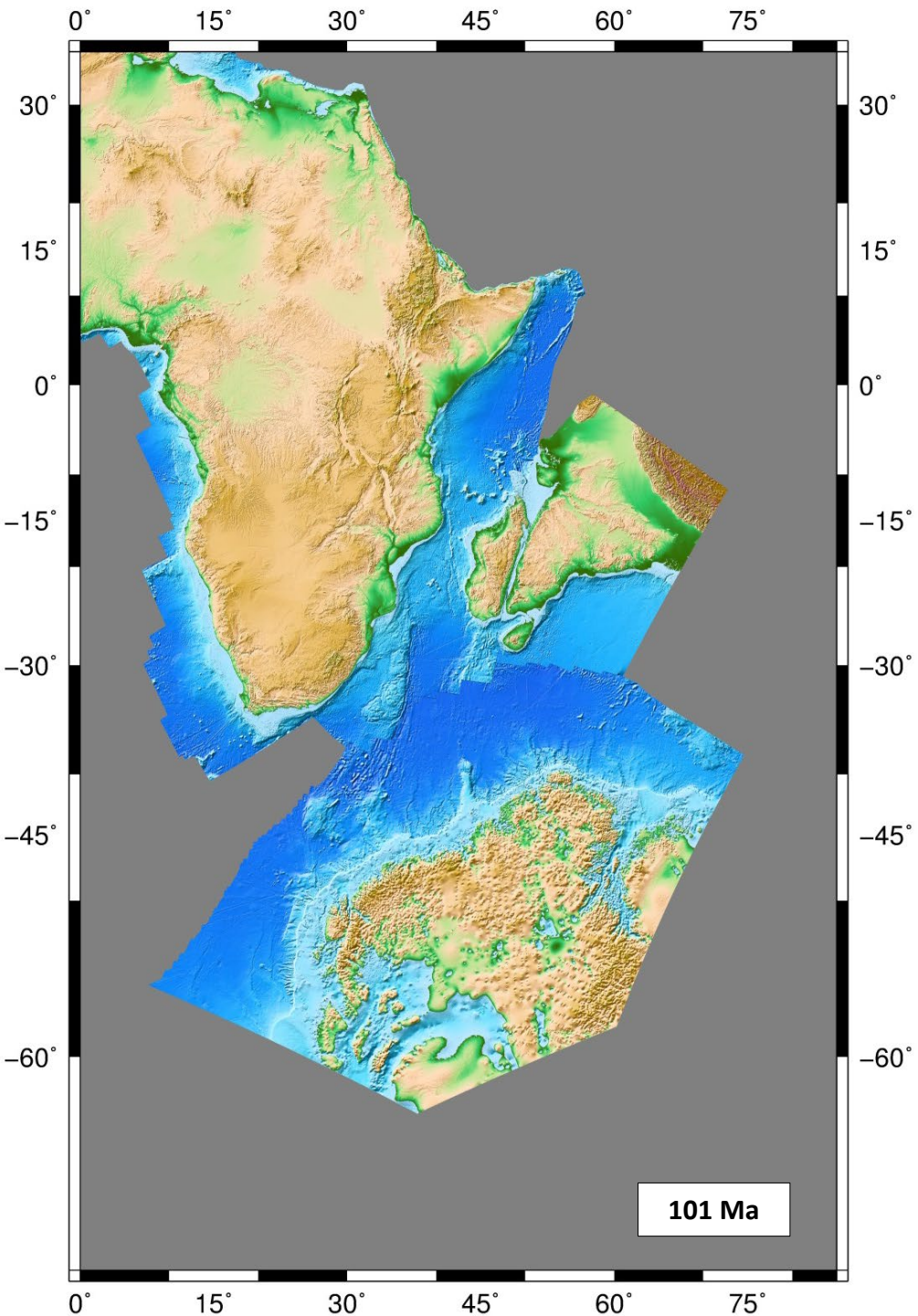
0˚
15˚
30˚
45˚
60˚
75˚
30˚
15˚
0˚
–15˚
–30˚
–45˚
–60˚
101 Ma

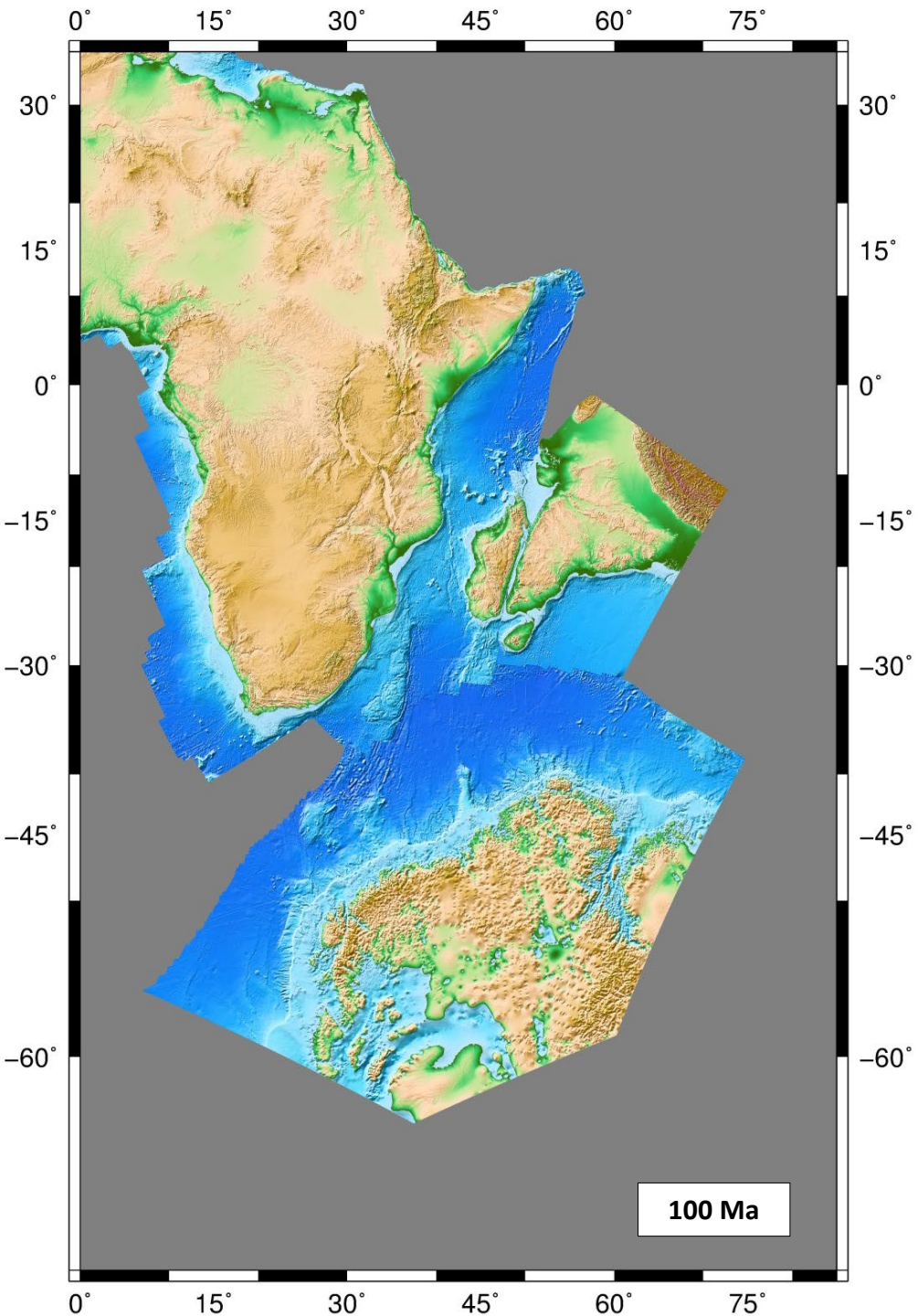
0°
15°
30°
45°
60°
75°
30°
15°
0°
−15°
−30°
−45°
−60°
100 Ma

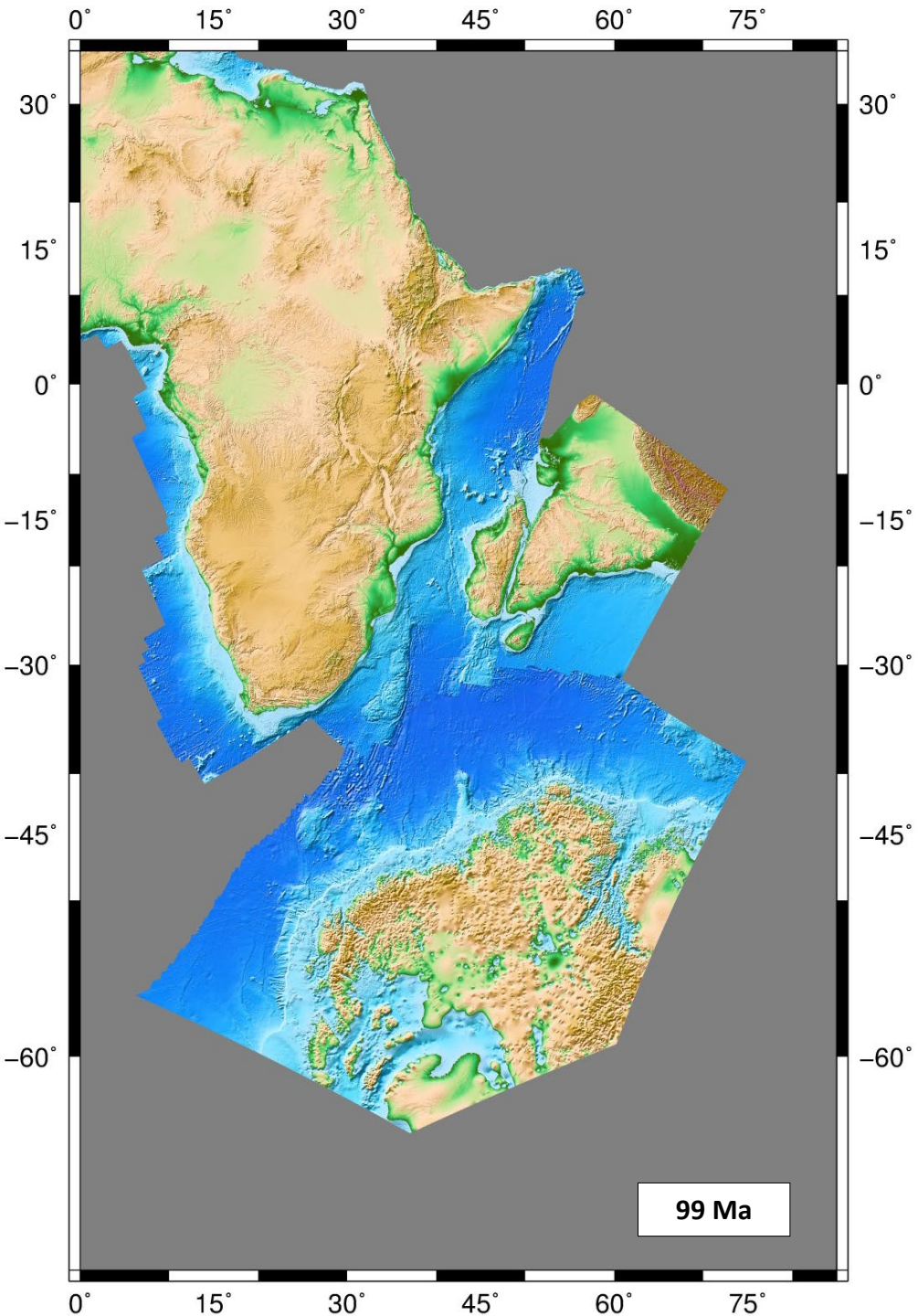
0°
15°
30°
45°
60°
75°
30°
15°
0°
−15°
−30°
−45°
−60°
99 Ma

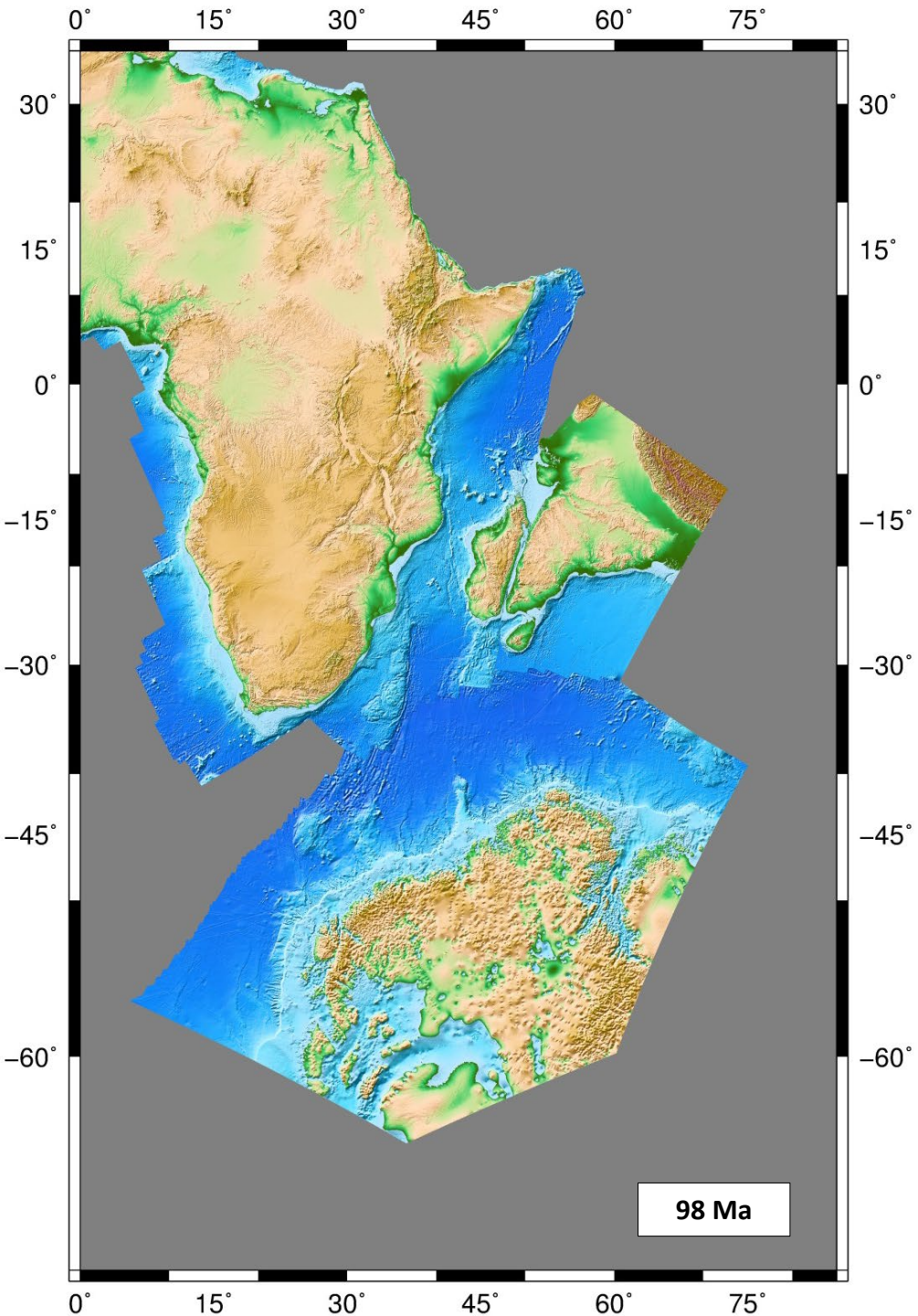
0°
15°
30°
45°
60°
75°
30°
15°
0°
−15°
−30°
−45°
−60°
98 Ma

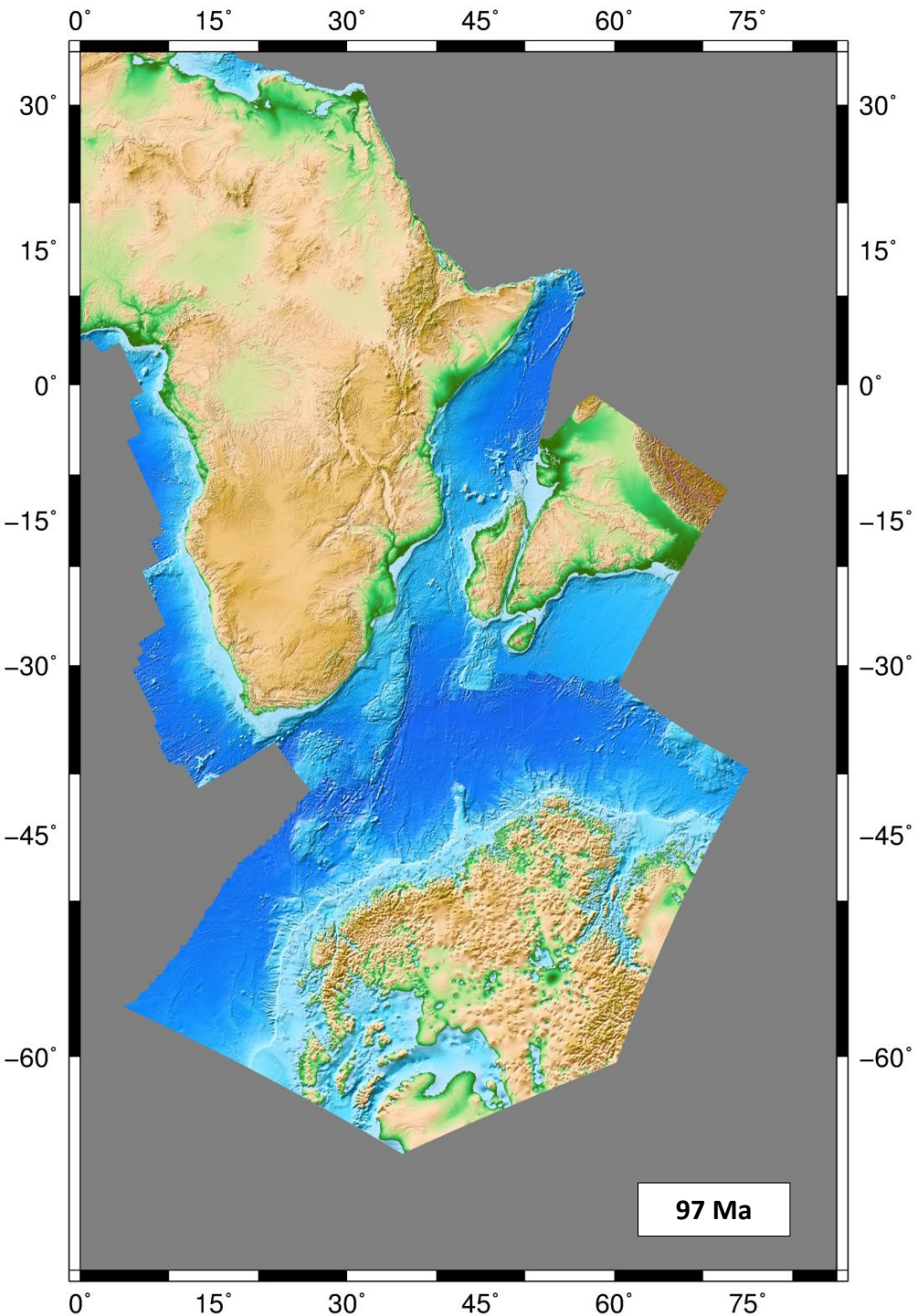
0°
15°
30°
45°
60°
75°
30°
15°
0°
−15°
−30°
−45°
−60°
97 Ma

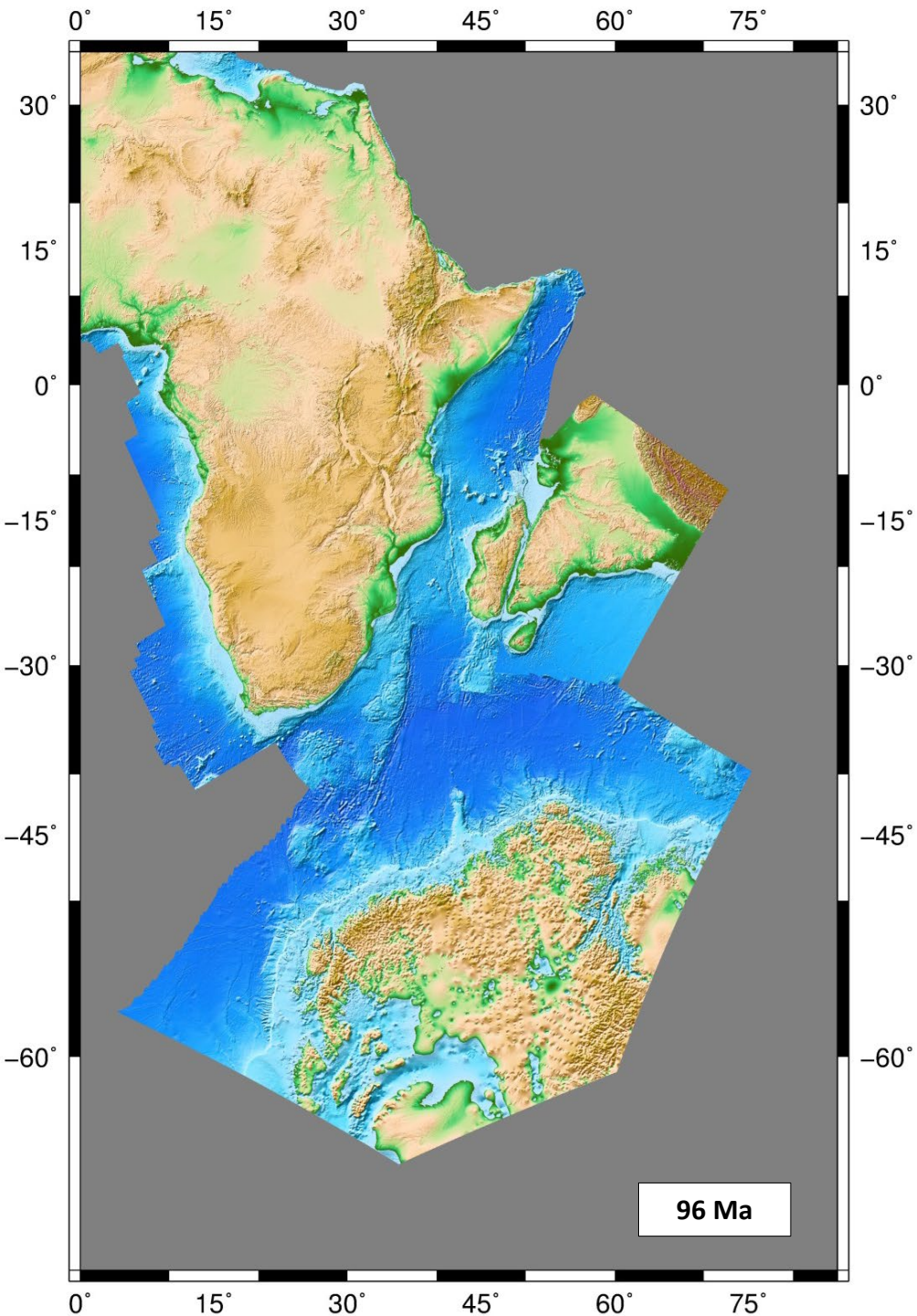
0°
15°
30°
45°
60°
75°
30°
15°
0°
−15°
−30°
−45°
−60°
96 Ma

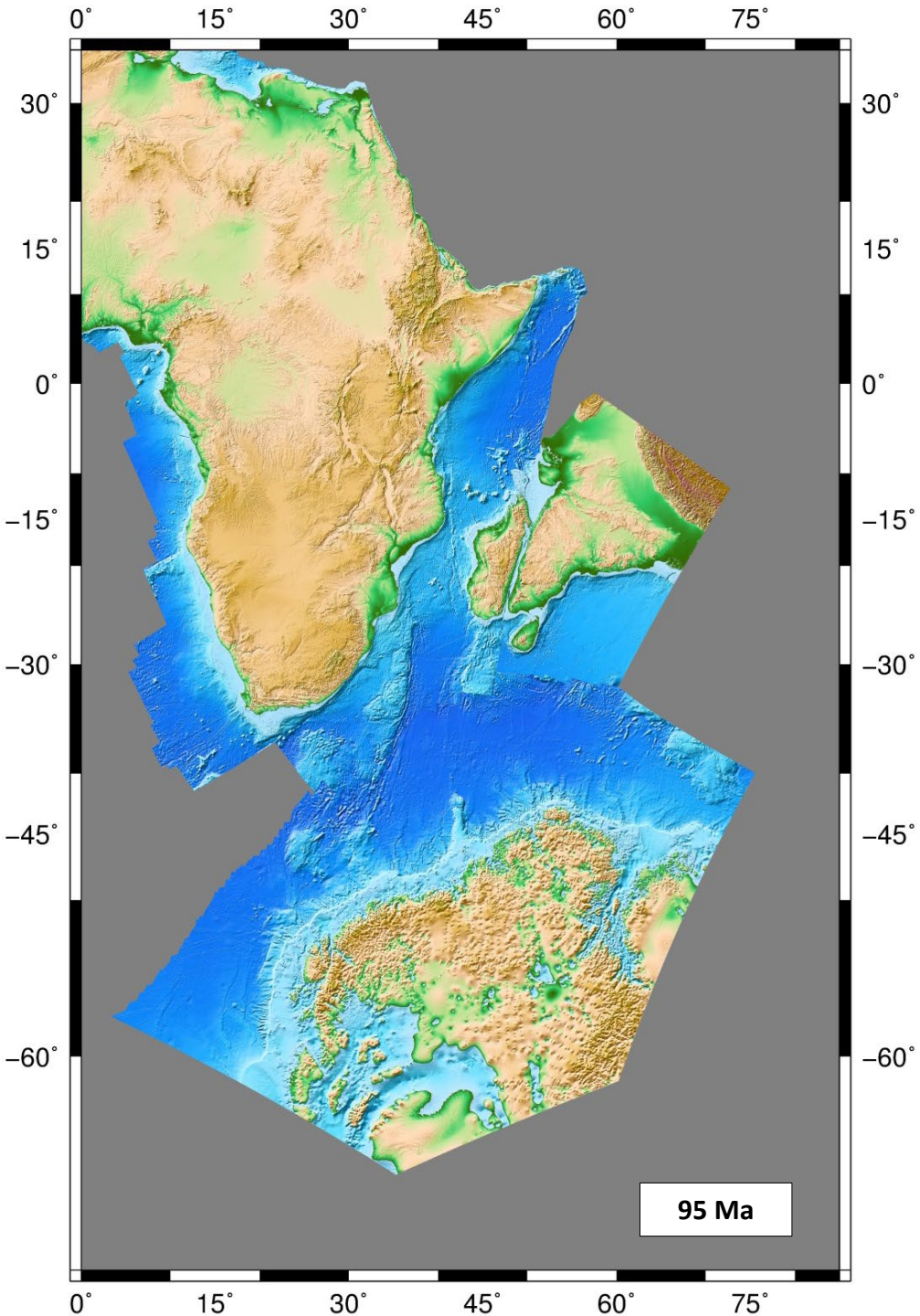
0˚
15˚
30˚
45˚
60˚
75˚
30˚
15˚
0˚
–15˚
–30˚
–45˚
–60˚
95 Ma

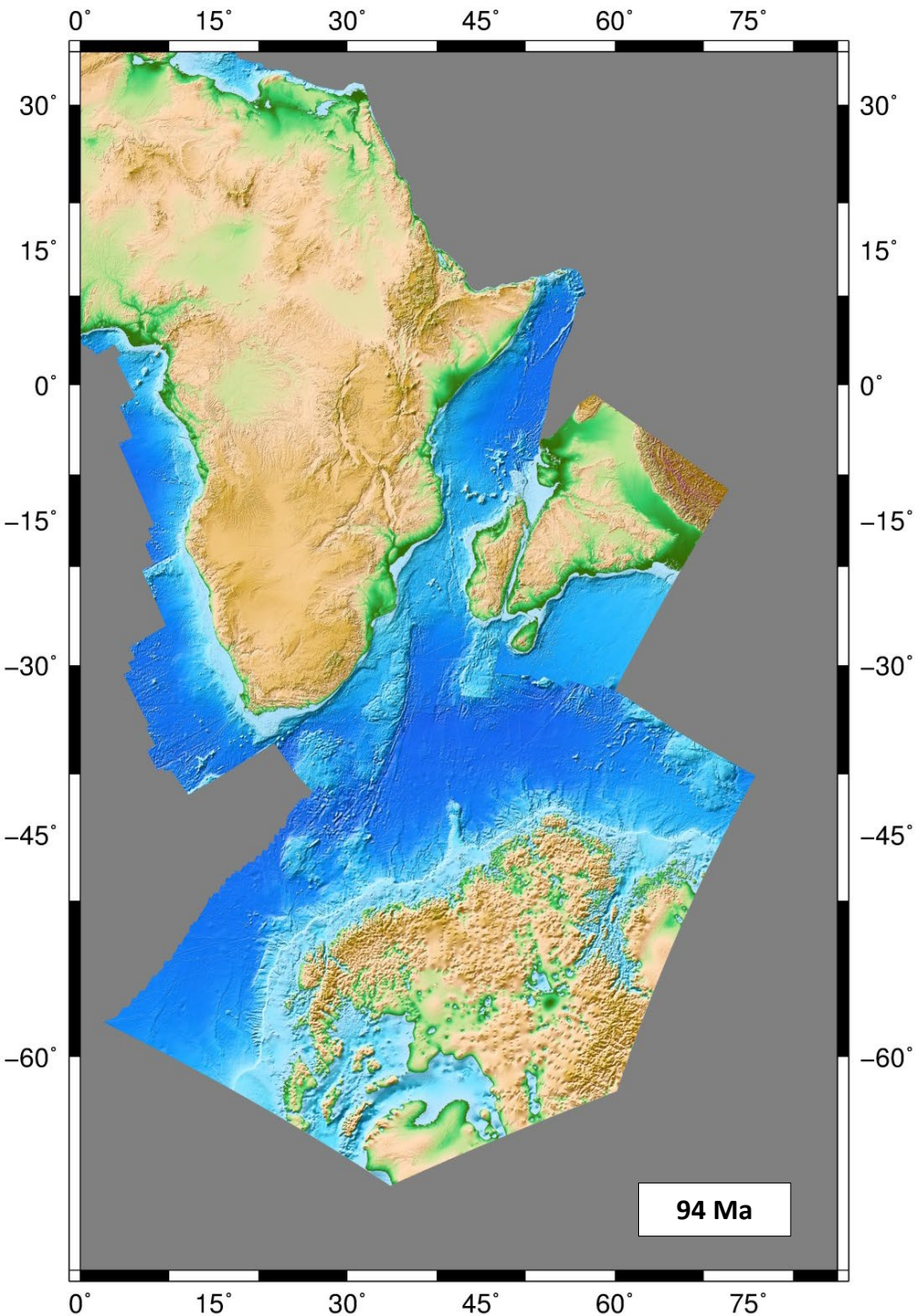
0˚
15˚
30˚
45˚
60˚
75˚
30˚
15˚
0˚
–15˚
–30˚
–45˚
–60˚
94 Ma

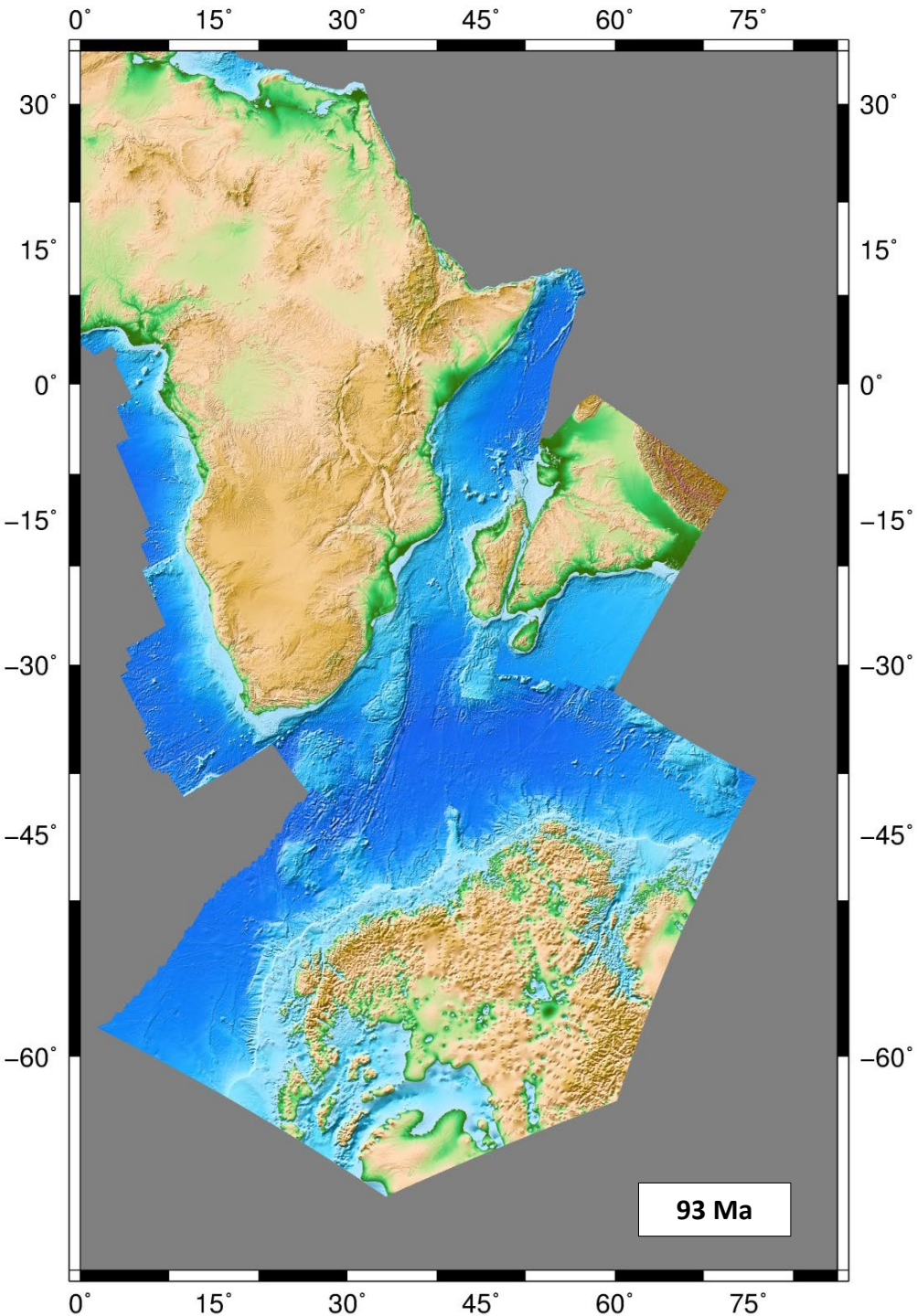
0°
15°
30°
45°
60°
75°
30°
15°
0°
−15°
−30°
−45°
−60°
93 Ma

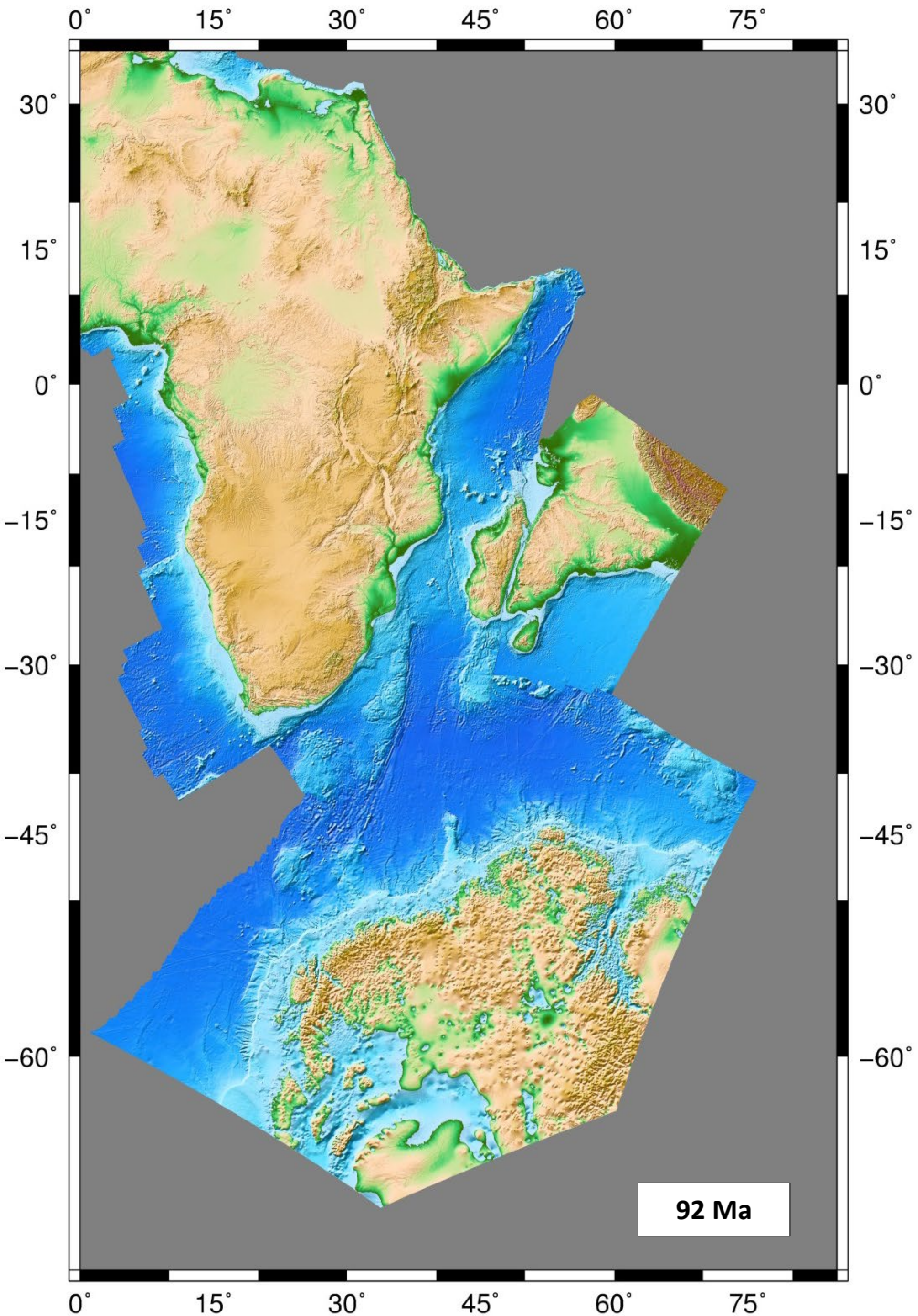
0°
15°
30°
45°
60°
75°
30°
15°
0°
−15°
−30°
−45°
−60°
92 Ma

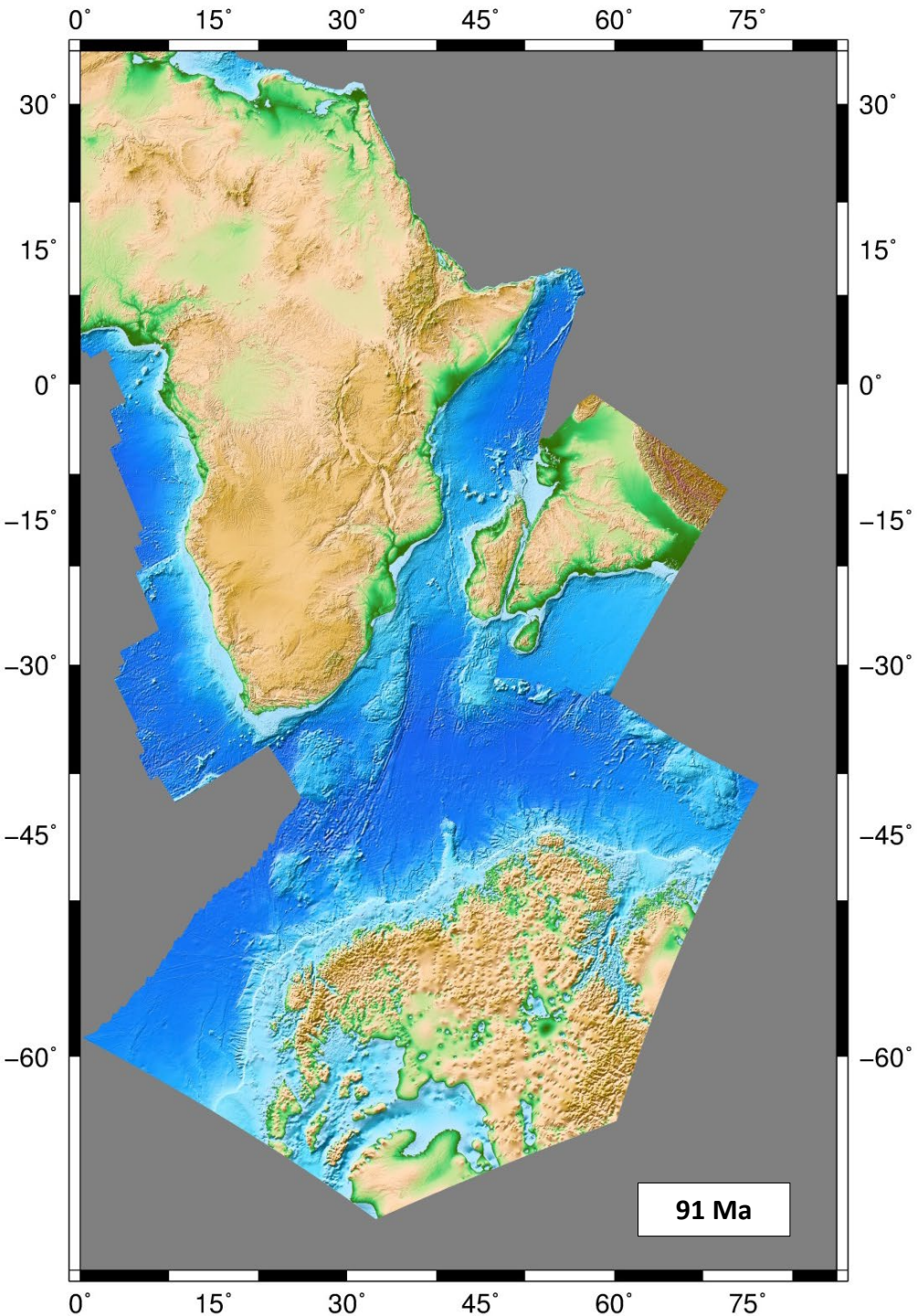
0˚
15˚
30˚
45˚
60˚
75˚
30˚
15˚
0˚
–15˚
–30˚
–45˚
–60˚
91 Ma

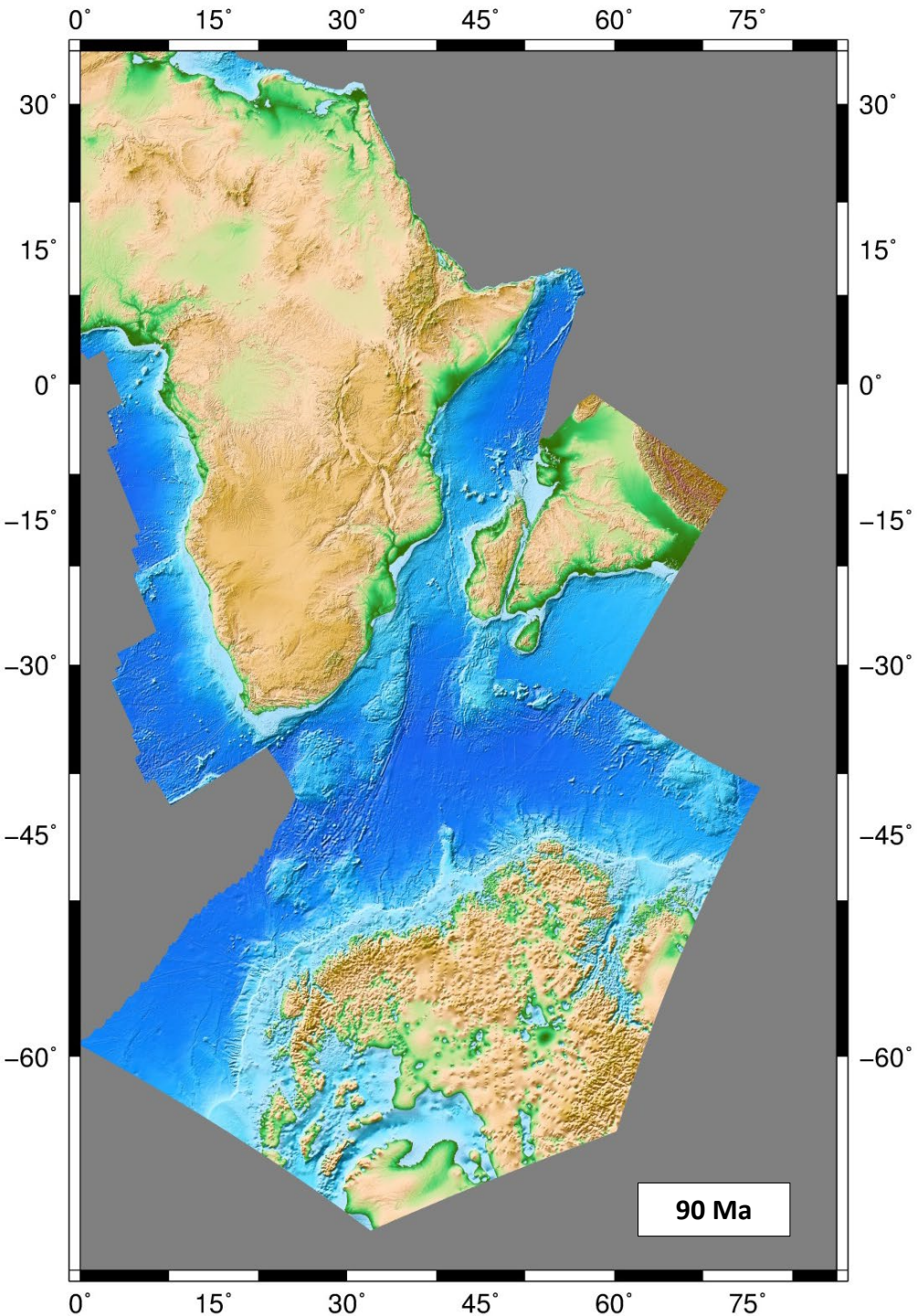
0°
15°
30°
45°
60°
75°
30°
15°
0°
−15°
−30°
−45°
−60°
90 Ma

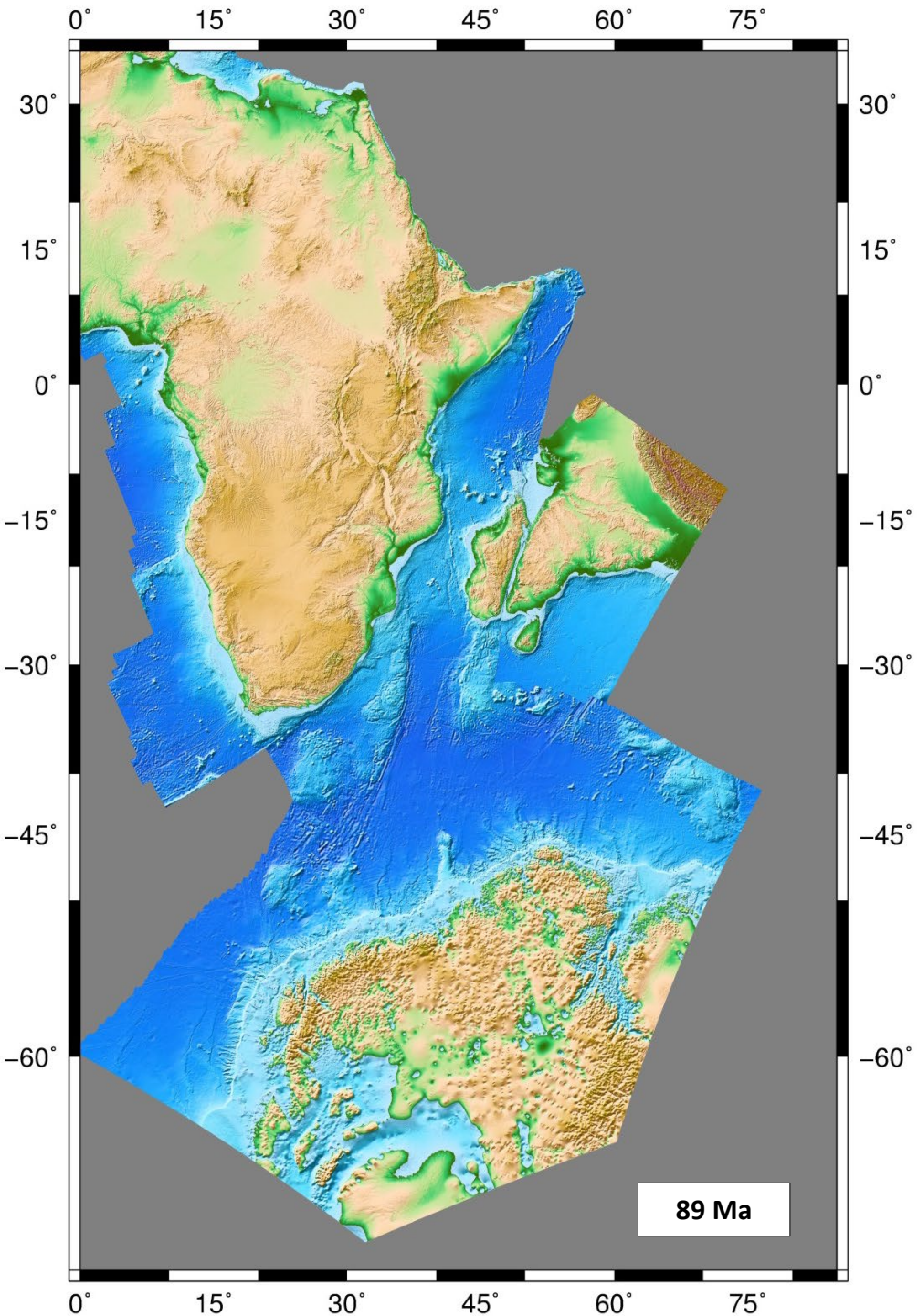
0°
15°
30°
45°
60°
75°
30°
15°
0°
−15°
−30°
−45°
−60°
89 Ma

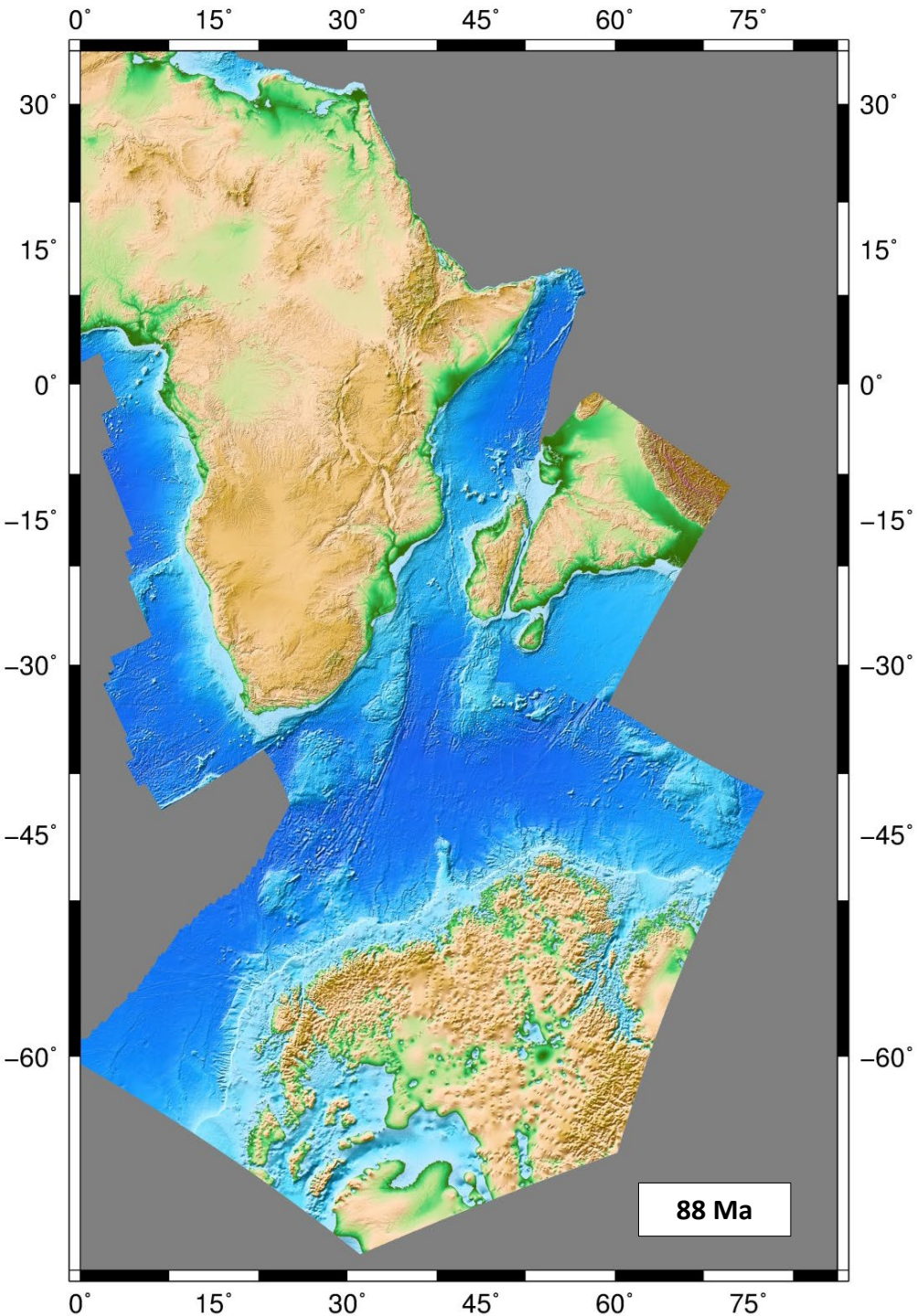
0°
15°
30°
45°
60°
75°
30°
15°
0°
−15°
−30°
−45°
−60°
88 Ma

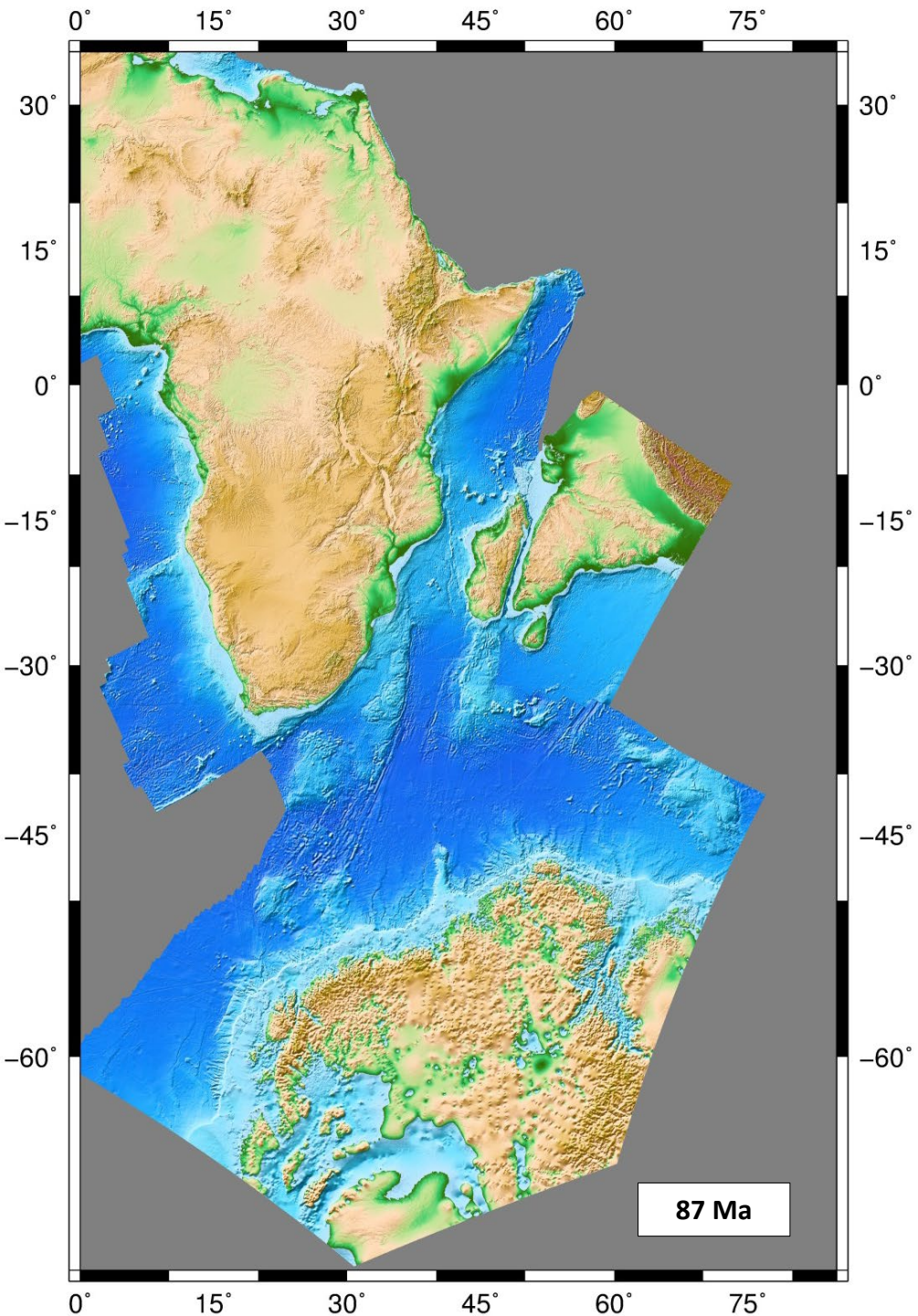
0°
15°
30°
45°
60°
75°
30°
15°
0°
−15°
−30°
−45°
−60°
87 Ma

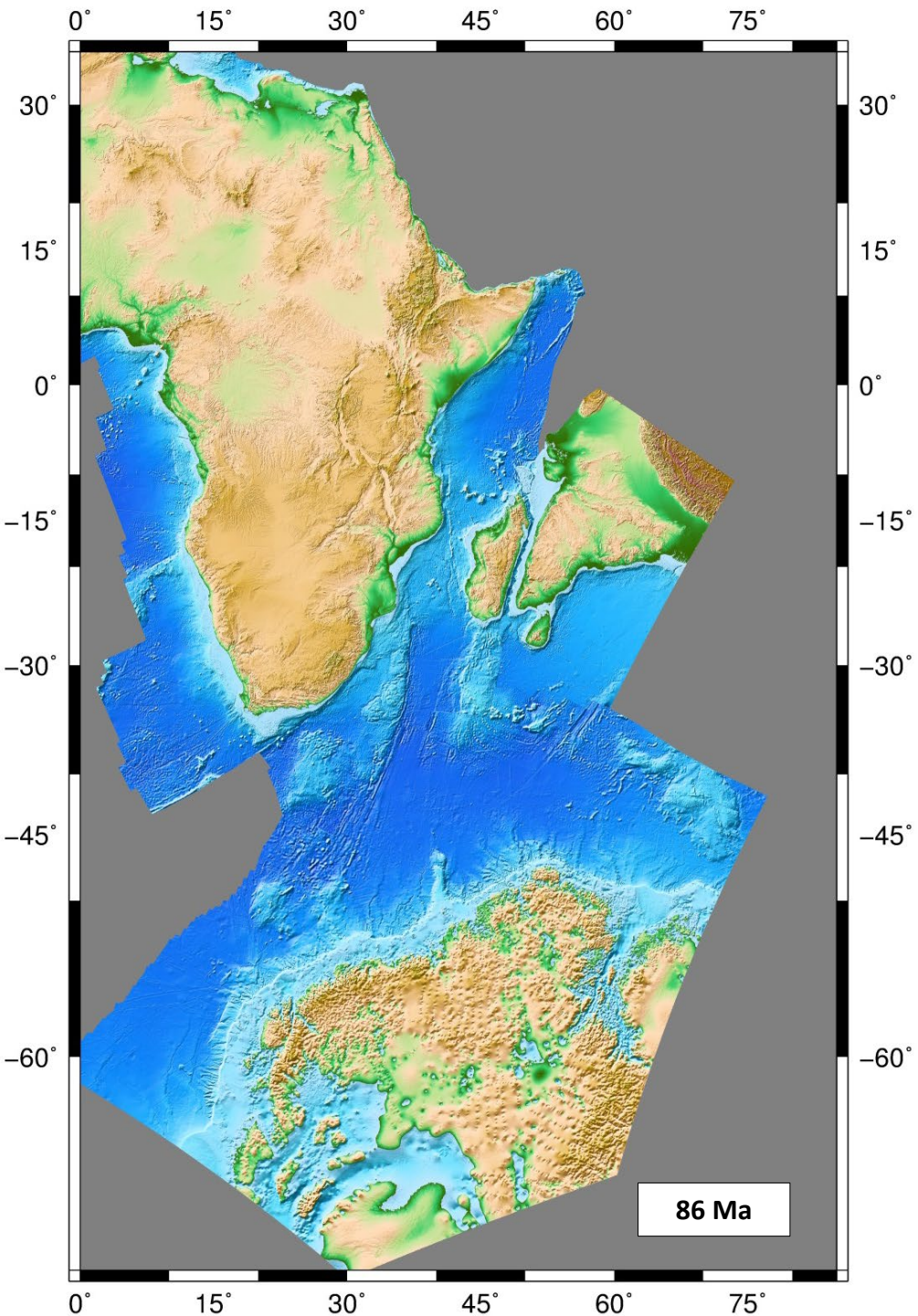
0˚
15˚
30˚
45˚
60˚
75˚
30˚
15˚
0˚
–15˚
–30˚
–45˚
–60˚
86 Ma

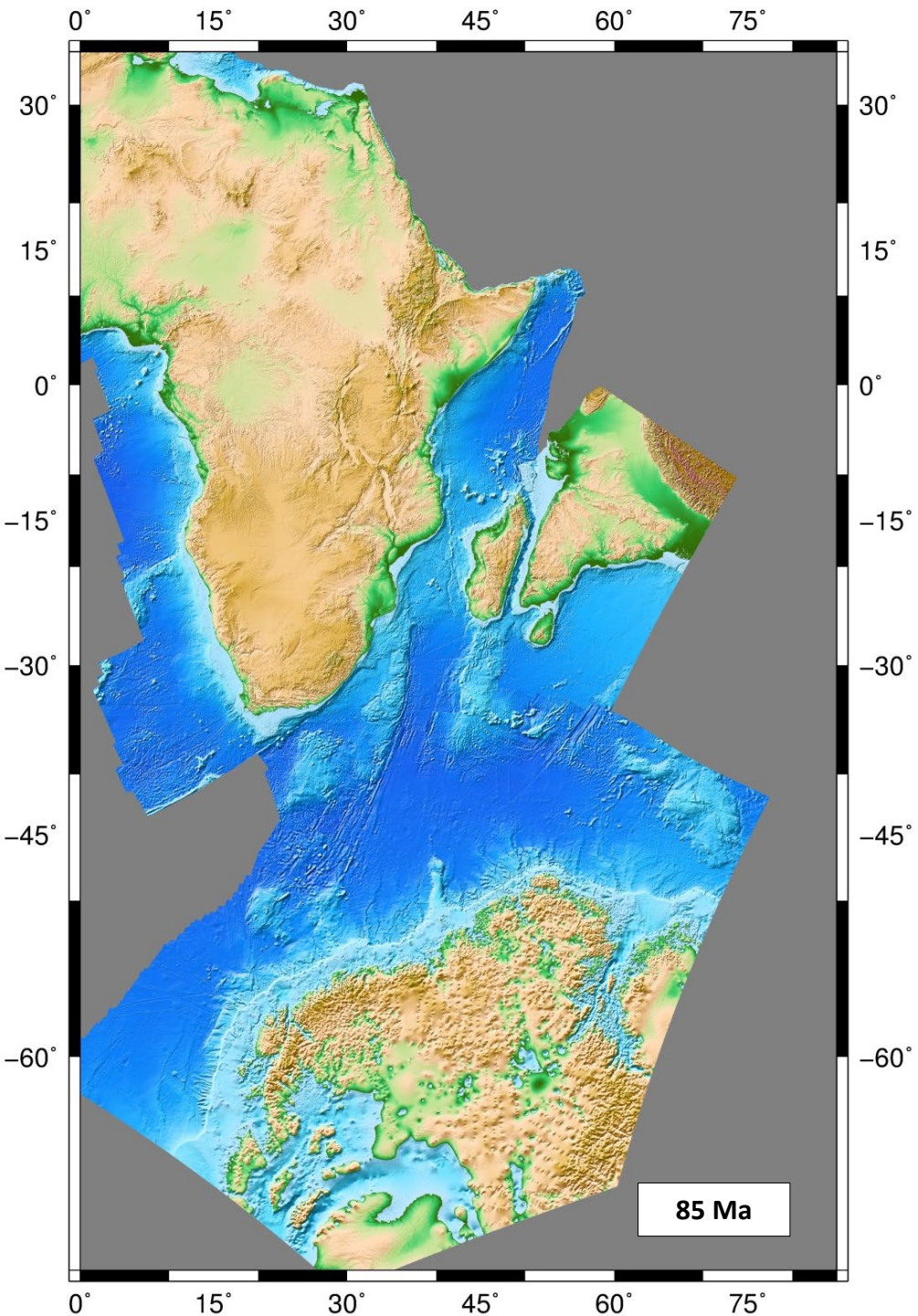
0°
15°
30°
45°
60°
75°
30°
15°
0°
−15°
−30°
−45°
−60°
85 Ma

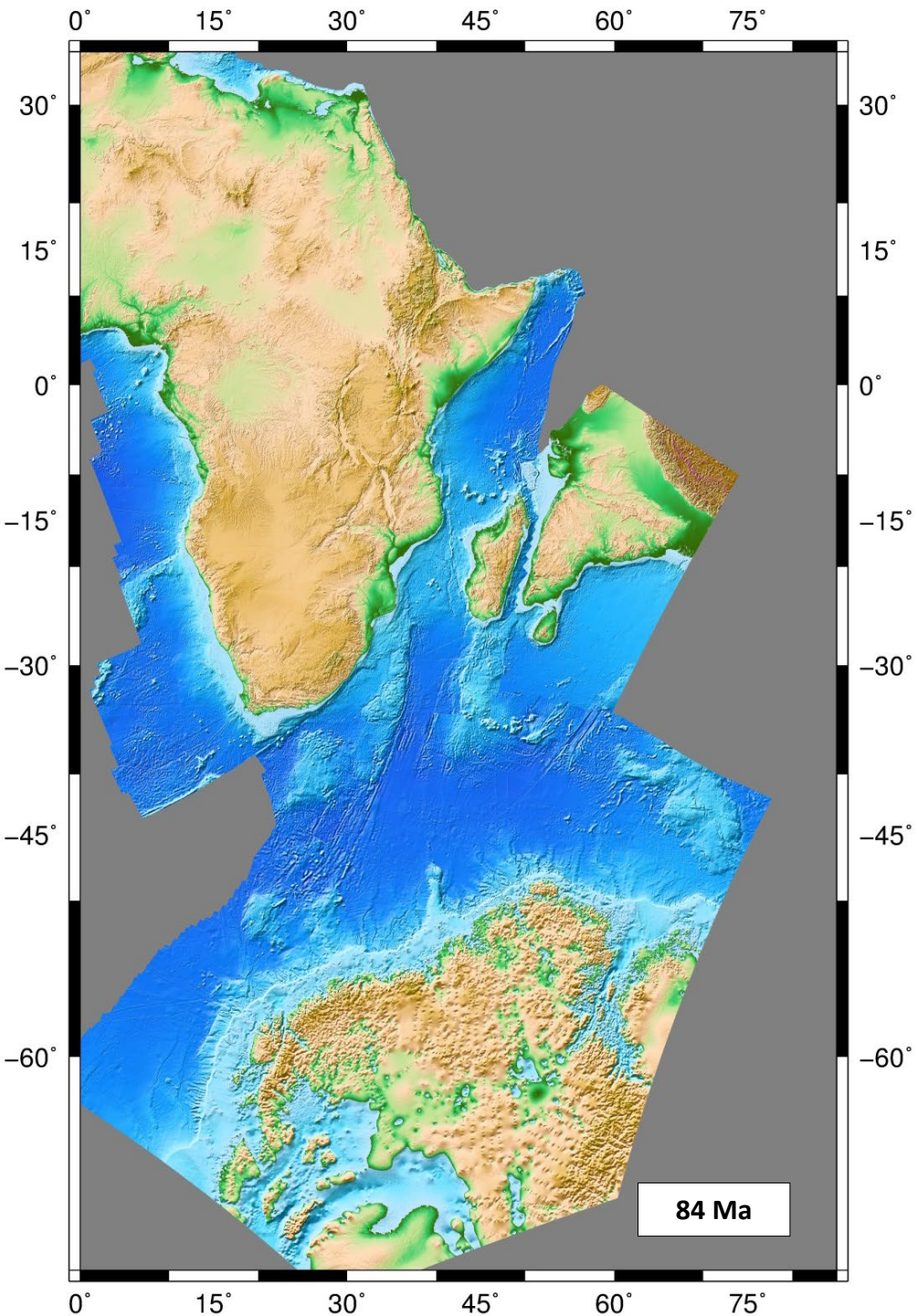
0°
15°
30°
45°
60°
75°
30°
15°
0°
−15°
−30°
−45°
−60°
84 Ma

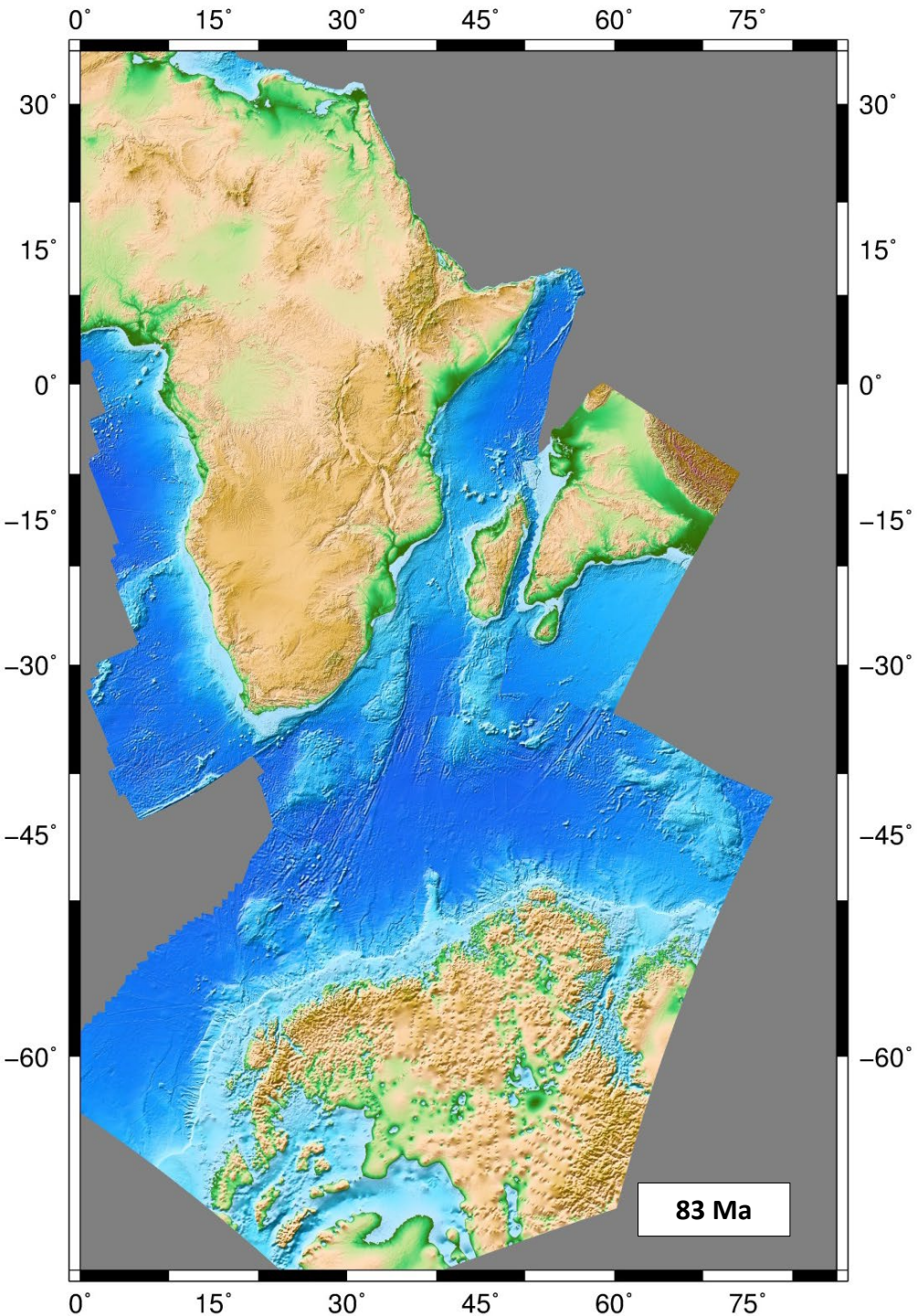
0°
15°
30°
45°
60°
75°
30°
15°
0°
−15°
−30°
−45°
−60°
83 Ma

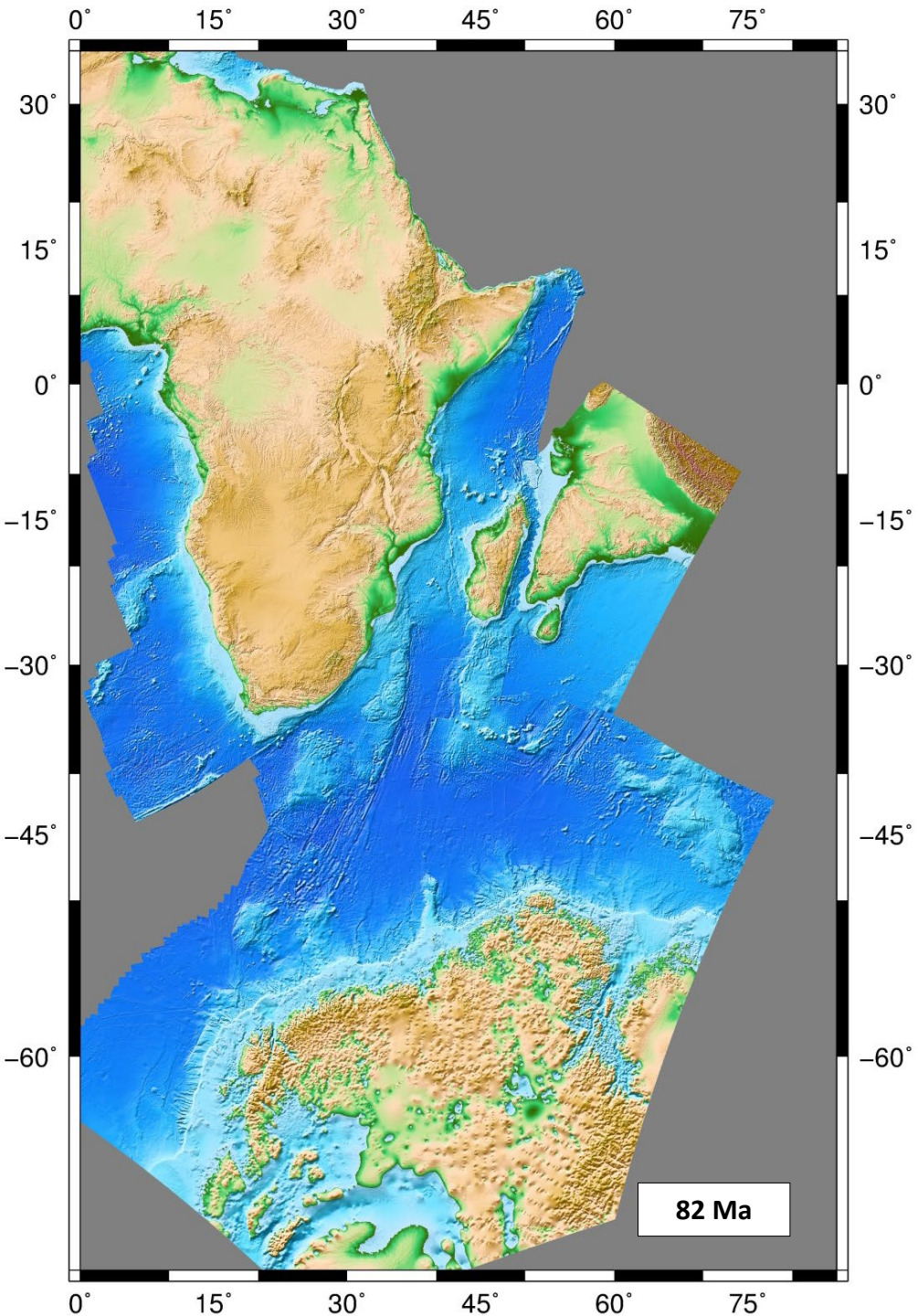
0°
15°
30°
45°
60°
75°
30°
15°
0°
−15°
−30°
−45°
−60°
82 Ma

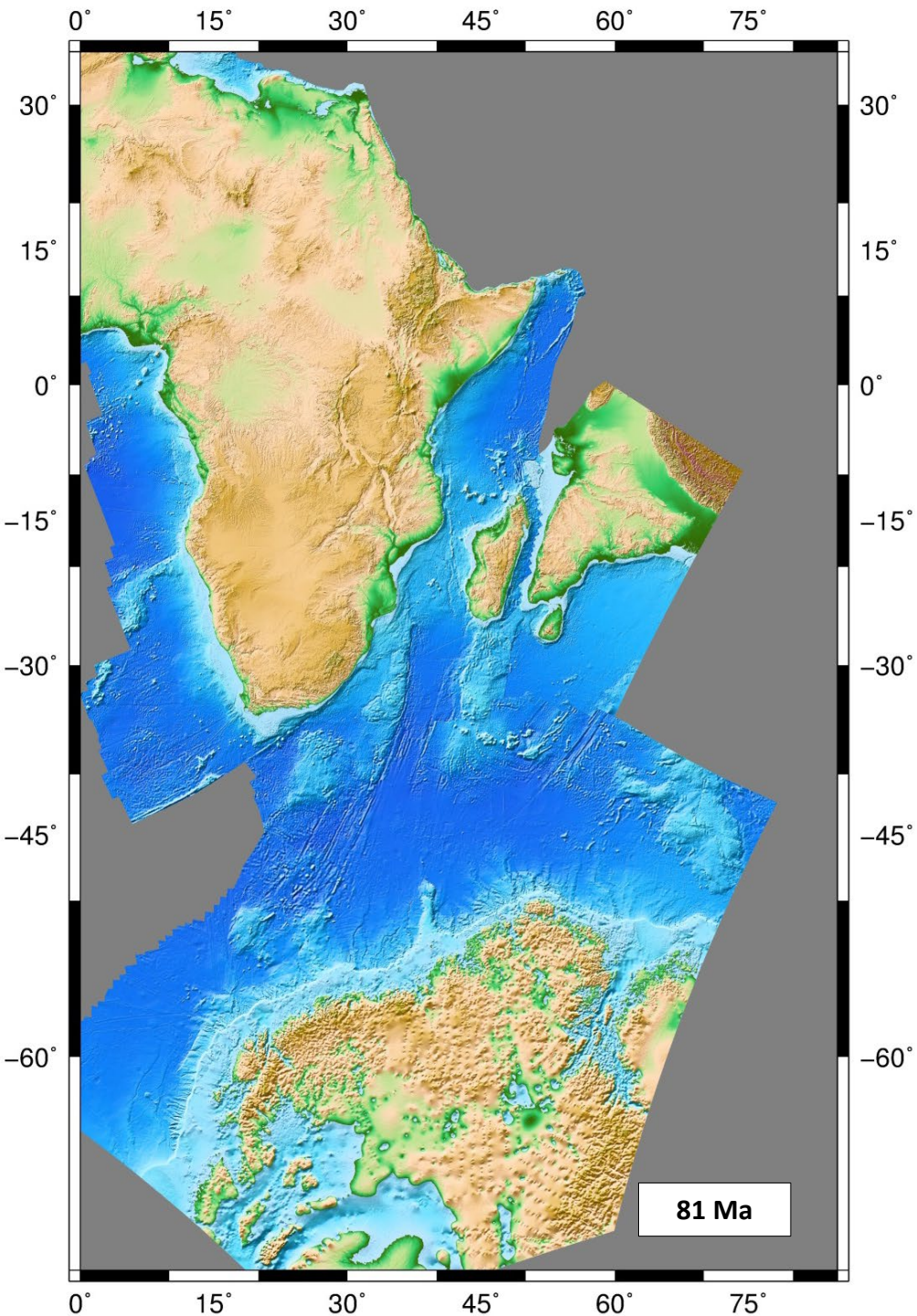
0°
15°
30°
45°
60°
75°
30°
15°
0°
−15°
−30°
−45°
−60°
81 Ma

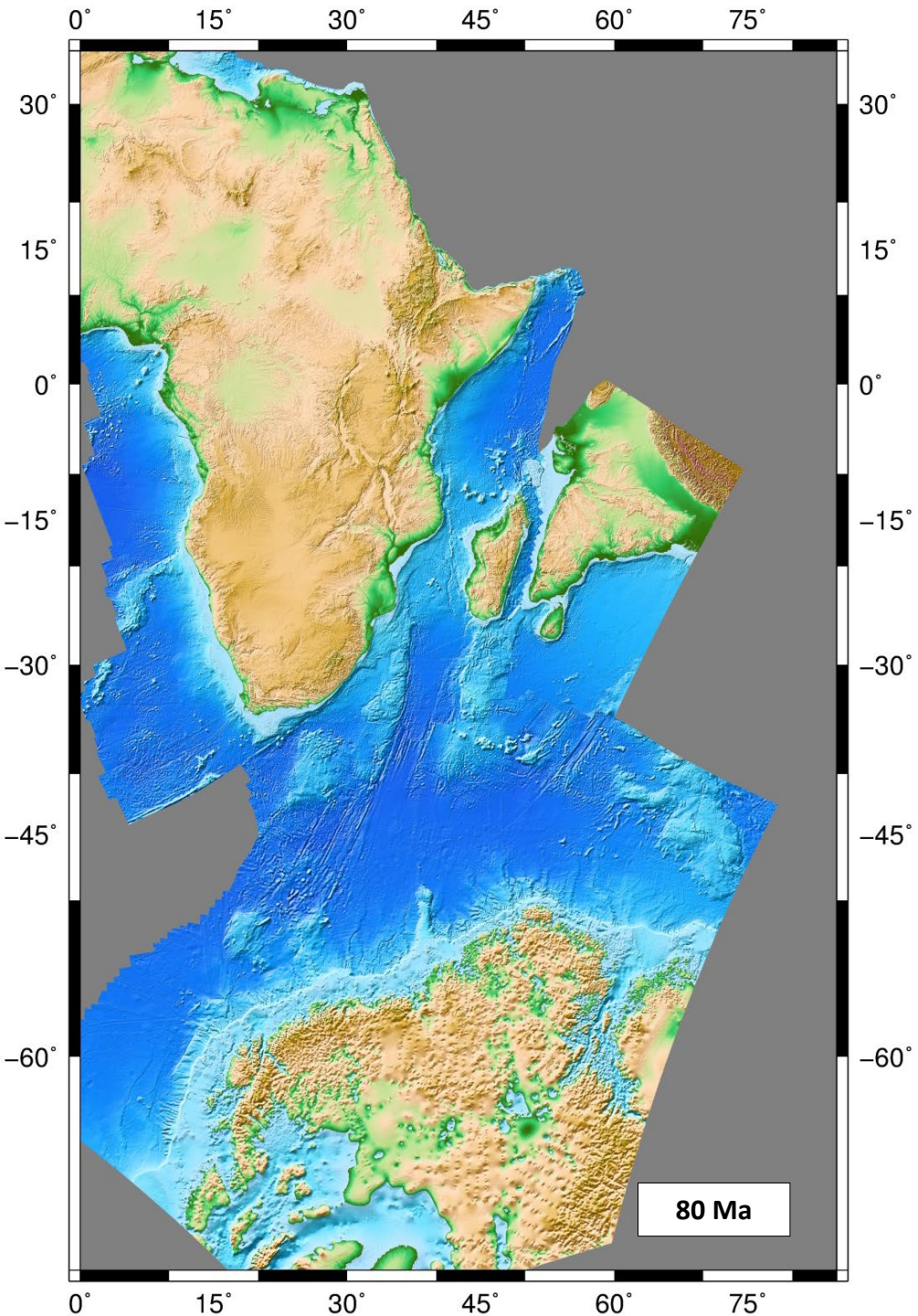
0°
15°
30°
45°
60°
75°
30°
15°
0°
−15°
−30°
−45°
−60°
80 Ma

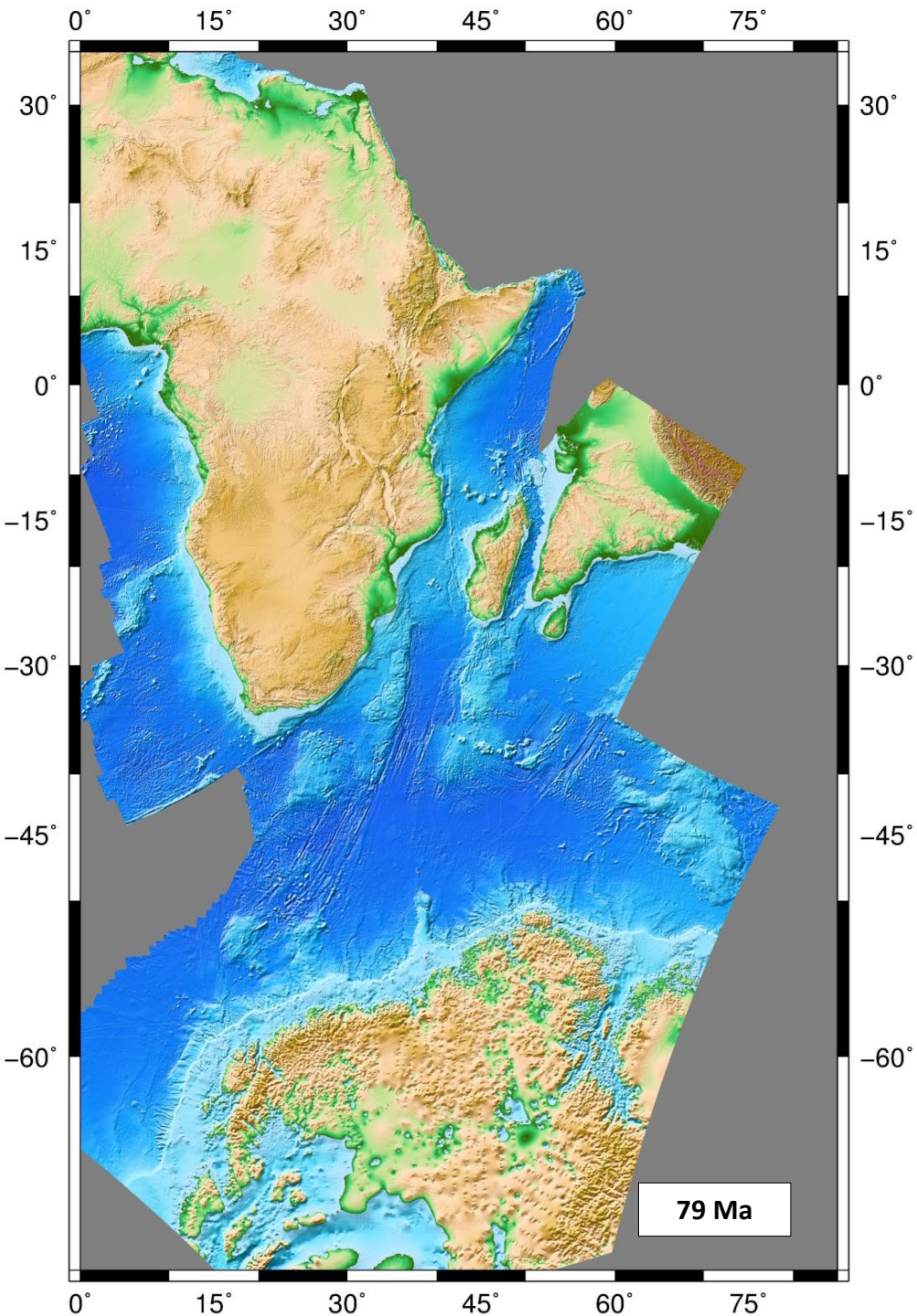
0°
15°
30°
45°
60°
75°
30°
15°
0°
−15°
−30°
−45°
−60°
79 Ma

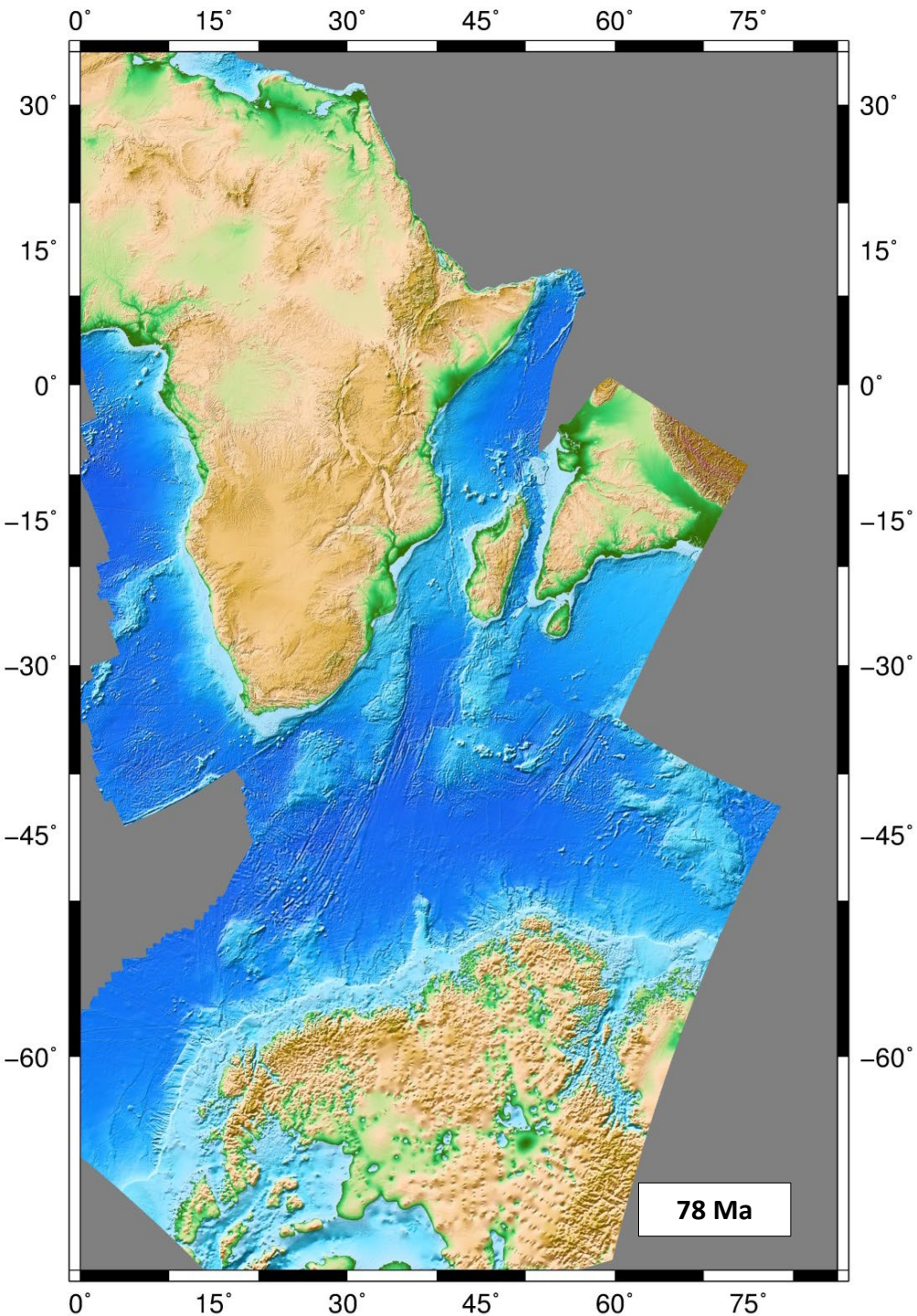
0°
15°
30°
45°
60°
75°
30°
15°
0°
−15°
−30°
−45°
−60°
78 Ma

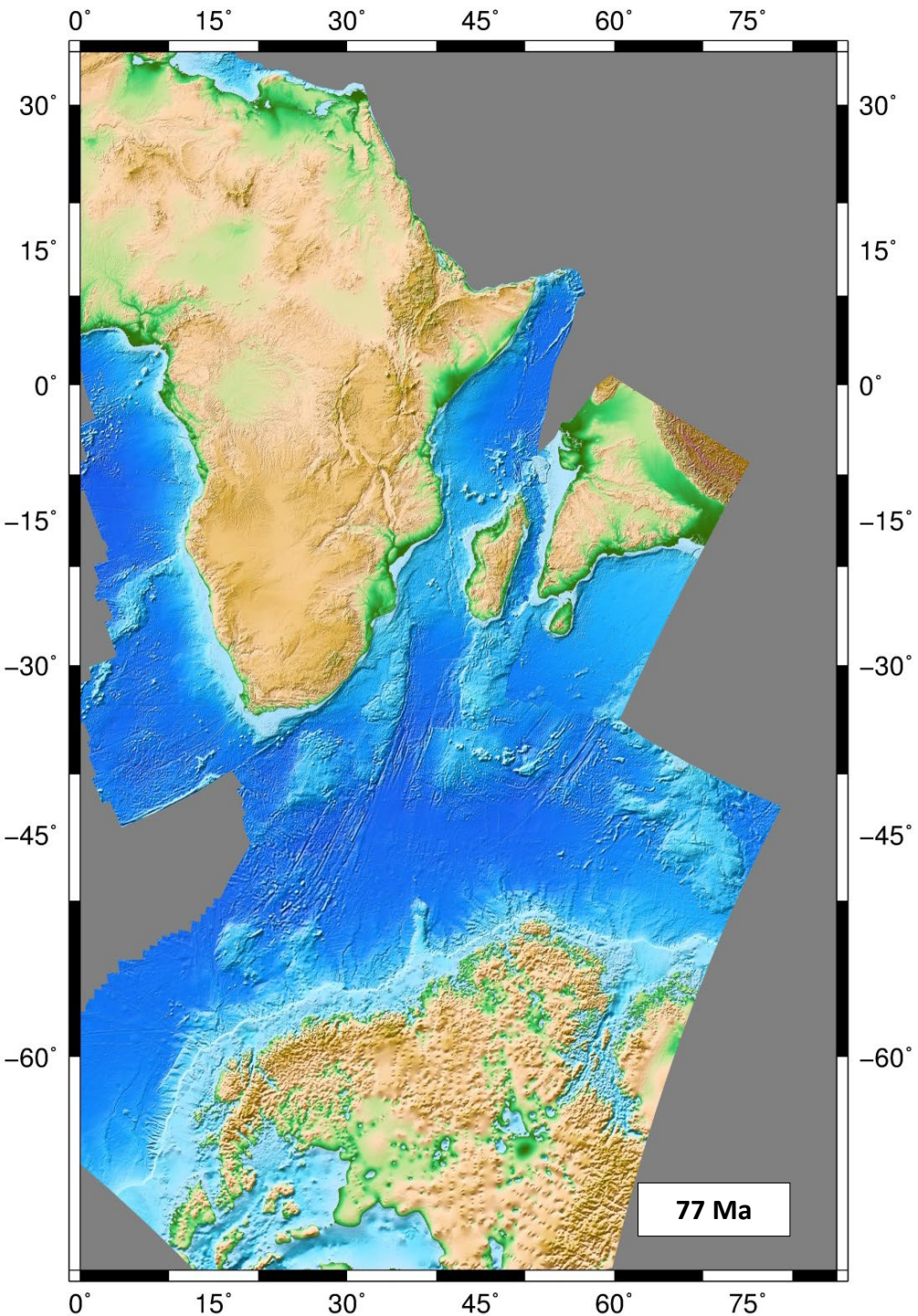
0°
15°
30°
45°
60°
75°
30°
15°
0°
−15°
−30°
−45°
−60°
77 Ma

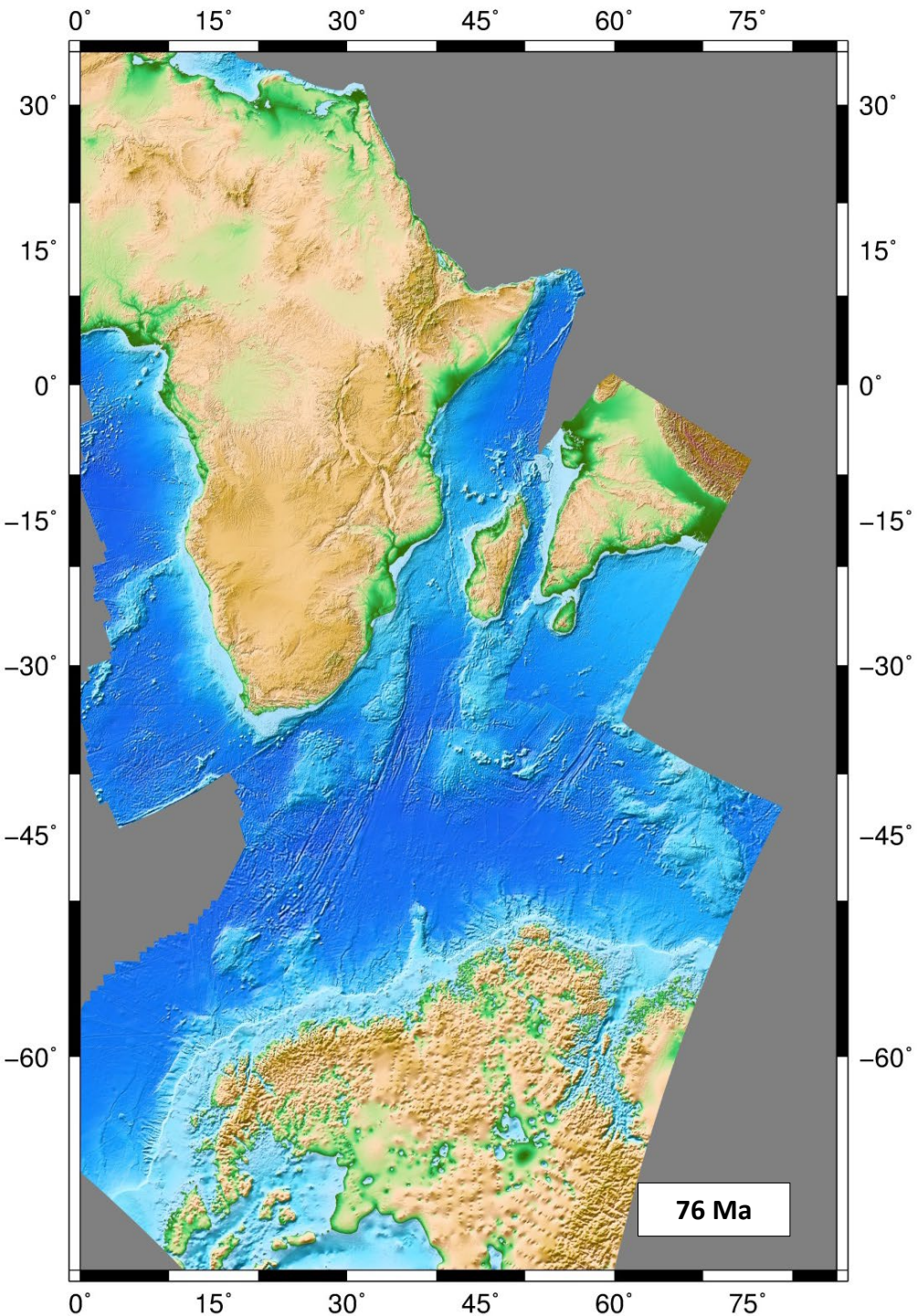
0°
15°
30°
45°
60°
75°
30°
15°
0°
−15°
−30°
−45°
−60°
76 Ma

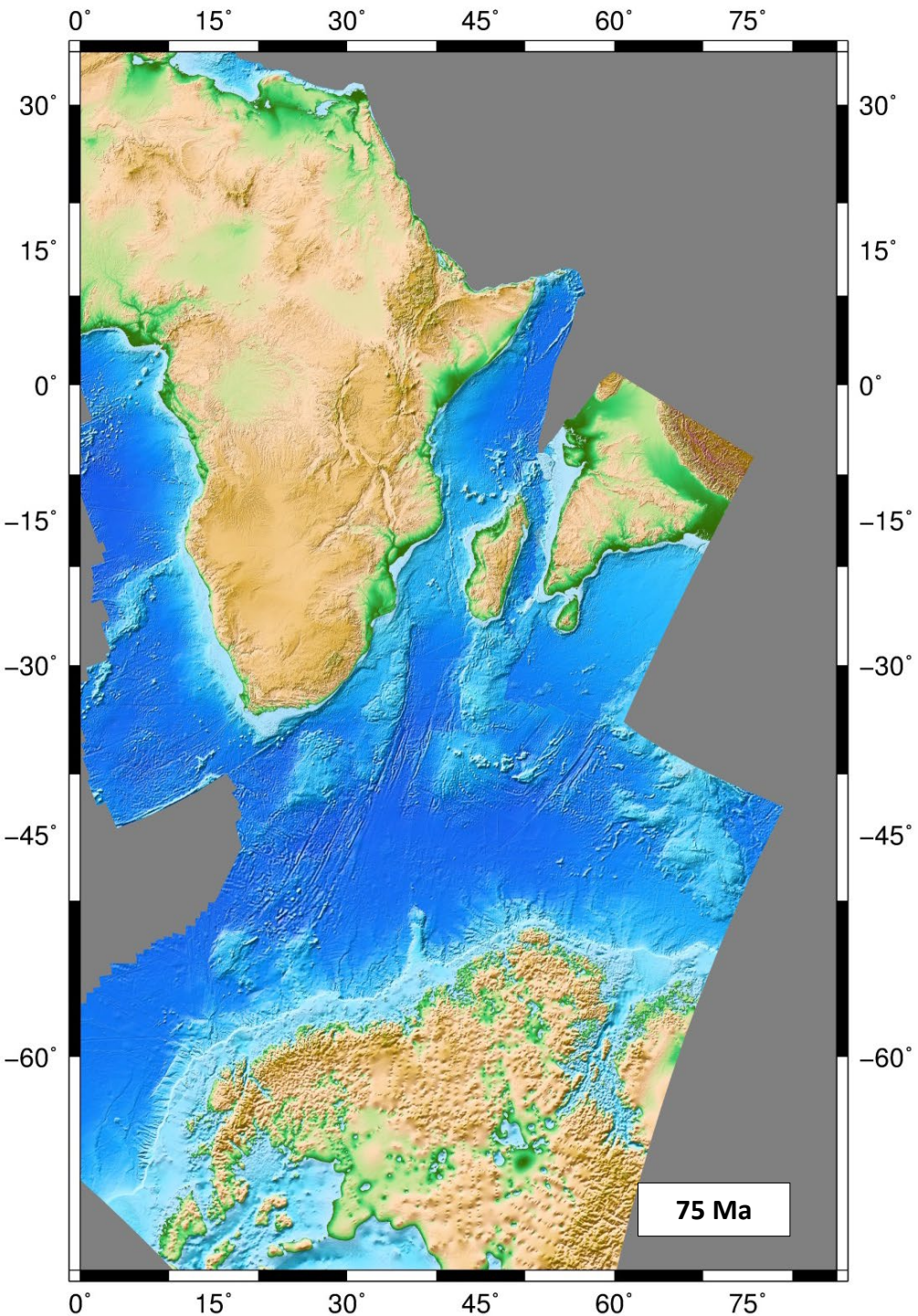
0°
15°
30°
45°
60°
75°
30°
15°
0°
−15°
−30°
−45°
−60°
75 Ma

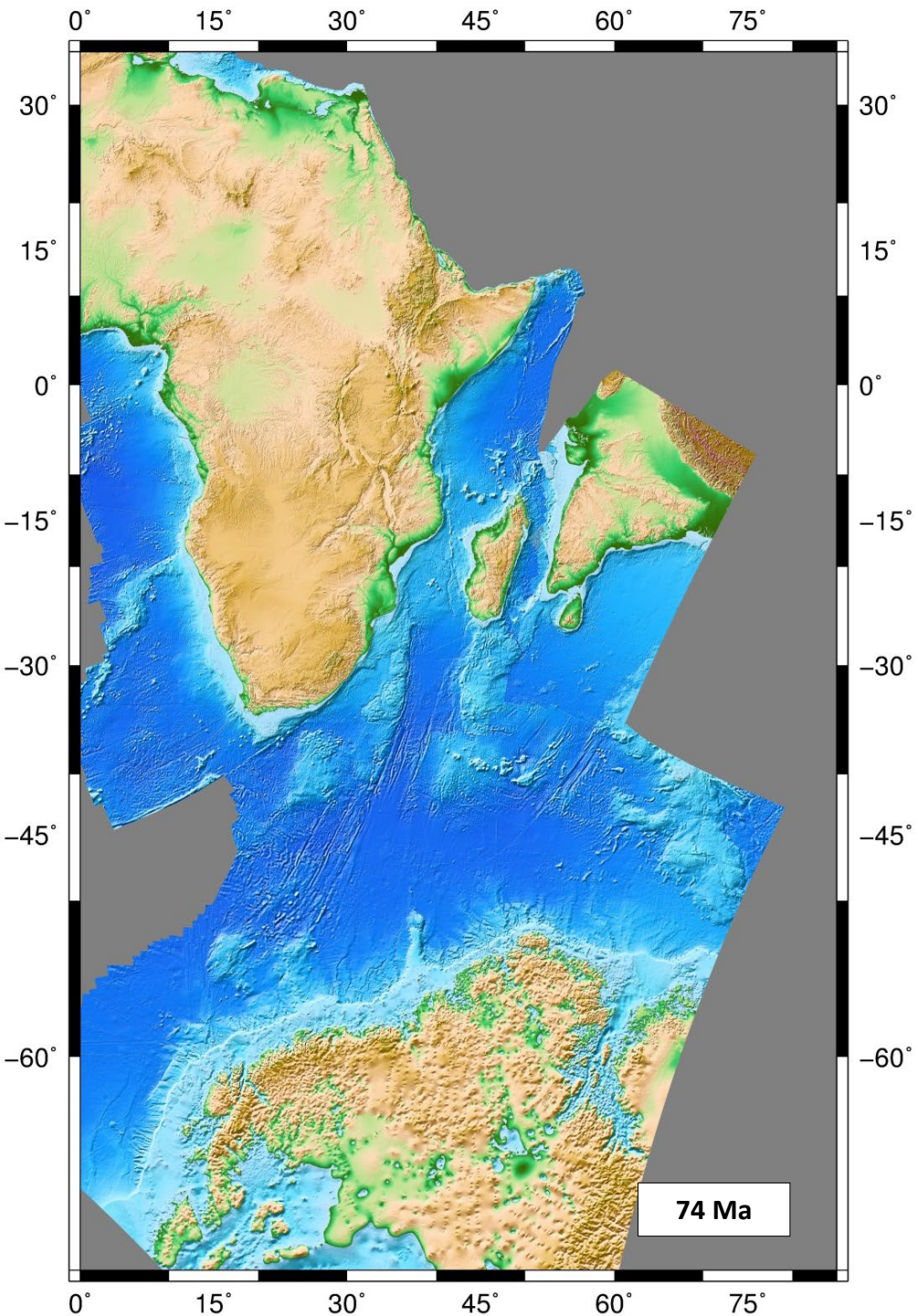
0˚
15˚
30˚
45˚
60˚
75˚
30˚
15˚
0˚
–15˚
–30˚
–45˚
–60˚
74 Ma

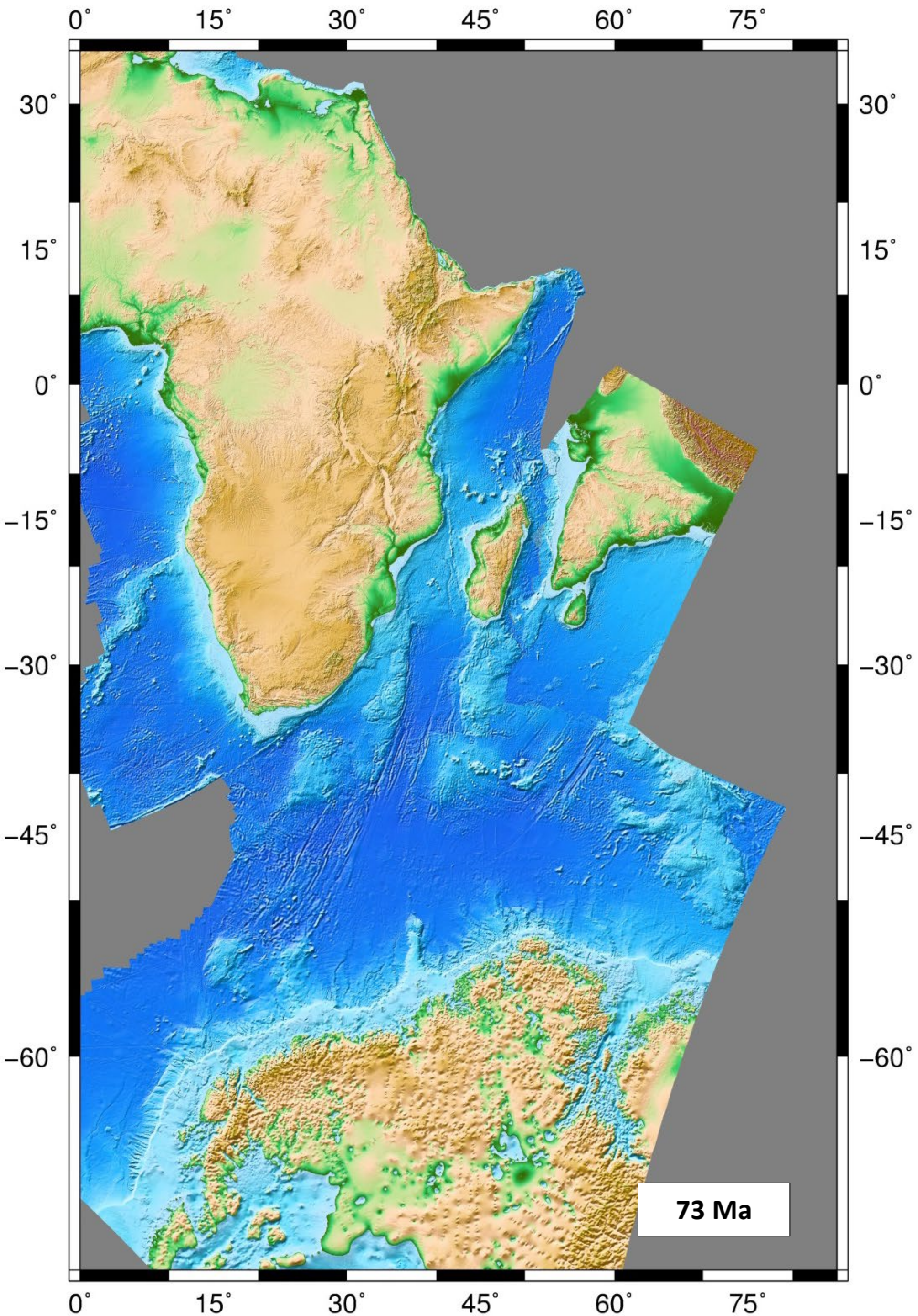
0°
15°
30°
45°
60°
75°
30°
15°
0°
−15°
−30°
−45°
−60°
73 Ma

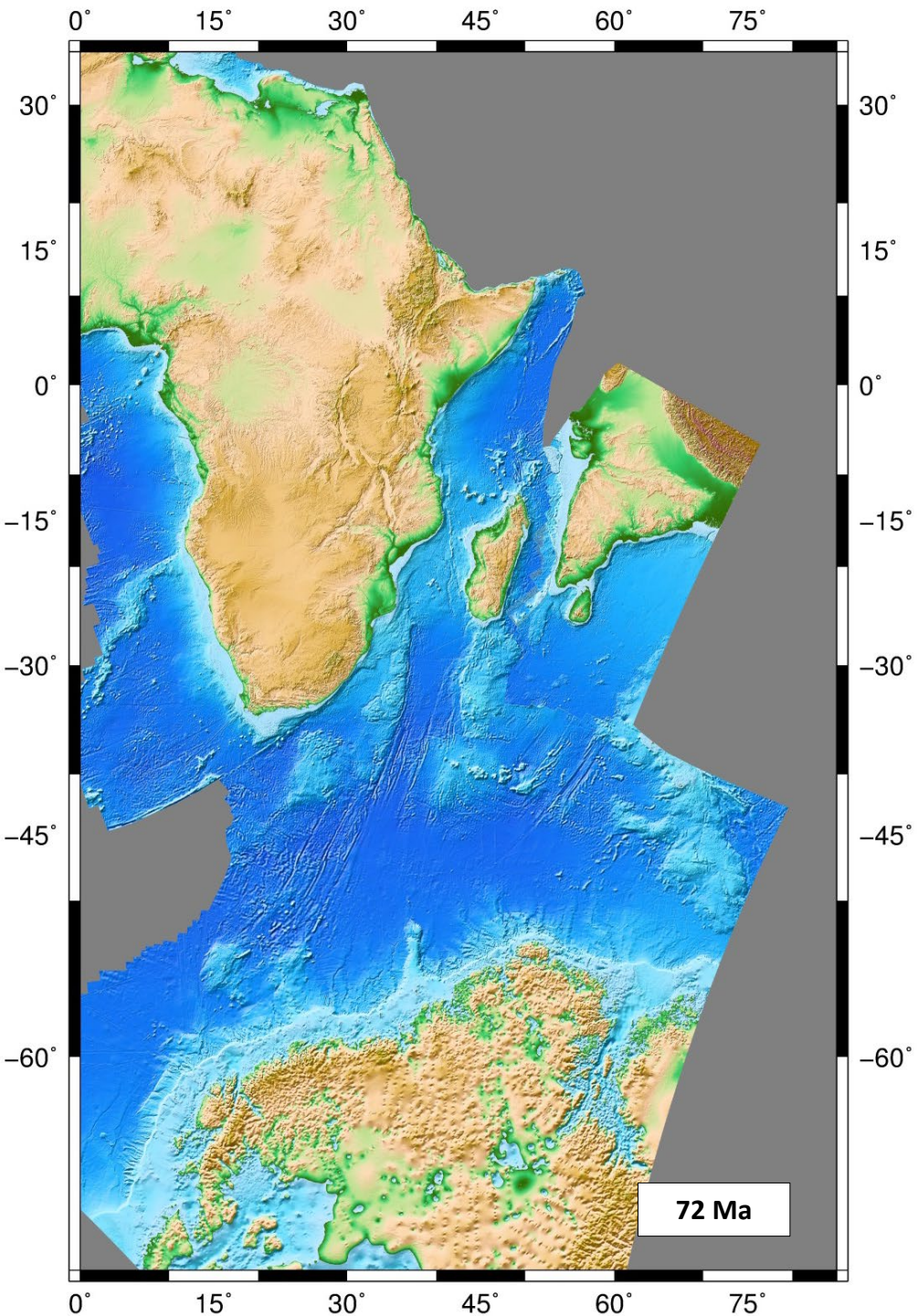
0°
15°
30°
45°
60°
75°
30°
15°
0°
−15°
−30°
−45°
−60°
72 Ma

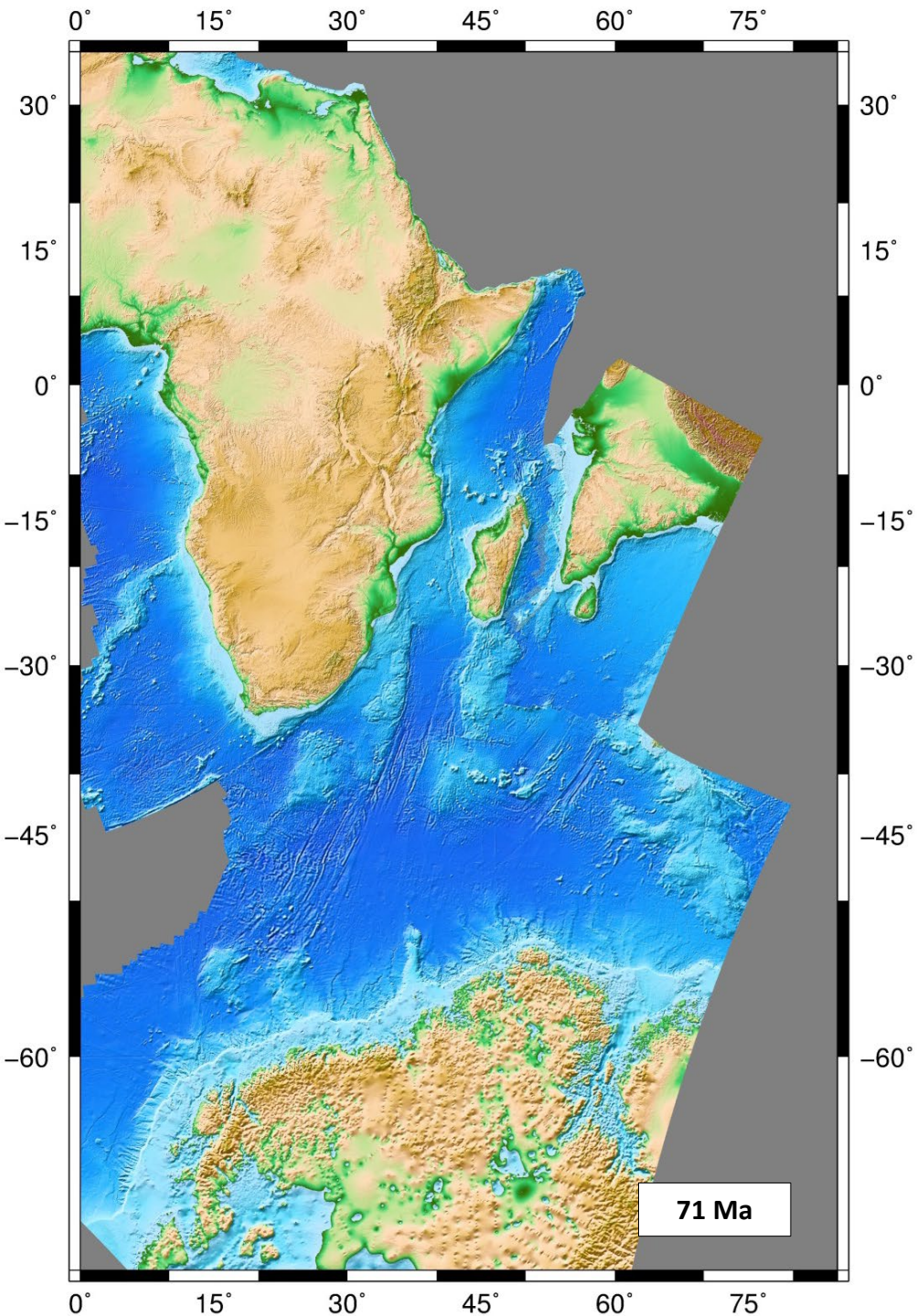
0˚
15˚
30˚
45˚
60˚
75˚
30˚
15˚
0˚
–15˚
–30˚
–45˚
–60˚
71 Ma

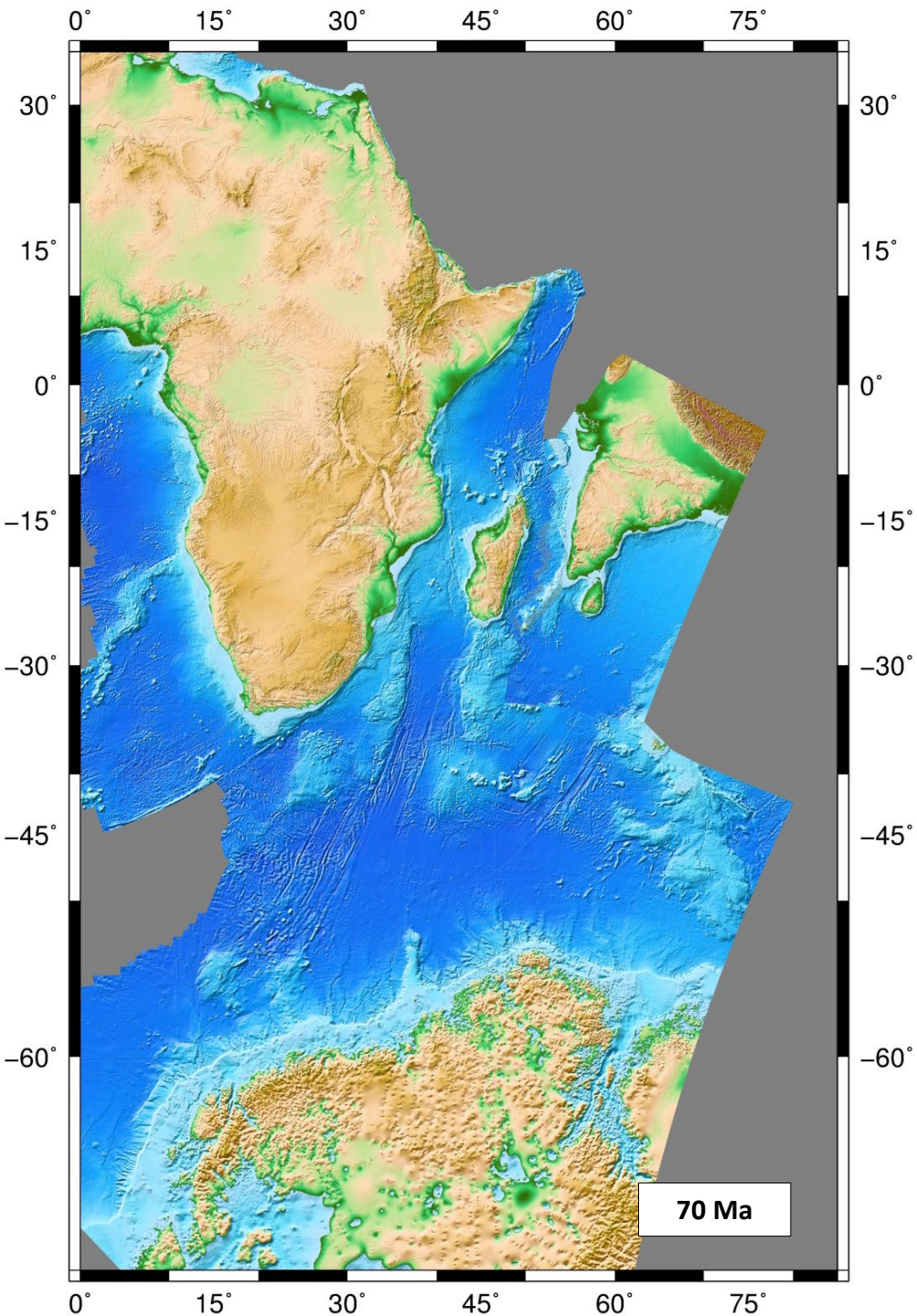
0°
15°
30°
45°
60°
75°
30°
15°
0°
−15°
−30°
−45°
−60°
70 Ma

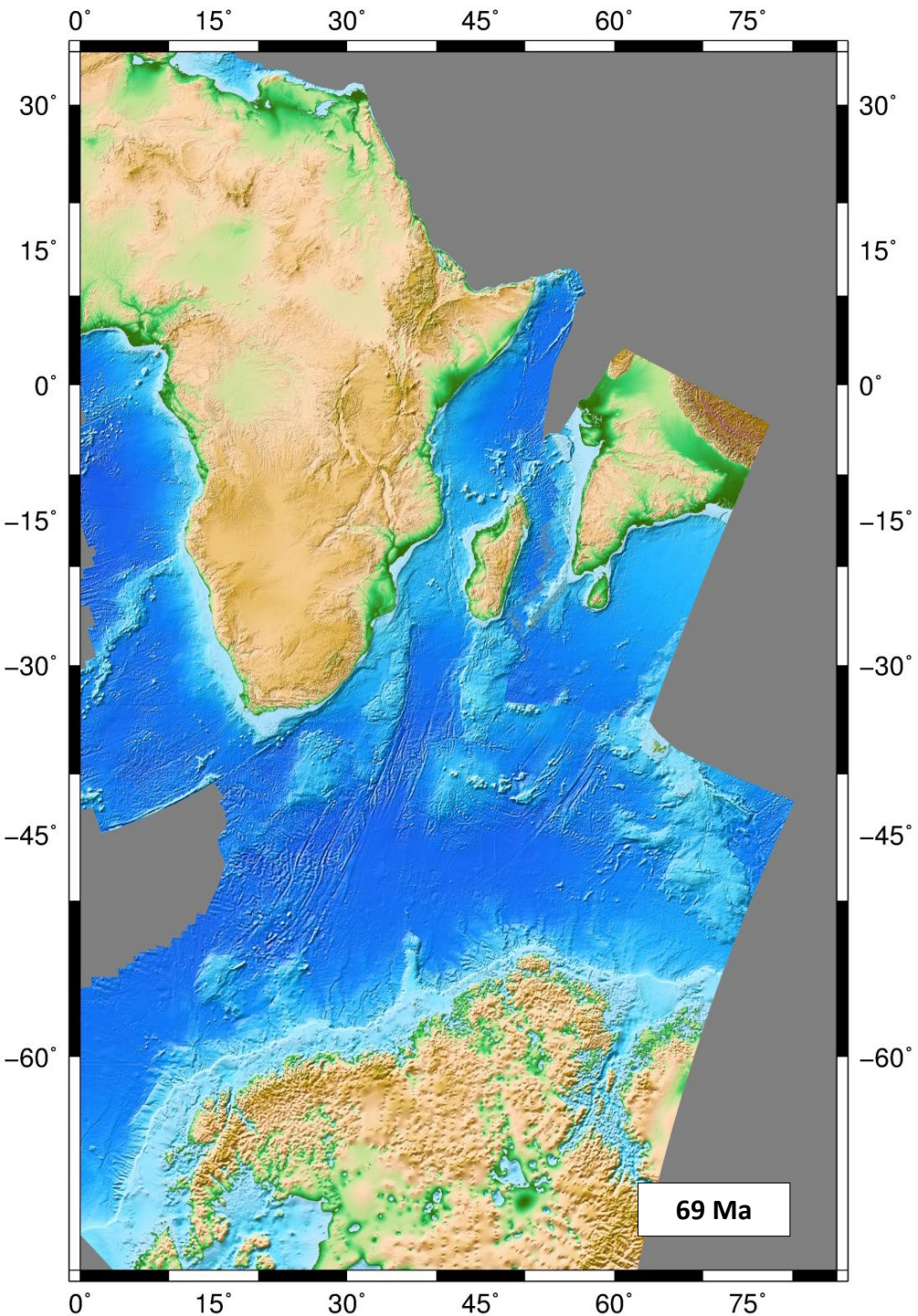
0°
15°
30°
45°
60°
75°
30°
15°
0°
−15°
−30°
−45°
−60°
69 Ma

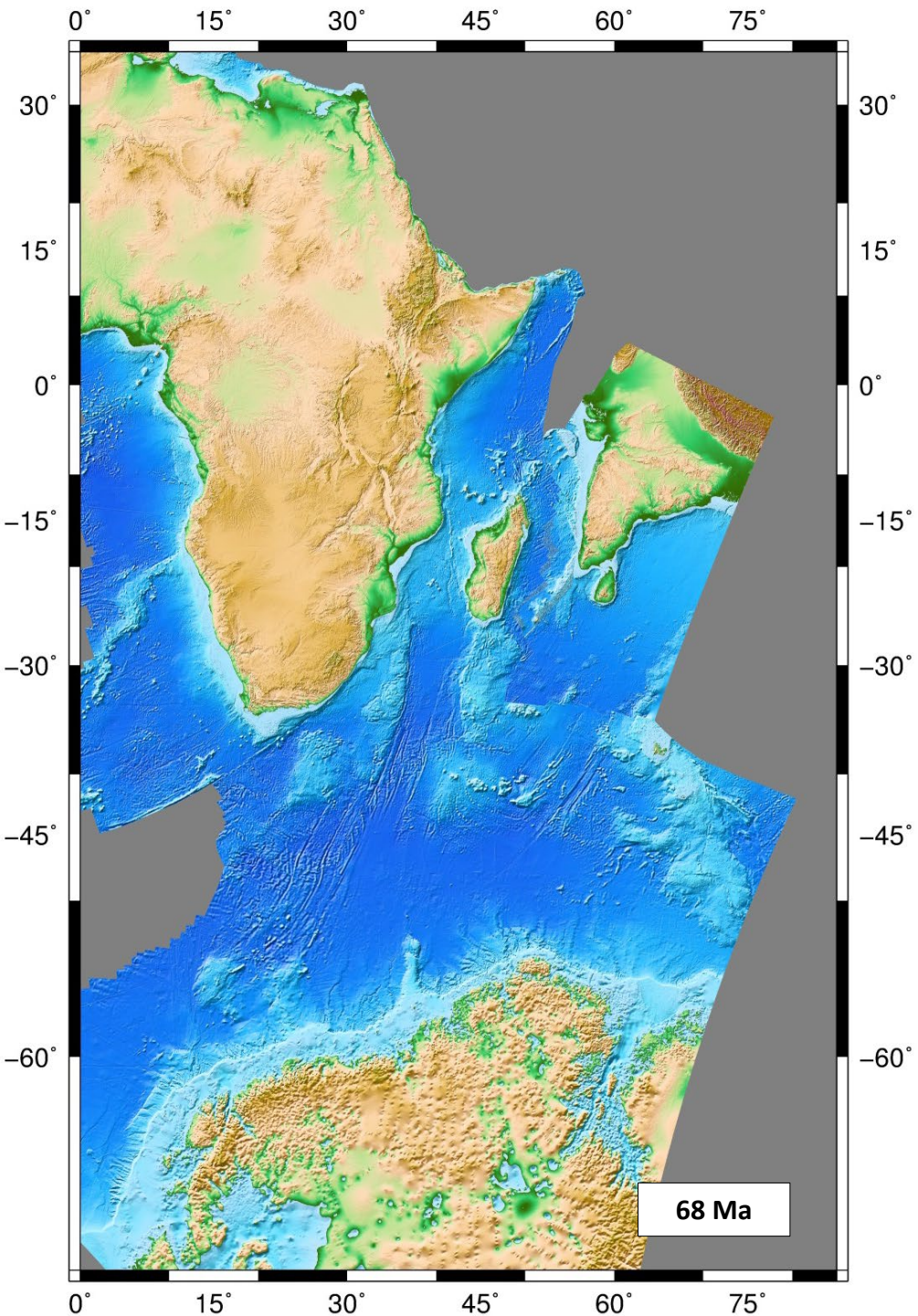
0°
15°
30°
45°
60°
75°
30°
15°
0°
−15°
−30°
−45°
−60°
68 Ma

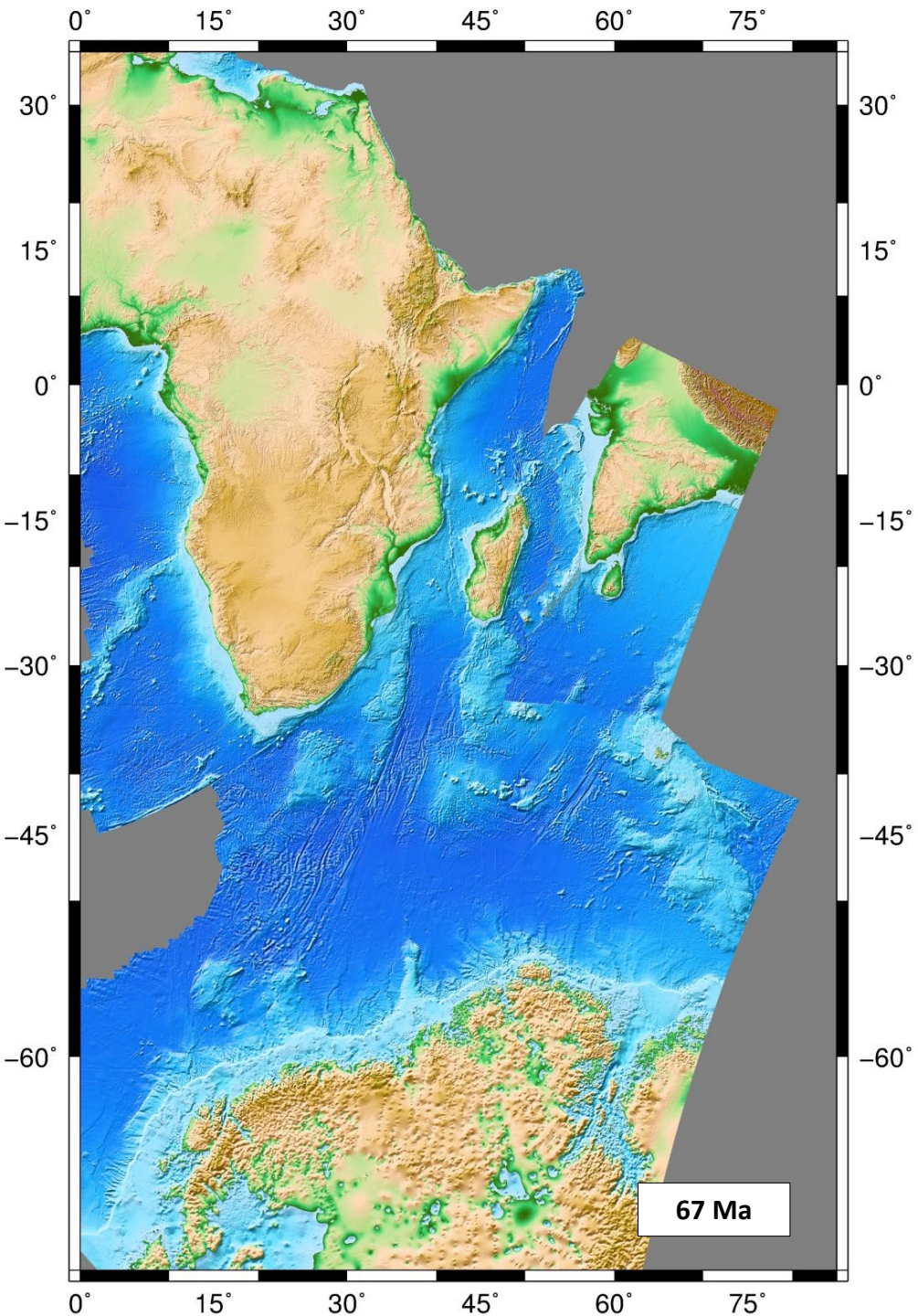
0°
15°
30°
45°
60°
75°
30°
15°
0°
−15°
−30°
−45°
−60°
67 Ma

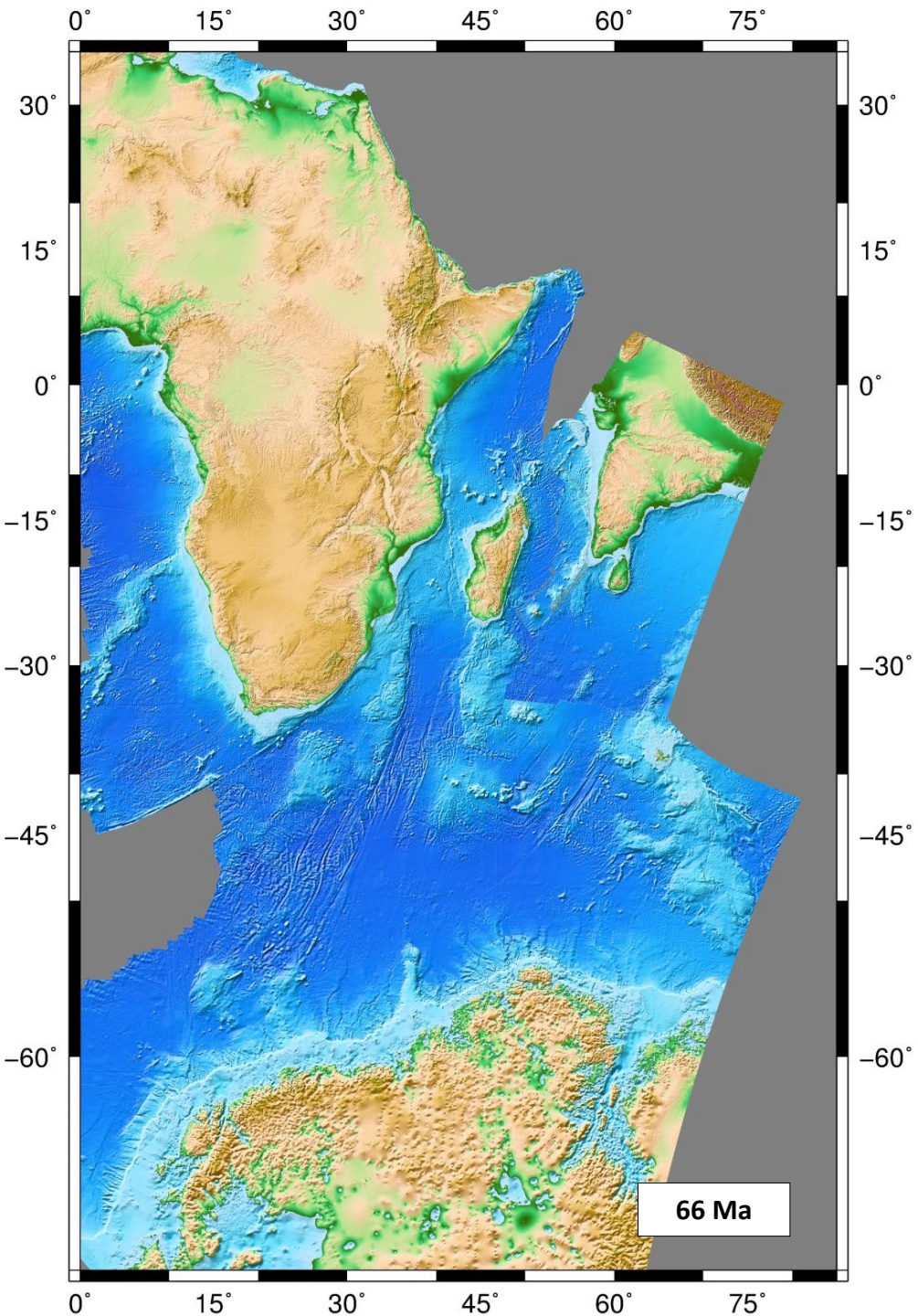
0°
15°
30°
45°
60°
75°
30°
15°
0°
−15°
−30°
−45°
−60°
66 Ma

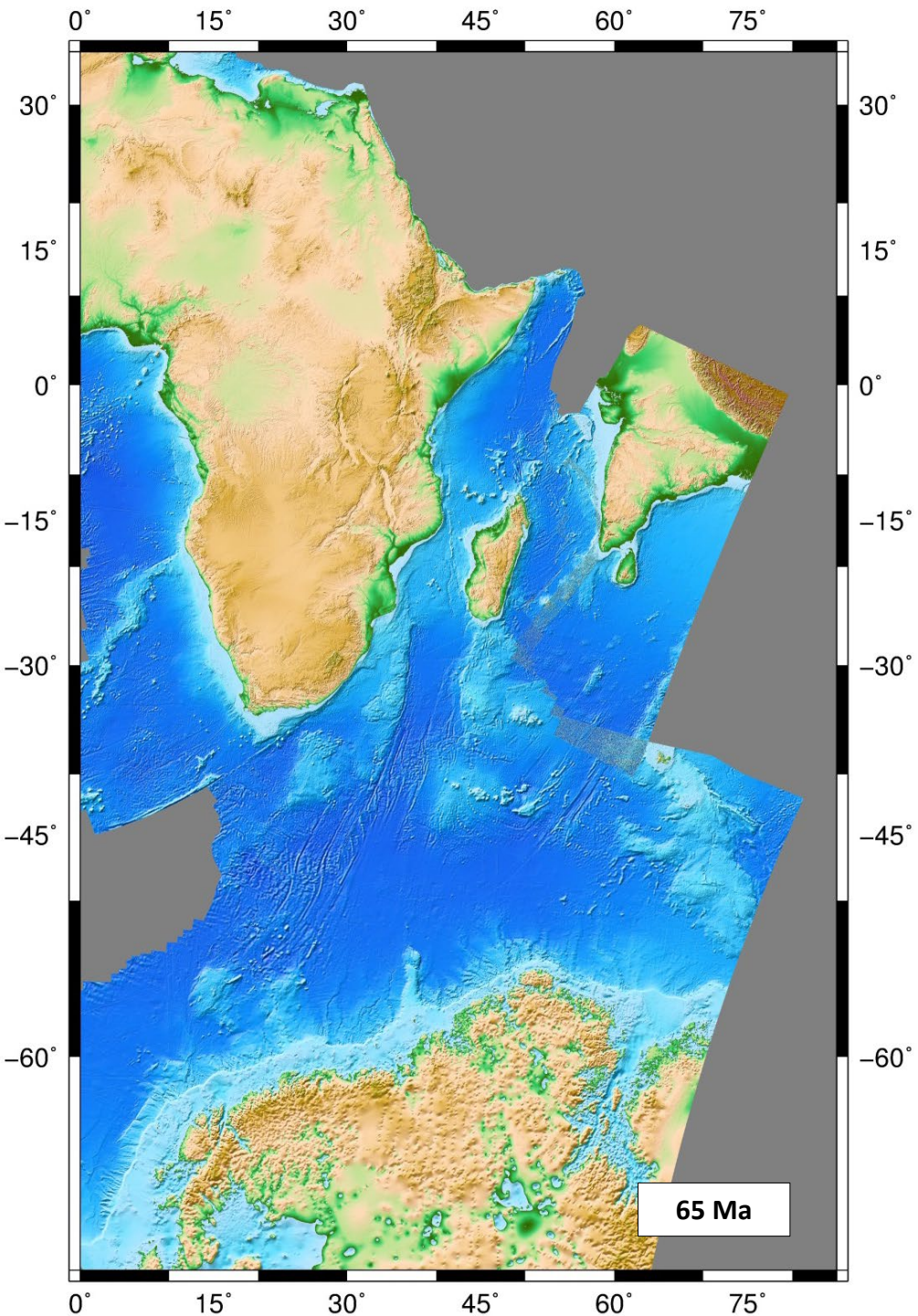
0°
15°
30°
45°
60°
75°
30°
15°
0°
−15°
−30°
−45°
−60°
65 Ma

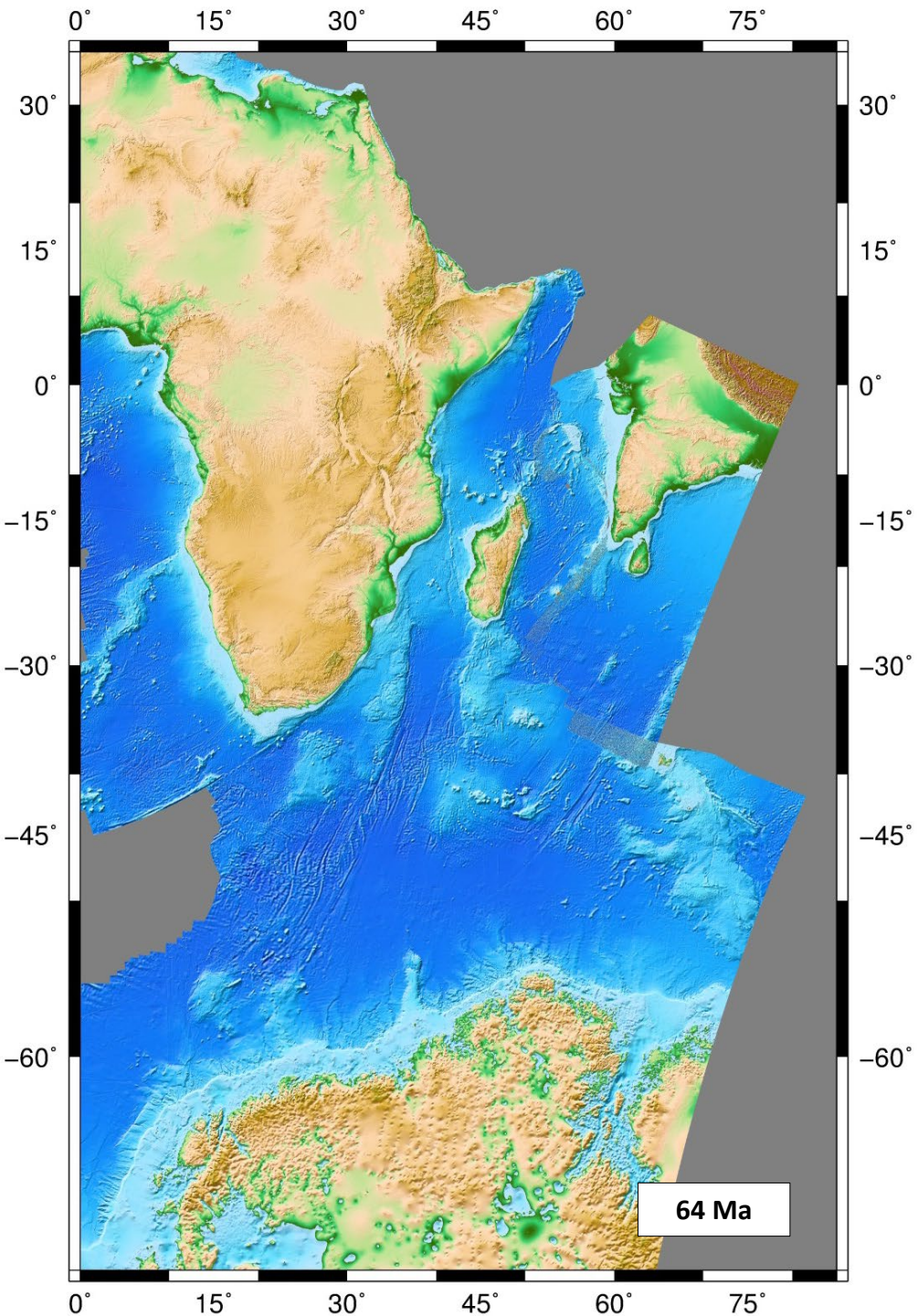
0˚
15˚
30˚
45˚
60˚
75˚
30˚
15˚
0˚
–15˚
–30˚
–45˚
–60˚
64 Ma

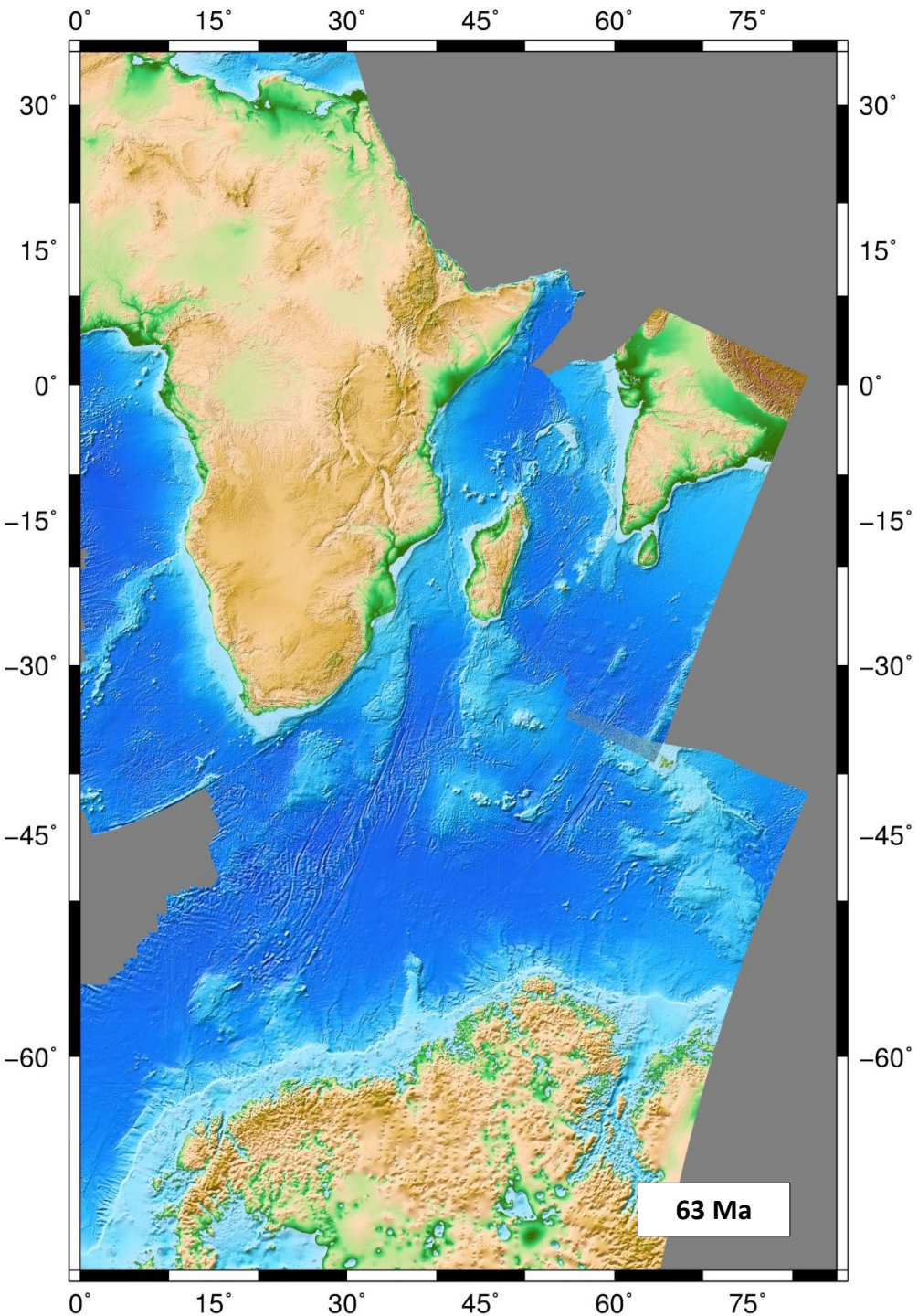
0˚
15˚
30˚
45˚
60˚
75˚
30˚
15˚
0˚
–15˚
–30˚
–45˚
–60˚
63 Ma

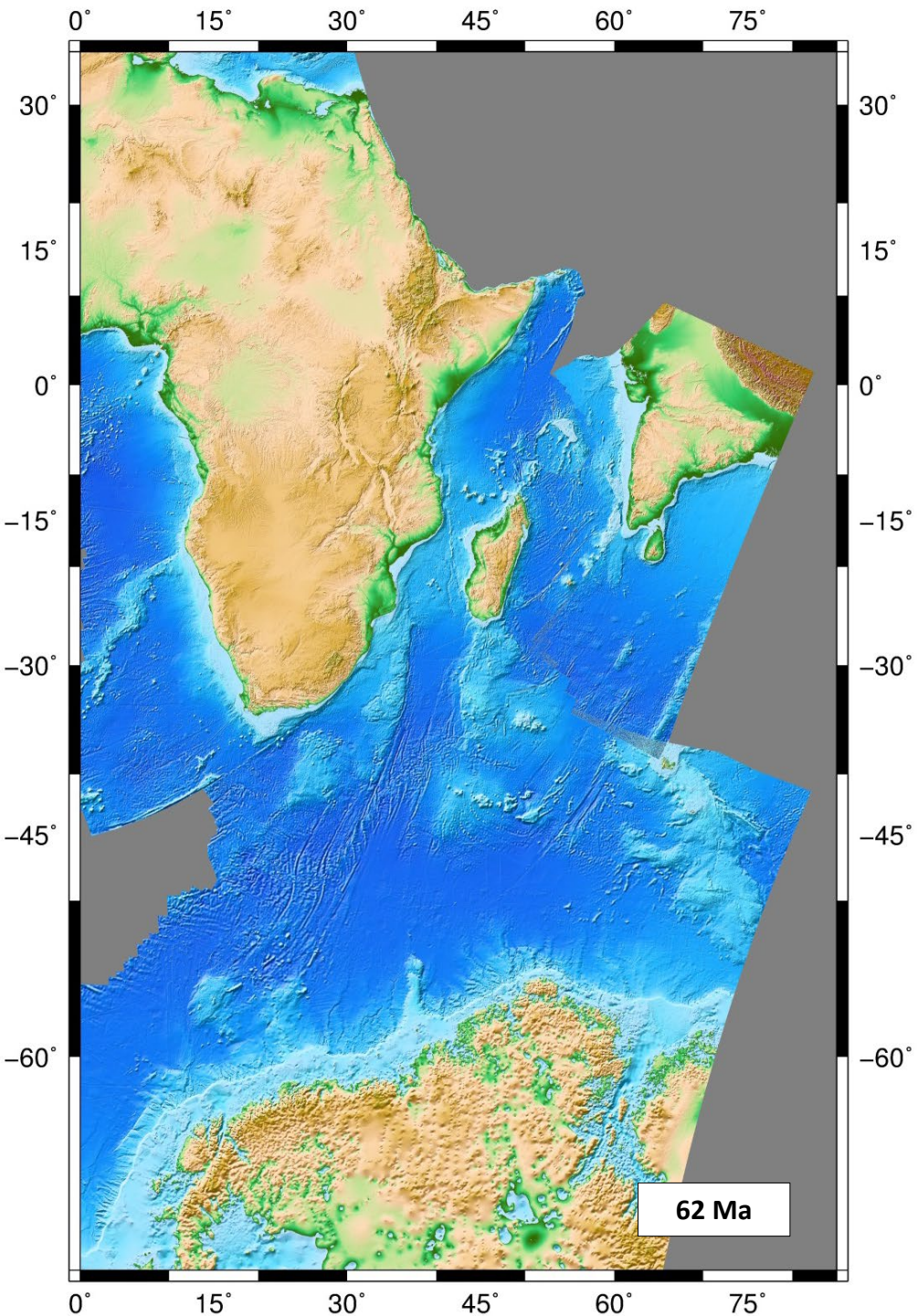
0˚
15˚
30˚
45˚
60˚
75˚
30˚
15˚
0˚
–15˚
–30˚
–45˚
–60˚
62 Ma

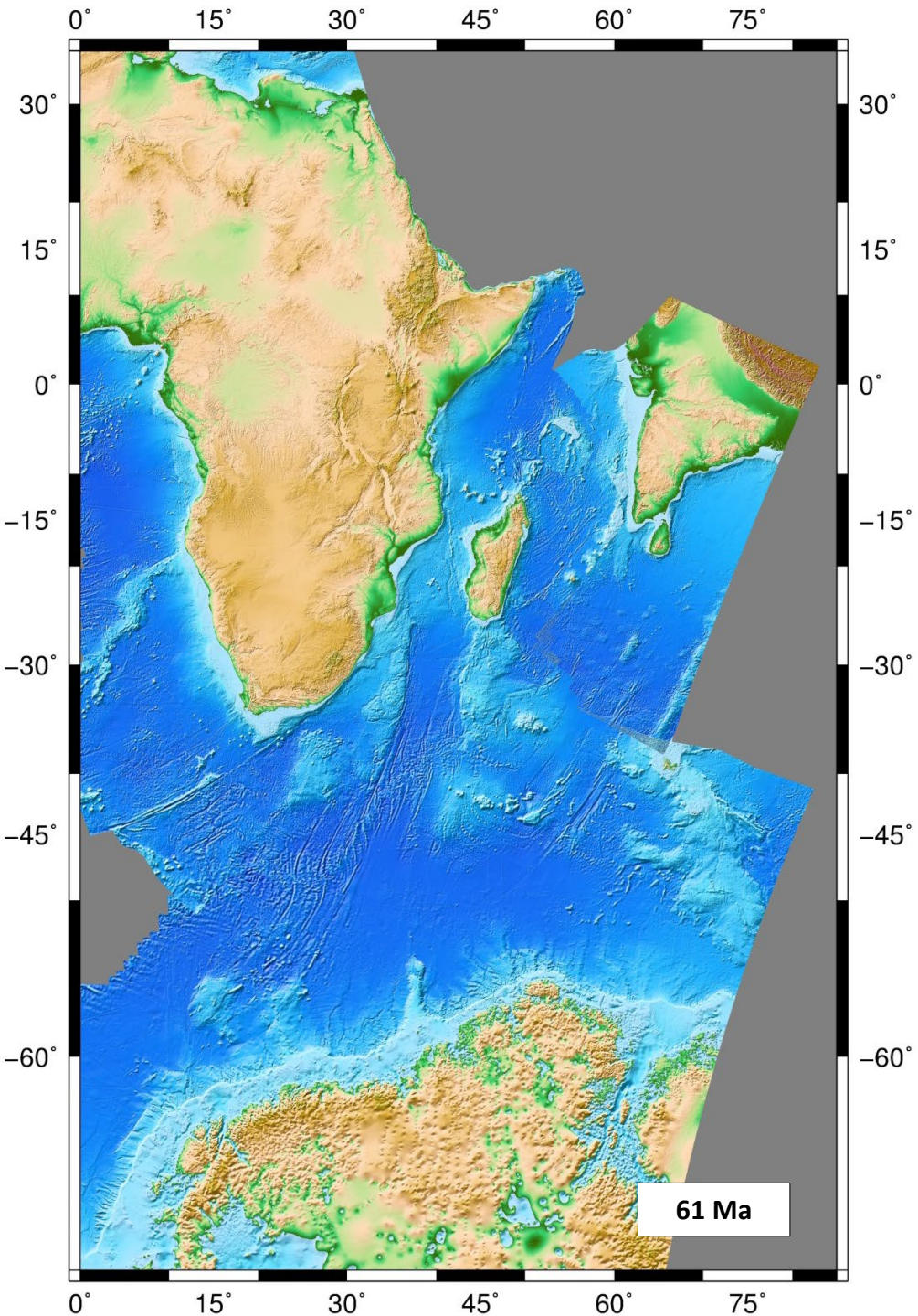
0˚
15˚
30˚
45˚
60˚
75˚
30˚
15˚
0˚
–15˚
–30˚
–45˚
–60˚
61 Ma

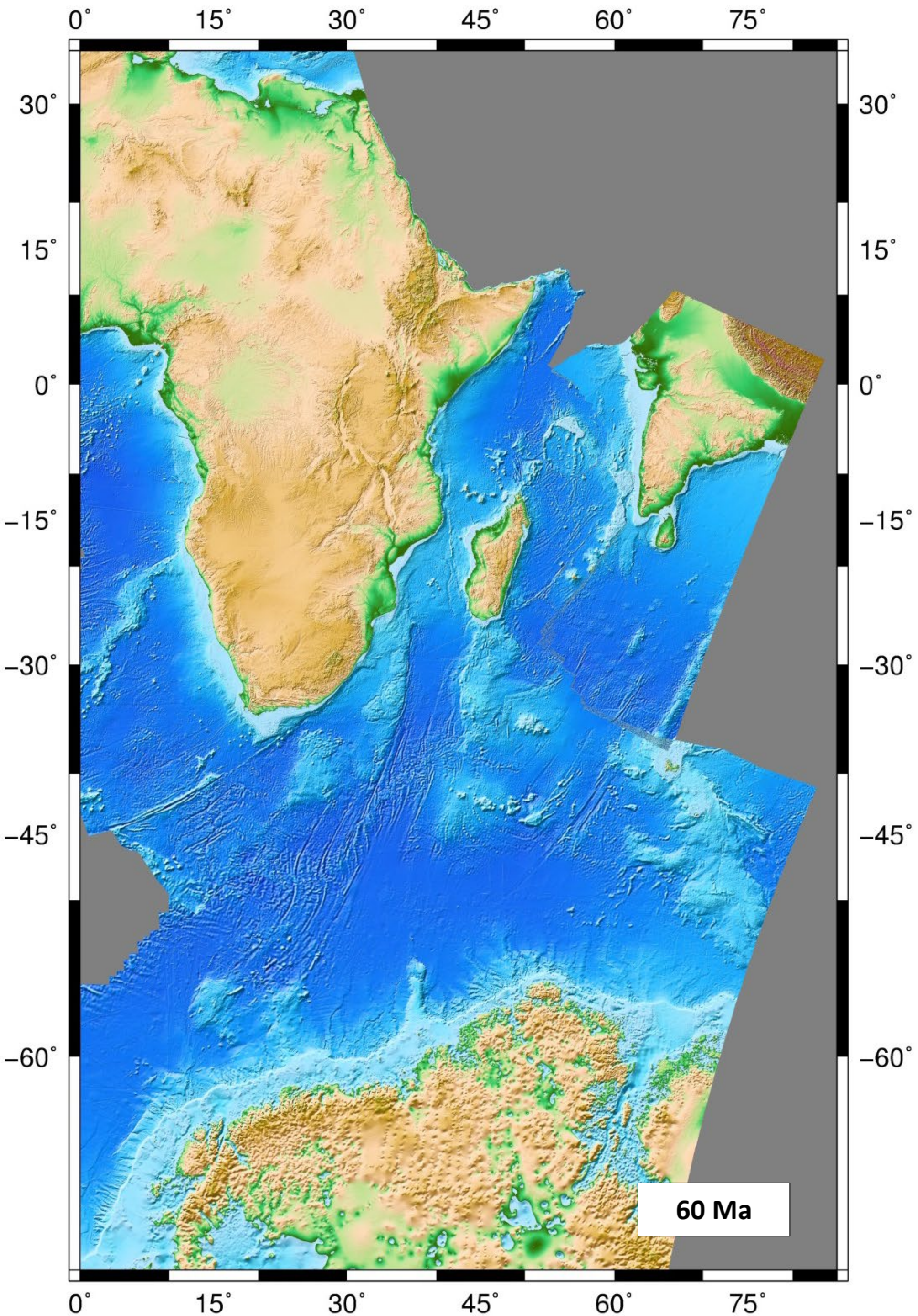
0°
15°
30°
45°
60°
75°
30°
15°
0°
−15°
−30°
−45°
−60°
60 Ma

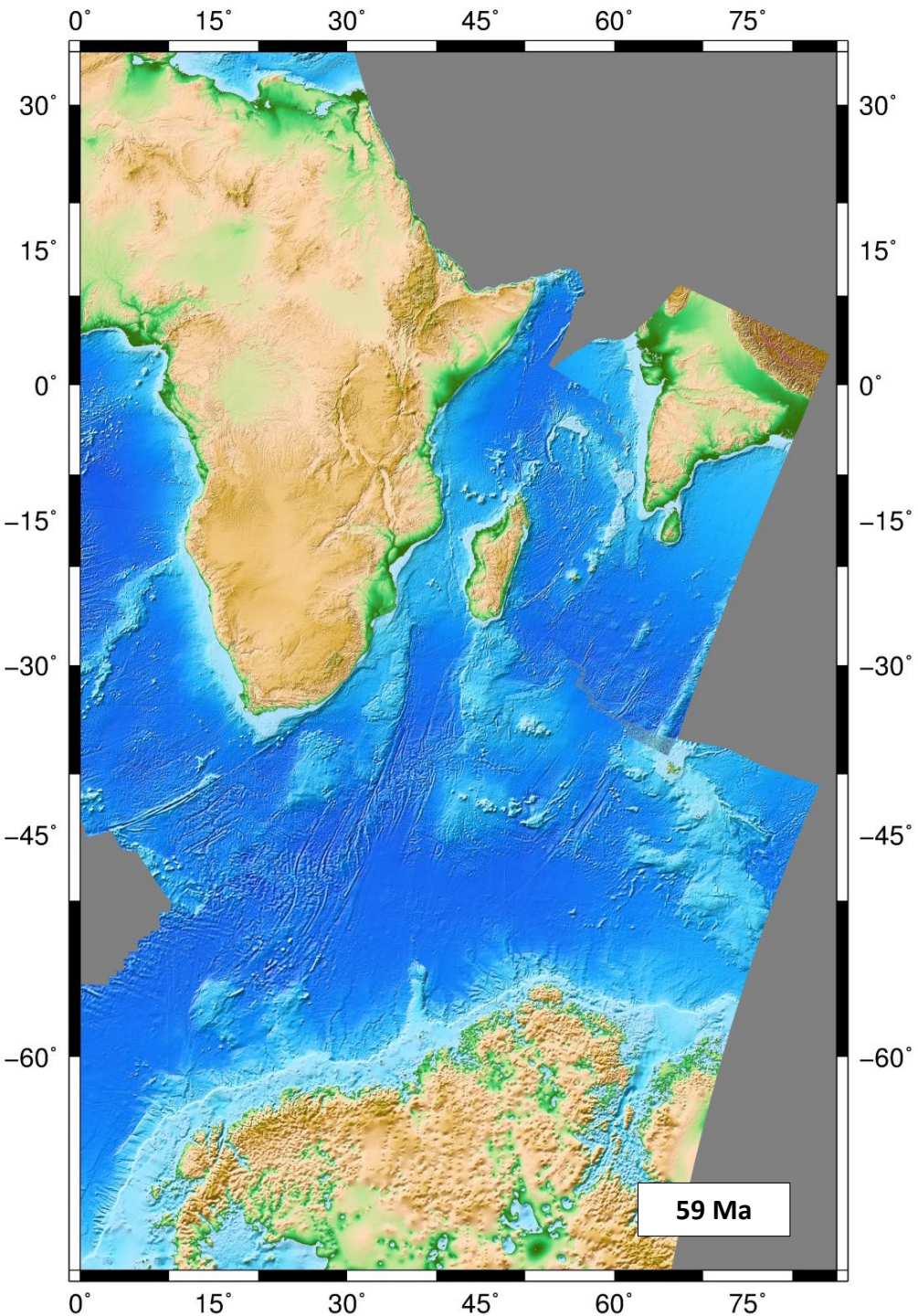
0°
15°
30°
45°
60°
75°
30°
15°
0°
−15°
−30°
−45°
−60°
59 Ma

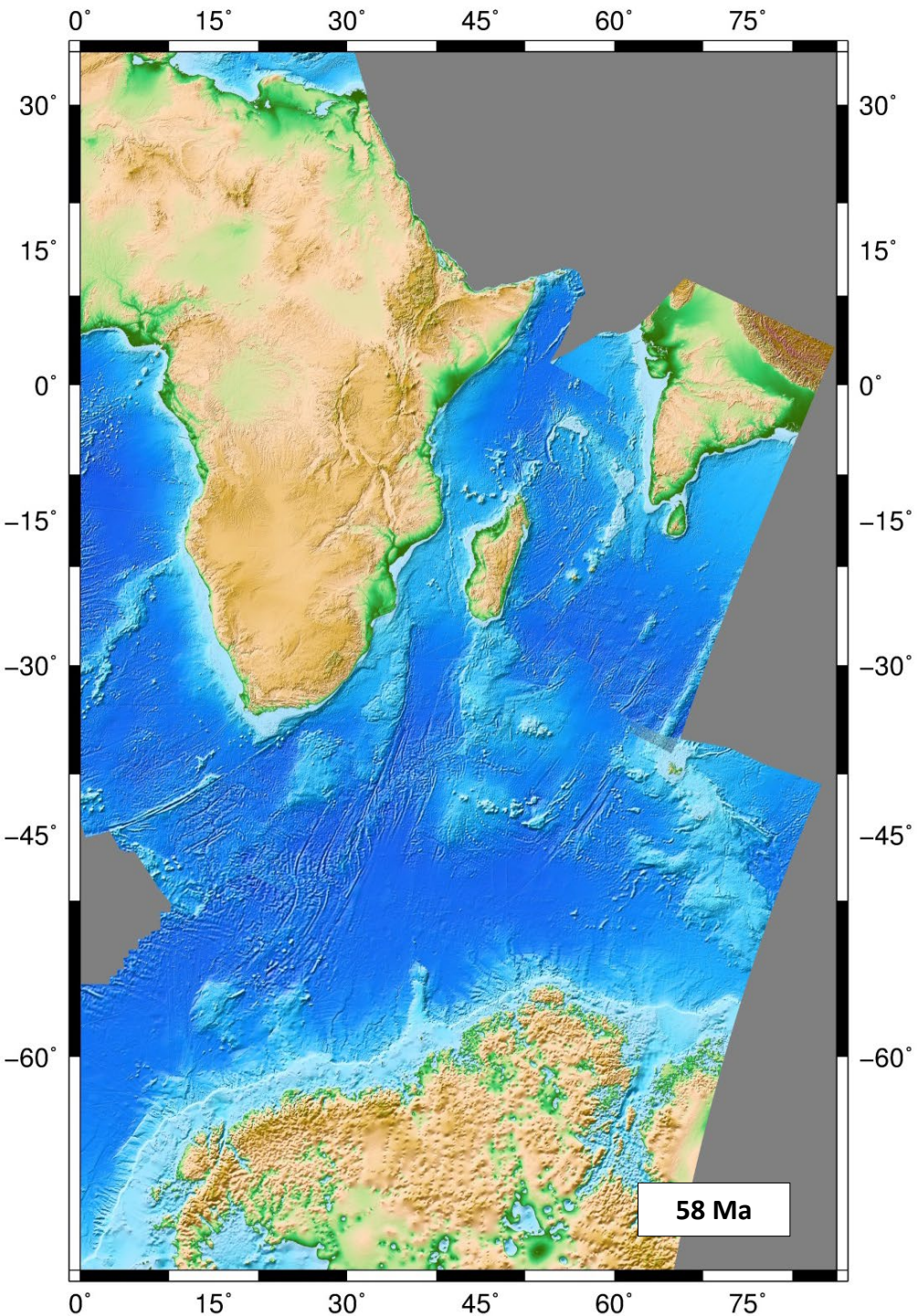
0°
15°
30°
45°
60°
75°
30°
15°
0°
−15°
−30°
−45°
−60°
58 Ma

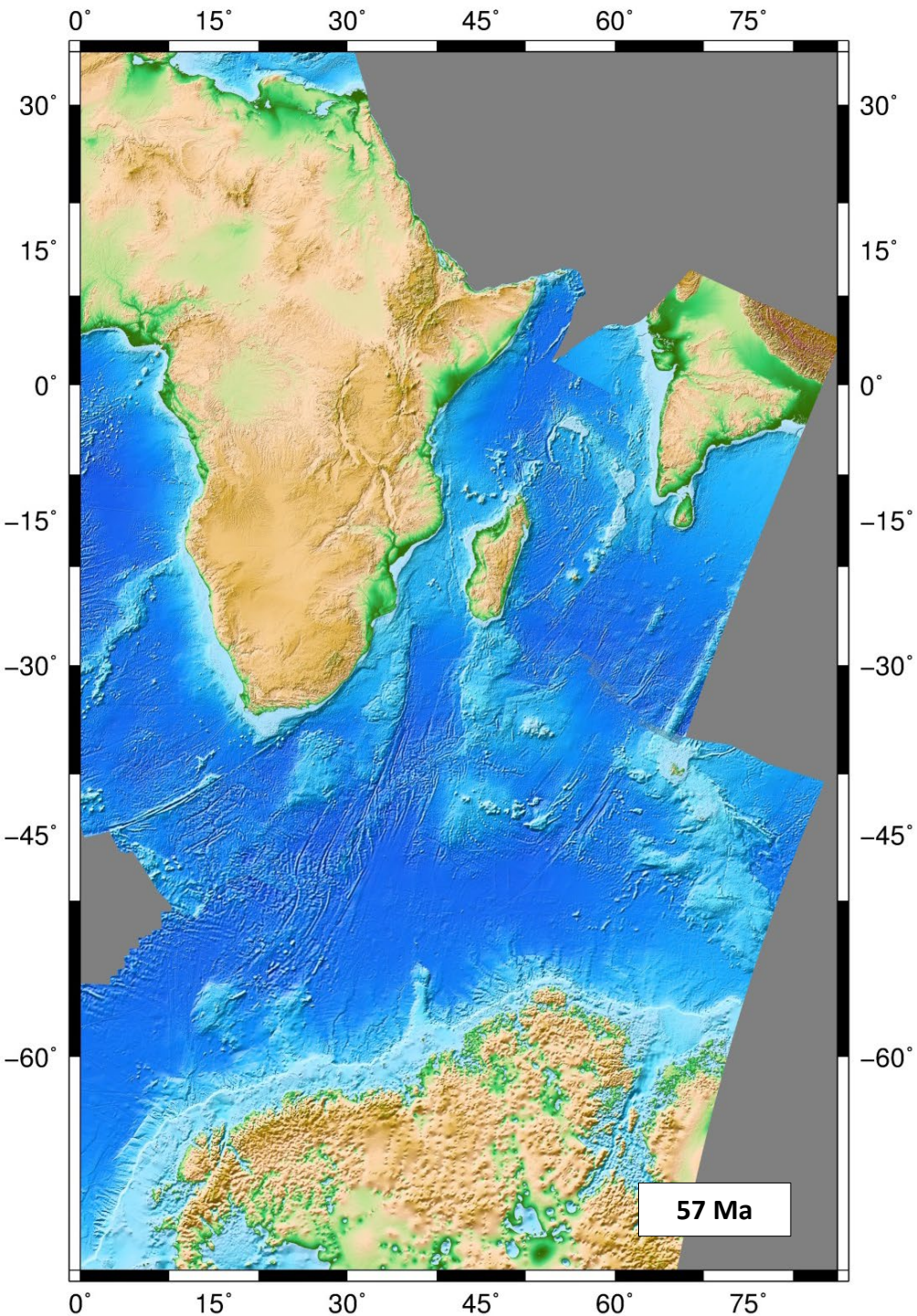
0°
15°
30°
45°
60°
75°
30°
15°
0°
−15°
−30°
−45°
−60°
57 Ma

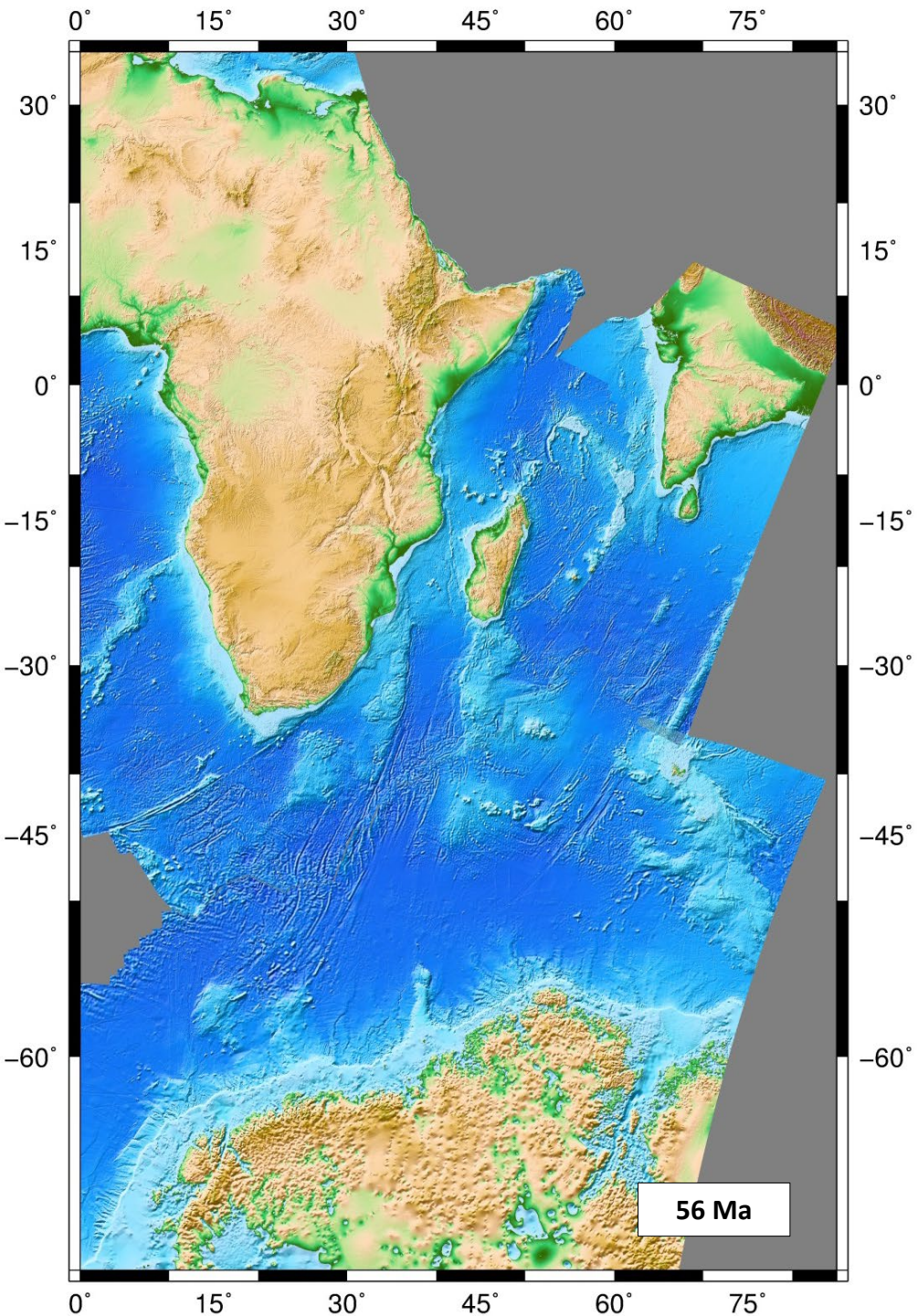
0°
15°
30°
45°
60°
75°
30°
15°
0°
−15°
−30°
−45°
−60°
56 Ma

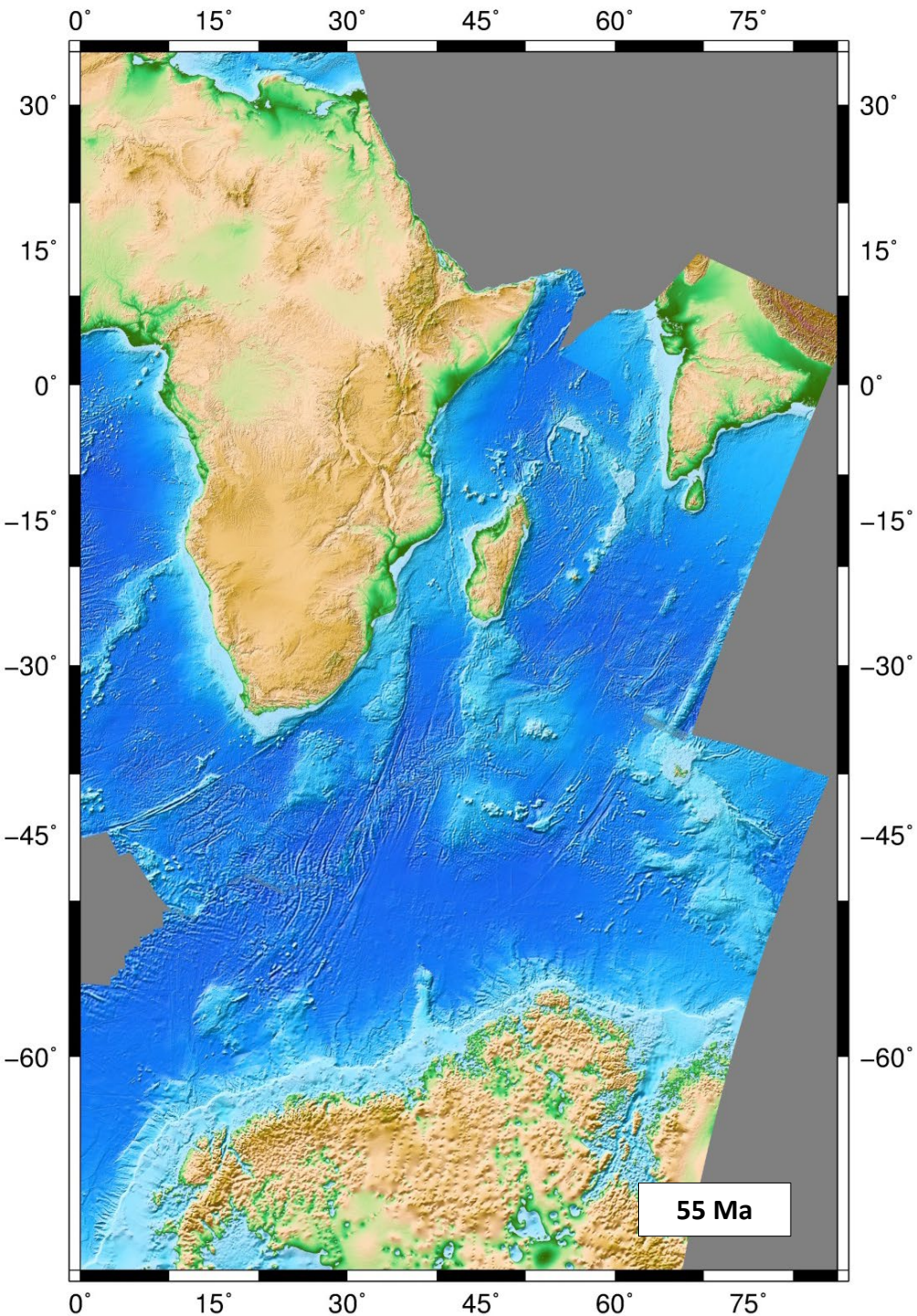
0°
15°
30°
45°
60°
75°
30°
15°
0°
−15°
−30°
−45°
−60°
55 Ma

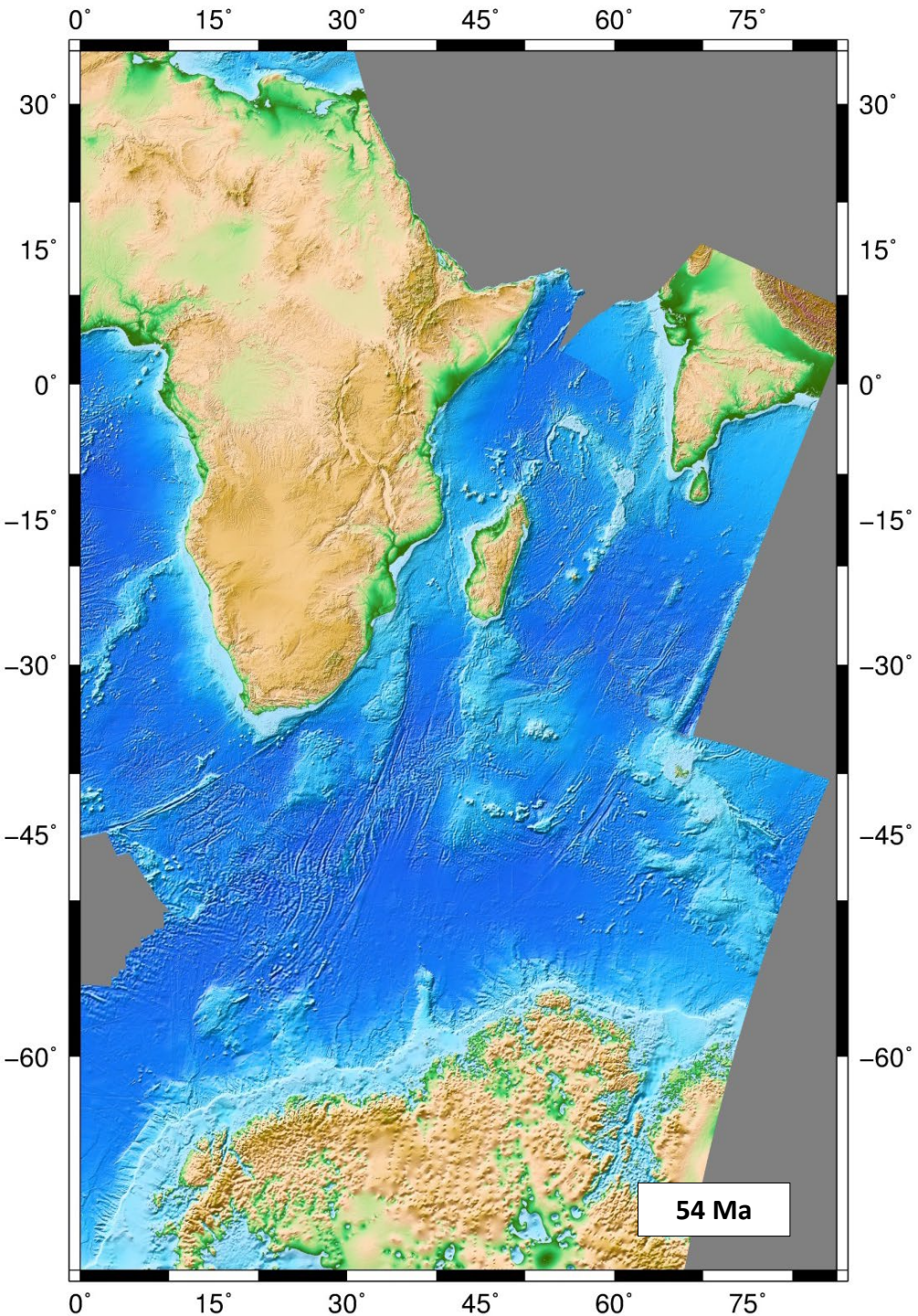
0°
15°
30°
45°
60°
75°
30°
15°
0°
−15°
−30°
−45°
−60°
54 Ma

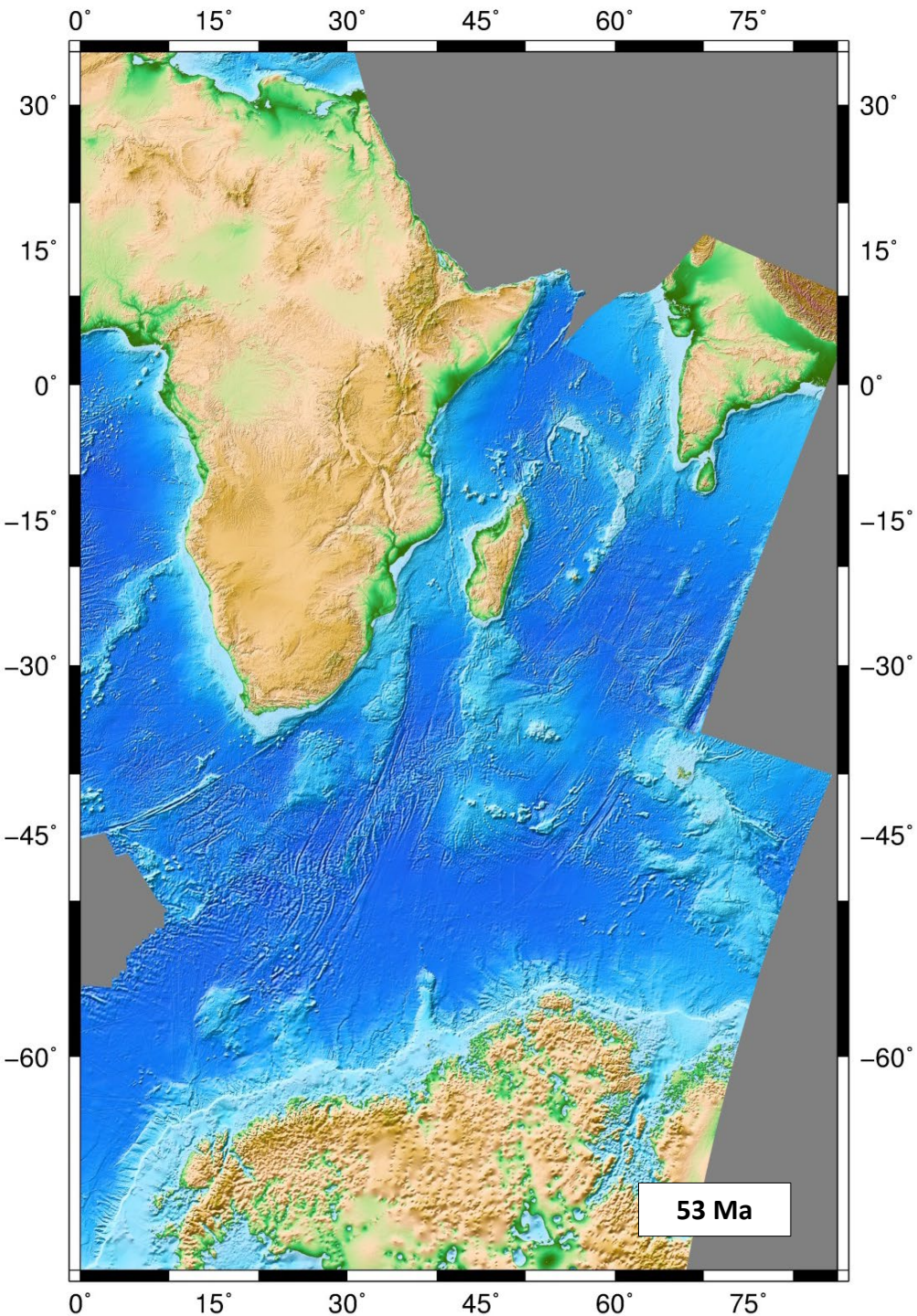
0°
15°
30°
45°
60°
75°
30°
15°
0°
−15°
−30°
−45°
−60°
53 Ma

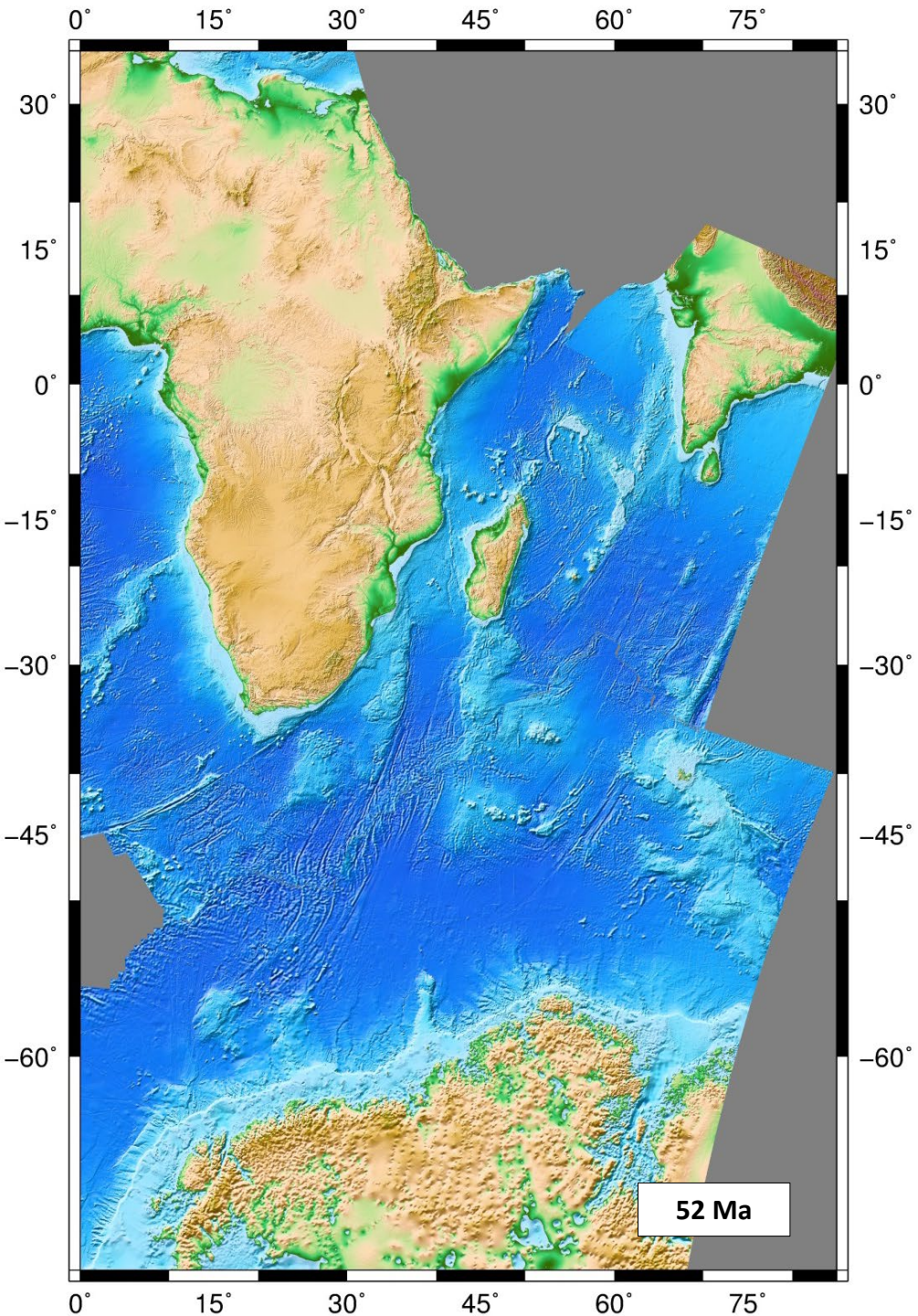
0˚
15˚
30˚
45˚
60˚
75˚
30˚
15˚
0˚
–15˚
–30˚
–45˚
–60˚
52 Ma

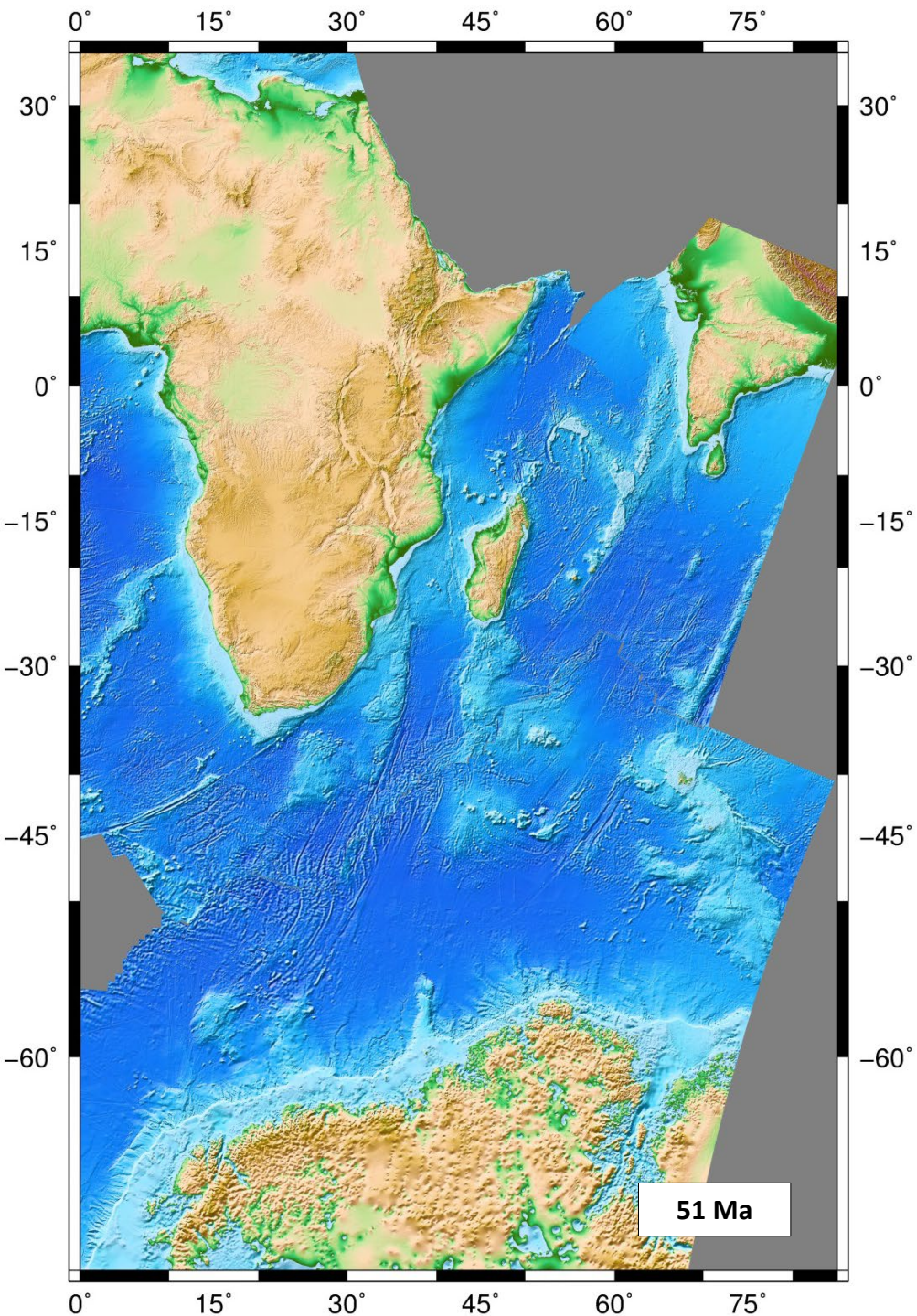
0°
15°
30°
45°
60°
75°
30°
15°
0°
−15°
−30°
−45°
−60°
51 Ma

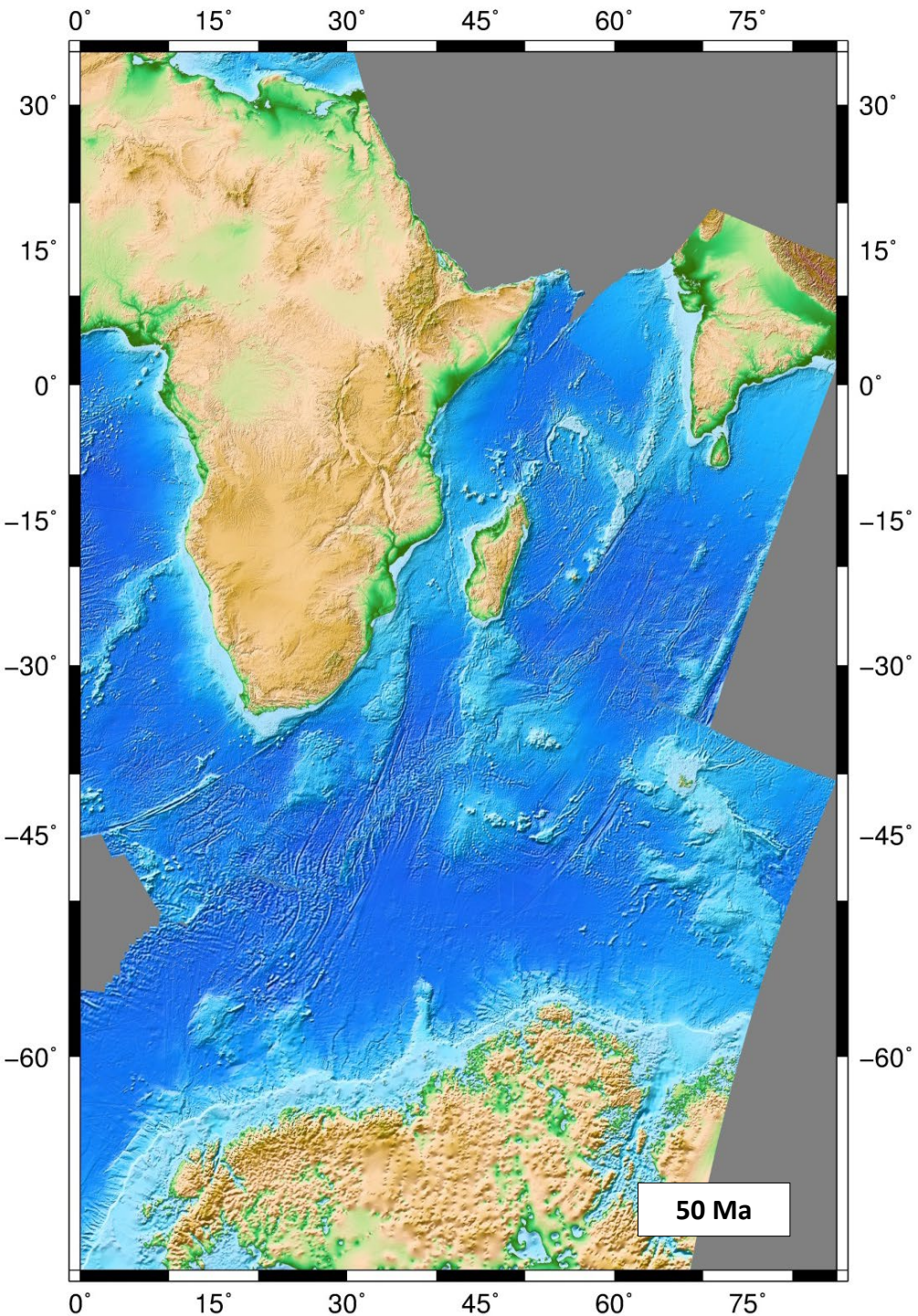
0˚
15˚
30˚
45˚
60˚
75˚
30˚
15˚
0˚
–15˚
–30˚
–45˚
–60˚
50 Ma

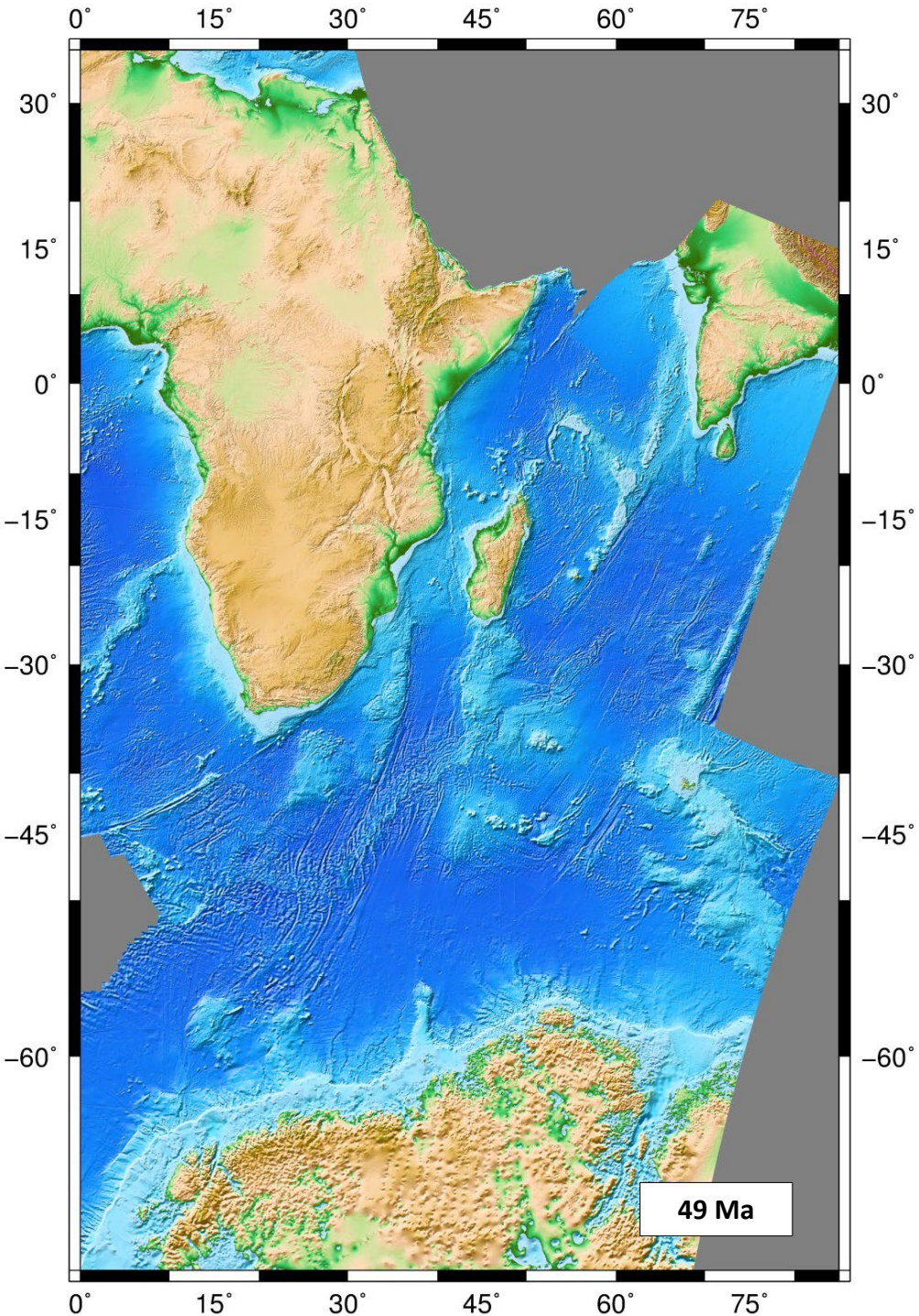
0°
15°
30°
45°
60°
75°
30°
15°
0°
−15°
−30°
−45°
−60°
49 Ma

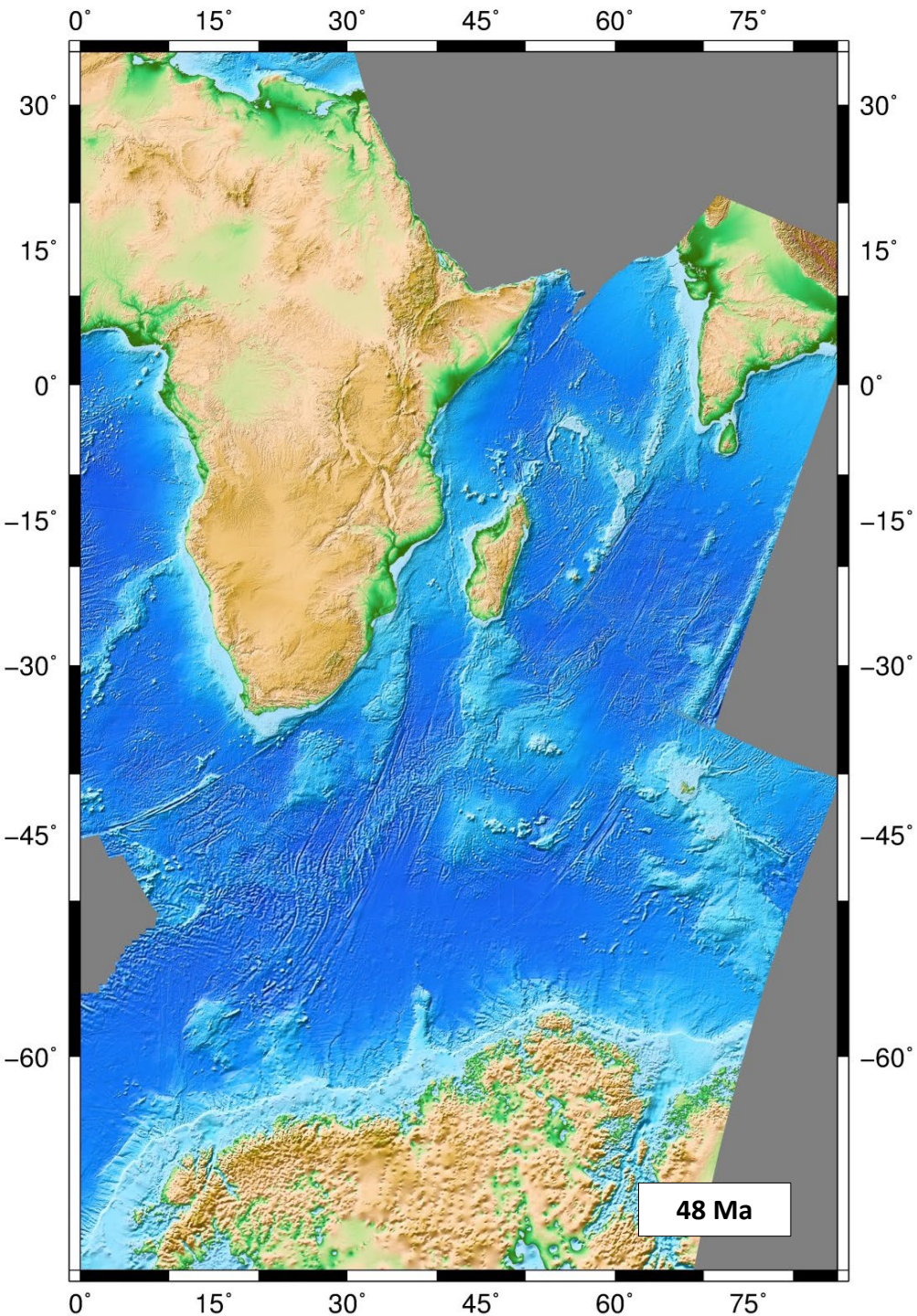
0°
15°
30°
45°
60°
75°
30°
15°
0°
−15°
−30°
−45°
−60°
48 Ma

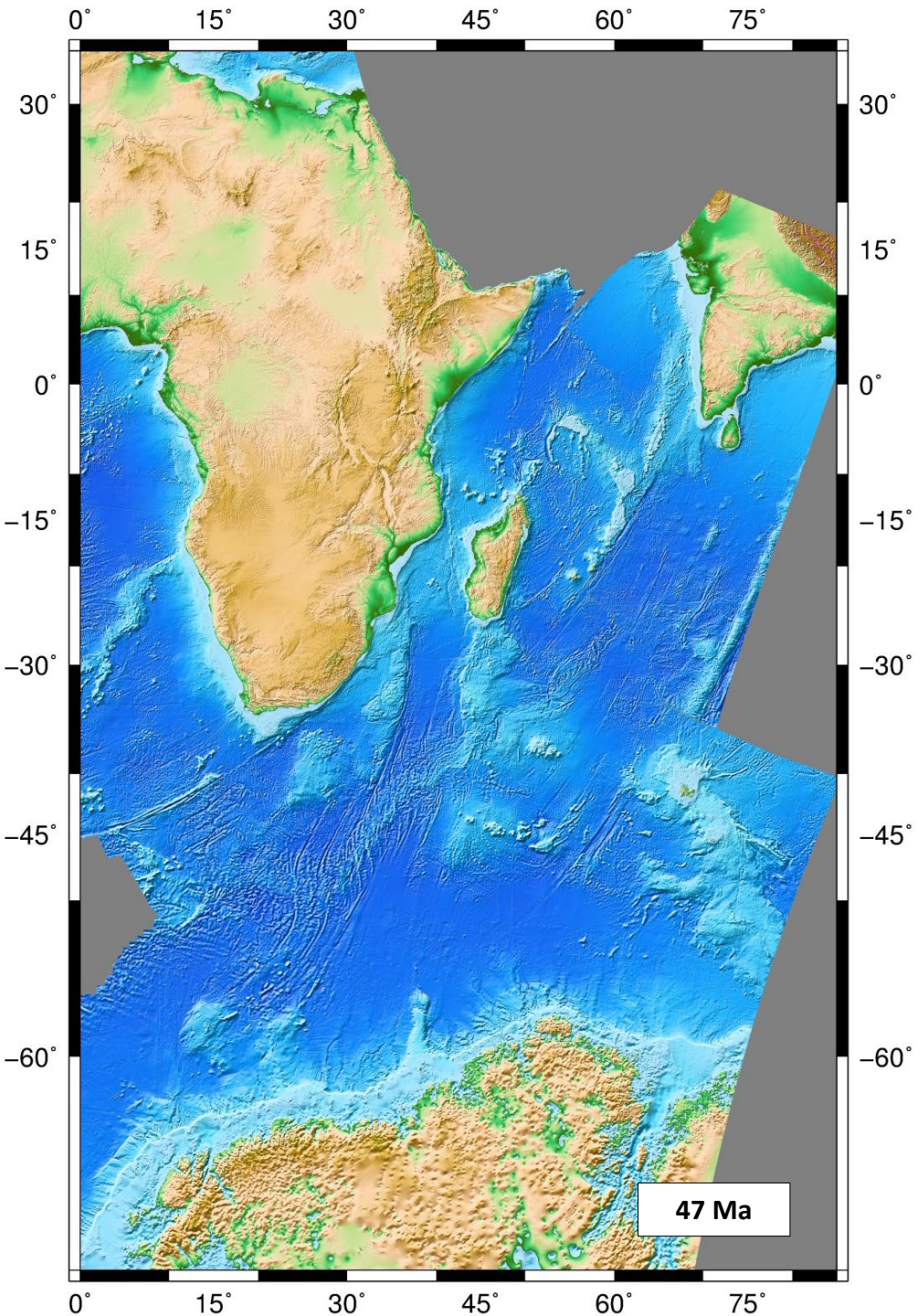
0°
15°
30°
45°
60°
75°
30°
15°
0°
−15°
−30°
−45°
−60°
47 Ma

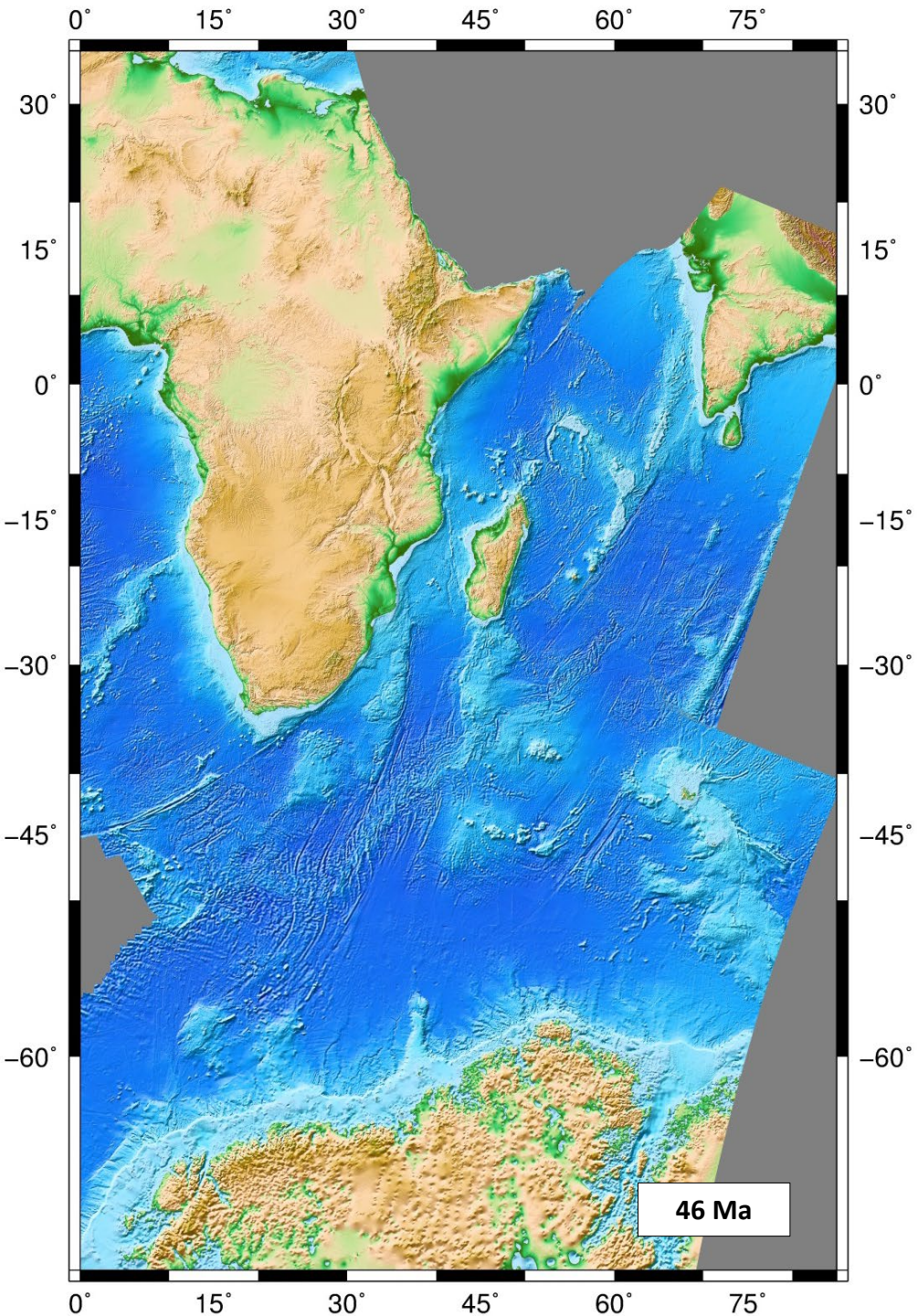
0°
15°
30°
45°
60°
75°
30°
15°
0°
−15°
−30°
−45°
−60°
46 Ma

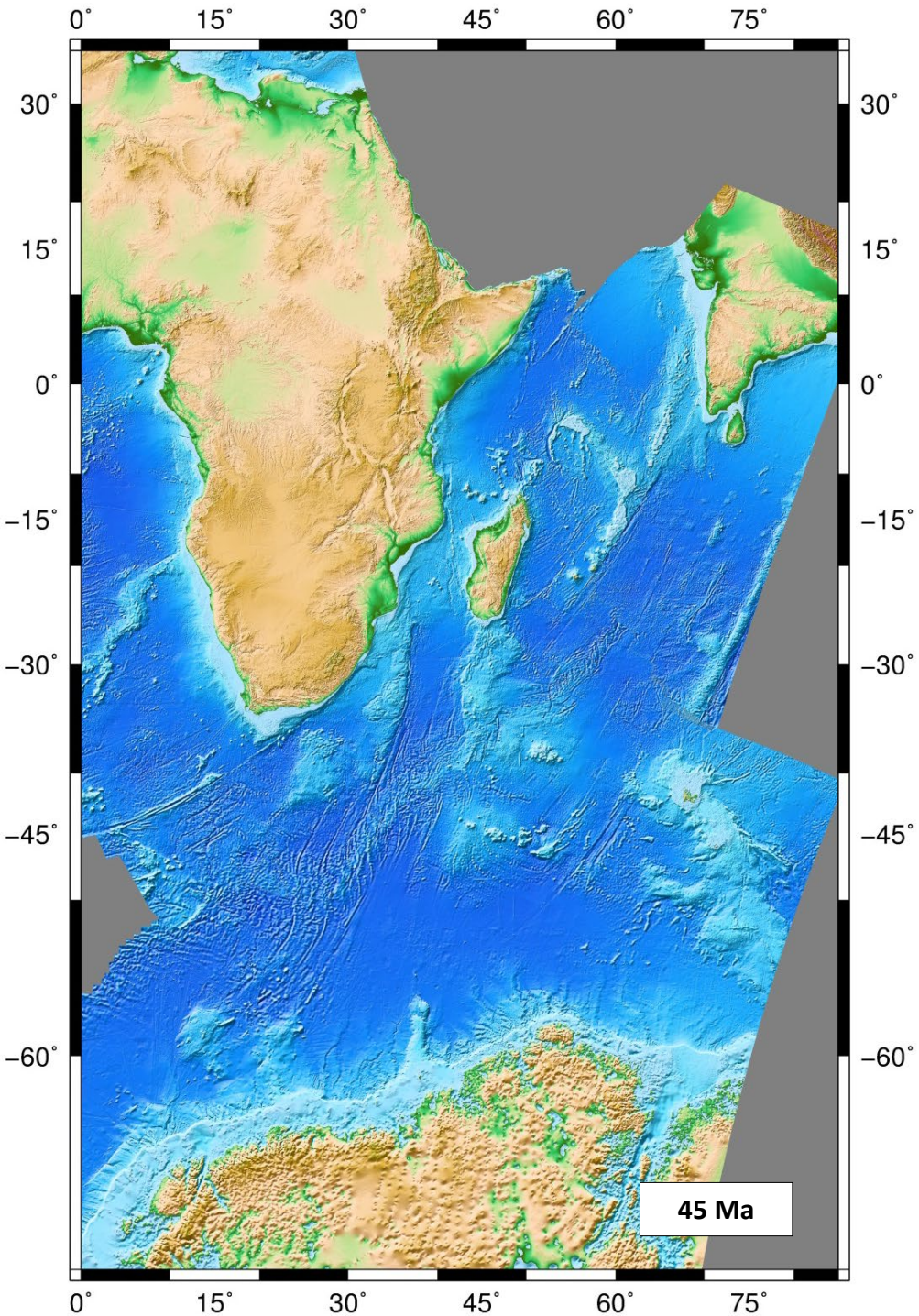
0°
15°
30°
45°
60°
75°
30°
15°
0°
−15°
−30°
−45°
−60°
45 Ma

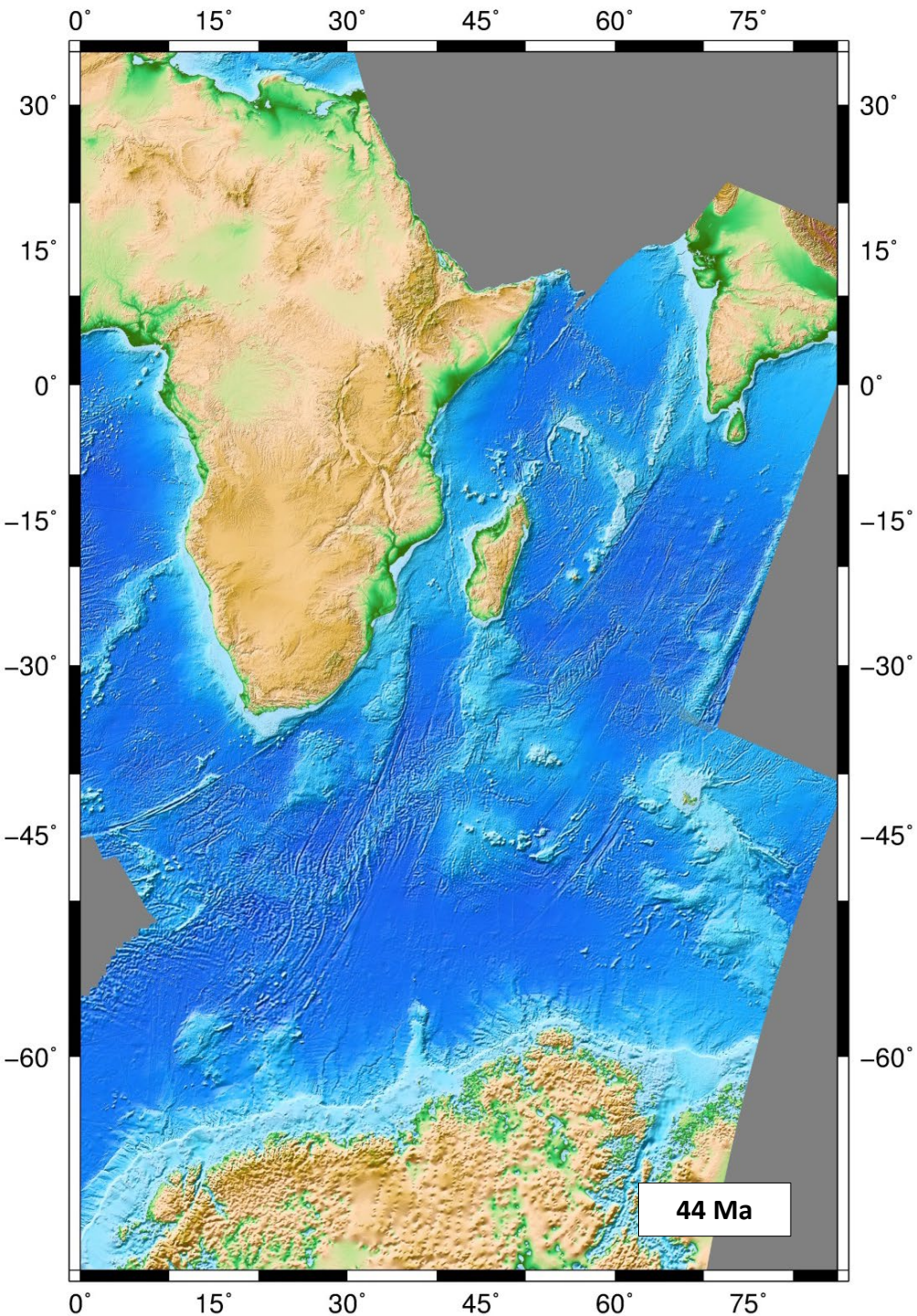
0°
15°
30°
45°
60°
75°
30°
15°
0°
−15°
−30°
−45°
−60°
44 Ma

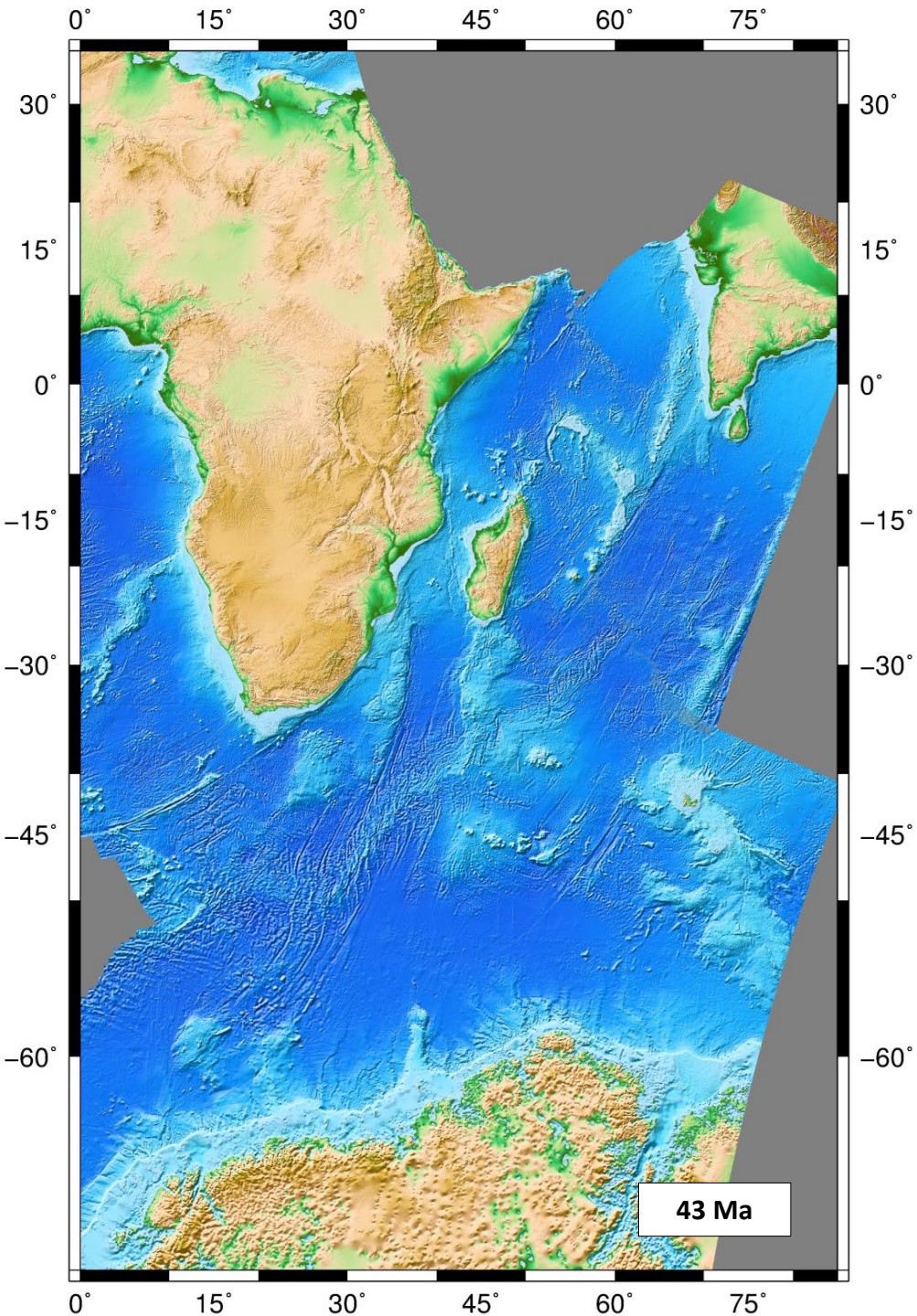
0°
15°
30°
45°
60°
75°
30°
15°
0°
−15°
−30°
−45°
−60°
43 Ma

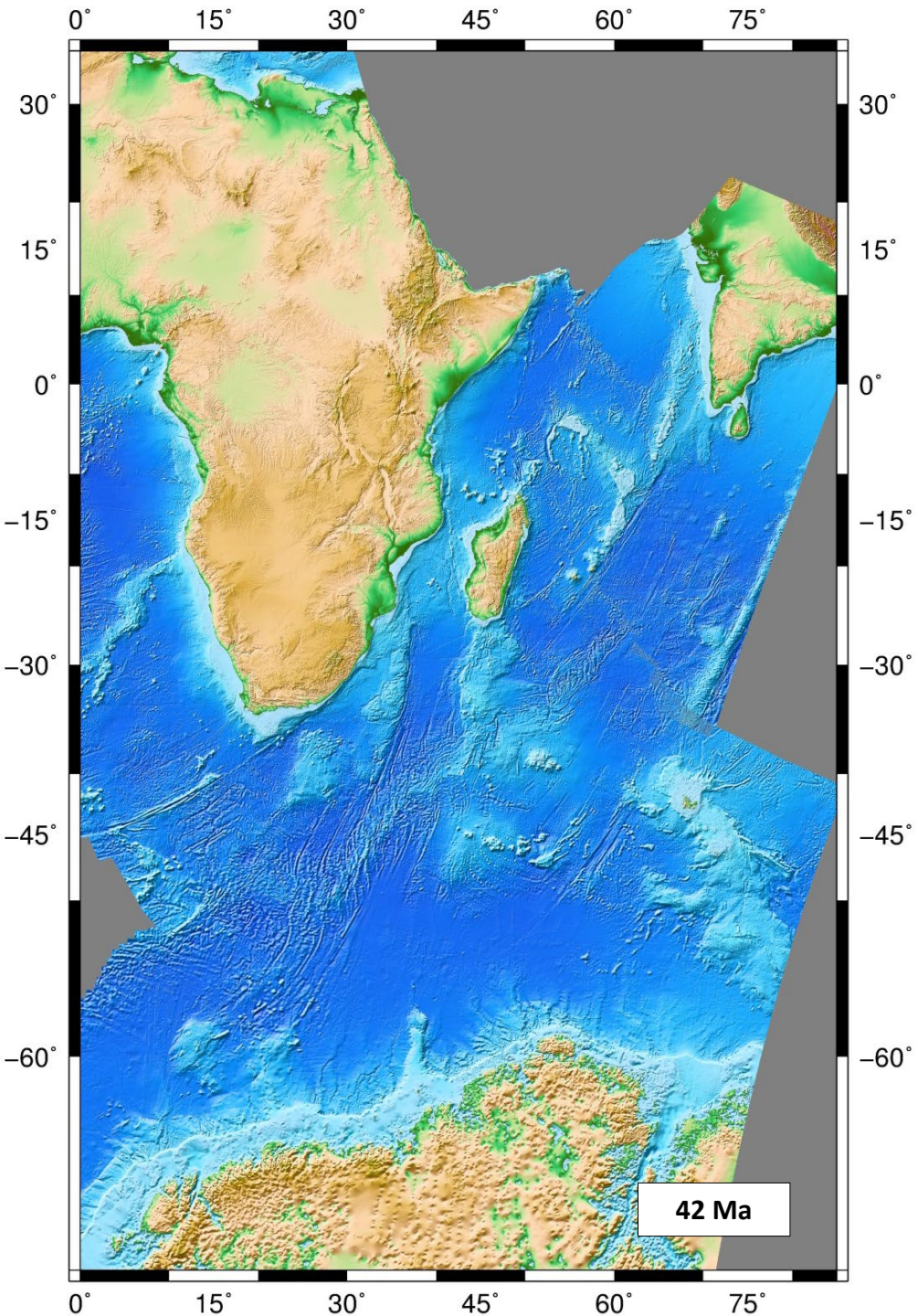
0°
15°
30°
45°
60°
75°
30°
15°
0°
−15°
−30°
−45°
−60°
42 Ma

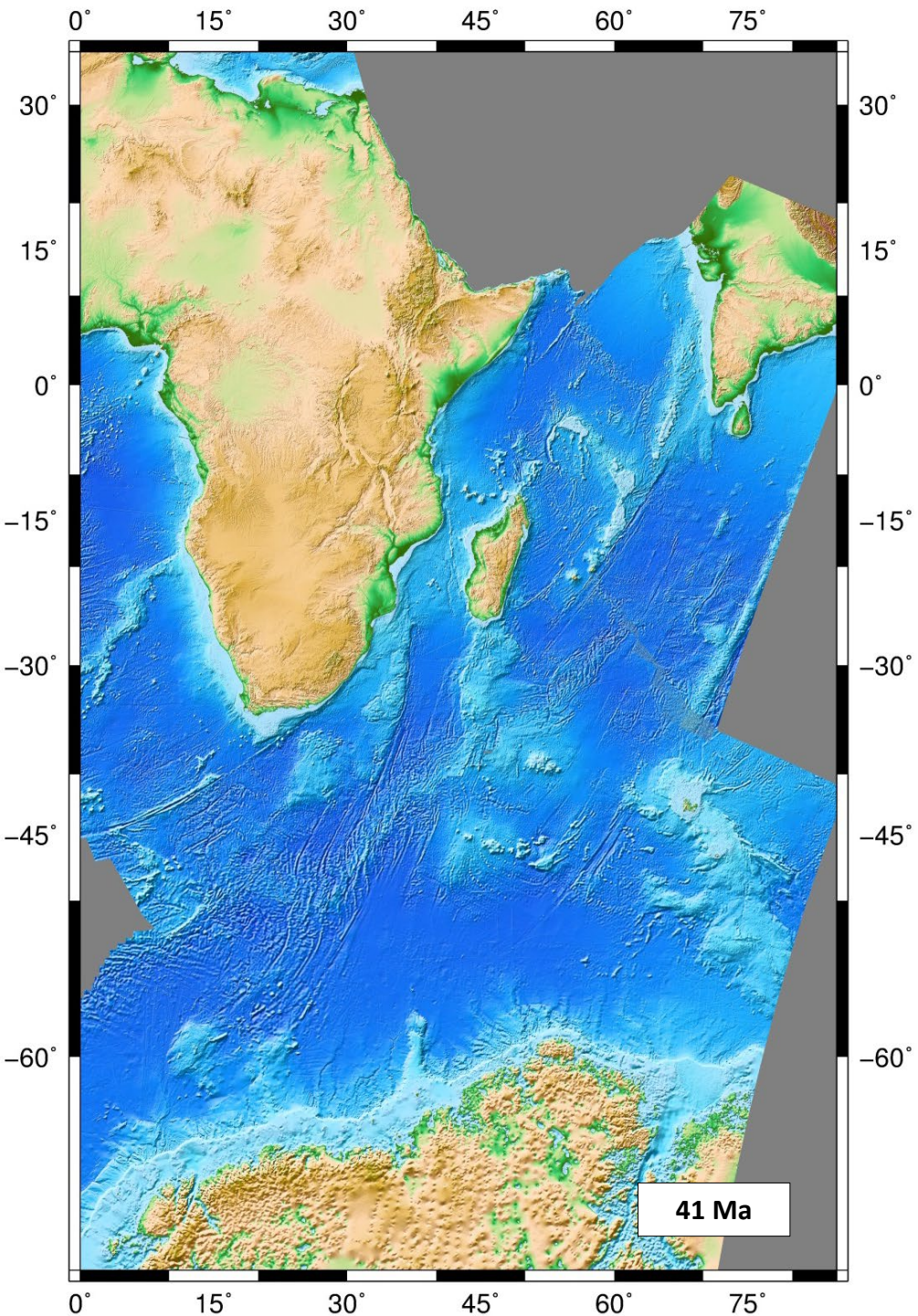
0°
15°
30°
45°
60°
75°
30°
15°
0°
−15°
−30°
−45°
−60°
41 Ma

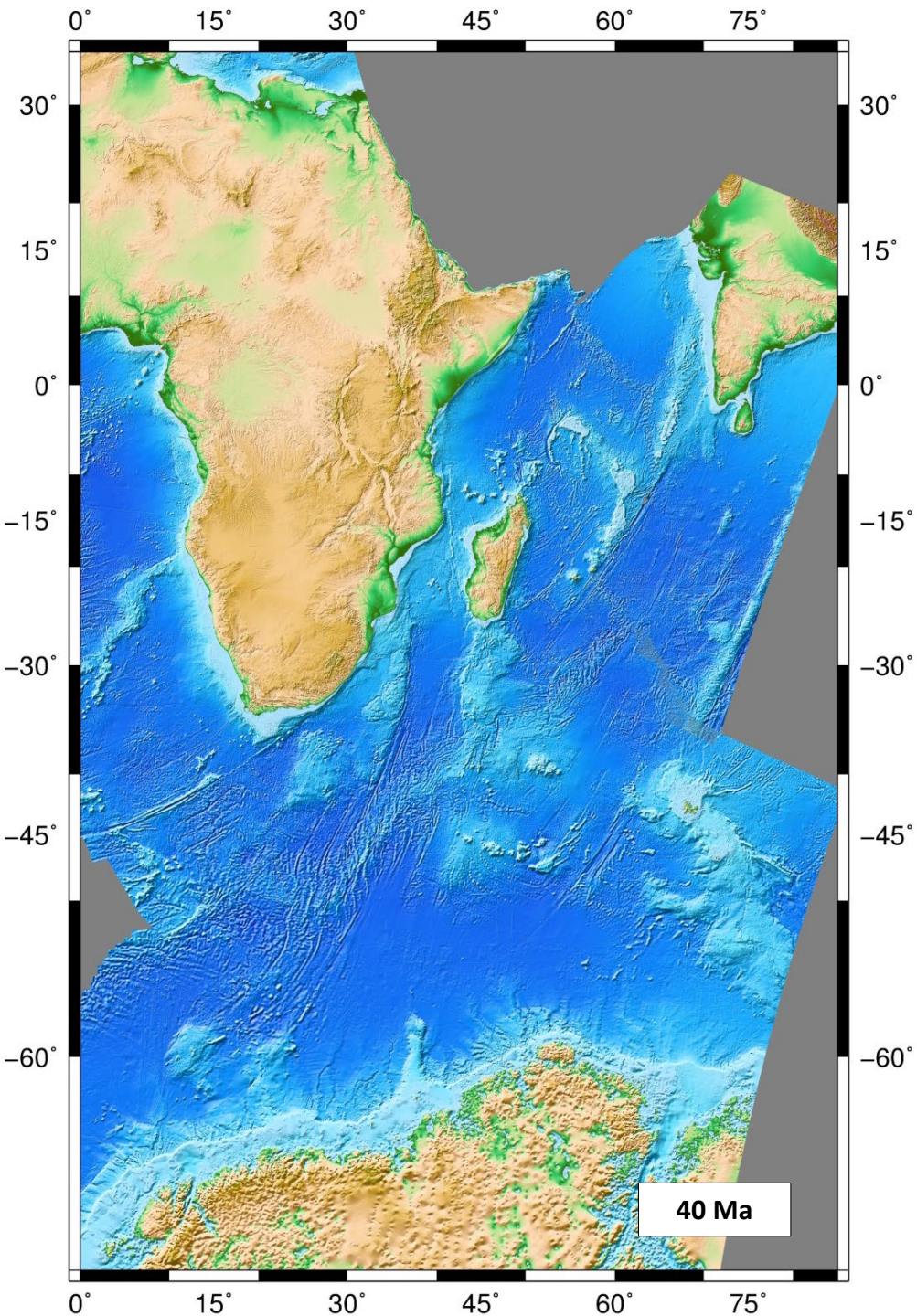
0°
15°
30°
45°
60°
75°
30°
15°
0°
−15°
−30°
−45°
−60°
40 Ma

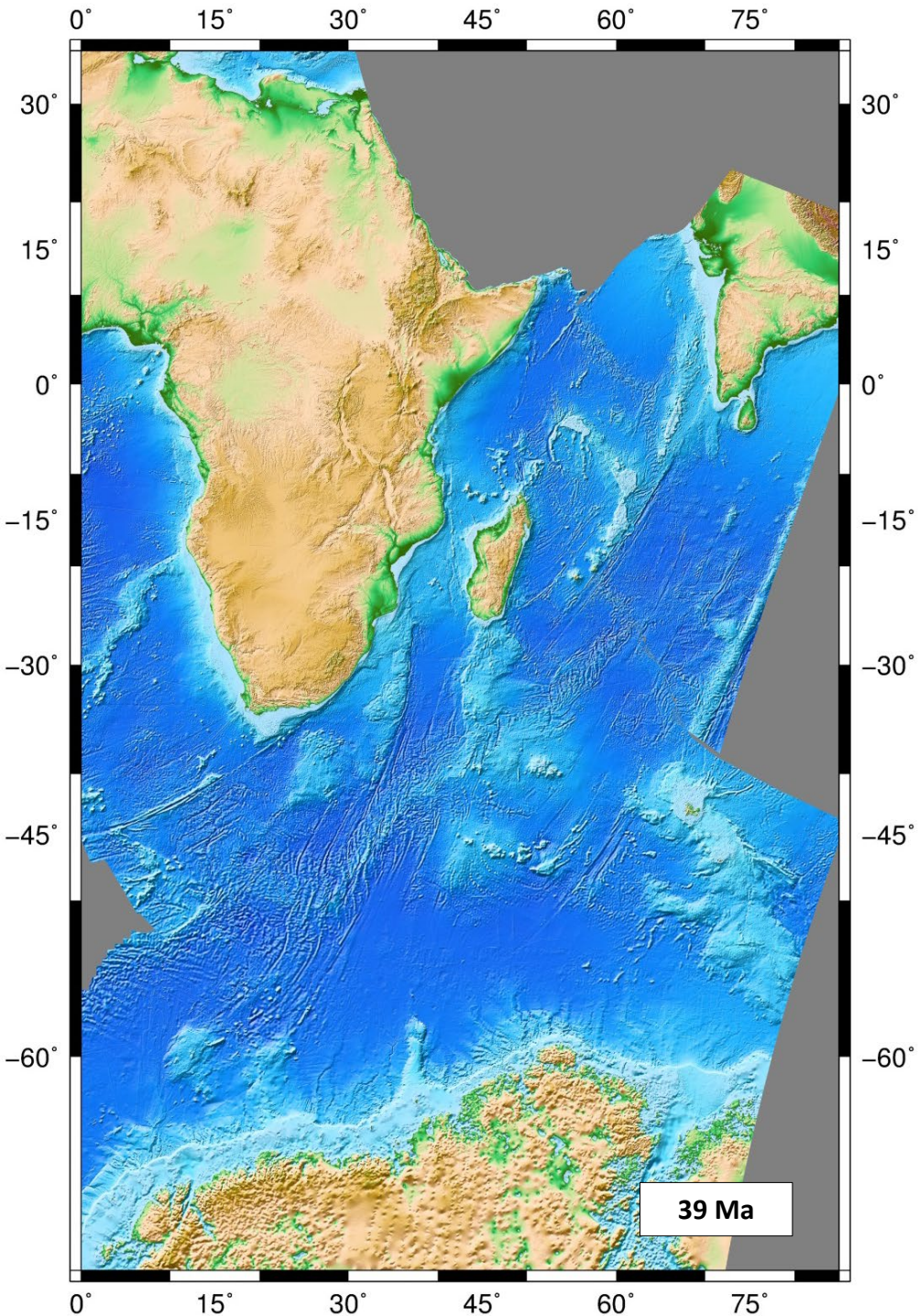
0°
15°
30°
45°
60°
75°
30°
15°
0°
−15°
−30°
−45°
−60°
39 Ma

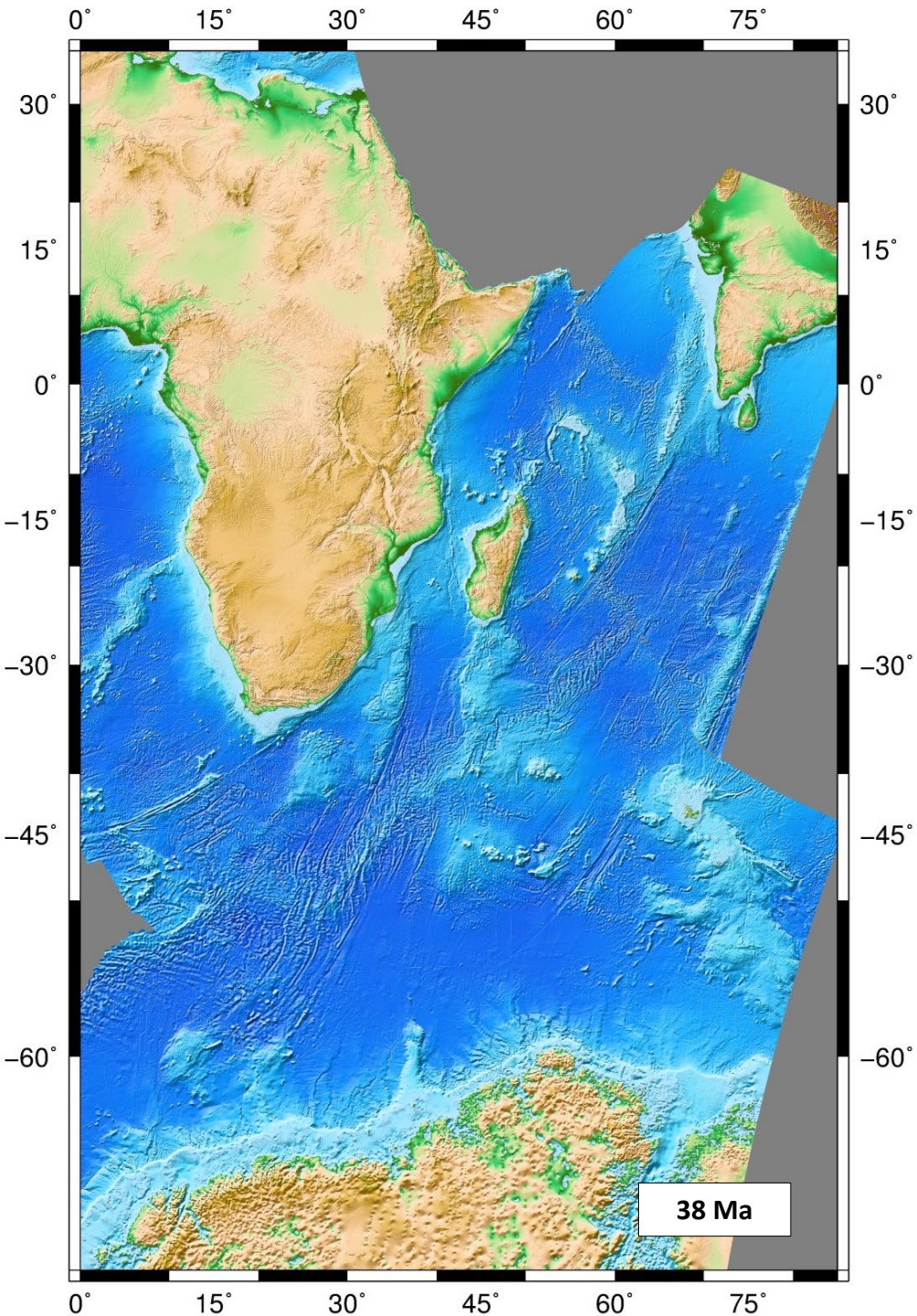
0°
15°
30°
45°
60°
75°
30°
15°
0°
−15°
−30°
−45°
−60°
38 Ma

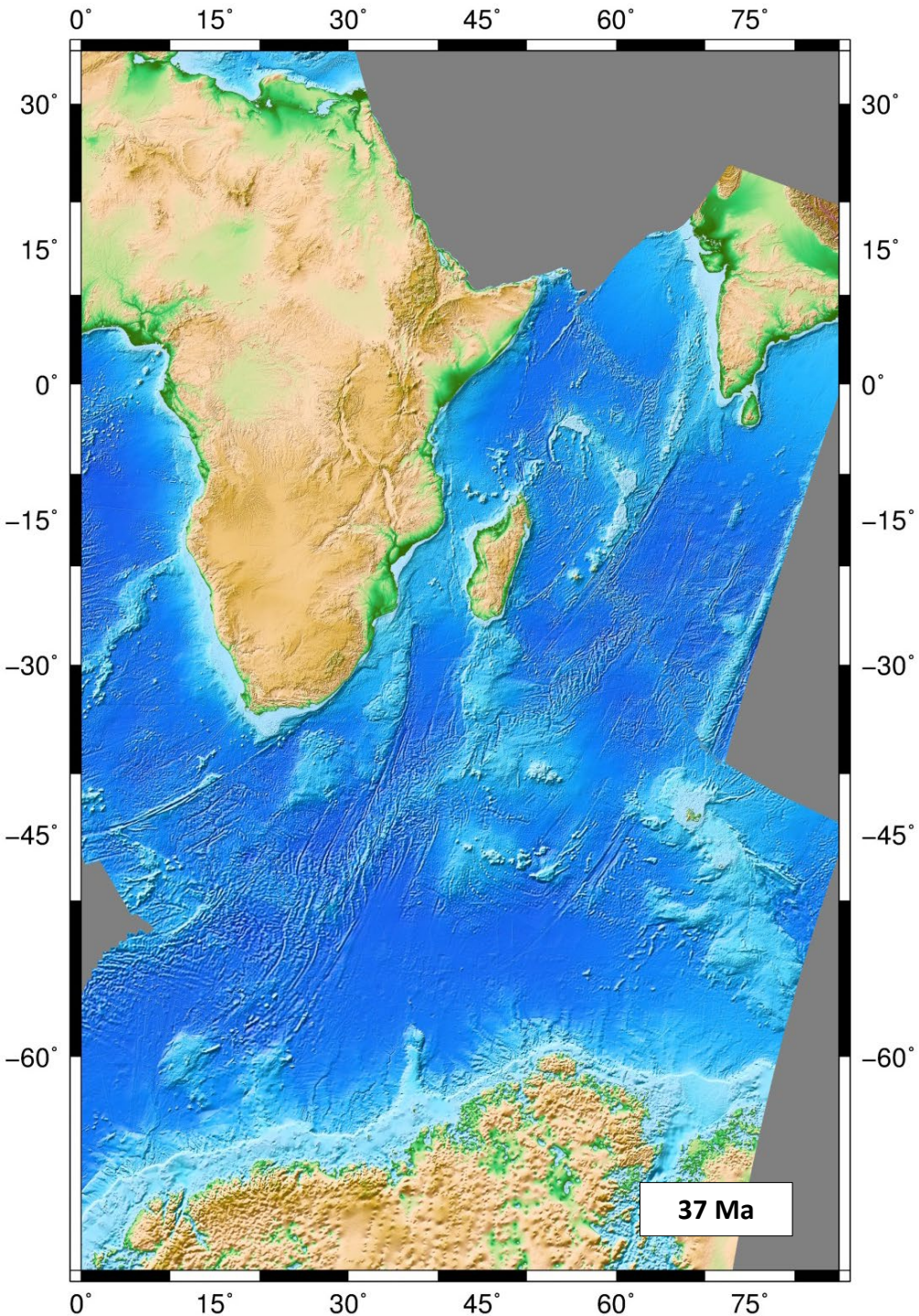
0˚
15˚
30˚
45˚
60˚
75˚
30˚
15˚
0˚
–15˚
–30˚
–45˚
–60˚
37 Ma

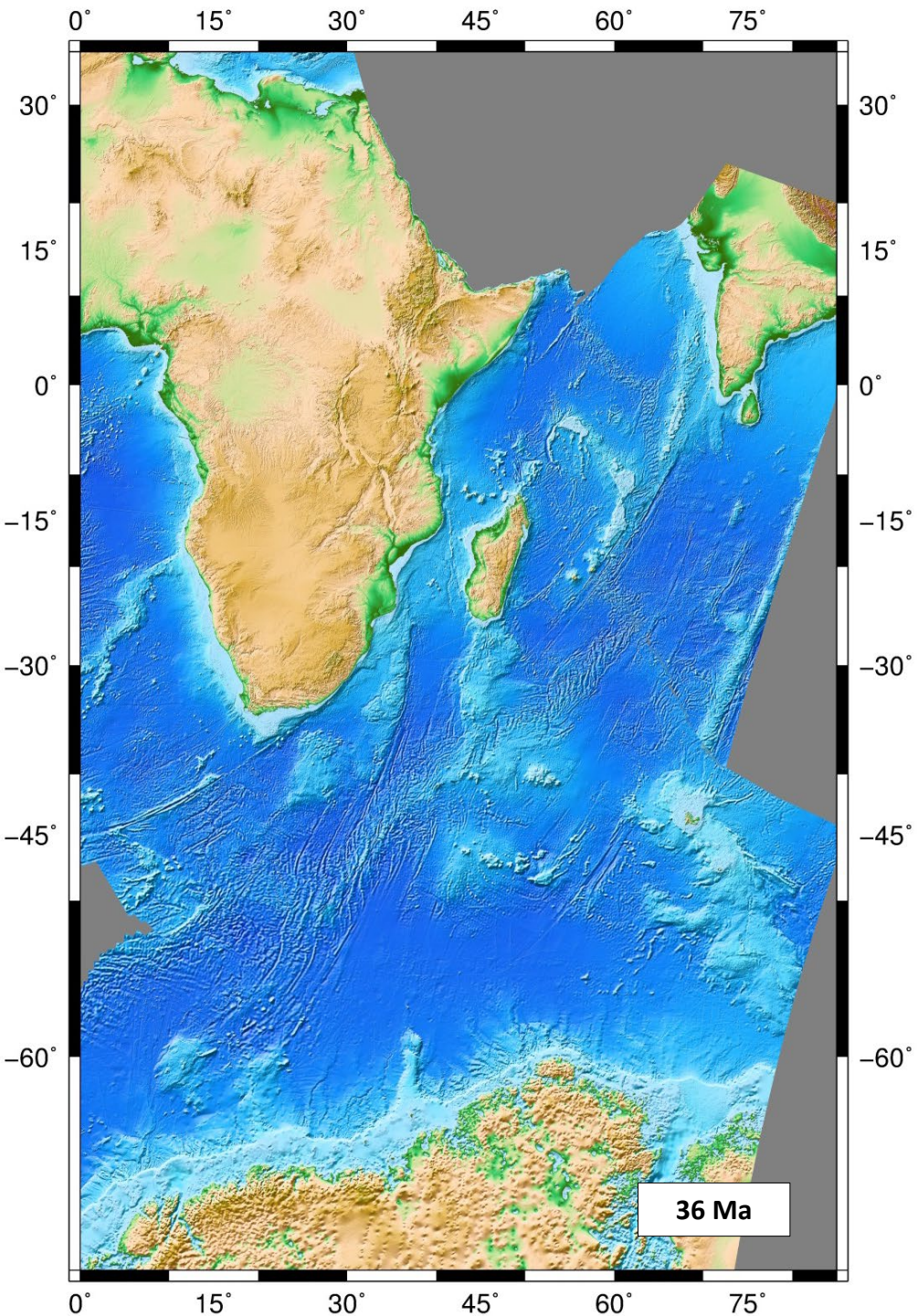
0°
15°
30°
45°
60°
75°
30°
15°
0°
−15°
−30°
−45°
−60°
36 Ma

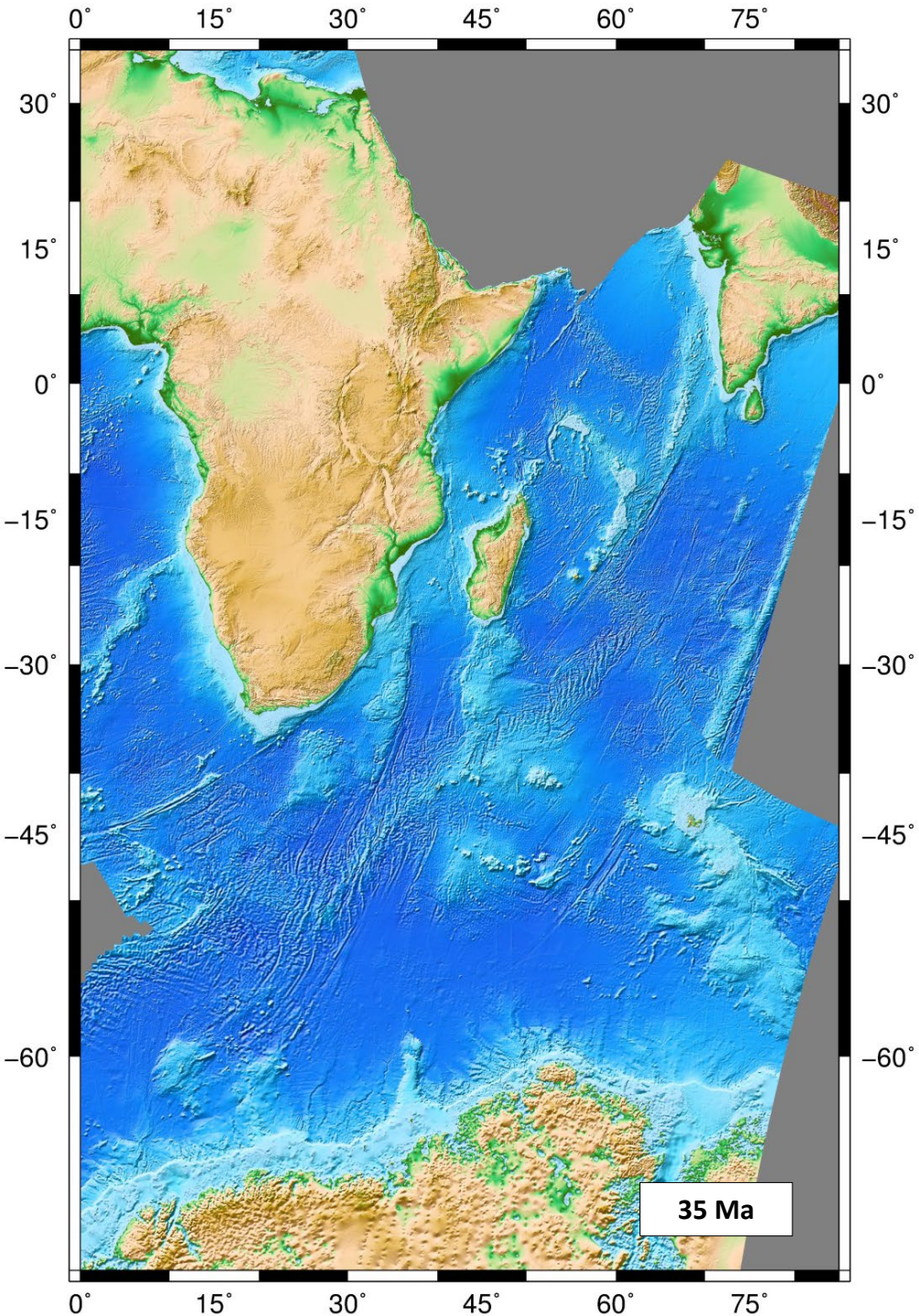
0°
15°
30°
45°
60°
75°
30°
15°
0°
−15°
−30°
−45°
−60°
35 Ma

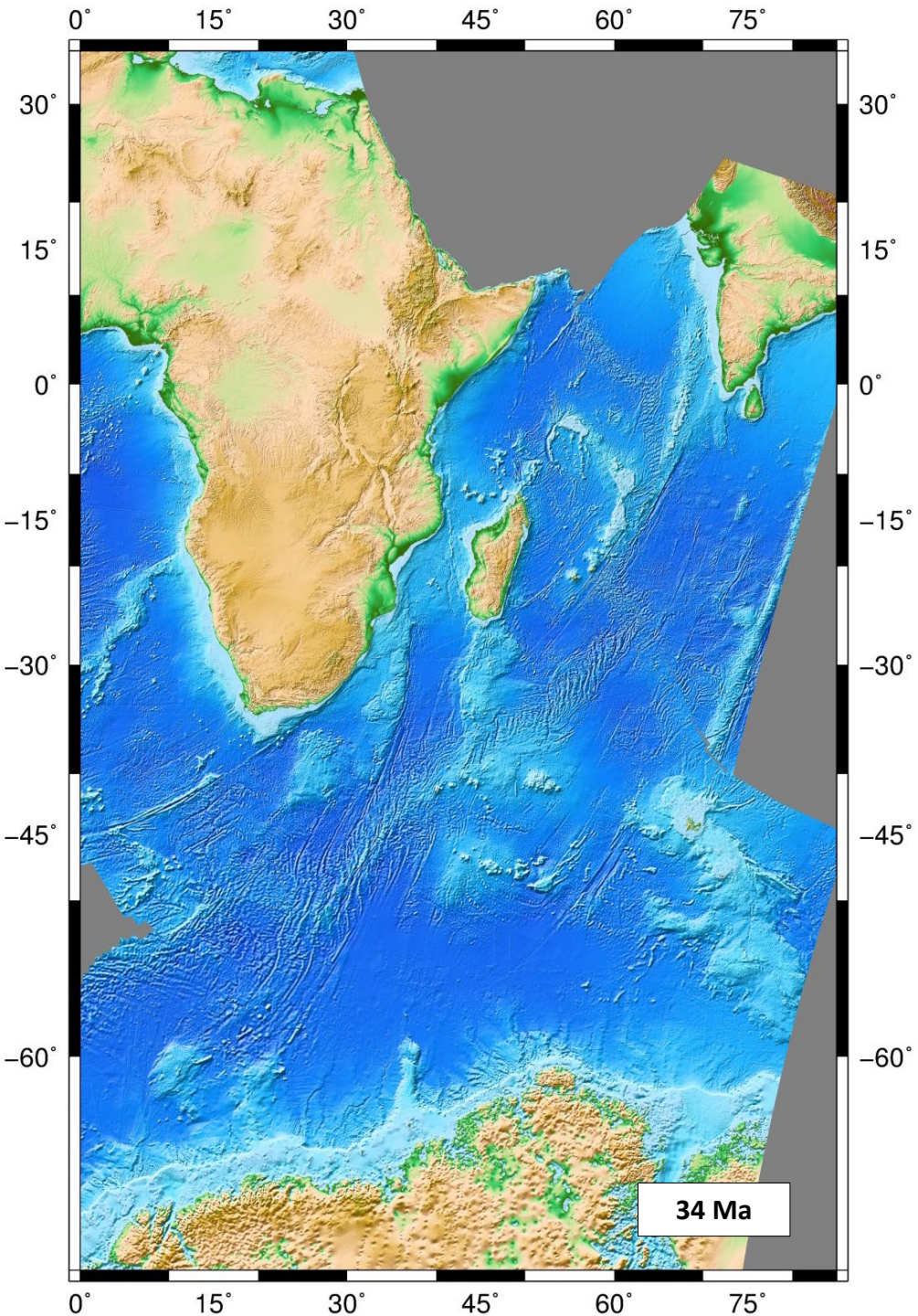
0°
15°
30°
45°
60°
75°
30°
15°
0°
−15°
−30°
−45°
−60°
34 Ma

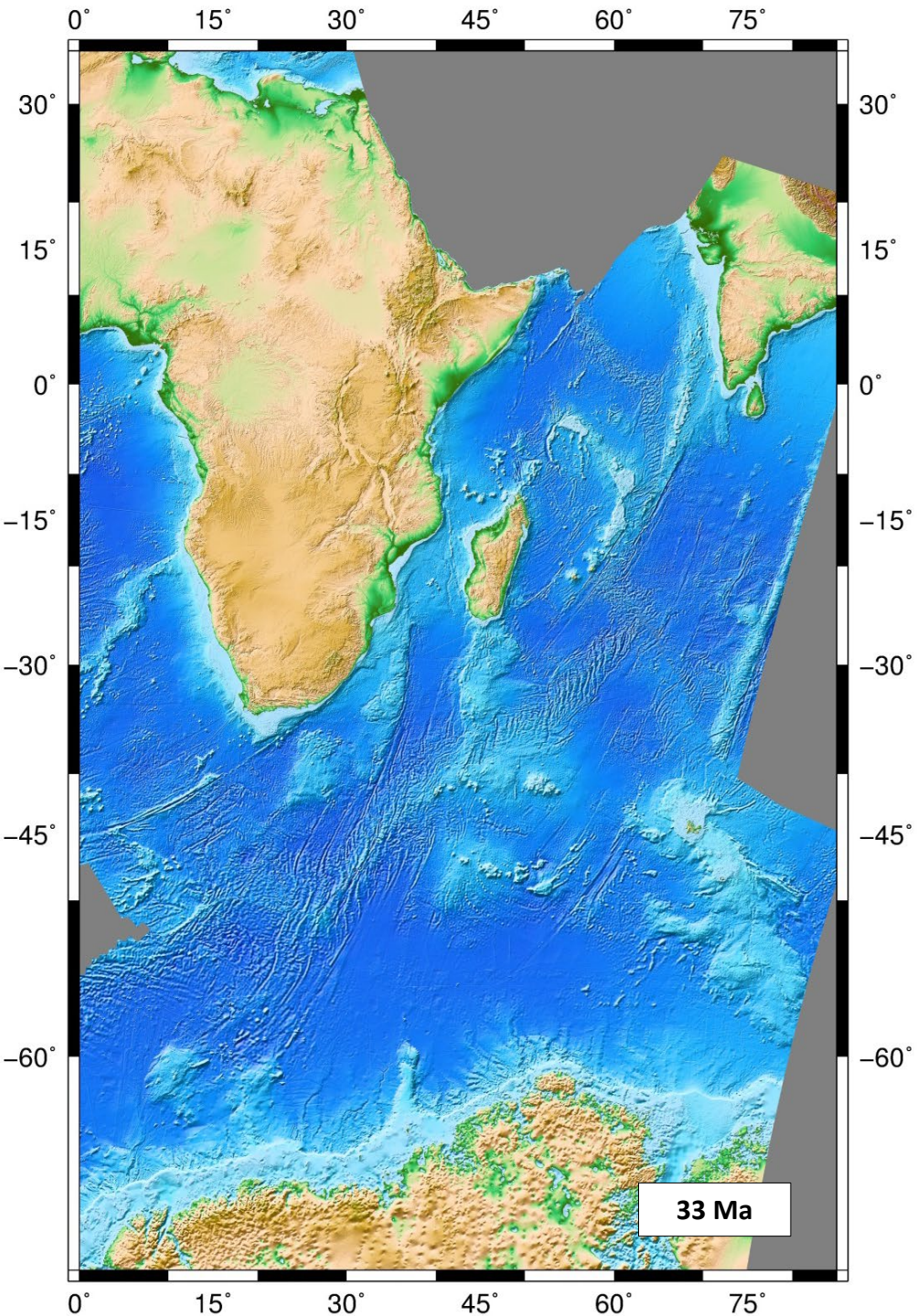
0˚
15˚
30˚
45˚
60˚
75˚
30˚
15˚
0˚
–15˚
–30˚
–45˚
–60˚
33 Ma

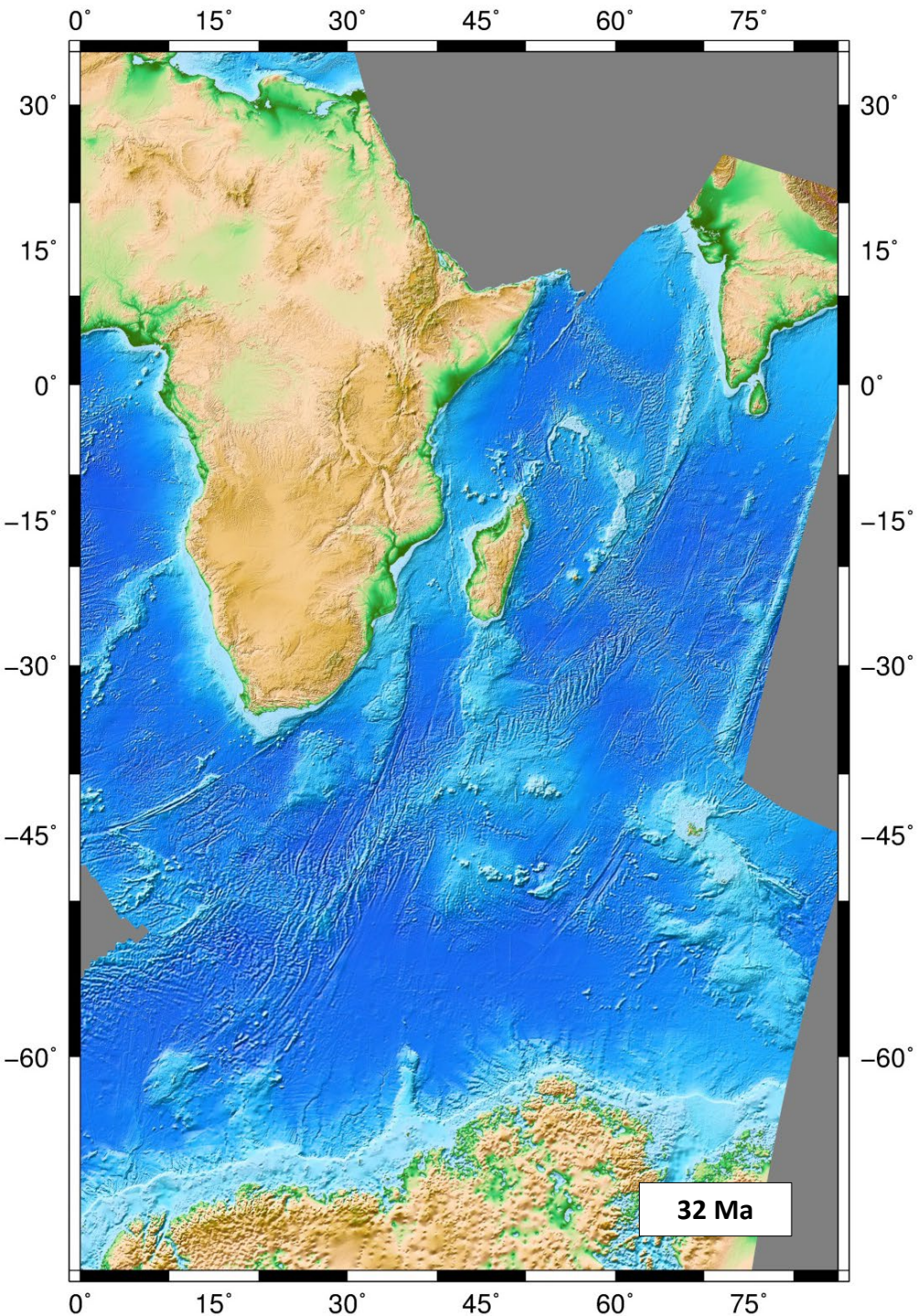
0°
15°
30°
45°
60°
75°
30°
15°
0°
−15°
−30°
−45°
−60°
32 Ma

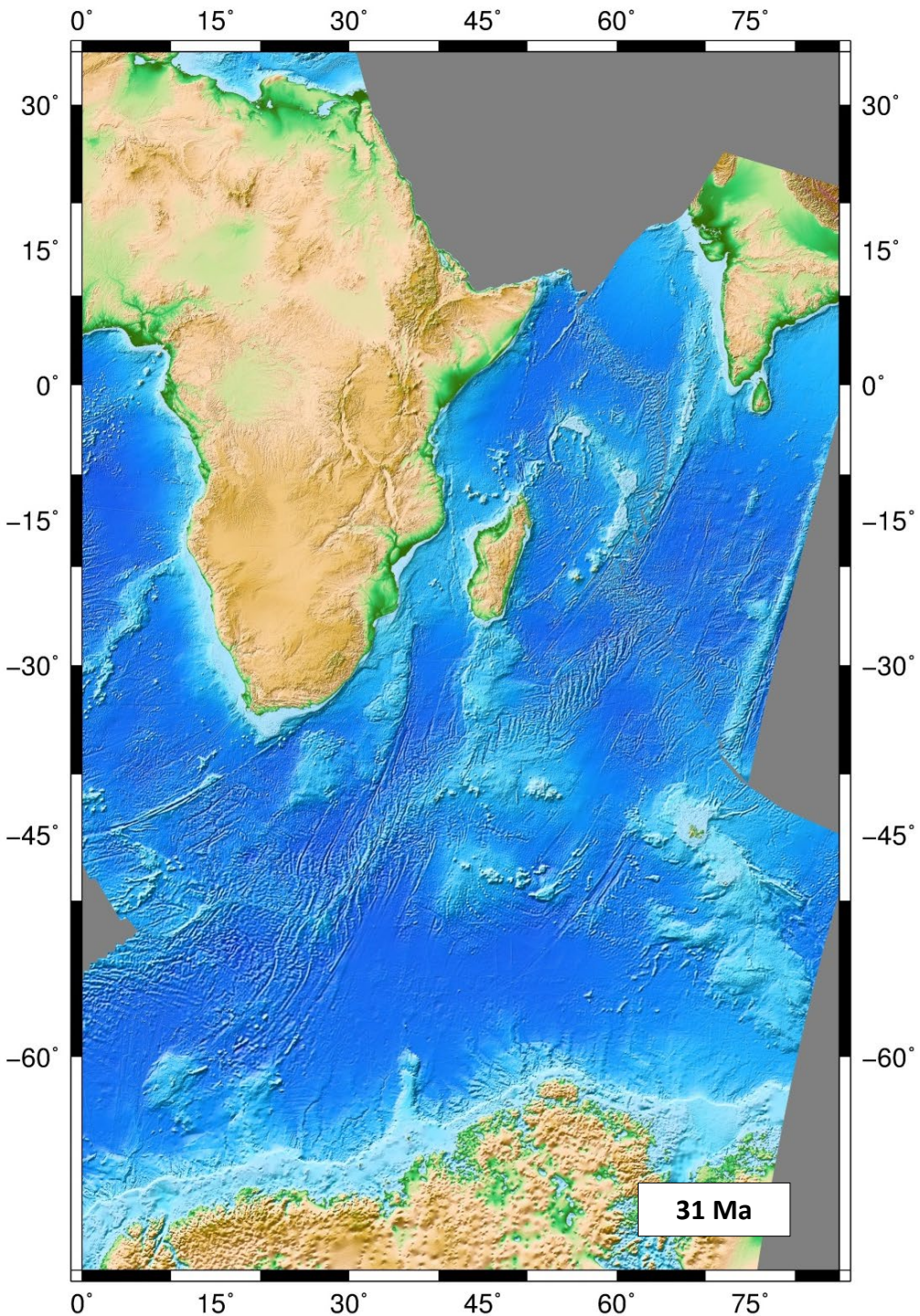
0˚
15˚
30˚
45˚
60˚
75˚
30˚
15˚
0˚
–15˚
–30˚
–45˚
–60˚
31 Ma

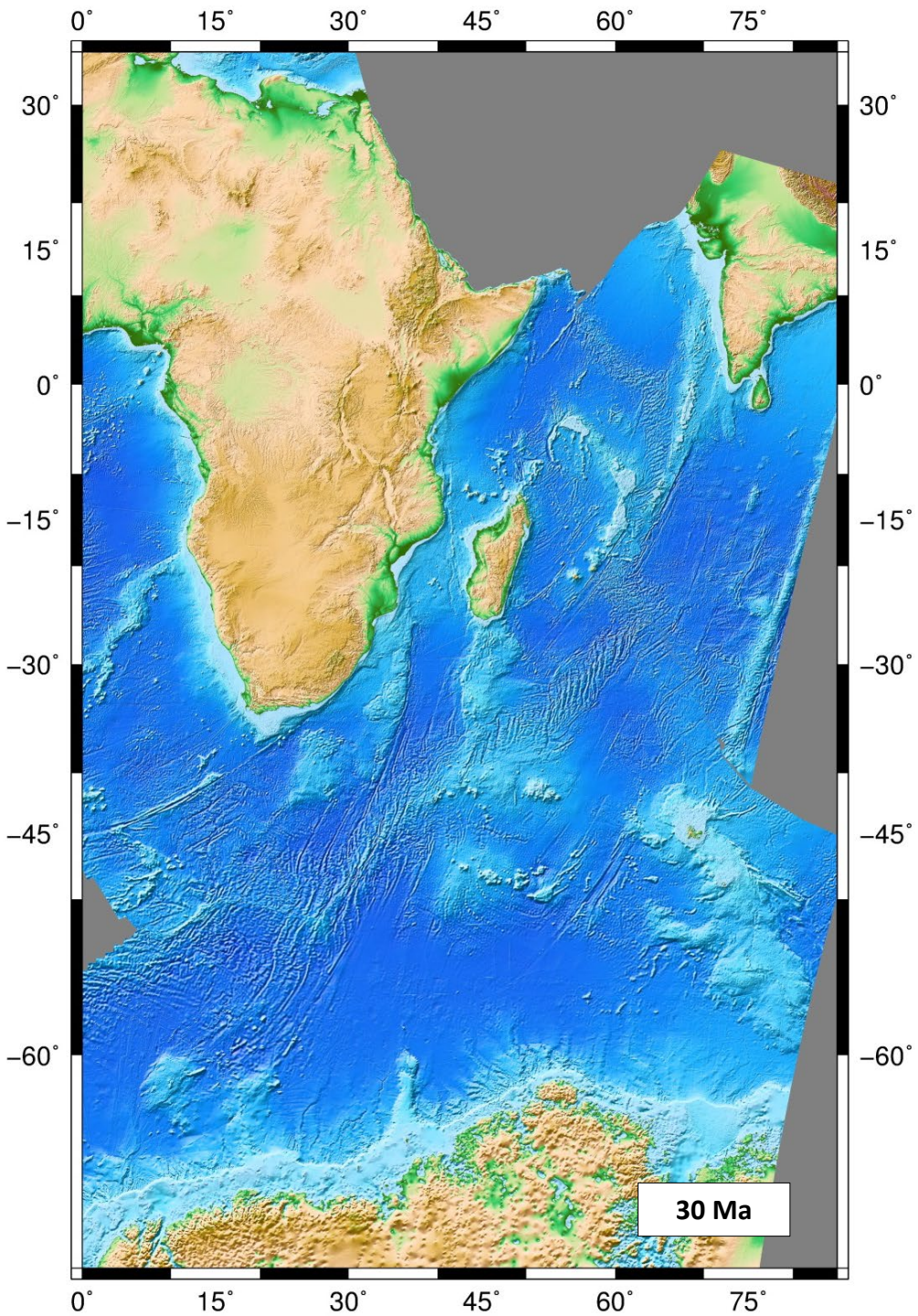
0˚
15˚
30˚
45˚
60˚
75˚
30˚
15˚
0˚
–15˚
–30˚
–45˚
–60˚
30 Ma

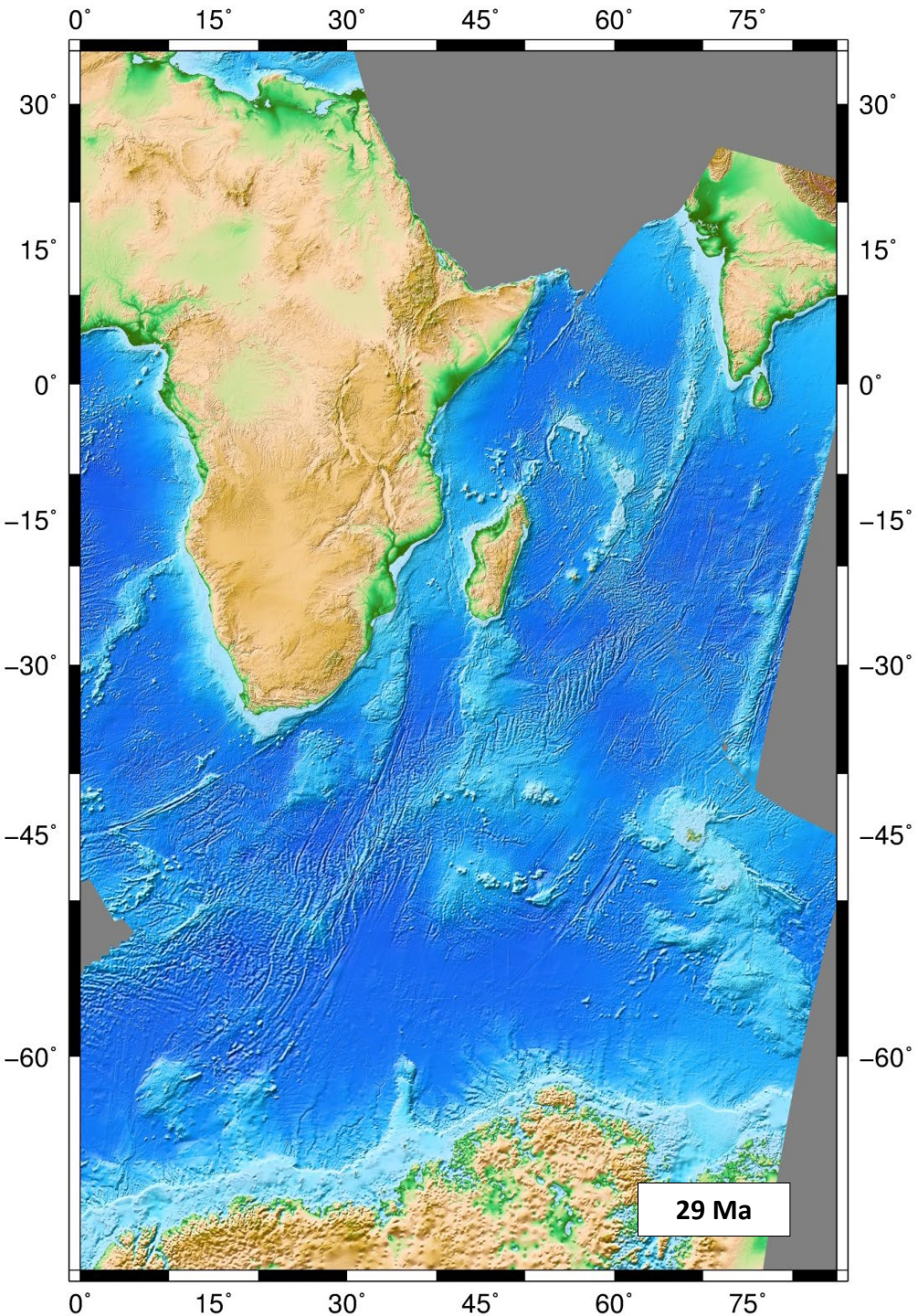
0°
15°
30°
45°
60°
75°
30°
15°
0°
−15°
−30°
−45°
−60°
29 Ma

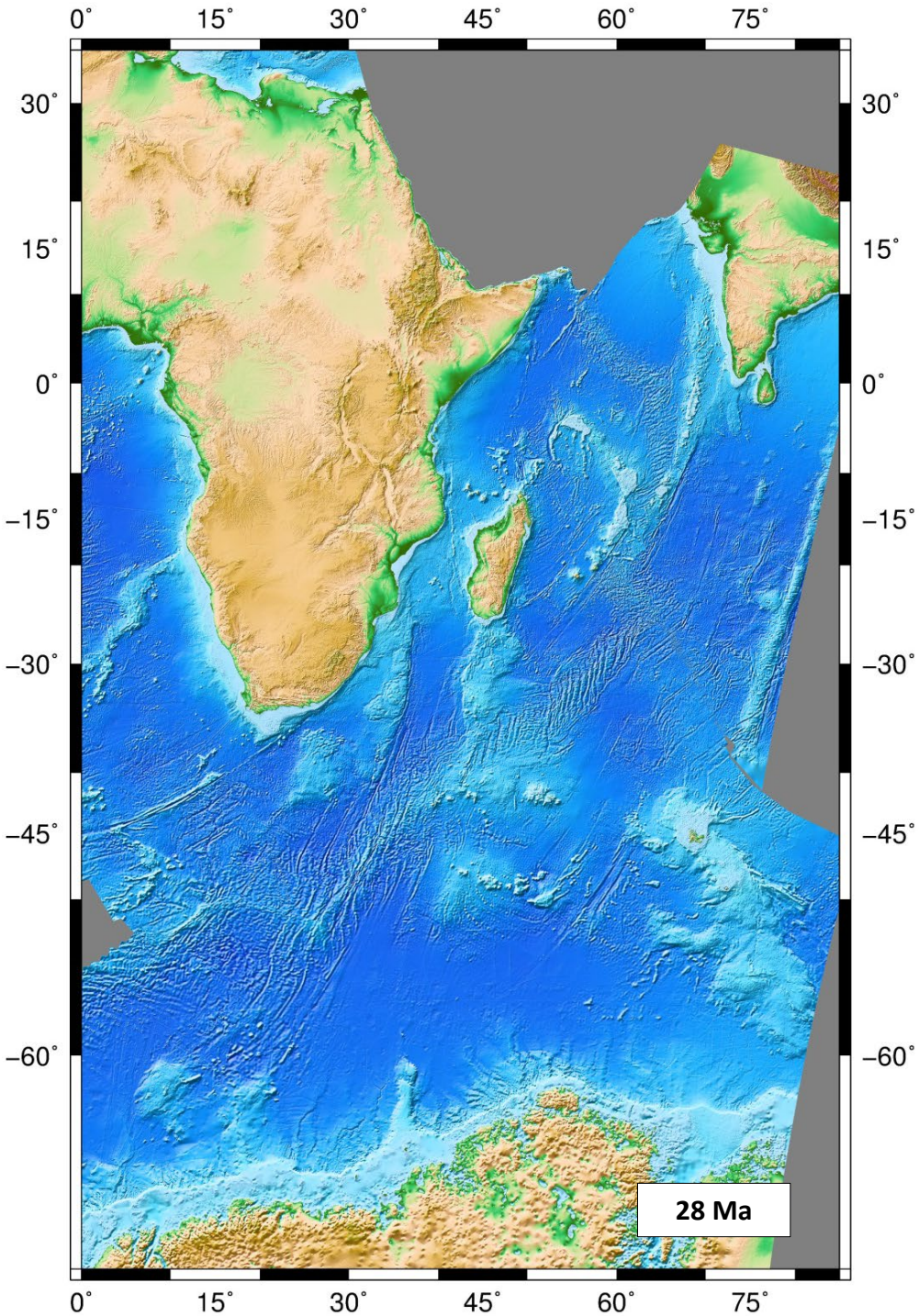
0°
15°
30°
45°
60°
75°
30°
15°
0°
−15°
−30°
−45°
−60°
28 Ma

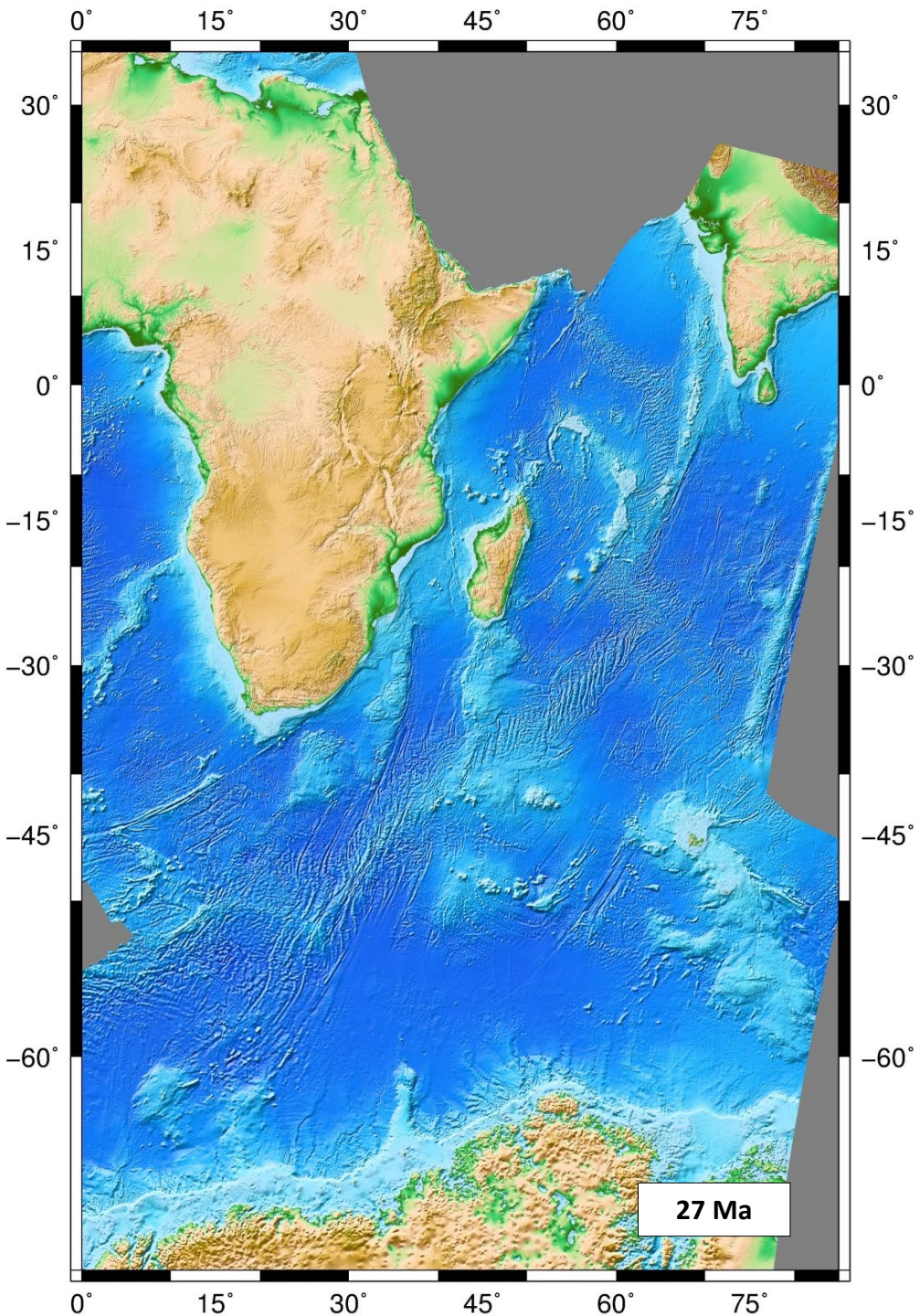
0˚
15˚
30˚
45˚
60˚
75˚
30˚
15˚
0˚
–15˚
–30˚
–45˚
–60˚
27 Ma

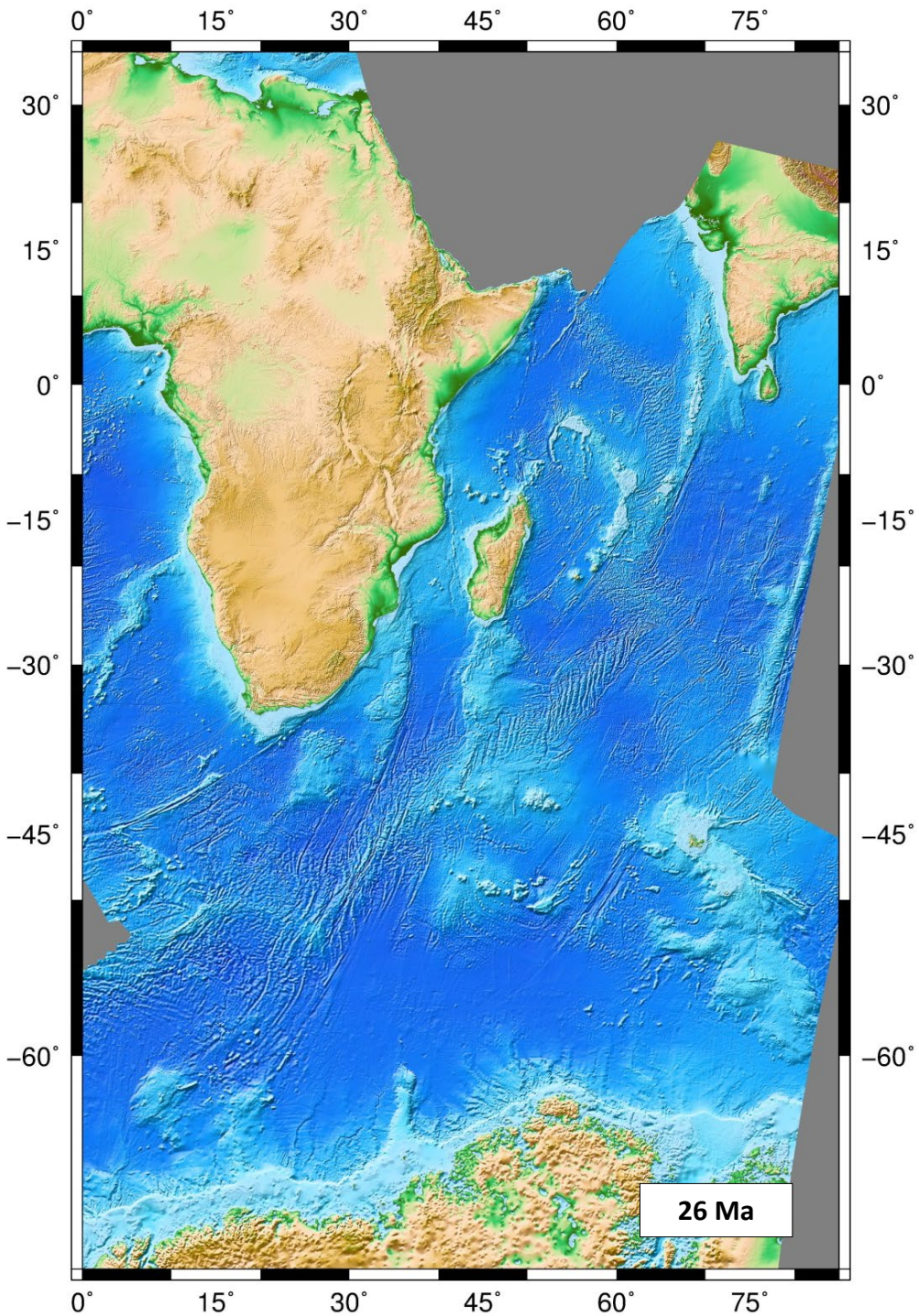
0°
15°
30°
45°
60°
75°
30°
15°
0°
−15°
−30°
−45°
−60°
26 Ma

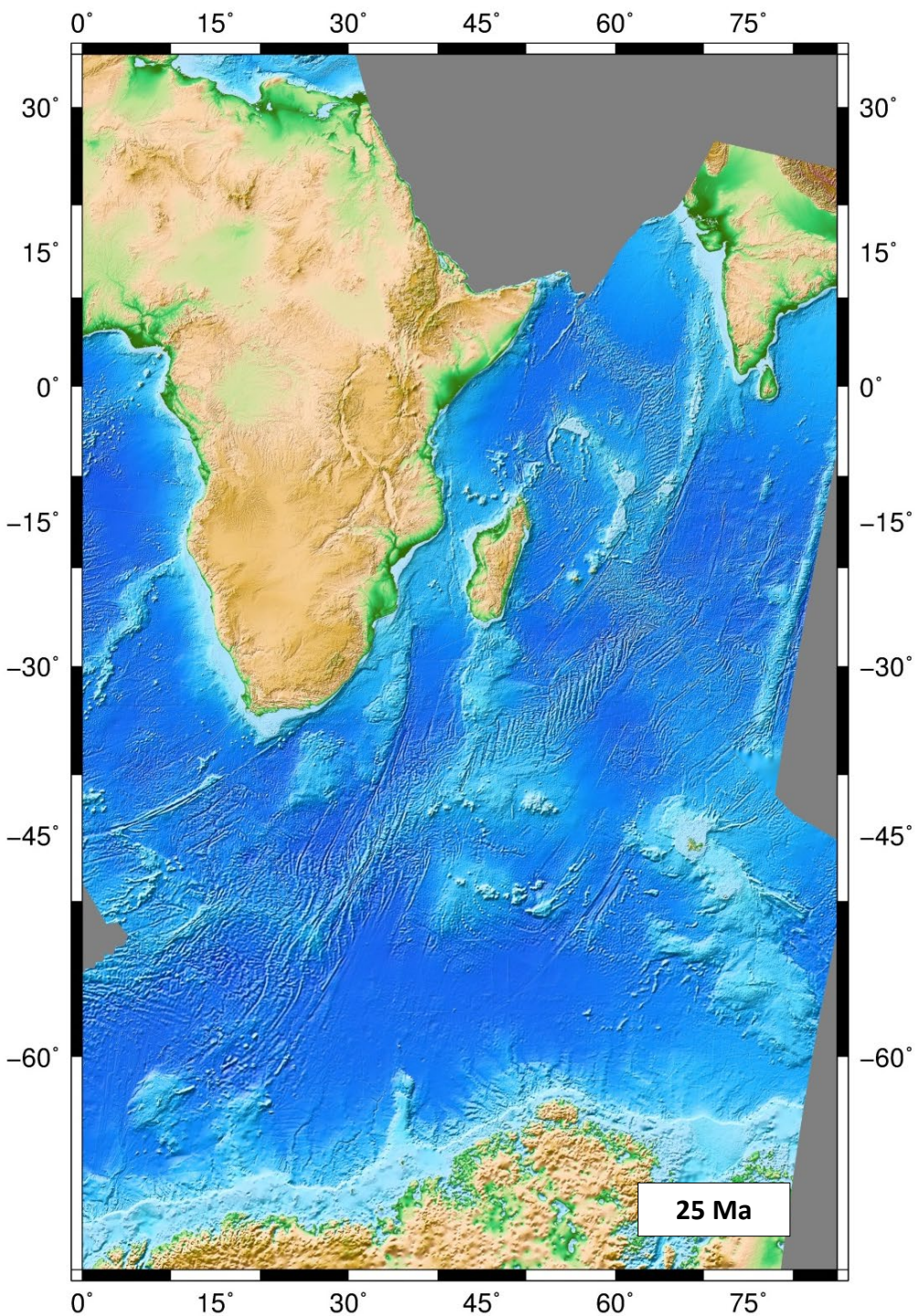
0°
15°
30°
45°
60°
75°
30°
15°
0°
–15°
–30°
–45°
–60°
25 Ma

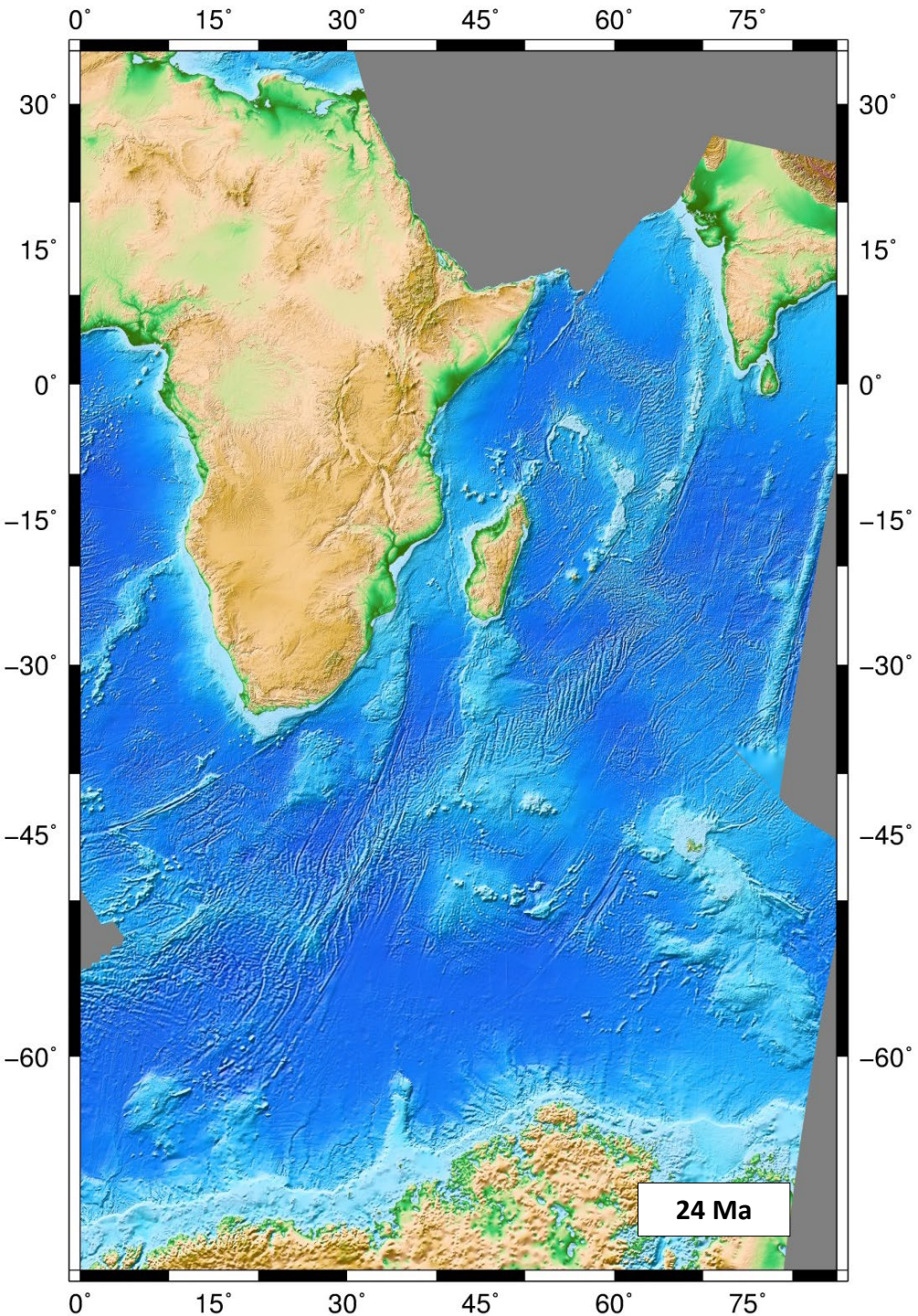
0˚
15˚
30˚
45˚
60˚
75˚
30˚
15˚
0˚
–15˚
–30˚
–45˚
–60˚
24 Ma

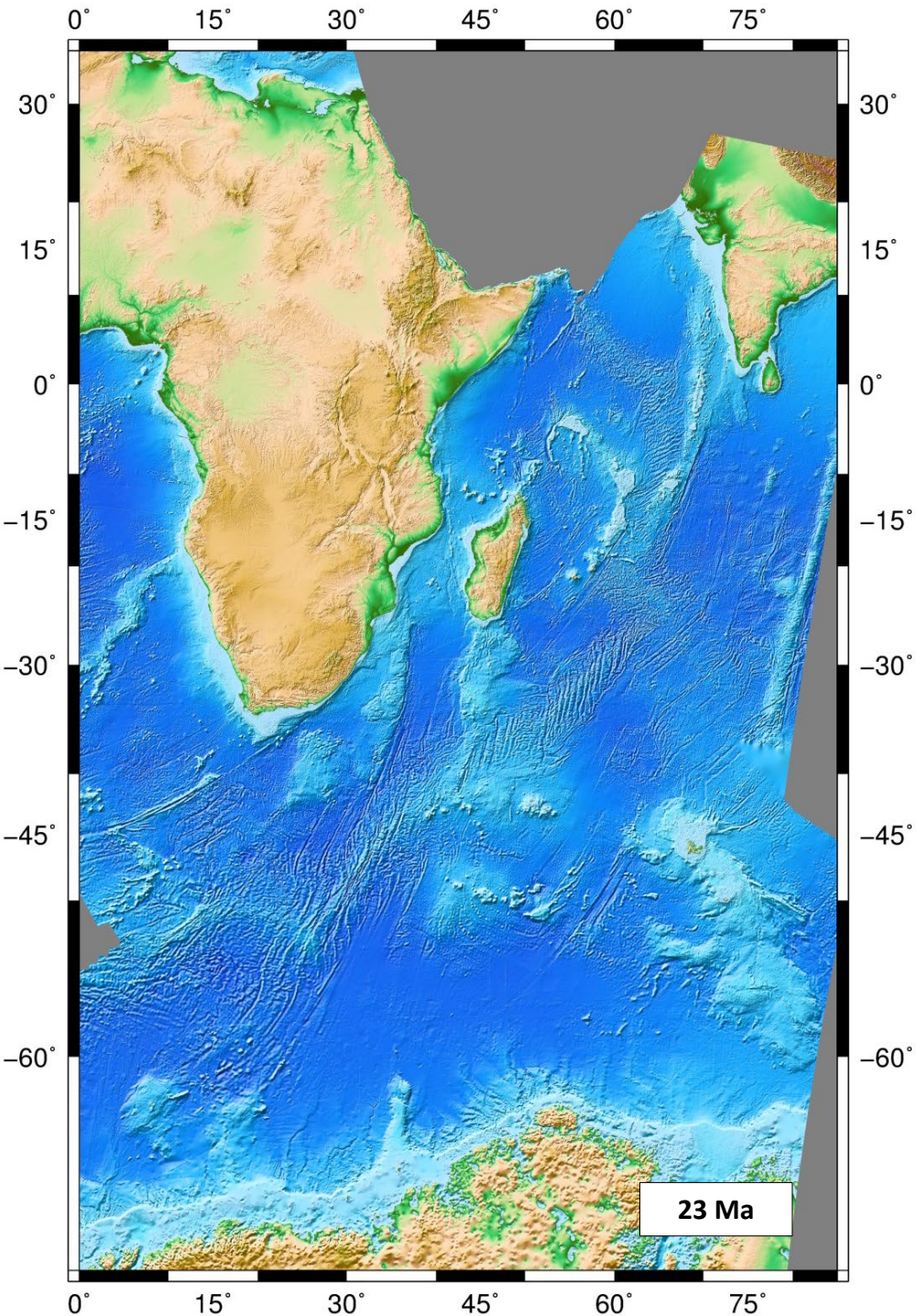
0°
15°
30°
45°
60°
75°
30°
15°
0°
−15°
−30°
−45°
−60°
23 Ma

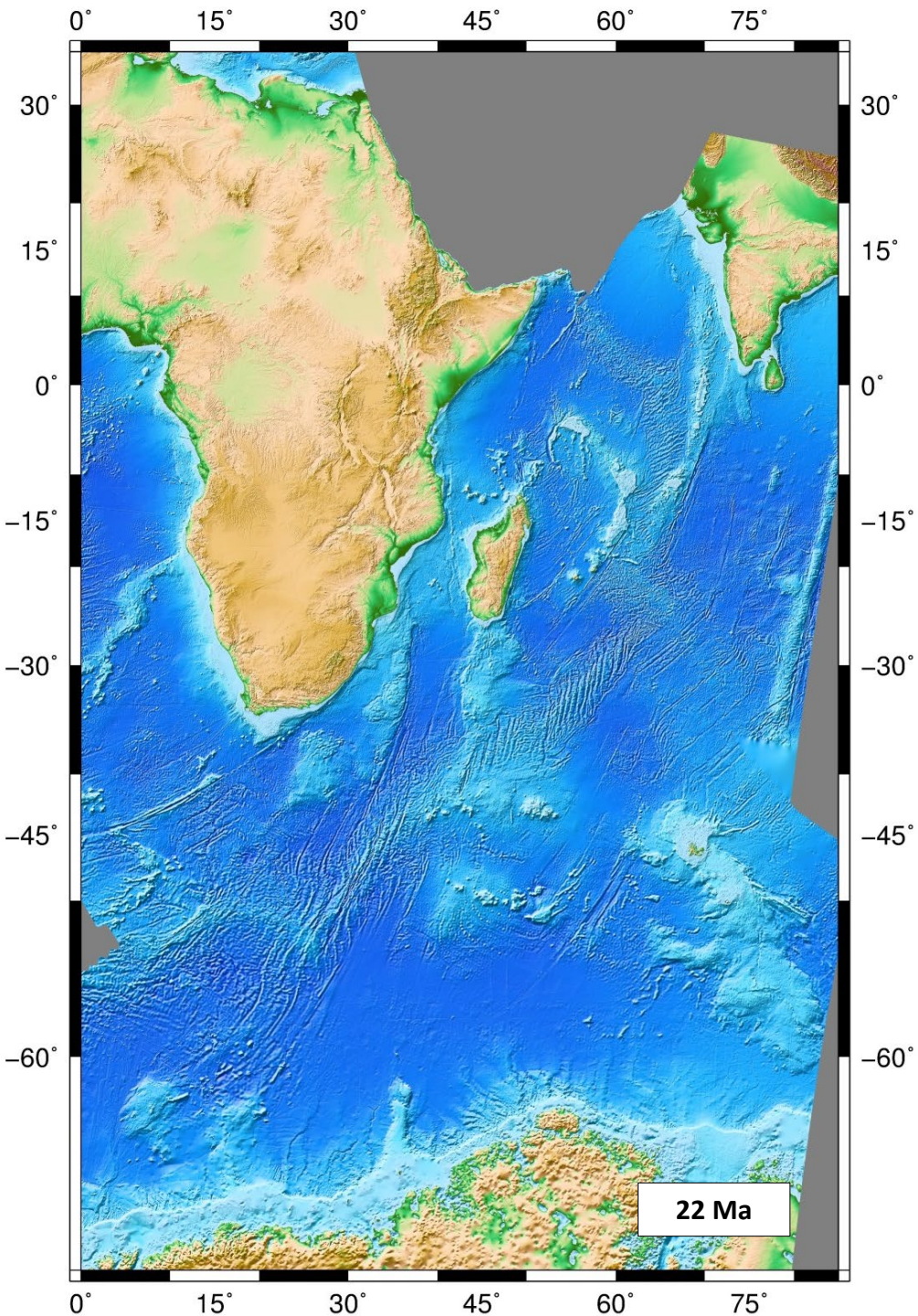
0˚
15˚
30˚
45˚
60˚
75˚
30˚
15˚
0˚
–15˚
–30˚
–45˚
–60˚
22 Ma

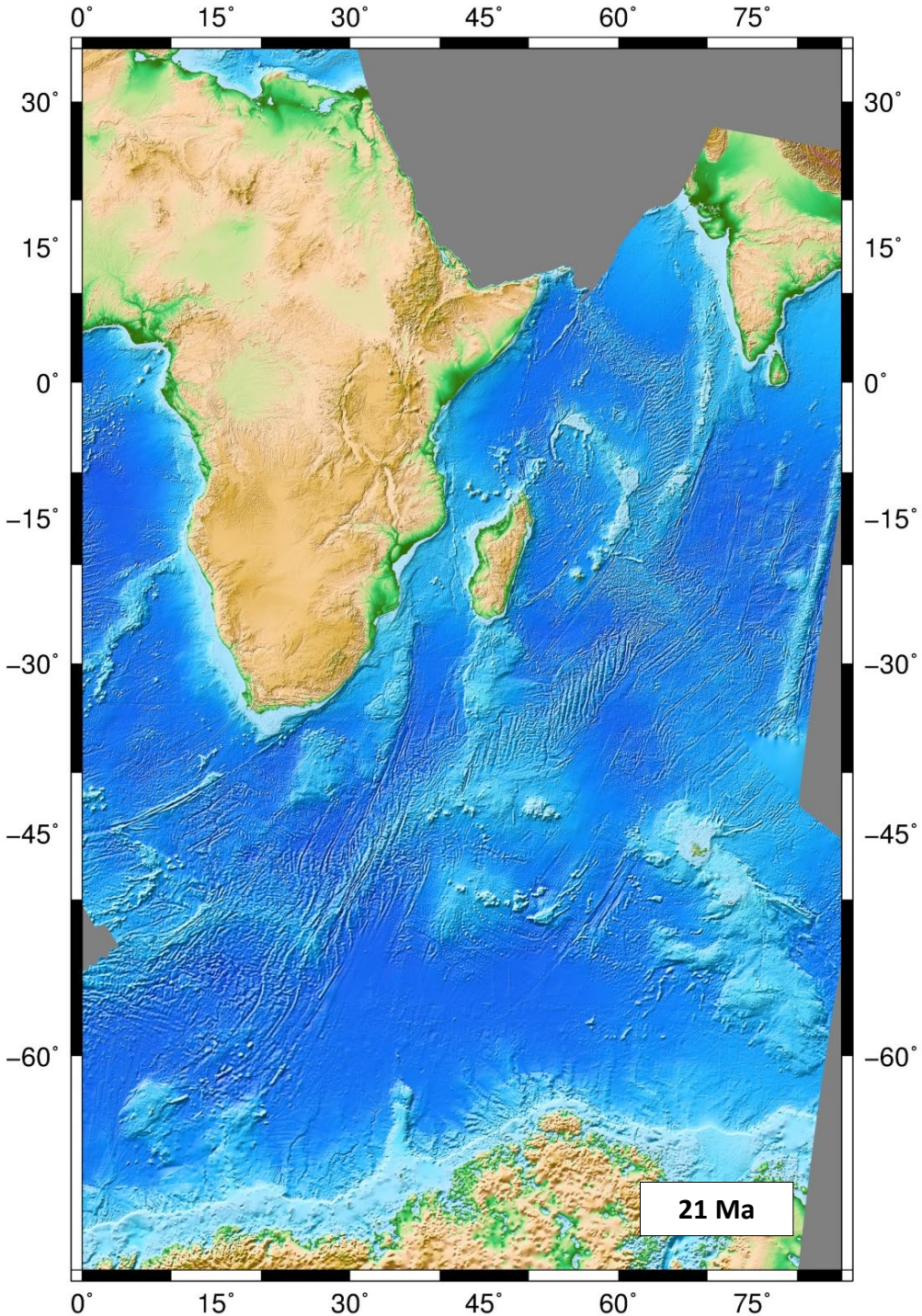
0°
15°
30°
45°
60°
75°
30°
15°
0°
–15°
–30°
–45°
–60°
21 Ma

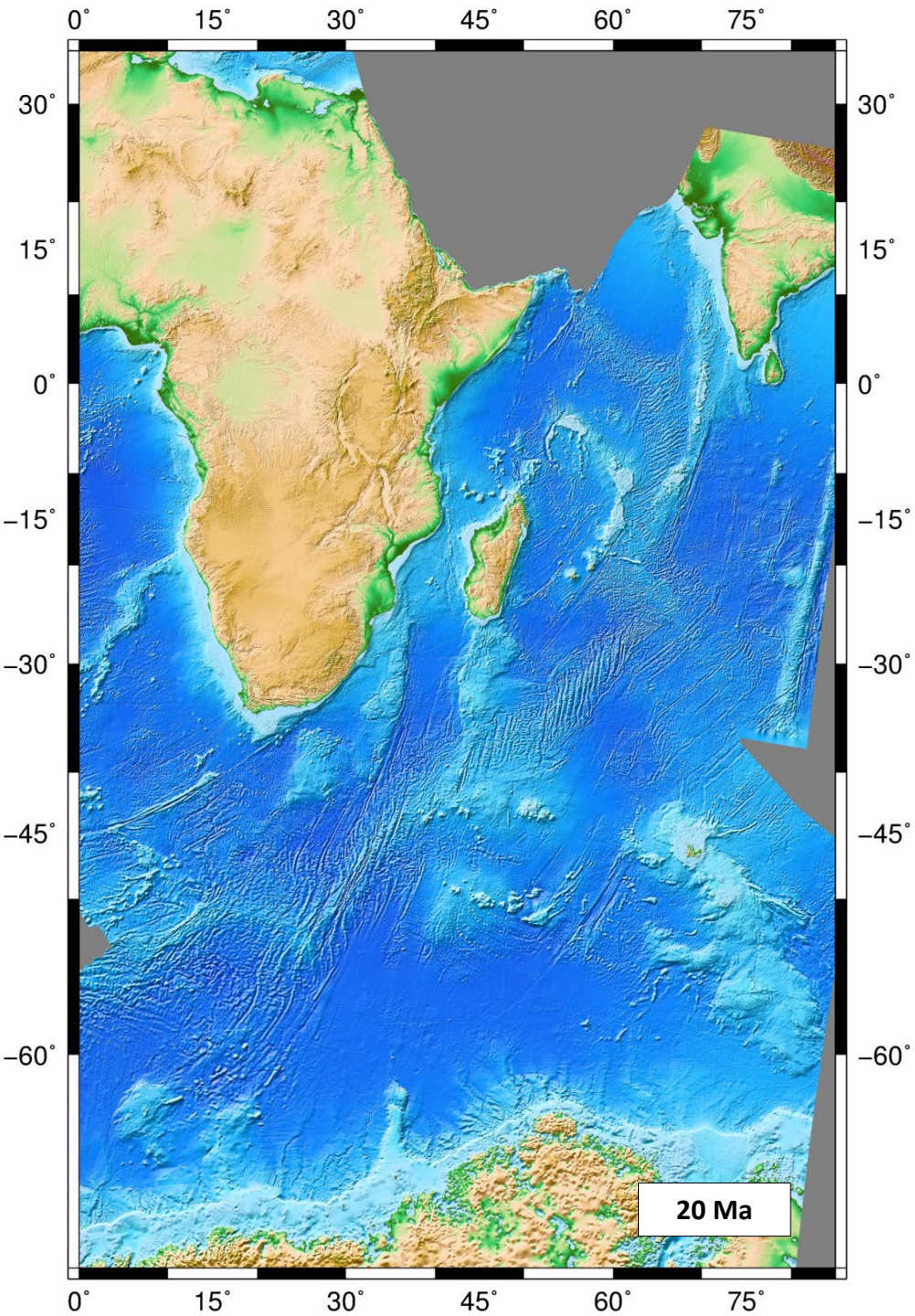
0˚
15˚
30˚
45˚
60˚
75˚
30˚
15˚
0˚
–15˚
–30˚
–45˚
–60˚
20 Ma

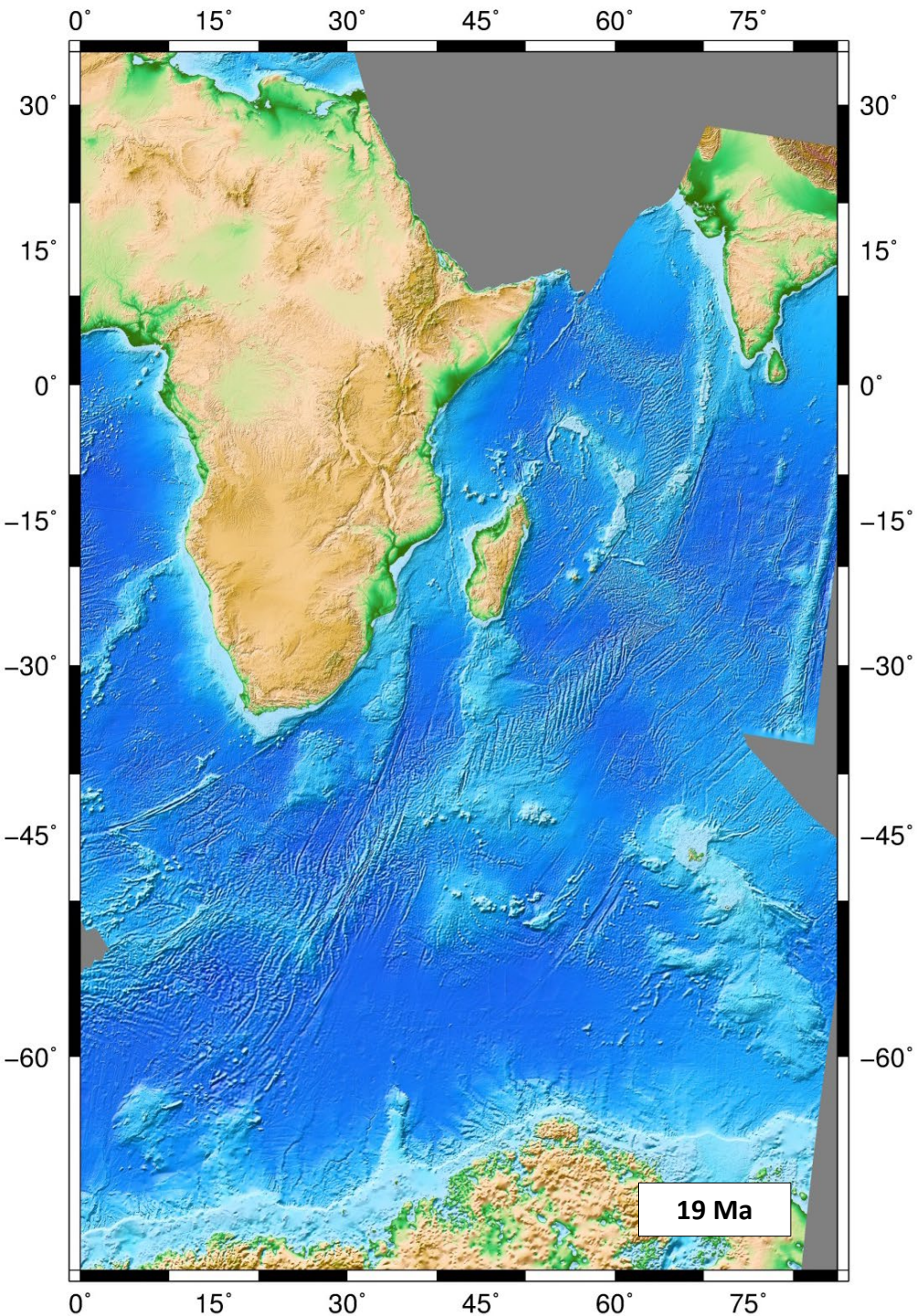
0°
15°
30°
45°
60°
75°
30°
15°
0°
−15°
−30°
−45°
−60°
19 Ma

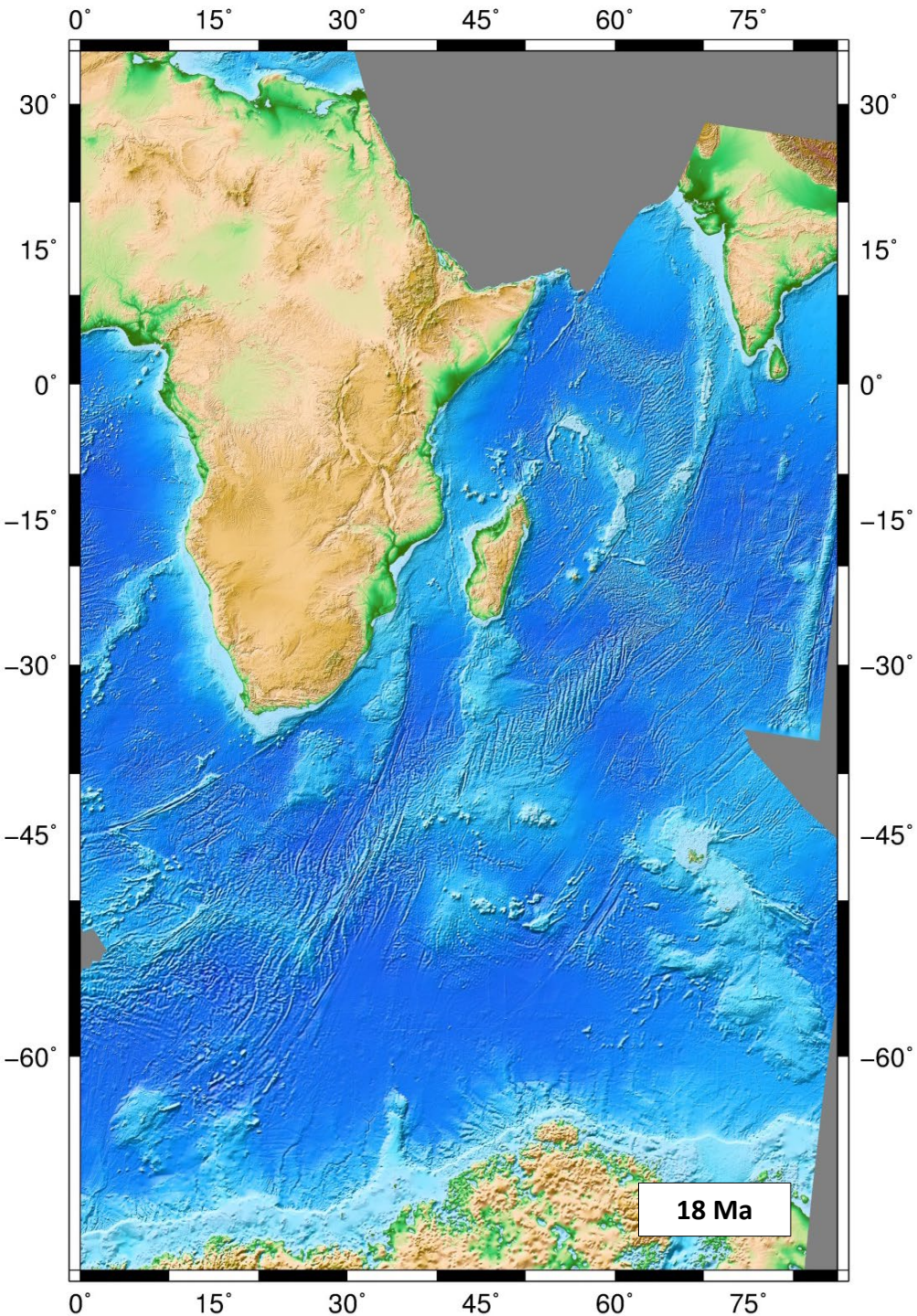
0°
15°
30°
45°
60°
75°
30°
15°
0°
−15°
−30°
−45°
−60°
18 Ma

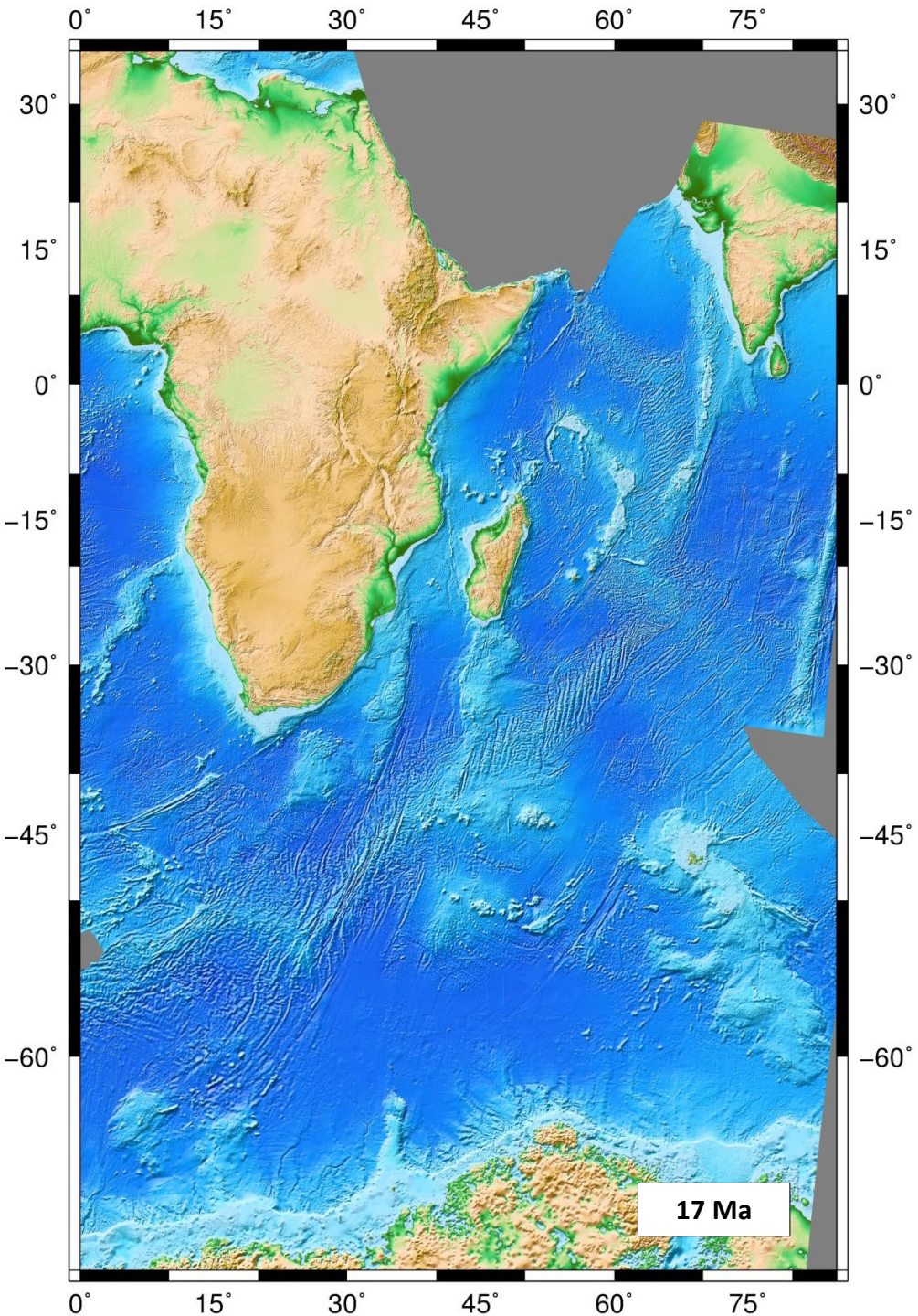
0°
15°
30°
45°
60°
75°
30°
15°
0°
−15°
−30°
−45°
−60°
17 Ma

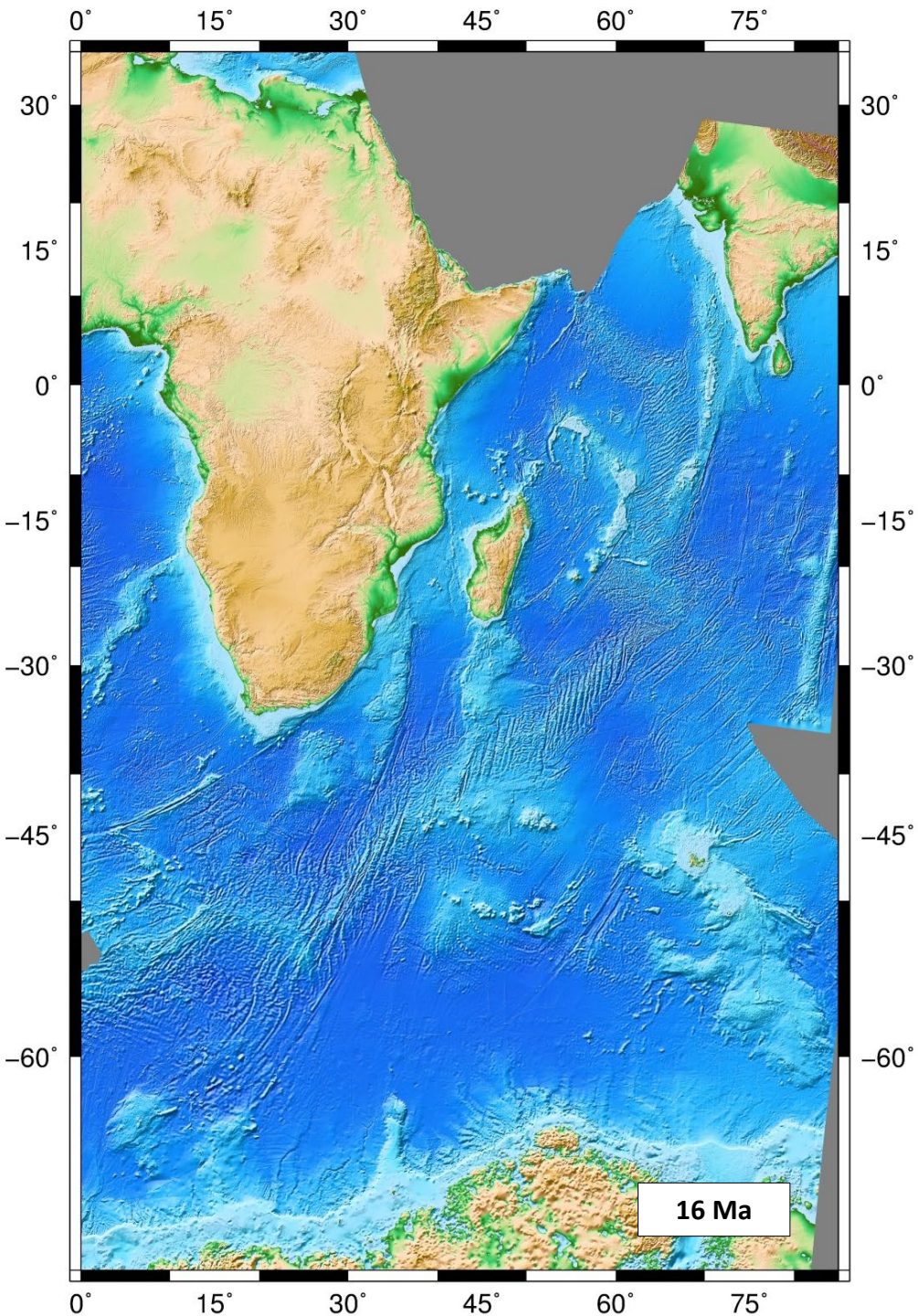
0˚
15˚
30˚
45˚
60˚
75˚
30˚
15˚
0˚
–15˚
–30˚
–45˚
–60˚
16 Ma

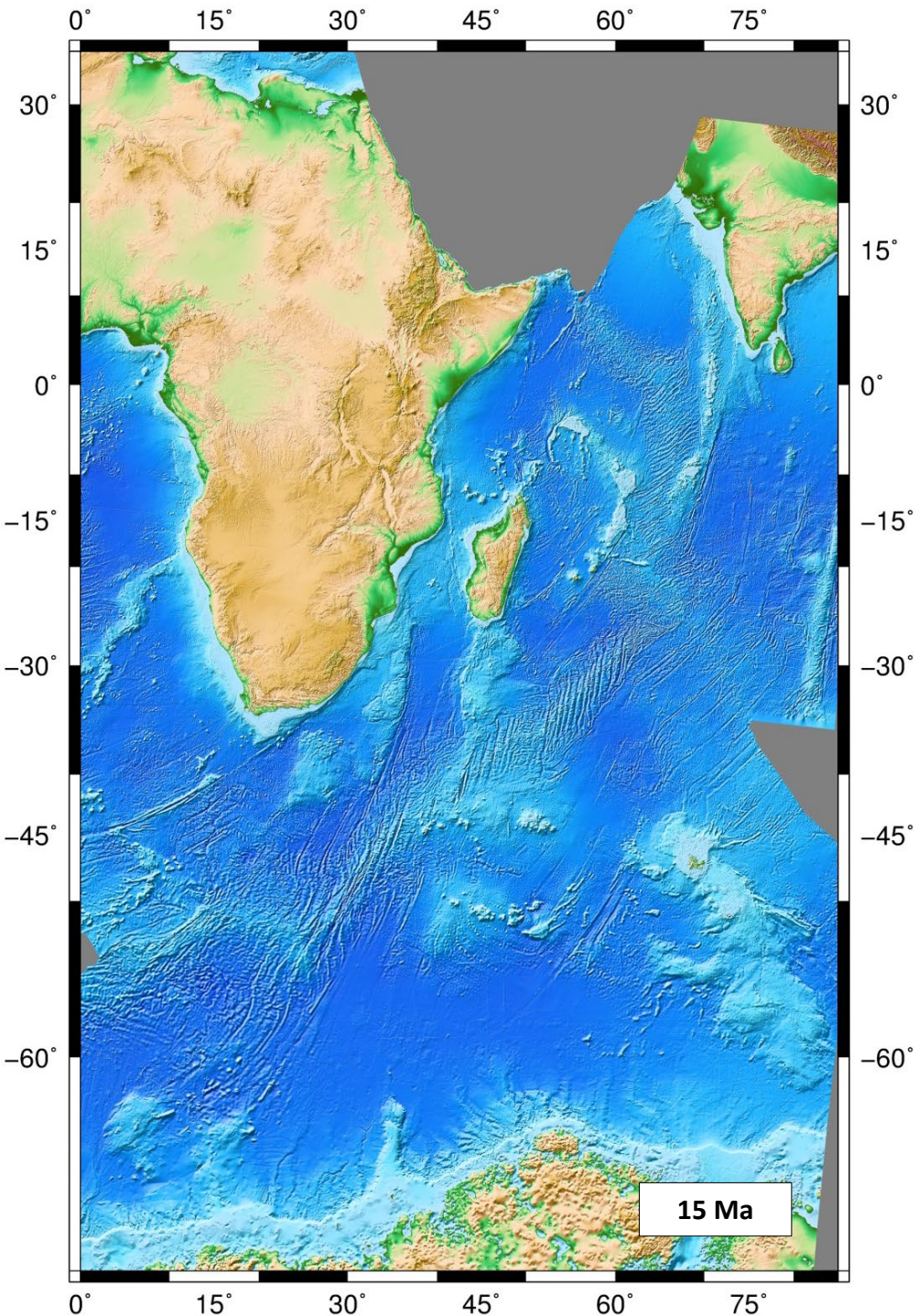
0°
15°
30°
45°
60°
75°
30°
15°
0°
−15°
−30°
−45°
−60°
15 Ma

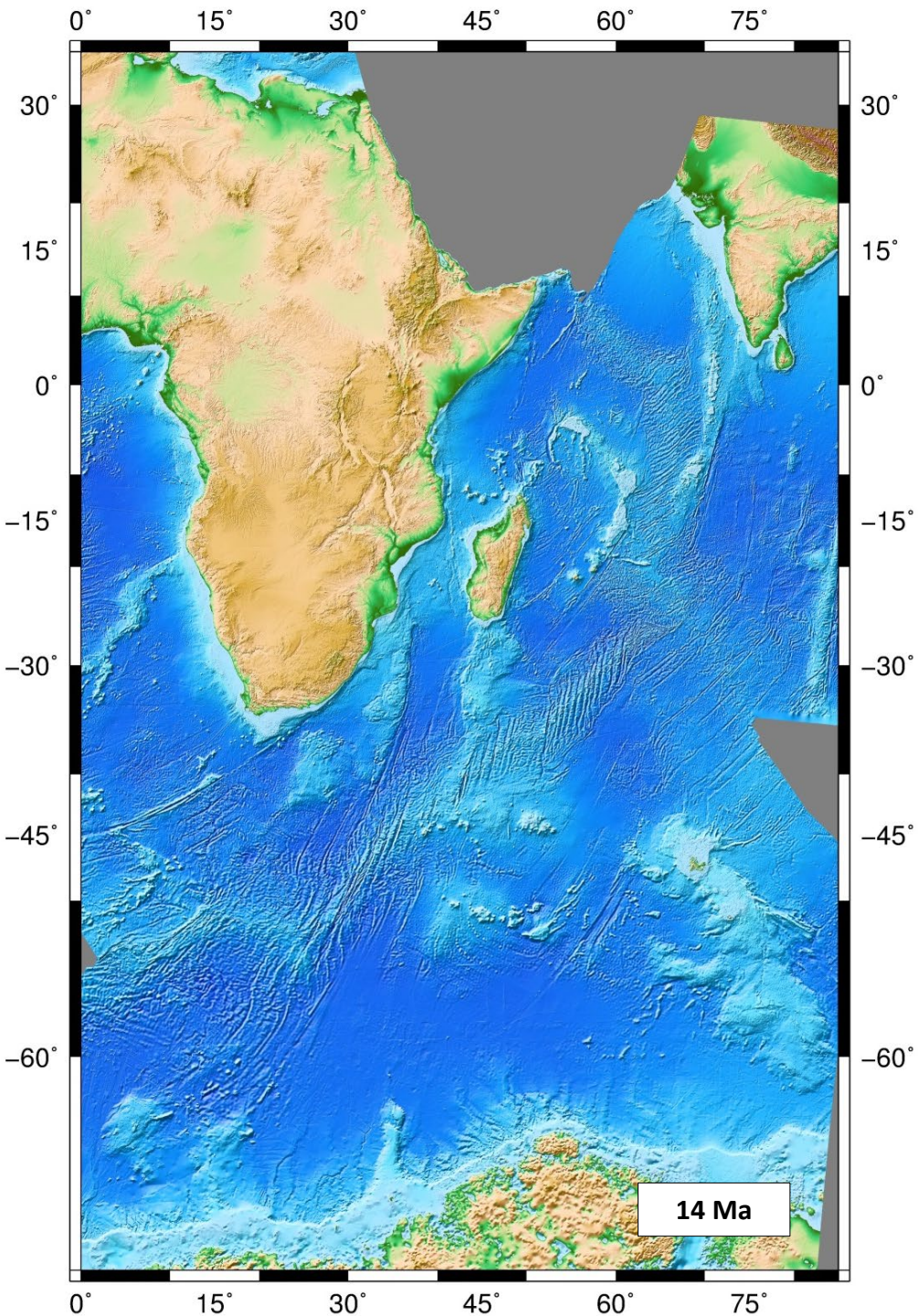
0˚
15˚
30˚
45˚
60˚
75˚
30˚
15˚
0˚
–15˚
–30˚
–45˚
–60˚
14 Ma

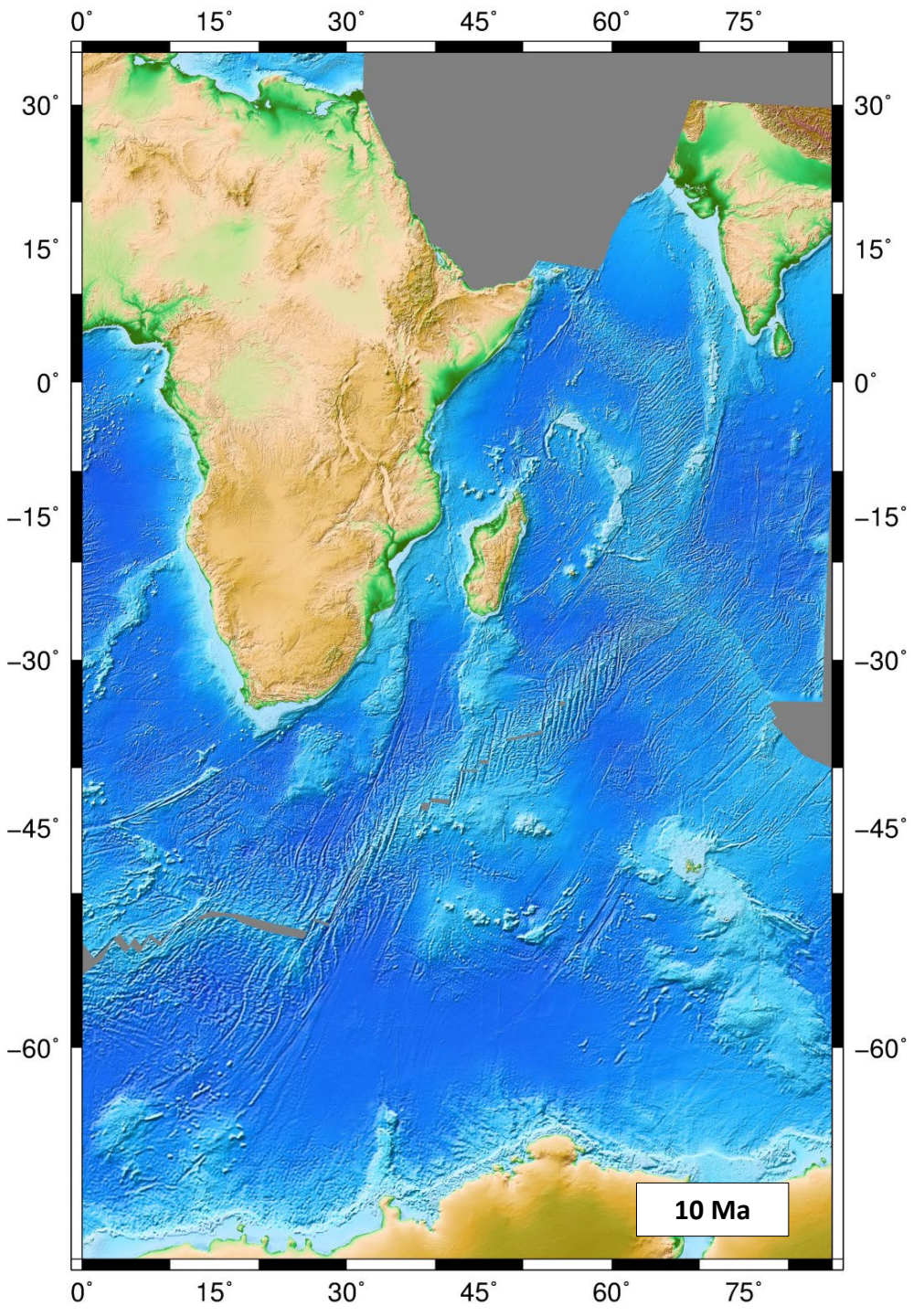
0˚
15˚
30˚
45˚
60˚
75˚
30˚
15˚
0˚
–15˚
–30˚
–45˚
–60˚
10 Ma

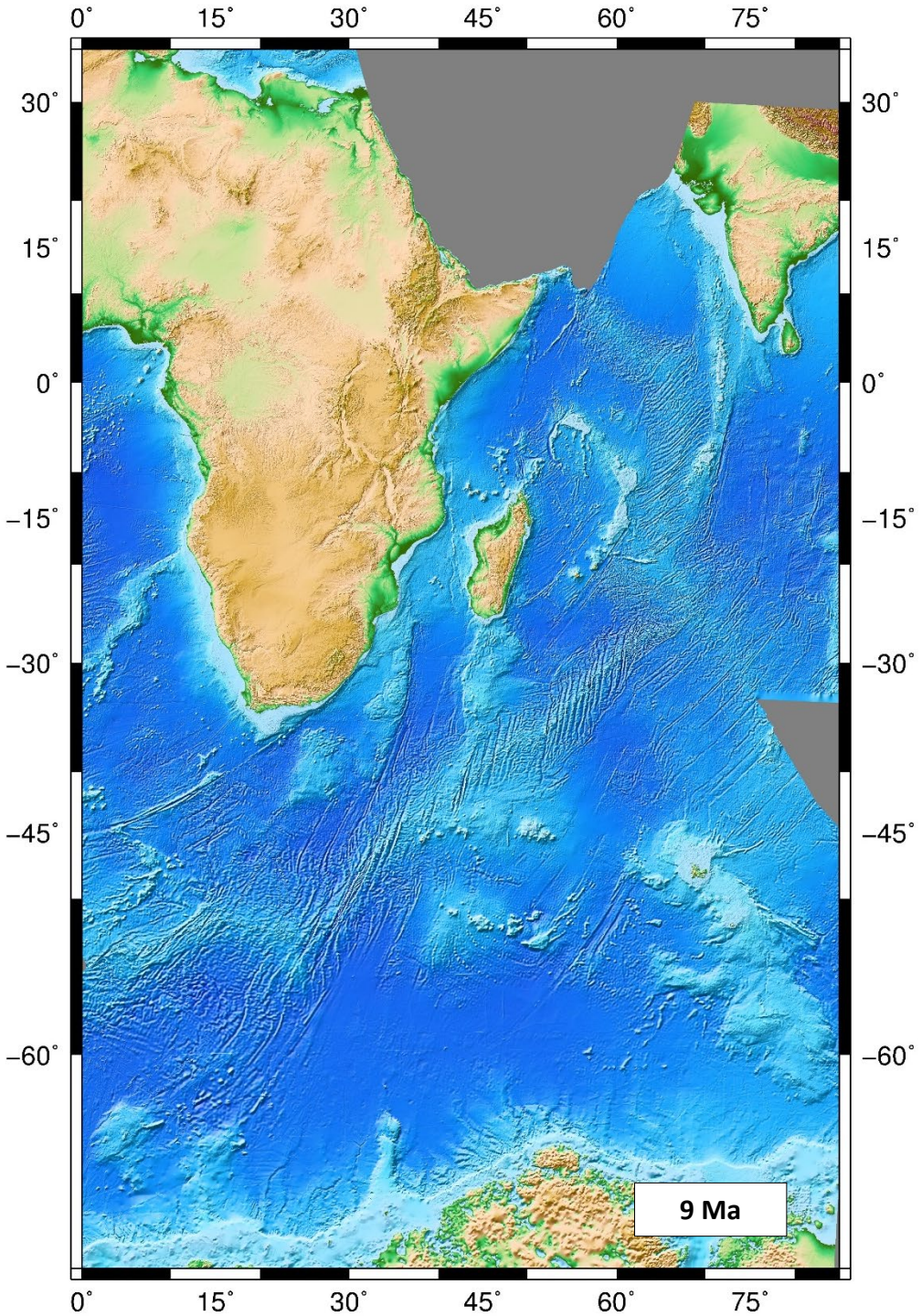
0°
15°
30°
45°
60°
75°
30°
15°
0°
−15°
−30°
−45°
−60°
9 Ma

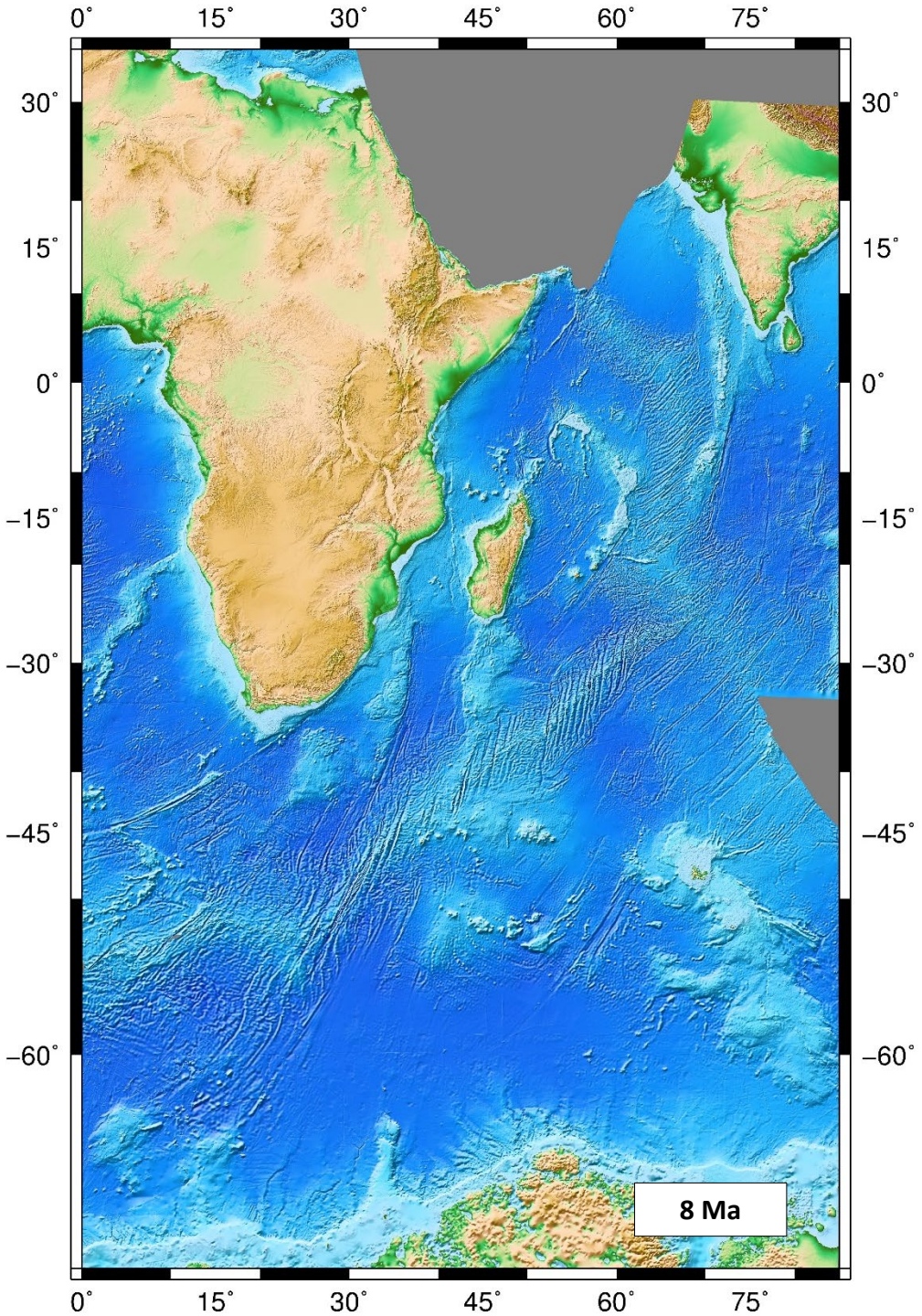
0°
15°
30°
45°
60°
75°
30°
15°
0°
−15°
−30°
−45°
−60°
8 Ma

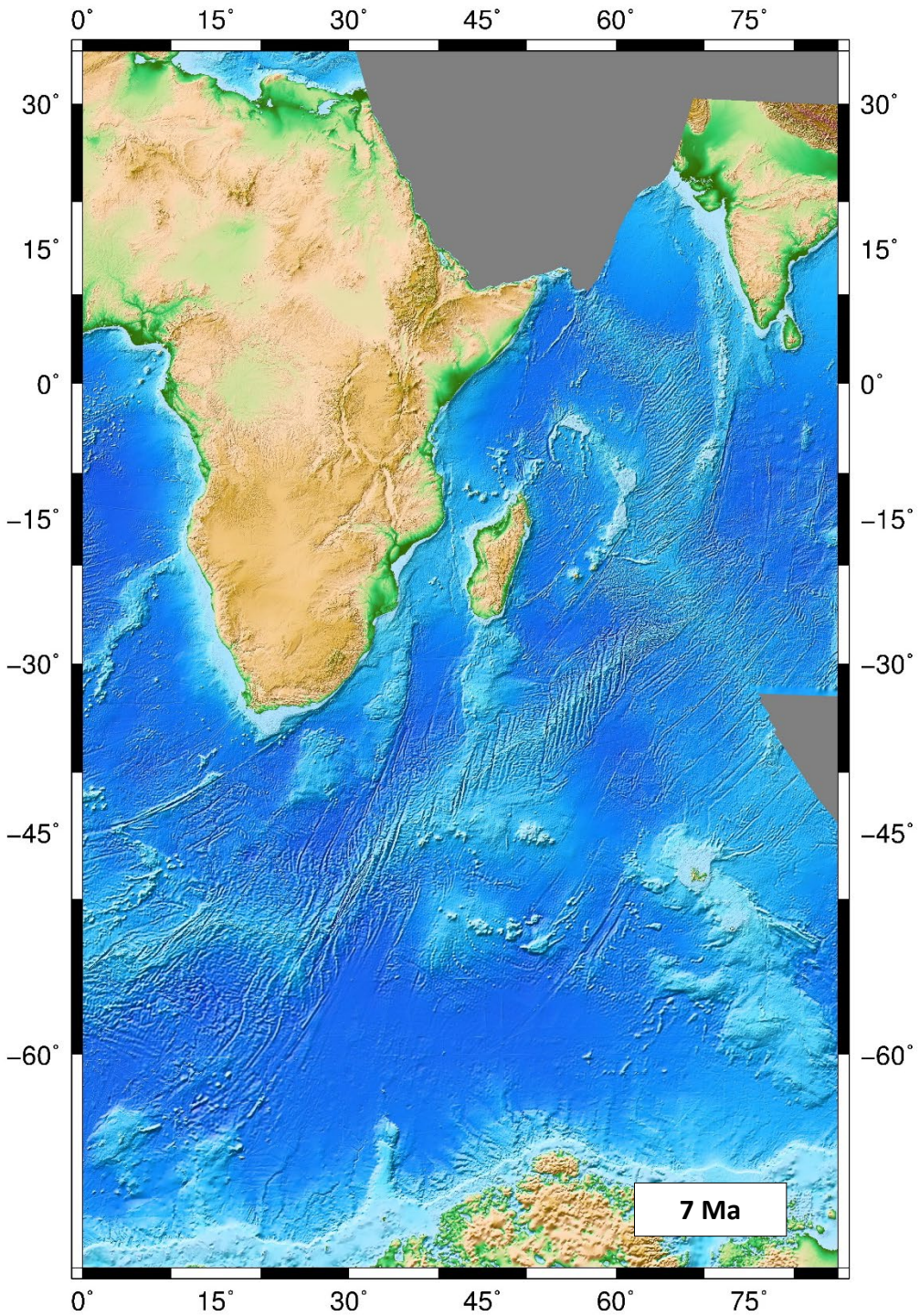
0°
15°
30°
45°
60°
75°
30°
15°
0°
−15°
−30°
−45°
−60°
7 Ma

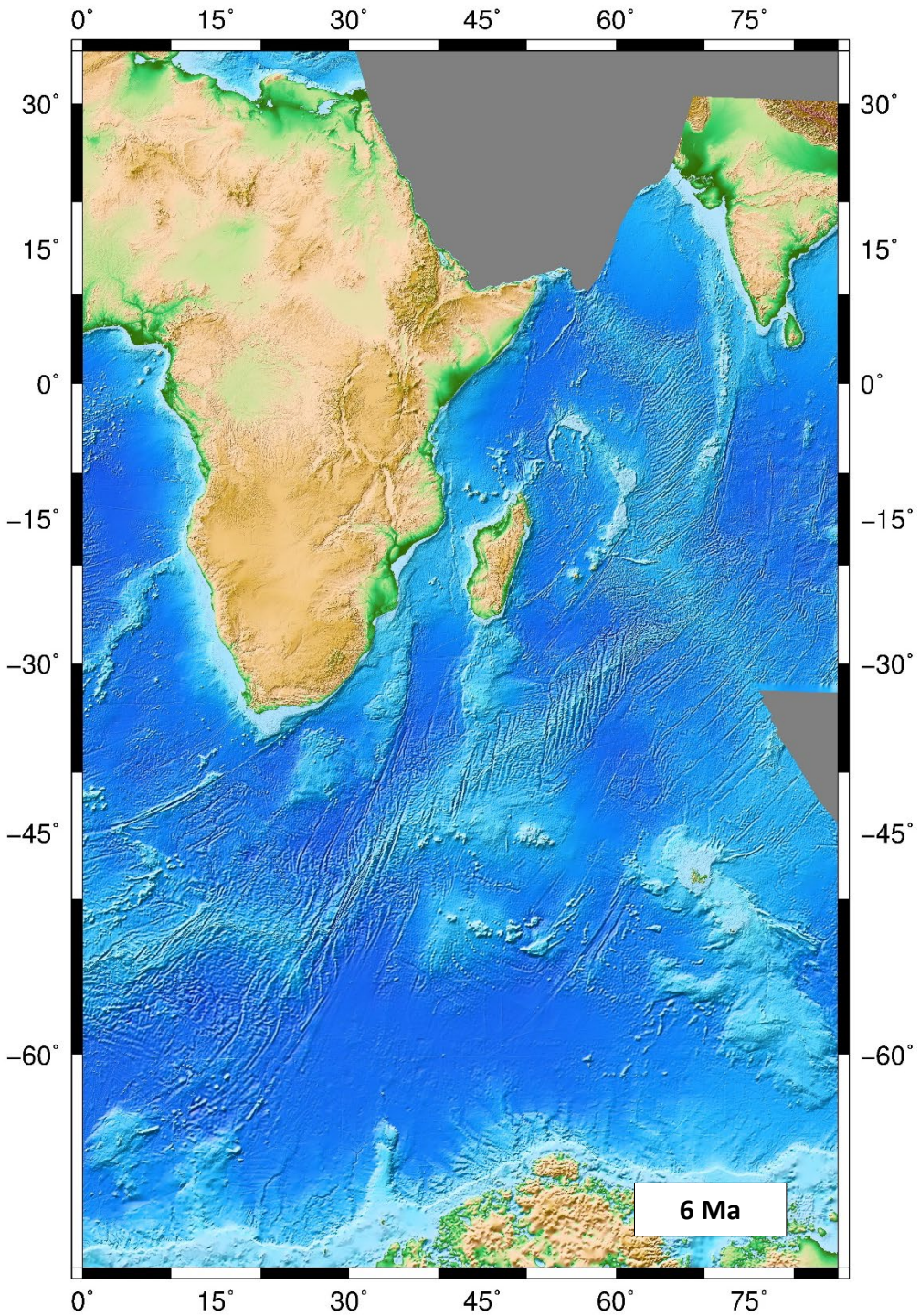
0°
15°
30°
45°
60°
75°
30°
15°
0°
−15°
−30°
−45°
−60°
6 Ma

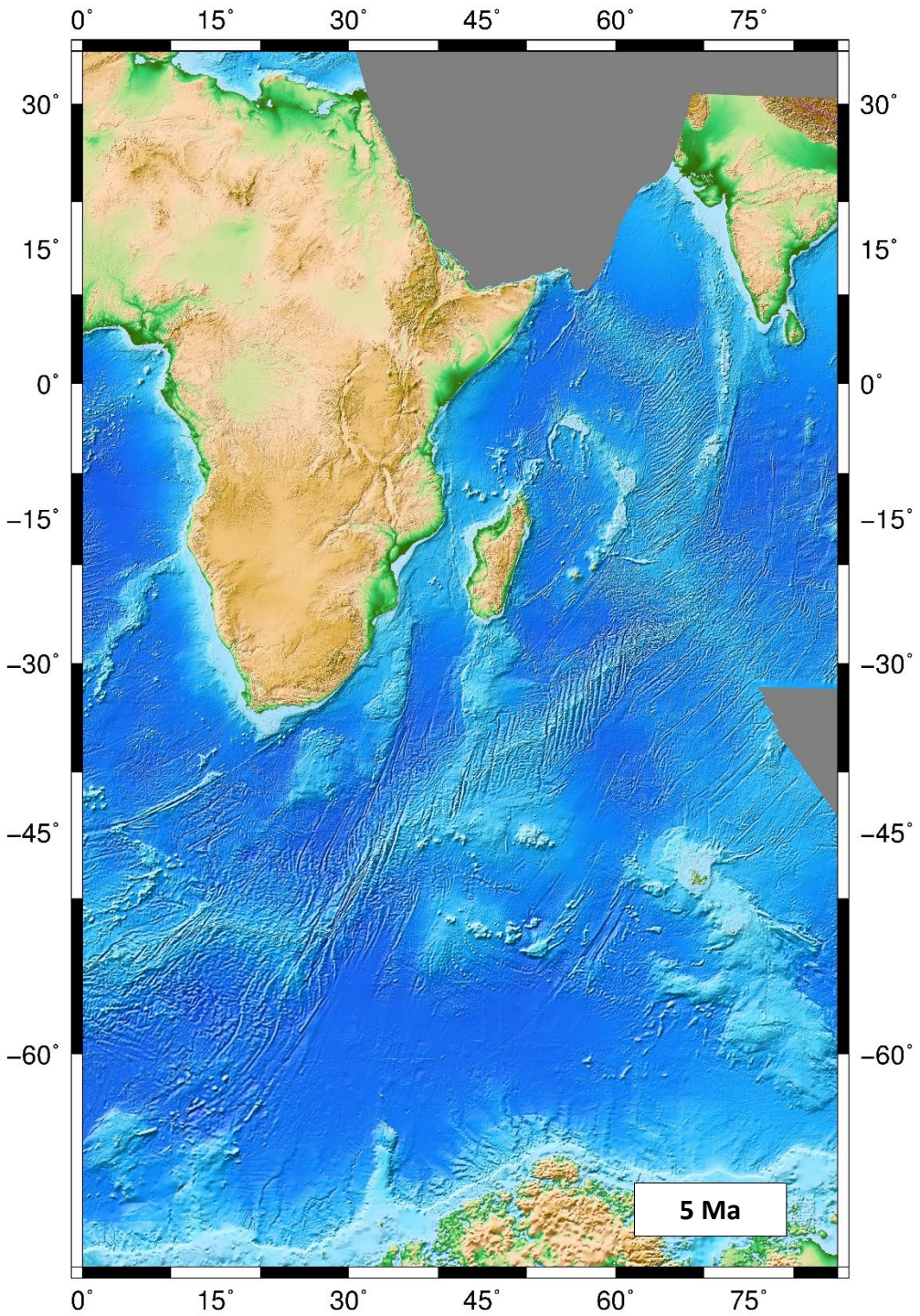
0˚
15˚
30˚
45˚
60˚
75˚
30˚
15˚
0˚
−15˚
−30˚
−45˚
−60˚
5 Ma

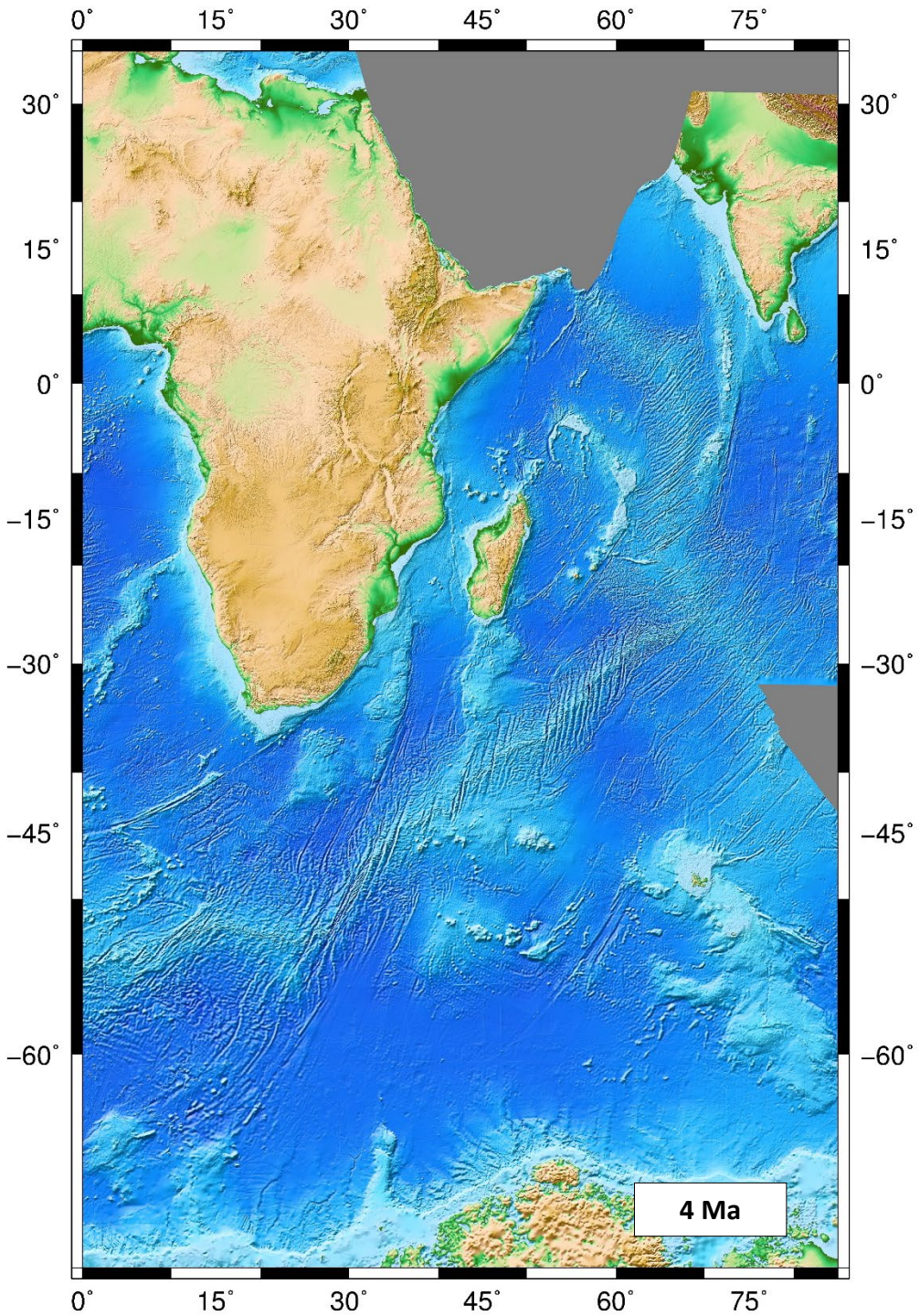
0°
15°
30°
45°
60°
75°
30°
15°
0°
−15°
−30°
−45°
−60°
4 Ma

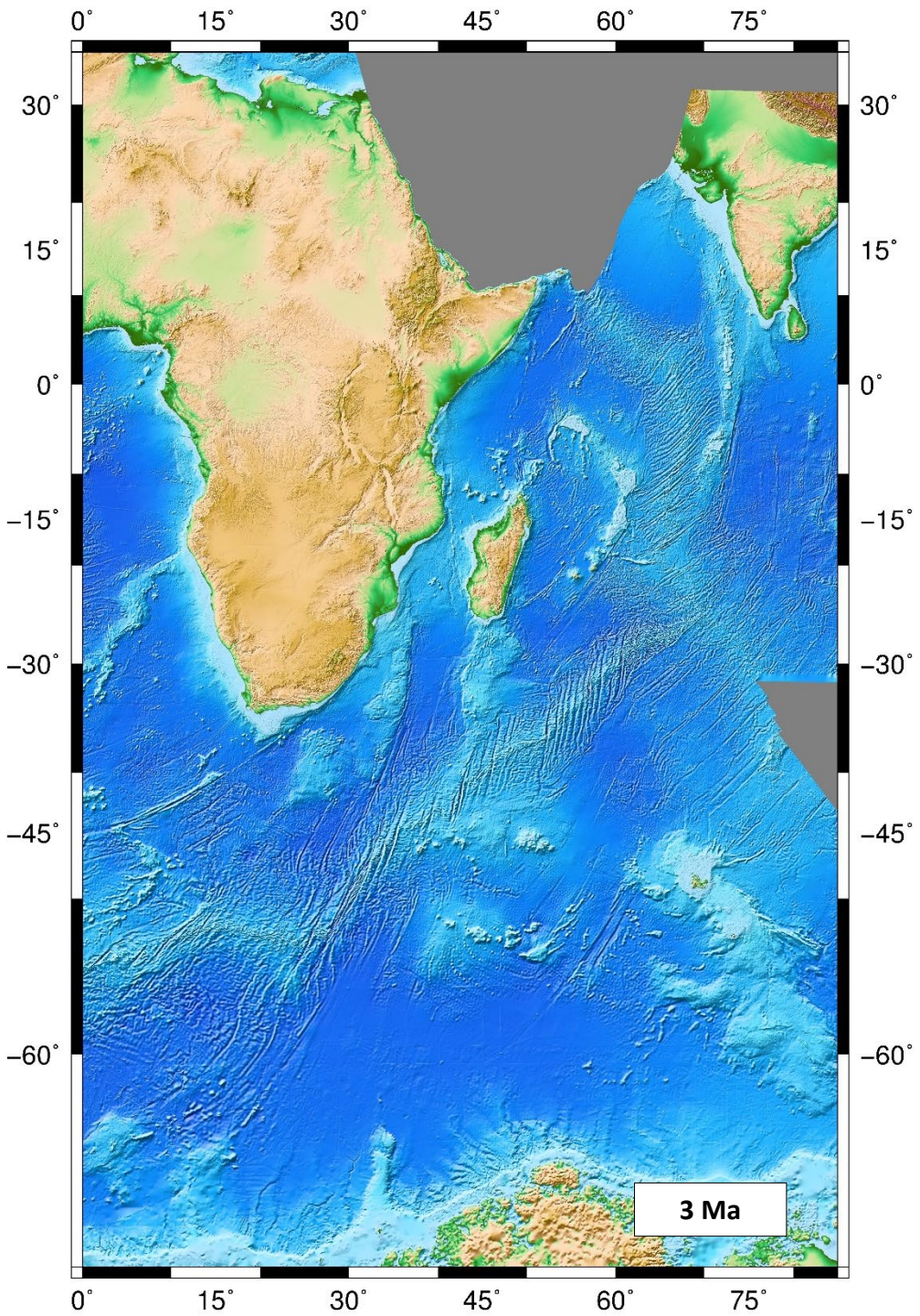
0°
15°
30°
45°
60°
75°
30°
15°
0°
−15°
−30°
−45°
−60°
3 Ma

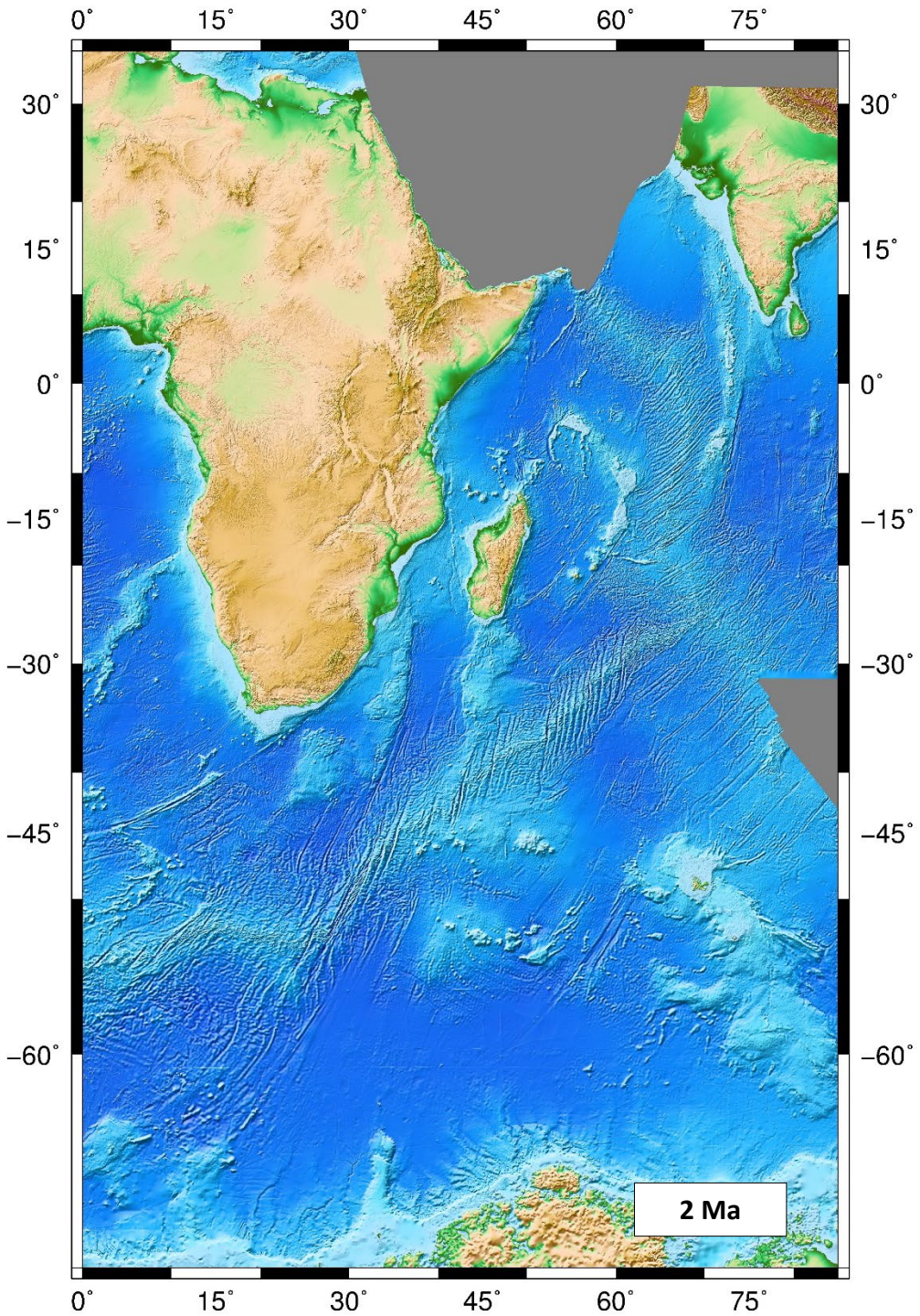
0°
15°
30°
45°
60°
75°
30°
15°
0°
−15°
−30°
−45°
−60°
2 Ma

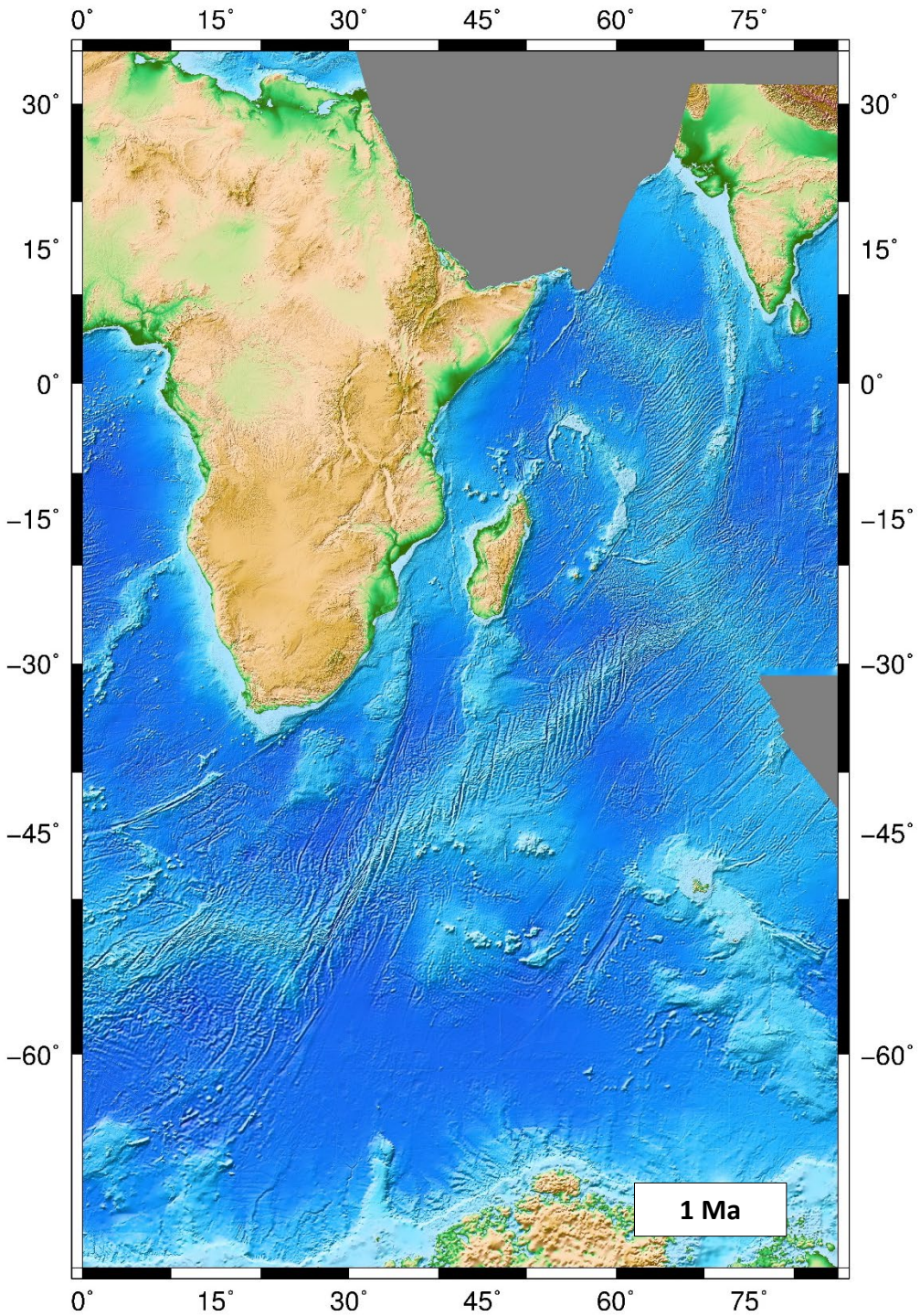
0°
15°
30°
45°
60°
75°
30°
15°
0°
−15°
−30°
−45°
−60°
1 Ma

Appendix B

Crustal Scale	Mega-sequence	Example Tectonic Setting	Mega-sequence Subdivision	Depositional Environment, Sedimentary Facies	Lithofacies	Petroleum System Type	Petroleum System Element	Petroleum System Element	Petroleum System Element	Petroleum System Element
Lithospheric architecture	*Tectonostrat. development*	*Tectonic evolution*	*Tectonostrat. development*	*Sedimentary response?*			*Source*	*Reservoir*	*Seal/charge*	*Trap*
Basin Fill	Modern Margin	Thermal subsidence Other Processes		Delta						
	Late Post-rift	Thermal subsidence Gravity spreading over Shale-detachments Transtensional rifts Active SF spreading	Marginal (Thermal) Sag	Clastics/delta, carbonate platforms	massive claystones foreset silts/clays hemipelagic–pelagic clays & turbidites porous & argillaceous limestones massive & bedded porous limestones	Late Postrift Regressive Delta	Source material transported into dw by turbidity currents Prodelta: Good SR in Foreset silts and clays (Type II/III) Distal: terrestrial organic matter, leaf litter with turbidites (Type III)	Regressive deltaic, coastal plain sands (aggradation or progradation) deep-marine turbidite sand downdip from deltas	regional marine shale seals	growth-faulted closures hanging-wall anticlines inversion structures toe-thrusted anticlinal folds
		Transpressional rifts Rift margin fault inversion Uplift and inversion	Post Inversion Syn Inversion	Active deltas progradation over transgressive sequence						
	Early Post-rift	Gravity gliding Thermal subsidence Active Seafloor spreading	Marginal (Thermal) Sag	Reg. transgression over basin margins and intra-basin highs open marine	carbonates and shales reefal build-up porous and argillaceous limestones massive and bedded porous limestones and dolomites	Early Postrift Marine	marine shale, lean gas-prone dispersed plant material in intra-deltaic neritic clays (Type II/III) turbiditic transport into deep water, Mangrove-derived OM with carbonate	open-marine carbonates carbonate platforms reefal build-ups	regional marine shale seals, often overpressured top, lateral and base seals inhibit vertical migration	
Break-up Unconformity (BCU)										
Basin Fill	Transitional Sag	Tectonic quiescence Thermal subsidence Structural sag	Interior Sag	Lacustrine Playa lake coastal plain coastal fluvio-marine restricted shelf extended beyond syn-rift grabens	evaporates clays, shales massive and bedded porous limestones and dolomites					
	Transitional Sag	Tectonic quiescence Thermal subsidence	Interior Sag	Fluvio-shallow marine sediments	fluvial channel sands overbank clays beach-barrier sands					
	Late Syn rift (Main Syn-rift)	Pure/oblique rifting Continued extension Sub-basins coalesced to complex networks and broader, symmetrical basins Back Arc extension Transtension	Interior Fracture	Transgressive fluviatile to deltaic sediments, more marine transgressive in distal basins	fluvial channel sands overbank clays beach-barrier sands deltaic top-set sands	Late Synrift Transgressive Delta	oil and gas-prone coals and coaly shales (Type II/III light oils with strong land plant imprint, some wet gas	fluvio-deltaic reservoirs and seals, transgressive deltaic sands often excellent quality. SR levels juxtaposed or interbedded	regional marine shale seals excellent top seals upward charge into shallower sequences is inhibited	
	Early Syn rift (Karoo Syn-rift)	Pure/oblique rifting Widespread faulting, Individual half-grabens Basement tilting Back Arc extension Transtension	Interior Fracture	Alluvial, lacustrine, fluviatile to deltaic sediments marginal lake swamp facies	alluvial fan sands conglomerates non-marine deltaic sands shallow-to deep-water lake clays	Early Synrift Lacustrine	strongly oil prone fluvio-lacustrine source SR algal organic material (Type I/II); minor gas from coals & coaly shale SR (Type III)	alluvial fans fluvio-lacustr. delta lacustrine turbidites lacustrine carbonates volcaniclastics fractured basement footwall blocks	laterally discontinuous non-marine shale seals charge leak into late syn-rift transgressive delta sequence Charging of fractured basement if lacustrine SR lap onto horsts	
Top basement unconformity										
Basement										

Appendix C – Stratigraphic reference reliability ratings

Margin Segment	Reference	Source of Info	Rating (A-C)
EA-IND	Bosellini, 1992	Well completion reports, geophysical reports, and geological reviews submitted to the government of Somalia by oil/gas operators, including Sinclair, Amerada, Hammar, ARCO, Burma, AGIP, Conoco, ELF, Gulf, Texaco, Exxon, Shell, BP, Mobil, Citco, Amoco, and several private laboratories. The writer has visited and/or investigated the Jurassic and Cretaceous of central and southern Somalia, the Jurassic and Cretaceous of the Aden coast (from Berbera to Bosaso), and the Oligocene-Miocene of the Indian Ocean coastal area, from Eil to the peninsula of Hafun.	A
	Coffin & Rabinowitz, 1988	Authors assembled available stratigraphy and structure studies, drilling results both onshore and offshore, and geophysical (seismic, magnetic, gravity) data for the region.	A
EA-MAD	Bosellini, 1992	Well completion reports, geophysical reports, and geological reviews submitted to the government of Somalia by oil/gas operators, including Sinclair, Amerada, Hammar, ARCO, Burma, AGIP, Conoco, ELF, Gulf, Texaco, Exxon, Shell, BP, Mobil, Citco, Amoco, and several private laboratories. The writer has visited and/or investigated the Jurassic and Cretaceous of central and southern Somalia, the Jurassic and Cretaceous of the Aden coast (from Berbera to Bosaso), and the Oligocene-Miocene of the Indian Ocean coastal area, from Eil to the peninsula of Hafun.	A
	Coffin & Rabinowitz, 1988	Authors assembled available stratigraphy and structure studies, drilling results both onshore and offshore, and geophysical (seismic, magnetic, gravity) data for the region.	A
	Nyagah, 1995	Geological and geophysical well data from fourteen wells drilled in the Lamu Basin. The subsurface lithological characteristics were assessed from well cuttings available for most of the wells and cores available from six wells.	A
	Cruciani & Barchi, 2016	Seismic stratigraphy and literature review.	A
	Kearns et al., 2016	Seismic data	A
	Mbede & Dualeh, 1997	Principal data used include well logs, geophysical, geochemical data and literature available.	A
	Nyaberi & Rop, 2014	Historical/existing well results and recent 2-D seismic data	B
	Coffin & Rabinowitz, 1988	Authors assembled available stratigraphy and structure studies, drilling results both onshore and offshore, and geophysical (seismic, magnetic, gravity) data for the region.	A
	Rais-Assa, 1988	Field work and literature review (location/extent of new data unclear)	B
	Hudson & Nicholas, 2014	Geological field surveys, analysis of outcrop samples, studies from available oil exploration data, and published materials.	A
	Nicholas et al., 2006	New field surveys combined with shallow drilling along the coast.	A
	Key et al., 2008	Field work (onshore)	B

Margin Segment	Reference	Source of Info	Rating (A-C)
	Nicholas et al., 2007	Structural field observations. 2nd hand seismic sections. Outcrop interpretation (onshore)	**B**
	Mahanjane & Franke, 2014	Seismic reflection data	**A**
	Franke et al., 2015.	Seismic reflection data and bathymetric data.	**A**
	Salman & Abdula, 1995	Results of oil and gas exploration activities including deep-drilling data and regional seismic lines both on- and offshore. Sections of all deep wells have been analysed, and the data on stratigraphy and lithology tied with seismic lines to produce a seismostratigraphic framework of the study area.	**A**
	Key & Reeves, 2012	Based on literature?	C
	Coffin & Rabinowitz, 1988	Authors assembled available stratigraphy and structure studies, drilling results both onshore and offshore, and geophysical (seismic, magnetic, gravity) data for the region.	**A**
MAD-EA	Papini & Benvenuti, 2008	Field work to establish stratigraphy (onshore).	**B**
	Geiger et al., 2004	Outcrop descriptions (onshore), thinsections and second hand seismic	**A**
	Clark, 1998	Review paper, unclear data source	C
	Geiger & Schwelgert 2006	Depositional models based on outcrop and literature data in combination with subsurface data sets	**A**
	Rerat, 1964	???	C
	Besairie & Collignon, 1972	Field work?	**B**
	Razafindrazaka et al., 1999	Literature review, some seismic	**B**
	Jeans & van Meerbeke, 1995	???	C
	Westcott & Diggens, 1997	?	C
	Mahanjane et al., 2014	Seismic reflection data tied to four wells	**A**
EA-ANT	Salman and Abdula, 1995	Results of oil and gas exploration activities including deep-drilling data and regional seismic lines both on- and offshore. Sections of all deep wells have been analysed, and the data on stratigraphy and lithology tied with seismic lines to produce a seismostratigraphic framework of the study area.	**A**
	Mahanjane, 2014	2-D seismic reflection data	**A**
	Salazar et al 2013	Seismic and gravity data	**A**
	Mahanjane, 2012	2-D seismic reflection data	**A**

Margin Segment	Reference	Source of Info	Rating (A-C)
	De Buyl & Flores, 1986	Detailed stratigraphy, but onshore and dated	B

A	Reliable
B	Some merit
C	Unsupported

Appendix D EA-IND Stratigraphy

			Megasequence	Sagaleh				N. Somalia (Mudugh Basin/Somali Embayment? Obbia Basin (offshore))				S. Somalia - Somali Coastal Basin, Coriole, Juba Basins (offshore)					
				Continent	Shelf	Basin		Continent	Shelf	Basin		Continent	Shelf	Basin	Continent	Shelf	Basin
												North			South (Juba)		
Quaternary			**Hafun Series:** Mainly carbonate sequence, product of depositional regression. It constitutes a 150-m-thick depositional sequence, called the Eil sequence by Bosellini et al. (1987), that prograded seaward for several kilometers (Bosellini, 1992). The Hafun Group is mainlycarbonate and unconformably overlies the Karkar Formation (Ali & Watts, 2015).	Terrestrial sediment (pediment, alluvial, caliche etc.)	Lagoonal and transitional sediment **(Scusciuban Fm**) / prograding carbonate platform **(Hafun series / Eil sequence)** represents a depositional regression. (Bosellini 1992). Somal equiv.?	deep-water mudstone and shale	**Somal / Merca Depositional Sequence**: By the end of the early Oligocene, most of Somalia was subareial. Possibly due to tectonic uplift. Angular unconformity below Somal/merca sequence. Widespread basaltic flows in the Mudugh region. Along the margin, first a general marine transgression (Somal Fm, base of Eil sequence) followed by Miocene depositional regression during highstand (Merca Fm, top of Eil sequence). (Bosellini, 1992)	Terrestrial sediment (pediment, alluvial, caliche etc.)	**Merca Fm**: regressive, shallow marineand continental sequence of sandstone, claystone, and sandy LST. Deltaic and shelf clastics / carbonate platforms. **Somal Fm:** Transgressive, shallow water carbonates. (Bosellini, 1992). Eil equiv.?	Deep-sea fan / Deep-water mudstone and shale **Garad Fm???** (Bosellini, 1992). Outer shelf to bathyal pelagic fossiliferous claystone.		Terrestrial sediment (pediment, alluvial, caliche etc.) (Bosellini, 1992)	**Somal / Merca Fm:** (Miocene to Pliocene) medium to fine grained sandstones and white microcrystalline limestones, with thin shale and anhydritic interbeds of littoral to shallow marine environment (Mbede & Dualeh, 1997). **Merca Fm:** regressive, shallow marineand continental sequence of sandstone, claystone, and sandy LST. Deltaic and shelf clastics / carbonate platform. prograding seaward (Bosellini, 1992). **Somal Fm:** Transgressive, shallow water carbonates. (Bosellini, 1992). Eil equiv.??	Deep-sea fan / Deep-water mudstone and shale (Bosellini, 1992). Outer shelf to bathyal pelagic fossiliferous claystone.	Terrestrial sediment (pediment, alluvial, caliche etc.)	**Somal / Merca Fm:** (Miocene to Pliocene) medium to fine grained sandstones and white microcrystalline limestones, with thin shale and anhydritic interbeds of littoral to shallow marine environment (Mbede & Dualeh, 1997) **Merca Fm:** regressive, shallow marineand continental sequence of sandstone, claystone, and sandy LST. Deltaic and shelf clastics / carbonate platform, prograding seaward (Bosellini, 1992) **Somal Fm:** Transgressive, shallow water carbonates. (Bosellini, 1992). Eil equiv.?	Deep-sea fan / Deep-water mudstone and shale **Garad Fm???** (Bosellini, 1992). Outer shelf to bathyal pelagic fossiliferous claystone.
Neogene	**Pliocene**	Piacenezian															
		Zanclean															
	Miocene	Messinian															
		Tortonian															
		Serravallian															
		Langhian															
		Burdigalian															
		Aquitanian															
Paleogene	**Oliocene**	Chattian															
		Rupelian		Missing?? Due to dramatic sea-level drop? (Bosellini, 1992), Or uplift due to onset of EARs				?									

		Megasequence	Sagaleh				N. Somalia (Mudugh Basin/Somali Embayment? Obbia Basin (offshore))				S. Somalia - Somali Coastal Basin, Coriole, Juba Basins (offshore)					
			Continent	Shelf	Basin		Continent	Shelf	Basin		Continent	Shelf	Basin	Continent	Shelf	Basin
											North			South (Juba)		
	Priabonian	**Auradu Supersequence:** records both tectonic and eustatic movements. These events are clear in the North but become more subdued further south, until they are overwhelmed by the high sedimentation rate of the Jubba delta. The Auradu represents a regional transgression. In middle Eocene the sea started to withdraw, hence the Taleh Fm (Bosellini, 1992). A late Paleocene or Early Eocene regional marine transgression terminated terrestrial conditions. Affected whole of the horn of Africa.	Alluvial and deltaic succession (provenance and transport direction from the NW)	**Karkar Fm:** (Late Eocene) As this does not occur across the Gulf of Aden could mark the onset of structural evolution of the Gulf itself. Marly, nodular, fosseliferous LST. (Bosellini, 1992)			Eroded (Bosellini, 1992)				Eroded (Bosellini, 1992)				Obbia Fm: Shale limestone and sandstone. Upper Eocene (Kearns, et al., 2016).
Eocene	Bartonian		**Taleh Fm:** (Middle Eocene) Represents regression. Consists of dense, massive to banded or laminated anhydrite, often smells like oil when freshly fractured. Often altered on the surface to gypsum and irregularly interbedded throughout with marls, shales, and thin LST bands. Little terrigenous sediment suggests a large, shallow evaporite bay surrounded by very arid land without substantial fluvial transport. (Bosellini, 1992)	**Marginal carbonates:** a marginal dolomitic belt of reefs and high-energy deposits (Bosellini, 1992)	**Obbia Fm:** Deep-water Eocene facies. Mostly clay and shale. (Bosellini, 1992)		**Taleh Equiv:** (Middle Eocene) Transitional area and carbonate platform. (Bosellini, 1992)	**Obbia Fm:** Deep-water Eocene facies. Mostly clay and shale. (Bosellini, 1992)			**Taleh Equiv:** Shallow marine sands (Bosellini, 1992)	**Obbia Fm:** Clay and shale (Bosellini, 1992)			**Scebeli Fm:** Shale, limestone and sandstone. Middle Eocene (Kearns, et al., 2016).
	Lutetian													Undifferentiated Clastics? (C & R, 1988)		

			Megasequence	Sagaleh				N. Somalia (Mudugh Basin/Somali Embayment? Obbia Basin (offshore))				S. Somalia - Somali Coastal Basin, Coriole, Juba Basins (offshore)					
				Continent	Shelf	Basin		Continent	Shelf	Basin		Continent	Shelf	Basin	Continent	Shelf	Basin
												North			South (Juba)		
		Ypresian		**Auradu LST:** (Early Eocene) Represents transgression. Thick shallow-water LST unit (mainly mudstone/wackstone), massive or thick bedded in lower part, with frequent iron-stained cherty concretions. Base is transgressive, older in the east and progressively younger in the west. (Bosellini, 1992)				**Auradu LST:** (Early Eocene) Represents transgression. Thick shallow-water LST unit (mainly mudstone/wackstone), massive or thick bedded in lower part, with frequent iron-stained cherty concretions. Base is transgressive, older in the east and progressively younger in the west. (Bosellini, 1992)				**Auradu Fm:** (Paleocene, continues into Eocene) finely crystalline, compact, hard, tan to lght brown LST with local, thin, grey shale (C & R, 1988). More shale to the south with calcareous, quartz SST beds and sills of spilitic basalt (C & R, 1988)	**Auradu Fm:** (Paleocene, continues into Eocene) deeper water facies. Shale (C & R, 1988)	Predoninantly terrigenous quartz SST interbedded with shale, mudstone, and some anhydrite (C & R, 1988)	**Coriole Fm:** Shale, limestone and sanstone. Loser Eocene (Kearns et al., 2016).
	Paleocene	Thanetian	**Yesomma depostional sequence:** (Late Maastrictian - Paleocene) Unconformity bounded. Facies changes from west to east. Further south, the Yesomma facies belt is replaced by a deltaic-marine sandy succession (Mogadishu and Juba Basins). Major crustal upwarping affected whole region prior to Yesomma deposition, it is time transgressive. Episode of uplift and block faulting (Bosellini, 1992)	**Yesomma sandstone proper:** ("Nubian" sandstone) Fluviatile sequence. Major unconformity at the base. Coarse. Lower part has clasts of underlying LST, and red, rusty colour. Fining-up sequneces topped by red-brown massive mudstone and shale. Cross-bedding is frequently tabular (sand waves), paleocurrents indicate east and southeast transport direction. (Bosellini, 1992).	Marginal belt of shale, sandstone, and carbonate, local lignite deposits / **Tisje Fm:** Shallow water carbonates (Bosellini, 1992)	**Sagaleh Fm:** Deep-water claystones and shale (Bosellini, 1992)		**Yesomma sandstone proper:** ("Nubian" sandstone) Fluviatile sequence. Major unconformity at the base. Coarse. Lower part has clasts of underlying LST, and red, rusty colour. Fining-up sequneces topped by red-brown massive mudstone and shale. Cross-bedding is frequently tabular (sand waves), paleocurrents indicate east and southeast transport direction. (Bosellini, 1992).	Marginal belt of shale, sandstone, and carbonate, local lignite deposits / **Tisje Fm:** Shallow water carbonates (Bosellini, 1992)	**Sagaleh Fm:** Deep-water claystones and shale (Bosellini, 1992)					**Yesomma Sequence:** continental Yesomma sandstone in the west and deltaic-marine sandy successions in the east (Bosellini, 1992). Paleo Deltas (Bosellini, 1992) equivalent to Yesomma. Paleocene (Kearns, et al., 2016).
		Selandian										**Yesomma Sandstone proper:** According to (Bosellini 1992). Should be same age etc. red, purple, and yellow cross-bedded quarts SST, with minor conglomerate and siltstone/shale beds. Commonly in fining-up sequences, interpreted as point bars. Bioturbation and root casts occur in overbank siltstones. Paleocurrents to the E & SE	**Tisje Fm:** Sallow water carbonates??	**Marai Ascia Fm:** (Paleocene) fossiliferous, transitional zone between the Sagaleh shale and the overlying Auradu LST. (C & R 1988)			
		Danian												**Sagaleh Fm:** (Upper Cretaceous) deep-water grey shale and marl, section thins seaward (C & R 1988)			
Cretaceous	**Upper**	Maastrichtian													Yesomma SST: Same as rest of Somalia? (Bosellini, 1992)	**Girs Supersequence**: Shale and Sandstone. Upper Cretaceous (Kearns et al., 2016). Mainly deltaic and transitional facies on the shelf. Deep-water mudstone and shale, Gira Fm. equivalent (Basin) (Bosellini, 1992)	
		Campanian	**Gira Supersequence:** Aptian transgression	Pediment and fluvial sandstones	Shallow water carbonate succession,	Deep-water mudstones, pelagic		Pediment and fluviale sandstone		Deep-water turbidite fan / **Gira Fm:** deep-water	**Gumburo Grp**	Pediment and fluviale sandstone	Mainly deltaic and transitional facies / Shallow water	Deep-water turbidite fan / **Gira Fm:** deep-water	Pediment and fluviale sandstone (Bosellini, 1992)		

			Megasequence	Sagaleh				N. Somalia (Mudugh Basin/Somali Embayment? Obbia Basin (offshore))				S. Somalia - Somali Coastal Basin, Coriole, Juba Basins (offshore)					
				Continent	Shelf	Basin		Continent	Shelf	Basin		Continent	Shelf	Basin	Continent	Shelf	Basin
												North			South (Juba)		
		Santonian			normally organised in shallowing-up cycles / Marginal, high-energy carbonates (sandy soals, reefs) (Bosellini, 1992)	shale (Bosellini, 1992)			Shallow water carbonate succession, normally organised in shallowing-up cycles / Marginal, high-energy carbonates (sandy shoals, reefs)	mudstones and shale		(Bosellini, 1992)	carbonate succession, normally organised in shallowing-up cycles / Marginal, high-energy carbonates (sandy shoals, reefs) (Bosellini, 1992)	mudstones and shale			
		Coniacian															
		Turonian															
		Cenomanian															
		Albian									Cotton Fm						
		Aptian															
		Barremian															
	Lower	Hauterivian	**Main Gysum depositional sequence** (Regression) unconformity bounded	**Missing** (Tilting/uplift and erosion)				**Main gypsum proper:** (Neocomian) dolostone and sulphates. Accumulated in sabkhas, lagoons and shallow sounds. (Bosellini 1992)	Shelf margin carbonates. A narrow high-energy belt of reefs and associated sandy shoals (Bosellini 1992)	Basinal mudstone and shale (Bosellini, 1992)		**Main gypsum proper:** (Neocomian) dolostone and sulphates. Accumulated in sabkhas, lagoons and shallow sounds. (Bosellini 1992) / **Cotton Fm:** Series of gypsum and LST. Unconformity bound top and bottom (C & R 1988).	Shelf margin carbonates. A narrow high-energy belt of reefs and associated sandy shoals (Bosellini 1992) / **Cotton Fm:** fore-reef LST. Unconformity bound top and bottom (C & R 1988)	Basinal mudstone and shale (Bosellini, 1992) / **Cotton Fm:** medium-depth neritic shale. Unconformity bound top and bottom (C & R 1988)	**Ambar Sandstone:** fluviatile system (paleocurrent from Kenya in the SW) / **Garbaharre Fm:** carbonates, evaporites, shale, and sandstone (Bosellini, 1992)	**Brava Fm:** (Middle Jurassic to Early Cretaceous) over 2000m of predominantly greenish shales, occasionally interbedded with limestones bands. (Mbede & Dualeh, 1997). / / deep-water basinal shale (Bosellini, 1992).
		Valanginian															
		Berriasian															
Jurassic	**Late**	Tithonian	**Uarandab depositional sequence** (sag	**North of the El Hamurre** trend (probs the site of reefs or liner carbonate sandy shoals) the Jurassic is mainly shallow water OR evaporite OR missing?? (Bosellini 1992)				**Gabredarre Fm:** (late Oxfordian/Kimmeridgian to early Tithonian) represents depostional regression. Well-		Deep-water basinal shale (Bosellini, 1992)		**Gabredarre Fm:** (Late Kimmeridgian-Tithonian) basinal dark grey and dark brown shale with some grey, finely crystalline		Deep-water basinal shale (Bosellini, 1992)	Open-marine, shelf marlstone, and shale (Bosellini, 1992)		

			Megasequence	Sagaleh				N. Somalia (Mudugh Basin/Somali Embayment? Obbia Basin (offshore))				S. Somalia - Somali Coastal Basin, Coriole, Juba Basins (offshore)					
				Continent	Shelf	Basin		Continent	Shelf	Basin		Continent	Shelf	Basin	Continent	Shelf	Basin
												North			South (Juba)		
		Kimmeridgian	phase?) Transgression					bedded LST sequence. (Bosellini 1992)				foraminifera-bearing LST. (C & R 1988)					
		Oxfordian						**Urandab Fm:** (late Callovian to late Oxfordian) represents a regional transgression. Greenish-grey and black fissile shale and micrite. (Bosellini 1992)				**Uarandab Fm:** (Oxfordian-Kimmeridgian) yellowish marly LST with belemnites and ammonites (C & R 1988)	**Uarandab Fm:** (Oxfordian-Kimmeridgian) basinal dark grey shale and grey marly Lst stringers (C & R 1988)				
	Middle	Callovian															
		Bathonian															
		Bajocian	Break up														
		Aalenian	Main syn-rift shallow marine transgressive sequence	**Hamanlei Fm:** (Pliensbachian to Callovian) Cabonate plateform margin. Mainly oolitic and pseudoolitic packstone-grainstone. Shallow water. (Bosellini 1992)				**Hamanlei Fm:** (Pliensbachian to Callovian) Cabonate plateform margin. Mainly oolitic and pseudoolitic packstone-grainstone. Shallow water. (Bosellini 1992)		**Meregh Fm:** thick, basinal dark mudstone, marlstone, and shale.Turbidity currents?? (Bosellini, 1992)		**Hamanlei Fm:** (Pliensbachian to Callovian) Cabonate plateform margin. Mainly oolitic and pseudoolitic packstone-grainstone. Shallow water. (Bosellini 1992)		Deep-water, basinal shale (Meregh Fm??) Turbidity currents?? (Bosellini, 1992)	**Hamanlei Fm?:** Shallow marine limestone (Kearns et al., 2016) with evaporites (Bosellini, 1992).		
		Toarcian															
	Early	Pliensbachian															
		Sinemurian	Top Agridat potential for Karoo syn-rift Top Karoo with U/C	**Adigrat Fm:** (Triassic - Early Jurassic) Karoo clastics. Terrigenous. Vast arid land. Mainly alluvial depositional environment. Coarse-grained clastics at the base, shale units towards the top. Absence of marine fossils. Presence of scattered plant debris? Lacustrine or coastal plain-deltaic areas as well as inland sabkas and eolian dune fields were locally present. Also fluviatile depostion. Very difficult to date boundaries. (Bosellini, 1992). The Adigrat Fm. ranges from continental alluvial, fluvial and coastal plain sediments with coarse-grained clastics at the base and shale units towards the top. They were deposited in a vast arid land with changeable depositional environments dominated by alluvial and fluvial settings with local lacustrine and coastal plain-deltaic areas as well as inland sabkas and eolian dune fields (Bosellini, 1992).				**Adigrat Fm:** (Triassic - Early Jurassic) Karoo clastics. Terrigenous. Vast arid land. Mainly alluvial depositional environment. Coarse-grained clastics at the base, shale units towards the top. Absence of marine fossils. Presence of scattered plant debris? Lacustrine or coastal plain-deltaic areas as well as inland sabkas and eolian dune fields were locally present. Also fluviatile depostion. Very difficult to date boundaries. (Bosellini, 1992).			**Adigrat Fm:** quartz SST with intercalations of gypsum and dark shale			**Karoo?????**		
		Hettangian															
Triassic	**Late**																
	Middle																
	Early																
Permian																	
Carboniferous																	

			Megasequence	Sagaleh				N. Somalia (Mudugh Basin/Somali Embayment? Obbia Basin (offshore))				S. Somalia - Somali Coastal Basin, Coriole, Juba Basins (offshore)					
				Continent	Shelf	Basin		Continent	Shelf	Basin		Continent	Shelf	Basin	Continent	Shelf	Basin
												North			South (Juba)		

Appendix E: EA-MAD Margin Segment Stratigraphy

			Megasequence	LAMU			Tanzania									Rovuma Basin		
							Ruvu (North)				Mandawa (South)							
				Continent	Shelf	Basin		Continent	Shelf	Basin	Continent	Shelf	Basin			Continent	Shelf	Basin
Quaternary																		
Neogene	**Pliocene**	Piacenezian	**Coastal Group** (Miocene to early Pliocene) lies on a major Late Oligocene unconformity. Deposited in the course of three late major cycles of sea-level change. Deposited in restricted shelf, middle to outer shelf, deep-marine and fluvial settings. Carbonate sequence associated with marine shales and an overlying siliciclastic sequence. The basal unconformity is marked offshore by starved-basin conditions (Nyagah, 1995). May extend down into the latest Oligocene.	**Marafa Fm:** Fining-upward sequence. Sandstones. very pale grey/orange medium to coarse grained poorly consolidated quartz sands with sandstones and kaolinitic clays (Nyagah, 1995)		**Simba Shales:** Lateral deep-marine equivalents of Lamu reefs. Green-grey to dark grey pyritic shales bearing numerous fossils. Calcareous sandstones, small to pebble-size sandy beds and clays are interspersed within this predomintly shale interval. Fossil indicate Miocene-Pliocene age (Nyagah, 1995)	**Regression:** above unconformity (Mbede & Dualeh, 1997)	Regressive estuarine fluviatile Plio-Pleistocene sands in existing depressions (Mbede & Dualeh, 1997)	Marine Pliocene deposits limited to present day offshore areas.		LSTs??		Regression followed, associated with Pliocene and later faulting with directly controls the modern topography		**Chinda Fm?:** Continental Sandstone. Lower sandstone unit with significant basal conglomerate beds, overlying an unconformity. Upper thicker, generally sandy section. Shallow marine or estaurine deposition environment. Onshore west. buff to very pale grey kaolinitic sandstone with pale kaolinitic mudstone clasts and small vugs. The formation comprises alluvial to possibly estuarine sediments deposited during Neogene uplift, partly as a lateral facies equivalent of the Mikindani Formation. The feldspar content appears to have been heavily altered in situ and the resulting kaolin redeposited during diagenesis in acidic groundwater (Key et al., 2008)	**Mikindani Fm:** Parlic clastices. Pale grey kaolintic SST with pale kaolinitic mudstone clastsand small vugs. Medium-grained, quartz, Pebbly SSTs with worm casts and burrows. Alluvial to possibly estuarine sediments deposited during Neogene uplift, partly lateral facies equivalent to Mikindani Beds. can be subdivided into two parts: a lower sandstone unit with significant basal conglomerate beds overlying an unconformity, and an upper thicker, generally sandy section. Shallow marine or estuarine with the upper unconsolidated red sands originating as offshore sand bars sourced from underlying sandstones. Unidirectional cross bedding indicates an east to east-south-east palaeoflow. The low angle channels down-cutting through interdistributary,	**Rovuma Delta Complex:** Marine shale, siltstones and sandstone. Marine sandstone. (Key et al., 2008). The offshore delta complex is characterized by sequences of marine shale, siltstone and sandstone which grade to paralic and continental clastics towards the onshore (Key et al., 2008).
		Zanclean																
	Miocene	Messinian																
		Tortonian																
		Serravallian																
		Langhian																
		Burdigalian					**Transgression**	Miocene sediments overstep older beds indicating renewed transgression and tectonic activity contemporaneous with the development of the EARs. Uplift and basinward tilting of hinterlands, together with intensive erosion and rapid basinal subsidence, resulted in the deposition of large prograding delta across the Dar-es-Salaam Embayment and Zanzibar channel. Accompanied by synsedimentary faults. deltaic deposition on pemba island. Marine limestones, silty mudstones and sands.				SSTs??		Trassgression in the Lower Miocene	**Songo Songo Group**				

		Aquitanian												
Paleogene	Oliocene	Chattian	**Tana Group** (Eocene to Oligocene) lies on regional unconformity. Deposited in fluvial, deltaic and restricted shelf settings. Deposited during three pulses of sea level change three pulses of sea-level rise and a single regressive phase of deposition, which coincide with tectonics in the Afar region (Cruciani & Barchi, 2016). The lithospheric assemblage comprises shelf-carbonates and fluvio-deltaic facies (Kipini Fm.), deposited by a paleo Tana river distributary system. The shelf carbonate facies that built up between periods of siliciclastic deposition are related to a tectonically influenced depositional pattern involving episodic uplift and subsidence which prevailed during the Palaeogene (Nyagah, 1995)	**Barren Beds Formation:** Comprises continental, fluvial "red beds" which are the lateral equivalents of the Kipini Fm. Middle Eocene through Late Oligocene. Thickens seaward where the SST units occur as fining-upward fluvial sandstone assemblages typical of point bar. (Nyagah, 1995)	**Kipini Formation:** (Early Eocene through part of the Late Oligocene) consists of two major clastic lithologies: sandstones that often grade into siltstones and are distinguished as the Sandstone Member of the Kipini Formation; and shales and mudstones that are distinguished as the shale Member of the Kipini Formation. The shales, which are delta-front facies, interbed with the limestones described below, to form clastic-carbonate couplets in the Pate embayment. Comprises shelf-carbonates and fluvio-deltaic facies (Kipini Fm.), including the Pate Limestone, Linderina Limestone and Dodori Limestone Members, which were deposited on the plunging crest of an intrabasinal high. **Pate Limestone:** Oldest thickest unit, onlapping Kofia sands. Early Eocene. alternating cycles of oolitic and nummulitic limestones, and dark grey to greenish shales. **Linderina Limestones:** Brief rise in sea level during the Middle Eocene. highly fossiliferous nummulitic limestone. **Dodori Limstone:** Shelf carbonate buildup Late Eocene. Nummulitic with shell fragments and interbeds of mudstones. Similar age correlative units are seen regionally to the northeast in Somalia. (Nyagah, 1995)	**Regression:** This regression may have resulted from isostatic adjustment due to active sea floor spreading related to development of the Owen fracture and widening of the Indian Ocean. It reflects building up of broad continental shelf and slope at a faster rate than the sudsidence which was probably continuous from the Late Cretaceous (Mbede & Dualeh, 1997).	Oligocene strata are largely missing (Mbede & Dualeh, 1997)						
		Rupelian												
	Eocene	Priabonian												
		Bartonian								Clastic sediments???	**Pande Fm:** Late Eocene to Early Oligocene. Soft, light olive grey or blue-grey clays mottled with yellowish orange sandy clay. Greenish black to dark greenish grey clay, or muddy clays developing a mild shaley parting.	Regression began in the middle Eocene and reached maximum in in the Oligocene.	**Kilwa Group**	bioturbated sandstones, and locally, with bi-directional crossbedding, suggest a fluctuating fluvial to tidally influenced delta-top environment in the upper part of the formation (Key et al., 2008)	**Delta Progradation t initiation of EARS Reeves, 201**
		Lutetian									**Masoko Fm:** Middle Eocene. Soft, light olive grey clays mottled with yellowish orange sandy clay. Mottled light olive grey to greyish olive grey clays. When fresh, dark greenish grey clays. Secondary lithologies: clay intervals are punctuated by occasional, massive, hard, sparry calcite cemented, limestone beds packed with *Nummulites*. These nummulitic limestones typically display normal grading in the *Nummulites* and some exhibit imbrication from unidirectional flow or cross-lamination at the top of the bed. These features suggest the beds are deposited from turbulent pulses exclusively sourcing sediment from shallow shelf areas. This may be consistent with these being storm deposits or tempestites (Nicholas et al., 2006).	Thick tertiary deposition		**Quissanga Fm:** Shallow water carbonates. Shallow water coasteal sediments (Key & Reeves, 2012). Lutetian to Priabonian. Calcareous sandstone and shelf carbonates. Lower SST unit overlain by reefel to micritic limestones. Lies unconformably on Mifume Fm?? Middle Eocene to Oligocene age. Shallow water, coastal sediments. A lower sandstone unit overlain by reefal to micritic limestones. A distinctive white, well-sorted, medium-grained sandstone with a kaolinitic cement is exposed in the type section and is considered to form the lower part of the formation. The sandstone is fairly massive but appears to have a low dip below conglomeratic and micritic limestones considered to form the upper part of the Quissanga Formation. In the road north of Quissanga (UTM 661677 8625418), fine-grained micritic limestone clasts are set in a sandstone matrix and beds of more massive shelly micritic limestone have karstic weathered surfaces. Unconformable on Mifume Fm. Shallow water coastal sediments (Key et al., 2008).	
		Ypresian									**Kivinji Fm:** Late Paleocene to Early Eocene. Hard/bloky olive grey claystones mottled with yellowish orange sandy clay. Rest on unconformity, needs confirmation? Greenish black to dark greenish grey claystone with fine quartz sandy partings and a dark greenish grey silty claystone to clayey siltstone (Nicholas et al, 2006).			**Alto Jingone Fm:** Shallow water carbonates (Key & Reeves, 2012). Danian to Ypresian. Mix of marl, shelf carbonate and calcareous sandstone. Interbedded bioclastic, variably sandy and locally gypsiferous sparry LSTs, calcareous siltstones, marls and mudstones, and variably bioturbated calcareous SSTs. Paleocene to early Eocene. Lower boundary unconformity. Deposited adjacent to reefs in an open shallow marine environment. interbedded bioclastic, variably sandy and locally gypsiferous sparry limestones, calcareous siltstones, marls	

	Paleocene	Thanetian	Erosional Unconformity (Nyagah, 1995)	Inversion-related???				Mainly deep marine dark grey to green clays with occasional sandy and silty intercalations (Mbede & Dualeh, 1997).						and mudstones, and variably bioturbated calcareous sandstones. Shell and other fossil fragments, calcareous nodules, mudstone clasts foraminifera including Nummulites were observed in these rocks as well as variably oriented, sand filled worm tubes (Figure 10c). Beds are up to 1 m in thickness, but commonly much thinner and are sub-horizontal or dip gently to the north-northeast. Local faulting has steepened bedding with westerly dips and there are calcite veins locally (Key et al., 2008).	
		Selandian													
		Danian													**Reduced sedimen Reduction in erosion interior**
Cretaceous	**Upper**	Maastrichtian	Uplift of Basement?? (Nyagah, 1995)	**Sabaki Group** Deposited in tide-influenced shelf and marine settings (Nyagah, 1995)	**Kofia Sands** Deltaic sediments represents reversion to a regressive depositional phase during the Turnian through Early Paleocene period. Thin well-cemented, white to pale grey, fine to medium grained sands with poor to fair porosity. The sand is intercalated with olive grey, calcareous claystones and medium to light grey calcareous silty claystones that grade in places into siltstone. interbedded calcite-cemented sandstones with poor to fair porosity, and calcareous shales with an abundance of carbonaceous plant remains. Siltstone lenses also occur in the interval.	**Walu Shale** Succession of bluish-grey to dark grey lots of marine plantonic fauna. The Walu Shale comprises both deep and shallow-water marine facies. Similar shales all along East Africa related to regional mid-Cretaceous transgressive phase (Nyagah, 1995)	The Neocomian regression was followed by a period of fluctuating water level, open marine conditions prevailed in response to gradual sibsidence and rising sea level. This middle Cretaceous deposition developed into full marine **transgression** during the Late Cretaceous.Tectonic activity	Silty mudstones and rare limestones deposited in an outer shell environment (Mbede & Dualeh, 1997).	**Nangurukuru Fm:** Late Cretaceous Santonian to Late Maastrichtian. Hard/blocky olive grey claystones mottled with yellowish orange sandy clay. Rest on unconformity.	Major depositional sequence (probs transgressive)		**Mifume Fm:** Marls/clays (Key & Reeves, 2012). Cenomanian to mid-Maastrichtian. Mainly marl, some marine sandstone calcareous sandstone. Grey marls or mudstones and calcareous sandstones (locally with detrital garnet and mudstone flakes) are the main lithologies. Some LSTs. The marls are strongly bioturbated and preserve worm burrows. Interbedded SSTs coarsen upwards and trough cross-bedding is present. Deposited in open-marine shelf environment above a diachronous unconformity above the Pemba Fm. West to east facies change from western near-shore sediments to eastern open sea sediments with eastern thickening of the formation. Sedimentation on continental margin and slope during rapid, global marine transgression.Grey marls or mudstones and calcareous sandstones (locally with detrital garnet and mudstone flakes) are the main lithologies, and limestones were also intersected in the Mocimboa-1 Borehole. The marls are strongly bioturbated and preserve worm burrows. Interbedded sandstones are up to ~70 cm in thickness and they coarsen upwards in places. Trough cross bedding is present in the sandstones (Key et al., 2008).
		Campanian													
		Santonian													
		Coniacian													
		Turonian			**Hagarso LST** (Albian through Maastrichtian) limestone with veins of calcite and			Marine clays, sandstones and limestones (Mbede & Dualeh, 1997).		**Kihuluhulu Fm:** (Hou) Clay/siltstones interbedded with		**Mavuji Group**		

					anhydrite. The limestone is interbedded with calcareous shales and mudstones. Shallow-water shelf deposition. (Nyagah, 1995)	**Freetown LST** (Cenomanian?) The limestones are calcarenites with shell fragments and possess calcite-lined vuggy porosity. Calcite filled fissures. (Nyagah, 1995)		at this time due to continued wrench faulting as Madagascar moved south, and the break up of South America and Africa (Mbede & Dulaleh, 1997).				fine to medium sandstones deposited in the outer shelf marine environment. Both are highly cemented by carbonate cements and dominated by calcite. SSTs thought to be turbidites						**Transgression (Key & 2012)**
		Cenomanian																	
		Albian	Transgressive Phase?? (Nyagah, 1995)						Limestones, marls and mudstones (Mbede & Dualeh, 1997).	**Makonde Fm:** (Hou) mouth bar depositional environment, with trough cross-stratification sediment ary structure.	**Kitunika Fm:** (Hou) shallow marine depositional environment. Formation dominated by reefal LST with calcarenites. Corals and foraminifera present.					**Macomia Formation?:** Mid Barremian to (inc.) Albian. Paralic clastics. High-energy reworked, proximal fluviatile sequence deposited in a braided channel system.Mostly marl, with bits of marine sandstone and calcareous sandstone. Mainly coarse to fine-grained quartzofeldspathetic or arkosic sandstones with local conglomeratic beds resting on Precambrian gneiss. The cement varies from calcareous and siliceous to kaolinitic. The kaolin is partly derived from in situ weathering of feldspar. Multi-storey sequences of trough cross-bedded sandstone in sets 30 cm-1 m thick are common (Figure 7c). Less common planar sets tend to be bimodal. (Key et al., 2008)	**Pemba Fm:** Oxfordian to Albian. Marine shale, siltstone and sandstone. Some marl. Records 3 marine transgressions. **3. Upper Pemba Fm.** - Aptian-Albian sedimentation during active sea floor spreading. Fluvial to shallow marine shoreface sequence. **2. Middle Pemba Fm**. - Basal Cretaceous sedimentation controlled during active sea floor spreading. Deltaic to open marine sediments. **1. Lower Pemba Fm.** - Upper Jurassic sedimentation controlled by incipient rifting. Proximal sediments deposited in shallow marine environment (presence of belemnites). Westerly. Sandstones and conglomerates interbedded with mudstones and limestones. (Key at al., 2008)
	Lower	Aptian			**Ewaso Sands** (Neocomian through Albian) Deltaic succession of alternating fine to coarse grained orthoquartzites, siltstones, shales and subordinate calcareous sandstones, arnaceous limestones and thin layers of anthracite. Progradational deposits of a tidally influenced delta formed in supratidal setting (Nyagah, 1995).			Aptian siltstones and inerbedded shales, indicate deposition in an open marine to outer shelf environment. To the north, upward fining sequences of grey calcareous sandstones, with minor siltstones and limestones, deposited in a marine mid-shelf environment (Mbede & Dualeh, 1997).				Mainly regressive				
		Barremian	Uplift? (Nyagah, 1995)						Regional unconformity at the base of the Aptian and Lower Albian section (Mbede & Dualeh, 1997).	**Nalwehe:** A Nalwehe sandstones member and a Nalwehe limestone member							
		Hauterivian						**Neocomian regression**	Regression resulted in the deposition of fluviatile sandstones that form a major reservoir along coastal Tanzania. Sandstones and deltaic bituminous sandstones interbedded with clay. Further south - septarian limestones and conglomeratic sandstones					**Mandawa Series**	Continental Clastics	
		Valanginian																

		Berriasian						crop out, indicating some tectonic activity at this time (apparently) (Mbede & Dualeh, 1997).						
Jurassic	Late	Tithonian			**Mtomkuu Fm:** Shales, Sinemurian – Bathonian, Inc. Bajocian Salt	**Late Jurassic transgression.** Quiet phase, deposition was mainly marine with predominantly clastic sediments (Mbede & Dualeh, 1997).	Predominantly maroine clastic sediments. These show an upward decrease in grain size from sand to clay throughout the Kimmeridgian. This low energy environment prevailed in most parts of coastal Tanzania for the whole of the Late Jurassic. Fluviatile deposition in soe parts of basin. In the North (around Tanga) 700m of Oxfordian to Kimmeridgian interbedded shales, sands and marls. Further south sandstones, limestones and mudstones (Mbede & Dualeh, 1997).	Deep marine deposition continued (Mbede & Dualeh, 1997).	**Mitole Fm:** Lower Mitole oolitic limestone member and sandstone member above (Hudson, 2011)	**Kipatimu Fm:** Sandstones (Hou)	Transgressive			
		Kimmeridgian												
		Oxfordian								**Mbaro Fm:** Sandstones and marls (Hudson, 2011)				**Kizimbani Shale equiv.** Marine shale, siltstone and sandstone (Mahanjane & Franke, 2014)
	Middle	Callovian			**Kibiongoni Beds:** sandy micaceous shale with thin, fin-grained sandstone. Rest conformably on the Kambe Fm. Callovian (Coffin & Rabinowitz, 1988)									
		Bathonian				**Full marine environment established:** Continued subsidence lead to the development of a shallow epicontinental sea by the end of the Bajocian and left the Karoo grabens along coastal Tanzania flooded with marine waters overstepping the basement (Mbede	**Amboni Limestone:** compact well bedded oolitic to pisolitic limestones. Reefal LST. Some calcareous sandstones and sandy oolitic limestones (Mbede & Dualeh, 1997).	Deep marine shales. **Posidonia Shales ?:** dark gray shales deposited in a restricted back reek environment (Mbede & Dualeh, 1997)	**Mtumbei Fm:** marine LST			**Makarawe Shale equiv.** Marine shale, siltstone and sandstone (Mahanjane & Franke, 2014)
		Bajocian		Break up	**Kambe Fm**: limestones. Inc. Rare LST, Rangani LST, Mwatchi LST. Dark grey oolitic limestone with abundant fauna (corel, ammanoids, and interbedded shale. Deep-water facies in the south, shallow-water facies in the north. Bajocian - Bathonian. (Coffin & Rabinowitz, 1988)									**Mtumbei LST equiv.** Carbonates / limestones (Mahanjane & Franke, 2014)

					& Dualeh, 1997).					
		Aalenian				**Ngerengere Beds:**Correlate with the Manzeras Sandstones of Kenya. Sequences within these beds are serarated by disconformities, indicating different cycles of deposition in response to tectonic control by bounding faults. Arkosic sandstones with occasional limestones, and shales reflecting a high energy environment, becoming much quieter with time (Mbede & Dualeh, 1997).	**Pindiro Group:** Top surface recognised as the Intra-Aalenian unconformity.**(1) Mbuo Fm:** (Upper Triassic) Older sandstone member (Mbuo sandstone member) - sandstone beds with fine to coarse sands alternating with silt- and claystones. Deposited in alluvial and fluvial environments. Younger Mbuo Claystone Member - mostly thick beds of claysstones alternating with thin dolomite beds. Deposited in lacustrine environment. **(2) Nondwa Fm**: (Upper Triassic to Lower Jurassic) evaporites and subordinate shales. Granular limestone and dolostone, gypsum and shales. Deposited in a restricted marine environment. **(3) Mihambia Fm**: (Toarcian to Aalenian) A sequence of clastic sediments with subordinate limestones. Transgressive over Nondwa evaporites. Alternating beds of sandy-siltstones and sandy-mudstones. Limestone beds. Basal sandstones with occasional carbonates, the top is open marine facies, namly limestones and shales. Indicates a shallow and marginal marine environment. (Hudson & Nicholas, 2014)	Active faulting up to middle Jurassic - Bajocian (Hudson & Nicholas, 2014)		**Rio Mecole Fm and N'Gapa Fm:** High-energy fluviatile, alluvial fan and scree slope sediments in intra-cratonic rift basins. (Key et al, 2008). **Rio Mecole Fm**: Conglomerate. The Rio Mecole is mainly continental, reddened coarse-grained siliciclastic conglomerates (Key et al., 2008). High-energy, fluviatile (and possibly alluvial fan sediments in the little basins). Paleoflow directions from the NE and NW, suggesting sediment transported by river-systems off the rift shoulders (Key et al., 2008). **N'Gapa Fm:** Sandstone and conglomerate, characteristically red-purple and sillicified (continental rift setting). They are preserved in small, isolated, fault controlled (NNW - SSE trending) basins located along the western limit of the Rovuma Basin. Poorly sorted nature – deposited in alluvial fan or on scree slopes within or on the shoulders of rift basins. The presence of fining upward beds in channels among the poorly sorted reddened sandstones, along with evidence for strong kaolinisation suggests fluviatile reworking of the sediments in a warm, humid climate. (Key et al., 2008).	Intra-cratonic rifti marine incursions (K 2008)
	Early	Toarcian		**Main Syn-Rift**	**Mazeras Sandstone:** Late Triassic to Lower Jurassic. Clean, coarse-grained, cross-bedded deltaic SST and grit with interbedded siltstone and silicified wood fragments (Coffin & Rabinowitz, 1988). **Lower:** Coarse SSTs, with silicified wood. **Upper:** Grits, SSTs. Both Deltaic to Aeolian. (Rias-Assa, 1988)					
		Pliensbachian								
		Sinemurian								
		Hettangian								
Triassic	**Late**									
	Middle		**Karoo Group**	**Karoo Syn-Rift**	**(Matolani Fm??:** Felspathetic SST at the top of thr Mariakani Fm) **Mariakani Fm:** Middle to Upper Triassic. Coarse-grained sandstones and shale lenses, intercalations of black shales and coals. Deltaic (Rais-Assa, 1988). SST - clean, fine-grained and flaggy contains local micaceous siltstone, silty shale and plant remains. Deltaic - indicated by current beds and ripple marks (C & R, 1988)	**Karoo Group:** Intermittent faulting	**Karoo:** Periodic fault movement initiated erosive phases that generated fluvial systems, deposited in fining-up sequences with conglomerates at the base. Pass up into high energy braided stream deposits then low energy meandering stream, flood plain and deltaic to swampy deposits. Karoo sedimentation terminated by a number of tectonic pulses. Interbedded continental sandstones, siltstones and shales with a basal conglomerate. Medium grained white quartzitic SST, red interbeds and grey silty claystones. lacustrine to braided stream deposits, evidence of occassional marine incursions, coaly beds and deltaic influence (Mbede & Dualeh, 1997).	**Karoo??**	???????? ???????? ???????? ????	**Karoo Supergroup** (Key et al., 2008). **Salman & Abdula (1995)** infer Karoo group by interpreting seismic and correlating with Selous and Madawa Basins in Tanzania. Selous Basin - more westerly. Continental syn-rift sediments overlying grabens. Continental conglomerate and sand with shale bands. Mandawa Basin - more easterly. Development of the basin began in Permo-Triassic and Early Jurassic times, as rifting resulted in differential subsidence and the formation of a semi-enclosed basin. Major salt bsain. likely to extend into Rovuma Basin. One can assume that in the Ruvuma Basin both types of Karoo facies are also found, their distribution related to buried rifts: on the west, continental syn-rift sediments similar to the Selous Basin; and on the east, lagoonal-evaporitic sediments of semi-enclosed basins similar to the Mandawa Basin. All (Salman & Abdula, 1995)!	Intra-cratonic rifting. 2008)
	Early				**Maji-ya-Chumvi Beds:** Late Permian to Early Triassic. Represents change from Fluviatile to Lacustrine environment. Silty shale, siltstone, and flaggy SST. Common ripple marks, cross-bedding, sun cracks and rain pits (C&R,1988). **Lower:** (Late Permian) SST & carboniferous shales. Lacustrine. (Rasi-Assa, 1988).					

Permian					Continental, contains plant fossils (C & R, 1988). **Middle:** (Lower Triassic) Marine sandy shales containing fish fossils (C & R, 1988; Rais-Assa, 1988). **Upper:** (Triassic) Argilaceous SSTs. Lacustrine (Rais-Assa, 1988). Presence of fresh water Brachiopod = fresh or possibly brackish lacustrine environment (C & R, 1988).					
					Taru Grits: Late Carboniferous to Early Permian. Fluviatile (possibly marine), 'fresh' feldspathetic grit and SST derived from basement to the west (Coffin & Rabinowitz, 1988) **Lower:** Tillite. Peri-glacial. Mild glacial episode. Mild unconformity between this and the middle Taru Grits. Above. **Middle:** Arkosic SST. Fluviatile. **Upper:** Arkose & Conglomerates. Fluviatile. (Rais-Assa, 1988).					
Carboniferous	**Late**										
	Early										

Appendix F Mad-EA Margin Segment Stratigraphy

				Megasequence	Ambilobe NE			Ambilobe SW				Majunga			Megasequence	Morondava				
					Continent	Shelf	Basin	Continent	Shelf	Basin		Continent	Shelf	Basin		Continent	Shelf	*Basin*		
Quaternary					This period is dominated by coastal dune and reef development; along with volcanism (basalt flows) that is probably continuous since Eocene time (Coffin & Rabinowitz, 1988).							Quaternary alluvial deposits (Coffin & Rabinowitz, 1988).				Continental Sandstone (Coffin & Rabinowitz, 1988)	Shale (Coffin & Rabinowitz, 1988)			
Neogene	**Pliocene**	Piacenezian			None reported, possibly volcanism (Coffin & Rabinowitz, 1988)							A regression during the Pliocene led to the deposition of continental cross-bedded sandstones intercalated with silty clay or rare sandy lacustrine limestone (Coffin & Rabinowitz, 1988).				Shallow water limestone and dolomite, Shale and thin sand, Dolomite, Limestone and thin sandstone (Coffin & Rabinowitz, 1988)				
		Zanclean																		
	Miocene	Messinian			A sequence of layered limestone, sandstone, and basaltic tuff Aquitanian to Burdigalian. Lava flows on top also considered Miocene in age (Coffin & Rabinowitz, 1988)							An Oligocene unconformity separates the Late Post-rift and the Modern Margin megasequences. Miocene sediments have been recognised along the shore of the basin as marine marls and limestone rich in fossils (Razafindrazaka et al., 1999; Coffin & Rabinowitz, 1988). Offshore, lower Miocene dolomite and limestone lie unconformably over mid-Oligocene sediments (Coffin & Rabinowitz, 1988).								
		Tortonian																		
		Serravallian																		
		Langhian																		
		Burdigalian																		
		Aquitanian																		
Paleogene	**Oliocene**	Chattian			None documented. Possible volcanic activity continuing from Eocene time (Coffin & Rabinowitz, 1988)							An Oligocene unconformity separates the Late Post-rift and the Modern Margin megasequences (Coffin & Rabinowitz, 1988).				Absent in the north of the basin. Present further south as marine limestone,calcareous shale, sand, and marl (Coffin & Rabiowitz, 1988)				

				Megasequence	Ambilobe NE			Ambilobe SW				Majunga			Megasequence	Morondava				
					Continent	Shelf	Basin	Continent	Shelf	Basin		Continent	Shelf	Basin		Continent	Shelf	*Basin*		
		Rupelian																		
		Priabonian																		
	Eocene	Bartonian			**Lower:** dolomite and basaltic tuff sequence. **Upper:** karst limestone of Lutetian age (Coffin & Rabinowitz, 1988).							The Eocene begins with fossil-rich Ypresian age limestone and marl, with sandy horizons (Coffin & Rabinowitz, 1988; Razafindrazaka et al., 1999). Offshore, the middle and upper Eocene sediments, including marl and limestones lie unconformably above Campanian marl or above Paleocene shale. Deposition of the Eocene sediment likely continued into the early Oligocene (Coffin& Rabinowitz, 1988).				Interbedded marine carbonate sequence and shale, thins to the north and loses marine character. Minor volcanic activity Offshore, Eocene shelf limestone and dolomite, calcareous shale with thin Limestone stringers, shallow water marl, marl and limestones, dolomites, shales, marls etc…. (Coffin & Rabinowitz, 1988)				
		Lutetian																		
		Ypresian																		
	Paleocene	Thanetian			No rock unequivocally identified as Paleocene. Possibly dolomite faoun at the base of the Eocene (Coffin & Rabinowitz, 1988)							Onshore, Paleocene sediments are predominantly marine, including marl, limestone, sandstone, dolomite and limestone commonly topped by a layer of red clay (Coffin & Rabinowitz, 1988; Razafindrazaka et al., 1999), whereas, offshore, the Epoch is represented by calcareous shale (Coffin & Rabinowitz, 1988).				Paleocene mostly missing in the north In the central and southern areas: marine sediments including dolomite, limestone and marl, with some shale. Eocene sediments lie unconformably above Upper Cretaceous sediments (Coffin & Rabinowitz, 1988)				
		Selandian																		

				Megasequence	Ambilobe NE			Ambilobe SW				Majunga			Megasequence	Morondava				
					Continent	Shelf	Basin	Continent	Shelf	Basin		Continent	Shelf	Basin		Continent	Shelf	*Basin*		
		Danian																		
		Maastrichtian			Sandstone and sandy marl with some limestone bands. Maastrichtian is represented by 40-80m of unfossiliferous sand and sandstone (Coffin & Rabinowitz, 1988)							The lava flows were followed by predominantly continental sediments such as cross-bedded sandstones from the Conacian to Campanian, with some thin, well-defined marine intervals consisting of a range of limestones, clays and conglomerates deposited in a lagonal environment and shales (Coffin & Rabinowitz, 1988). Fully marine conditions became established again during the Maastrichtian with a unit of fossiliferous marly limestone or chalky marl that persisted through to the Eocene (Coffin & Rabinowitz, 1988). Offshore, the Maastrictian is usually missing and middle to upper Eocene sediments rest unconformably on Coniacian through Campanian marine marls (Coffin & Rabinowitz, 1988).				Shale and Marl, with interbedded volcanic rocks (Coffin & Rabinowitz, 1988)				
		Campanian																		
		Santonian																		
	Upper	Coniacian																		
Cretaceous		Turonian			The Lower Turonian id marked by a sudden change to fossiliferous continental sandstone. Presence of trachyte in conglomerates marks an important episode of volcanism commencing in the early Turonian. A return to marine conditions in late Turonian time is indicated by sandstone succeeded by shaly limestone. (Coffin & Rabinowitz, 1988)							The Turonian is marked by extensive lava flows, averaging 50 m but ranging to as much as 200 m in thickness. Most of the flows are subaerial, although some were extruded in lacustrine and marine environments. In the southern Majunga Basin, the flows are underlain by 20 m of coarsegrained, unfossiliferous sandstone, and overlain by 5 m of fossiliferous clay, marl, and limestone (C&R, 1988).				In southern and central Morondava is represented by thick continental to marine sand grading rapidly offshore to shale (Coffin & Rabinowitz, 1988)				
		Cenomanian			Marl rich in microfauna (Coffin & Rabinowitz, 1988)							The Cenomanian was an age of transition (although not synchronous basin-wide) from marine to continental facies. As much as 100 to 120 m of shale with limestone horizons underlies as much as 370 m of coarse, cross-bedded pebbly sandstone. By the end of Cenomanian time, the Sahondralava-Ihopy horst's role as a north-south partition between subbasins ceased (C&R, 1988).								
	Lower	Albian			Lower Albian shale and Middle and Upper Albian marl (Coffin & Rabinowitz, 1988)							The Albian is an entirely marine facies, rich in fossils, made up of 150 to 250 m of shale and marl with calcareous or ferruginous nodules and commonly glauconite in the north, and 50 to 100 m of marl in the south. The Sofia 1 well (M4 in Fig. 1) recovered 1,165 m of Lower Cretaceous massive shale with thin sandstone beds (Coffin & Rabinowitz, 1988).				**Sitampiky Fm:** Continental sandstone (Coffin & Rabinowitz, 1988)	**Duvalia Marls:** (Geiger, 2004) Early Cretaceous mudstones (Valangian - Earliest Aptian?) interbedded with thin silt- / sandstones, as well as limestones containing calcareous and iron-oolites (Geiger, 2006).		
		Aptian			Sandstone, up top of angular unconformity (Coffin & Rabinowitz, 1988)							Hauterivian and Aptian time marked by a change to predominantly continental conditions. To the north the Hauterivian is a marine epicontinental facies 400m thick consisting of shale commonly containing							**Transgression (Luger?)**	

				Megasequence	Ambilobe NE			Ambilobe SW				Majunga			Megasequence	Morondava			
					Continent	Shelf	Basin	Continent	Shelf	Basin		Continent	Shelf	Basin		Continent	Shelf	*Basin*	
		Barremian										ferruginous nodules or pellets, and rare glauconitic sand with some lignite horizons. In the south the Hauterivian comprises 250m of continental cross-bedded sandstone. The Aptian records several marine horizons (faunally) in a predominantly continental section. To the north, 25 m of glauconitic sandstone are found beneath 340 m of poorly consolidated, continental cross-bedded sandstone. The Aptian interval in the south, from bottom to top, consists of 110 m of continental lignitic sandstone, 55 m of continental sandstone, 20 m of glauconitic sandstone, and 30 m of gypsiferous marl (Coffin & Rabinowitz, 1988).						
		Hauterivian			Fossiliferous marl and shale (Coffin & Rabinowitz, 1988)														**Transgression (Luger?)**
		Valanginian																	
		Berriasian																	
Jurassic	**Late**	Tithonian			**East:** interfingered marine and continental sediments, silty, commonly calcareous, fossiliferous sediments, with influxes of coarse-grained, calcareous intervals and sudden facies changes (Coffin & Rabinowitz, 1988)			**West:** epicontinental, marine, fauna-rich sandy marl and limestone (Coffin & Rabinowitz, 1988)				Predominantly marine. 10m of fauna-rich Lower Oxfordian marl and limestone, succeeded by 30m of Kimmeridgian marl, glauconitic or gypsiferous, and clay. In the north, the Tithonian consists of 70m marl and gypsyferous clay, whereas in the south this interval is represented by 25m glauconitic marl. Also shale (in Sofia-1 well) (Coffin & Rabinowitz, 1988). In the north: Berriasian - clay with gypsum 150m and Valanginian - shale and marl 100m. In the south marly limestone and marl for those intervals. A major Upper Jurassic transgression flooded the carbonate platform and led to the deposition of marine clastics, limestones, marls and clays often containing glauconite or gypsum during the Late Jurassic reflecting post-rift subsidence (Coffin & Rabinowitz, 1988; Jeans & Meerbeke, 1995). Marine deposition continued into the earliest part of the Cretaceous (Neocomian) (Coffin & Rabinowitz, 1988).				
		Kimmeridgian																	
		Oxfordian																	
	Middle	Callovian						**Unit F:** (Lavalohalika Formation, Rerat, 1964) Dark grey sandy clay with fine to coarse sandstones at the top deposited in a coastal plain environment. Barren Callovian. (Papini & Benvenuti, 2008).							**Mudstones?** Dysoxic basinal mudstones (shales and marls) with a thick intercalated? Late Callovian – Early Oxfordian Sandstone (Geiger, 2006).		In the Early Callovian, deeper and distal shelf conditions transgressed far landward and formed a thick mudstone succession. (Geiger, 2006)

			Megasequence	Ambilobe NE			Ambilobe SW				Majunga			Megasequence	Morondava								
				Continent	Shelf	Basin	Continent	Shelf	Basin		Continent	Shelf	Basin		Continent	Shelf	*Basin*						
							Unit E: (Komamery Formation, Rerat, 1964; Besairie and Collignon, 1972) Alternation of whitish medium-fine sandstone and grey claystone passing upward to marls. Bathonian – Callovian (Papini & Benvenuti, 2008).														
		Bathonian				**Unit 5:** Alternation of oolitic limestone , marls and cross-stratified coarse-medium sandstones . . Similar to Bemaraha/ Sakaraha formations described in the Morondava basin by Geiger *et al.,* 2004. Aalenian - Callovian (Papini & Benvenuti, 2008).				By the end of the Middle Jurassic, the West Madagascan Margin was covered by shallow-water carbonate platforms and this most likely extended to the Majunga Basin. Razafindrazaka et al., (1999) describe open marine facies comprising marls, limestones (Ankara and Kelifely Limestones) and argillites.					**Ankazoabo Fomation:** Sandstones rest on Sakaraha Fm with an erosional base (Geiger, 2004). Sandstones of fluvial and deltaic origin **Sakanavaka Formations** (Geiger, 2004)						
															Bemaraha Formation: Predominantly massive limestones, including carbonate mudstones, pelletoidal-grainstones or oolitic-grainstones. Bajocian to Bathonian in age. Lies unconformably on Andafia Fm. (Geiger, 2004). Coastal barrier / lagoon complex (Clark & Ramanampisoa, 2002). Marginal carboate platform, deposition environments ranging from barrier islands with beaches and tidal deltas, to lagoons, upper intertidal flats and supratidal sabkhas. A wedge composed of millimetre- and centimetre-bedded carbonate mudstones occurs basinward of the platform. This wedge is interpreted as an anoxic, submarine slope deposit. A thin unit of millimetre-bedded mudstones is present basinwards of the mud wedge. These sediments probably accumulated in a more offshore, deeper water, anoxic, basin–plain environment (Gieiger, 2004). **Sakaraha Formation:** Found in Southern Morondava basin, in the north it has been removed by erosion. Mixture of siliciclastics and carbonates. The carbonates are similar to the Bemaraha Formation, whereas the siliciclastics comprise varying admixtures of shale, marl, siltstone and sandstone. Oolitic grainstone. Thinly-bedded succession of marls, sandstones and limestones. The sandstones are composed of quartz and are generally cemented by carbonate. Calcareous ooids and bioclasts occur in some of the sandstones as well as in some of the limestones. (Geiger, 2004). Intertidal to shallow subtidal, open lagoonal environment.						
		Bajocian					**Unit D:** (Andrahibo Formation, Ampasimena Formation according to Rerat, 1964) Alternation of whitish sandstone and dark grey claystone. Sandstone are cross bedded indicating palaeocurrents to SW. Bajocian – Bathonian (Papini & Benvenuti, 2008).														
		Aalenian					**Unit C:** (Ampasimena Formation according to Rerat, 1964) Dark grey calcilutite and marl with		**Syn-rift II**	**Beronono Fm?:** Shales. Lower part - shales and marls, interbedded with a few thin beds of sandstones and shelly limestones. Middles part - sandstones (shell fragments) with thin shale beds. Sandstones followed			**Syn-Rift II**	**Andafia Fm:** Rests unconformably on the Isalo Fm**.** Predominantly marine shales and marls, together with thin limestones and cross-bedded sandstones (Geiger, 2004).						

				Megasequence	Ambilobe NE			Ambilobe SW				Majunga			Megasequence	Morondava				
					Continent	Shelf	Basin	Continent	Shelf	Basin		Continent	Shelf	Basin		Continent	Shelf	*Basin*		
						Unit3: Marly limestone, subordinate calcarenitic beds, followed by **Unit 4:** limestones and clayey-silty marlstones (Unit 4). A mixed carbon-terrigenous ramp controlled by relative sea-level fluctuations. Aalenian (Papini & Benvenuti, 2008).		subordinate cross-bedded sand indicating palaeocurrent direction toward NE. Deposited in a coastal plain and shallow marine environment. Toarcian - Aalenian (Papini & Benvenuti, 2008).		by shales and marls, with thin sandstones and limestones beds, and capped by sandstones bed with oyster shells and bone fragments. Upper part - shale with oyster fragments and a few thin bioclastic limestones, Syn-rift. Toarcian - Aalenian (Geiger *et al.*,2004).				Seismic, borehole and outcrop data suggest these sediments onlap tilted and rotated fault blocks of Isalo Sandstone to form wedge-shaped bodies within half-grabens (Clark 1996).		
				During Late Toarcian-Early Aalenian, basin underwent depositional differentiation with activation of asymmetric sub-basins bounded by steep faults.																
	Early	Toarcian				**Unit 2:** (Marivorahona Series and the Ankarabo Sandstone,		**Unit B:** (Jangoa Limestone, Rerat, 1964; Besairie and Collignon,												
				Early Toarcian marked by																

			Megasequence	Ambilobe NE			Ambilobe SW				Majunga			Megasequence	Morondava				
				Continent	Shelf	Basin	Continent	Shelf	Basin		Continent	Shelf	Basin		Continent	Shelf	*Basin*		
			widespread transgression.		Rerat, 1964; Besairie & Collignon, 1972) A mix of silty claystones, clayey sandstones and marly limestones, followed by fluvio-deltaic sandstones deposited in a mixed carbonate – terrigenous ramp. Toarcian (Papini & Benvenuti, 2008)		1972) Limestone interbedded with fine sandstones and claystones deposited on a mixed carbonate-terrigenous ramp. Lower - Middle Toarcian. (Papini & Benvenuti, 2008)										
		Pliensbachian			**Isalo Group** Cross-laminated whitish medium-course, locally microconglomeritic, quartzitic sandstones in bedsets up to 10 m thick. Reddish mudstones may be embedded within the sandstones. Alluvial plain, with fluvial deposition (Papini & Benvenuti, 2008). The sandstone varies greatly in grain size, contains a few conglomerate bands and thin, sandy shale horizons, and continues into the upper Lower Jurassic (Coffin & Rabinowitz, 1988).			**Karoo**	**Isalo Formation:** (Lower Jurassic). The lower sequence, Isalo I, consists of continental fluviatile, cross-bedded sandstones (Razafindrazaka et al., 1999) and sandy red beds with local flood plain shales (Jeans and Meerbeke, 1995).The Middle and Upper Isalo sequences, Isalo II and Isalo III respectively, indicate increasing marine influence. The Isalo II: reddish sandstones and argillites with numerous marine beds, and the Isalo III: lagoonal and marine beds intercalated with terrestrial sandstone (Razafindrazaka et al., 1999). At this time, it has been suggested that salt was deposited in the Ambilobe Basin to the north (Clark, 1998), so it is possible that the salt in the Majunga Basin was also deposited at this time.						
		Sinemurian																	
		Hettangian																	
Triassic	**Late**										**Upper Sakamena:** records a return to continental conditions with the deposition of predominantly fine red sandstones, with crossed laminations and reddish argillites (Razafindrazaka et al., 1999).			**Karoo Group Syn-Rift I**	**Isalo Fm:** Cross_bedded sandstones and conglomerates with locally developed root horizons and petrified tree trunks (Wescott and Diggens, 1998; Piqué et al., 1999). (Geiger, 2004)				
	Middle														**Sakamena Group:** **Lower Sakamena Sandstone**: Middle-Late Permian. Predominantly sandstones and conglomerates, with subordinate siltstones,				

				Megasequence	Ambilobe NE			Ambilobe SW				Majunga			Megasequence	Morondava			
					Continent	Shelf	Basin	Continent	Shelf	Basin		Continent	Shelf	Basin		Continent	Shelf	*Basin*	
																			mudstones and shales, together with some stromatolitic, pisolitic, oolitic and bioclastic limestones in the upper part. The sandstones and conglomerates were deposited as series of alluvial fans and fan-deltas that spread progressively into developing half grabens (Wescott, 1988; Clark, 1996; Montenat et al., 1996; Wescott and Diggens, 1998). Shallow marine conditions prevailed in the halfgrabens, with thick offshore mudstones being deposited in the deeper, more central parts, and deltas prograding in from the margins to form coalescing sheets. The limestones are interpreted as shallow marine sand shoals, inter-tidal beach deposits and algal reefs that formed around the marine fringes of fan-delta complexes (Clark, 1996). **Middle Sakamena Shale:** Early Triassic. Dark grey shales and nodular or laminated mudstones, together with local heterolithiic and cross-bedded sandstones. Rests unconformably on Lower Sakamena Fm, progressively onlaps it. Deposited in probably varied from marine in lower part of the middle Sakamena Formation, to fluvio- deltaic in the middle and, finally, lacustrine in the upper part. **The Upper Sakamena Sandstone:** Early-Middle Triassic. Predominatly sandstones. Conformable on middle Sakamena. Deposited in a range of shallow marine, shoreface, deltaic and fluvial environments. These include distributary channel and mouth bar environments on the delta front and delta plain, interdistributary bay and crevasse splay environments, and braided and low-sinuosity fluvial channels in an alluvial plain environment (Wescott, 1988; Nichols and Daly, 1989; Vroon ten Hove, 1993; Wescott and Diggens, 1998).(Geiger, 2004) **Sakoa Group:** succession of tillites, sandstones, shales, limestones and coals of Late Carboniferous–Early Permian age (Geiger, 2004). Stephanian (Late Carboniferous) age from the base of the succession (Wescott & Diggens, 1997) The top of the Sakoa is marked by the shallow marine Vohitolia limestone, which contains Early Permian palynomorphs (Wescott and Diggens, 1997)
	Early																		
				Vertical crustal movement during the Late Permian and Early Triassic is recorded as a discordance between Permian and Triassic strata, and it preserved Permian sediments in grabens (Coffin & Rabinowitz, 1988).	Dominated by the deposition of marine shale. Separated by an angular unconformity from overlying continental sandstones. 20 to 100 m thick. Correlative with Isalo facies of Morondava basin (Coffin & Rabinowitz, 1988).														
Permian	**Upper**				Massive coarse-grained, dolomite-cemented sandstone (to 500 m thick), containing coral and other fossils, with angular conglomerate bands at the base; gray, yellow, or black fossilbearing shale (100 to 250 m thick) with dolomitic or quartzite bands; green sandstone (50 to 100 m thick); interbedded sandy and massive shale (120 to 150 m thick) (Coffin & Rabinowitz, 1988).								**Middle Sakamena:** consists of (Upper Permian to Early Triassic) argillites and limestones, which are often bituminous (Razafindrazaka et al., 1999). They were deposited as tectonic movement slowed during the Upper Permian, and record a marine incursion (Jeans and Meerbeke, 1995).						
	Middle				**Middle Permian Marine Beds the oldest recorded in the basisn**(Coffin & Rabinowitz, 1988). There are three major subbasins withing the Deigo Basin which record different stratigraphic seqences although all are similar to the Sakamena facies of the Mjunga Basin. The following in the stratigraphy of the best known one, dated by microfossils, from base to Upper Permian. Tectonic breccia overlying basement (Coffin & Rabinowitz, 1988)								**Sakoa(?) and Lower Sakamena:** thick sequences of fluvio-deltaic, coal swamp, and terrestrial immature clastics deposited in grabens during extensional faulting (Jeans and Meerbeke, 1995)						
	Lower																		
Carboniferous	**Late**																		
	Early																		

				Megasequence	Ambilobe NE			Ambilobe SW				Majunga			Megasequence	Morondava				
					Continent	Shelf	Basin	Continent	Shelf	Basin		Continent	Shelf	Basin		Continent	Shelf	*Basin*		

Appendix G EA-ANT Margin Segment Stratigraphy

				Megasequence	Mozambique								
					Angoche Basin			Zambezi Delta Depression			Southern Mozambique Basin		
					Onshore	Offshore		Onshore	Offshore		Central	Southern	
Quaternary						Shallow-water/shelf terrigenous (Mahanjane, 2014)			**Zambezi Deltaic Complex:** The Zambezi Deltaic complex is the largest Cenozoic deltaic complex on the east coast of Africa, reaches 4000m thick. Formed of interbedded conglomerate, sand and clay with characteristic deltaic superposition of layers and numerous intraformational interruptions and erosional inlets. During the Oligocene, Neogene and Quaternary the depression was filled with terrigenous sediments. Rate of deposition was higher than rate of subsidence. As a result the delta plain prograded towards the east (Salman & Abdula. 1995).		**Dunes Fm:** Pliocene deposits were formed at a period of extensive marine regression and occur over the greater part of the Mozambique Basin as continental deposits of ancient dunes, river terraces and lakes (Salman & Abdula. 1995).	**Limpopo Deltaic Complex:** Marked by a considerable reduction in the amount of terrigenous material deposited in the marine basin. Deposition is mainly concentrated in the coastal plain with the formation of a sub-aerial delta (Salman & Abdula. 1995).	
Neogene	**Pliocene**	Piacenezian				Shelf Carbonates (Mahanjane, 2014)							
		Zanclean											
	Miocene	Messinian				Paralic sandstone, with channel fill sandstones (Mahanjane, 2014)					**Jofane Fm:** Occurs primarily as marine carbonate: limestone, calcarinite and arenaceous limestone, which are distributed practically everywhere within the coastal plain. Thickness up to 200m (Salman & Abdula. 1995).		
		Tortonian											
		Serravallian											
		Langhian											
		Burdigalian									**Inharrime Fm:** Lies unconformably over the Cheringoma deposits. Occurs as a layer of red dolomite, red clay and sandstone with individual bands of anhydrite. Deposited in a restricted lagoonal environment, whose central part comprises a thick, qypsum-bearing sequence identified as the **Temane Formation.** Thickness 100 – 350m (Salman & Abdula. 1995).		
		Aquitanian											
Paleogene	**Oliocene**	Chattian				Shelf carbonates, followed by shaly siltstone with basin floor fans. Unconformity at the base (Mahnajane, 2014)							
		Rupelian											
	Eocene	Priabonian				Shale with basin floor fans, Unconformity at the top (Mahanjane, 2014)			**Middle – Late Eocene reef:** • Shallow-water carbonate shelf deposits, mainly stacked nummulitic limestone and marl • Margin barrier reef is shifted west with respect to earlier reefs. • Margin reef developed progradational stratification of Eocene sediments on its outer shelf (Salman & Abdula, 1995).		**Cheringoma Fm:** West, shallow-water facies – Nummulitic limestones with bands of clay and calcareous sandstone. East, deeper-water formations – calcarenitic and calcilutitic which formed in conditions of a continental slope and continental rise. Along the outer edge of the shelf, a chain of reef massifs is present (Salman & Abdula, 1995)		
		Bartonian											
		Lutetian											

				Megasequence	Mozambique									
					Angoche Basin			Zambezi Delta Depression			Southern Mozambique Basin			
					Onshore	Offshore		Onshore	Offshore		Central	Southern		
		Ypresian							In the area of the Zambezi Delta depression, the Paleocene – Eocene sediments occur as deep-water facies comprising marls, shales and calcilutites. In the area of the Zambezi Delta depression, the Upper Grudja Formation is made up of 2 reef levels**. Lower Fm – Paleocene reef:** Shallow-water shelf represented by interbedded sandstone, arenaceous limestone and marl of the lower part of the Upper Grudja Formation. **Upper Fm – Early Eocene Reef:** Interbedded, stacked arenaceous limestone, sandstone and marl (Salman & Abdula, 1995)			**Upper Grudja Fm:** Sequence of glauconitic sand, clay and marl with bands of limestones (Salman & Abdula, 1995)		
	Paleocene	Thanetian				Unconformity at the base. Layers of shaly siltstone, shelf carbonates with basin floor fans, and then marly-shaly siltstones (Mahanjane, 2014)								
		Selandian												
		Danian												
Cretaceous	**Upper**	Maastrichtian				**Lower Grudja equiv.**			**Lower Grudja Fm:**		**Lower Grudja Fm:** Spread widely in the central part of the basin. Commercial gas pools have been found in different layers. A layer of clay with bands of glauconitic-quartzose sandstone. Sandstone layers up to 50m, overall thickness 1100-1200m in the centre and decreases at the periphery. The formation has been eroded so it is absent from the elevated areas and horsts in the south. The SST beds are buried shoals and bars which had formed in a shallow-water shelf environment. In the east, the sandy bodies gradually disappear from the section and synchronous deposits occur as a thick uniform layer of Upper Cretaceous shale deposited on a continental palaeoslope. In the west, the fm. grades into continental sands and conglomerates (Salman & Abdula, 1995)		**These sediments form a self-contained cycle of sedimentation associated with the development of the East African continental margin. Typified by a consistent marine transgression (Salman & Abdula, 1995).**
		Campanian												
		Santonian				**Upper Domo Shale equiv.**			**Upper Domo Shale Fm**		**Upper Domo Shale Fm:** Turonian to Santonian. Sequence of dense clays, in the south(?). Also found in the central part of the basin where it grades into continental sandstones and becomes part of the Sena Formation towards northwest (Salman & Abdula, 1995)			
		Coniacian												
		Turonian				**Domo Sand equiv.:** Paralic sandstones, deposited during regression. Slope fan or basin floor fan (Mahanjane, 2014).		**Sena Fm:** Found in central and northern parts of the basin. Continental rock sequence of variegated fluvial and alluvial formations: arkose sandstones, conglomerates and argillites enriched with coaly detritus. Hauterivian to			**Domo Sandstones Fm:** Cenomanian. Primarily quartzose sandstone, interbedded with dark argillite. Distributed in the central parts of the basin. Towards the south and east the sandstones decrease in importance and the section becomes primarily argillaceous (Salman & Abdula, 1995)		
		Cenomanian												

				Megasequence	Mozambique									
					Angoche Basin			Zambezi Delta Depression			Southern Mozambique Basin			
					Onshore	Offshore		Onshore	Offshore		Central	Southern		
	Lower	Albian				Lower Domo Shale equiv.: Further south in the Mozambique Basin the Domo shale is regarded as a potential sources rock, dark grey to black, thinly bedded, marly shale (Nairn et al., 1991).		Upper Cretaceous (Cenomanian – Turonian) (Salman & Abdula, 1995).			Lower Domo Shale Fm: Distributed in the southern and central areas of the basin, both on- and offshore, where it occurs as dark marine argilites with occasional bands of arkose sandstones. The argillites contain Aptian – Albian and Cenomanian fauna. The Maputo and Lower Domo shales are the marine equivalent of the Sena Formation. Eastwards the Lower Domo Shales grade into continental slope and rise sediments where fan complexes are widespread (Salman & Abdula, 1995).			
		Aptian												
		Barremian									Maputo Fm: (Salman & Abdula, 1995). Neocomian. A Cretaceous transgressive marine sequence begins with the Maputo Formation. Found in the southern and central areas of the basin. Occurs as a layer of glauconitic-quartzose sandstones and arenaceous limestones, interbedded with argillites. Shallow water marine sandstones and limestones of the Maputo fm. overlie eroded Stormberg basalts or the Red beds fm. May be assigned as Neocomian (Salman et al., 1985; Salman & Abdula, 1995).			
		Hauterivian				Pemba Fm equiv.: Shale and paralic sandstones (Mahanjane, 2014).								
		Valanginian						Lupata Fm: Northwestern equivalent of the Red Beds Fm. Tithonian to Hauterivian. Continental sandstones. Towards the east the facies change from continental sandstones of the Lupata Formation to deposits of the ancient delta (Salman & Abdula, 1995)						Transgression? (Salman & Abdula, 1995)
		Berriasian			Red Beds Fm?						Red Beds: Red, continental sediments found in the southern part of the basin, onshore. Oxfordian to Berriasian (Salman & Abdula, 1995)	Stormberg Series: Aalenian to Barremian layers of Rhyolitic tuff to basalts (Salman & Abdula, 1995)		
Jurassic	Late	Tithonian				J-Unit I: shale, J-Unit II: paralic sandstone and J-Unit III: shale (Mahanjane, 2014).			Lupata Fm equiv. (Early Marine shale)??? Mahanjane et al., 2014)					
		Kimmeridgian												
		Oxfordian												
	Middle	Callovian												
		Bathonian				Makarawe Shale equivalent & Mtumbei LST equivalent			Belo Fm: Bajocian/Bathonian. Volcanic, Rhyolites (Salman & Abdula, 1995)					
		Bajocian		Break up										
		Aalenian												
	Early	Toarcian		Also Karoo Group???				Stormberg Series - Lebata Basalts equiv. Early Jurassic (Salman & Abdula, 1995). A volcanic sequence of Early Jurassic age, Basalts (Salman & Abdula, 1995) If it's the same as the Lebata formation described by Ellam & Cox (1990) then it's picritic basalts and forms part of the Karoo Igneous Province.			Stormberg Series - Lebata Basalts equiv. Early Jurassic (Salman & Abdula, 1995). A volcanic sequence of Early Jurassic age, Basalts (Salman & Abdula, 1995) If it's the same as the Lebata formation described by Ellam & Cox (1990) then it's picritic basalts and forms part of the Karoo Igneous Province.			
		Pliensbachian												
		Sinemurian												
		Hettangian												

				Megasequence	Mozambique									
					Angoche Basin			Zambezi Delta Depression			Southern Mozambique Basin			
					Onshore	Offshore		Onshore	Offshore		Central	Southern		
Triassic	Late			Karoo Group	Beaufort Series			Karoo Group	**Beaufort Series:** Triassic (Salman & Abdula, 1995). Not well known in the Mozambique basin due to lack of outcrop but can be generally described as fluvial, continental, terrigenous deposits with dispersed coaly material (Salman & Abdula, 1995)		Karoo Group	**Beaufort Series:** Triassic (Salman & Abdula, 1995). Not well known in the Mozambique basin due to lack of outcrop but can be generally described as fluvial, continental, terrigenous deposits with dispersed coaly material (Salman & Abdula, 1995)		
	Middle													
	Early													
Permian														
					Ekka Series				**Ekka Series:** Early Permian (Salman & Abdula, 1995). Typically terrestrial depositional settings, inc. lacustrine and fluvial mudstones and shales of overbank settings in the rift basins, also fluvial to fluvial-lacustrine sandstones and siltstones (Catuneanu et al., 2005). In this series there are widely developed, commercially viable seams of hard coal (Salman & Abdula, 1995)			**Ekka Series:** Early Permian (Salman & Abdula, 1995). Typically terrestrial depositional settings, inc. lacustrine and fluvial mudstones and shales of overbank settings in the rift basins, also fluvial to fluvial-lacustrine sandstones and siltstones (Catuneanu et al., 2005). In this series there are widely developed, commercially viable seams of hard coal (Salman & Abdula, 1995)		
Carboniferous	Late				Dwyka Series				**Dwyka Series:** Late Carboniferous to earliest Permian (Salman & Abdula, 1995). Tillites combined with periglacial and deglaciation sequences deposited by the Late Carboniferous – earliest Permian glaciation which reached into Northwest Africa (Catuneanu et al., 2005).			**Dwyka Series:** Late Carboniferous to earliest Permian (Salman & Abdula, 1995). Tillites combined with periglacial and deglaciation sequences deposited by the Late Carboniferous – earliest Permian glaciation which reached into Northwest Africa (Catuneanu et al., 2005).		
	Early													

Appendix H: Rotation Parameters

Africa fixed! All rotations back to Africa

Age (Ma)	India			Mascarene Plateau			Seychelles			Madagascar			Sri Lanka			Antarctica			
	Longitude	Latitude	Angle	Longitude	Latitude	Angle	Longitude	Latitude	Angle	Longitude	Latitude	Angle	Longitude	Latitude	Angle	Longitude	Latitude	Angle	
1	-146.585	-22.192	0.449													136.680	-7.462	-0.170	
2	-146.585	-22.192	0.897													136.680	-7.462	-0.339	
3	-146.585	-22.192	1.346													137.001	-7.602	-0.496	
4	-146.585	-22.192	1.794													137.531	-7.832	-0.634	
5	-146.585	-22.192	2.243													137.871	-7.979	-0.772	
6	-146.585	-22.192	2.691													138.108	-8.081	-0.911	
7	-146.585	-22.192	3.140													138.283	-8.157	-1.049	
8	-146.585	-22.192	3.588													138.417	-8.214	-1.187	
9	-146.585	-22.192	4.037													138.523	-8.260	-1.325	
10	-146.585	-22.192	4.485													138.684	-8.355	-1.466	
11	-145.369	-21.771	5.024													139.065	-8.627	-1.618	
12	-143.319	-21.036	5.664													139.381	-8.852	-1.770	
13	-141.701	-20.433	6.309													139.647	-9.041	-1.922	
14	-140.393	-19.931	6.958													139.874	-9.203	-2.074	
15	-139.314	-19.508	7.610													140.070	-9.342	-2.226	
16	-138.411	-19.147	8.264													140.242	-9.463	-2.378	
17	-137.643	-18.835	8.921													140.393	-9.570	-2.530	
18	-136.983	-18.563	9.579													140.527	-9.664	-2.682	
19	-136.409	-18.324	10.238													140.521	-9.863	-2.836	
20	-135.906	-18.113	10.898													140.162	-10.363	-2.996	
21	-135.461	-17.925	11.559													139.838	-10.812	-3.155	
22	-135.065	-17.756	12.220													139.545	-11.218	-3.316	
23	-134.710	-17.604	12.882													139.278	-11.586	-3.476	
24	-134.390	-17.466	13.545													139.034	-11.921	-3.637	
25	-134.100	-17.340	14.208													138.810	-12.227	-3.798	
26	-133.836	-17.226	14.871													138.245	-13.017	-4.002	
27	-133.595	-17.120	15.535													137.695	-13.780	-4.211	
28	-133.374	-17.023	16.199													137.195	-14.469	-4.422	
29	-133.171	-16.934	16.863													136.737	-15.095	-4.634	
30	-132.983	-16.851	17.527													136.317	-15.665	-4.846	
31	-132.808	-16.774	18.192													135.930	-16.186	-5.059	
32	-132.646	-16.702	18.856													135.573	-16.665	-5.273	
33	-132.495	-16.634	19.521													135.242	-17.106	-5.487	
34	-132.354	-16.572	20.186													135.371	-16.610	-5.731	
35	-132.222	-16.513	20.851													135.561	-16.006	-5.980	
36	-132.099	-16.457	21.517													135.735	-15.450	-6.230	
37	-131.982	-16.405	22.182													135.894	-14.938	-6.481	
38	-131.872	-16.356	22.848													136.041	-14.463	-6.732	
39	-131.769	-16.309	23.513													136.242	-14.074	-6.956	
40	-131.671	-16.265	24.179													136.535	-13.787	-7.134	
41	-131.578	-16.223	24.844													136.812	-13.514	-7.313	
42	-131.824	-16.324	25.271													137.076	-13.254	-7.493	
43	-132.548	-16.623	25.358													136.626	-13.530	-7.724	
44	-133.270	-16.918	25.449													135.912	-14.004	-7.978	
45	-133.989	-17.209	25.544													135.238	-14.447	-8.234	
46	-134.705	-17.494	25.643													134.966	-14.484	-8.481	
47	-135.417	-17.775	25.746													135.630	-13.552	-8.704	
48	-136.349	-17.941	26.270													136.257	-12.665	-8.930	
49	-137.307	-18.062	26.928													136.849	-11.821	-9.159	
50	-138.552	-18.189	27.686													137.408	-11.017	-9.390	
51	-139.969	-18.311	28.529													137.937	-10.251	-9.624	
52	-141.308	-18.416	29.385													138.439	-9.521	-9.861	
53	-142.461	-18.416	30.485													138.674	-8.739	-10.030	
54	-143.393	-18.301	31.903													138.510	-7.838	-10.088	
55	-144.549	-18.397	32.842													138.348	-6.947	-10.148	
56	-145.643	-18.481	33.791													138.189	-6.066	-10.211	
57	-146.750	-18.652	34.714													138.032	-5.196	-10.276	
58	-147.943	-18.996	35.574													137.878	-4.338	-10.344	
59	-149.000	-19.329	36.303	-163.664	-15.991	0.000										137.732	-3.482	-10.416	
60	-149.970	-19.652	36.954	-163.664	-15.991	0.032	-125.390	1.460	6.596							137.728	-2.452	-10.539	End of Mascarene Basin
61	-150.912	-19.959	37.614	-163.664	-15.991	0.356	-125.390	1.460	13.192							137.723	-1.447	-10.666	
62	-151.847	-20.360	38.229	-162.112	-17.084	0.928	-125.787	2.386	20.847							137.719	-0.465	-10.796	
63	-152.804	-20.947	38.755	-160.817	-17.979	1.961	-126.444	3.914	30.487							137.716	0.493	-10.929	
64	-154.019	-21.592	39.675	-161.724	-17.330	2.926	-126.057	5.131	41.088							137.488	0.962	-11.115	
65	-155.108	-22.293	41.193	-162.367	-17.125	4.814	-123.826	6.181	39.704							137.055	0.969	-11.352	
66	-155.420	-22.436	42.304	-158.360	-15.228	7.141	-125.020	5.600	40.388							136.640	0.976	-11.589	
67	-155.625	-22.503	43.349	-158.731	-16.213	8.579	-126.057	5.131	41.088							136.519	1.049	-11.828	
68	-155.821	-22.567	44.395	-159.270	-17.273	9.785	-127.059	4.675	41.803							136.584	1.162	-12.066	
69	-155.936	-22.596	45.444	-160.141	-18.757	10.478	-127.978	4.267	42.569							136.646	1.271	-12.305	
70	-155.853	-22.539	46.503	-160.428	-19.590	11.235	-128.731	3.960	43.448							136.706	1.376	-12.544	
71	-155.763	-22.480	47.557	-160.700	-20.326	11.981	-129.444	3.671	44.336							136.763	1.477	-12.782	
72	-155.453	-22.307	48.523	-161.384	-21.185	12.421	-129.904	3.547	45.272							136.905	1.509	-13.069	
73	-155.156	-22.139	49.490	-162.028	-21.982	12.864	-130.347	3.429	46.210							137.110	1.489	-13.395	
74	-154.992	-22.066	50.233	-162.979	-23.099	13.136	-130.714	3.285	46.900							137.304	1.470	-13.721	
75	-155.000	-22.115	50.667	-164.413	-24.702	13.178	-130.994	3.106	47.246							137.437	1.222	-14.055	
76	-155.007	-22.163	51.101	-165.873	-26.280	13.237	-131.269	2.929	47.594							137.542	0.884	-14.393	
77	-155.014	-22.210	51.535	-167.357	-27.827	13.312	-131.540	2.755	47.943							137.641	0.562	-14.731	
78	-155.021	-22.257	51.969	-168.865	-29.338	13.404	-131.807	2.583	48.294							137.736	0.254	-15.069	
79	-155.029	-22.303	52.404	-170.394	-30.810	13.512	-132.073	2.412	48.646							137.827	-0.041	-15.408	
80	-155.033	-22.338	52.741	-171.627	-31.953	13.645	-132.274	2.282	48.921							138.192	-0.154	-15.821	
81	-155.035	-22.361	52.965	-172.491	-32.731	13.796	-132.406	2.197	49.104							138.854	-0.072	-16.321	
82	-155.037	-22.384	53.188	-173.350	-33.486	13.952	-132.536	2.112	49.287							139.476	0.006	-16.822	
83	-155.039	-22.407	53.411	-174.205	-34.218	14.113	-132.666	2.027	49.470							140.062	0.079	-17.326	
84	-155.040	-22.430	53.630	-175.055	-34.928	14.277	-132.791	1.944	49.650							140.493	0.025	-17.857	
85	-155.042	-22.452	54.104	-175.900	-35.615	14.446	-133.064	1.794	50.045							140.686	-0.239	-18.435	
86	-155.044	-22.474	54.578	-176.739	-36.280	14.619	-133.333	1.647	50.442							140.868	-0.487	-19.014	
87	-155.046	-22.496	55.052	-177.572	-36.924	14.795	-133.597	1.501	50.840							141.040	-0.720	-19.593	
88	-155.048	-22.518	55.526	-178.399	-37.548	14.976	-133.933	1.850	51.312							141.202	-0.940	-20.172	
89	-155.050	-22.540	56.000				-134.115	1.214	51.639							141.354	-1.148	-20.752	Opening of the Mascarene Basin
90	-155.050	-22.540	56.000				-134.115	1.214	51.639				-155.050	-22.540	56.000	141.499	-1.345	-21.333	
91	-155.050	-22.540	56.000				-134.115	1.214	51.639				-153.892	-21.852	56.946	141.636	-1.531	-21.913	
92	-155.050	-22.540	56.000				-134.115	1.214	51.639				-152.780	-21.178	57.914	141.766	-1.708	-22.494	
93	-155.050	-22.540	56.000				-134.115	1.214	51.639				-151.711	-20.517	58.905	141.890	-1.876	-23.076	
94	-155.050	-22.540	56.000				-134.115	1.214	51.639				-150.684	-19.870	59.917	142.007	-2.036	-23.657	
95	-155.050	-22.540	56.000				-134.115	1.214	51.639				-149.696	-19.237	60.948	142.119	-2.188	-24.239	
96	-155.050	-22.540	56.000				-134.115	1.214	51.639				-148.745	-18.619	61.998	142.226	-2.334	-24.821	
97	-155.050	-22.540	56.000				-134.115	1.214	51.639				-147.829	-18.014	63.065	142.329	-2.472	-25.404	
98	-155.050	-22.540	56.000				-134.115	1.214	51.639				-146.948	-17.424	64.150	142.426	-2.605	-25.986	
99	-155.050	-22.540	56.000				-134.115	1.214	51.639				-146.098	-16.848	65.250	142.520	-2.732	-26.569	
100	-155.050	-22.540	56.000				-134.115	1.214	51.639				-145.278	-16.285	66.366	142.609	-2.853	-27.152	
101	-155.050	-22.540	56.000				-134.115	1.214	51.639				-144.487	-15.737	67.497	142.681	-2.740	-27.642	
102	-155.050	-22.540	56.000				-134.115	1.214	51.639				-143.724	-15.201	68.641	142.750	-2.630	-28.133	
103	-155.050	-22.540	56.000				-134.115	1.214	51.639				-142.986	-14.679	69.798	142.817	-2.523	-28.624	
104	-155.050	-22.540	56.000				-134.115	1.214	51.639				-142.273	-14.169	70.968	142.882	-2.421	-29.114	
105	-155.050	-22.540	56.000				-134.115	1.214	51.639				-141.583	-13.672	72.149	142.944	-2.321	-29.605	
106	-155.050	-22.540	56.000				-134.115	1.214	51.639				-140.915	-13.187	73.342	143.005	-2.225	-30.096	
107	-155.050	-22.540	56.000				-134.115	1.214	51.639				-140.268	-12.714	74.545	143.063	-2.132	-30.587	
108	-155.050	-22.540	56.000				-134.115	1.214	51.639				-139.641	-12.252	75.759	143.120	-2.042	-31.079	
109	-155.050	-22.540	56.000				-134.115	1.214	51.639				-139.033	-11.801	76.982	143.175	-1.954	-31.570	
110	-155.050	-22.540	56.000				-134.115	1.214	51.639				-138.444	-11.361	78.215	143.229	-1.869	-32.062	
111	-155.050	-22.540	56.000				-134.115	1.214	51.639				-137.871	-10.932	79.456	143.281	-1.787	-32.553	
112	-155.050	-22.540	56.000				-134.115	1.214	51.639				-137.315	-10.512	80.705	143.331	-1.706	-33.045	
113	-155.050	-22.540	56.000				-134.115	1.214	51.639				-136.775	-10.102	81.963	143.380	-1.629	-33.536	
114	-155.050	-22.540	56.000				-134.115	1.214	51.639				-136.249	-9.702	83.228	143.427	-1.553	-34.028	
115	-155.050	-22.540	56.000				-134.115	1.214	51.639				-135.737	-9.311	84.501	143.474	-1.479	-34.520	
116	-155.050	-22.540	56.000				-134.115	1.214	51.639				-135.239	-8.928	85.780	143.519	-1.408	-35.012	
117	-155.050	-22.540	56.000				-134.115	1.214	51.639				-134.754	-8.554	87.066	143.562	-1.338	-35.504	
118	-155.050	-22.540	56.000				-134.115	1.214	51.639				-134.281	-8.188	88.358	143.605	-1.271	-35.996	
119	-155.050	-22.540	56.000				-134.115	1.214	51.639				-133.820	-7.830	89.656	143.646	-1.205	-36.488	
120	-155.050	-22.540	56.000				-134.115	1.214	51.639				46.630	7.480	-90.960	143.624	-0.991	-36.912	
121	-155.050	-22.540	56.000				-134.115	1.214	51.639				46.630	7.480	-90.960	143.603	-0.783	-37.337	
122	-155.050	-22.540	56.000				-134.115	1.214	51.639				46.630	7.480	-90.960	143.582	-0.579	-37.762	
123	-155.050	-22.540	56.000				-134.115	1.214	51.639				46.630	7.480	-90.960	143.561	-0.379	-38.187	
124	-155.050	-22.540	56.000				-134.115	1.214	51.639				46.630	7.480	-90.960	143.541	-0.184	-38.613	
125	-155.050	-22.540	56.000				-134.115	1.214	51.639				46.630	7.480	-90.960	143.579	0.039	-39.023	
126	-155.050	-22.540	56.000				-134.115	1.214	51.639				46.630	7.480	-90.960	143.704	0.306	-39.409	
127	-155.050	-22.540	56.000				-134.115	1.214	51.639				46.630	7.480	-90.960	143.827	0.569	-39.796	
128	-155.050	-22.540	56.000				-134.115	1.214	51.639				46.630	7.480	-90.960	143.948	0.826	-40.184	
129	-155.050	-22.540	56.000				-134.115	1.214	51.639				46.630	7.480	-90.960	144.066	1.079	-40.572	
130	-155.050	-22.540	56.000				-134.115	1.214	51.639				46.630	7.480	-90.960	144.182	1.327	-40.962	
131	-155.050	-22.540	56.000				-134.115	1.214	51.639				46.630	7.480	-90.960	144.298	1.555	-41.368	
132	-155.050	-22.540	56.000				-134.115	1.214	51.639				46.630	7.480	-90.960	144.419	1.719	-41.838	
133	-155.050	-22.540	56.000	Mascarene			-134.115	1.214	51.639	Madagascar			46.630	7.480	-90.960	144.537	1.879	-42.308	End of Seafloor spreading in the Somali Basin (between 133-134Ma)
134	-155.097	-23.857	55.118				-133.448	0.052	50.666	1.625	-26.201	1.512	-133.291	-8.353	90.103	145.261	3.074	-43.423	
135	-154.952	-24.069	54.915				-133.174	-0.111	50.523	-1.460	-22.719	1.791	-133.177	-8.511	89.965	145.382	3.136	-43.713	
136	-154.806	-24.281	54.714				-132.900	-0.273	50.382	-3.594	-20.142	2.077	-133.063	-8.669	89.829	145.502	3.197	-44.003	
137	-154.544	-24.504	54.540				-132.540	-0.444	50.311	-7.575	-17.510	2.374	-132.898	-8.845	89.758	145.537	3.186	-44.348	
138	-154.190	-24.734	54.389				-132.116	-0.624	50.299	-12.214	-14.954	2.694	-132.693	-9.035	89.740	145.505	3.121	-44.736	
139	-153.834	-24.963	54.242				-131.692	-0.803	50.290	-15.774	-12.880	3.029	-132.487	-9.223	89.725	145.473	3.056	-45.123	
140	-153.473	-25.193	54.096				-131.267	-0.983	50.283	-18.564	-11.198	3.378	-132.281	-9.412	89.709	145.442	2.993	-45.511	
141	-153.110	-25.424	53.952				-130.843	-1.162	50.278	-20.797	-9.812	3.735	-132.075	-9.601	89.695	145.412	2.931	-45.899	
142	-152.744	-25.654	53.811				-130.418	-1.342	50.277	-22.628	-8.662	4.098	-131.869	-9.790	89.683	145.382	2.870	-46.287	
143	-152.285	-25.895	53.687				-129.927	-1.530	50.327	-24.928	-7.393	4.503	-131.622	-9.995	89.715	145.300	2.762	-46.724	
144	-151.817	-26.137	53.567				-129.433	-1.719	50.383	-26.875	-6.320	4.919	-131.373	-10.201	89.752	145.216	2.654	-47.164	
145	-151.345	-26.377	53.450				-128.939	-1.907	50.443	-28.510	-5.400	5.341	-131.123	-10.406	89.790	145.134	2.547	-47.605	
146	-150.880	-26.627	53.328				-128.448	-2.103	50.494	-29.774	-4.683	5.772	-130.877	-10.616	89.818	145.065	2.456	-48.049	
147	-150.594	-27.073	53.044				-127.976	-2.464	50.304	-28.713	-5.254	6.297	-130.699	-10.928	89.625	145.210	2.624	-48.557	
148	-150.305	-27.523	52.764				-127.501	-2.827	50.119	-27.809	-5.735	6.824	-130.520	-11.241	89.433	145.353	2.789	-49.066	
149	-150.010	-27.976	52.488				-127.022	-3.193	49.938	-27.034	-6.148	7.353	-130.341	-11.554	89.244	145.493	2.951	-49.576	
150	-149.710	-28.434	52.215				-126.540	-3.561	49.762	-26.359	-6.504	7.884	-130.160	-11.869	89.057	145.631	3.110	-50.086	
151	-149.560	-28.940	51.909				-126.145	-3.975	49.492	-25.033	-7.296	8.390	-130.050	-12.195	88.786	145.847	3.384	-50.550	
152	-149.448	-29.462	51.598				-125.770	-4.405	49.199	-23.669	-8.113	8.895	-129.959	-12.524	88.496	146.081	3.684	-51.004	
153	-149.336	-29.991	51.292				-125.391	-4.841	48.911	-22.448	-8.844	9.407	-129.867	-12.856	88.207	146.311	3.980	-51.460	
154	-149.220	-30.526	50.988				-125.006	-5.282	48.627	-21.346	-9.493	9.924	-129.774	-13.189	87.920	146.538	4.271	-51.918	
155	-149.108	-30.866	50.867				-124.775	-5.579	48.522	-21.096	-9.986	10.236	-129.718	-13.405	87.814	146.596	4.442	-52.203	
156	-149.000	-31.089	50.853				-124.637	-5.791	48.520	-21.296	-10.411	10.426	-129.685	-13.551	87.813	146.556	4.546	-52.386	
157	-148.891	-31.312	50.840				-124.498	-6.003	48.520	-21.492	-10.820	10.617	-129.652	-13.698	87.812	146.516	4.649	-52.570	
158	-148.782	-31.534	50.827				-124.360	-6.214	48.520	-21.681	-11.213	10.807	-129.618	-13.843	87.812	146.476	4.751	-52.753	
159	-148.672	-31.756	50.815				-124.220	-6.425	48.521	-21.863	-11.590	10.999	-129.585	-13.989	87.812	146.437	4.852	-52.937	
160	-148.560	-31.980	50.805				-124.081	-6.638	48.524	-22.044	-11.959	11.192	-129.551	-14.136	87.814	146.397	4.953	-53.121	
161	-148.449	-32.203	50.794				-123.942	-6.850	48.527	-22.215	-12.312	11.385	-129.517	-14.282	87.815	146.358	5.053	-53.305	
162	-148.337	-32.425	50.785				-123.803	-7.060	48.530	-22.379	-12.651	11.578	-129.483	-14.428	87.816	146.320	5.152	-53.489	
163	-148.225	-32.648	50.777				-123.663	-7.272	48.535	-22.543	-12.983	11.772	-129.450	-14.574	87.818	146.281	5.251	-53.674	
164	-148.112	-32.870	50.769				-123.524	-7.483	48.541	-22.698	-13.302	11.966	-129.416	-14.720	87.820	146.243	5.349	-53.858	
165	-147.999	-33.093	50.761				-123.384	-7.695	48.547	-22.849	-13.613	12.161	-129.382	-14.866	87.823	146.205	5.447	-54.043	
166	-147.884	-33.315	50.755				-123.244	-7.905	48.554	-22.999	-13.910	12.356	-129.348	-15.012	87.826	146.167	5.543	-54.228	
167	-147.769	-33.538	50.750				-123.105	-8.117	48.562	-23.143	-14.203	12.552	-129.314	-15.159	87.830	146.129	5.640	-54.413	
168	-147.653	-33.759	50.745				-122.965	-8.327	48.571	-23.282	-14.481	12.747	-129.280	-15.304	87.834	146.092	5.735	-54.598	
169	-147.537	-33.983	50.741				-122.824	-8.539	48.580	-23.416	-14.757	12.945	-129.246	-15.451	87.838	146.055	5.831	-54.784	
170	-147.420	-34.205	50.739				-122.685	-8.749	48.591	-23.549	-15.020	13.141	-129.212	-15.597	87.843	146.018	5.925	-54.969	
171	-147.303	-34.427	50.736				-122.544	-8.960	48.602	-23.678	-15.277	13.338	-129.178	-15.743	87.848	145.981	6.019	-55.155	
172	-147.184	-34.649	50.734				-122.403	-9.170	48.614	-23.802	-15.524	13.536	-129.143	-15.889	87.853	145.945	6.112	-55.341	
173	-147.066	-34.871	50.734				-122.264	-9.380	48.627	-23.925	-15.768	13.733	-129.109	-16.035	87.859	145.908	6.205	-55.527	
174	-146.946	-35.092	50.735				-122.123	-9.590	48.641	-24.044	-16.002	13.931	-129.075	-16.180	87.866	145.872	6.297	-55.713	
175	-146.827	-35.314	50.736				-121.983	-9.800	48.656	-24.159	-16.232	14.129	-129.041	-16.326	87.872	145.836	6.389	-55.899	
176	-146.706	-35.536	50.737				-121.842	-10.010	48.671	-24.269	-16.453	14.328	-129.006	-16.472	87.879	145.801	6.480	-56.085	
FIT 183 - 177 Ma	-146.576	-35.748	50.740				-121.697	-10.209	48.692	-24.402	-16.638	14.523	-128.967	-16.614	87.890	145.763	6.560	-56.271	